Fyziologie hmyzu

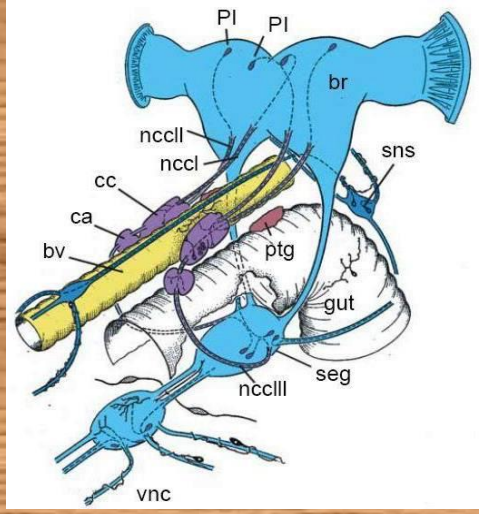

Dalibor Kodrík

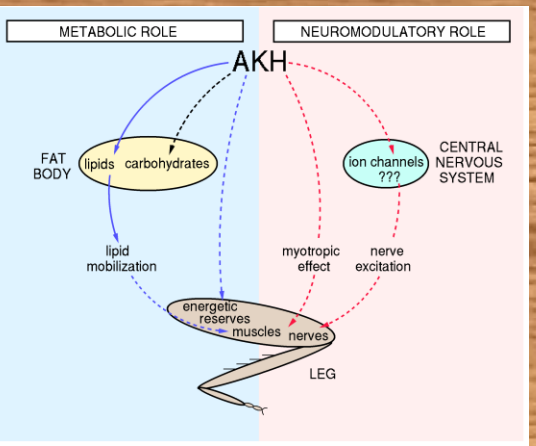

http://rum.prf.jcu.cz/public/fyziologie_hmyzu/

Fyziologie hmyzu - Dalibor Kodrík

Hodinová dotace (př/cv): 2/2 (cvičení – 2 dny za semestr), doporučené prerekvizity: FFZ 230 - Fyziologie živočichů a člověka, počet kreditů: 6

Přednáška seznamuje studenty se základními poznatky z fyziologie a funkční anatomie hmyzu. Klade důraz na základní rozdíly mezi fyziologickými mechanismy u hmyzu a u obratlovců:

1. Růst a pohyb (kutikula, svlékání, fyziologie svalů, typy hmyzí lokomoce - plazení, chůze, plavání, let a klikový mechanismus)
2. Trávení živin (typy trávení, peritrofická membrána, mikroorganismy, tukové těleso)
3. Dýchání (tracheální soustava, výměna plynů, tracheální žábry, fyzikální žábry, plastron)
4. Exkrece (toxické produkty metabolismu, Malpighické trubice, tvorba moči, kryptonefrický systém, osmoregulace)
5. Oběh tělních tekutin (hemolymfa, cirkulace, činnost srdce, imunita)
6. Bioluminiscence (mechanismus a funkce světelných orgánů)
7. Vnější faktory ovlivňující fyziologické děje (teplota těla a termoregulace, fotoperioda a diapauza)
8. Nervová činnost (nervová soustava a její činnost, mediátory, funkce CNS a činnost mozku, reflexní činnost)
9. Fyziologie smyslové soustavy (mechano-, chemo-, termo- a fotoreceptory)
10. Endokrinní soustava (význam, funkce a mechanismus působení hormonů, ekdysteroidy, juvenilní hormony a juvenoidy, peptidické neurohormony, feromony)
11. Činnost pohlavních orgánů a rozmnožování (samičí a samčí pohlavní systém, kopulace a fertilizace, kladení vajíček, vitellogenéza)
12. Hmyzí produkty využitelné člověkem (snovací žlázy a hedvábí, produkce medu, vosků, laků a jedů)

Seznam základní literatury:

1. Kodrík D.: Fyziologie hmyzu, učební texty, ENTÚ AVČR a BF JU Č. Budějovice, 2000 a jejich aktualizace na: http://rum.prf.jcu.cz/public/
2. Chapman N.F.: The Insects. Structure and Function. 4th edition, Cambridge University Press, Cambridge, 1998
3. Nation J.L.: Insect Physiology and Biochemistry, CRC Press, Boca Raton, 2002
4. Gullan P.J. and Cranston P.S.: The Insects: An Outline of Entomology, Chapman & Hall, London, 1995
5. Gilbert L.I., Iatrou K. and Gill S.S. Comprehensive Molecular Insect Science, Pergamon, 2005
6. Klowden M.J.: Physiological Systems in Insects, 2nd edition, Elsevier, Amsterodam, 2007

***Kontakt*:**

Dalibor Kodrík
Entomologický ústav AVČR, 2. patro, dveře č. 219 nebo 222, Branišovská 31, 370 05 České Budějovice
Telefon: 387 775 271, E-mail: kodrik@entu.cas.cz

Úvod
Fyziologie hmyzu - historie

- **starověk** - Aristoteles - znal a popsal fenomén hmyzí metamorfózy

- **17. a 18. století** - zakladatelé mikroskopických technik Robert Hooke, Marcello Malpighi, Anton van Leeuwenhoek, René de Réaumur, Pieter Lyonet - často používali hmyz jako pokusný objekt - začíná se poznávat struktura a funkce jednotlivých hmyzích orgánů

- **18. a 19. století** - Claude Bernard, John Lubbock, Henri Fabre - provádějí první funkční analýzy hmyzu, i když hlavní zájem je soustředěn na morfologii a systematiku

- **20. století: 1917-22** - Polák Stephan Kopeč - zakladatel hmyzí endokrinologie a objevitel existence hmyzích hormonů, prováděl operace a extirpace mozků a studoval jejich vliv na metamorfózu. Zavedl metodu ligatury, která se používá dodnes.

- **1934** - Angličan V.B. Wigglesworth - zakladatel hmyzí fyziologie jako samostatného oboru vydává v tomto roce knihu hmyzí fyziologie "Insect Physiology" a v roce 1947 základní dílo "Principles of Insect Physiology", které se od té doby dočkalo mnoha renovací a reedicí

- **40. a 50. léta 20. století** (a dále) - obrovský rozvoj biochemie a jejích metod znamená vznik a rozvoj biochemie hmyzu (Butenandt, Fraenkel, Fukuda, Piepho, Scharrer, Snodgrass, Williams)

- **60. léta** - Němec Peter Karlson a kolektiv - objevují steroidní hormony ekdysteroidy a naznačují mechanismus jejich působení na úrovní genu
  - Čech Karel Sláma - objevuje při své stáži v USA analogy juvenilního hormonu - juvenoidy (paper factor)

- **70. léta** - začínají se provádět sekvenace hmyzích peptidů - jako první je sekvenován adipokinetický hormon I ze saranče stěhovavé (Locusta migratoria) (Locmi-AKH-I).

- **80. a 90. léta až dnes** - obrovský rozvoj molekulární biologie, biochemie a chemie organických látek vede k poznání molekulární podstaty řady biologických procesů v hmyzím těle včetně metamorfózy

1. Růst a pohyb

Obr. 1

Stavba integumentu

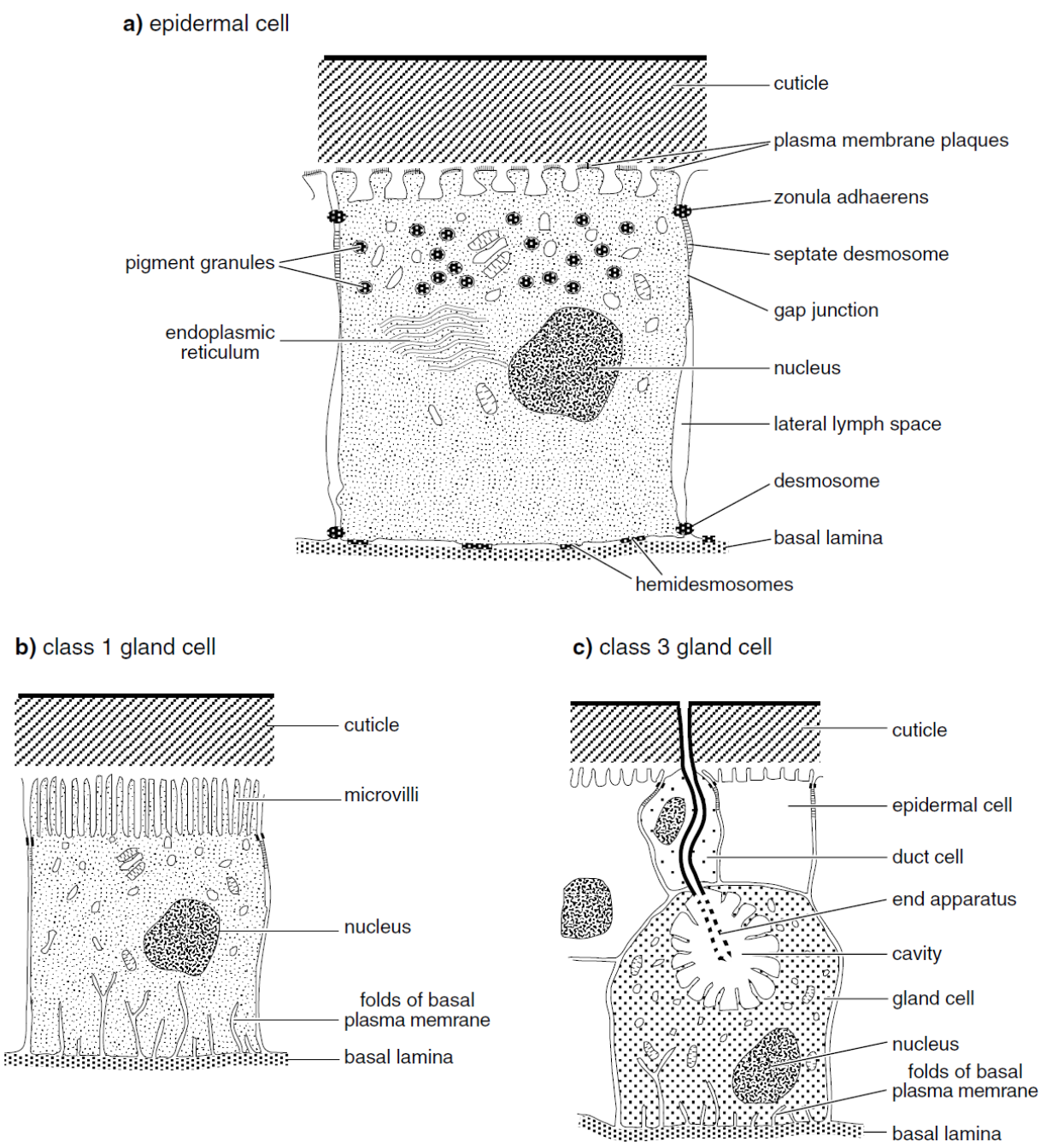

Fig. 16.1. Epidermal cells. **(a)** Principal features of an epidermal cell during the intermolt period. **(b)** Class 1 gland cell with no duct to the exterior (based on Noirot & Quennedey, 1974). **(c)** Class 3 glandular unit (based on Noirot & Quennedey, 1974).

Obr. 2 Jednotlivé části hmyzího integumentu

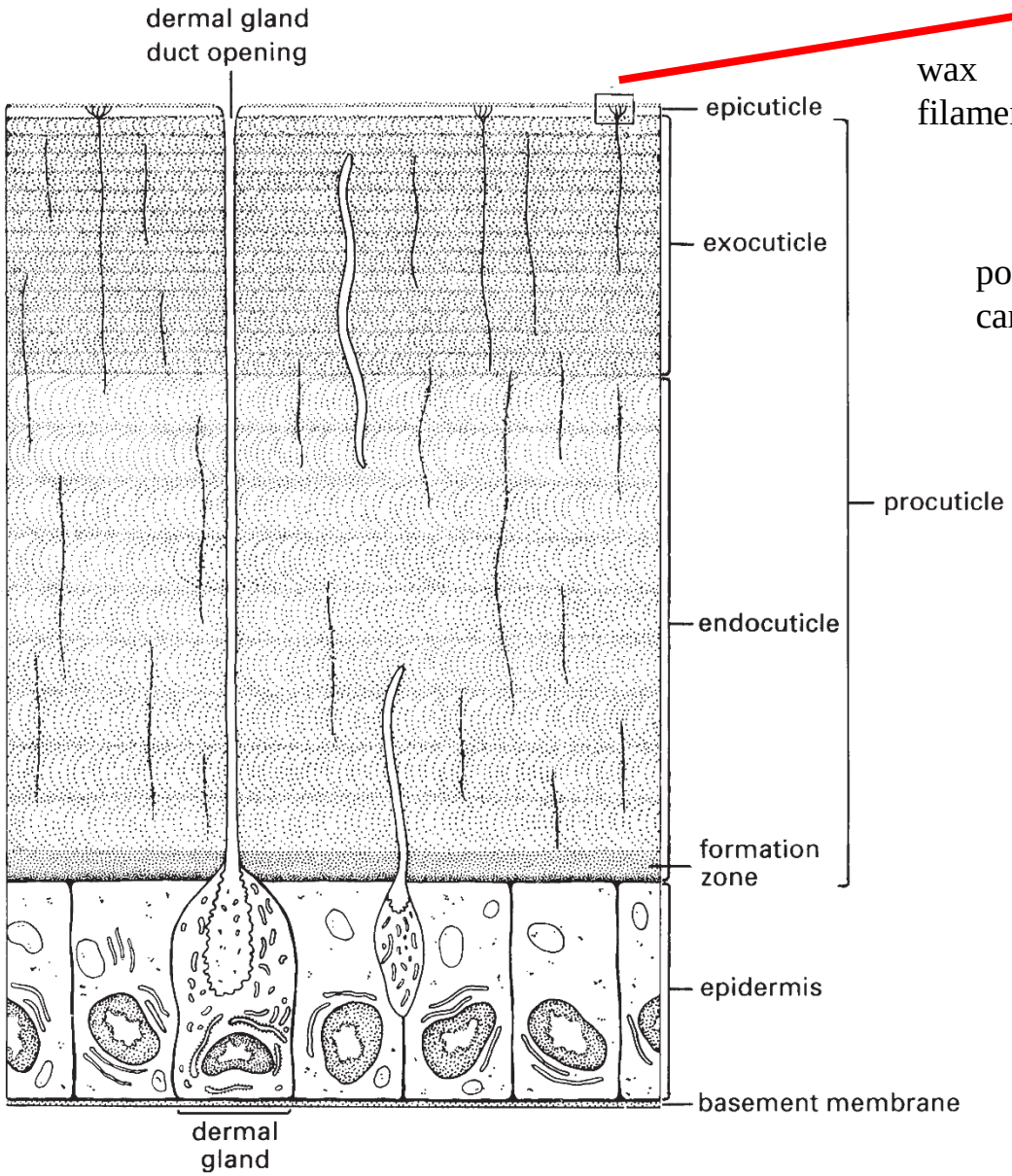

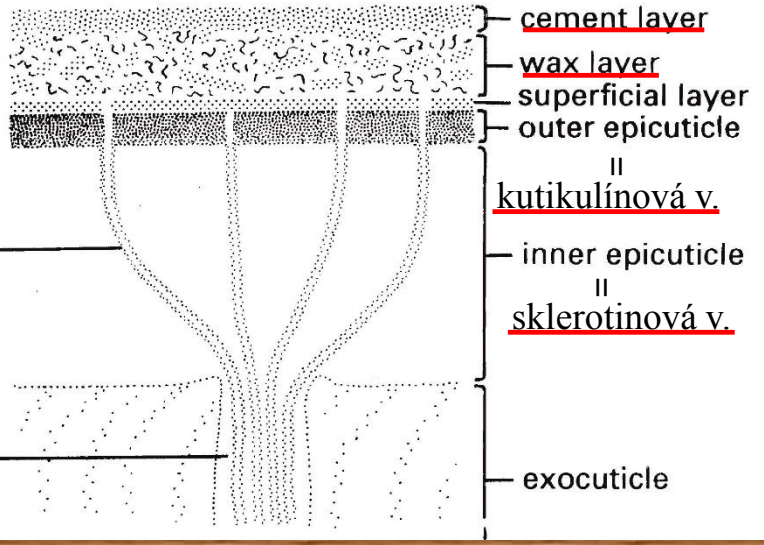

Obr. 3 Detail epikutikuly

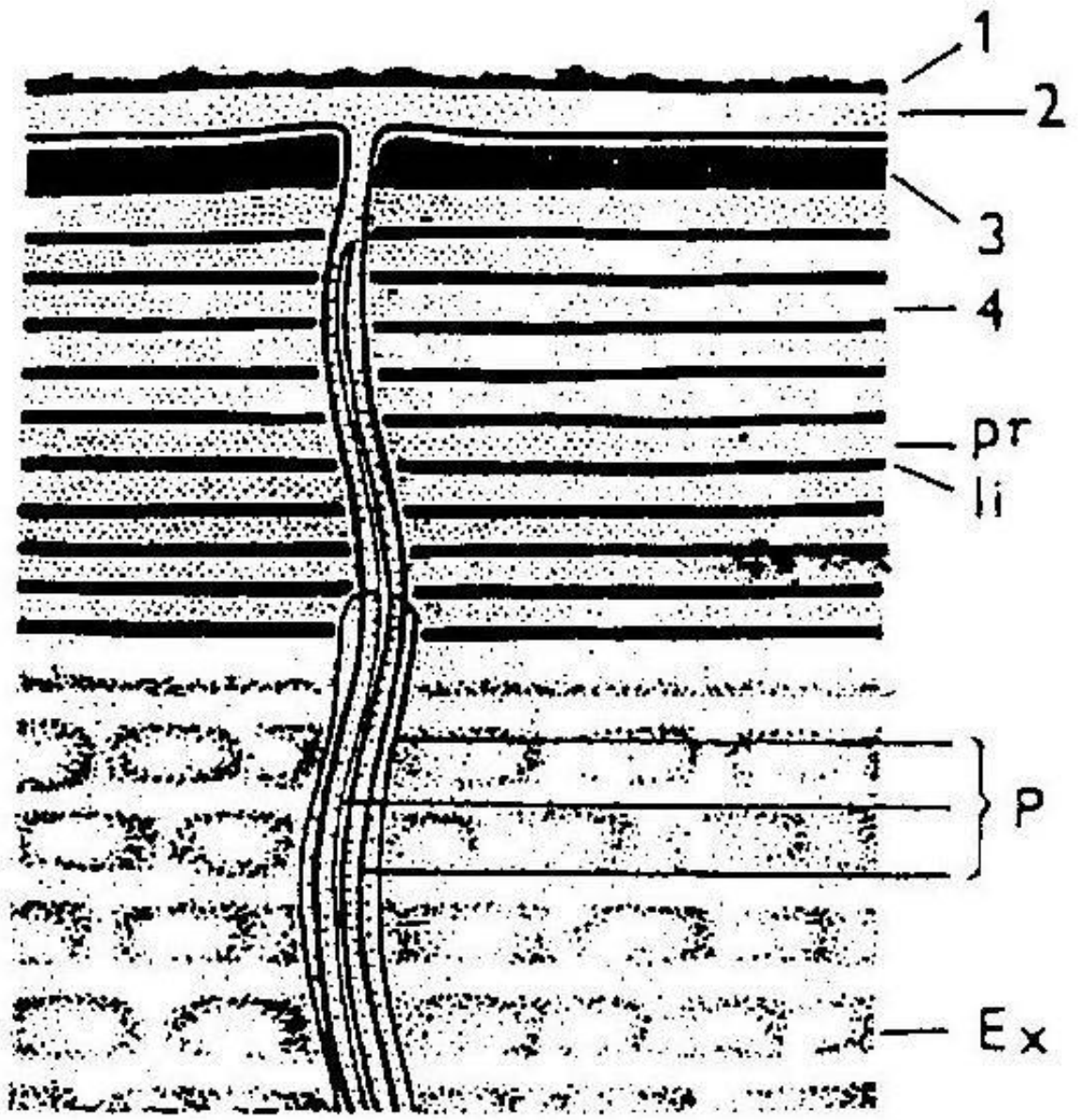

1 - cementová vrstva
2 - vosková vrstva
3 - kutikulínová vrstva
4 - sklerotinová vrstva
pr - proteiny
li - lipoidy
p - kanálek
Ex - exokutikula

Obr. 4 Složení voskové vrstvičky epikutikuly u vybraných druhů hmyzu

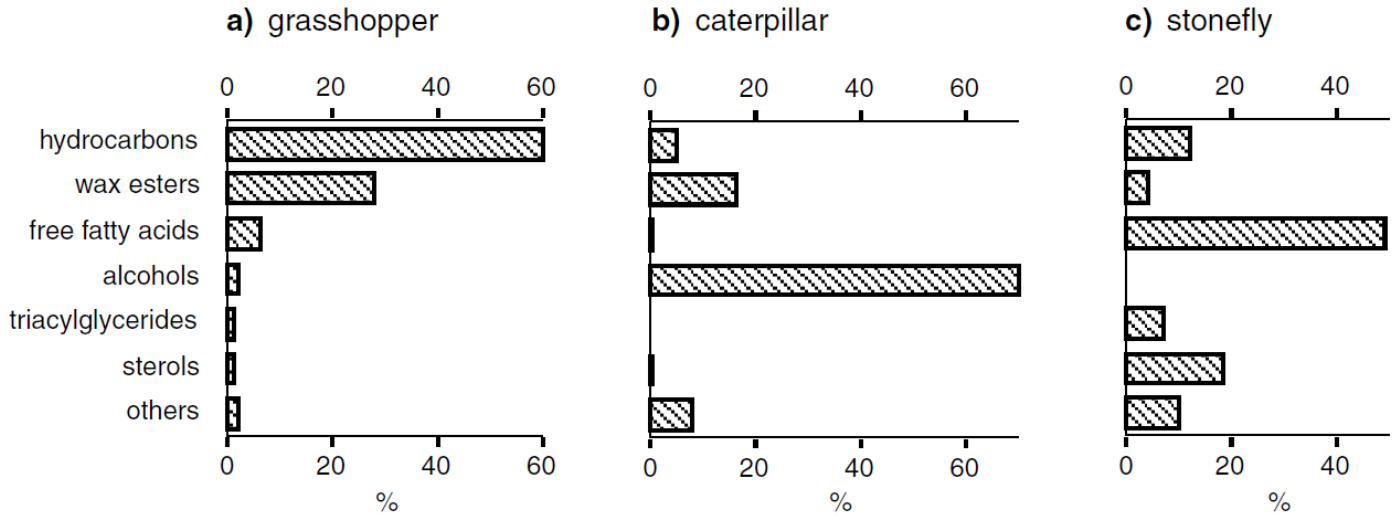

d)

		chain lengths (values of x)
hydrocarbons	$CH_3 - (CH_2)_X - CH_3$	12-37
wax esters	$CH_3 - (CH_2)_X - O - \overset{\overset{O}{\|\|}}{C} - (CH_2)_X - CH_3$	-
free fatty acids	$CH_3 - (CH_2)_X - \overset{\overset{O}{\|\|}}{C} - OH$	10-22
alcohols	$CH_3 - (CH_2)_X - CH_2 - OH$	12-34
triacylglycerides	$\begin{array}{l} CH_2 - O - \text{fatty acid} \\ \quad\vert \\ CH - O - \text{fatty acid} \\ \quad\vert \\ CH_2 - O - \text{fatty acid} \end{array}$	-
sterols	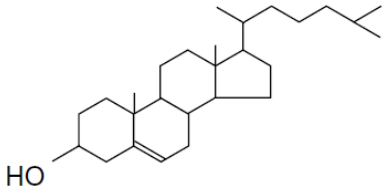	-

Obr. 5

Ukázky elastických částí kutikuly

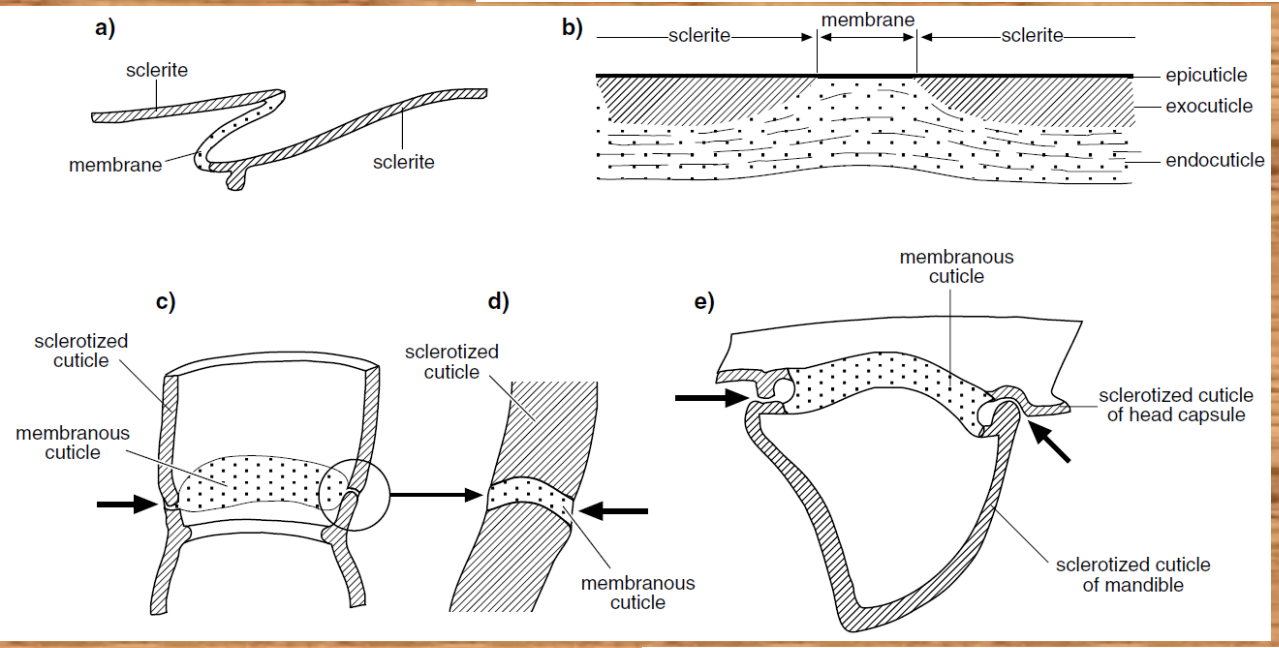

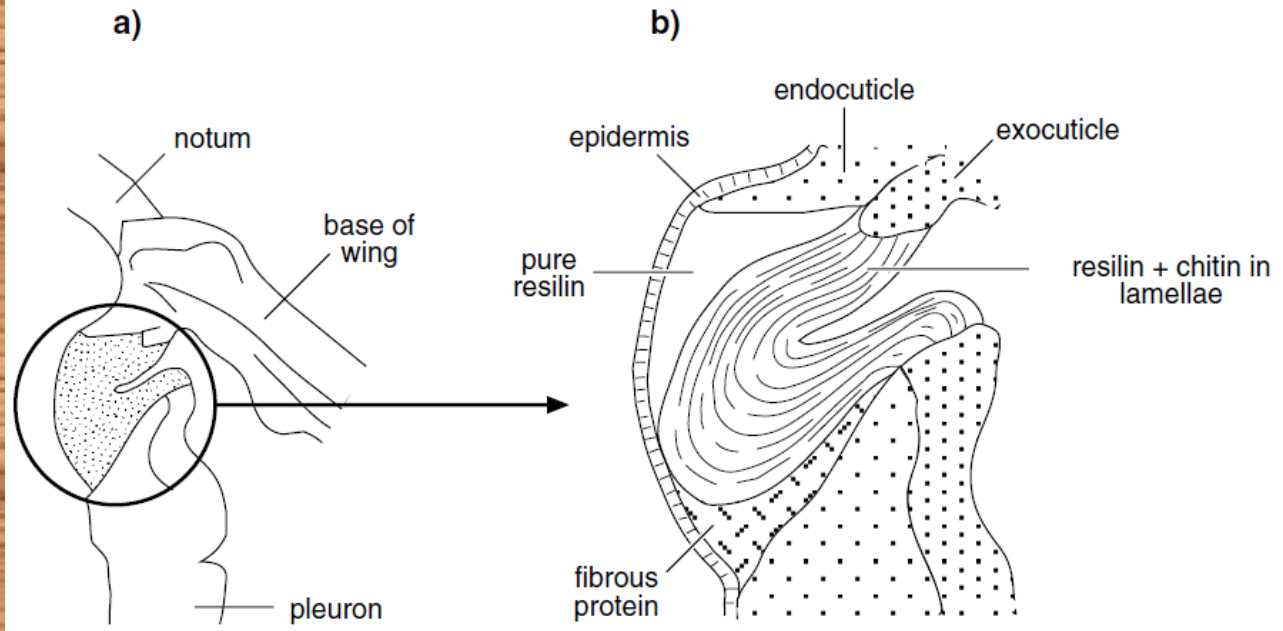

Obr. 6 Struktura chitinu

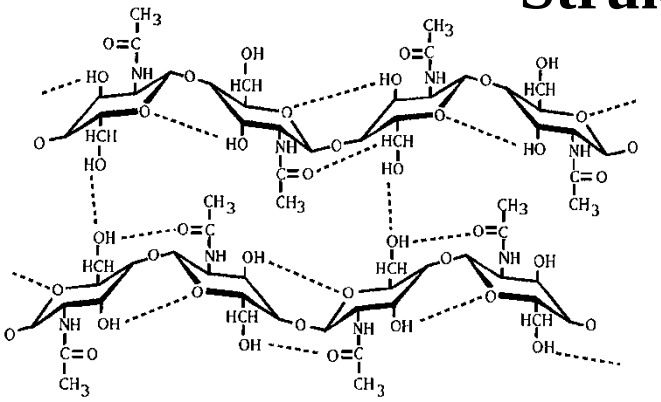

alpha-chitin

FIGURE 4.9 An illustration of the chemical structure of α-chitin chains and the anti-parallel arrangement of (two) chains that is typical in insect cuticles. Hydrogen bonds, some of which are intrachain and some interchain bonds, are represented by the dotted lines. Not shown are hydrogen bonds between chains in adjacent layers of chitin.

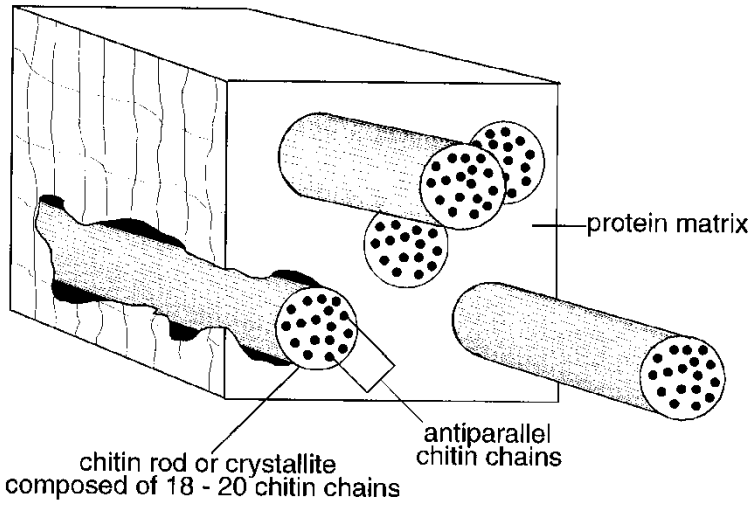

FIGURE 4.10 Chitin chains (about 20 typically in antiparallel arrangement) held together by hydrogen bonds to form chitin rods or crystallites embedded in a protein matrix in cuticle. (Modified from a model presented in Giraud-Guille and Bouligand, 1986.)

Obr. 7

Chitinové struktury v kutikule

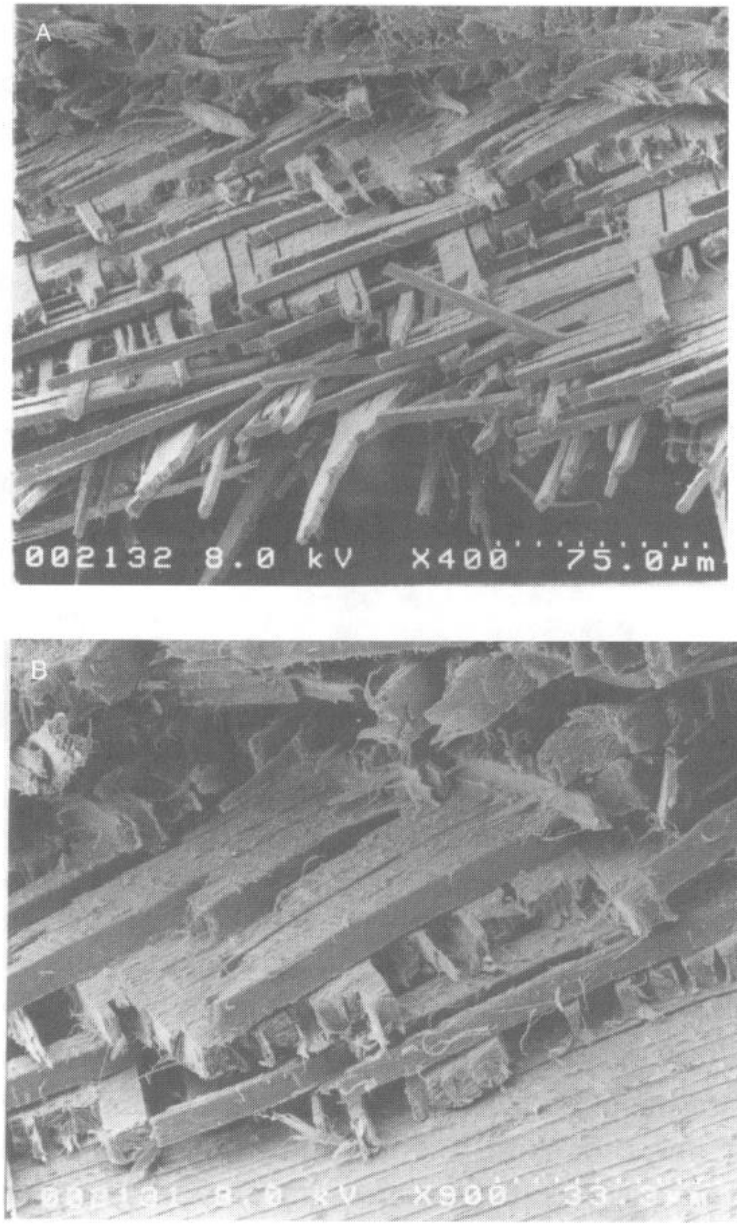

FIGURE 4.12 Freeze-fractured break in the thoracic cuticle of the weevil *Rhynchophorus cruentatus* showing plywood-like arrangement of cuticle layers that gives the cuticle added strength. (Magnification: ×400 (A), ×900 (B).) (Photographs courtesy of Robin Giblin-Davis.)

Stavba integumentu

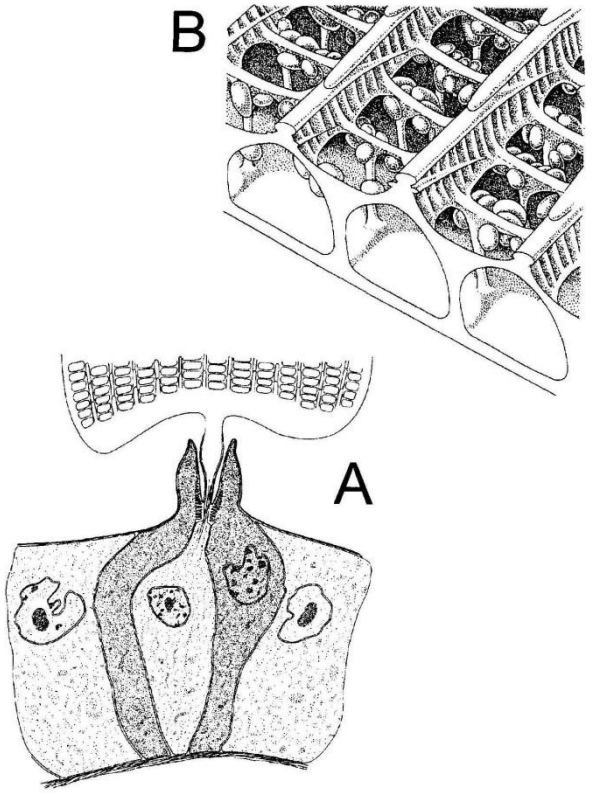

FIGURE 2.15. (A) An epidermal cell on a lepidopteran wing forming a scale. The ribs and lamellae on the scale (B) diffract the light and produce structural colors. Reprinted with permission from Ghiradella (1991).

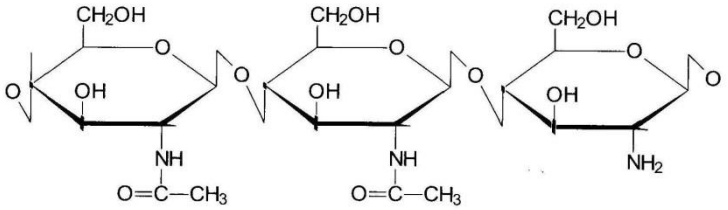

FIGURE 2.16. A portion of the chitin chain, showing two residues of N-acetyl-D-glucosamine and one of glucosamine.

Obr. 8

Obr. 9 **Motýlí šupina - na mikrostrukturách žeber vznikají kovově lesklé barvy**

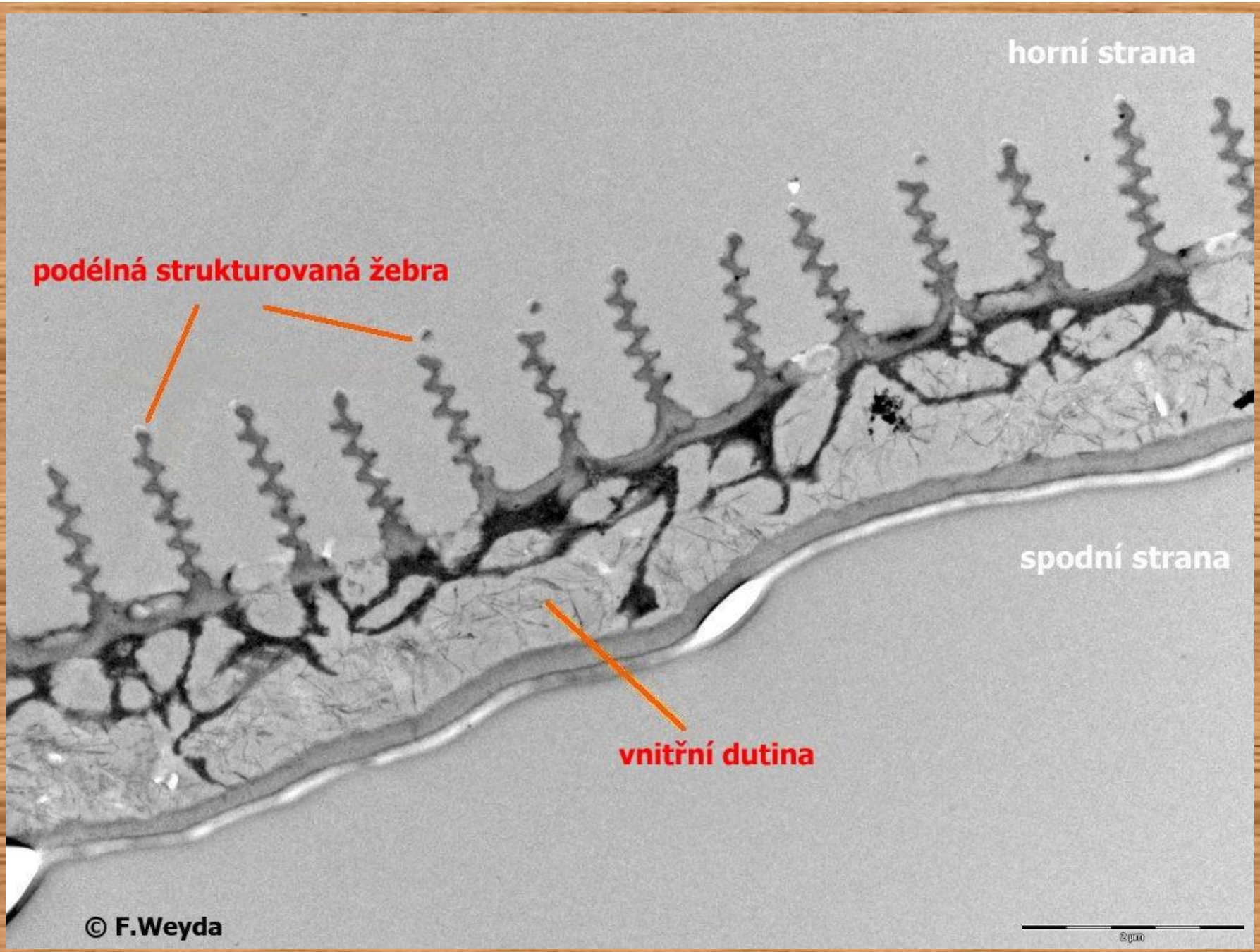

Barva	Barvivo	Taxon
černá	aphiny	Homoptera, Aphididae
	melanin	Coleoptera, Diptera, Lepidoptera (larvy)
červená	omochromy	Odonata
	pteriny a karotenoidy	Hemiptera, Homoptera
	antrachinony	Hemiptera, Coccoidea
	karotenoidy	Coleoptera, Coccinellidae
	porfiriny	Diptera, Chironomodae (larvy)
	ommochromy	Lepidoptera
hnědá	ommochromy	Lepidoptera
	ommochromy-pteriny	mnohé řády
oranžová	pteriny	Hemiptera, Homoptera
žlutá	karotenoidy, flavonoidy	Orthoptera, Acrididae
	pteriny	Hemiptera, Homoptera
	papiliochromy	Lepidoptera, Papilionidae
mosazně žlutá	interferenční barva	Lepidoptera
bronzová	interferenční barva	Coleoptera, Scarabaeidae
zlatá	interferenční barva	Coleoptera, Cassidinae, Lepidoptera, Danaidae
zelená	insectoverdin (karotenoid-bilin)	Orthoptera, Lepidoptera (larvy)
	interferenční barva	Lepidoptera, Zygaenidae
	bilin	Diptera, Chironomidae (imága)
modrá	Tyndalův rozptyl	Odonata
	interferenční barva	Lepidoptera
	karotenoidy	Orthoptera, Acrididae
fialová	interferenční barva	Lepidoptera, Pieridae
bílá	kyselina močová	Hemiptera, Homoptera
	rozptýlené pteriny	Lepidoptera, Pieridae
	flavonoidy	Lepidoptera, Satyridae
stříbrná	interferenční barva	Lepidoptera, Danaidae (kukly)
měňavá	difrakce	Coleoptera
	interferenční barva	Coleoptera, Scarabaeidae

Porfyrin

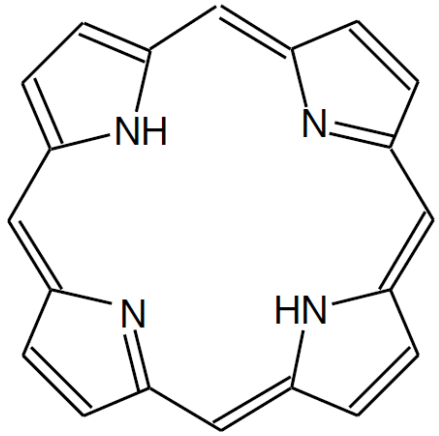

Bilin

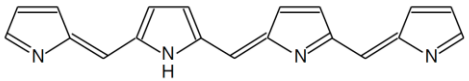

Obr. 10

Obr. 11

Změny v kutikule během svlékání

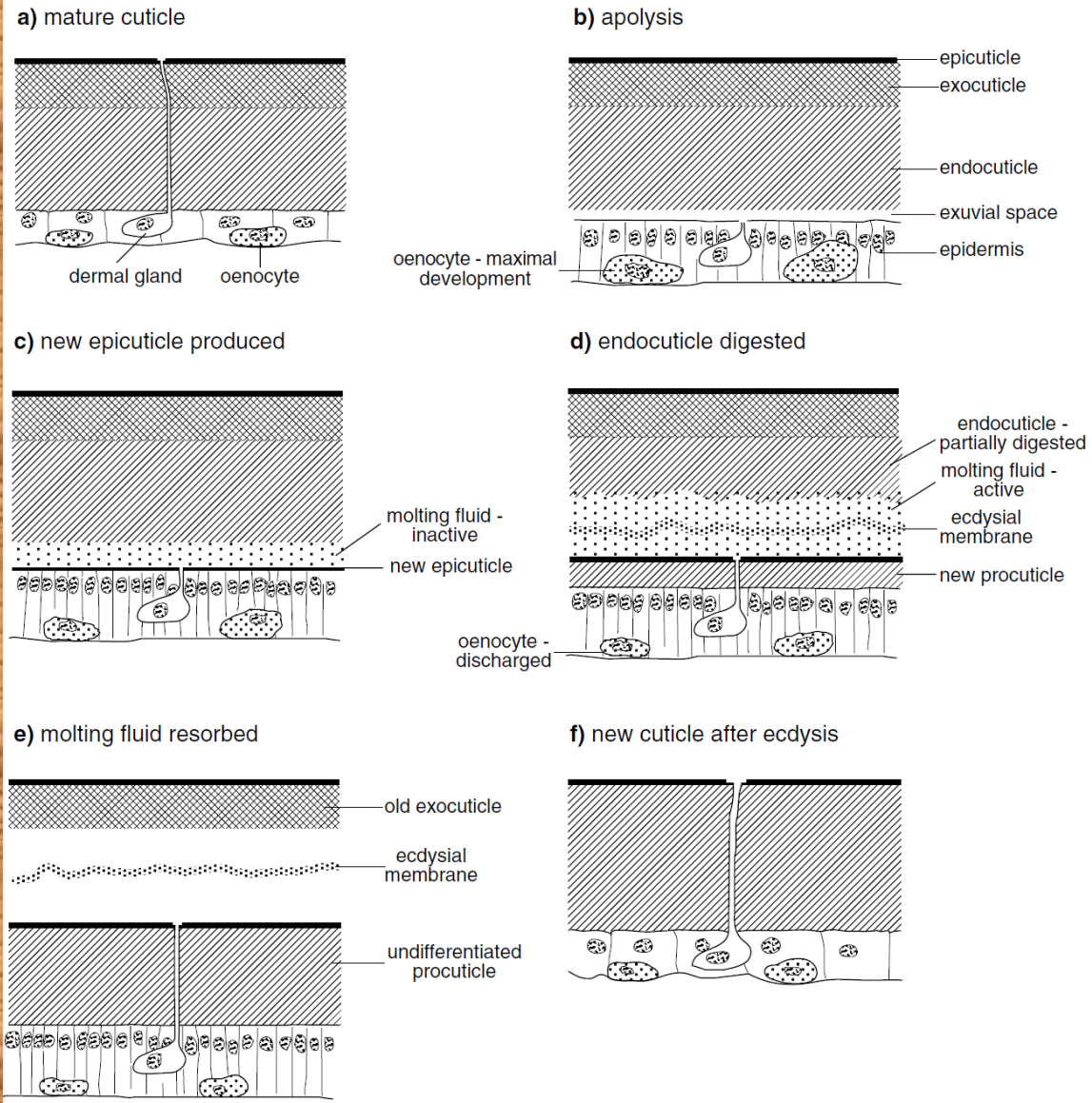

Fig. 16.17. Changes in the integument over a molt. **(a)** Mature cuticle. **(b)** Apolysis follows cell division and the change in cell shape. **(c)** Molting fluid is produced. At first, the enzymes it contains are inactive. The new outer and inner epicuticles are produced. **(d)** The enzymes in the molting fluid are activated and start to digest the old endocuticle. At the same time new procuticle is laid down. **(e)** All the old endocuticle is digested and resorbed. New procuticle becomes thicker. **(f)** After ecdysis the new cuticle expands and the epidermal cells change shape. The procuticle is still undifferentiated.

Obr. 12

Změny tvaru epidermálních buněk během ekdyze

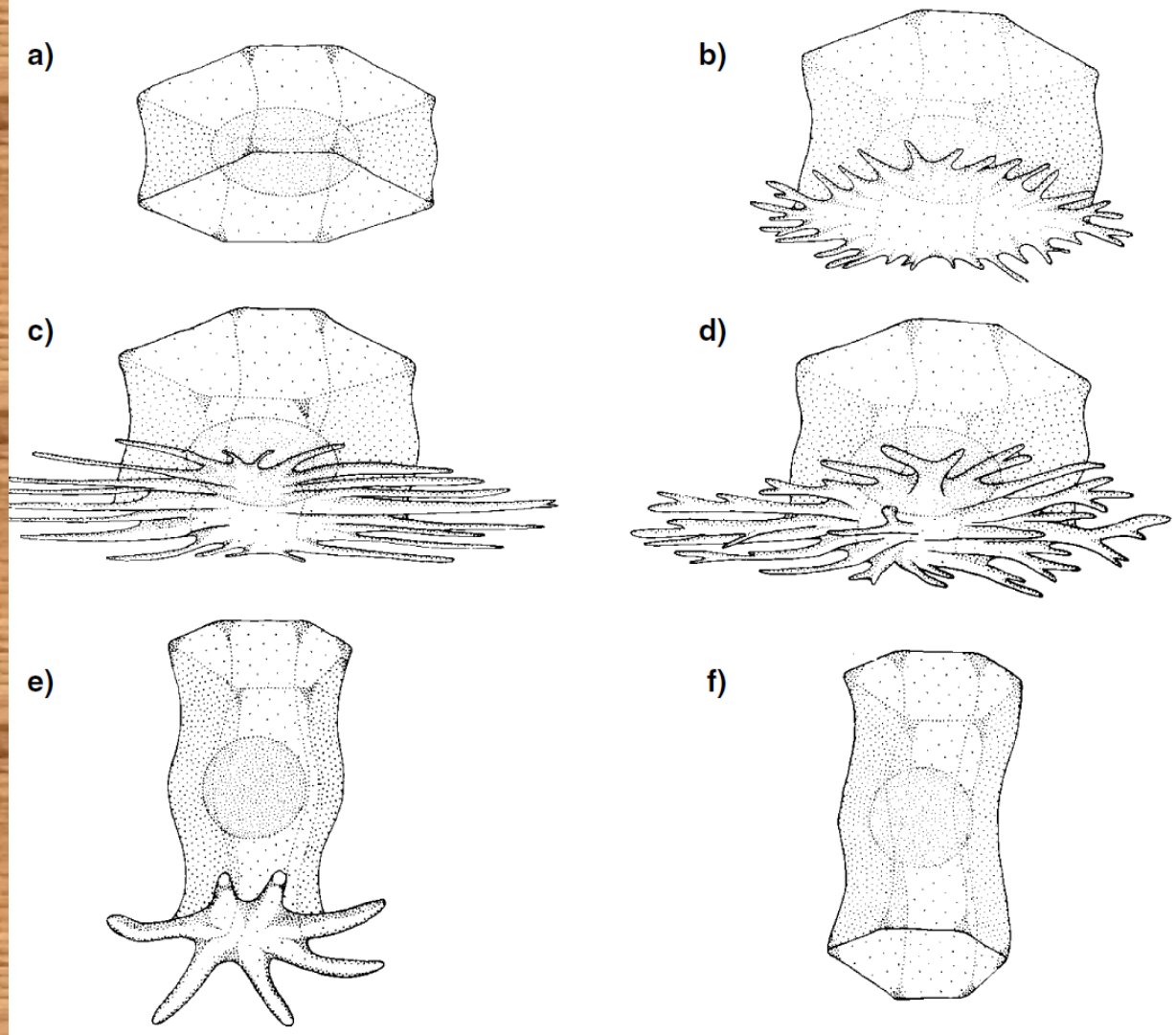

Fig. 16.16. Changes in the shape of epidermal cells during the final larval stage of *Calpodes* (Lepidoptera) (after Locke, 1985b): **(a)** 36 hours after ecdysis from the fourth stage; **(b)** 72 hours after ecdysis. Cell growth keeps pace with the increasing size of the larva; **(c)** the larva has reached its maximum size and the cell has extensive feet; **(d)** the feet begin to shorten as the larva shortens in the period before pupation; **(e)** cell area and the extent of feet is greatly reduced as shortening continues, but cell depth increases as the cells become crowded; **(f)** about 20 hours before ecdysis to the pupa.

Obr. 13 Mechanismus hlavních kroků vedoucích k tvorbě tmavých (melanin) a tvrdých (sklerotin) součástí kutikuly

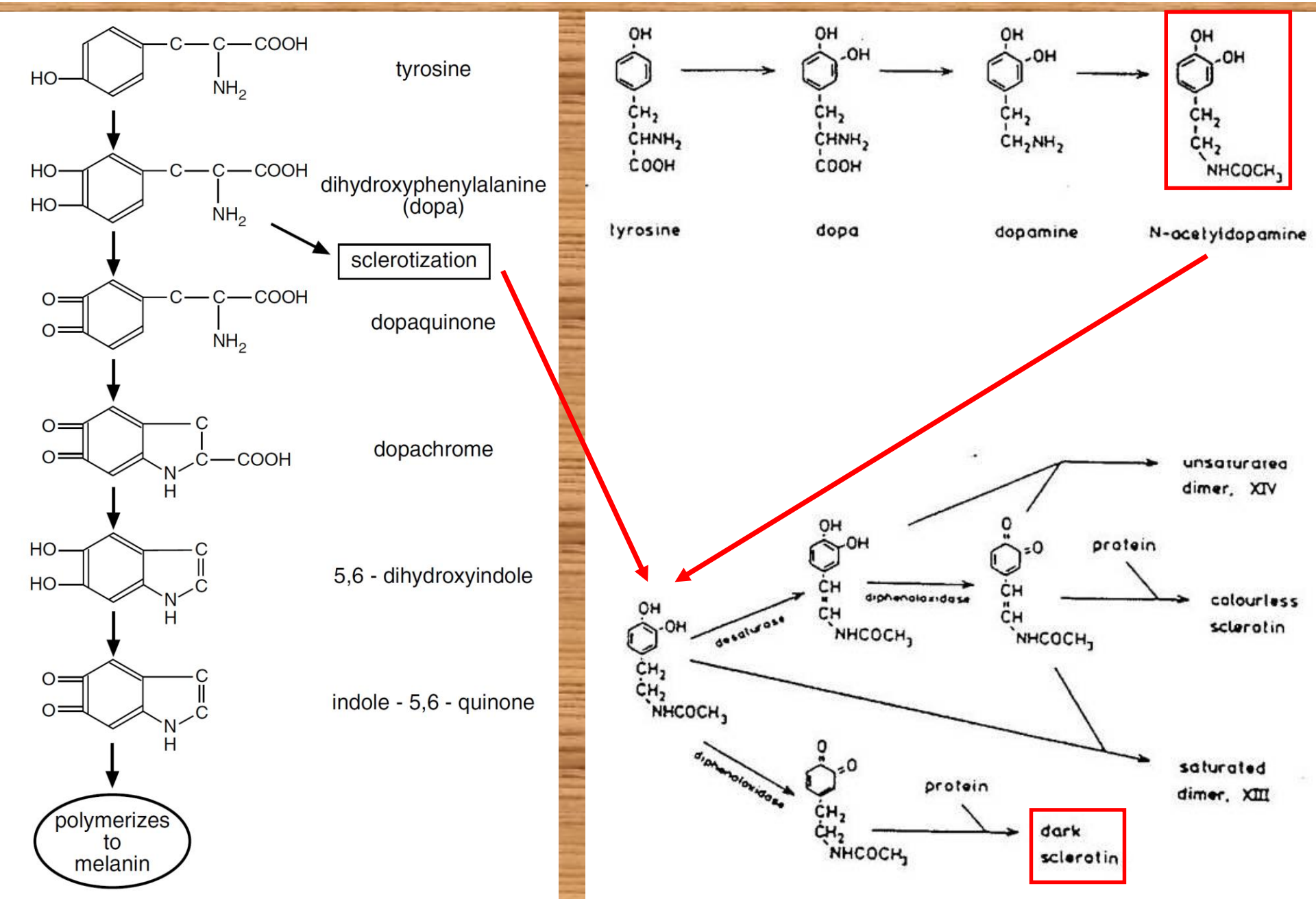

Tmavnutí a tvrdnutí kutikuly

Obr. 14

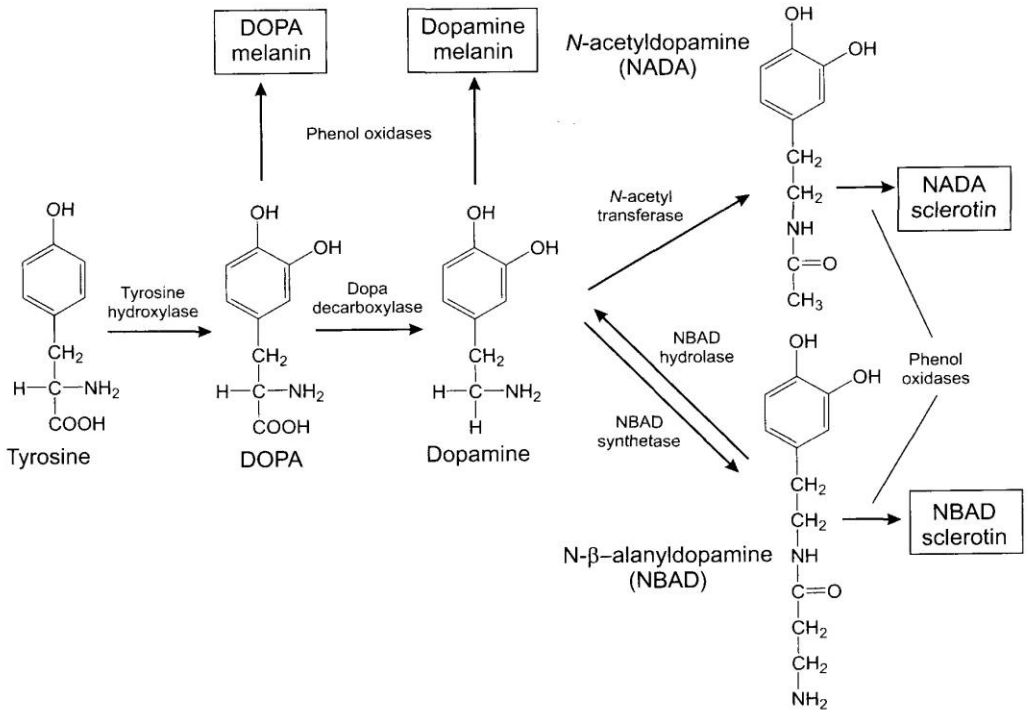

FIGURE 2.19. The steps in the synthesis of cuticular tanning precursors.

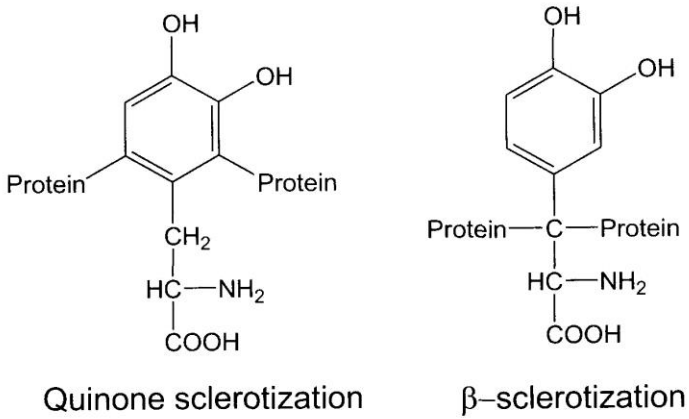

FIGURE 2.20. Differences between quinone sclerotization and β-sclerotization in where the cross-linked proteins are attached.

Obr. 15

Ukázka expanze nové kutikuly po ekdyzi

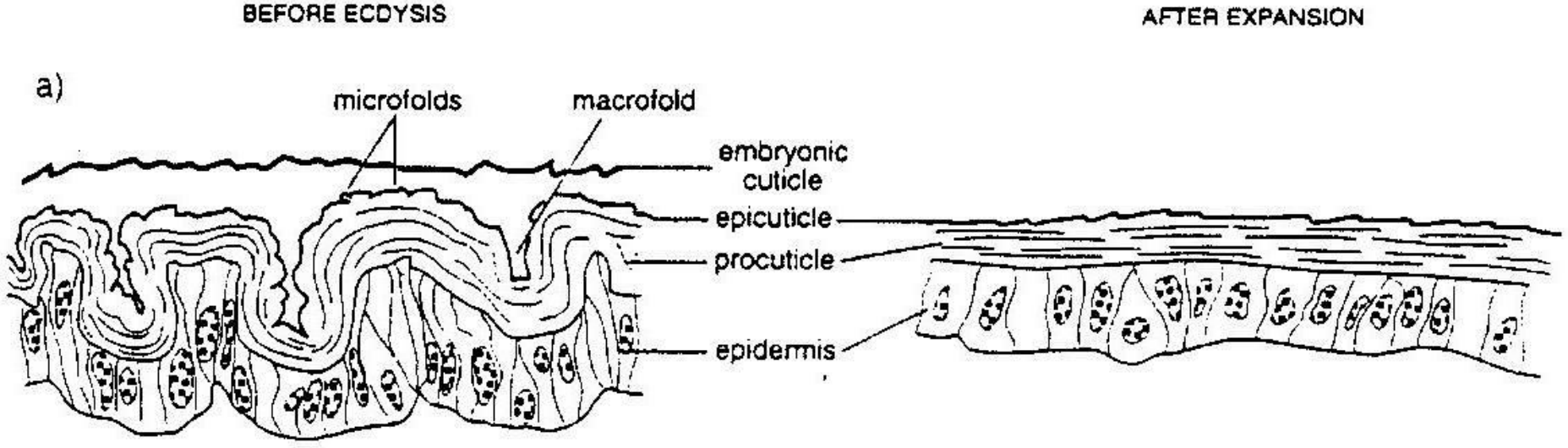

Schéma svlékání kutikuly: http://www.youtube.com/watch?v=QfeEZl0VGs0

- Svlékání cikády: http://www.youtube.com/watch?v=2A1i10ZIB-w

- Svlékání housenky: http://www.youtube.com/watch?v=NsMPxvsdDdk&feature=endscreen&NR=1

Obr. 16

Exo- a endoskelet

Schéma exoskeletu hmyzu

a = tergum, b = intersegmentální membrána, c = sternum, d = končetinový článek, e = hlavová schránka

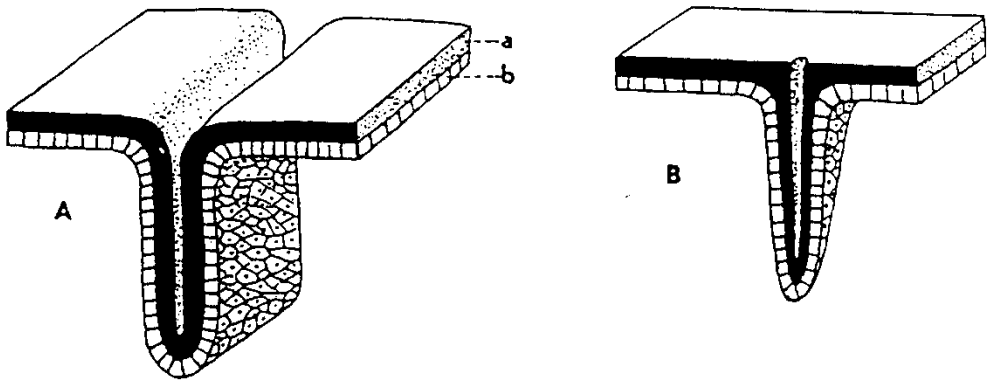

Endoskeletní útvary hmyzu

A - endoskeletní lišta, B - apodema; a = kutikula, b = epidermis

Obr. 17

Intersegmentální membrána

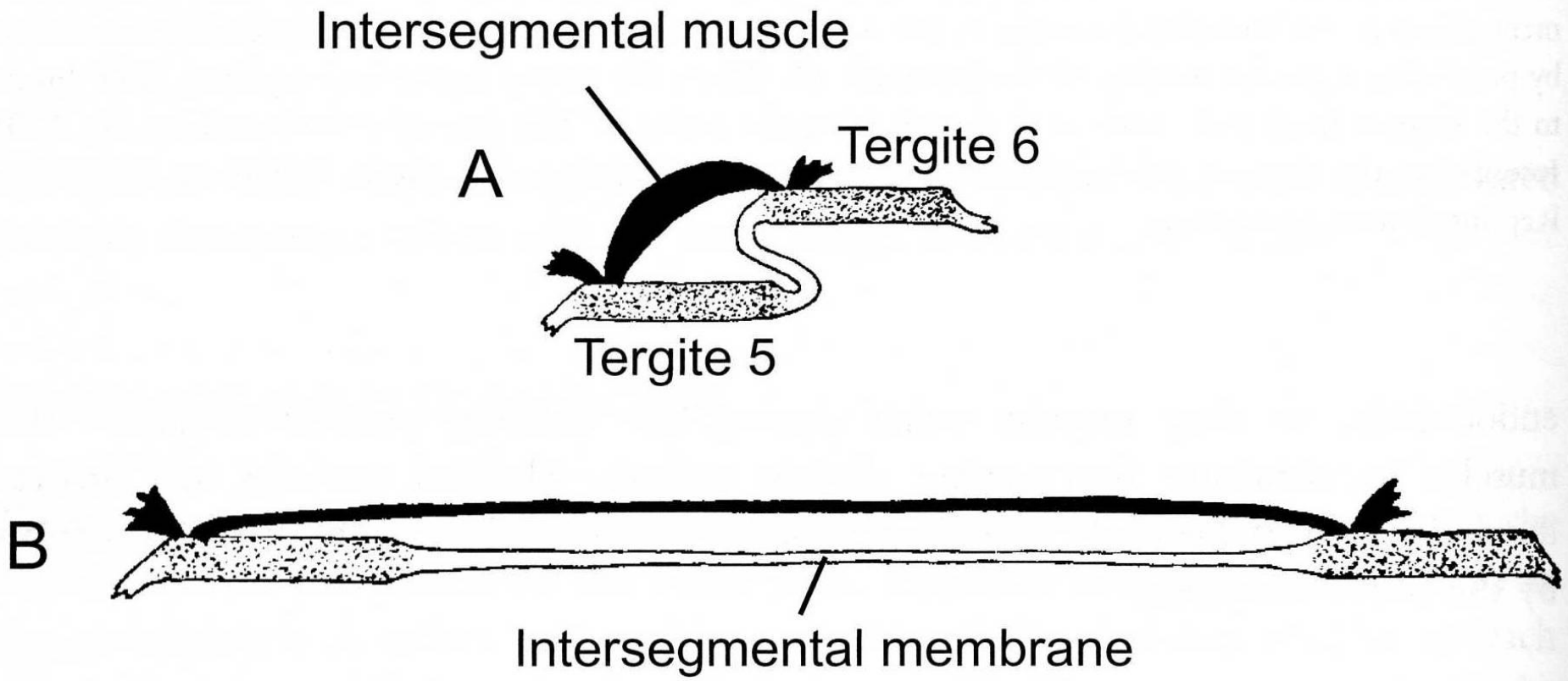

FIGURE 10.15. Intersegmental muscles allow for the supercontraction (A) and the superextension (B) and of the body segments. Reprinted from Jorgensen W.K., M.J. Rice. 1983. Superextension and supercontraction in locust ovipositor muscles. J. Insect Phys. 29: 437–448. Copyright 1983, with permission from Elsevier Science.

Příklady různých druhů úponů svalů na kutikulu

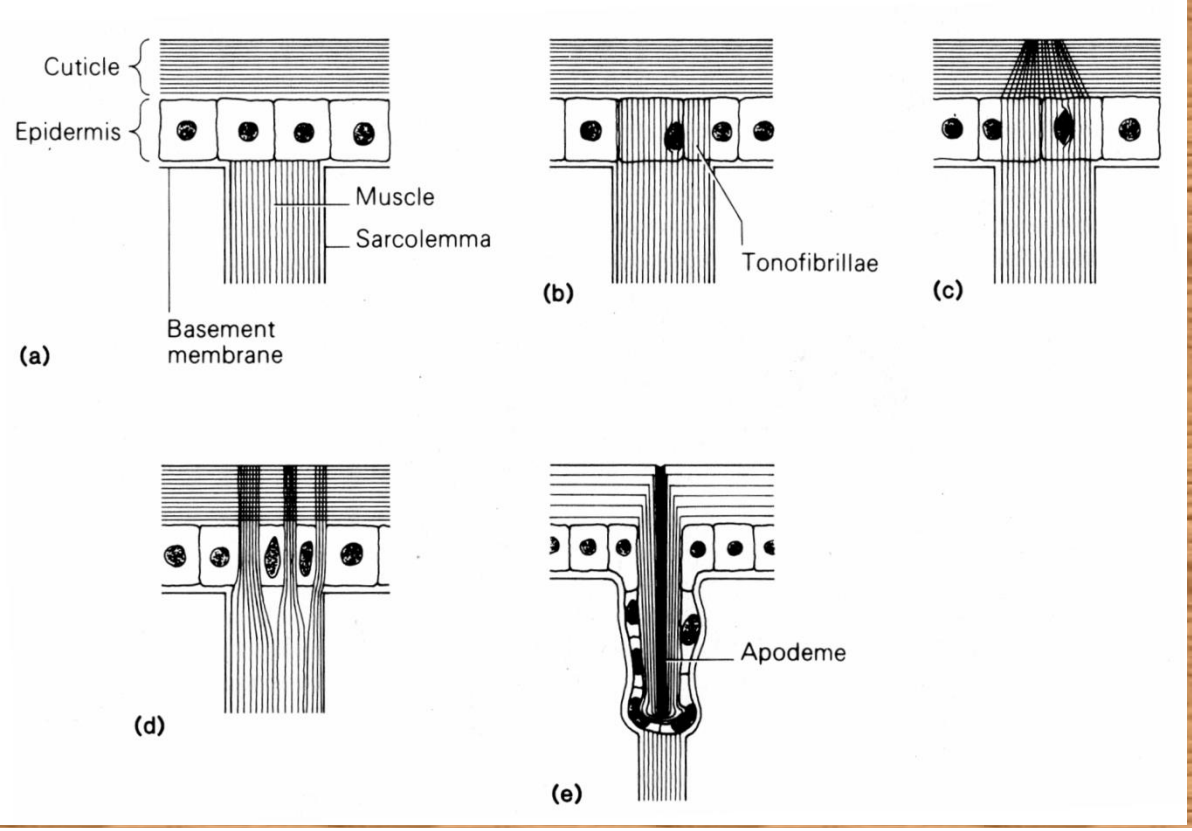

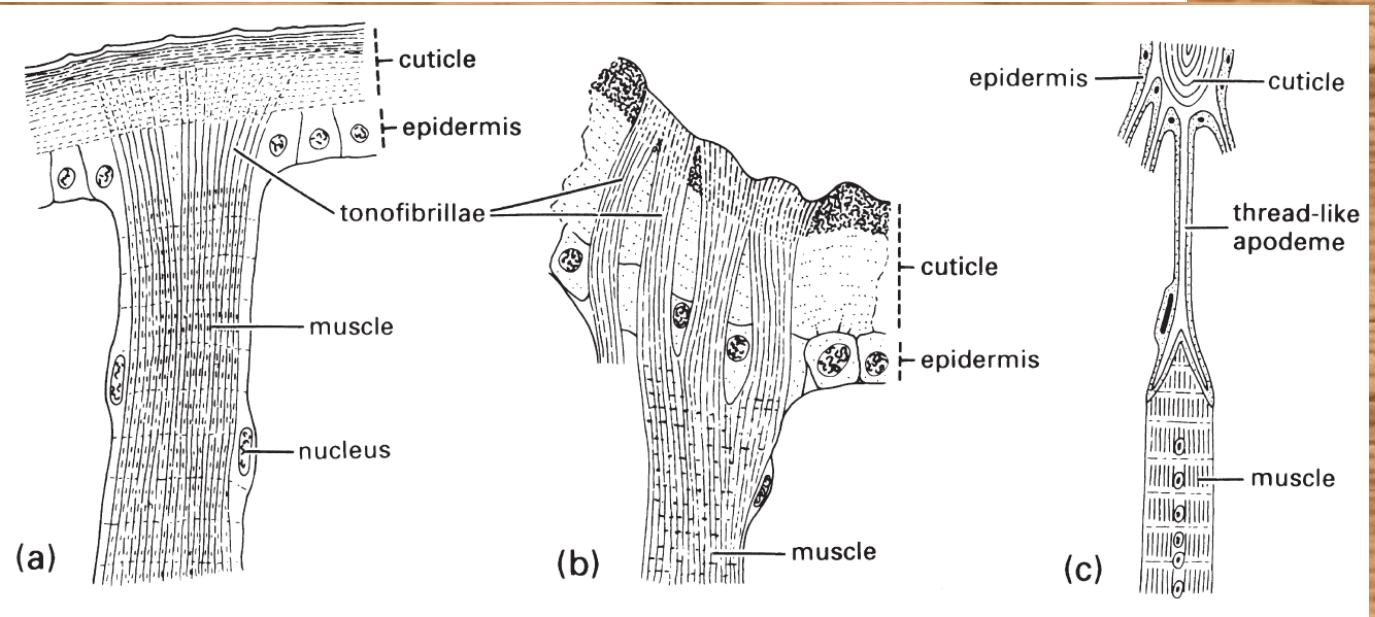

Obr. 18

Obr. 19

Detail úponu svalu na kutikulu

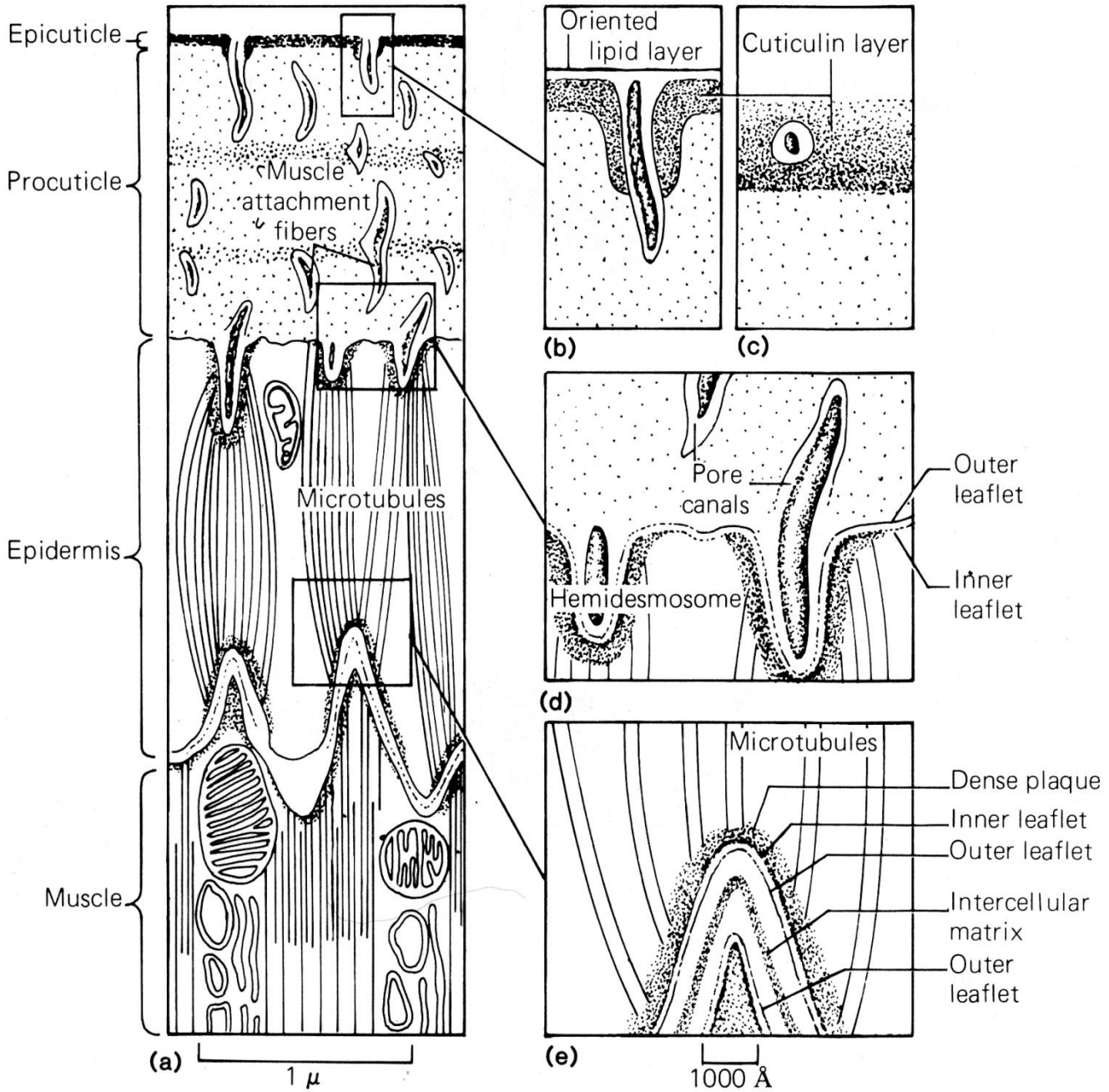

Obr. 20 Připojení svalu ke kutikule

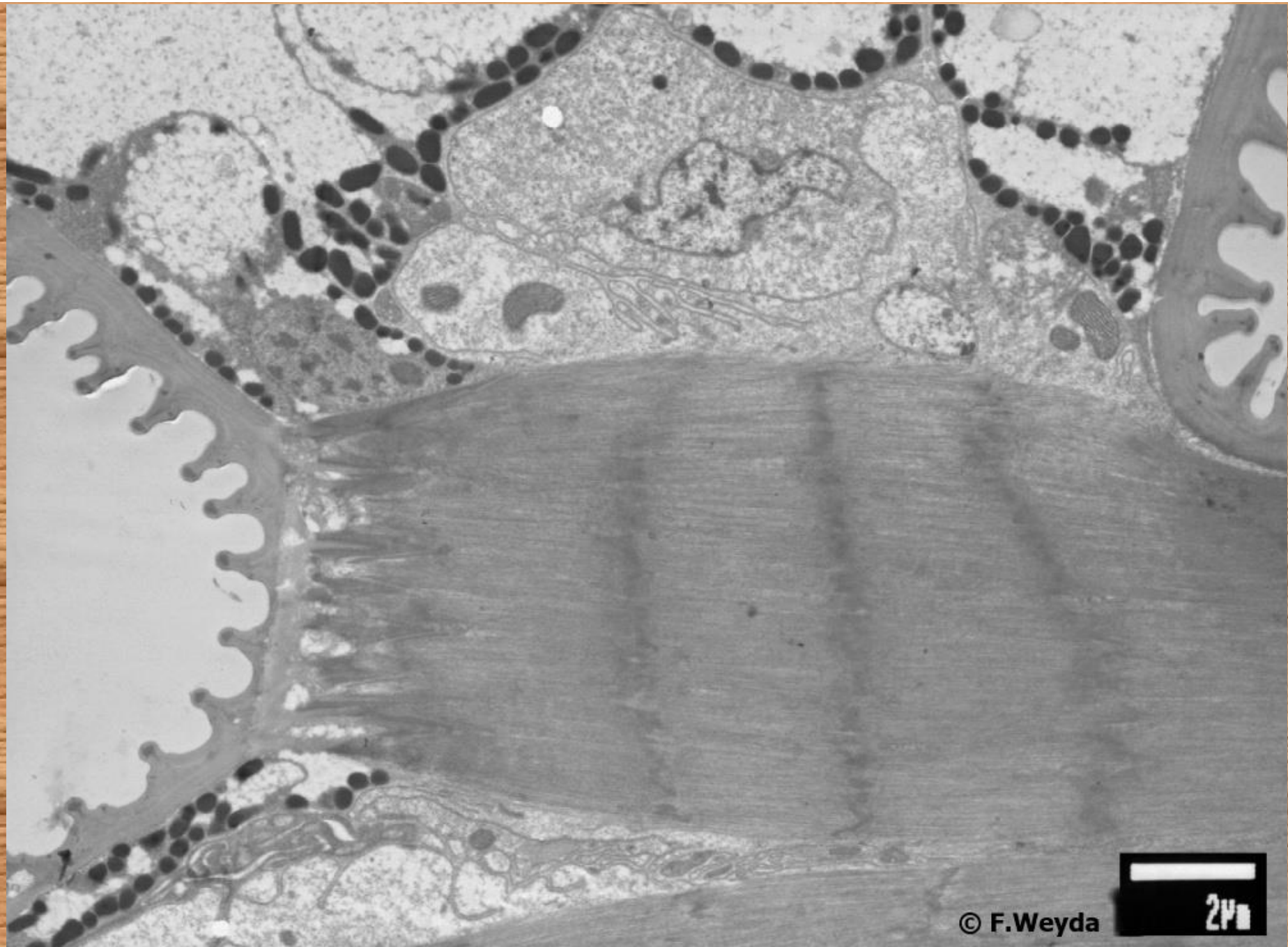

Obr. 21

Uspořádání a inervace hmyzích svalů

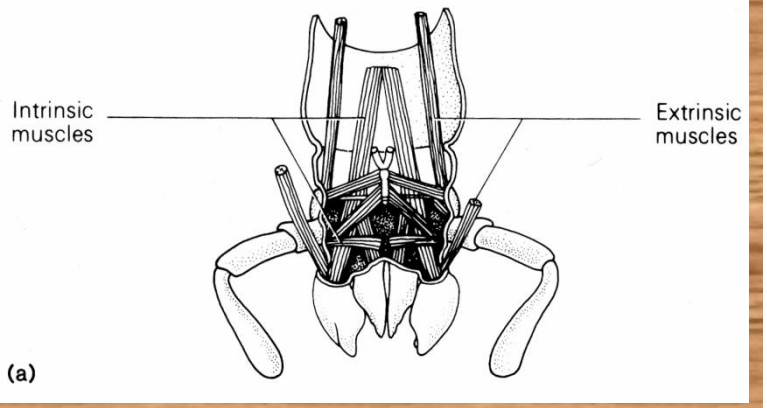

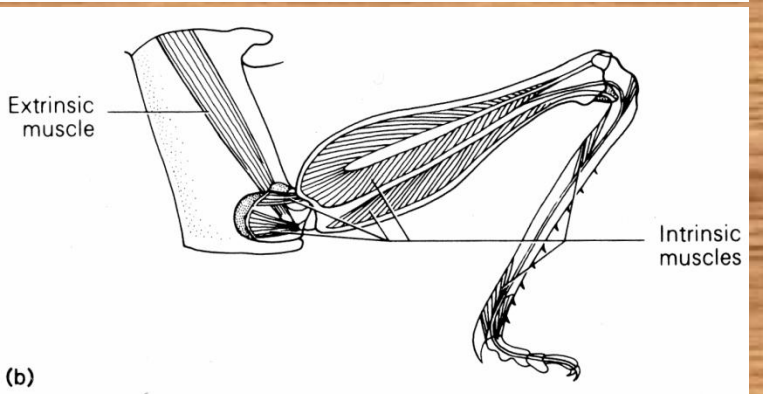

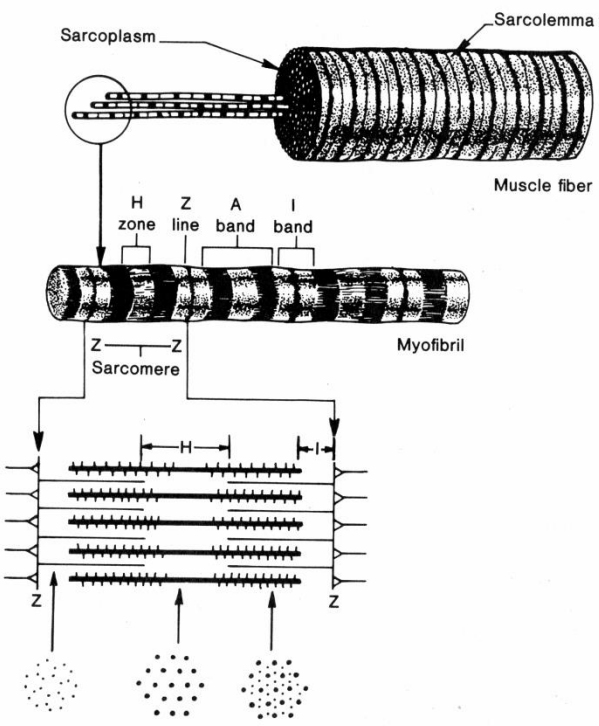

Figure 3.25 Innervation of a typical muscle unit showing fast and slow axons and multiterminal endings. *Redrawn from Hoyle, 1965.*

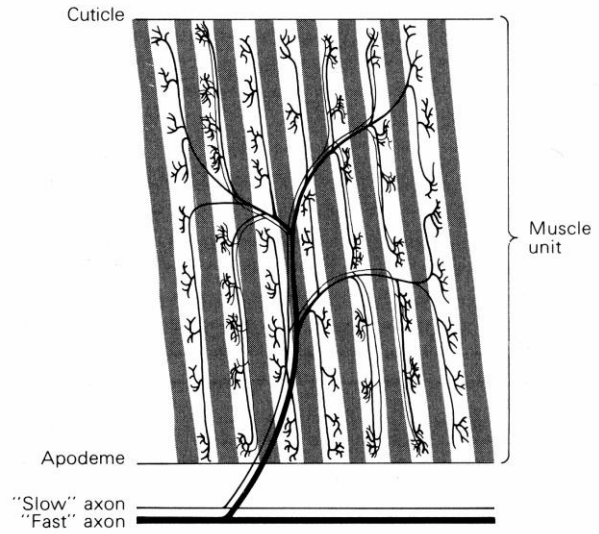

Figure 3.24 Ultrastructure of skeletal muscle in the mosquito *Aedes aegypti*. (*a*) Cross section (9600×): 1, center of a single myofibril; 2, mitochondria. (*b*) Longitudinal section (25,400×): 1–2 and 3–4, I-bands; 5, mitochondrion; the dark, thick (myosin) and thin (actin) parallel, horizontal lines between 2 and 3 myofilaments. (*c*) Portions of cross sections of myofibrils showing arrays of thick (myosin) and thin (actin) myofilaments (73,000×): 1, parts of T-system. *Courtesy of M. Catherine Walker.*

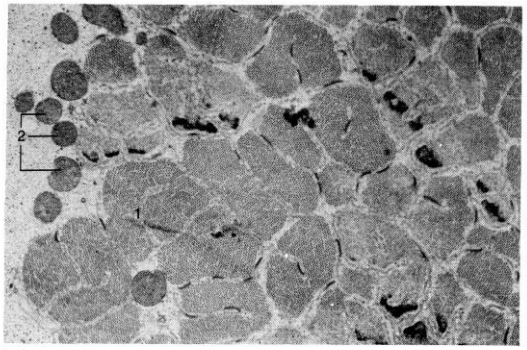

(a)

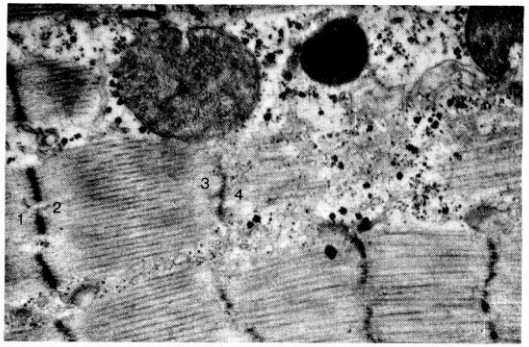

(b)

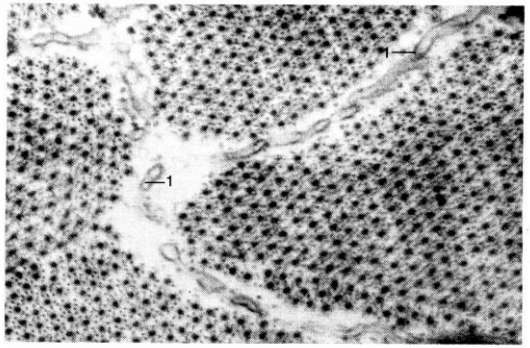

(c)

Obr. 21a Hrudní létací svaly octomilky obecné *Drosophila melanogaster*
foto - F. Weyda

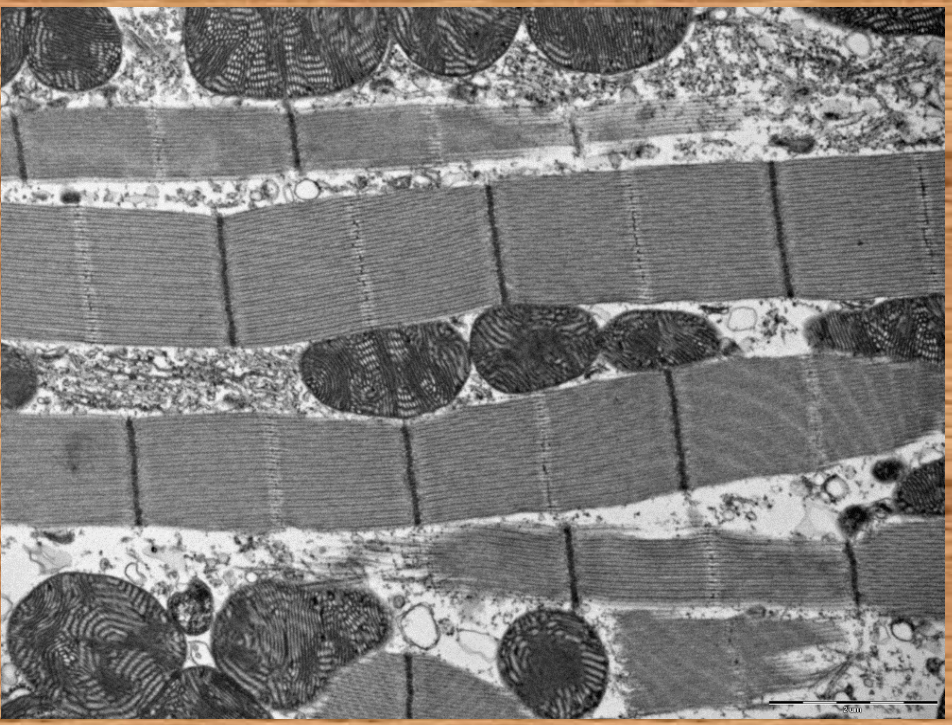

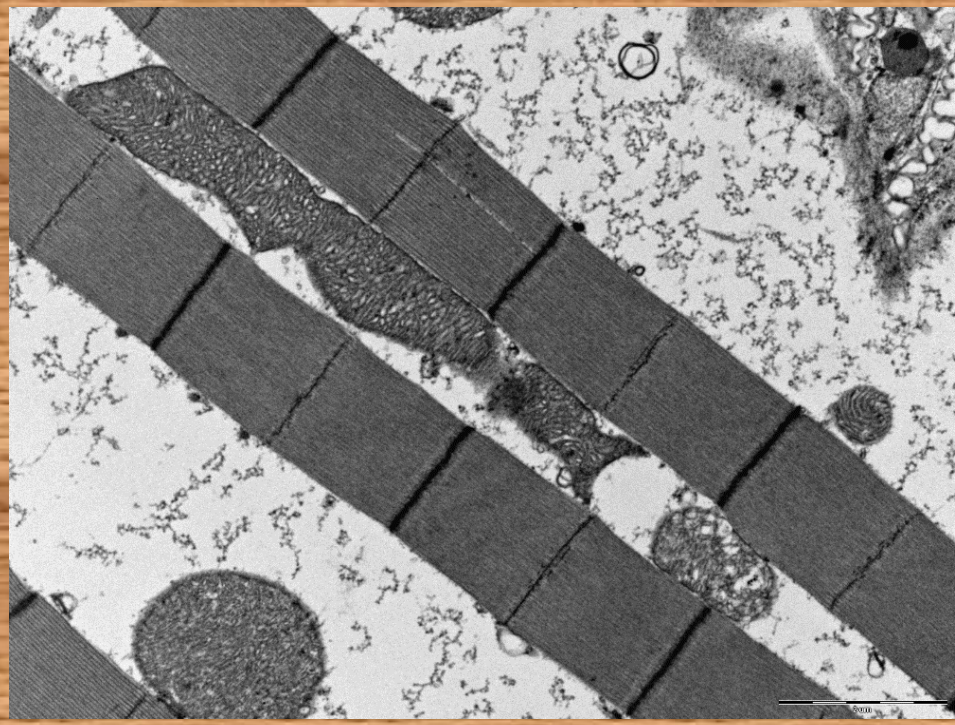

Obr. 22 Pohyb larev s měkkým povrchem těla

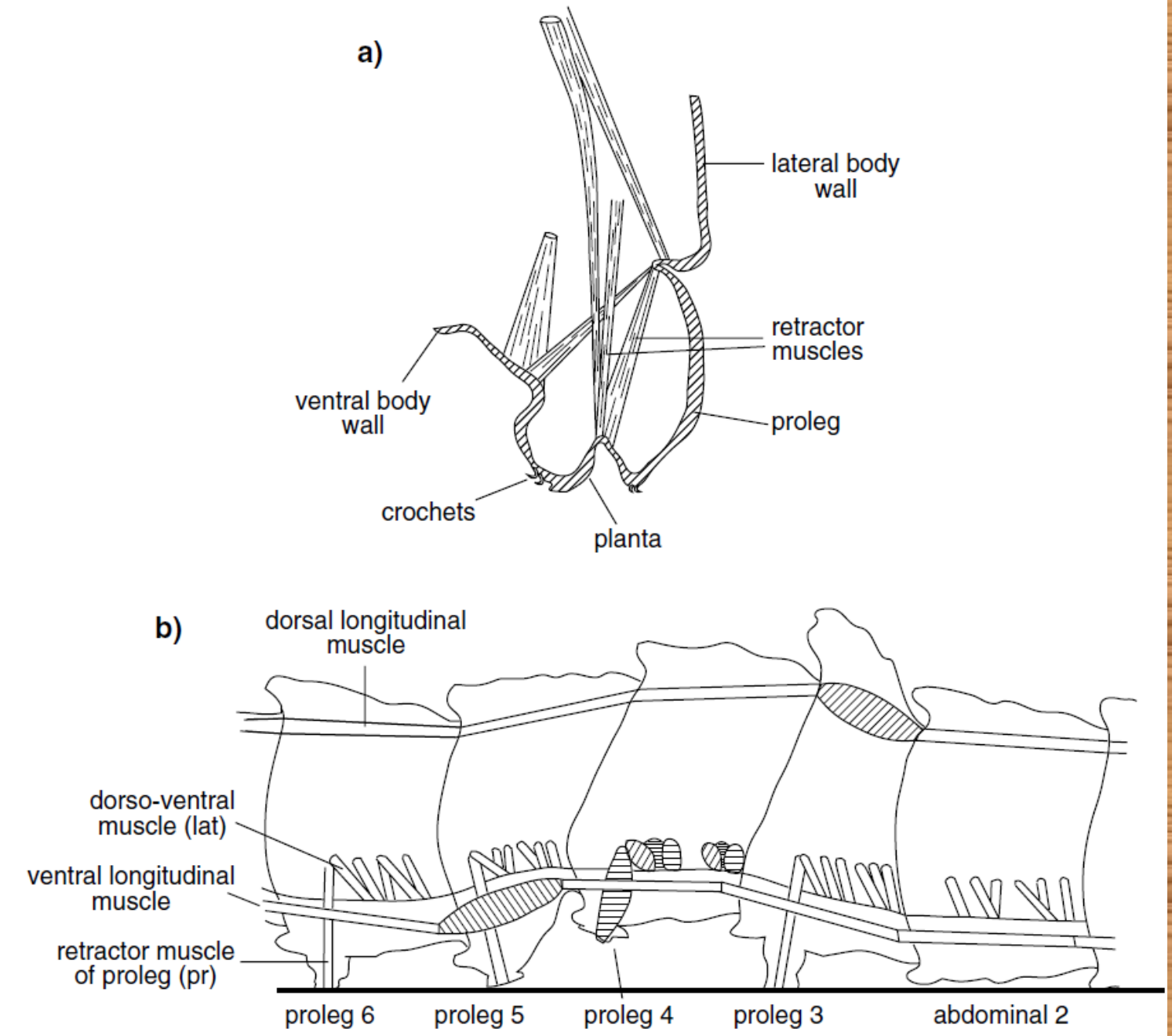

Fig. 8.27. Caterpillar crawling. **(a)** Transverse section through part of an abdominal segment of a caterpillar showing a proleg (after Hinton, 1955). **(b)** Longitudinal section through the abdomen of a caterpillar showing a wave of contraction which passes along the body from behind forwards (left to right) and produces forward movement. Contracted muscles are shown hatched. There are no prolegs on abdominal segment 2 (based on Hughes, 1965). **(c)** Central nervous

Obr. 23

Příklad klátivé chůze

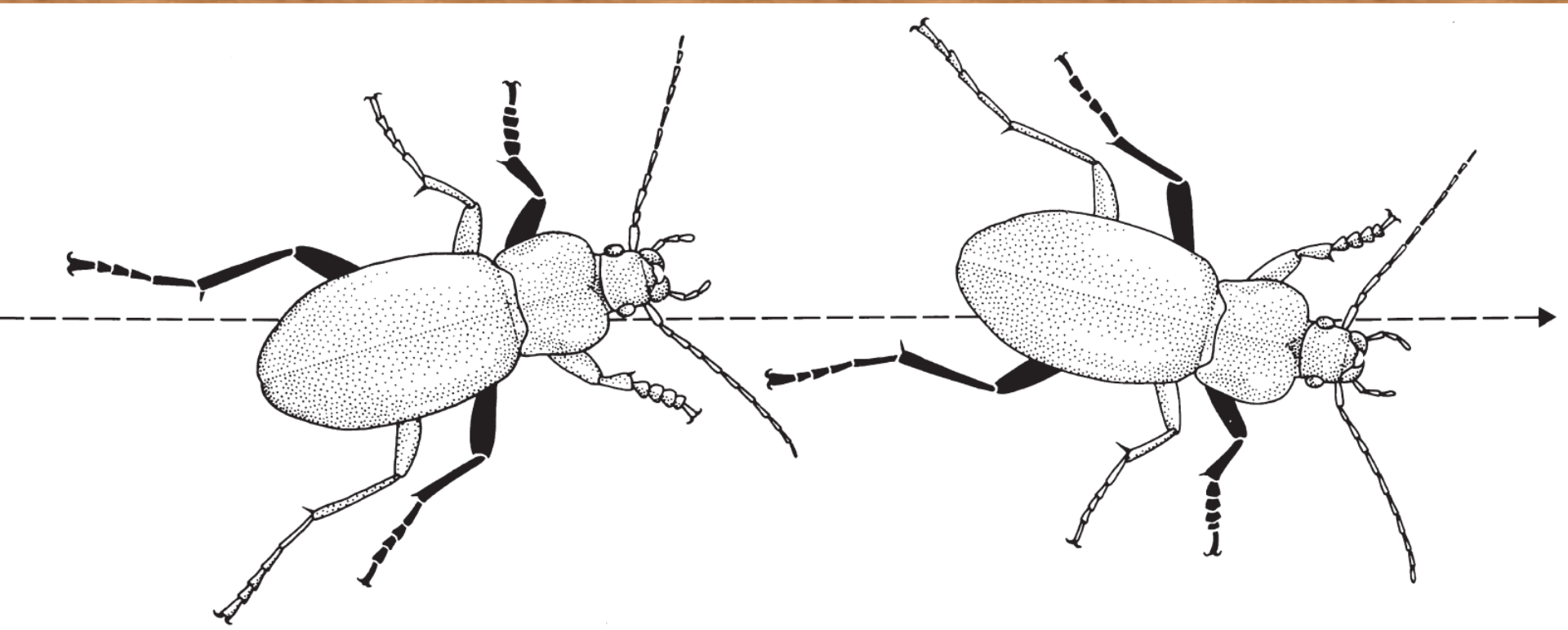

Fig. 3.3 (*right*) A ground beetle (Coleoptera: Carabidae: *Carabus*) walking in the direction of the broken line. The three blackened legs are those in contact with the ground in the two positions illustrated – (a) is followed by (b). (After Wigglesworth 1972.)

Variabilní zastoupení hlavních organel svalových buněk u různých typů svalů

Obr. 24

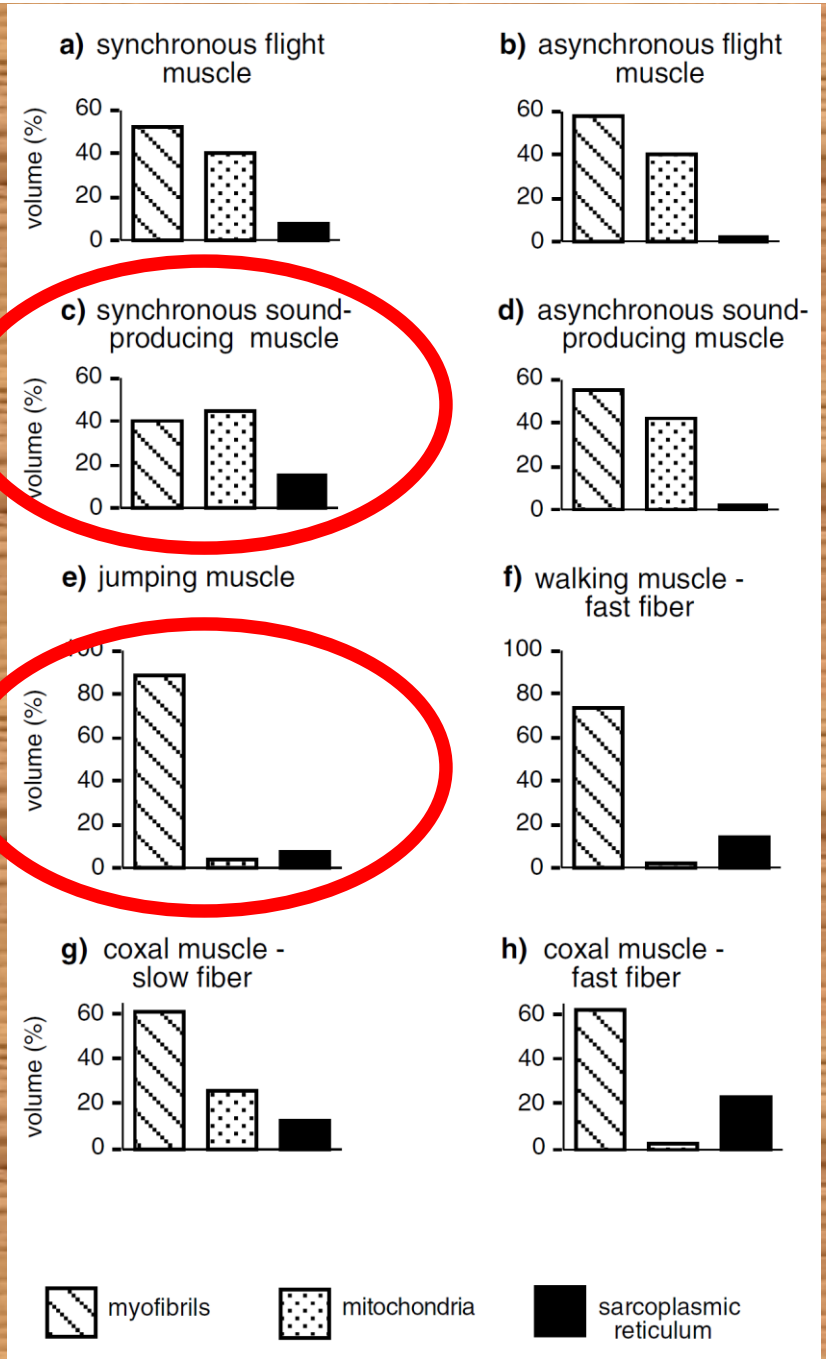

Obr. 25 Typy pohybu u vodního hmyzu

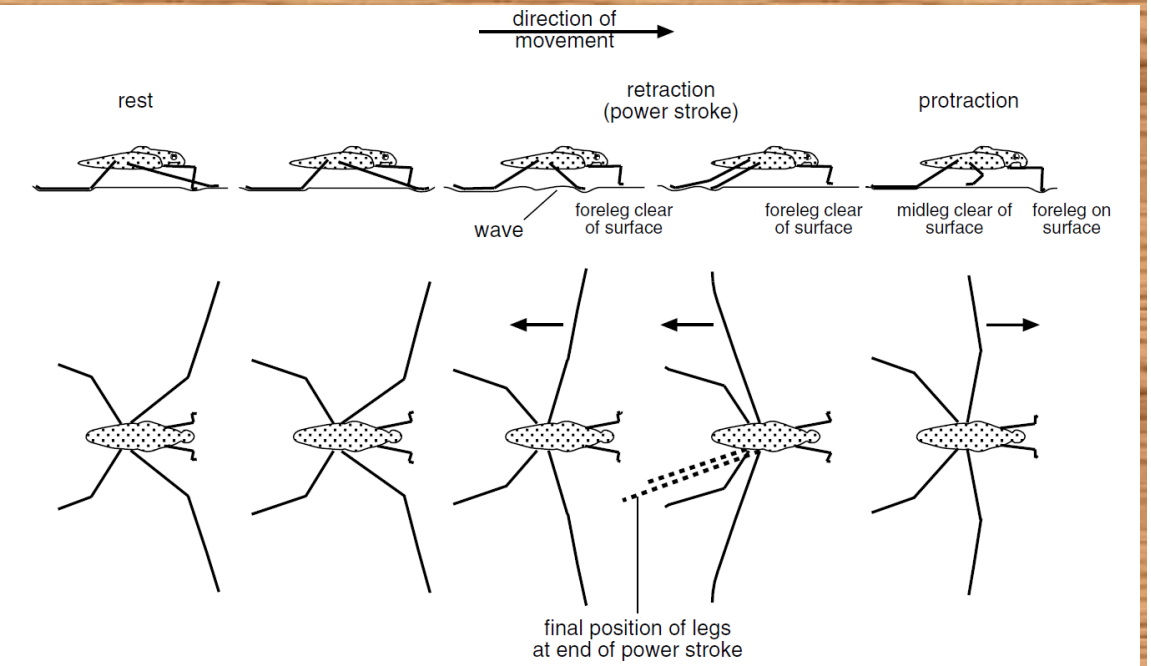

Fig. 8.29. Movement on the water surface. Positions of the legs of *Gerris*. Arrows show the directions of movement of the legs relative to the body; insect moving from left to right (after Nachtigall, 1974).

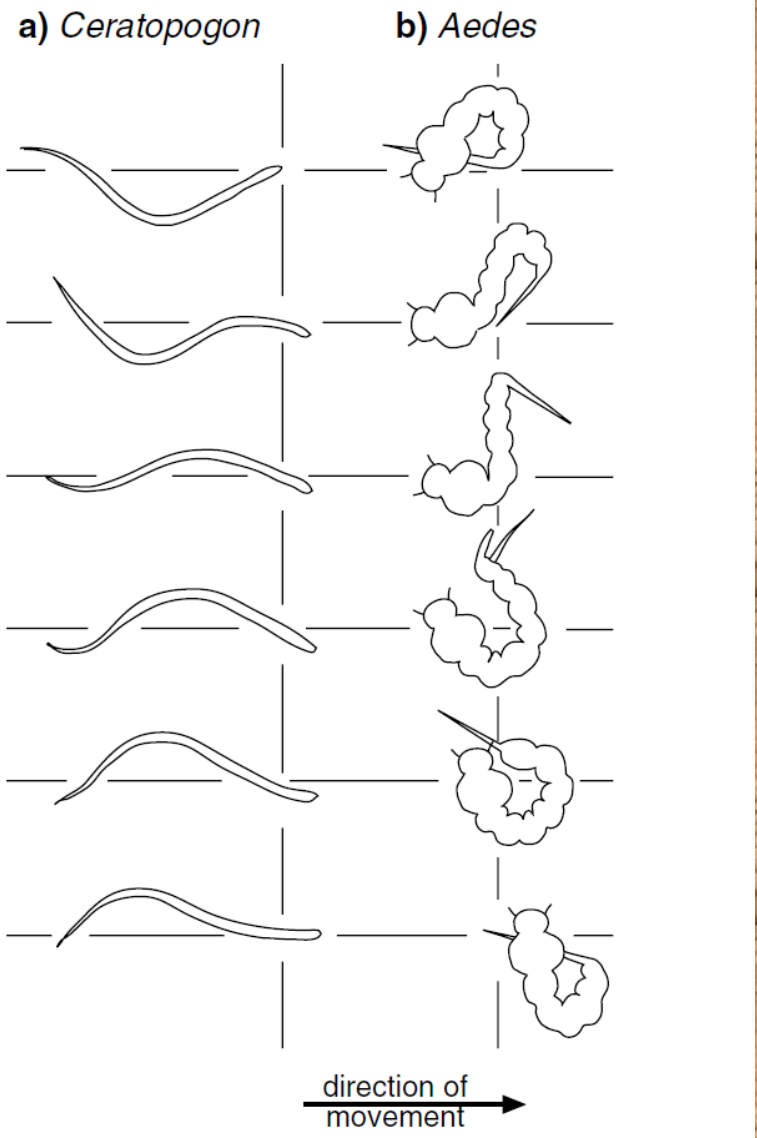

Fig. 8.36. Swimming by larval Diptera (after Nachtigall, 1965): (a) *Ceratopogon*, (b) *Aedes*.

Obr. 26

Hmyzí létací svaly

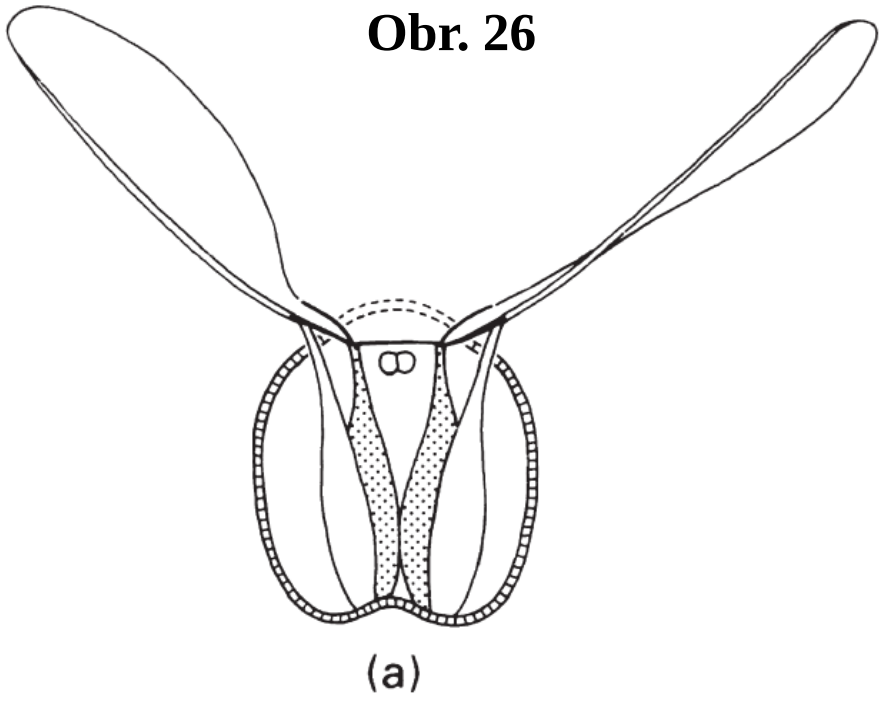

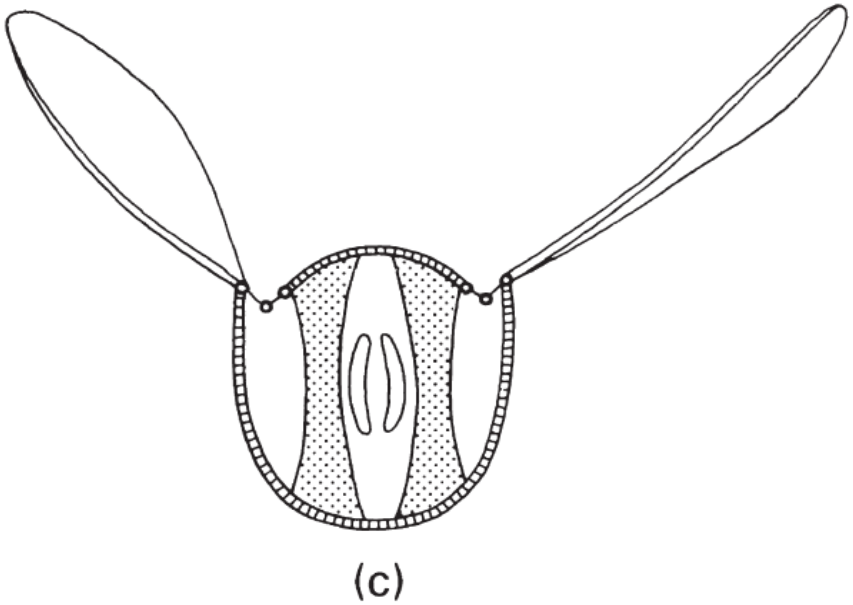

Přímé létací svaly

Nepřímé létací svaly

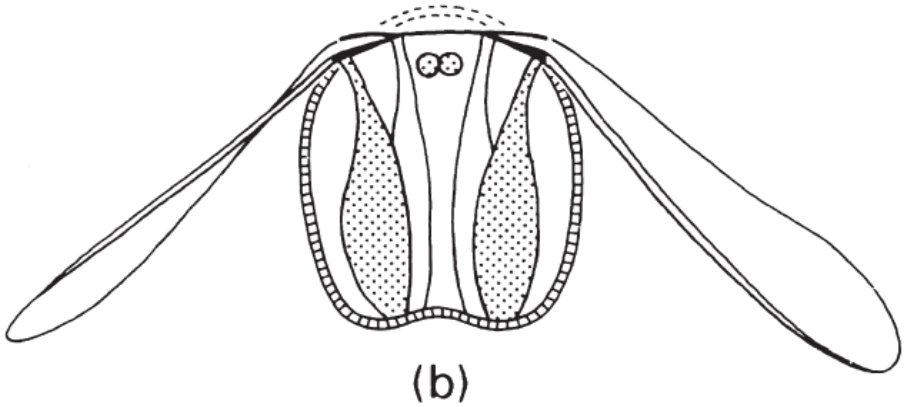

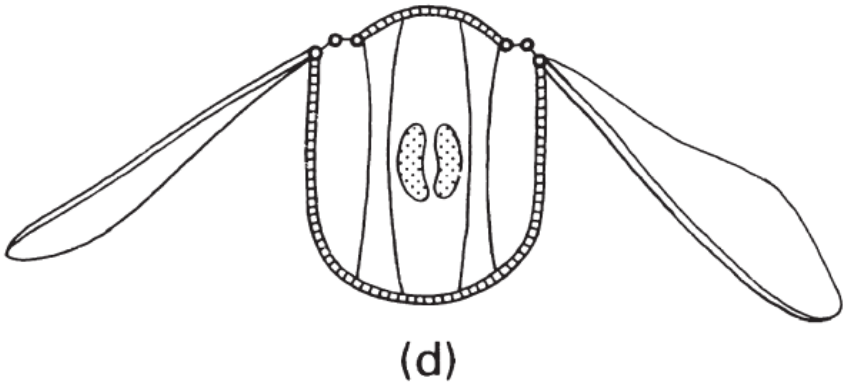

Fig. 3.4 Direct flight mechanisms: thorax during (a) upstroke and (b) downstroke of the wings. Indirect flight mechanisms: thorax during (c) upstroke and (d) downstroke of the wings. Stippled muscles are those contracting in each illustration. (After Blaney 1976.)

Obr. 27

Hmyzí létací svaly

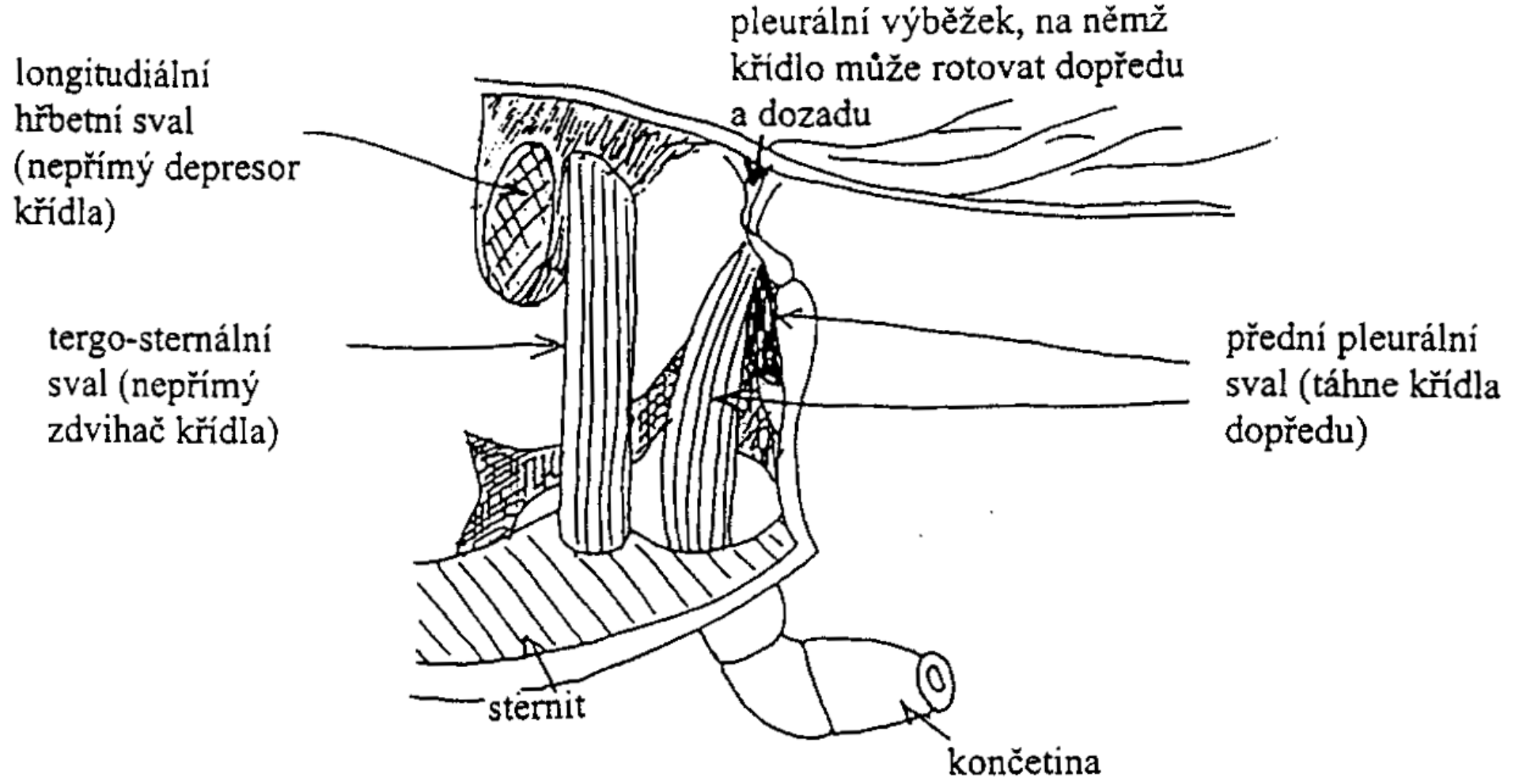

Obr. 28

Hmyzí létací svaly

Sagitální řez: hlava

vážka

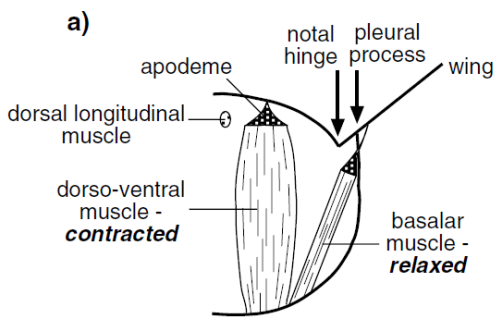

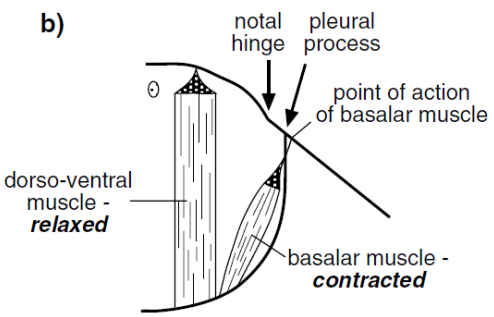

moucha

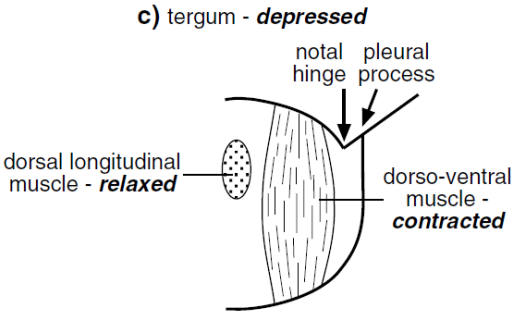

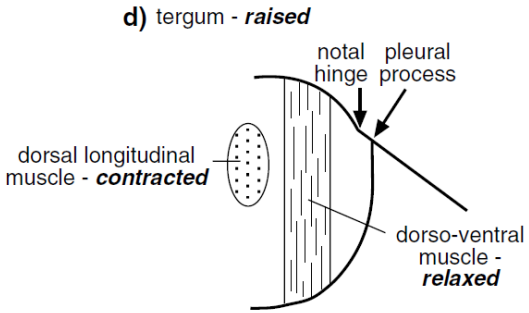

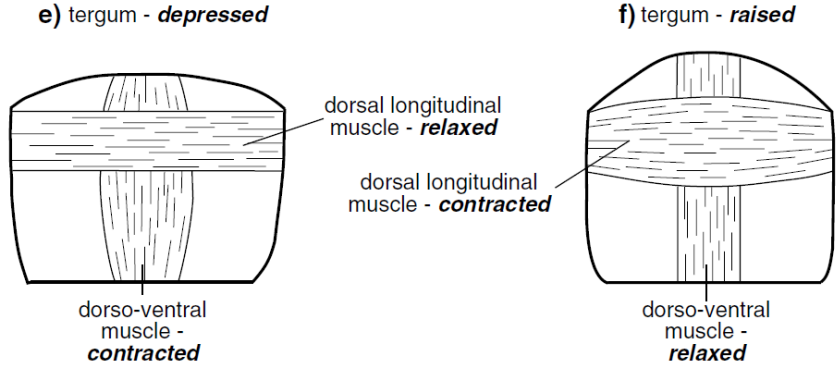

Fig. 9.17. Muscular basis of wing movements. **(a), (b)** In an insect, such as a dragonfly, in which the direct wing muscles cause depression of the wings. **(a)** Indirect dorso-ventral muscles cause wing elevation. **(b)** Direct dorso-ventral muscles cause depression. **(c)–(f)** In an insect, such as a fly, in which both up and down movements of the wing are produced by indirect muscles. **(c), (d)** Cross-sections of the thorax. **(e)** and **(f)** Sagittal sections of the wing-bearing segment from the inside corresponding with **(c)** and **(d)**, respectively. In **(f)**, contraction of the dorsal longitudinal muscles raises the tergum (as seen in cross-section in d) and the wing flaps down.

Obr. 29 **Frekvence mávání křídel u různých skupin hmyzu**

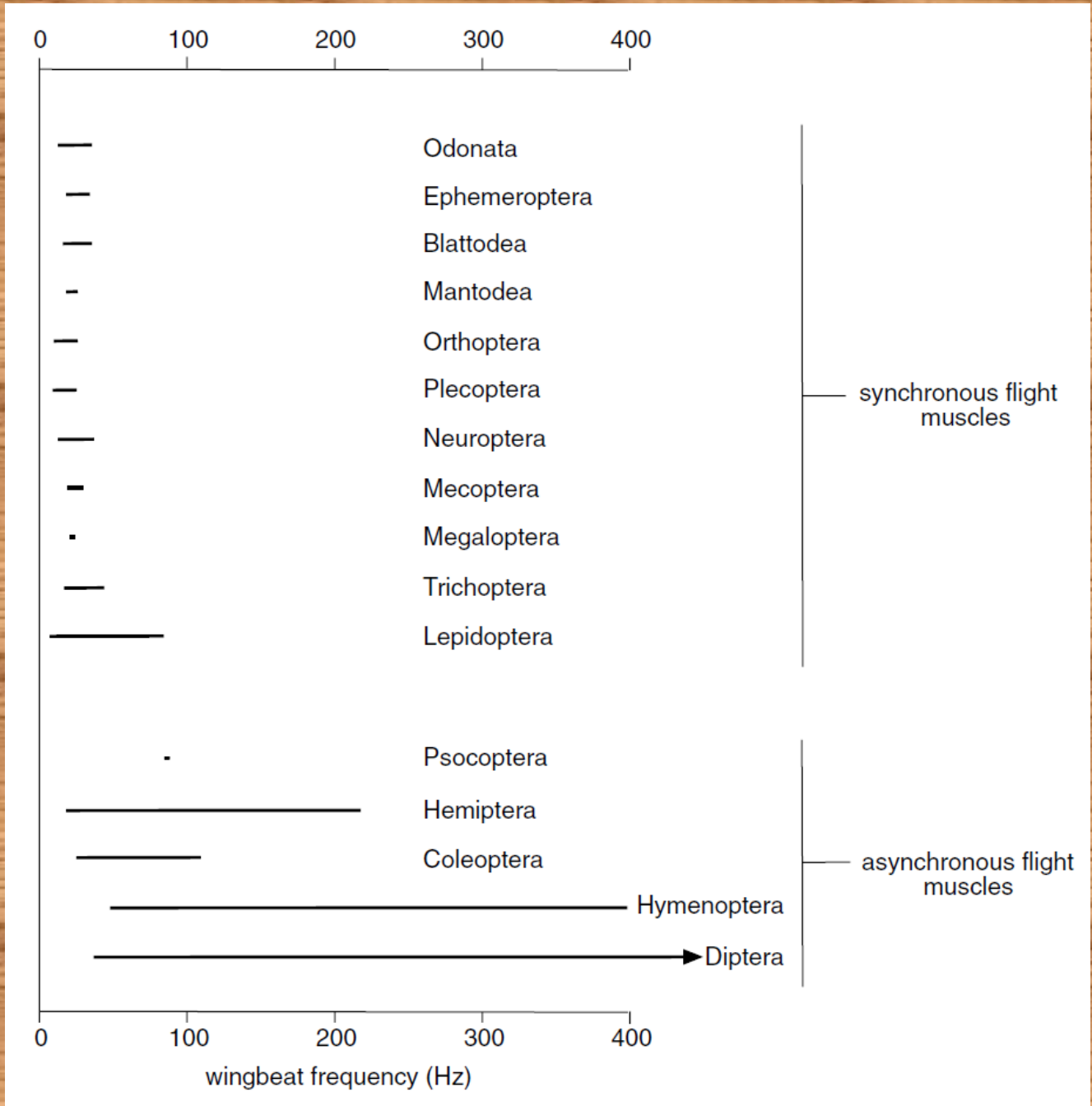

Hmyzí létací svaly: http://www.youtube.com/watch?v=iUNRkvwIUQ0&feature=plcp

Obr. 30 Aerodynamika hmyzího letu

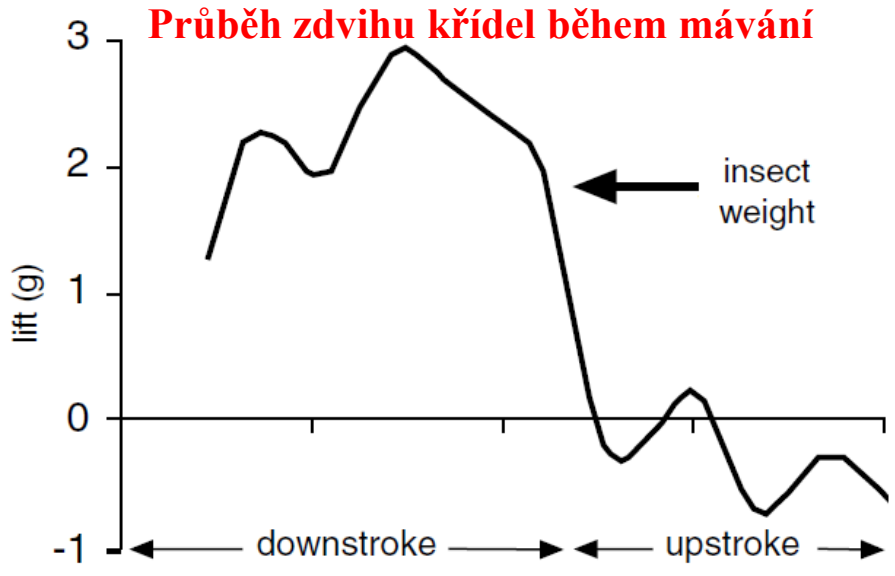

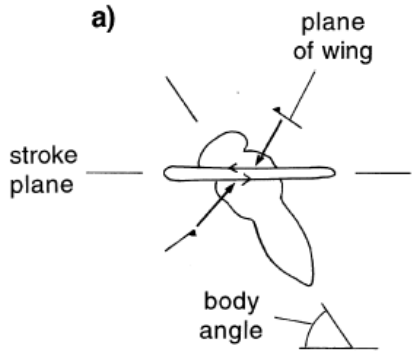

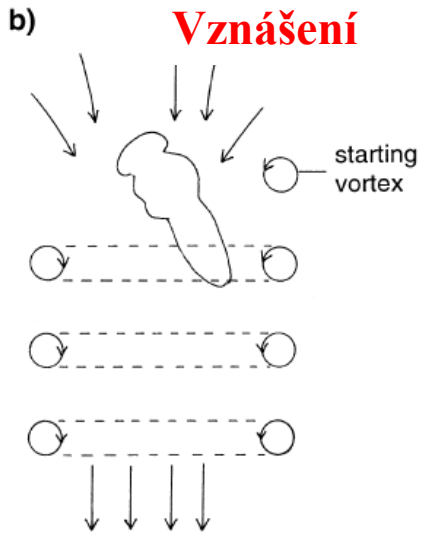

Obr. 31 Nervové řízení hmyzího letu

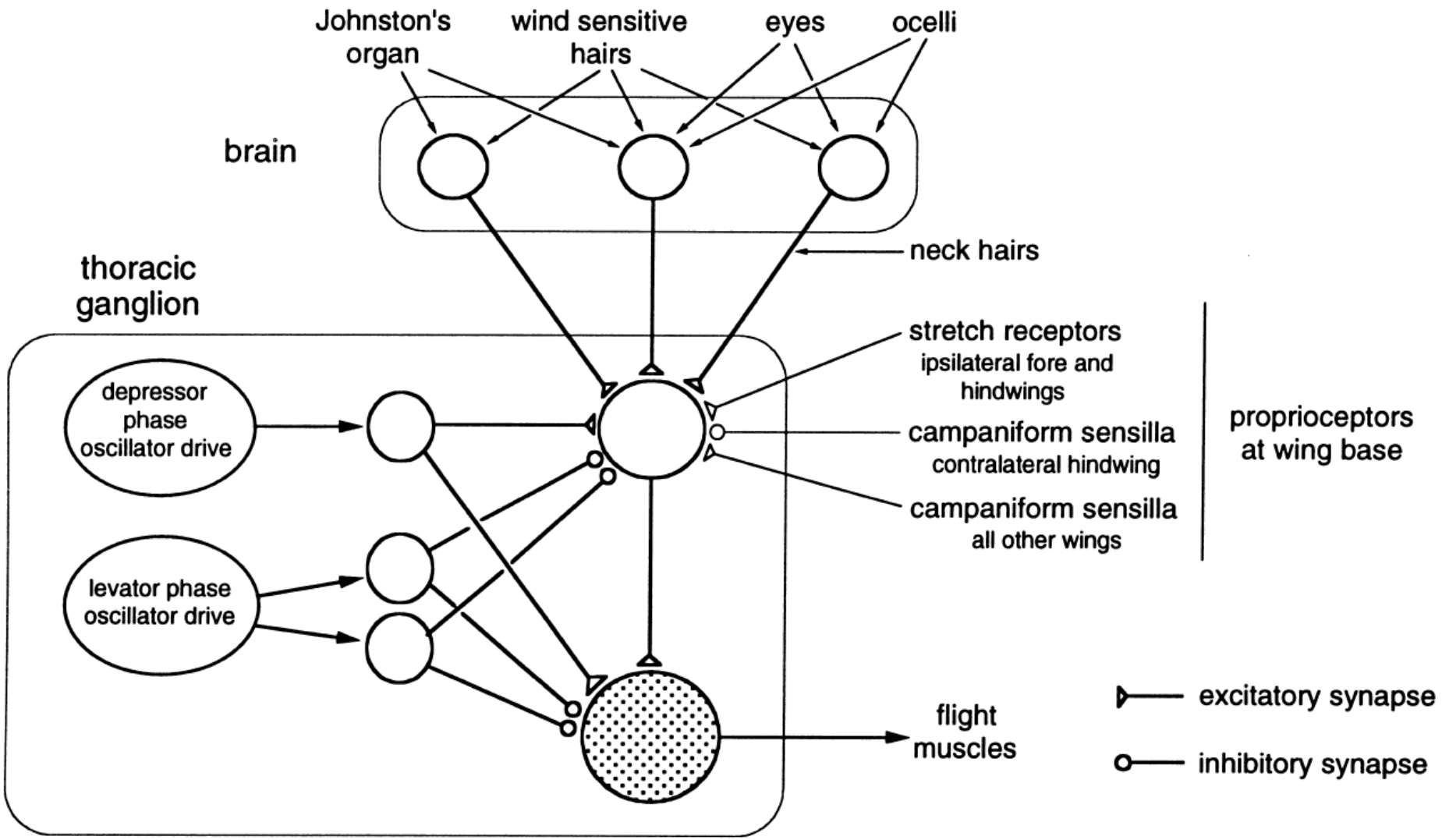

Energetické krytí hmyzího letu

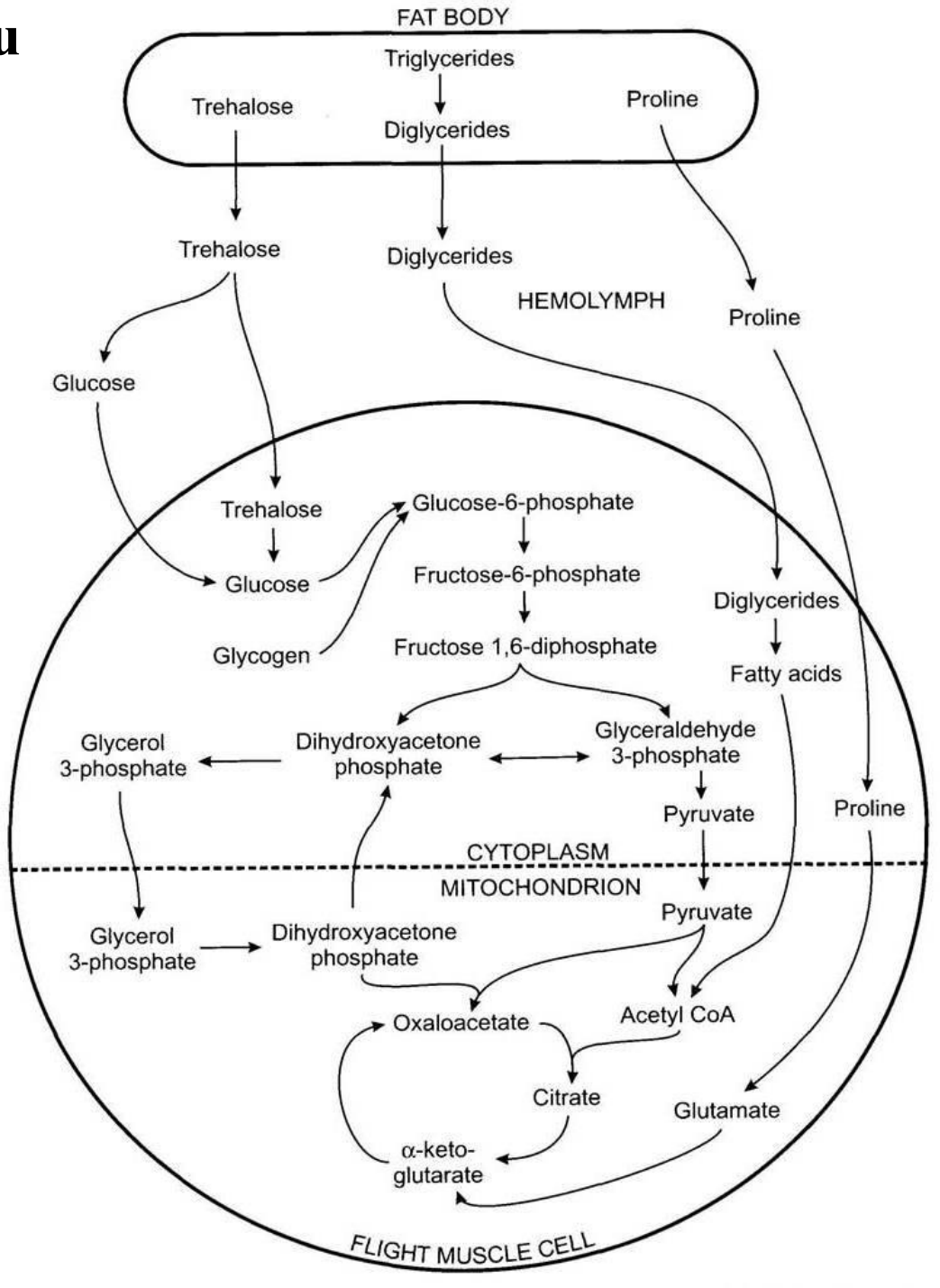

Obr. 32

Obr. 33 Energetické zdroje hmyzího letu saranče a mouchy

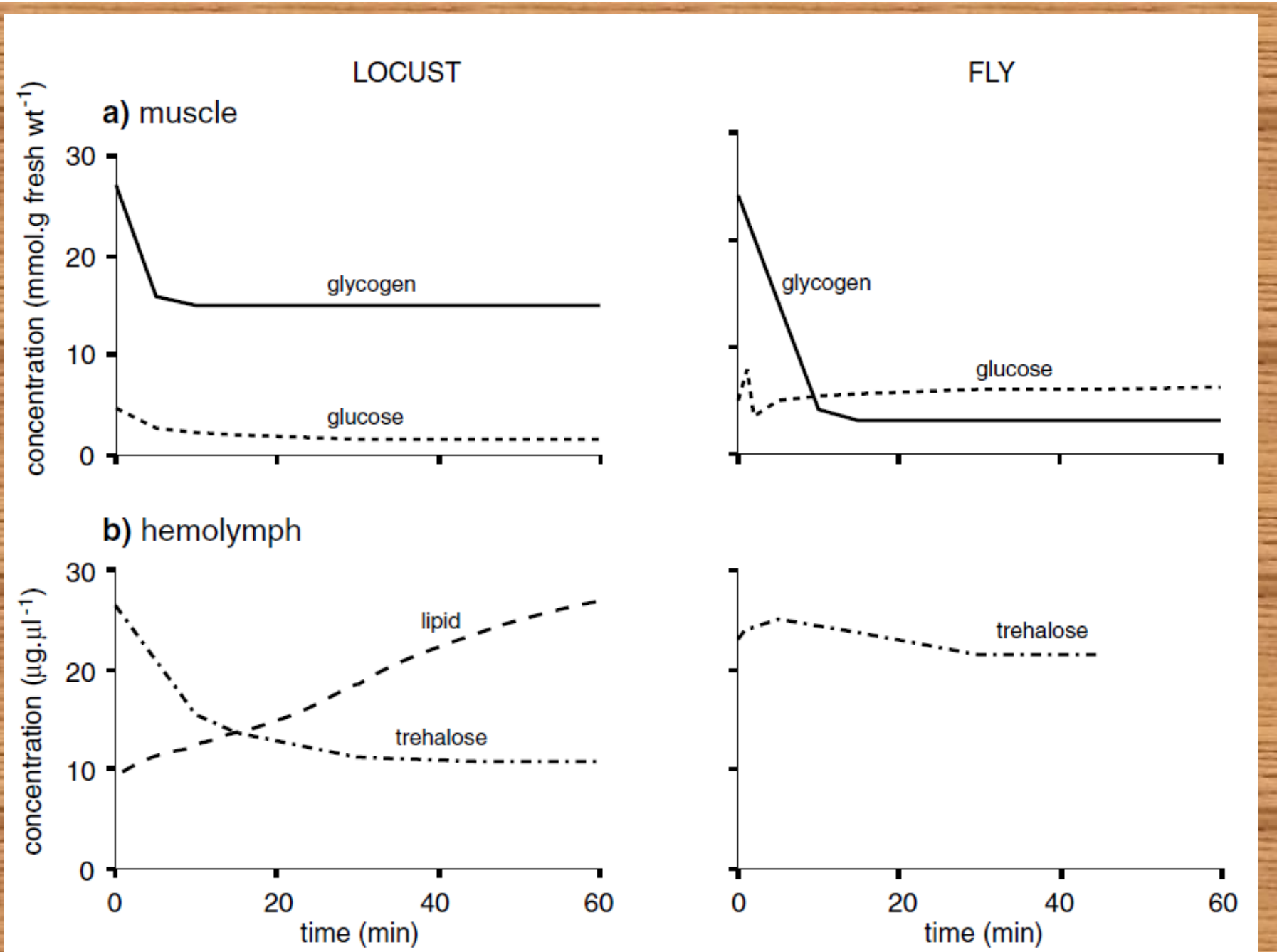

2. Trávení živin

Obr. 1

Čtyři hlavní typy hmyzí potravní specializace a přechody mezi nimi

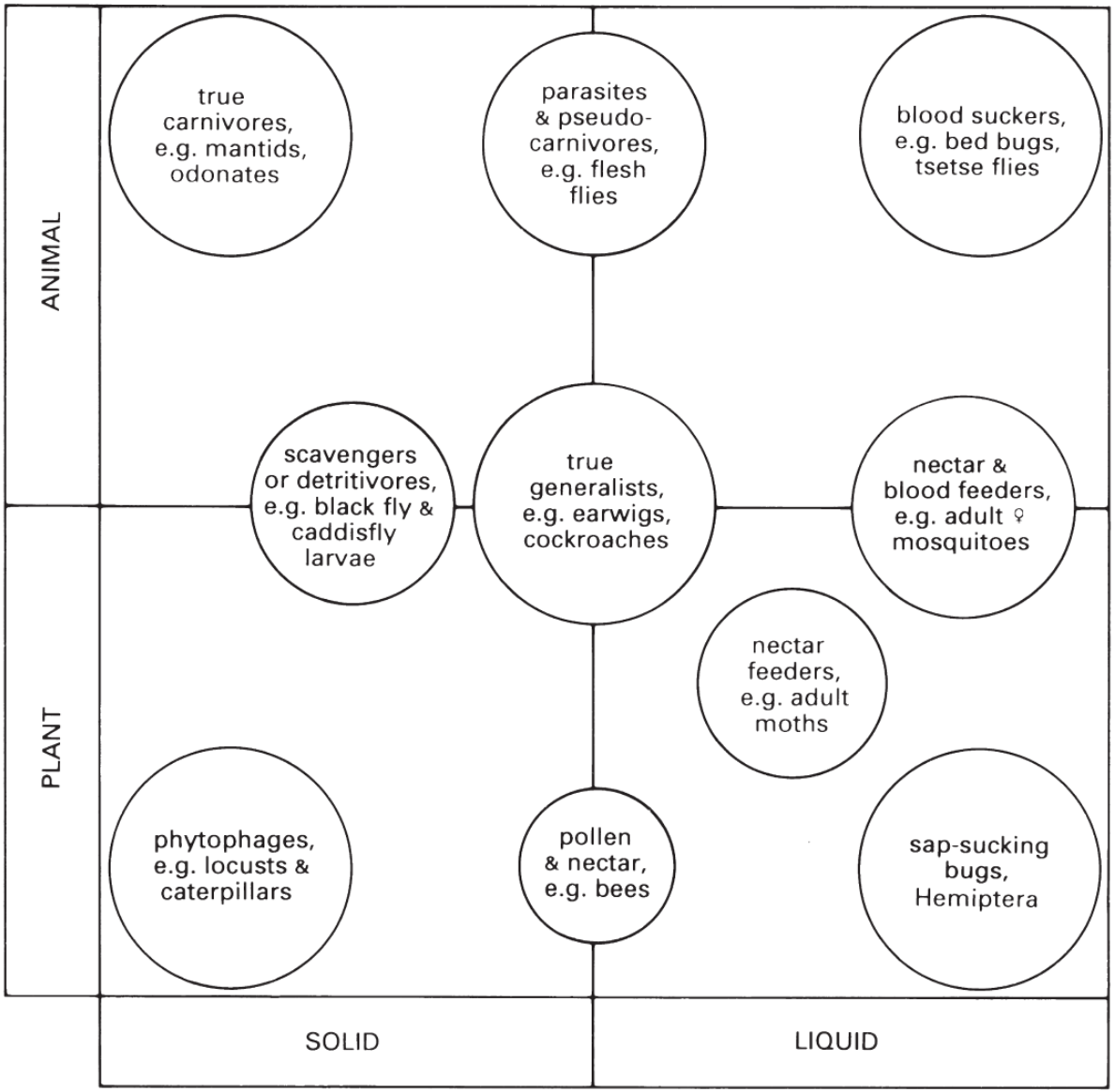

Fig. 3.12 The four major categories of insect feeding specialization. Many insects are typical of one category, but others cross two categories (or more, as in generalist cockroaches). (After Dow 1986.)

Obr. 2 Hmyzí trávící soustava

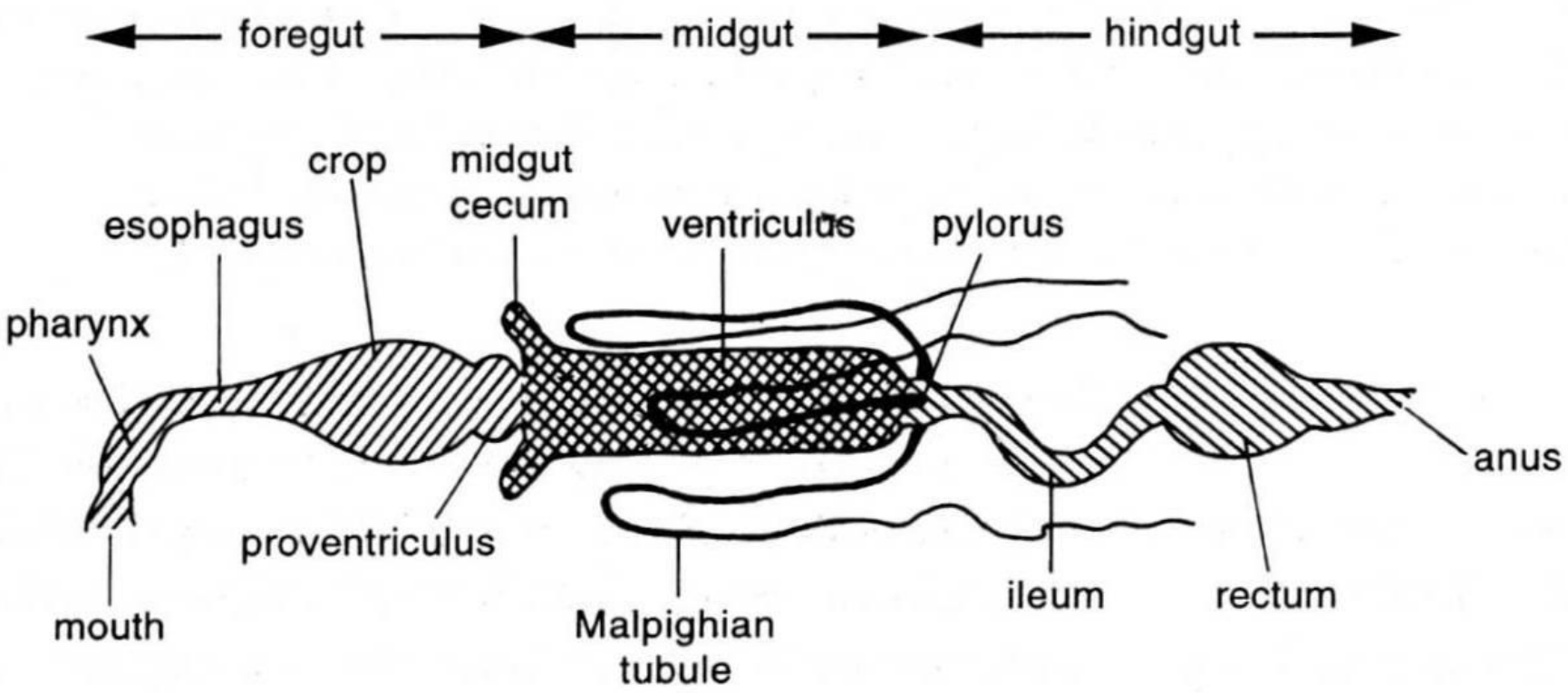

Obr. 3

Trávicí soustava hmyzu

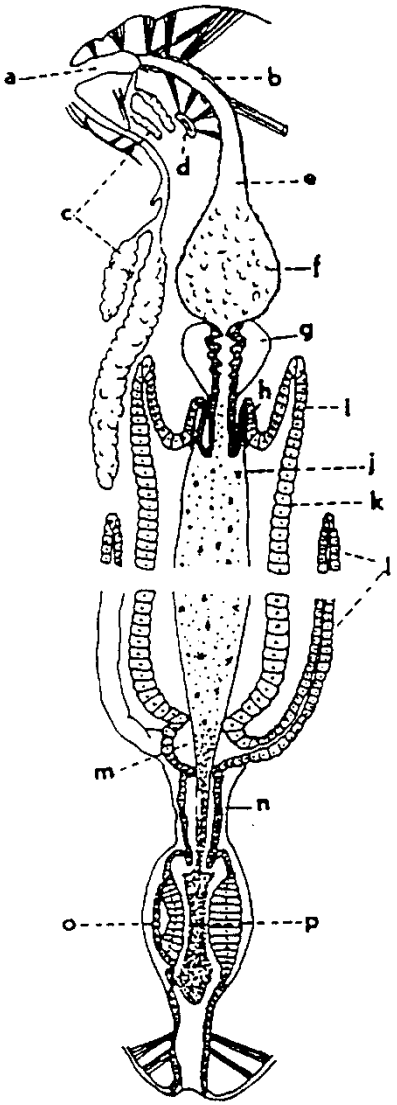

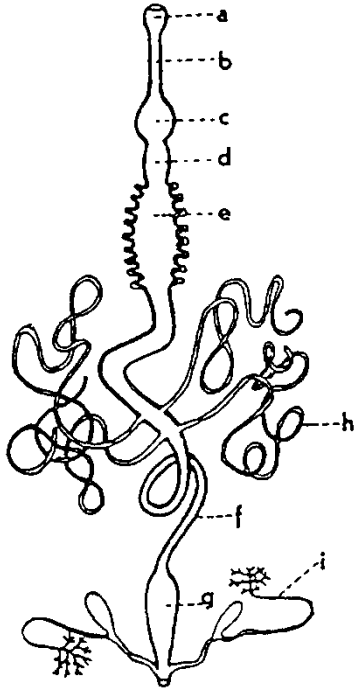

Trávicí soustava hmyzu (střevlík)

a = dutina ústní, b = jícen, c = vole, d = žvýkací žaludek, e = žlaznatý žaludek, f = střevo, g = kloaka, h = Malpighiovy žlázy, i = análné žlázy

Obecné schéma trávicí soustavy hmyzu

a = dutina ústní (cibarium), b = hltan, c = slinné žlázy, d = tentorium, e = jícen, f = vole, g = žvýkací žaludek, h = valvula cardiaca, i = slepé střevo, j = peritrofická membrána, k = mesenteron (žlaznatý žaludek nebo střední oddíl střeva), l = Malpighiova trubice, m = pylorus (tlusté střevo), n = rovné nebo tenké střevo, o = rektální papila, p = konečník

Obr. 4 Slinné žlázy ruměmice pospolné *Pyrrhocoris apterus* foto - F. Weyda

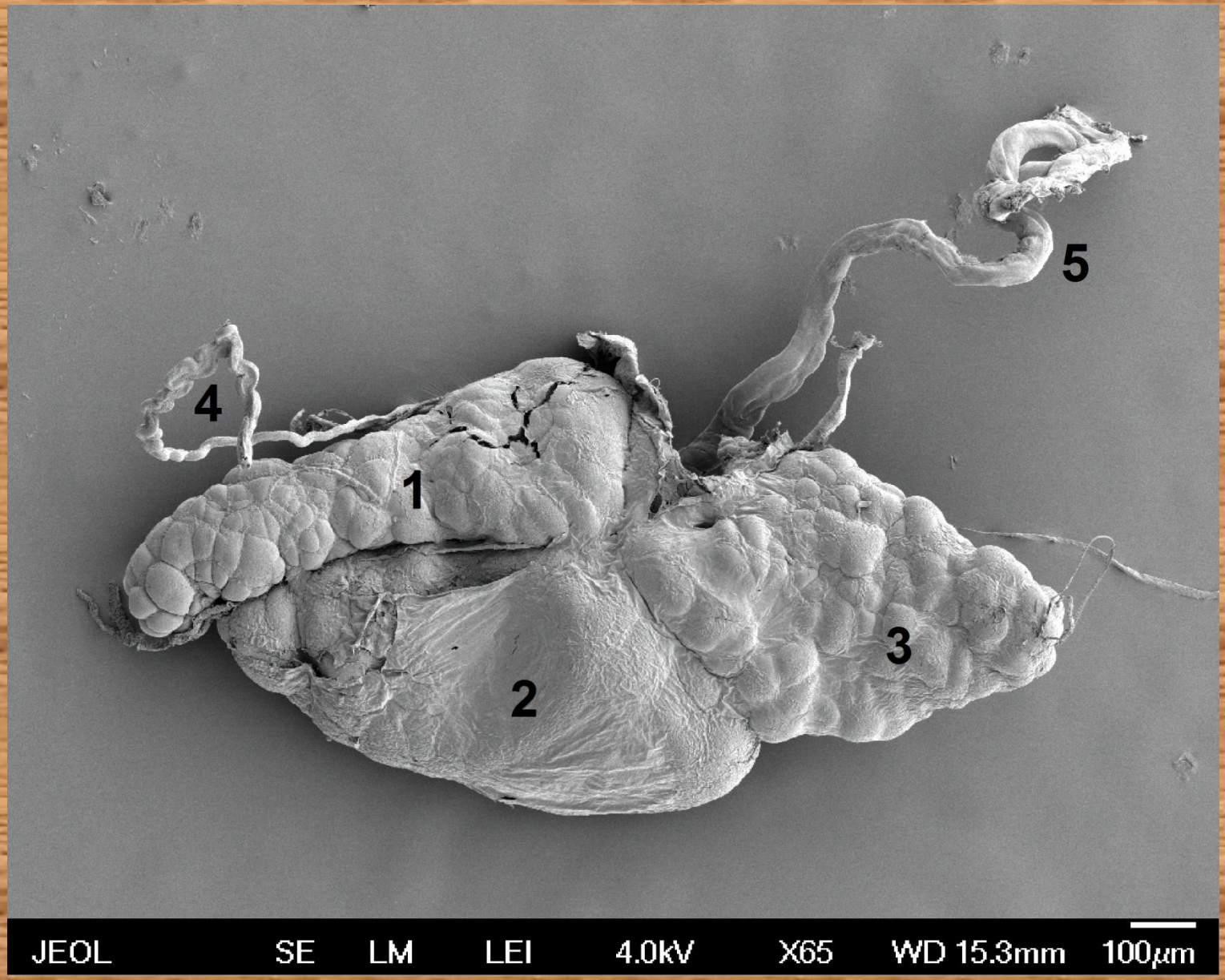

1. Přední lalok, 2. střední lalok, 3. zadní lalok, 4. přídatná žláza, 5. vývod slinné žlázy

Obr. 5 **Detail volete (crop) a žvýkacího žaludku (proventriculus)**

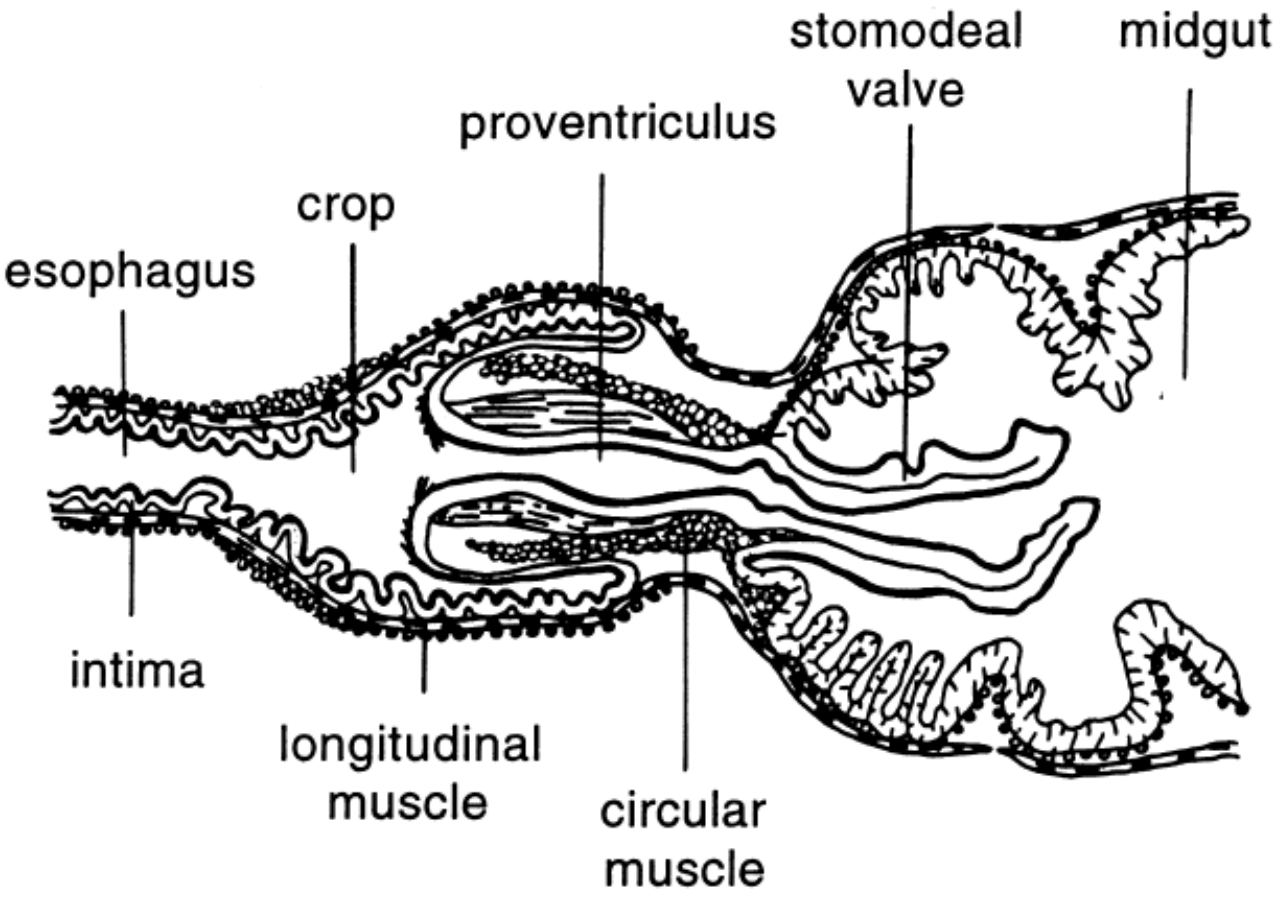

Fig. 3.4. Foregut of a worker honeybee in longitudinal section showing the development of the proventriculus. The anteriorly directed part enables the insect to extract pollen grains from nectar in the crop; the posterior part, projecting into the midgut, forms a valve (after Snodgrass, 1956).

Obr. 6 Žvýkací žaludek (proventriculus)

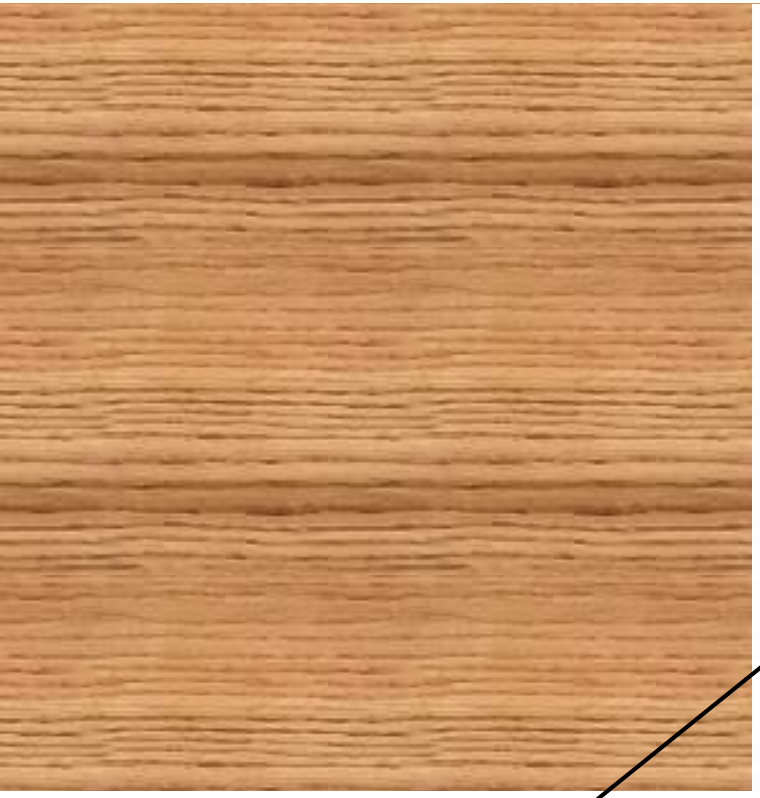

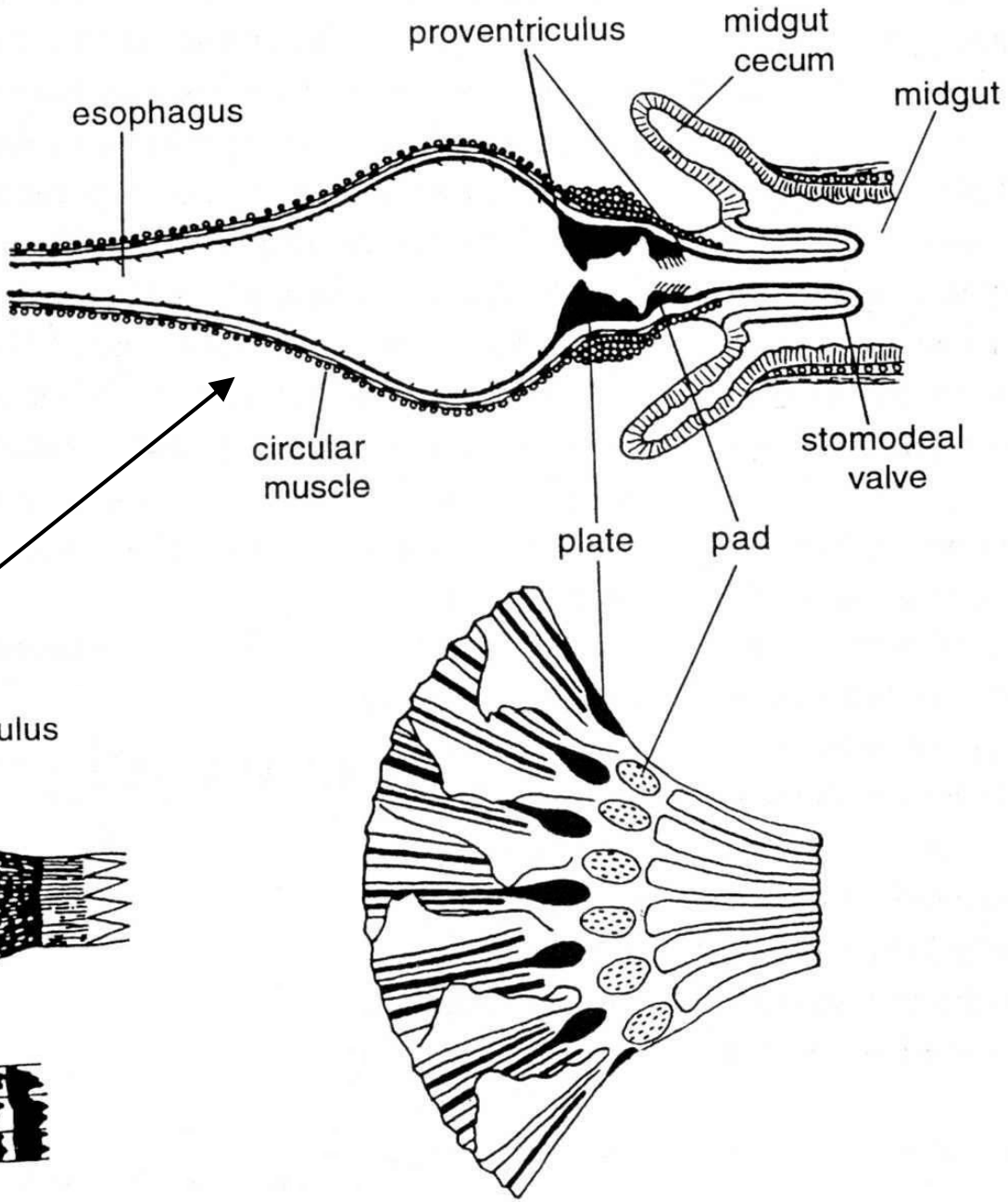

Obr. 7 Střevo švába amerického *Periplaneta americana*, SEM, foto - F. Weyda

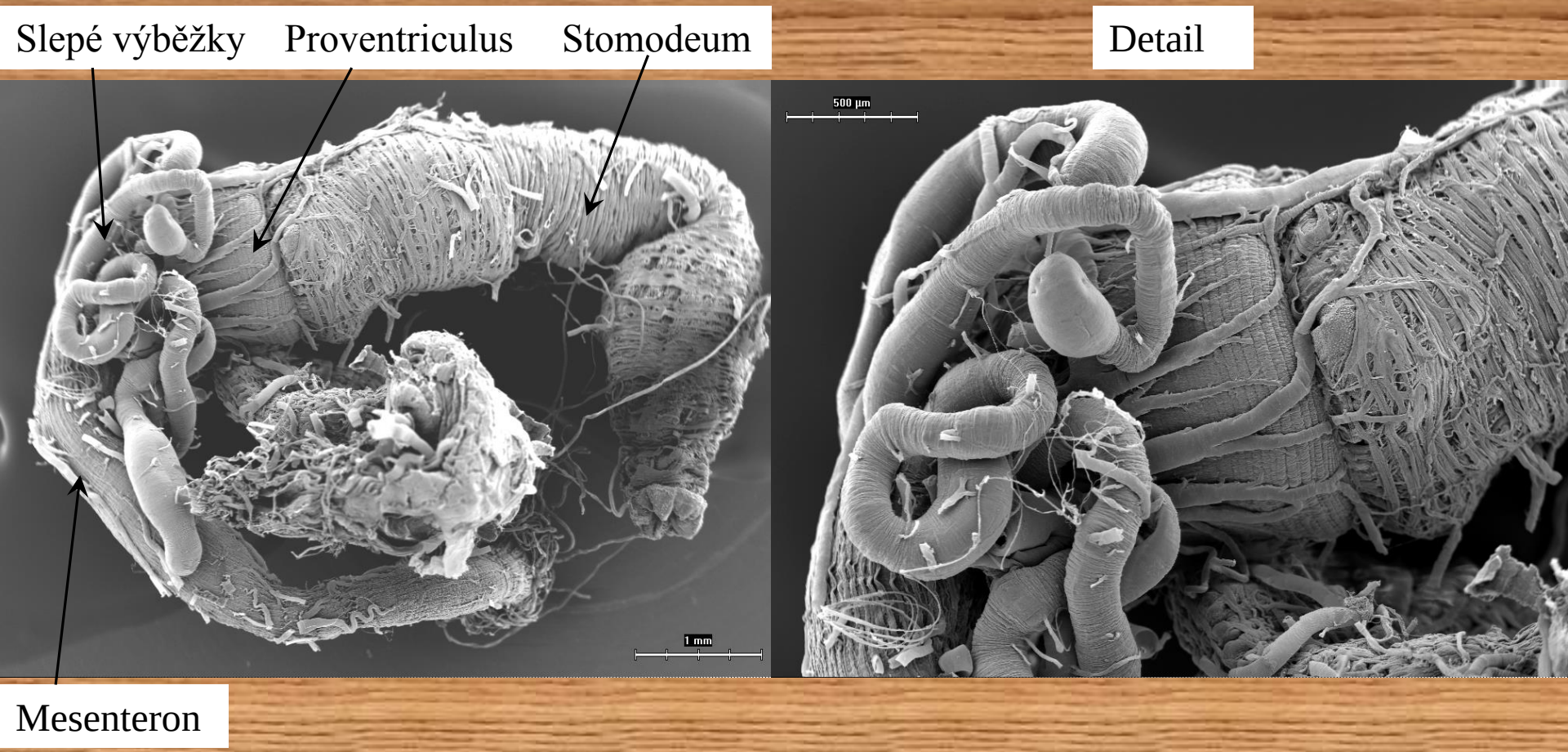

Obr. 8 Mesenteron

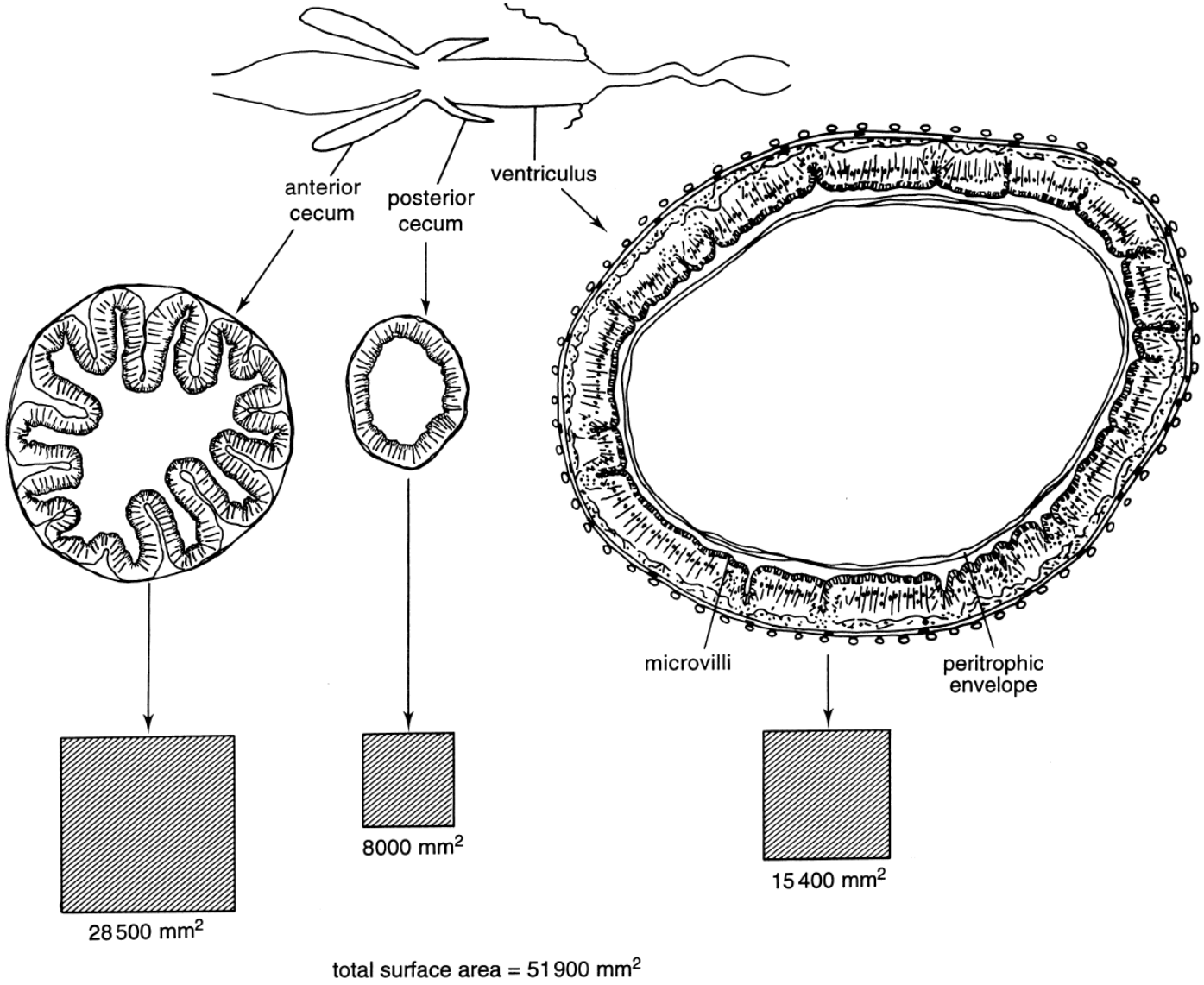

Fig. 3.6. Midgut surface area of a grasshopper. Outline of gut about twice natural size. Sections, all to same scale, through various parts of the midgut showing the extent of folding of the epithelium. The cells of all parts of the midgut have microvilli apically and so have very large surface areas. The boxes below show, to scale, the surface area of each part including the area produced by the microvilli.

Obr. 9

Typická hlavní buňka středního střeva

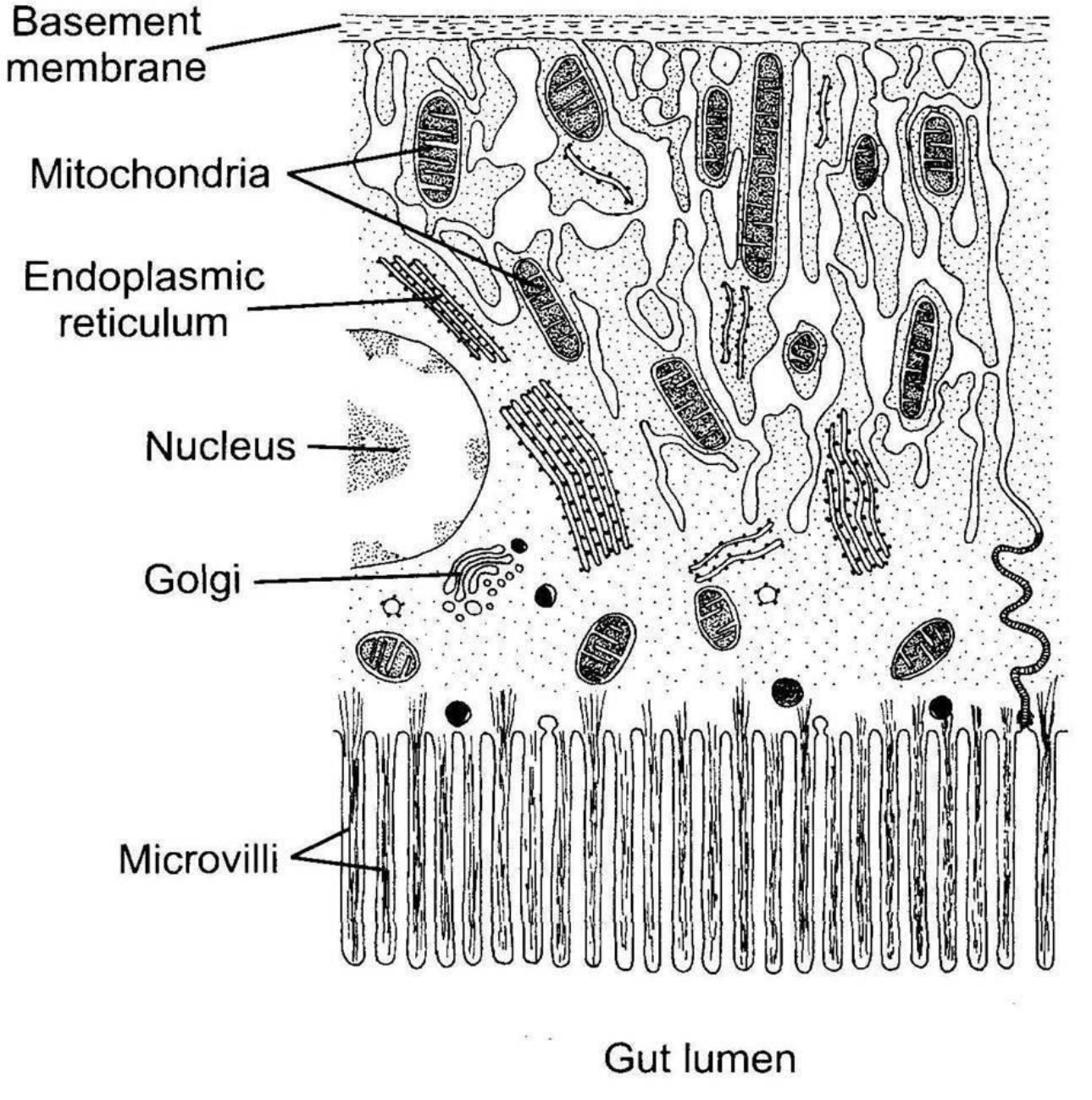

Obr. 10 Detaily stavby středního střeva

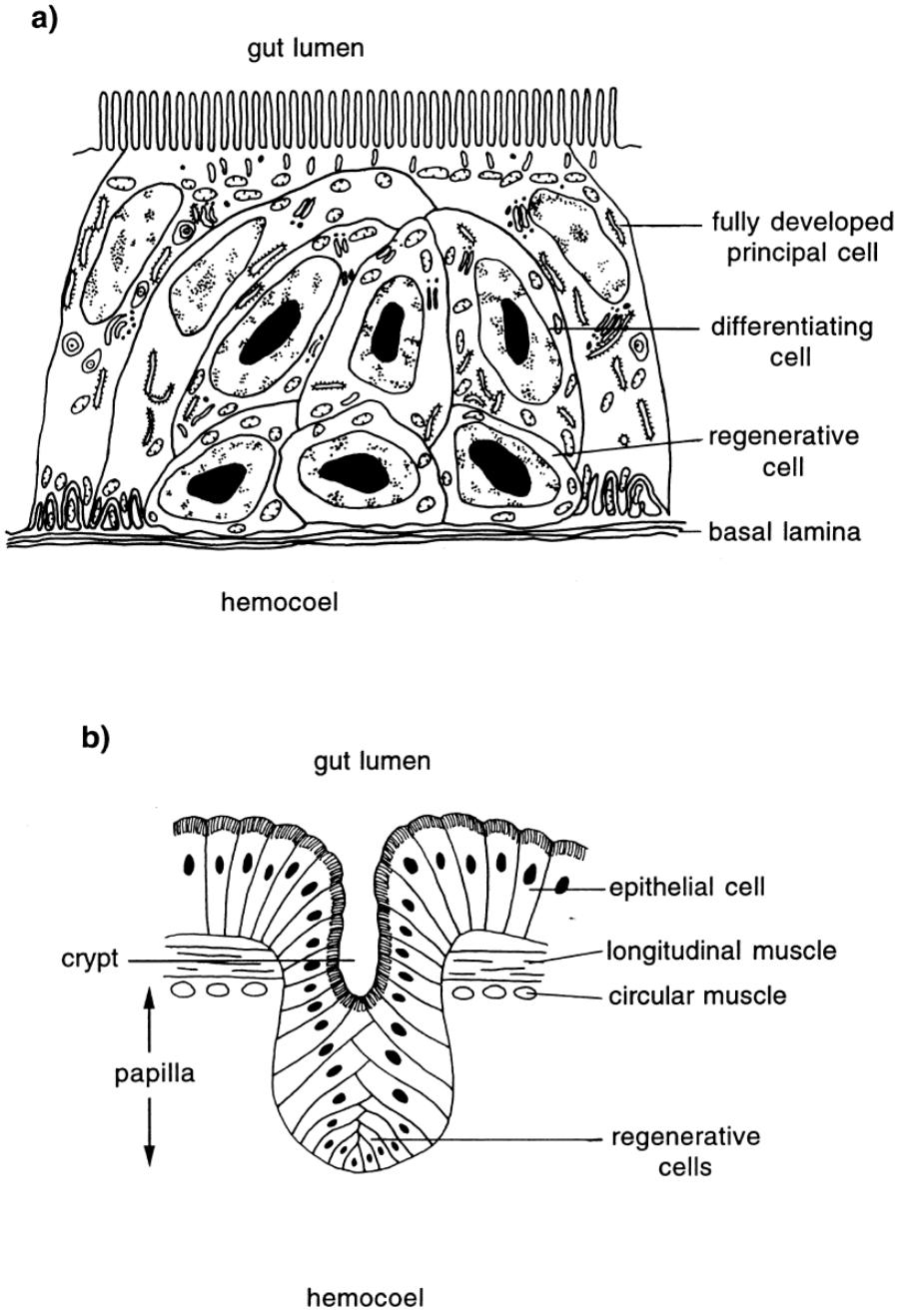

Fig. 3.7. Regenerative cells of the midgut. **(a)** Diagram of a nidus at the base of the midgut epithelium showing the differentiation of principal cells (after Fain-Maurel, Cassier & Alibert, 1973). **(b)** Diagram of a midgut crypt in a beetle extending through the muscle layer to form a papilla (after Snodgrass, 1935).

Obr. 11

Pohárková buňka středního střeva

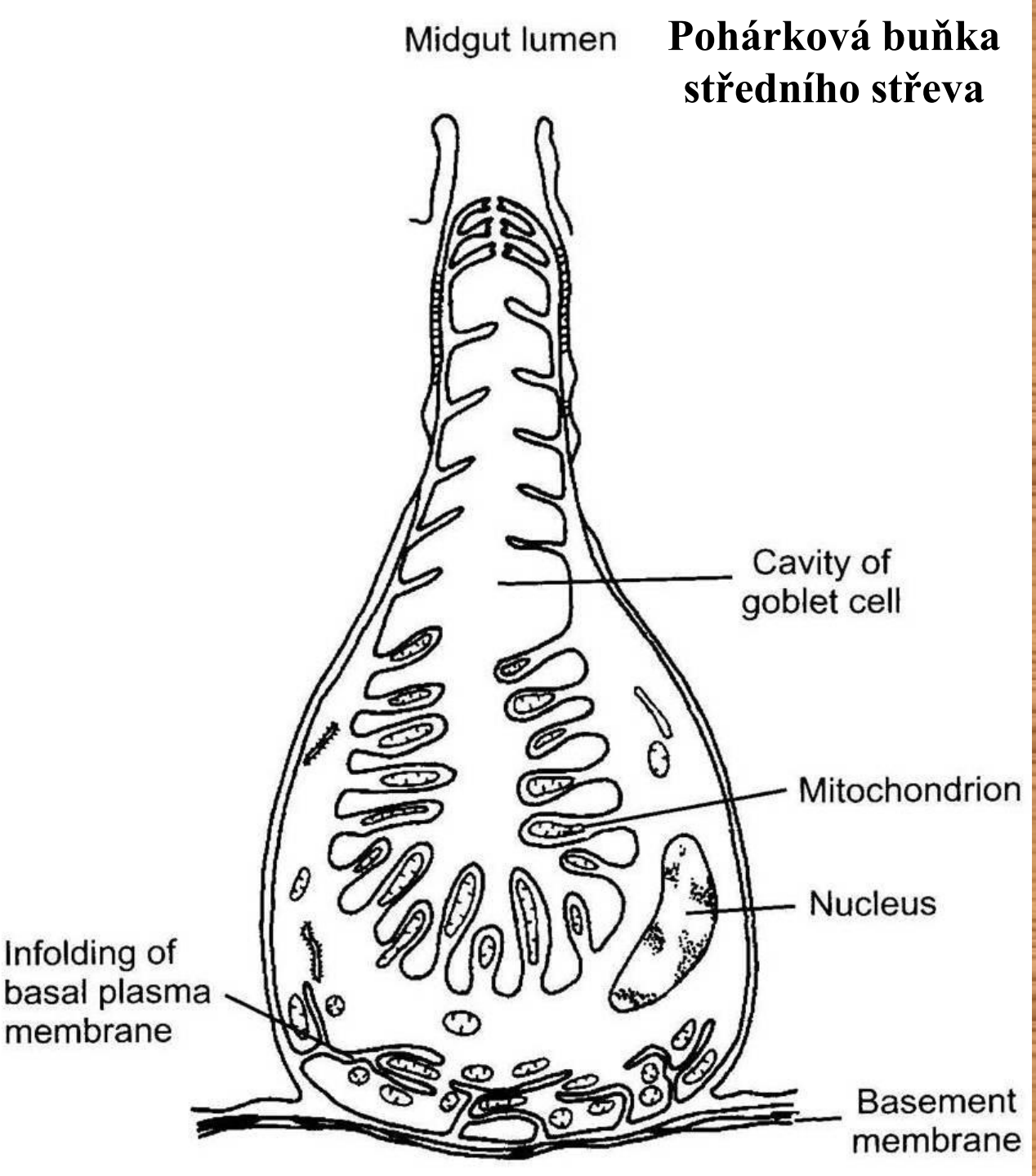

Obr. 12

Protonová pumpa

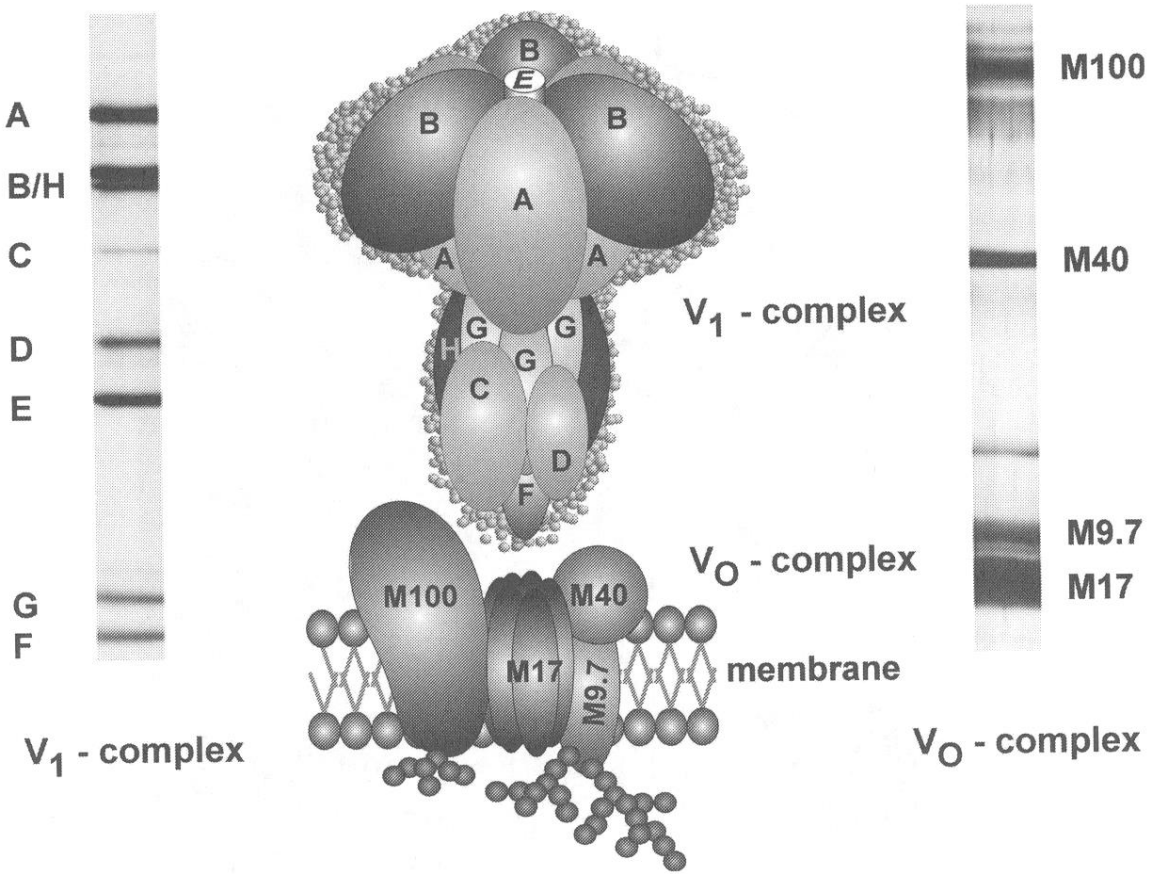

FIGURE 2.10 Projected complex of subunits comprising the proton pump (V-ATPase) that drives H^+ into the lumen of goblet cells in *Manduca sexta*. The head part of the pump, designated V_1, is located within the goblet cell cytoplasm, and the pump base (Vo) forms a transmembrane channel through which protons are pumped into the goblet cell cavity. ATP hydrolysis in the V_1 part of the pump provides the energy for the pumping of protons across the cell membrane. A separate mechanism in the goblet cell membrane that has not been elucidated yet exchanges K^+ for H^+ in the goblet cell cavity. The proton pump is the driving force for the concentration of K^+ against a concentration gradient in the goblet cell cavity. Eventually, the K^+ is released into the gut lumen, creating high pH in the lumen. The relative sizes of the various protein subunits are indicated in the gel bands shown on each side of the pump. (Illustration provided by William Harvey. Reproduced with permission from Wieczorek et al., 2000.)

Obr. 13 Peritrofické membrána a její formování na začátku středního střeva

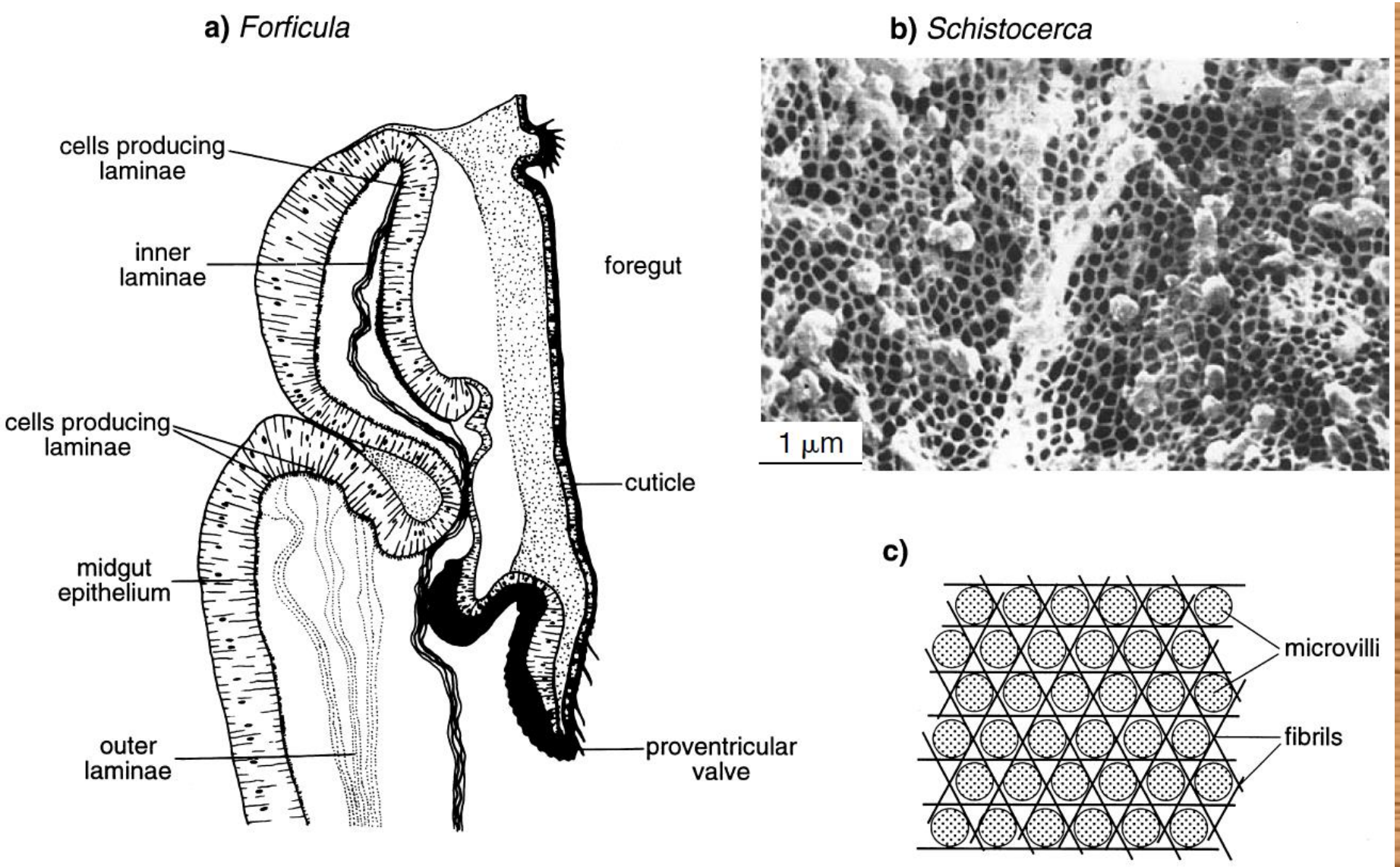

Fig. 3.10. Peritrophic envelope. **(a)** Diagram showing the origin of the peritrophic envelope in cells at the anterior end of the midgut of *Forficula* (after Peters *et al.*, 1979). **(b)** Scanning electron micrograph of the peritrophic envelope of *Schistocerca*. The envelope has been washed so that only the chitinous lattice remains (after Chapman, 1985a). **(c)** Diagram showing how the fibers which will form the lattice of the peritrophic envelope are laid down round the microvilli.

Obr. 14 Střední střevo švába amerického *Periplaneta americana* - peritrofická membrána, SEM, foto - F. Weyda

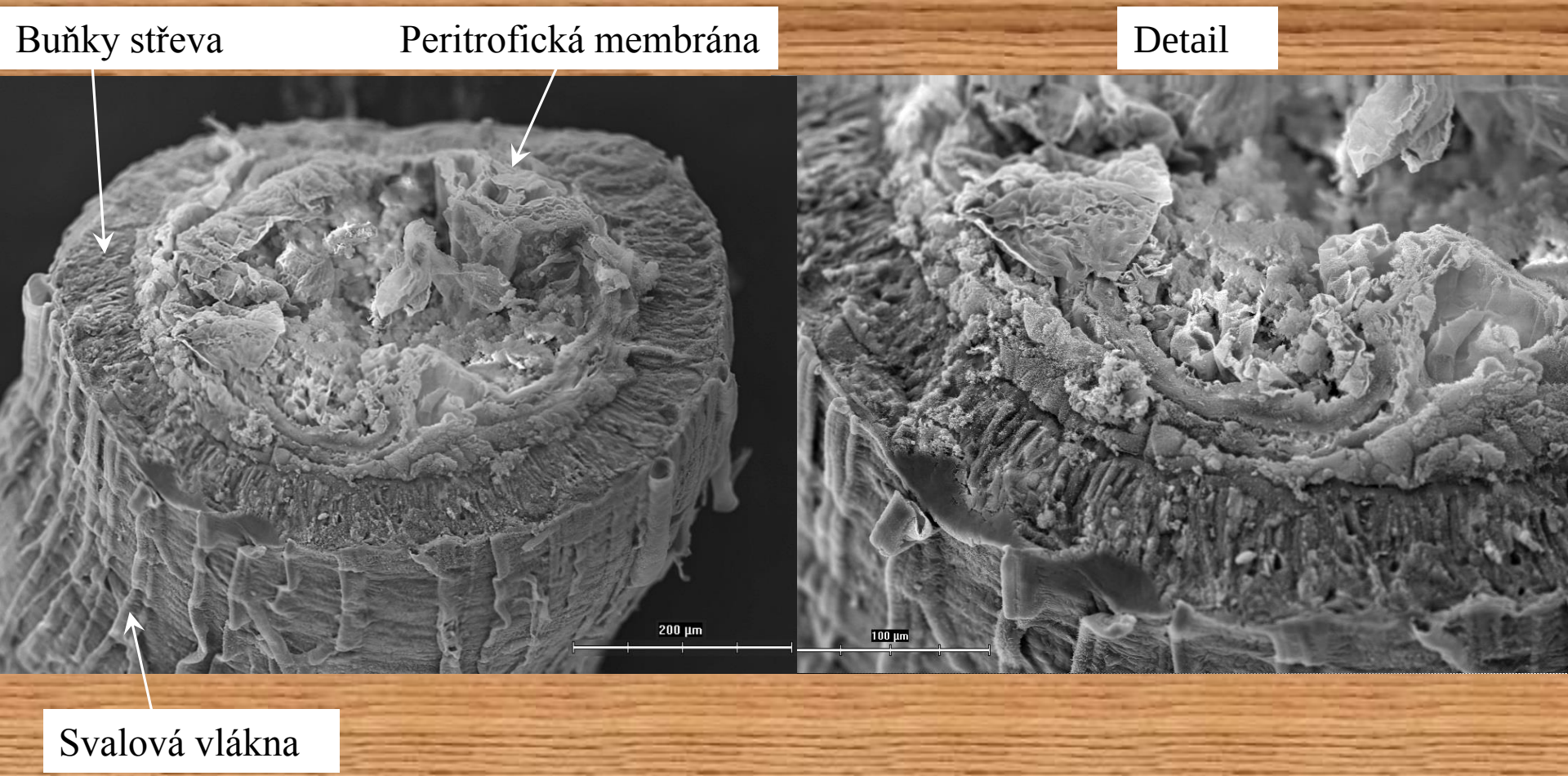

Obr. 15 Peritrofická membrána ve středním střevě

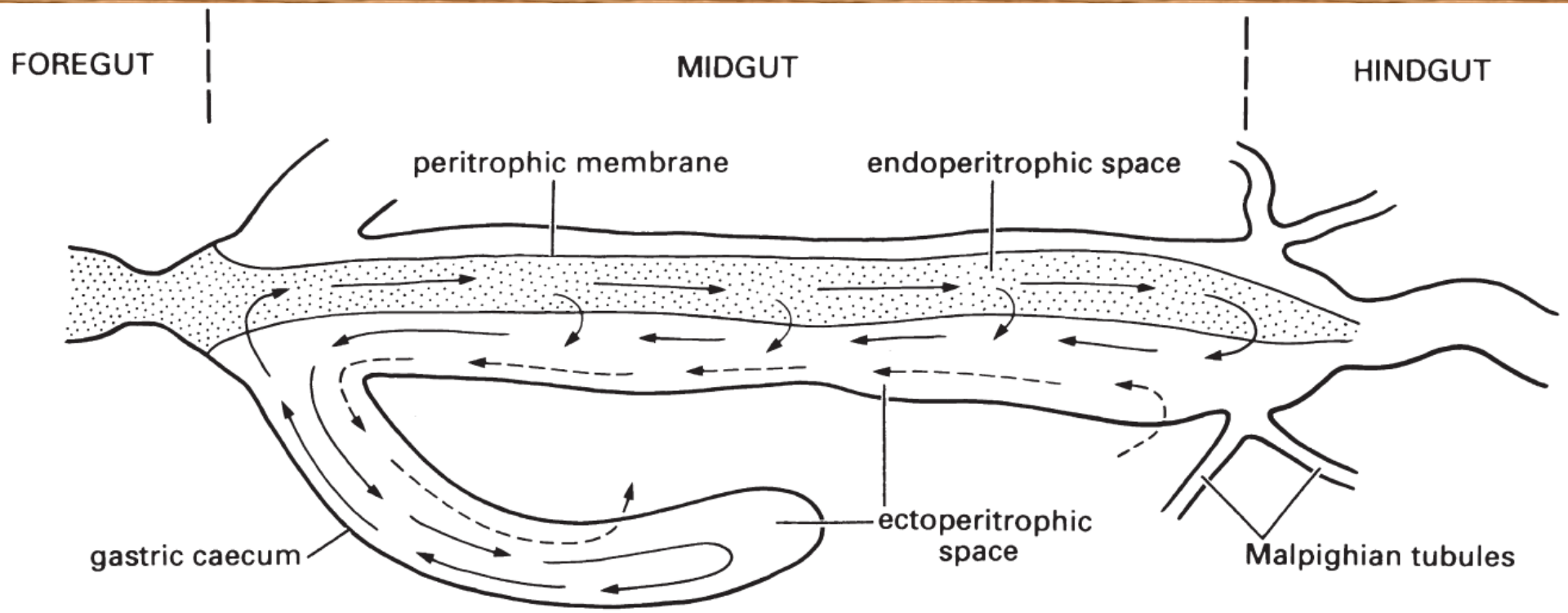

Fig. 3.16 Generalized scheme of the endo–ectoperitrophic circulation of digestive enzymes in the midgut. (After Terra & Ferreira 1981.)

Obr. 16 Celkový pohled na trávící soustavu hmyzu

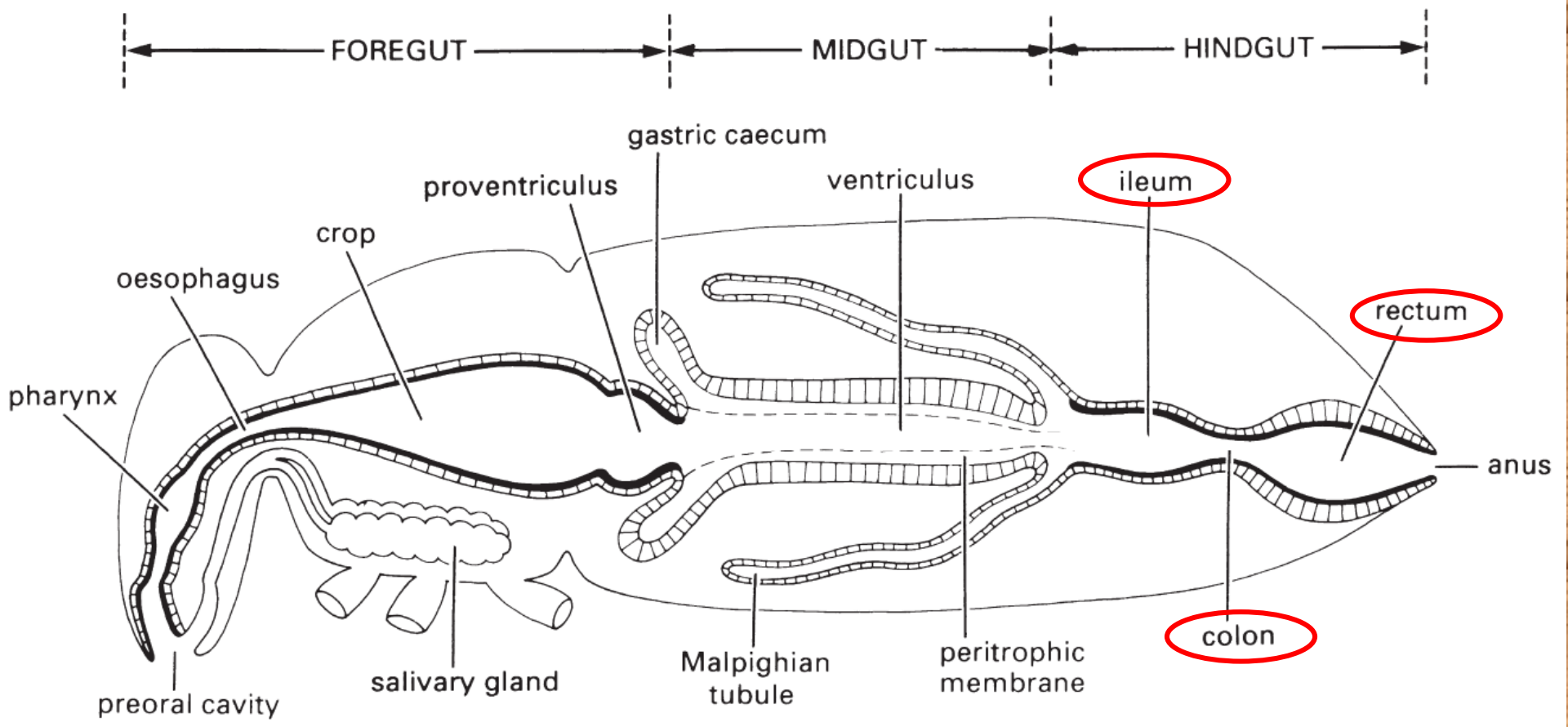

Fig. 3.13 Generalized insect alimentary canal showing division into three regions. The cuticular lining of the foregut and hindgut are indicated by thicker black lines. (After Dow 1986.)

Obr. 17 Svalovina ve střevě švába amerického *Periplaneta americana*, SEM, foto - F. Weyda

Příčná svalovina

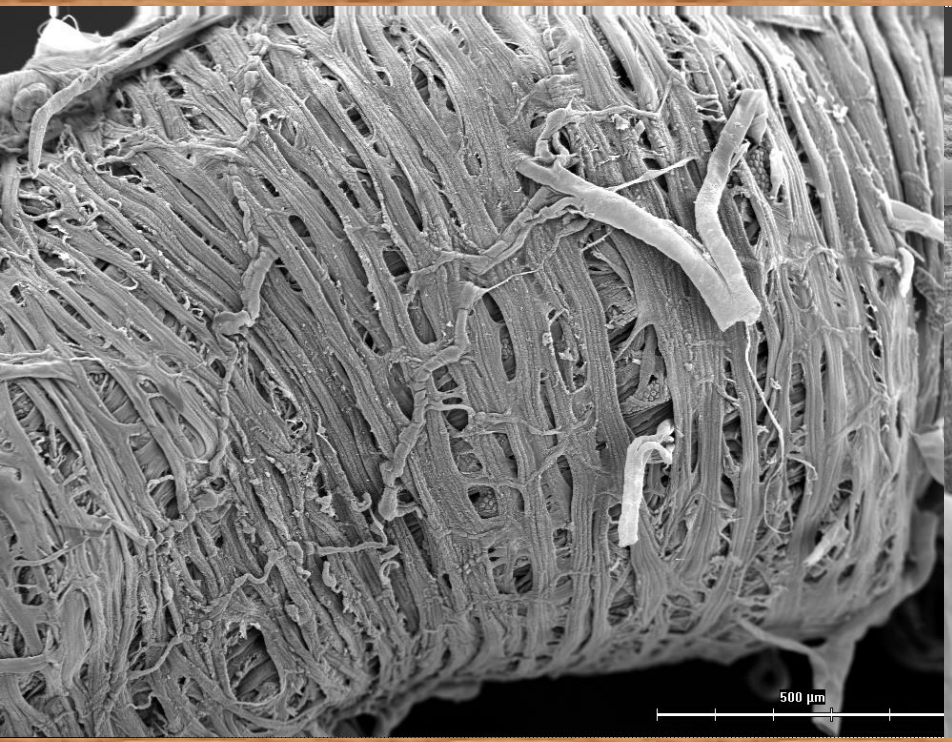

Podélná svalovina

Trachea

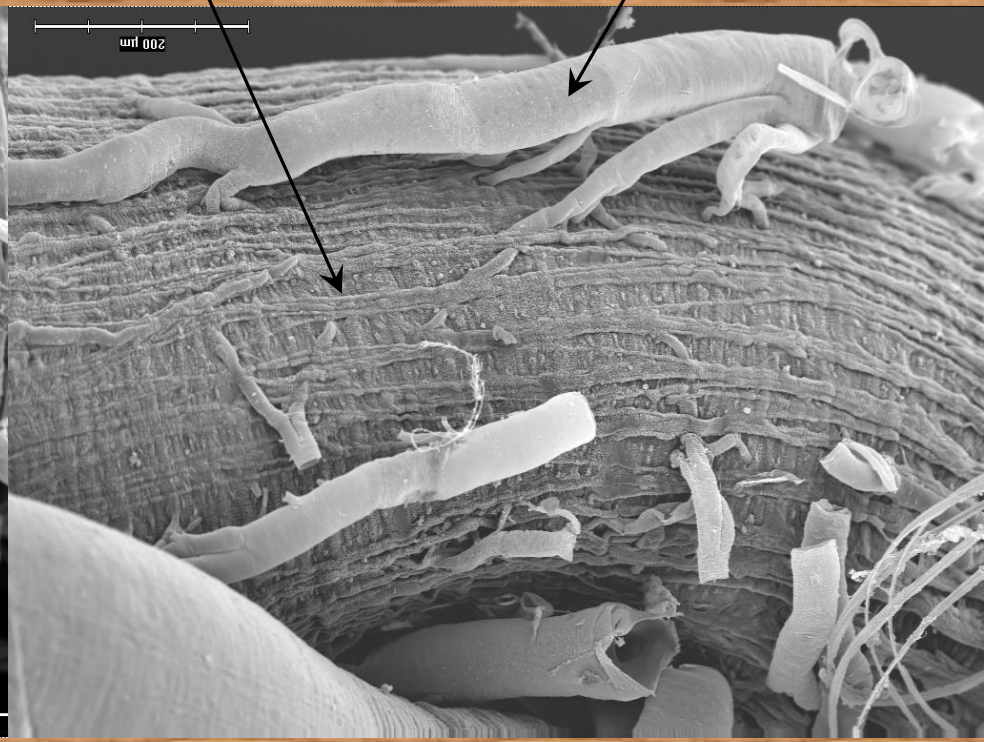

Trávení hmyzu: http://www.youtube.com/watch?v=5IdSruWQG5k&feature=plcp

Obr. 18 Filtrační komora

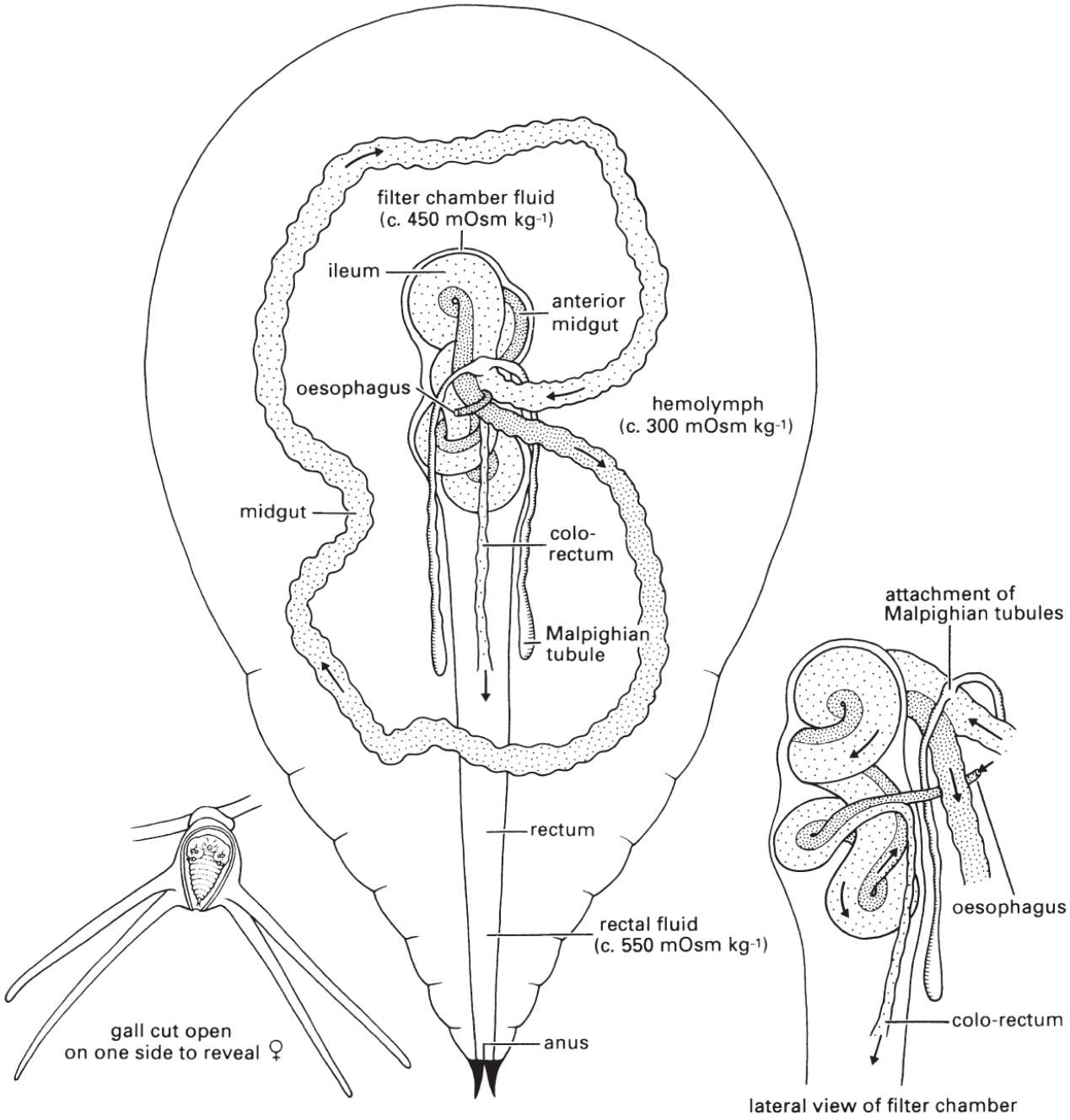

Obr. 19

Extraintestinální trávení

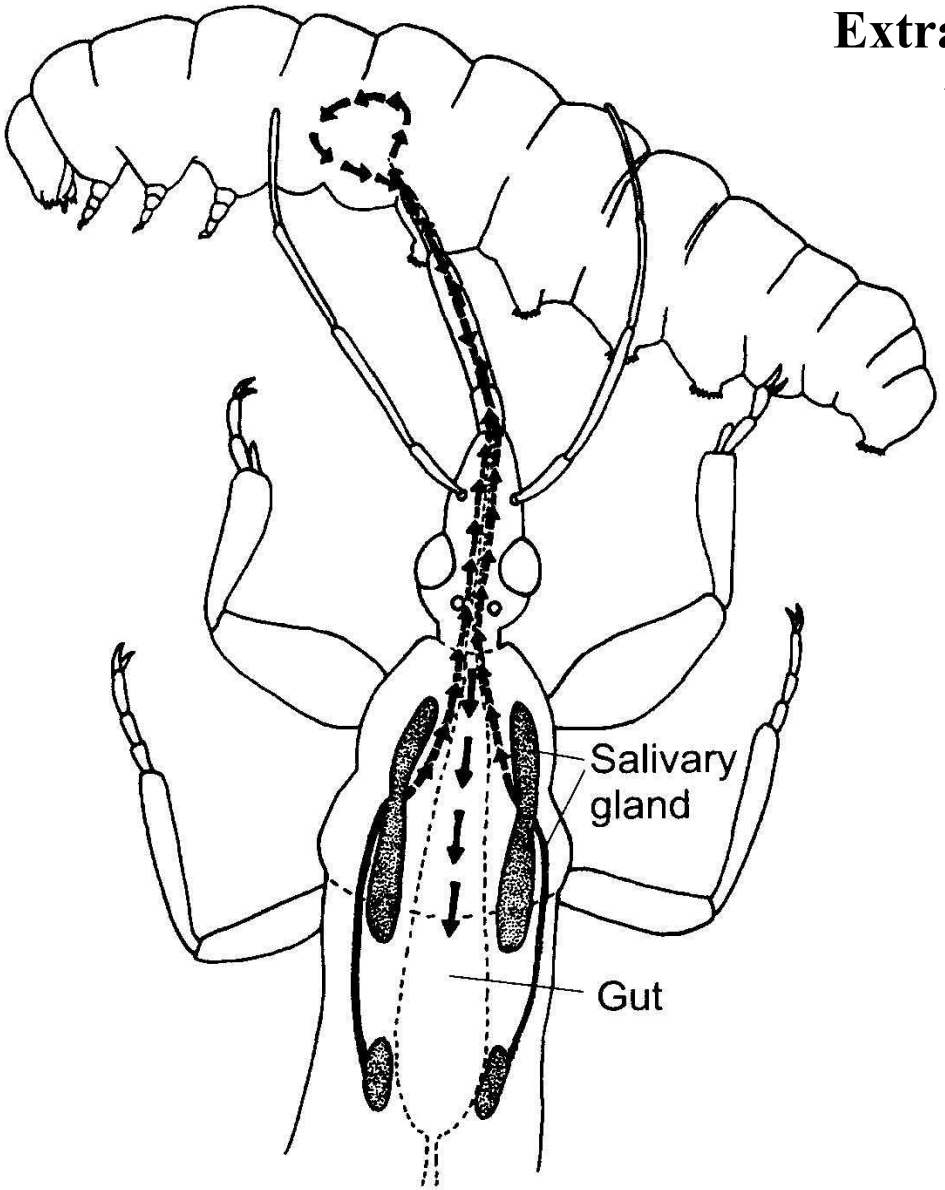

FIGURE 6.2. Extra-oral digestion, in which salivary gland components are injected into prey and then sucked into the gut. The arrows show the flow of digestive materials. From Cohen (1998). Reprinted with permission.

Činnost peptidáz

Obr. 20

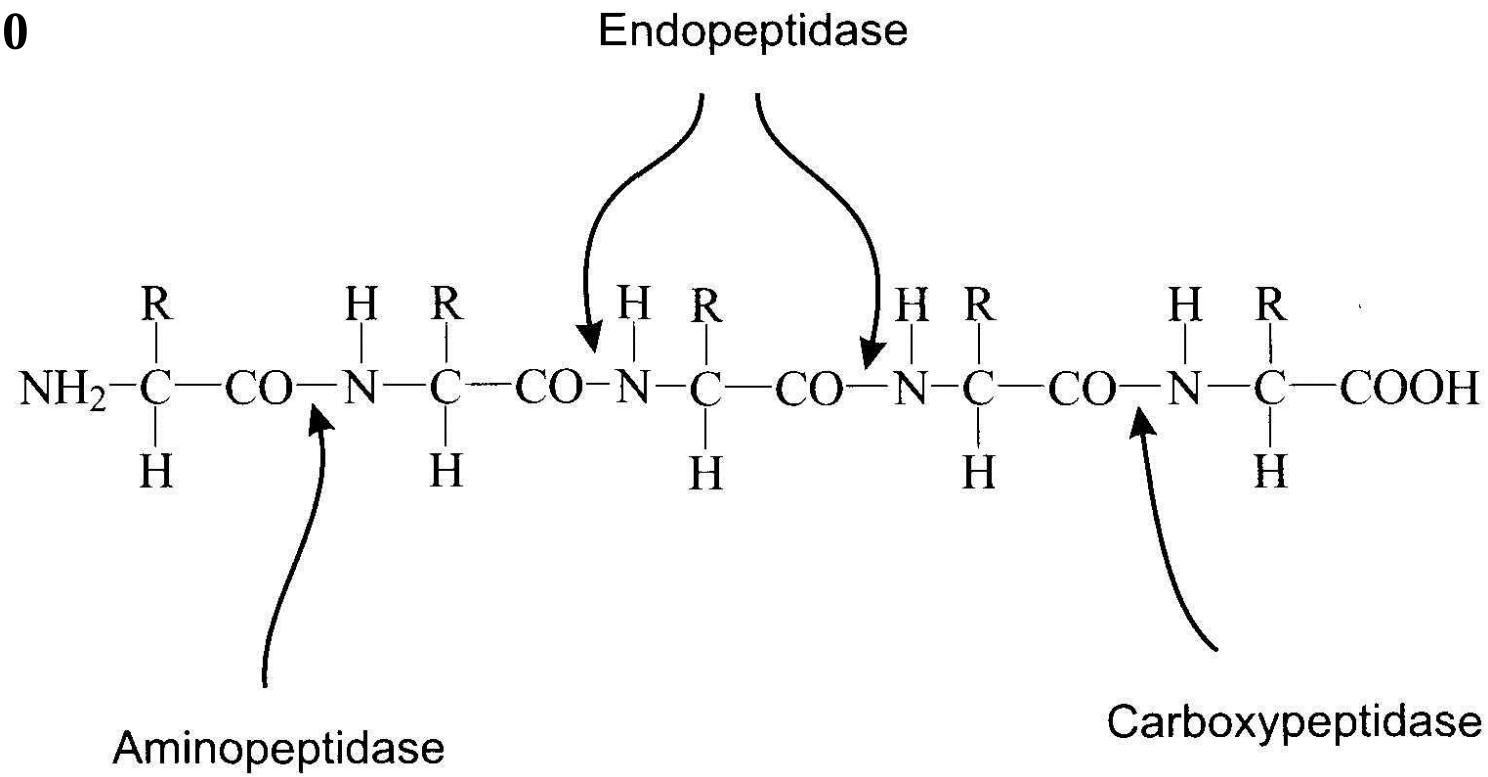

FIGURE 6.13. The action of aminopeptidases, endopeptidases, and carboxypeptidases on a polypeptide chain.

Obr. 21

Činnost trypsinu u komárů

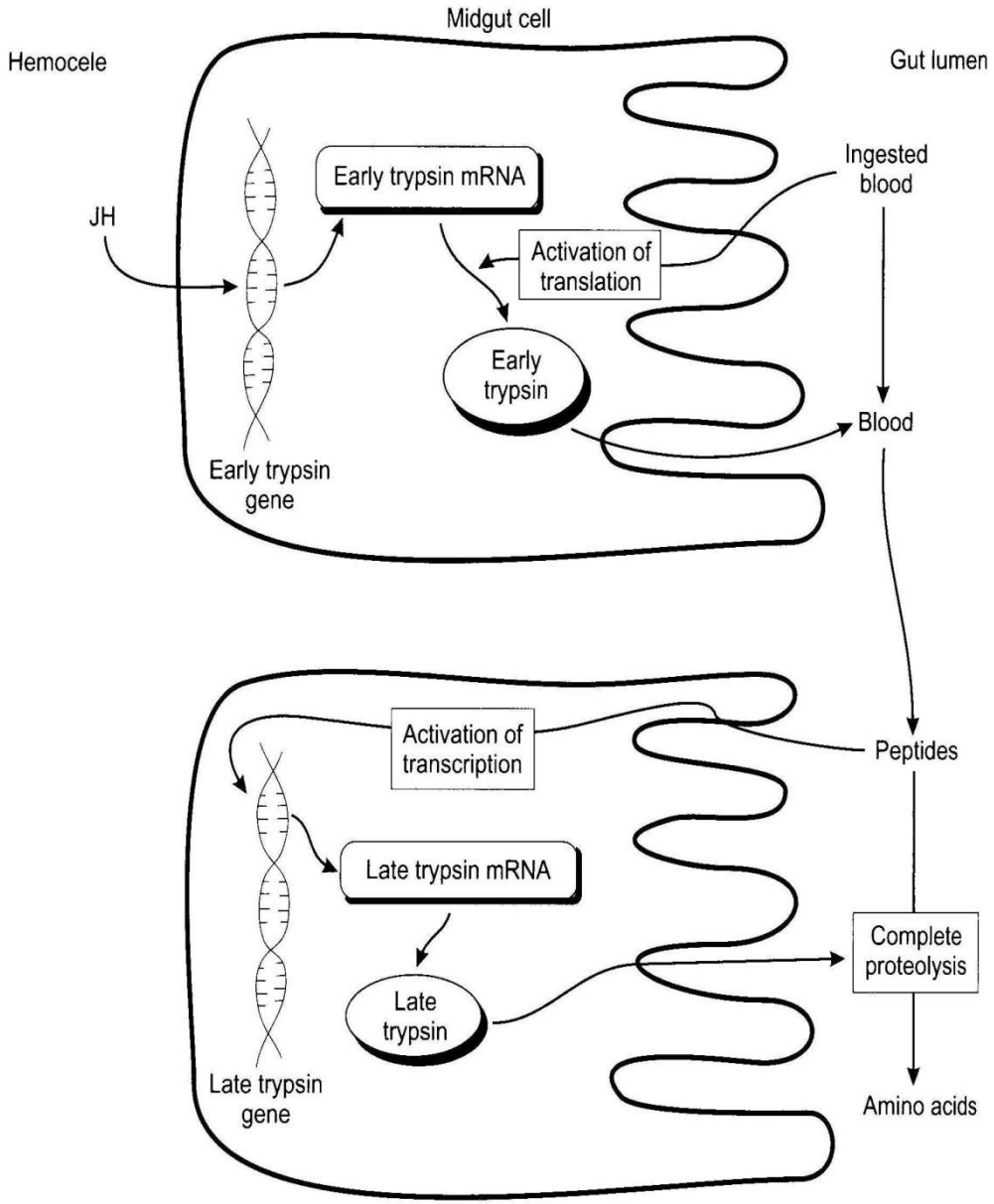

FIGURE 6.14. Mechanism of proteolytic digestion in mosquitoes. JH activates an early trypsin gene resulting in early trypsin mRNA. A newly ingested blood meal activates its translation to early trypsin, which digests the blood to peptides. The peptides activate transcription of late trypsin mRNA, and this late trypsin breaks the peptides down to amino acids.

Obr. 22 **Trávení tuků**

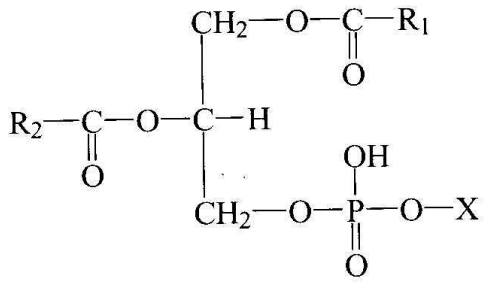

Phosphoglyceride

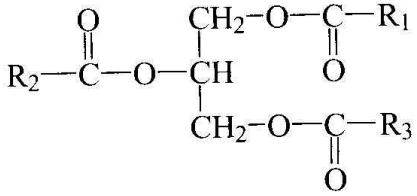

Triacylglycerol

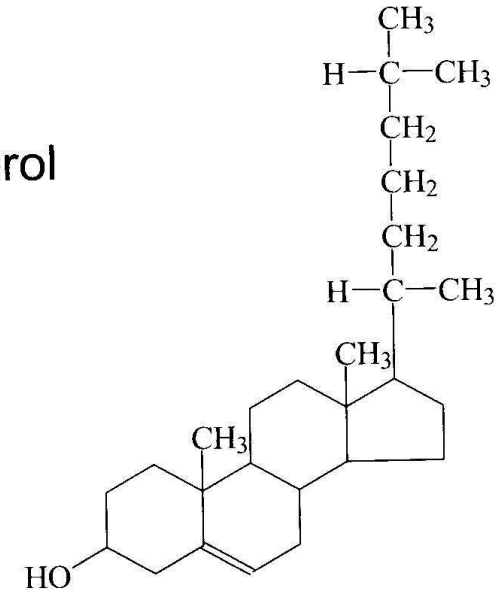

Cholesterol

FIGURE 6.17. The major types of animal lipids. X = alcohol in phosphoglyceride.

Obr. 23 Tukové těleso hmyzu

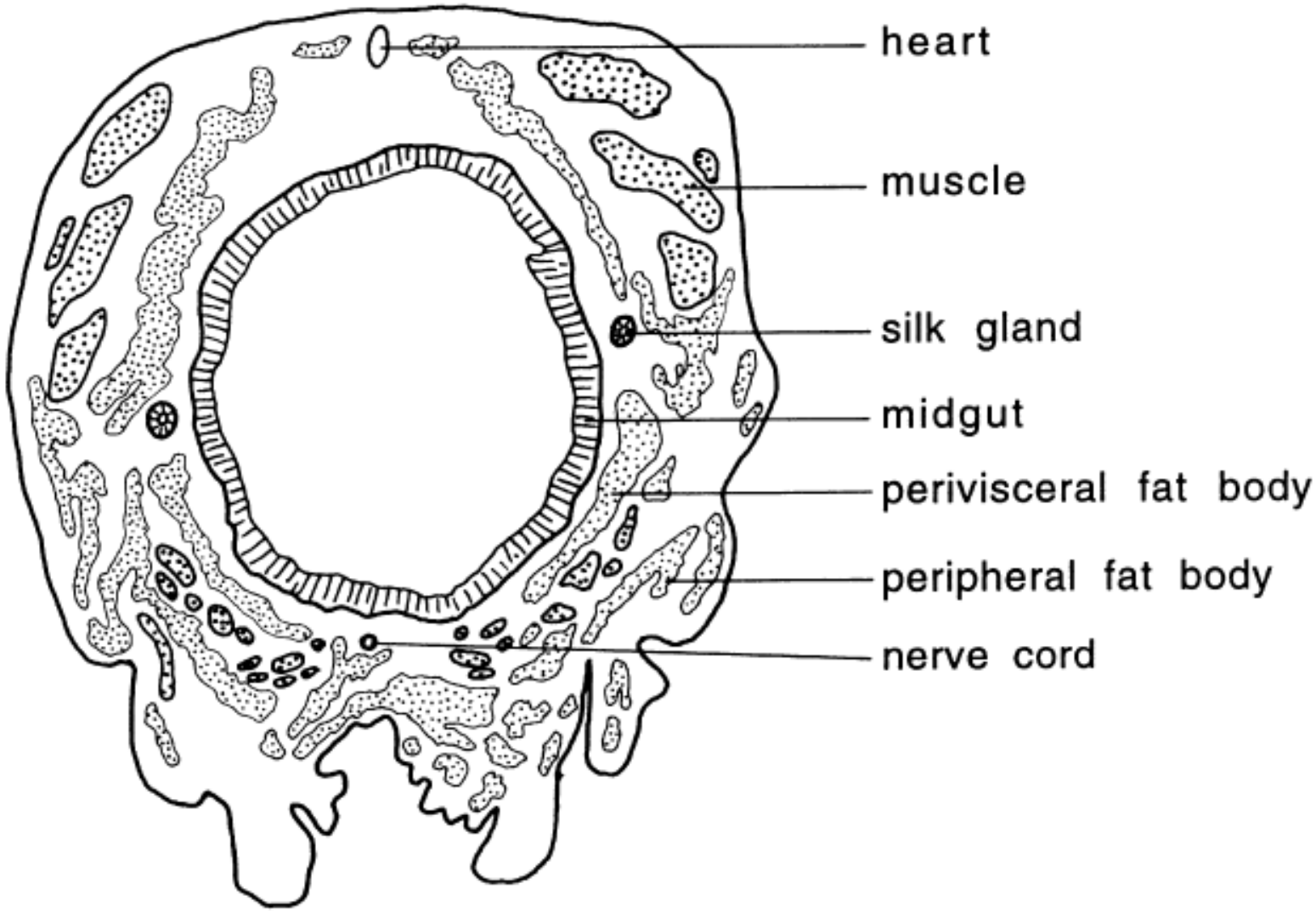

Fig. 6.1. Distribution of fat body in a caterpillar in transverse section of the abdomen.

Obr. 24 Schéma vstřebávání cukrů pomocí cyklu glukóza-trehalóza

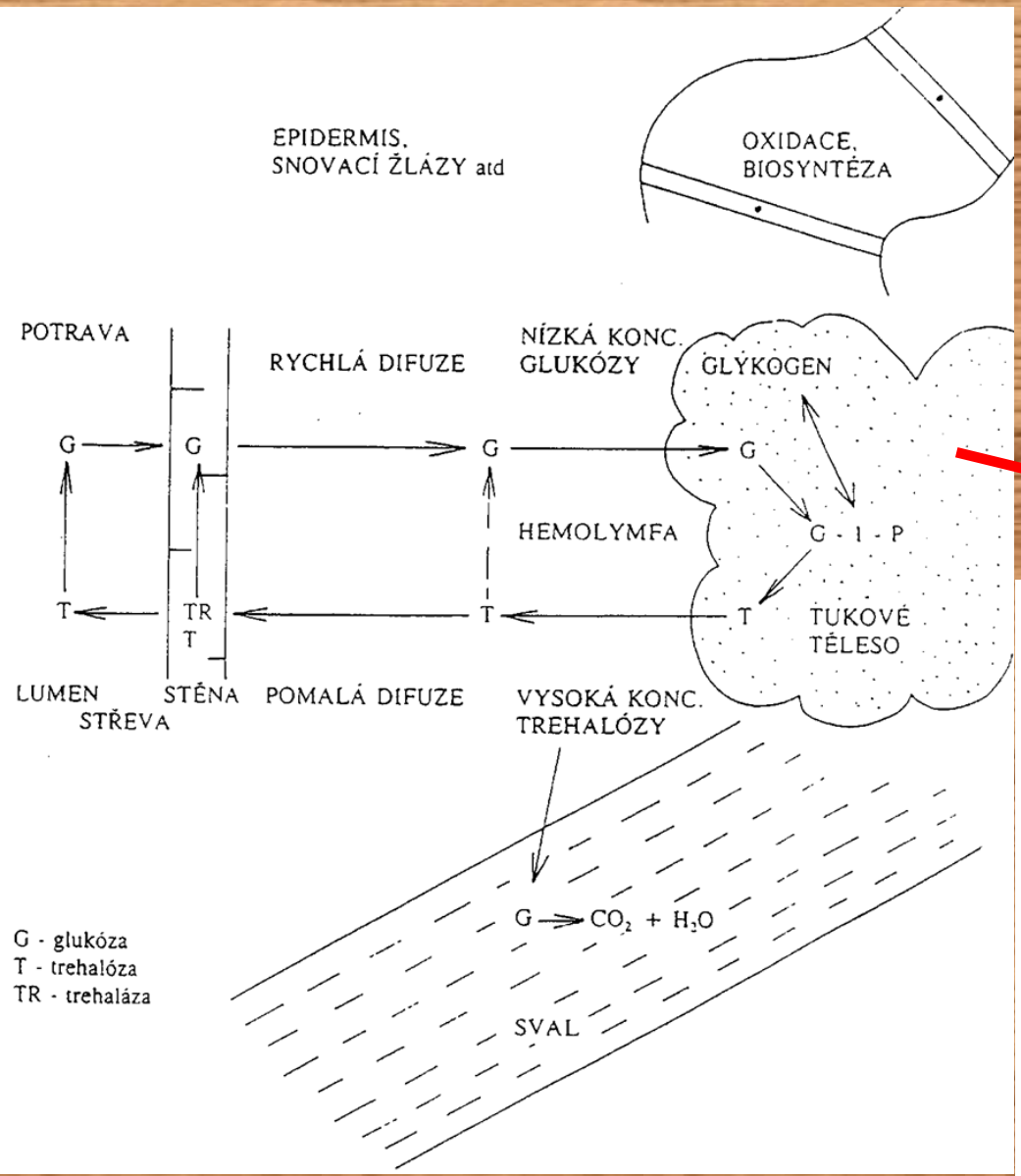

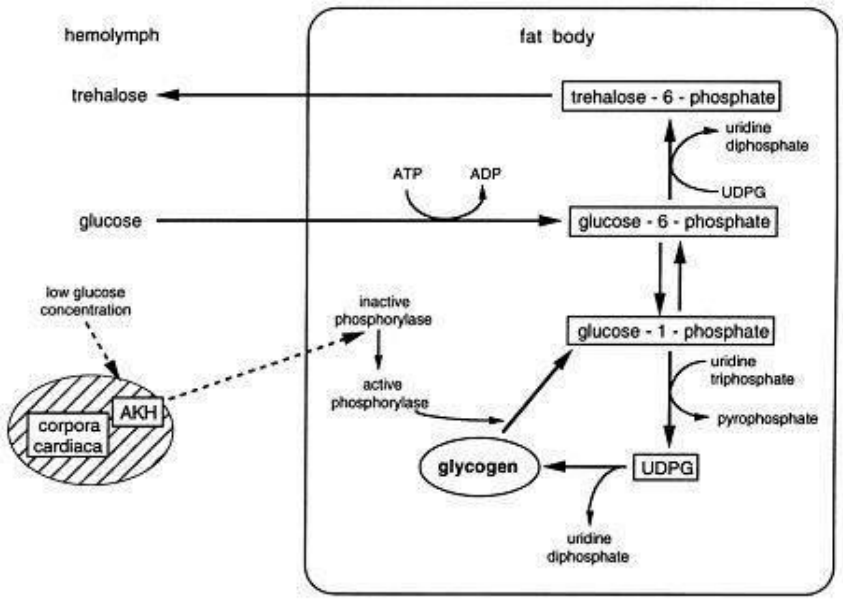

AKH – adipokinetic hormone, UDPG - uridine diphosphate glucose

Tukové těleso: http://www.youtube.com/watch?v=NU1GTKjpSnM&feature=plcp

3. Dýchání

Obr. 1

Tracheální soustava hmyzu

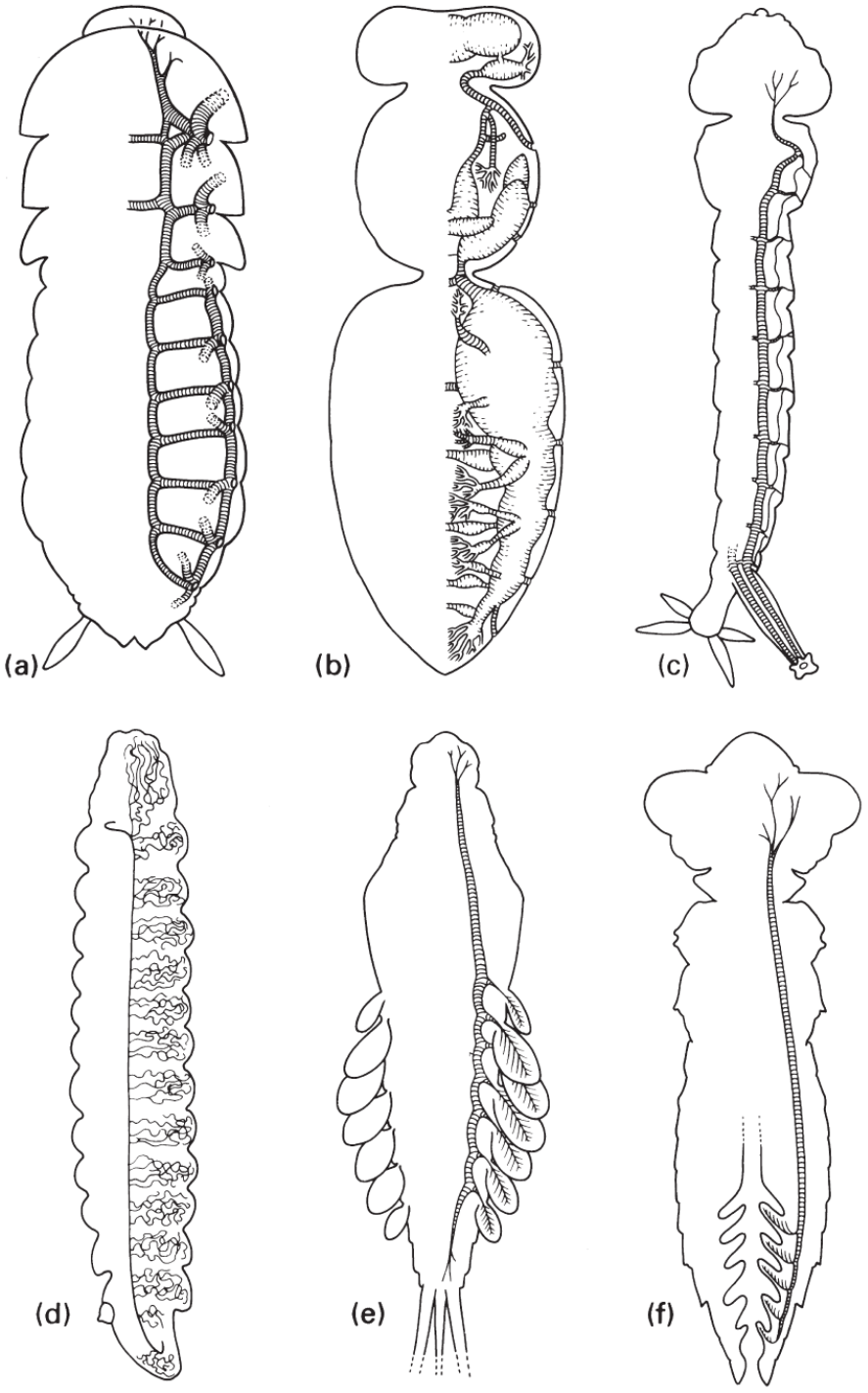

Fig. 3.11 Some basic variations in the open (a–c) and closed (d–f) tracheal systems of insects. (a) Simple tracheae with valved spiracles, as in cockroaches. (b) Tracheae with mechanically ventilated air sacs, as in honey bees. (c) Metapneustic system with only terminal spiracles functional, as in mosquito larvae. (d) Entirely closed tracheal system with cutaneous gas exchange, as in most endoparasitic larvae. (e) Closed tracheal system with abdominal tracheal gills, as in mayfly nymphs. (f) Closed tracheal system with rectal tracheal gills, as in dragonfly nymphs. (After Wigglesworth 1972; details in (a) after Richards & Davies 1977, (b) after Snodgrass 1956, (c) after Snodgrass 1935, (d) after Wigglesworth 1972.)

Obr. 2 Tracheální soustava hmyzu

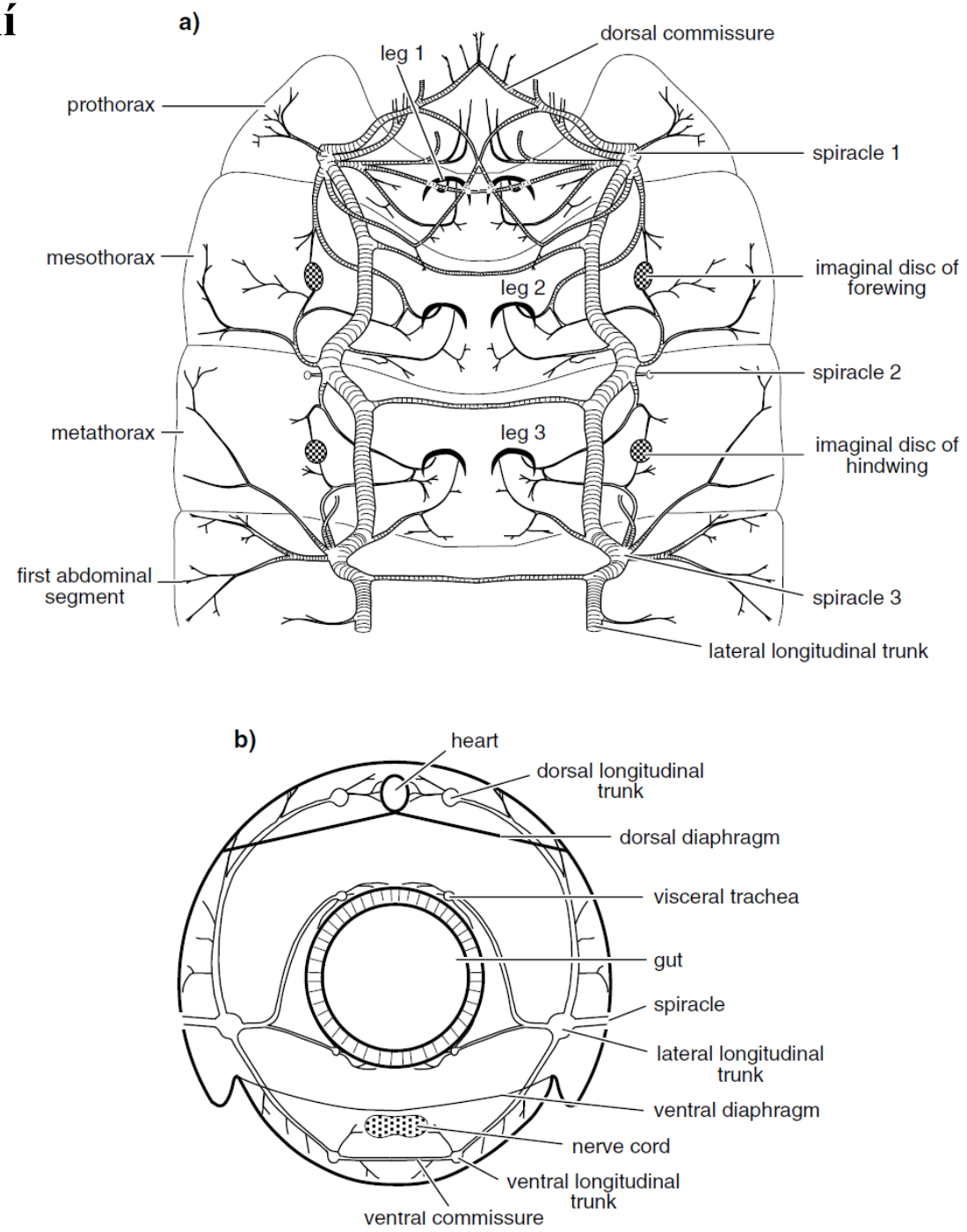

Obr. 3 Spirakulum a jeho stavba

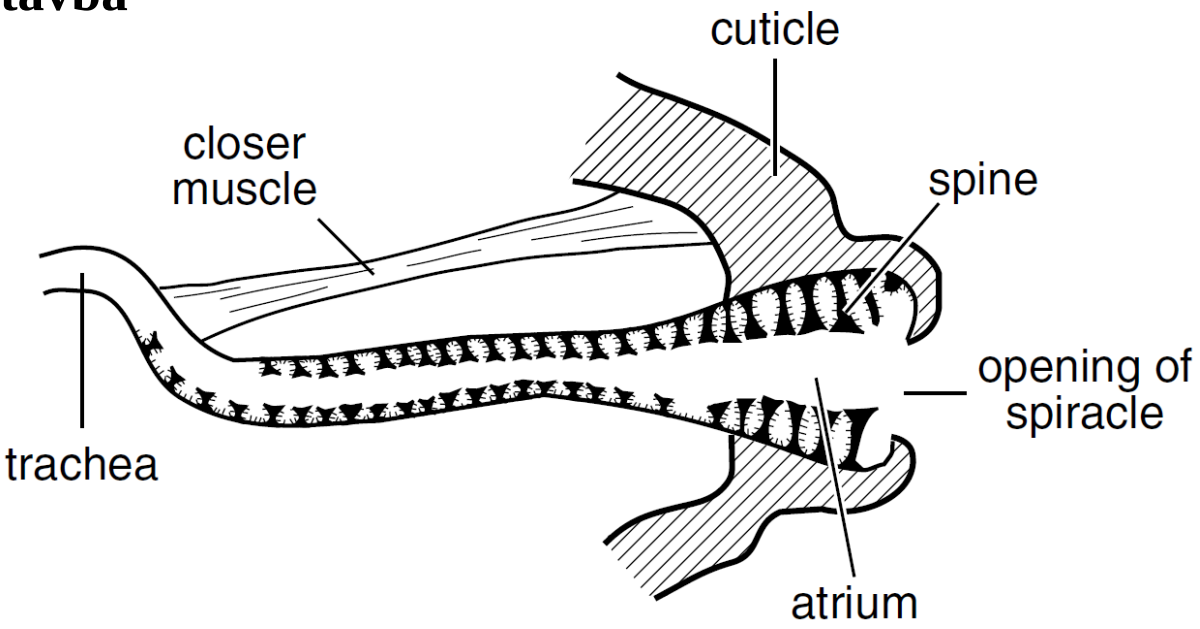

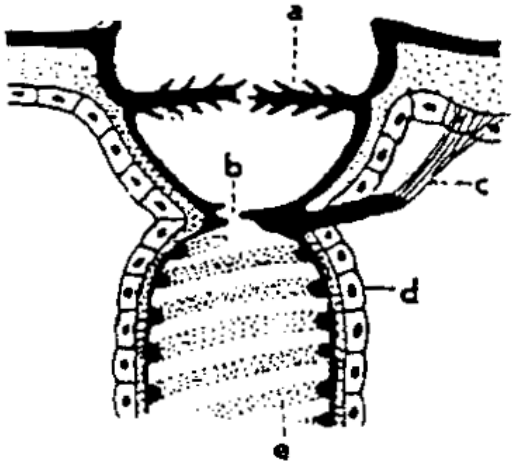

Stavba průduchu
a = filtrační ústrojí, b = uzavíratelný otvor průduchu, c = otevírací sval, d = tracheální epitel, e = taenidium

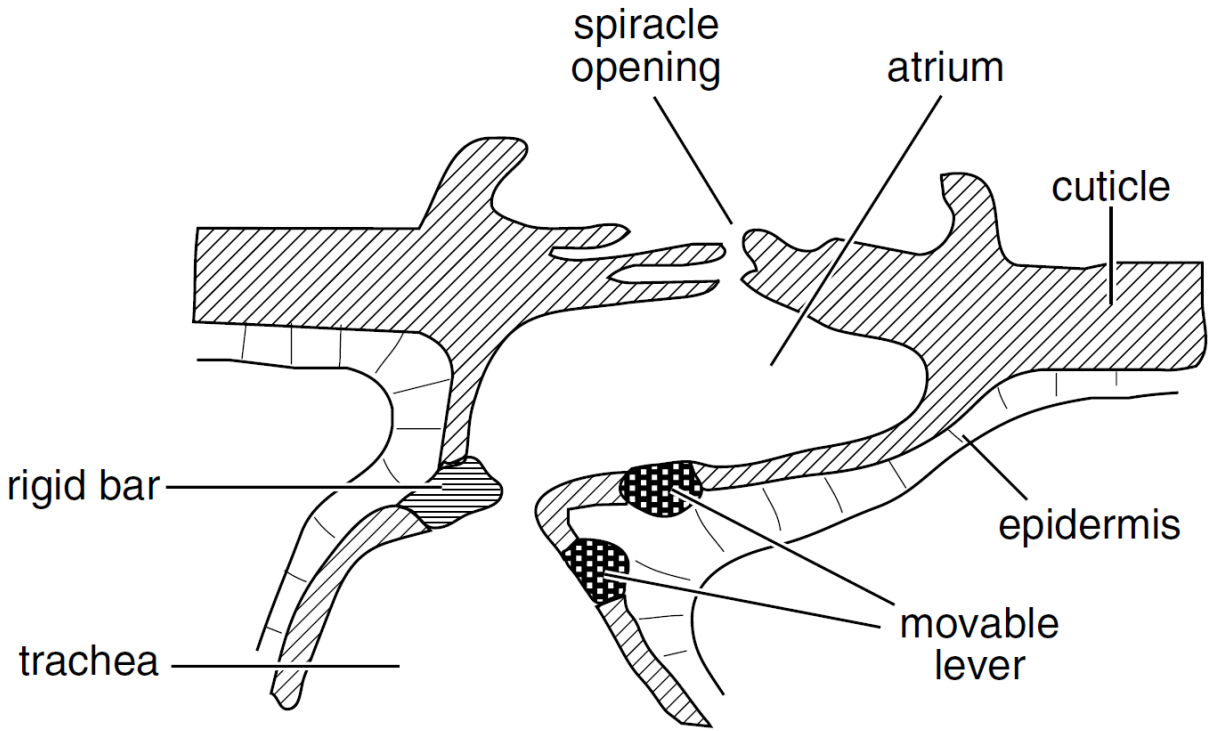

Obr. 4 Vzdušnice a jejich stavba

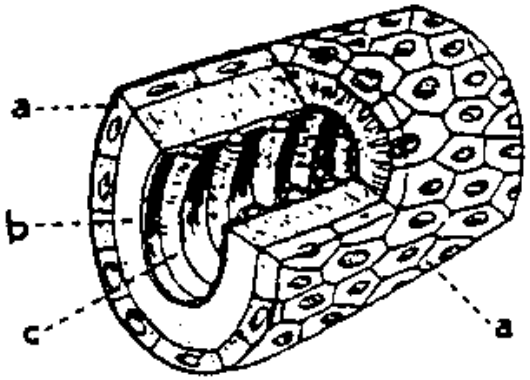

Stavba vzdušnice

a = buňky tracheálního epitelu, b = intima, c = taenidium

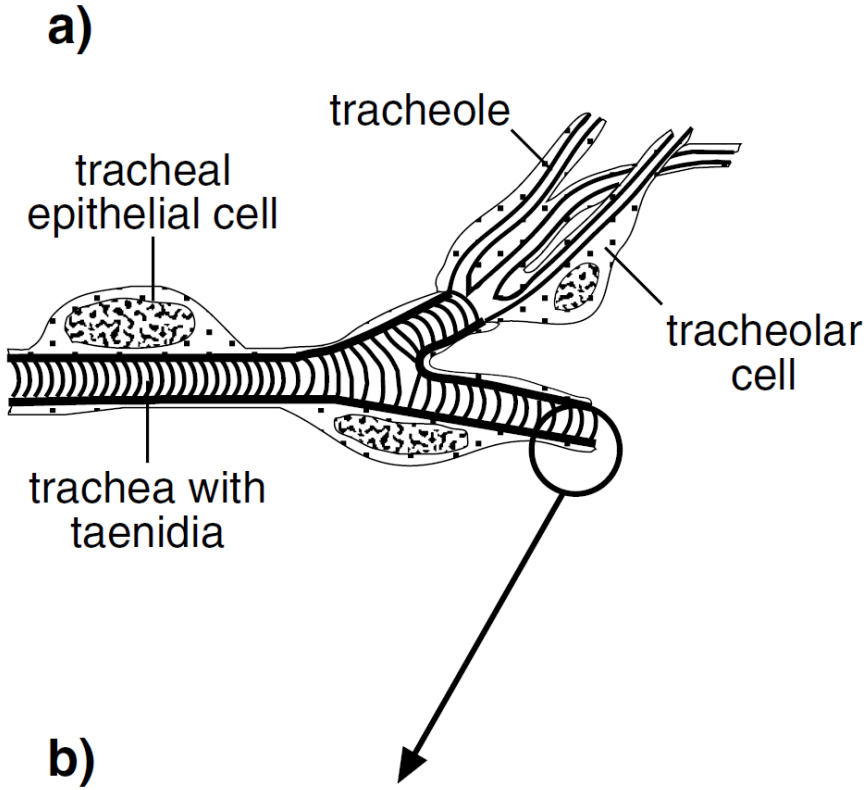

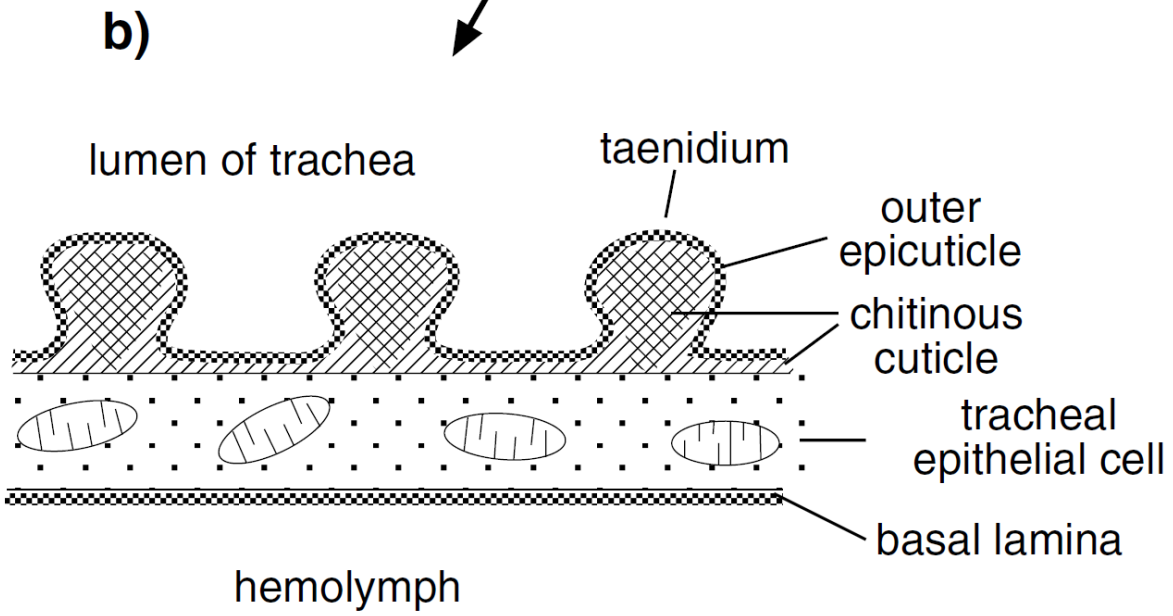

Obr. 5a Hmyzí trachea – podélný řez, TEM

Obr. 5a Tracheizace femuru ploštice *Pyrrhocoris apterus* – podélný řez, TEM, foto F. Weyda

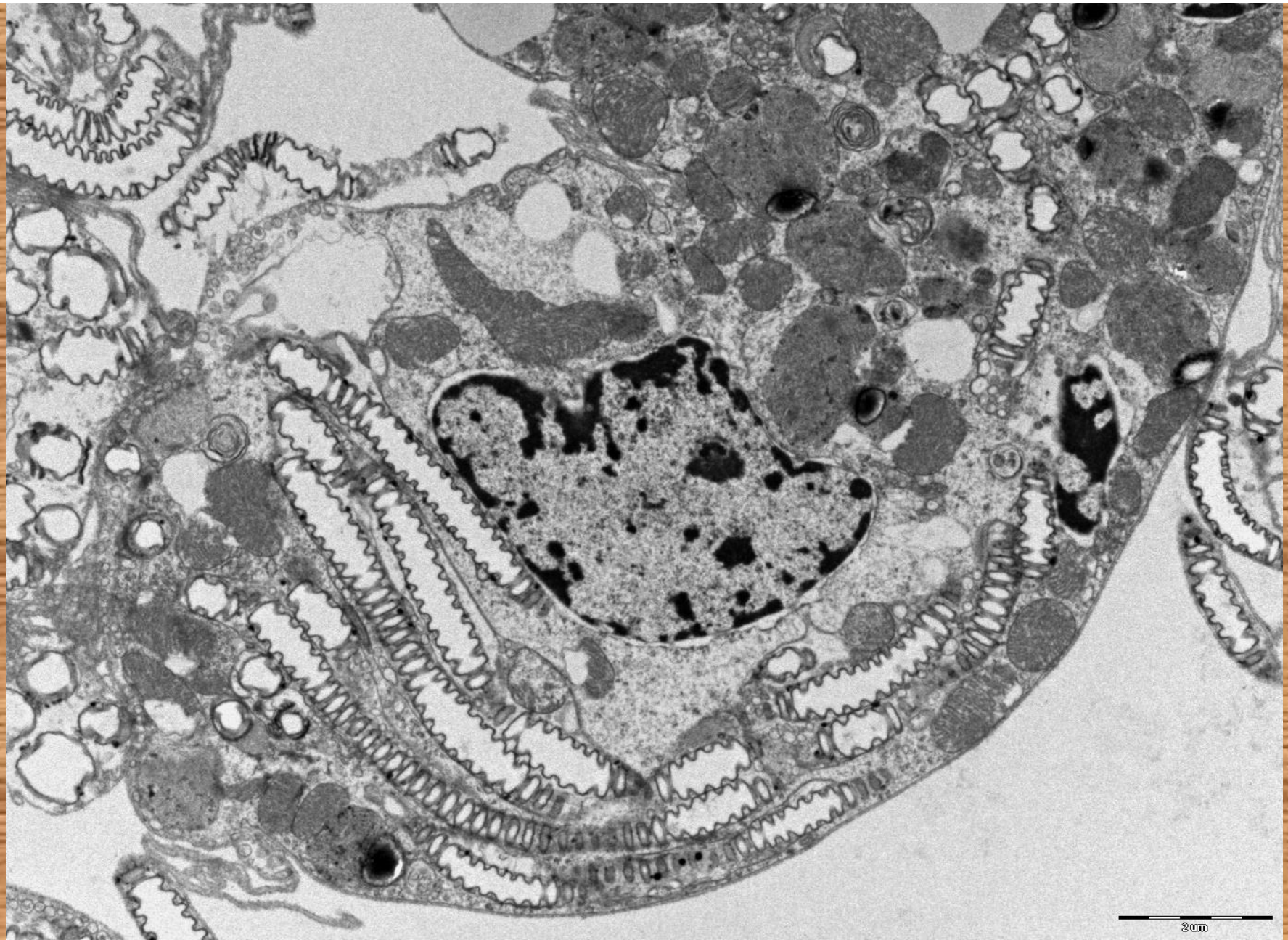

Obr. 5c Trachea ve střevě včely – elektronová mikroskopie, technika FESEM, foto F. Weyda

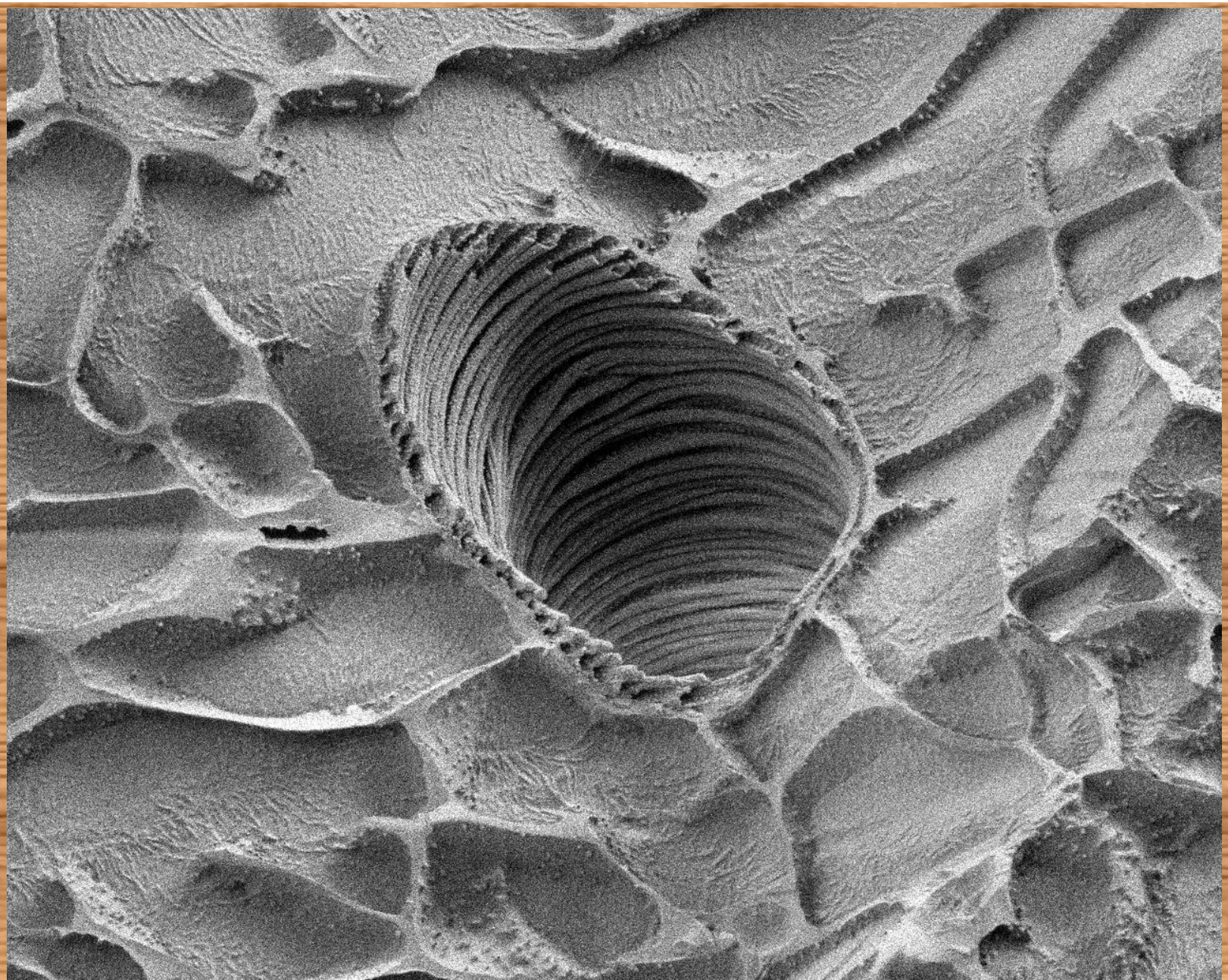

Obr. 6 Tracheální vaky u saranče pustinného *Schistocerca gregaria*

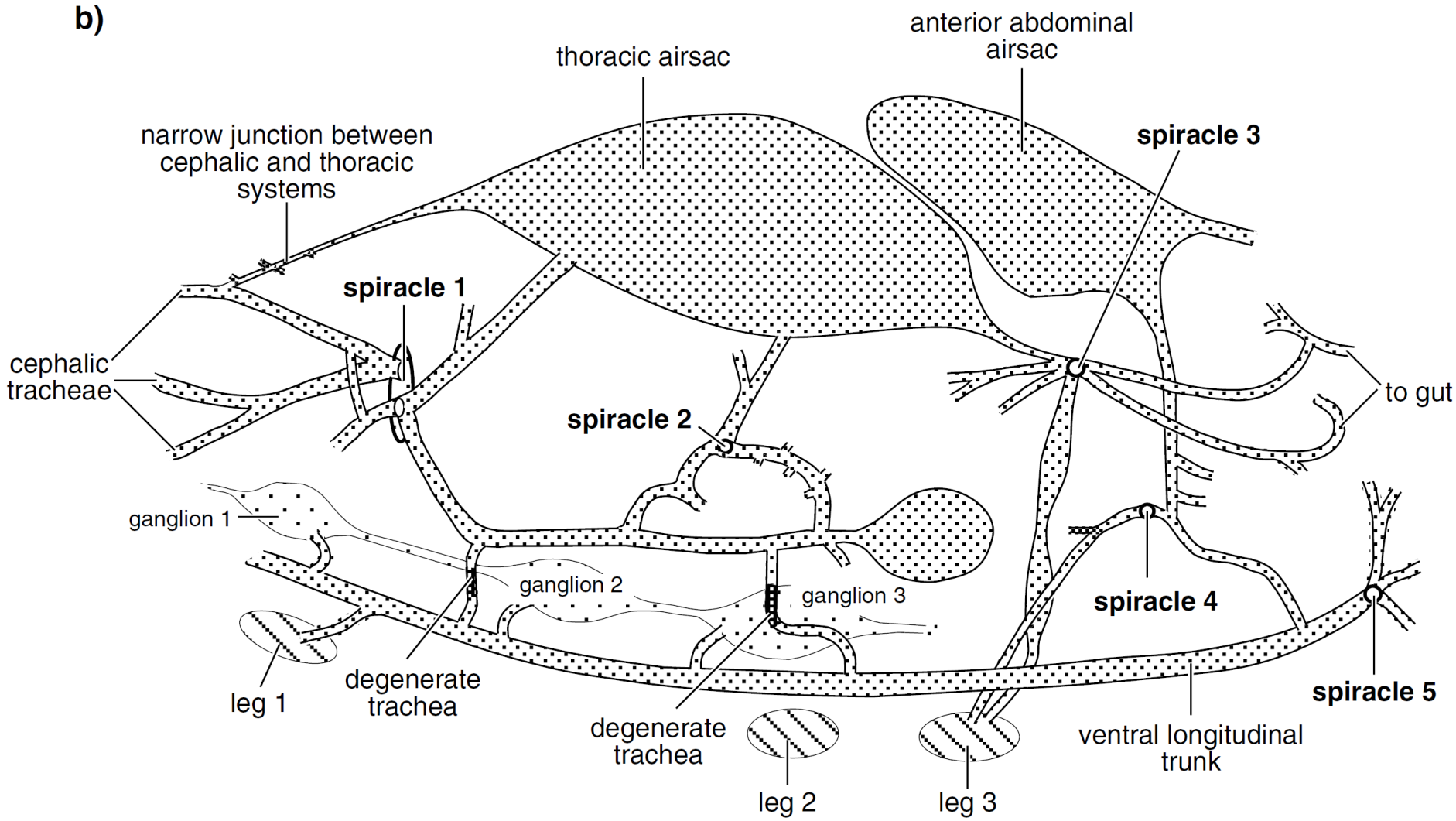

Obr. 7

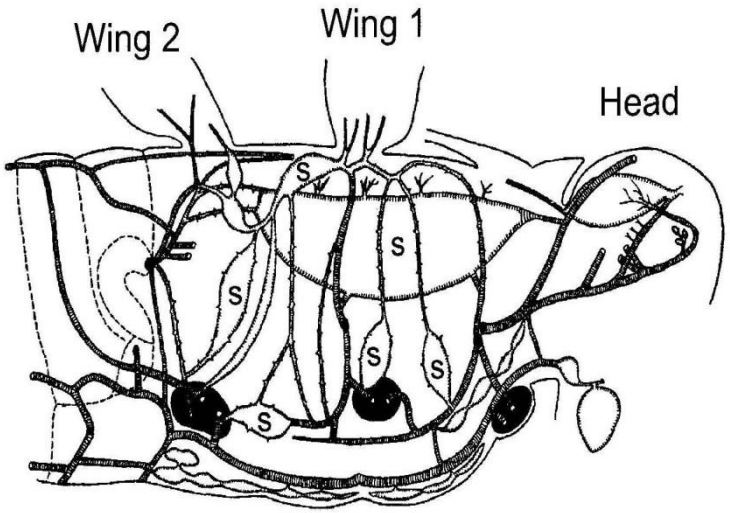

Stavba tracheálního vaku

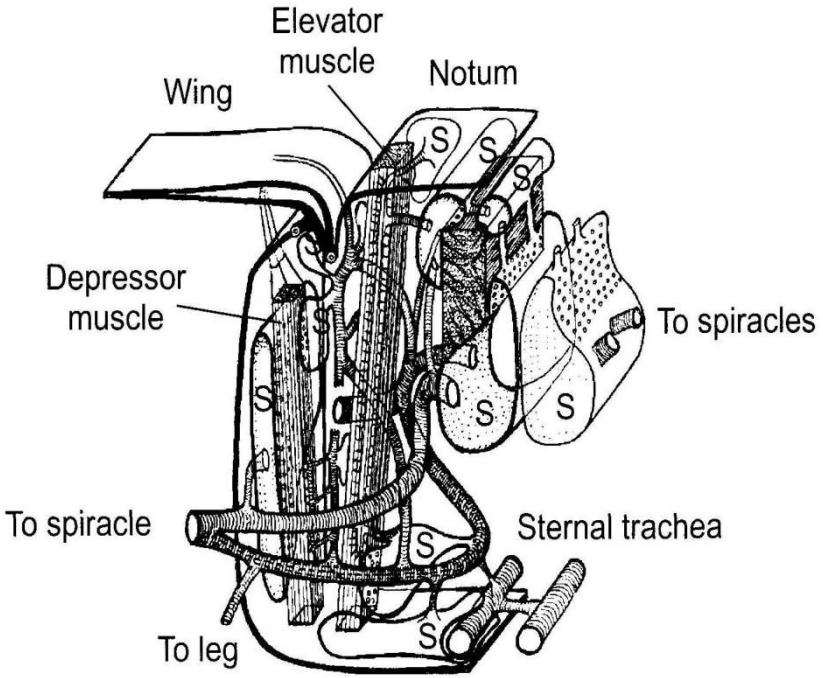

FIGURE 9.14. Tracheal air sacs(s) within the tracheal system can be increased and decreased in volume to pump air through the system. From Albrecht (1953). Reprinted with permission.

Obr. 8

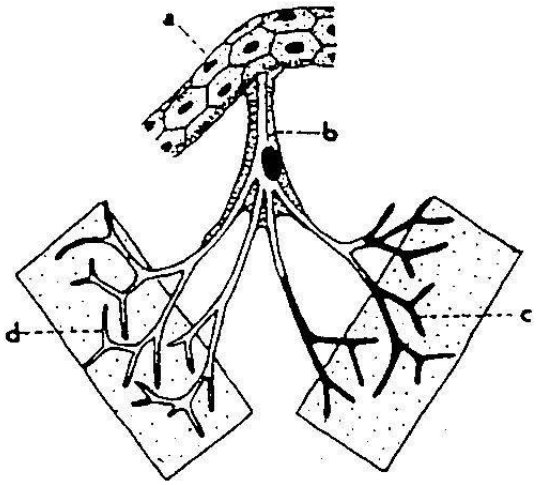

Stavba a funkce tracheol

a = koncová větévka trachee, b = tracheální buňka rozvětvená v tracheoly, c = tracheoly vyplněné krvomízou v nečinné tkáni, d = tracheoly bez krvomízy, rozvětvené ve tkáni, která spotřebovává kyslík

Stavba a vývoj tracheoly

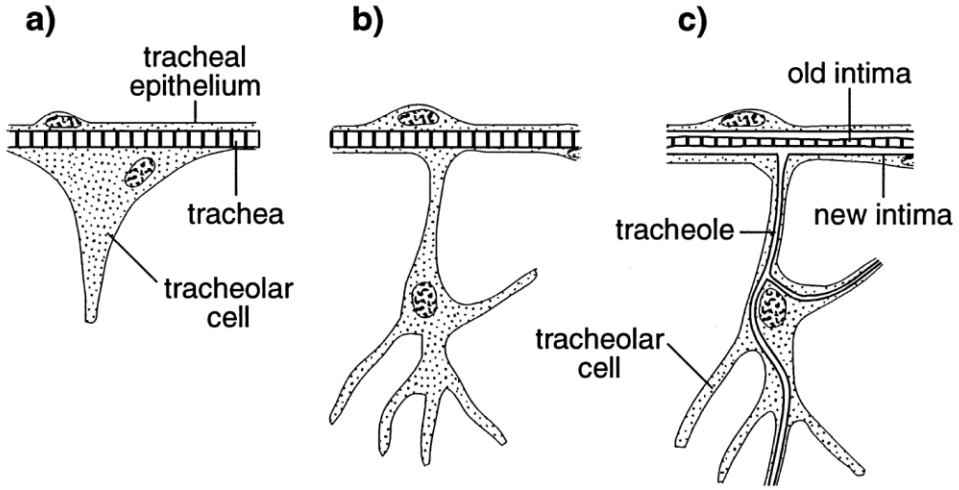

Fig. 17.2. Development of a tracheole (after Keister, 1948). **(a)** Tracheolar cell developing from the tracheal epithelium. **(b)** Tracheolar cell with extensive cytoplasmic processes. **(c)** Tracheole within tracheolar cell and becoming connected to existing trachea at a molt.

Obr. 9

Dýchací pohyby abdomenu

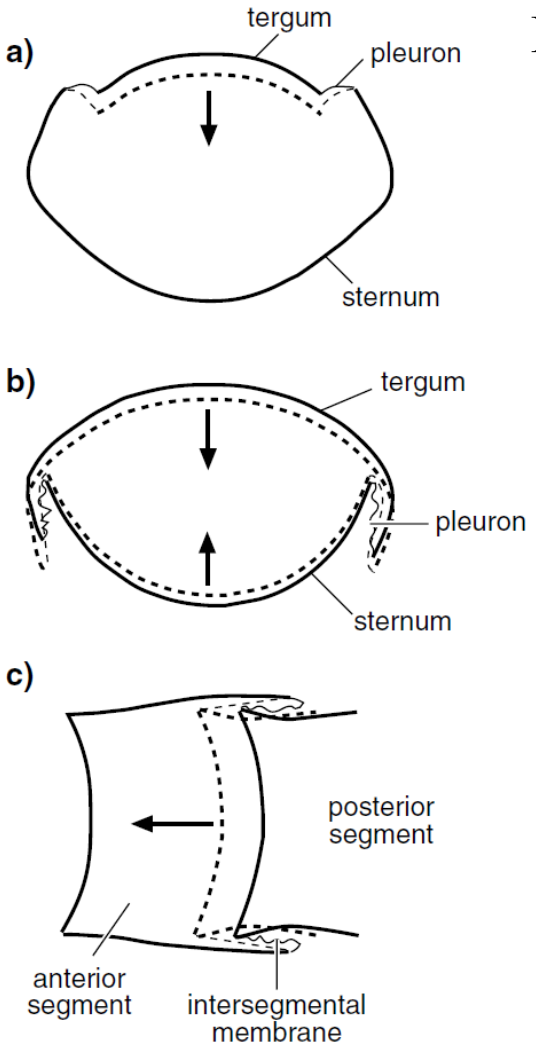

Fig. 17.14. Ventilatory movements of the abdomen. Dashed lines represent the contracted position, compressing the abdominal airsacs and causing expiration. Arrows indicate directions of movement in the compression phase (from Snodgrass, 1935). **(a)** Dorso-ventral compression involving tergal depression, transverse section. **(b)** Dorso-ventral compression involving both tergum and sternum, transverse section. **(c)** Longitudinal compression by telescoping one segment within another anterior to it, horizontal section.

Obr. 10

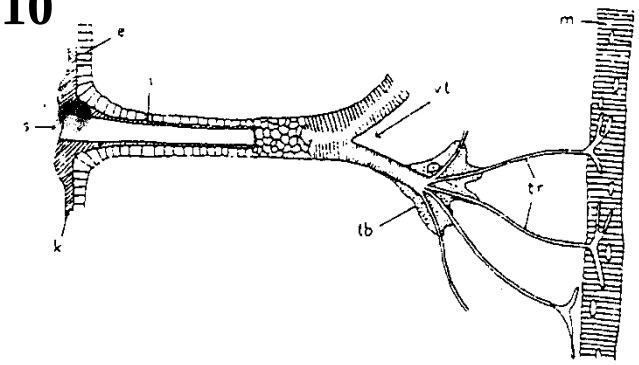

Obr.131.Schéma jednotlivých částí vzdušnice. (k - kutikula povrchu těla, s - dýchací otvor, e - epitel, i - tracheální intima, vt - větvení tracheí na stále tenčí trubice ..., tb - tracheální buňka, tr - tracheoly zásobující orgány kyslíkem, m - sval).

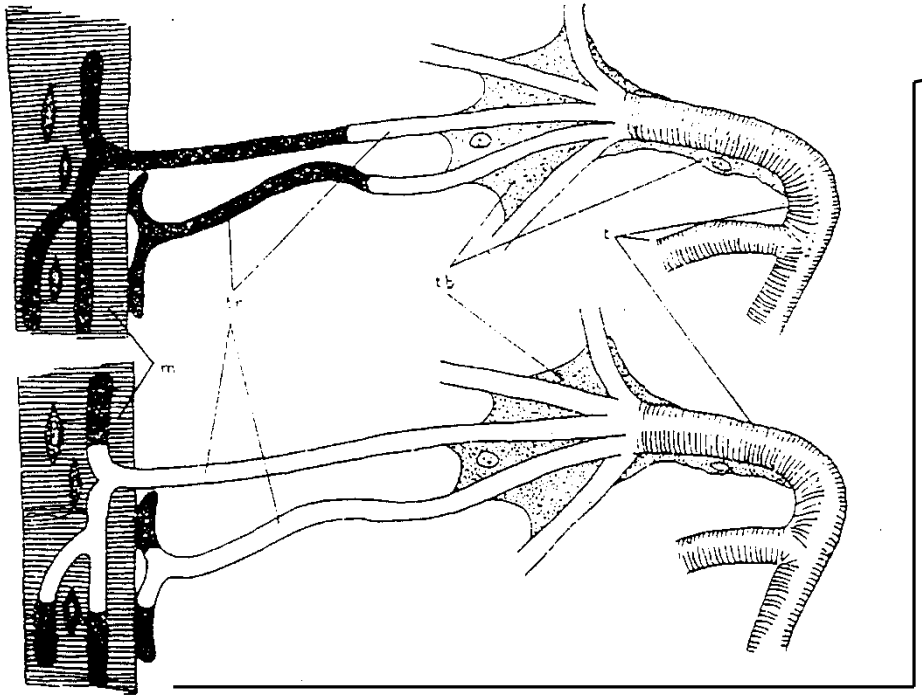

Obr.132.Schéma vysvětlující přívod kyslíku do svalu. (t - trachea, tb- tracheální buňka, tr - tracheoly; bíle: partie obsahující vzduch, černě: konečné partie tracheol obsahující serosní tekutinu a spojené přímo se svalem, m - sval). - Nahoře: Stav klidu. Vzduch je vysoko stoupající tekutinou daleko odloučen od svalu. - Dole: Sval v činnosti. Unavující se sval vtahuje do sebe tekutinu z konců tracheol a tato je absorbována svalem do té míry, že vzduch se dostává přímo do styku s unaveným svalem, který nyní potřebuje oxidaci a je svalem přímo osmoticky odebírán z konečků tracheol.

Tracheoly a výměna plynů v tkáních

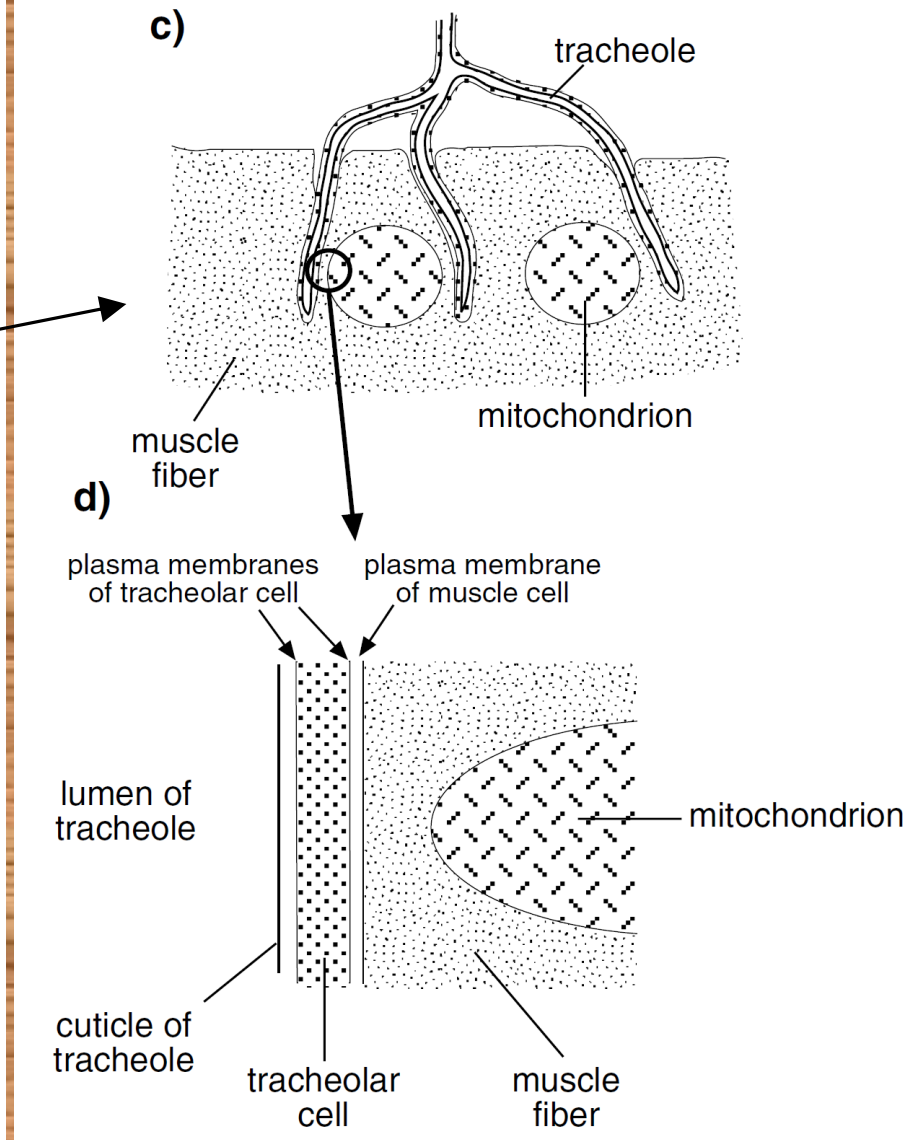

Obr. 11 Záznam periodické výměny dýchacích plynů

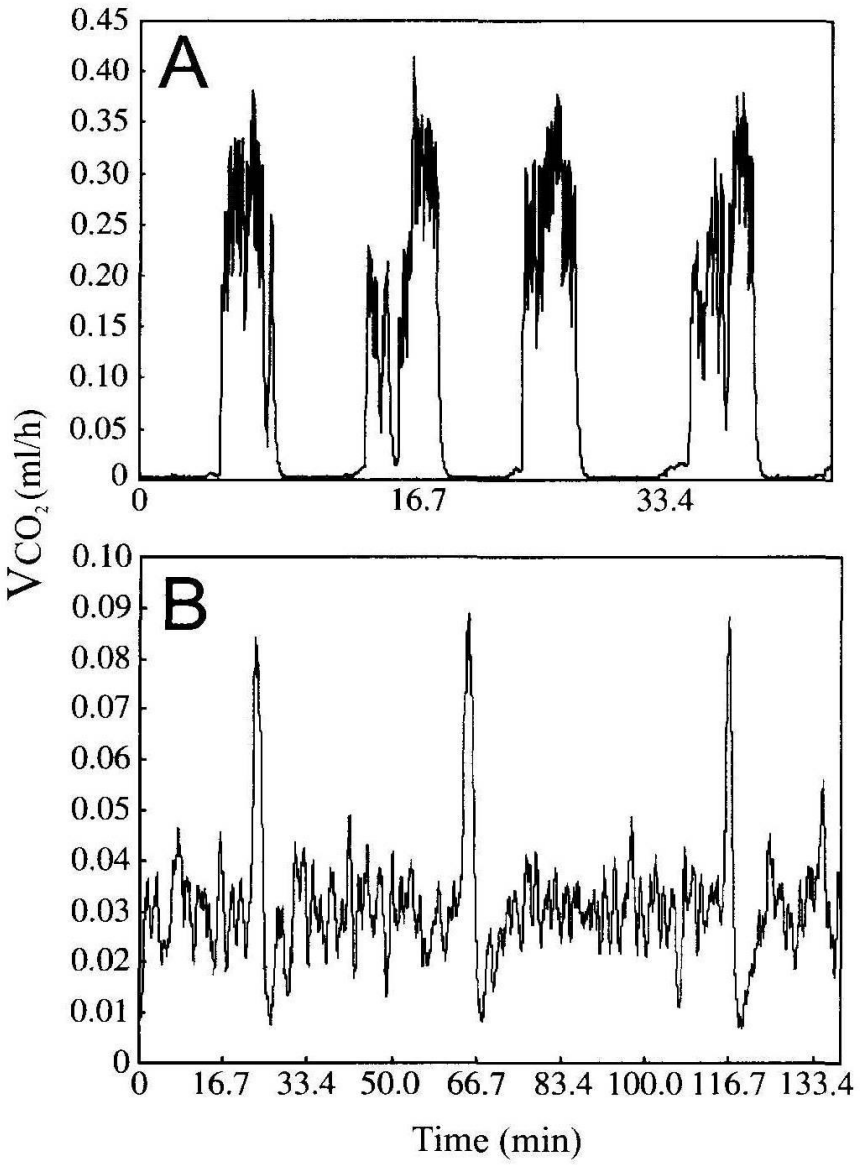

FIGURE 9.16. A. Discontinuous respiration from a cockroach. B. Cyclical respiration from a dragonfly. From Marais et al. (2005). Reprinted with permission.

Obr. 12 Záznam periodického otvírání a zavírání spirakula a dýchacích pohybů

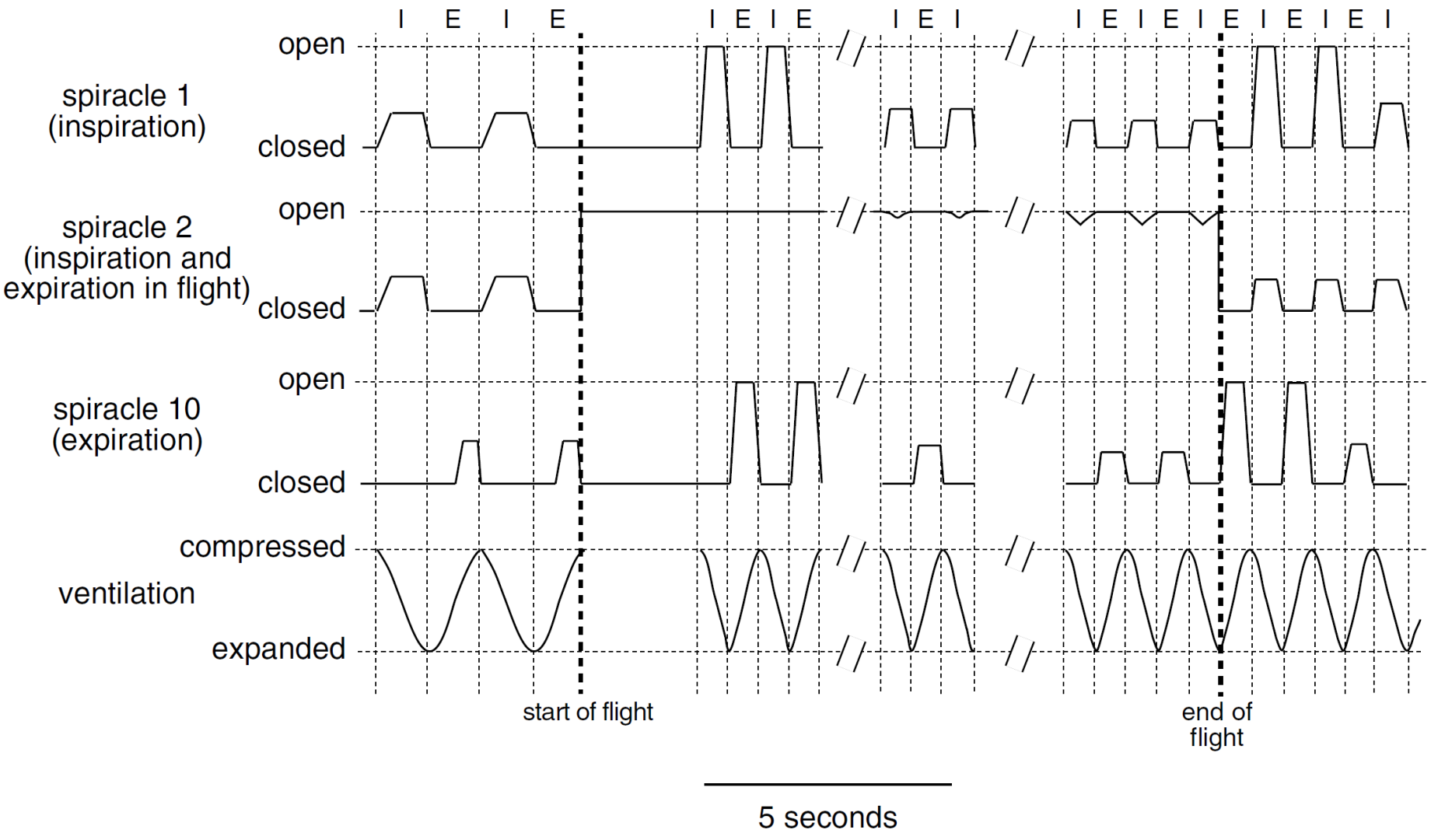

Obr. 13 Nervová kontrola dýchání

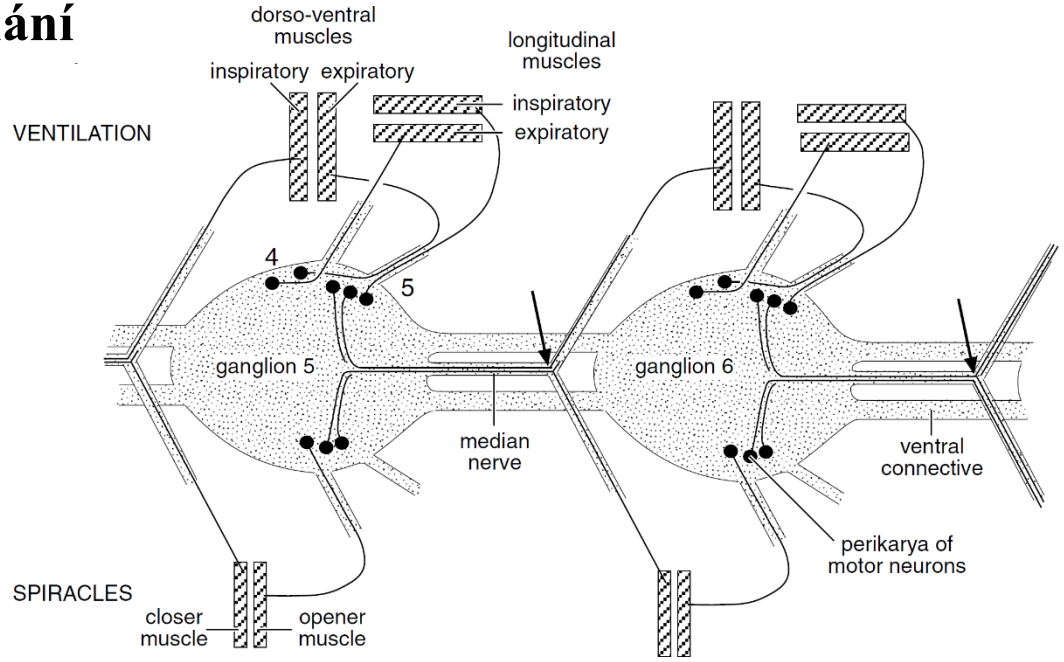

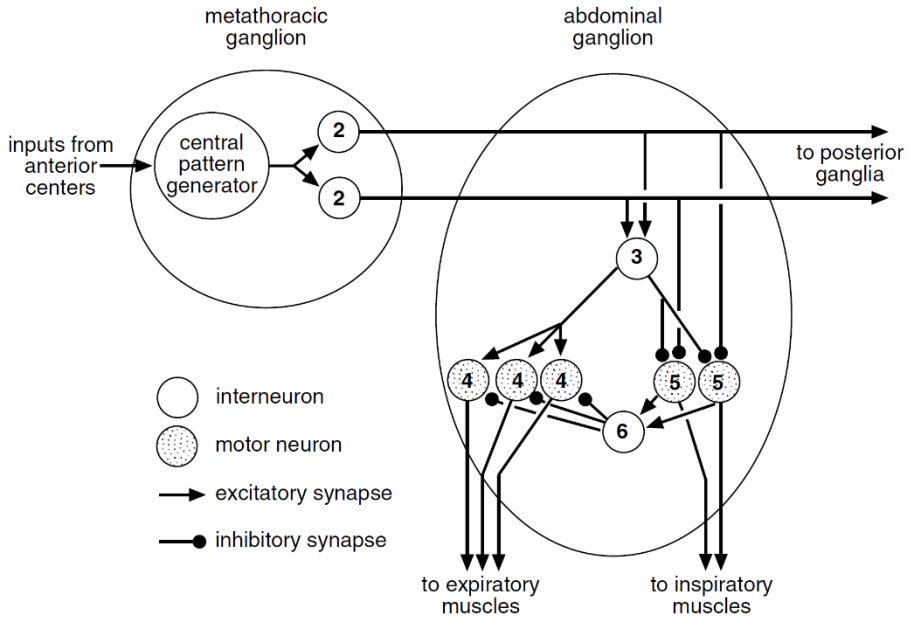

Dýchání:
http://www.youtube.com/watch?v=quwhcgkVO3c&feature=plcp

https://www.youtube.com/watch?v=S5xwtddjq9o

Obr. 14 **Základní kroky energetického metabolismu**

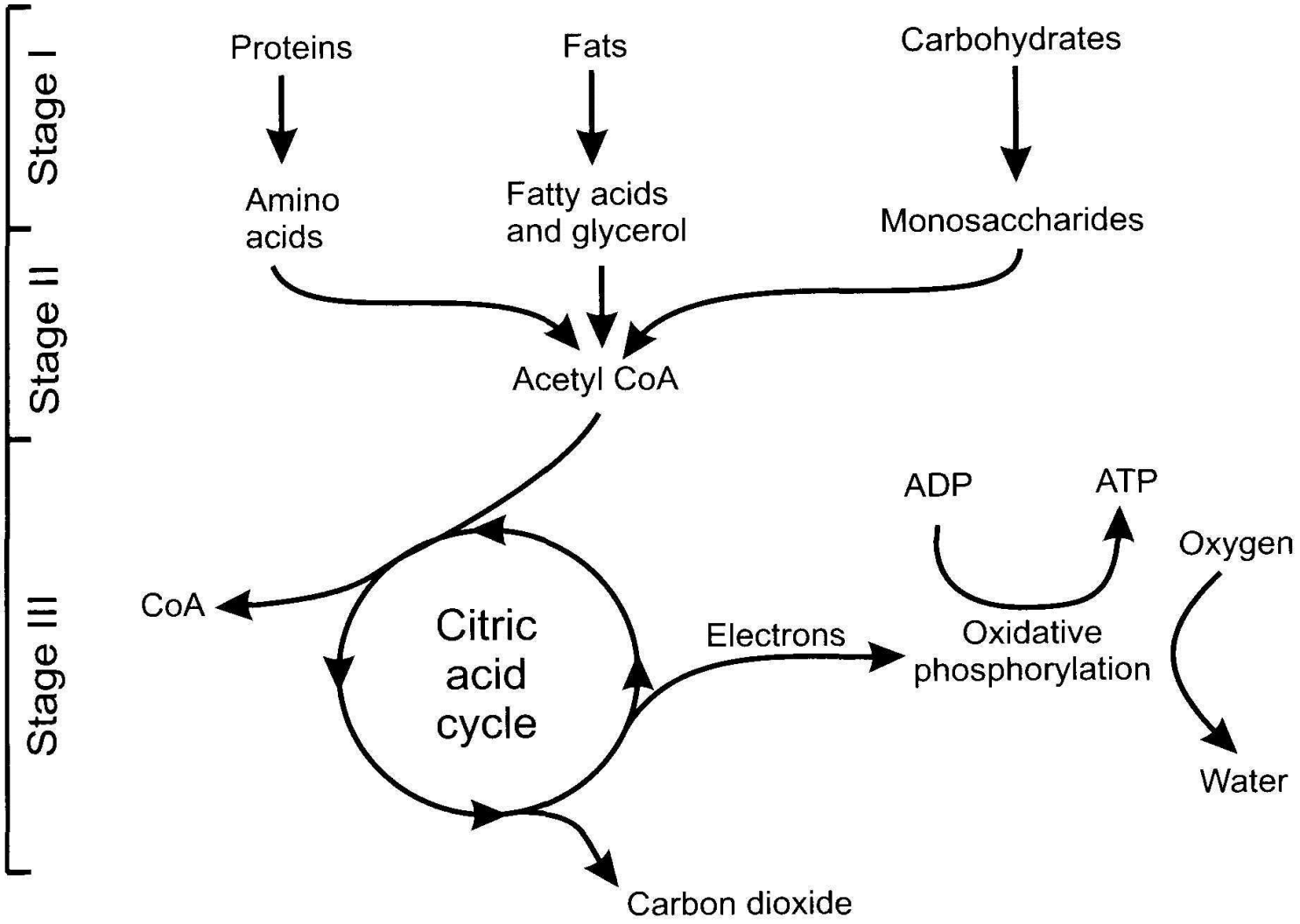

FIGURE 6.19. Stages in the oxidation of food. In stage I, proteins, fats, and carbohydrates are broken down into their constituents. In stage II, these building blocks are reduced to two carbon molecules for entry in the citric acid cycle. In stage III, the two carbon molecules enter the citric acid cycle, with carbon dioxide and water produced along with the bulk of the energy transfer to ATP.

Obr. 15 Citrátový cyklus a cytochromový systém v mitochondriích

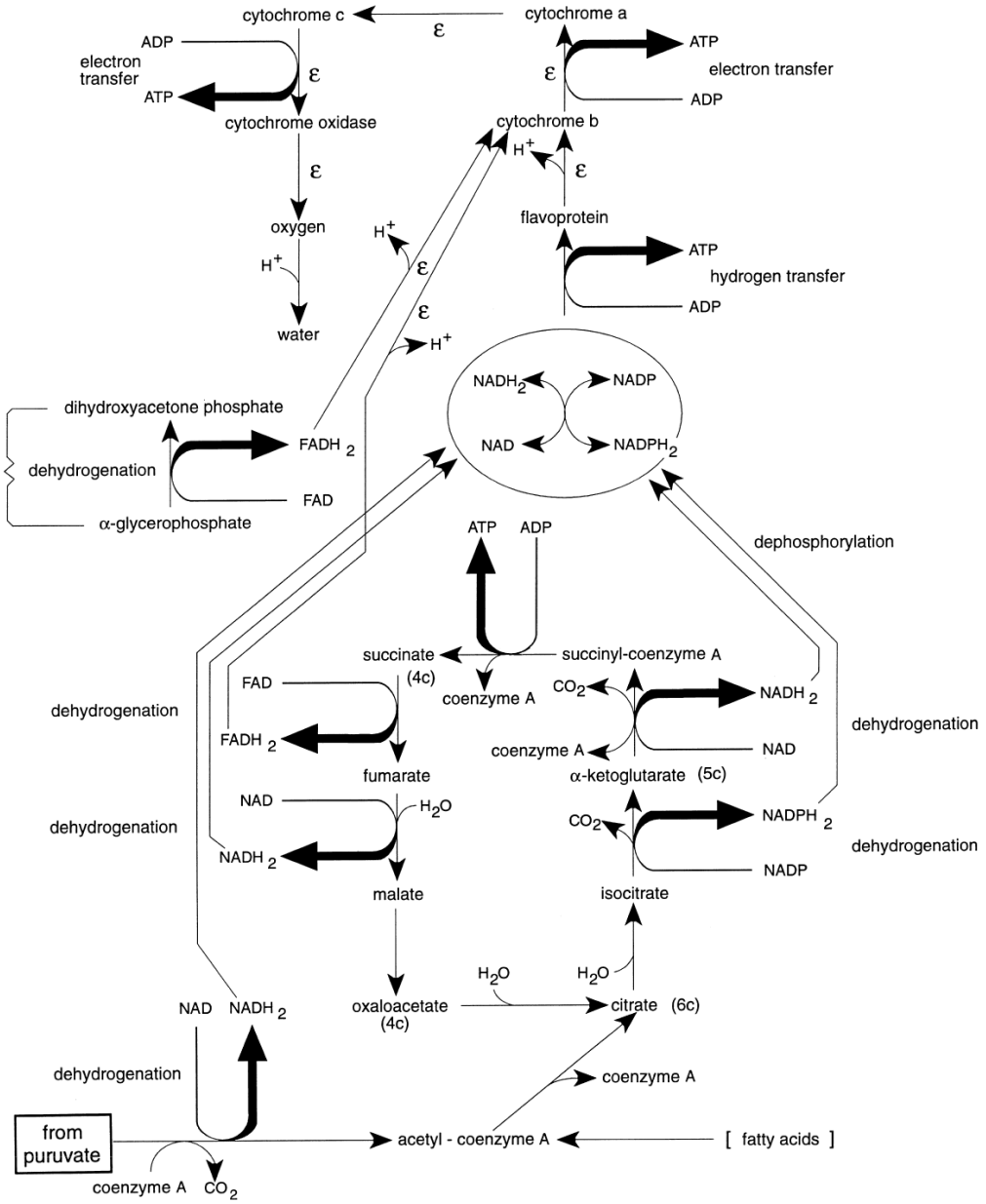

Fig. 9.39. The citric acid cycle and terminal oxidation in the mitochondria. Notice how the glycerol phosphate shuttle, which channels virtually all carbohydrate metabolism via pyruvate (see Fig. 9.40), results in the greatest production of ATP. Bold, curved arrows show energy conserving steps. Fatty acids are introduced into the citric acid cycle via acetyl-coenzyme A.

Obr. 16 **Detail reakce označené na předchozím obrázku (Obr. 46) - !: redukce dihydroxyacetonfosfátu na glycerol-3-fosfát (= α-glycerofosfát) za katalytického působení glycerofosfátdehydrogenázou (tento enzym je ve schématu označen - *). Při reakci dochází k regeneraci pyridinnukleotidu: NADH2 → NAD**

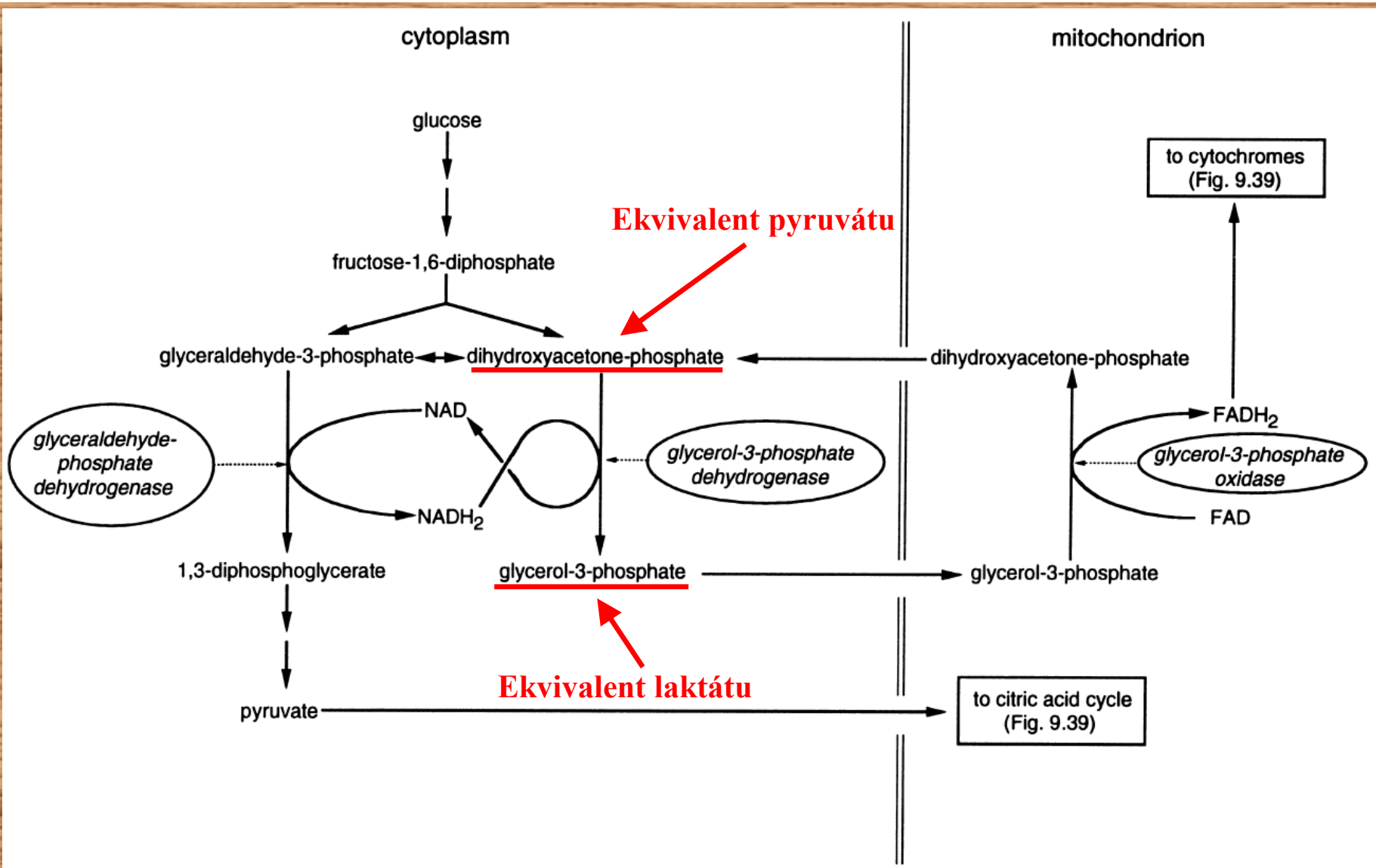

Fig. 9.40. The glycerol phosphate shuttle. Enzymes referred to in table 9.2 are shown in italics. The points at which they are active are indicated by broken arrows.

Obr. 17 Tracheální žábry

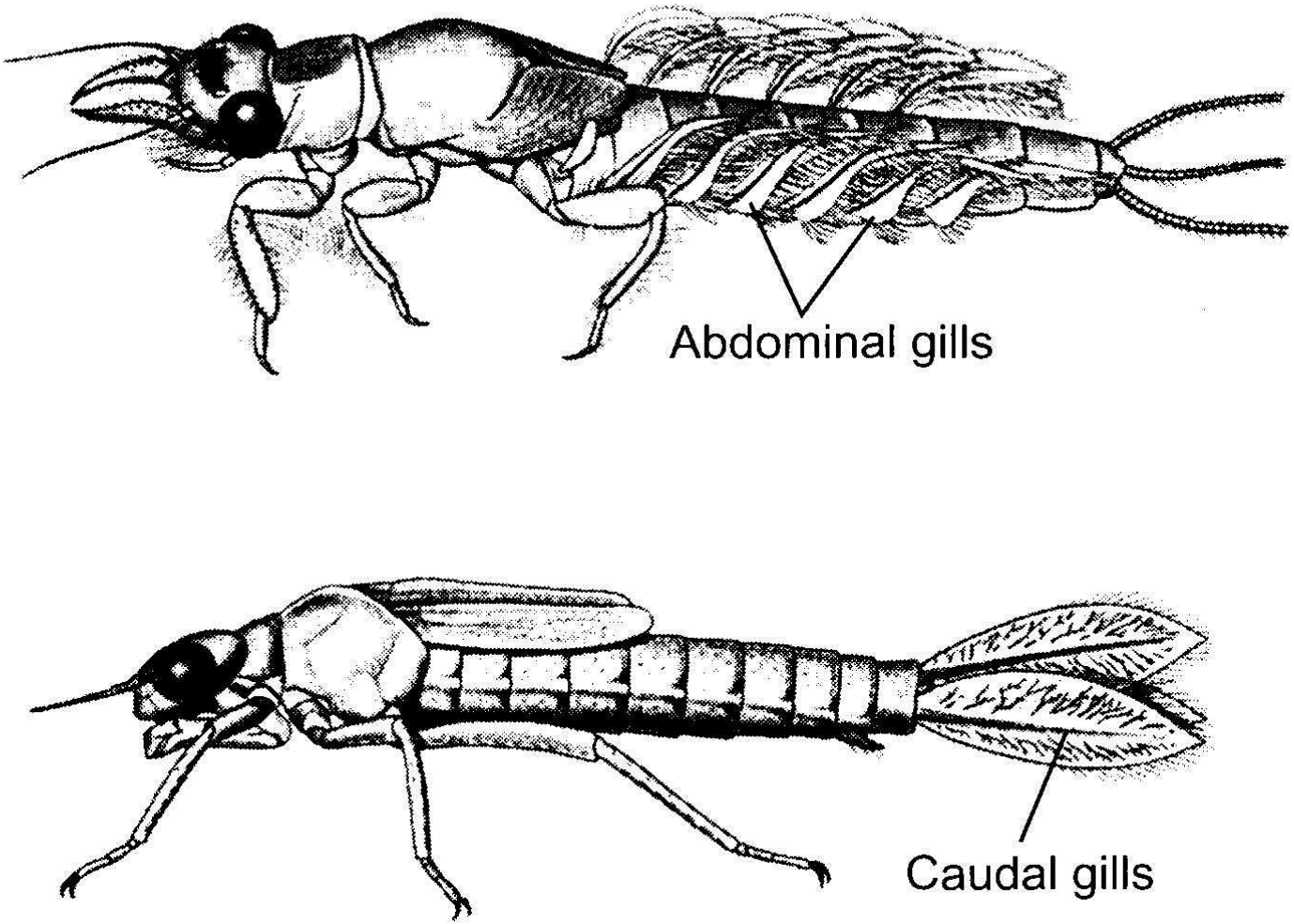

FIGURE 9.18. Abdominal gills of the mayfly. From McCafferty (1981). Reprinted with permission.

Obr. 18 Střevní tracheální žábry

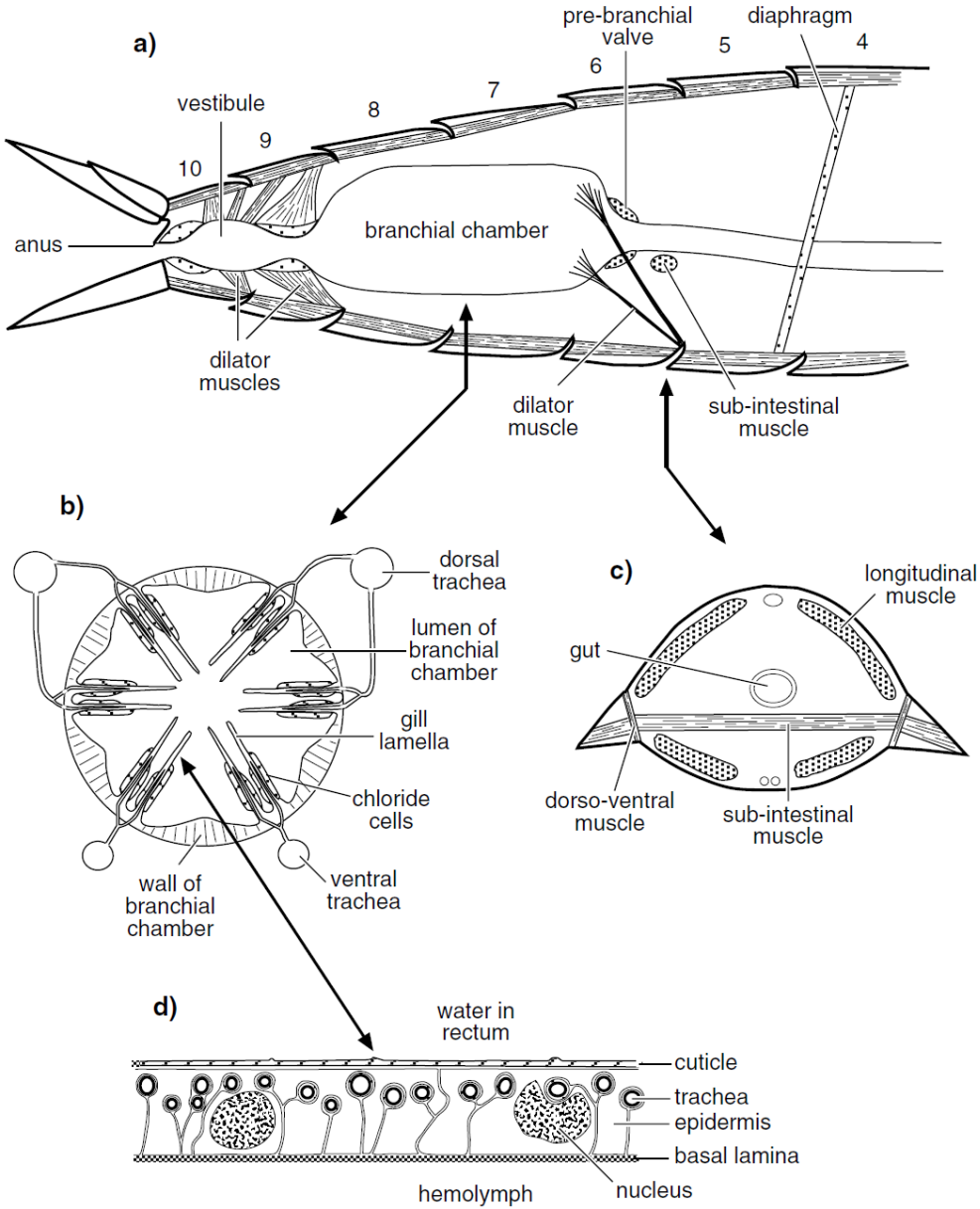

Fig. 17.29. Tracheal gills in the rectum of a dragonfly larva (after Mill & Pickard, 1972; Tillyard, 1917). **(a)** Longitudinal section through the abdomen. Numbers indicate abdominal segments. **(b)** Transverse section through the branchial chamber **(c)** Transverse section through abdominal segment 6 showing the subintestinal muscle. **(d)** Detail of gill epithelium showing the tracheae close beneath the cuticle (after Schmitz & Komnich, 1976).

Obr. 19 Hmyzí hemoglobinové buňky

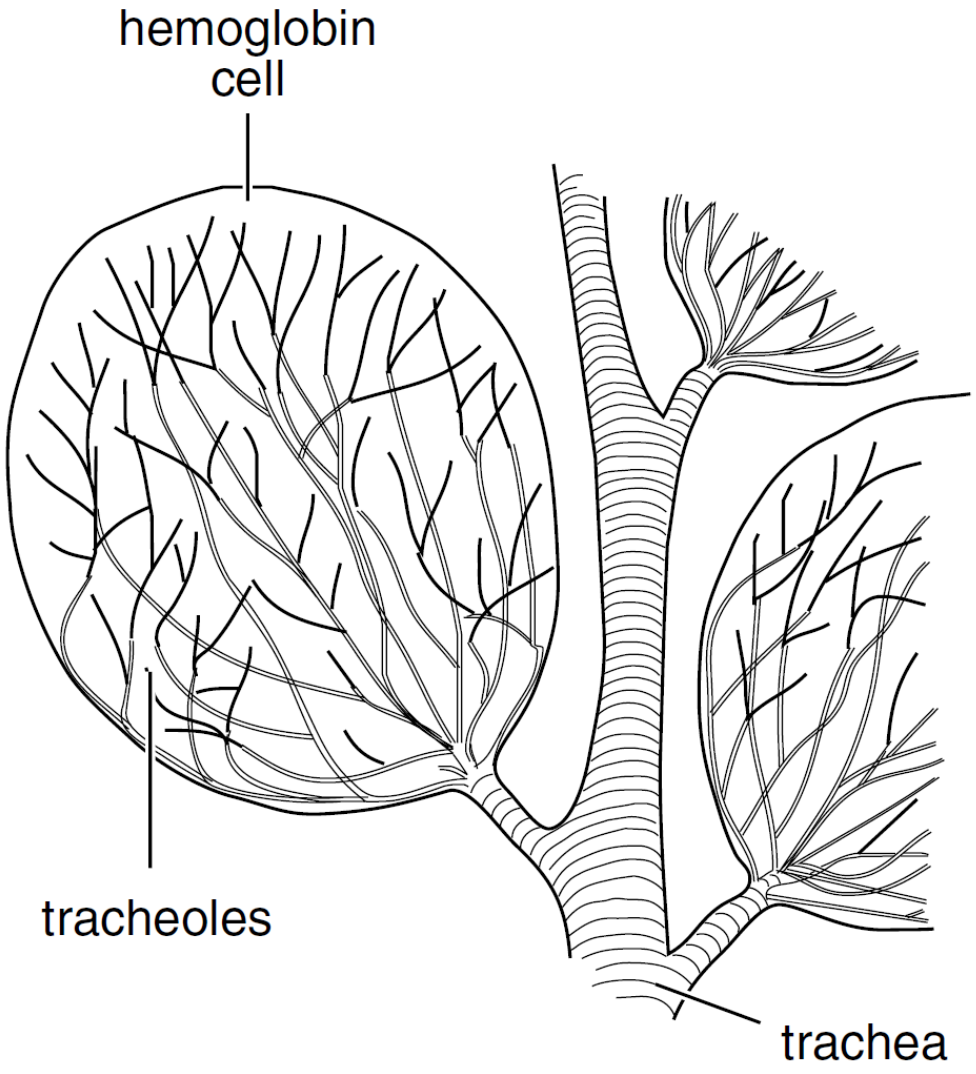

Fig. 17.36. Hemoglobin occurs in hemoglobin cells of the larva of the bot fly, *Gasterophilus* (after Keilin, 1944).

Obr. 20 Stavba a funkce dýchací bubliny u vodního hmyzu

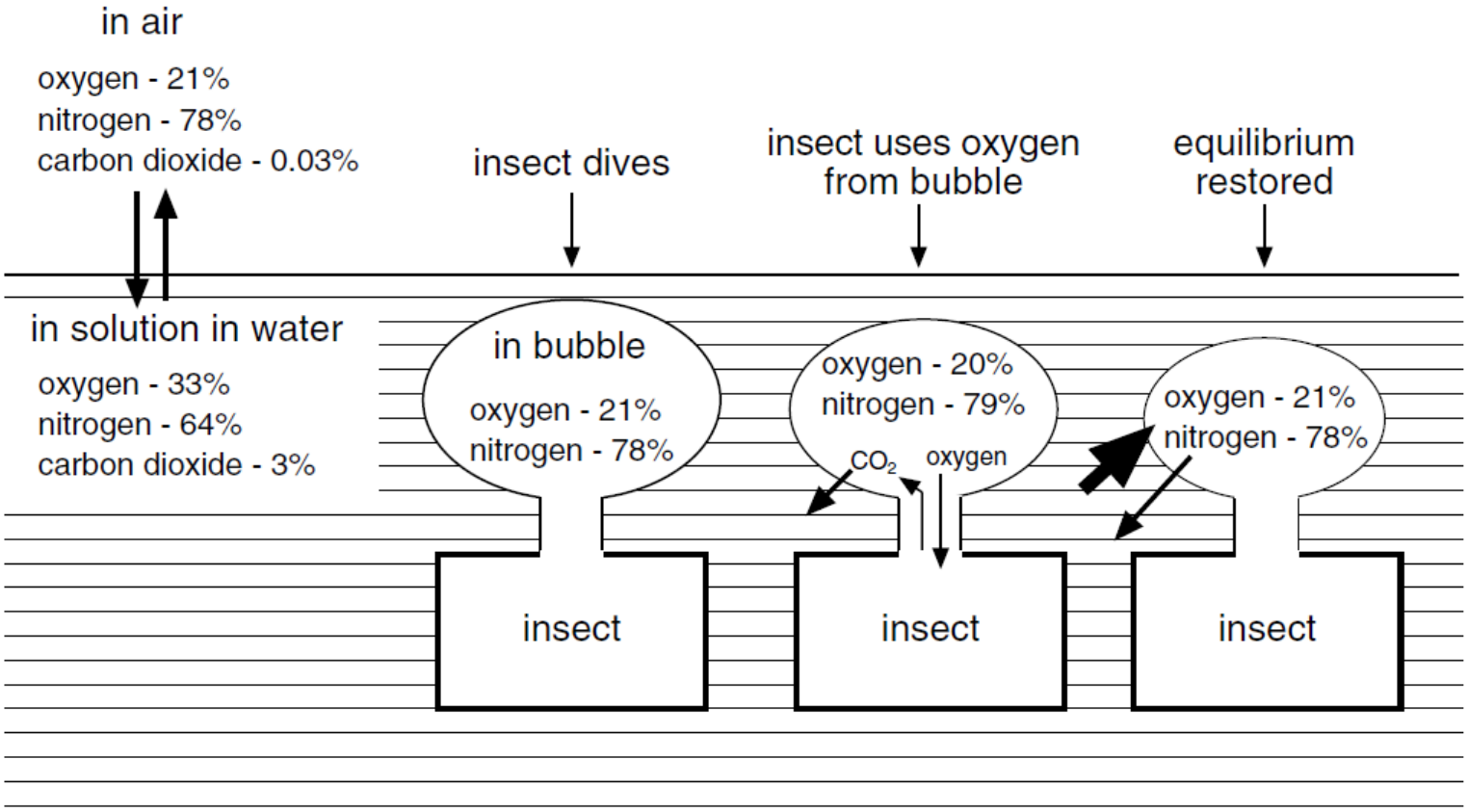

Fig. 17.26. Diagram of an air bubble acting as a physical gill. As the insect dives, the gases in the bubble are in equilibrium with those dissolved in the water. As the insect uses oxygen, the equilibrium is perturbed. It is restored by the inward movement of oxygen and the outward movement of nitrogen. This is a continuous process; it is shown as two separate steps for clarity. Note that carbon dioxide produced by the insect is immediately dissolved in the water. Oxygen comes out of solution faster than nitrogen goes in. The bubble shrinks continuously as nitrogen goes into solution.

http://ww2.kqed.org/science/wp-content/uploads/sites/35/2015/11/DL_WaterBeetles_bubble_720.gif

Obr. 21 Plastron

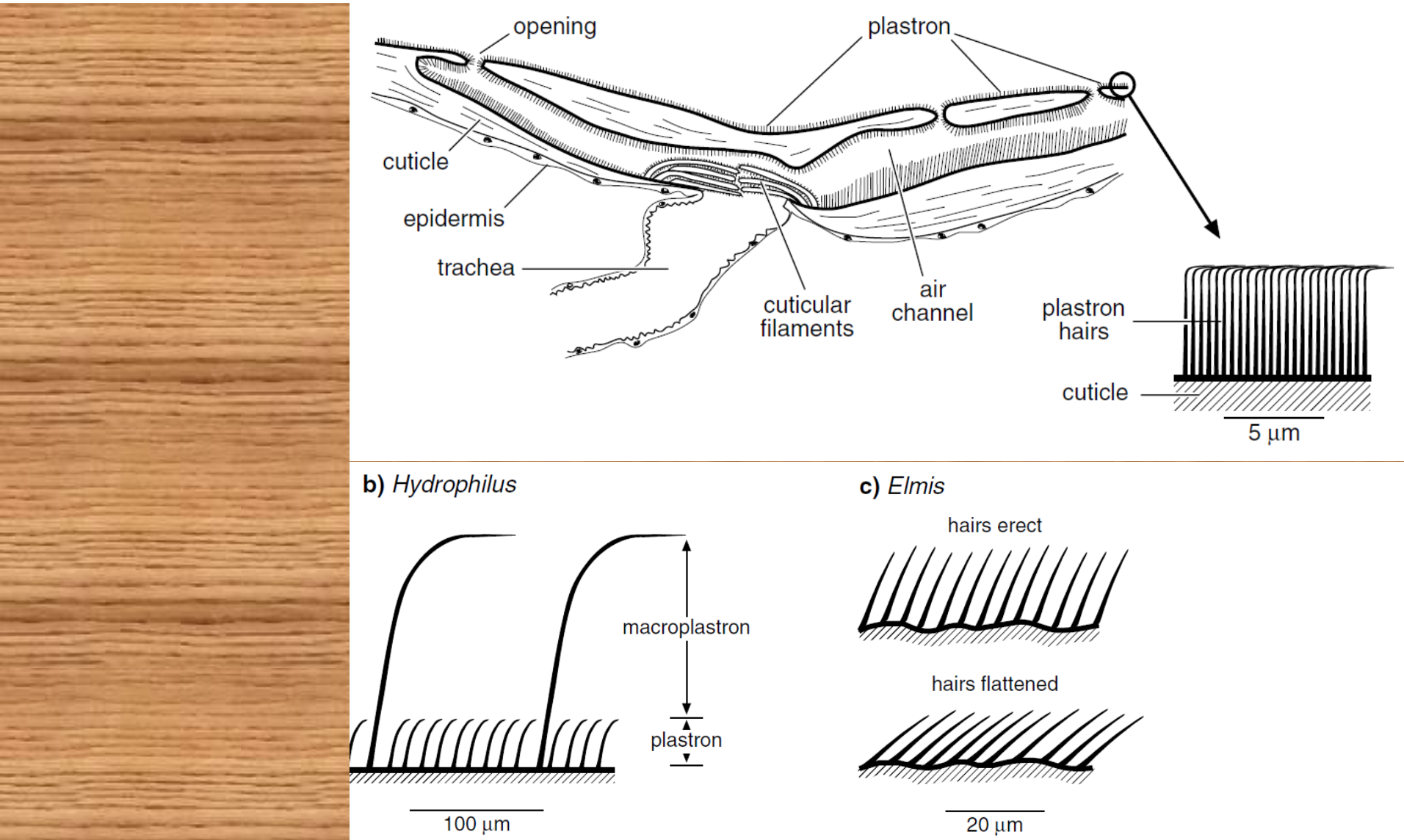

Fig. 17.31. Plastron. **(a)** Plastron of *Aphelocheirus* (Hemiptera). Section through a spiracular rosette showing the junction of a trachea with a system of channels in the cuticle connecting with the plastron. Below right, detail of the plastron (after Thorpe & Crisp, 1947a). **(b)** Macroplastron of *Hydrophilus* (Coleoptera) (after Thorpe & Crisp,1949). **(c)** Macroplastron of *Elmis* (Coleoptera) showing the hairs erect, forming a macroplastron (above) and with the hairs compressed so that only the true plastron remains (after Thorpe & Crisp, 1949).

Obr. 22 Schematické znázornění funkce hydrofobních chloupků u vodního hmyzu

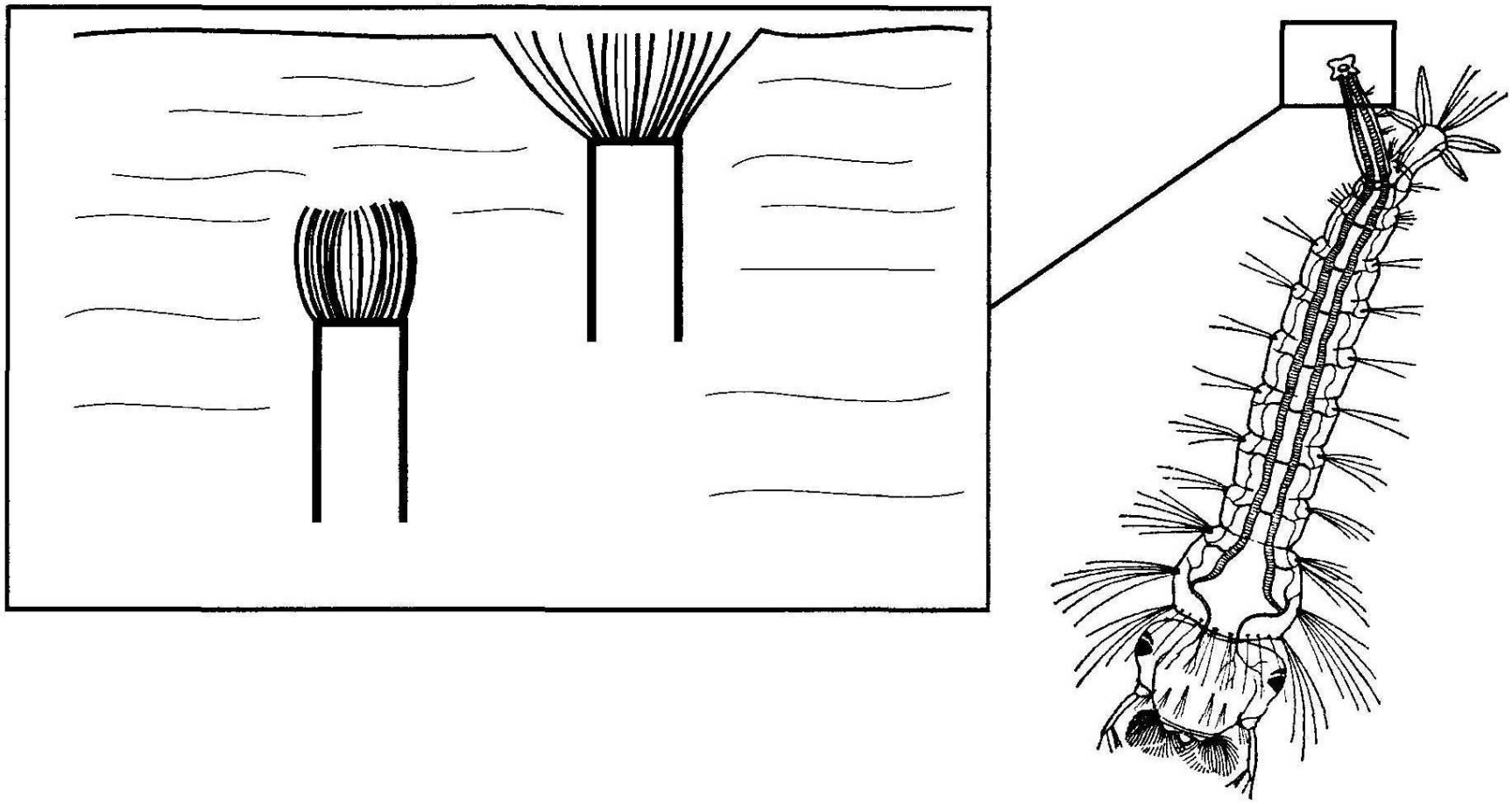

FIGURE 9.17. Hydrofuge hairs on the tip of the siphon tube of an aquatic insect. When underwater, the hairs remain over the spiracular opening and prevent water from entering. At the surface, the hairs open up and allow air to enter.

4. Osmoregulace a exkrece toxických produktů metabolismu

Obr. 1 **Odpadní produkty dusíkatého metabolismu**

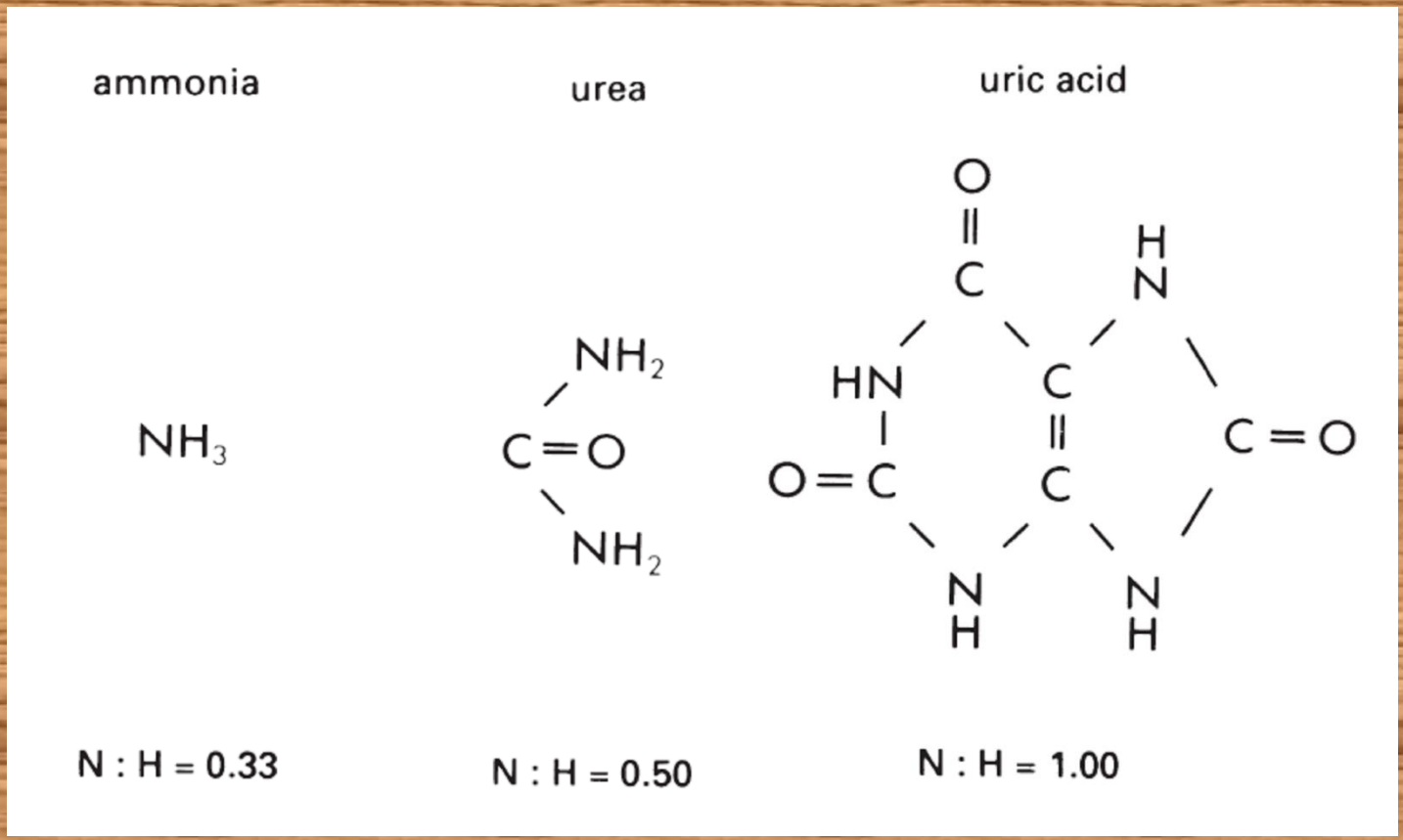

Fig. 3.19 Molecules of the three common nitrogenous excretory products. The high N : H ratio of uric acid relative to both ammonia and urea means that less water is used for uric acid synthesis (as hydrogen atoms are derived ultimately from water).

Malpighické trubice

Obr. 2

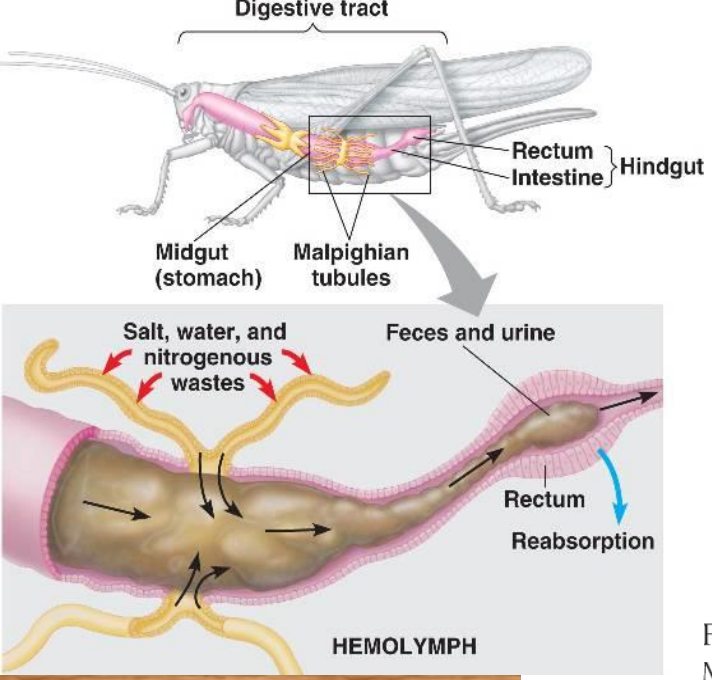

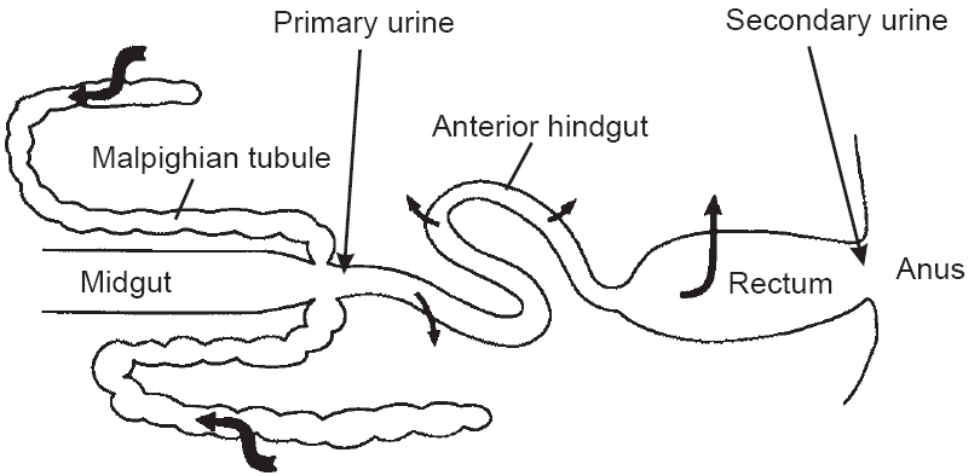

FIGURE 8.10. The formation of primary and secondary urine in the excretory system. From Maddrell (1981). Reprinted with permission.

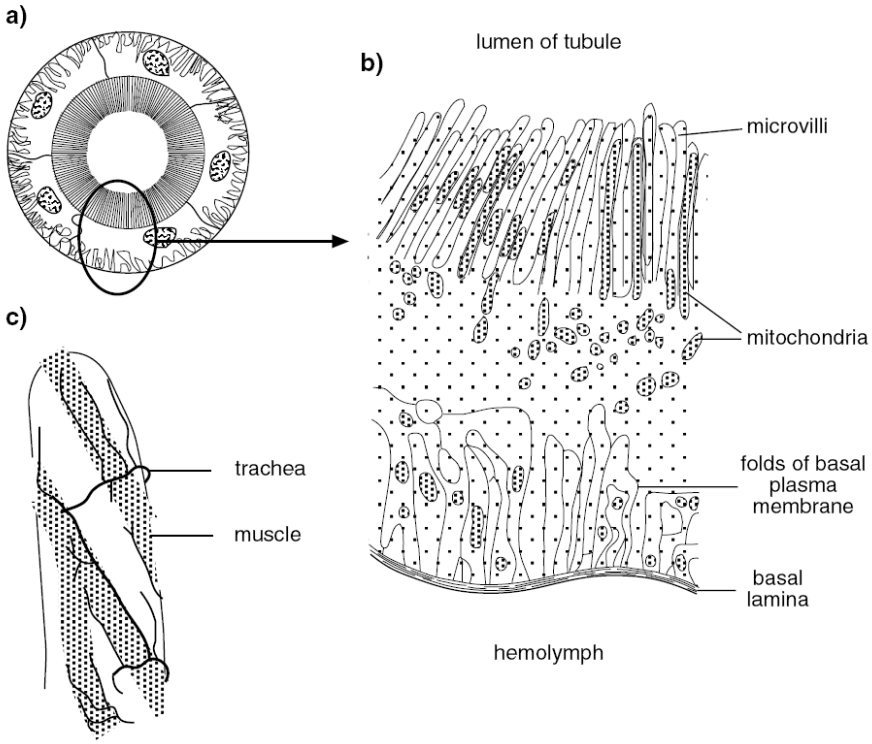

Obr. 2a Malpighické trubice

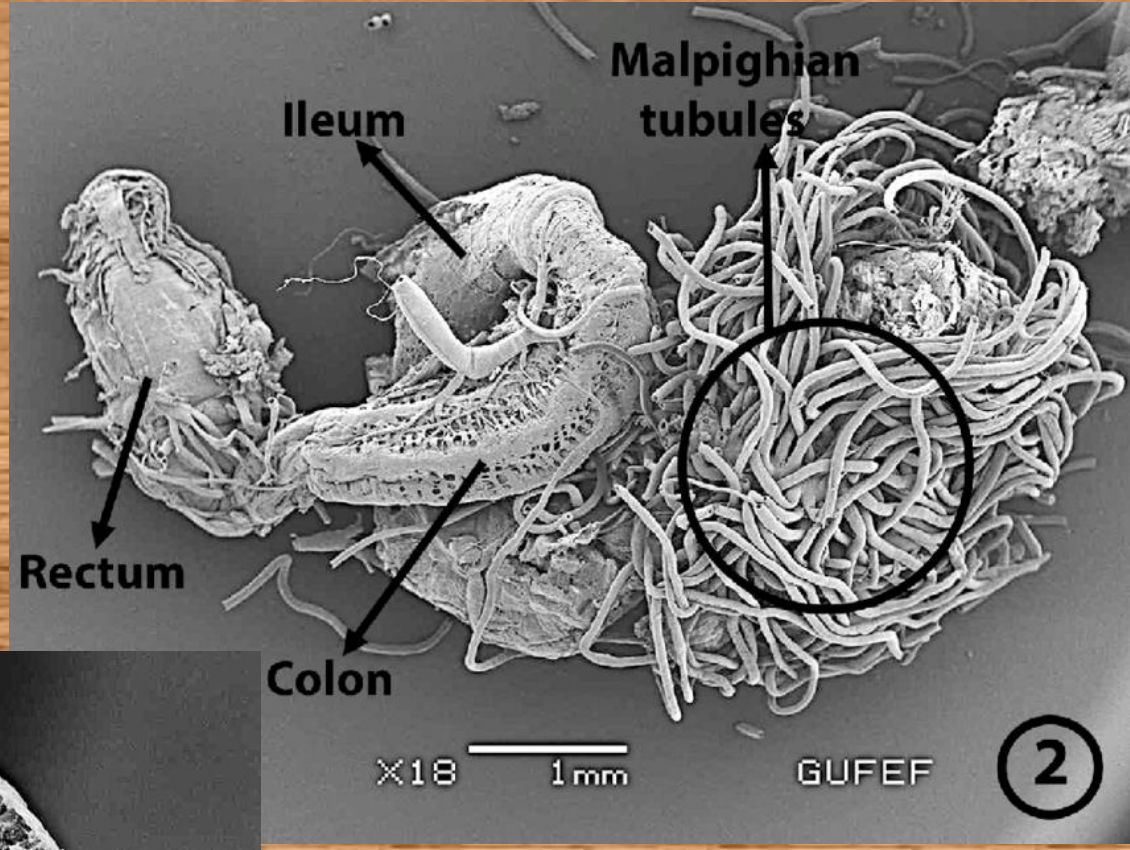

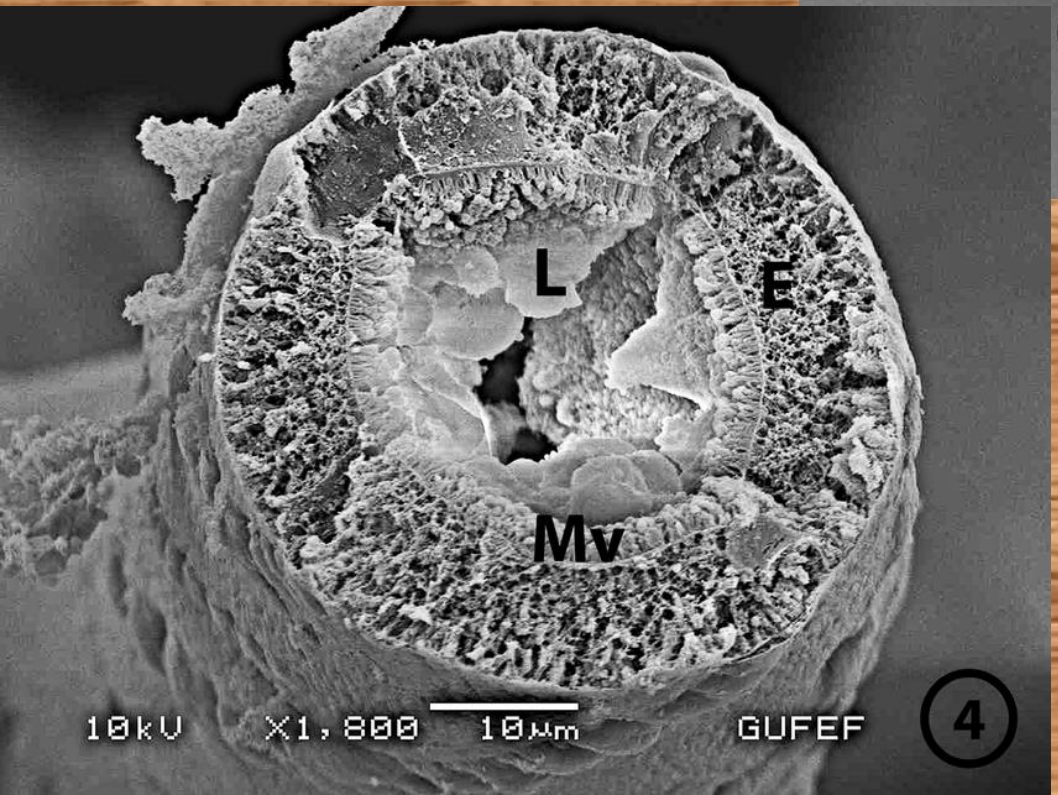

Obr. 3 Svalové vlákno na Malpighické trubici – označeno šipkou

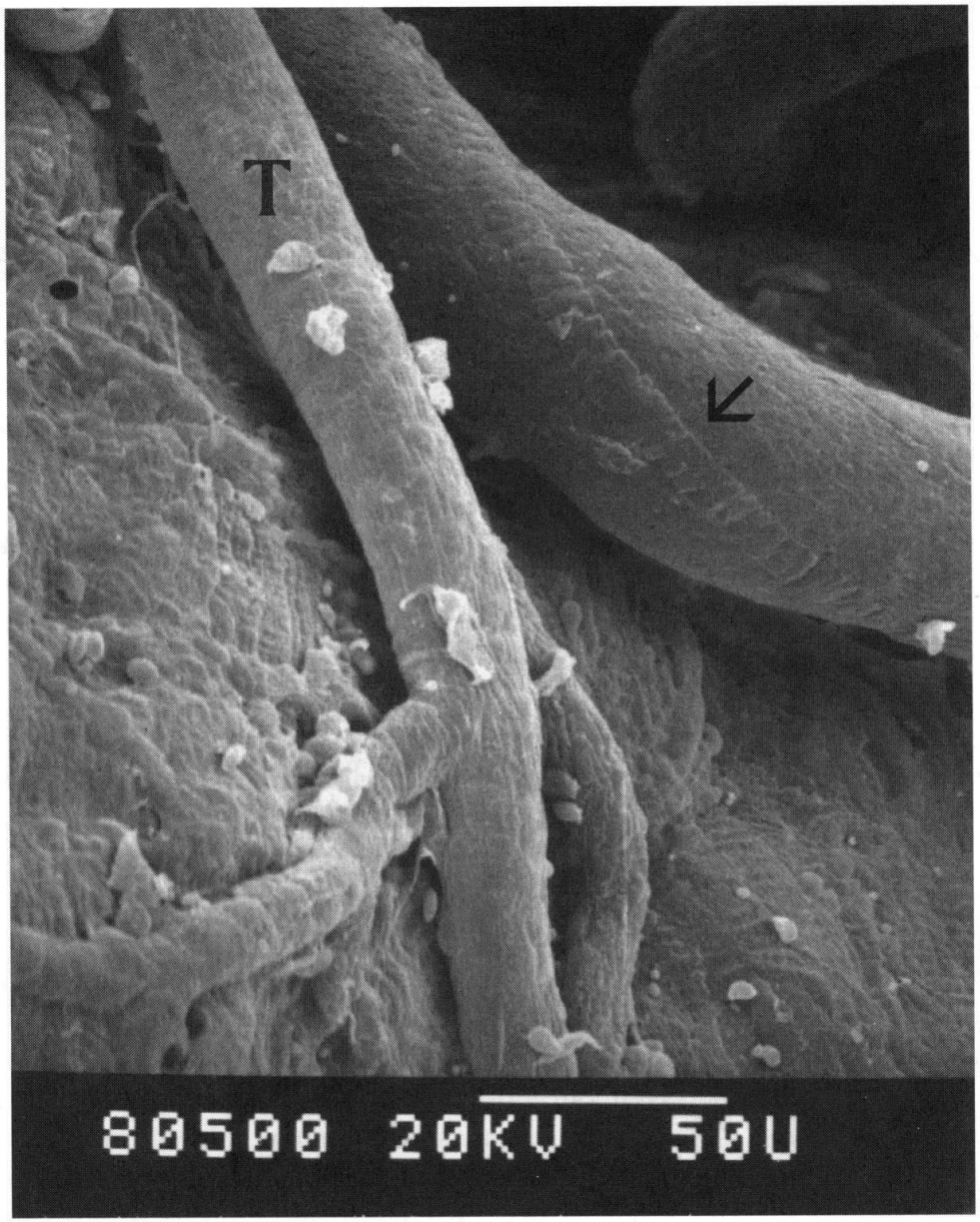

FIGURE 13.3 An SEM photo of the small muscle (arrow) that often spirals along the length of a Malpighian tubule of some insects, in this case, the cricket *Gryllus assimilis*. Contraction of the muscle throws the tubules into tight coils in some insects. The muscle probably serves to keep the tubule moving through the hemolymph. (Photograph by the author.)

Obr. 4 Schéma funkce Malpighické trubice

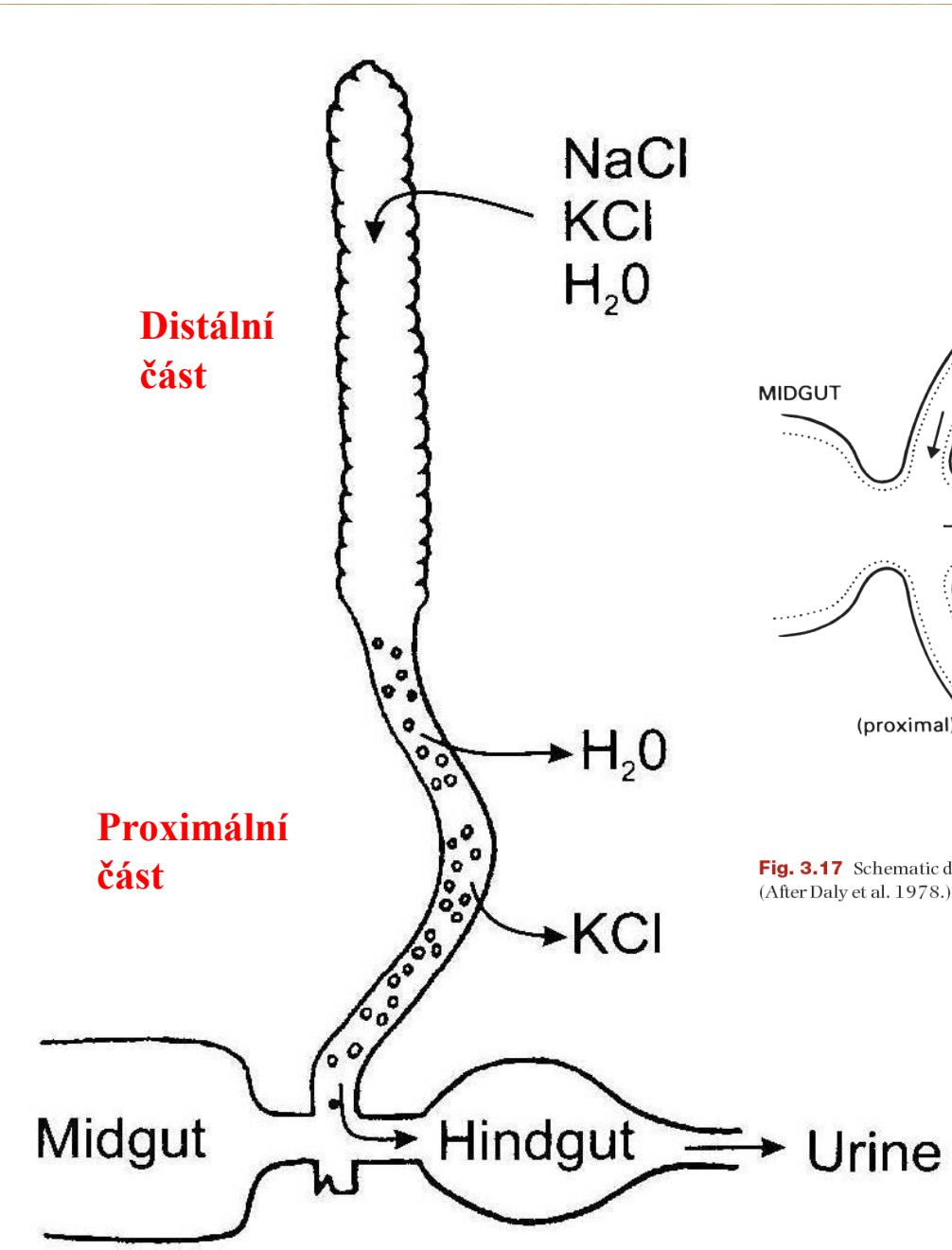

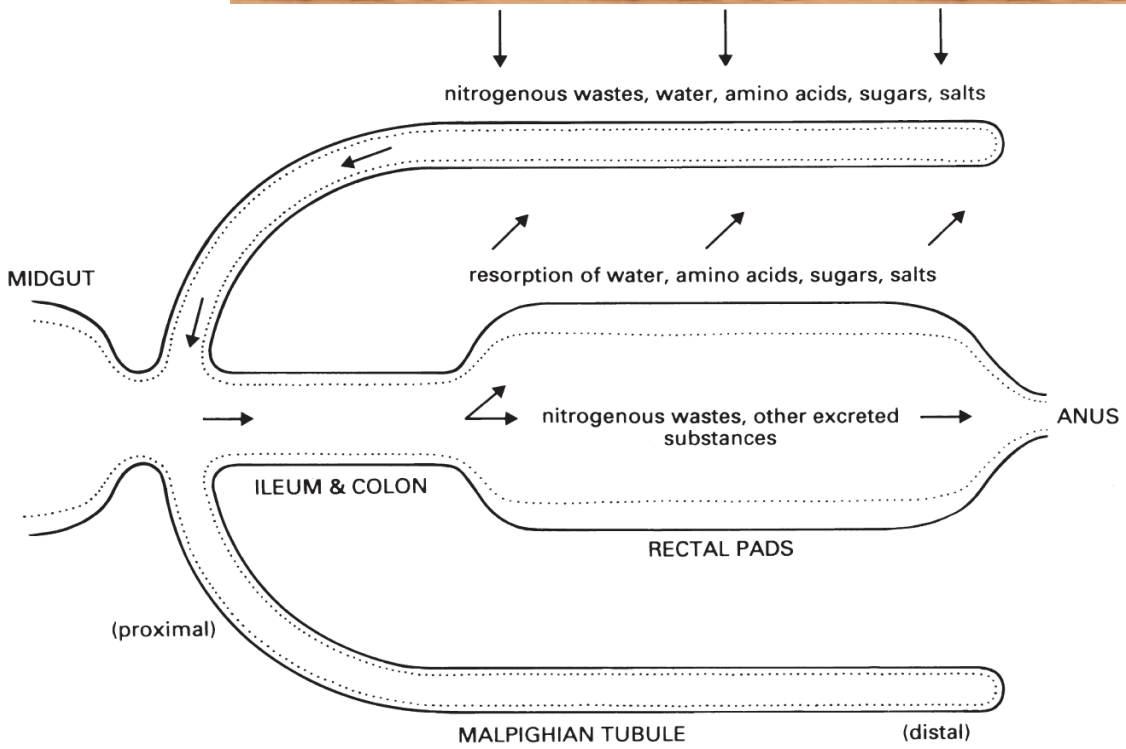

Fig. 3.17 Schematic diagram of a generalized excretory system showing the path of elimination of wastes. (After Daly et al. 1978.)

Syntéza kyseliny močové a z ní odvozených produktů

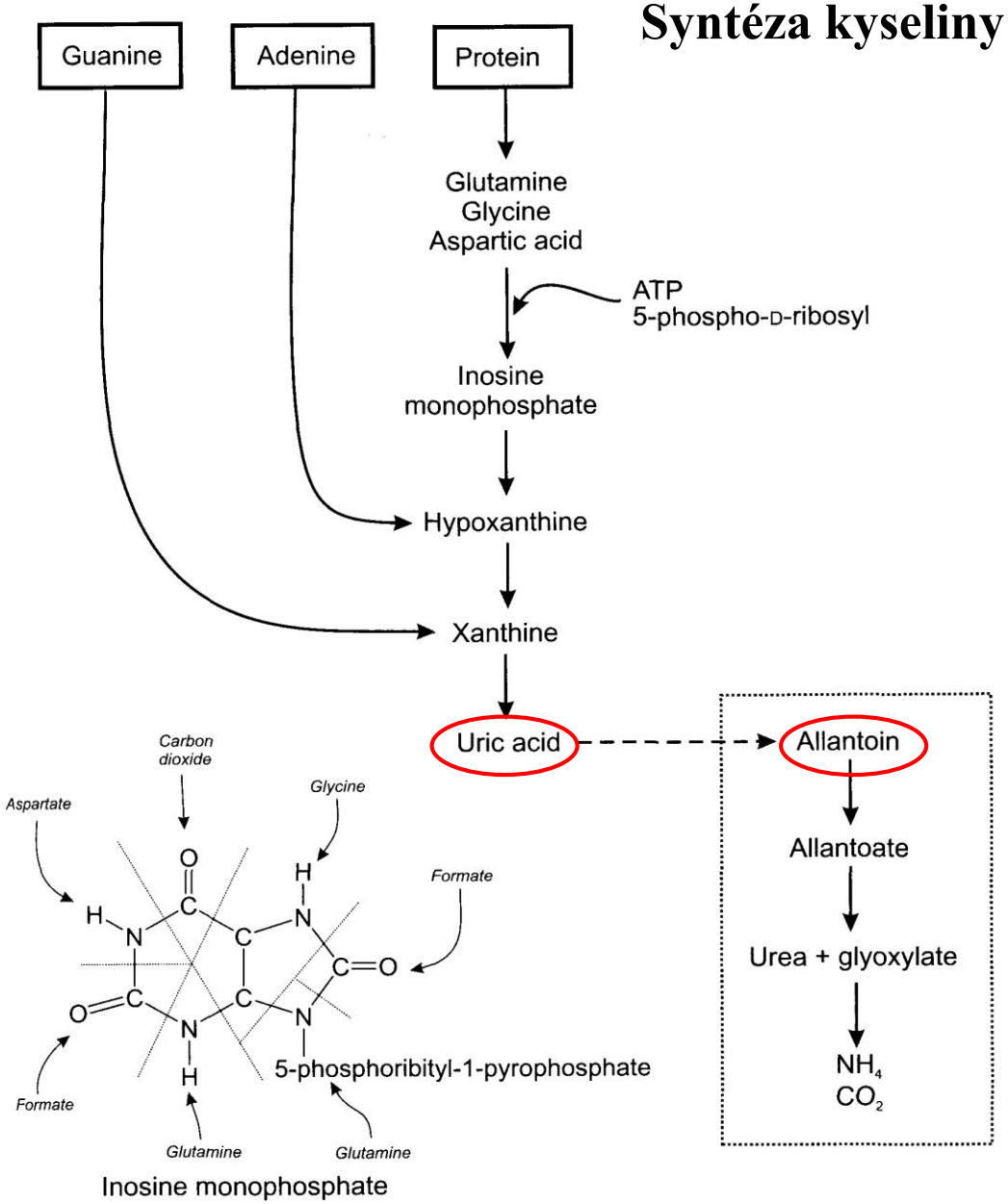

Obr. 5

Přeměna kyseliny močové na alantoin a kyselinu alantoovou

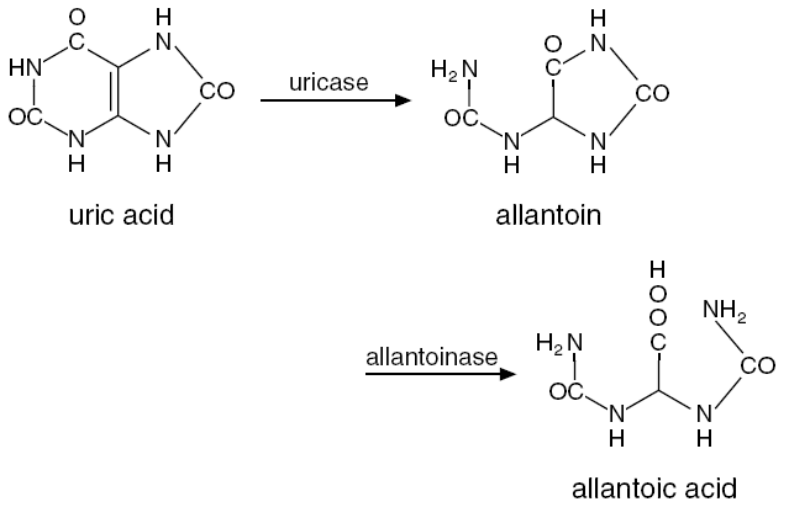

Obr. 6 **Schéma produkce primární moči**

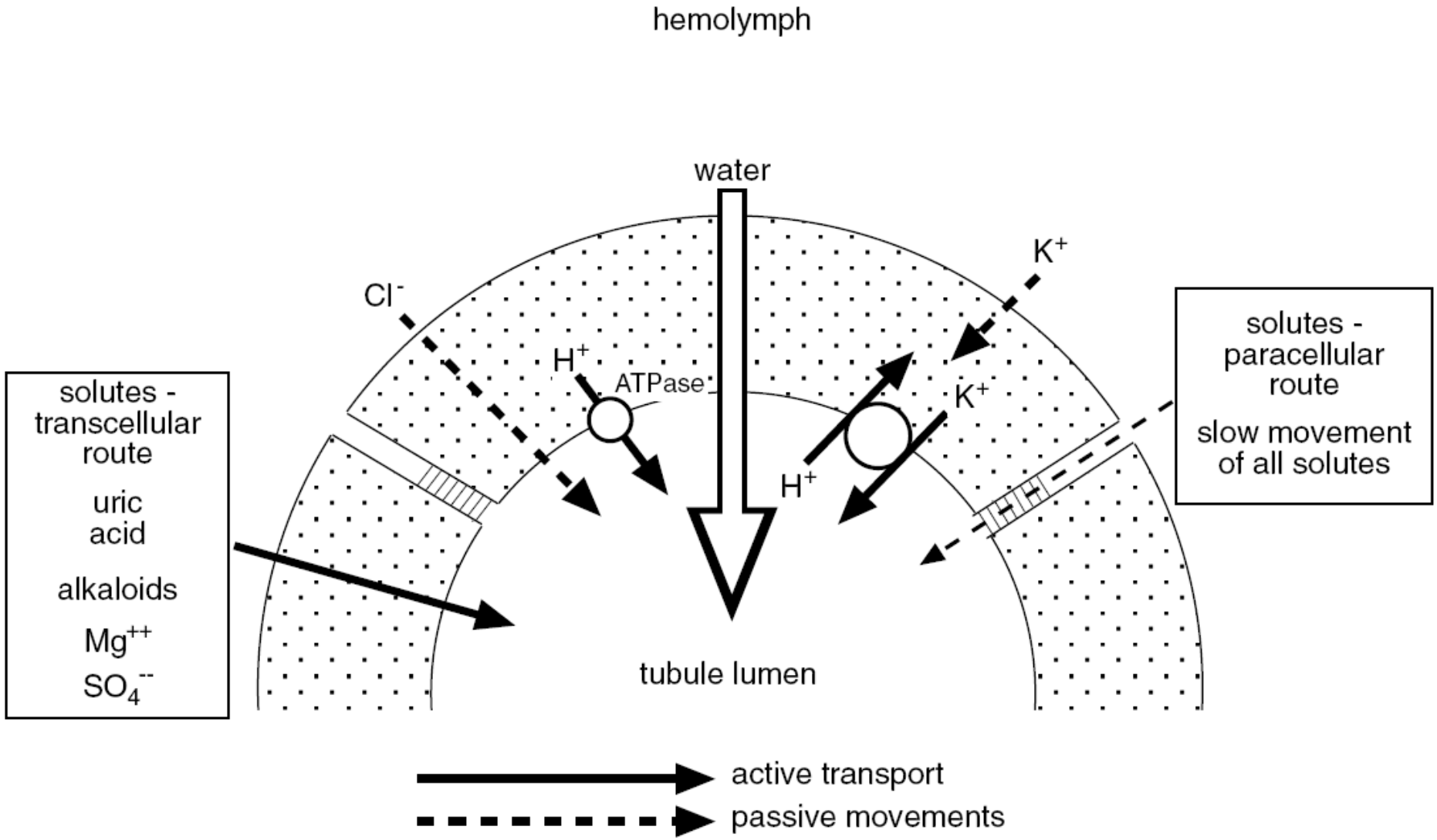

Obr. 7 Umístění a struktura chloridových buněk, analní papily

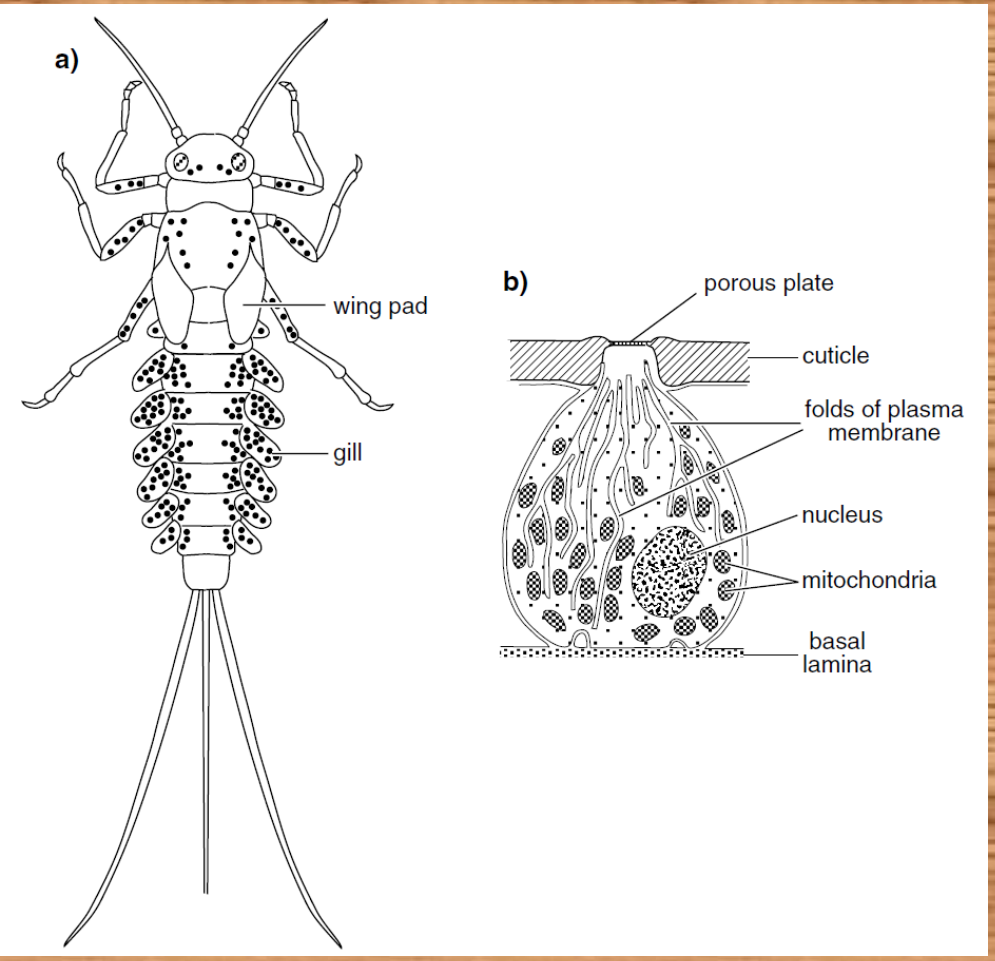

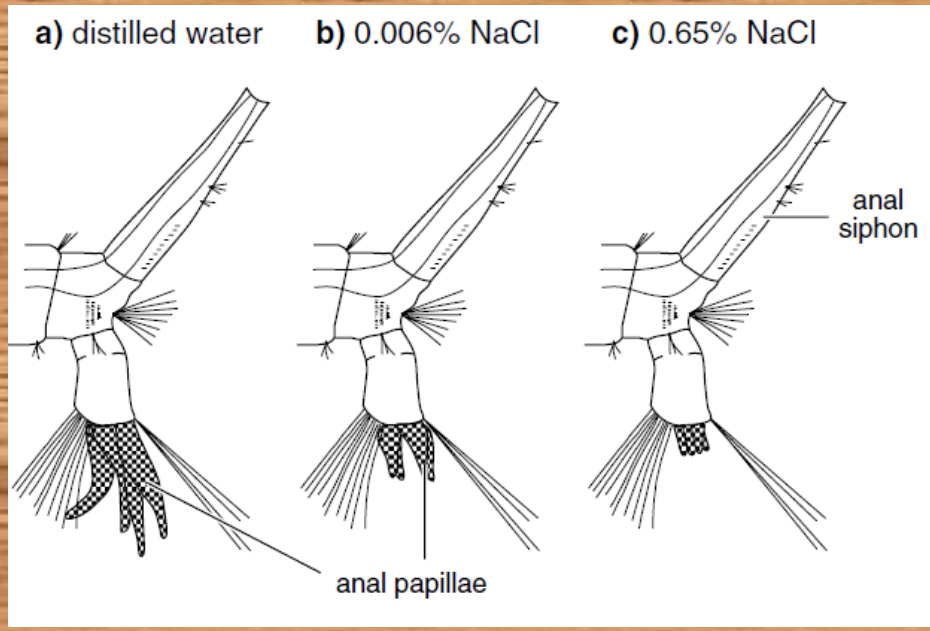

Obr. 8

Kryptonefrický systém

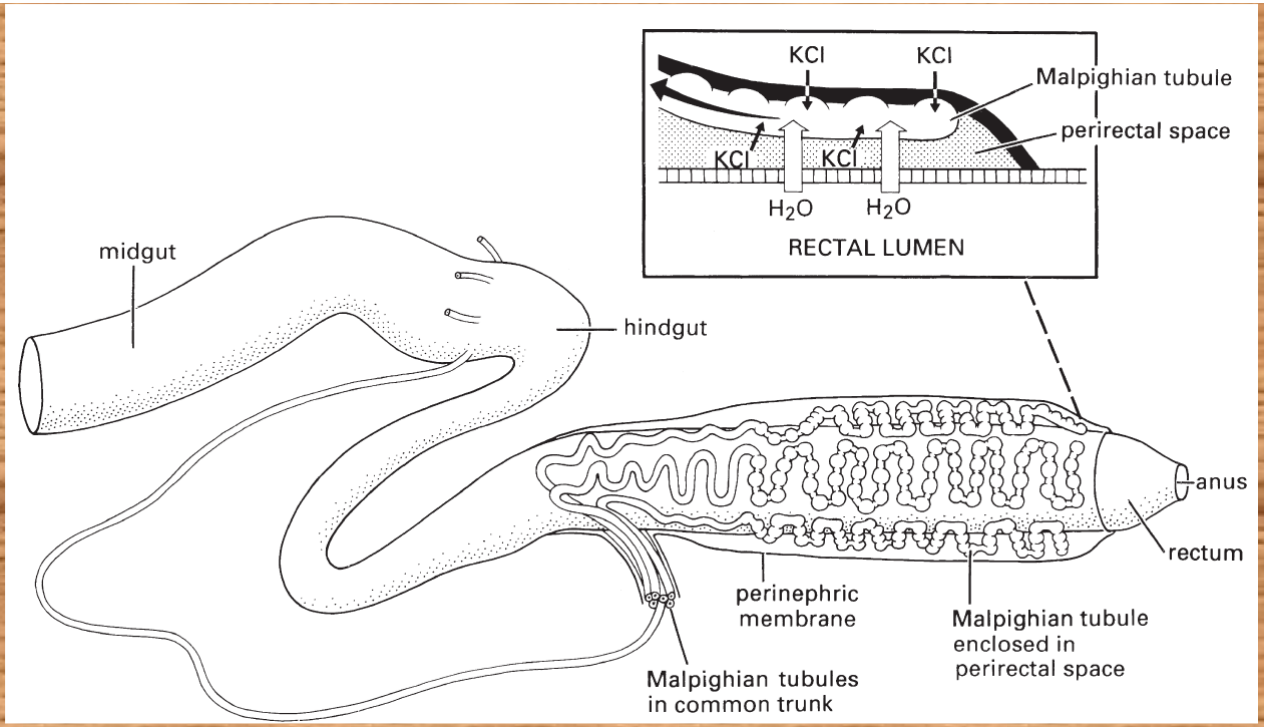

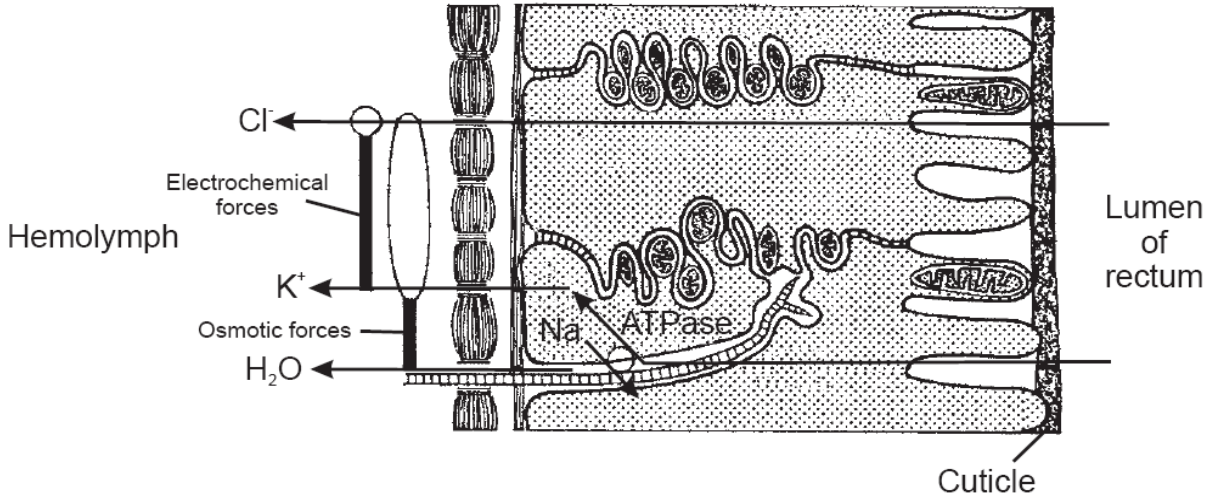

FIGURE 8.13. A rectal cell and its ion transport. From Hevert (1984). Reprinted with permission.

Obr. 9 Absorbce vzdušné vlhkosti v rektu potemníka

Fig. 18.14. Absorption of water vapor from the rectum of a beetle larva (*Tenebrio*). **(a)** Transverse section of the cryptonephridial complex (after O'Donnell & Machin, 1991). **(b)** Diagrammatic representation of ionic and water movements. It is assumed that ions are pumped into the Malpighian tubules from the hemolymph, but not via the leptophragmata, whose function is unknown. Numbers show the osmotic pressure in Osmol kg^{-1}. Note the very high levels in the Malpighian tubule (based on Machin, 1983; O'Donnell & Machin, 1991).

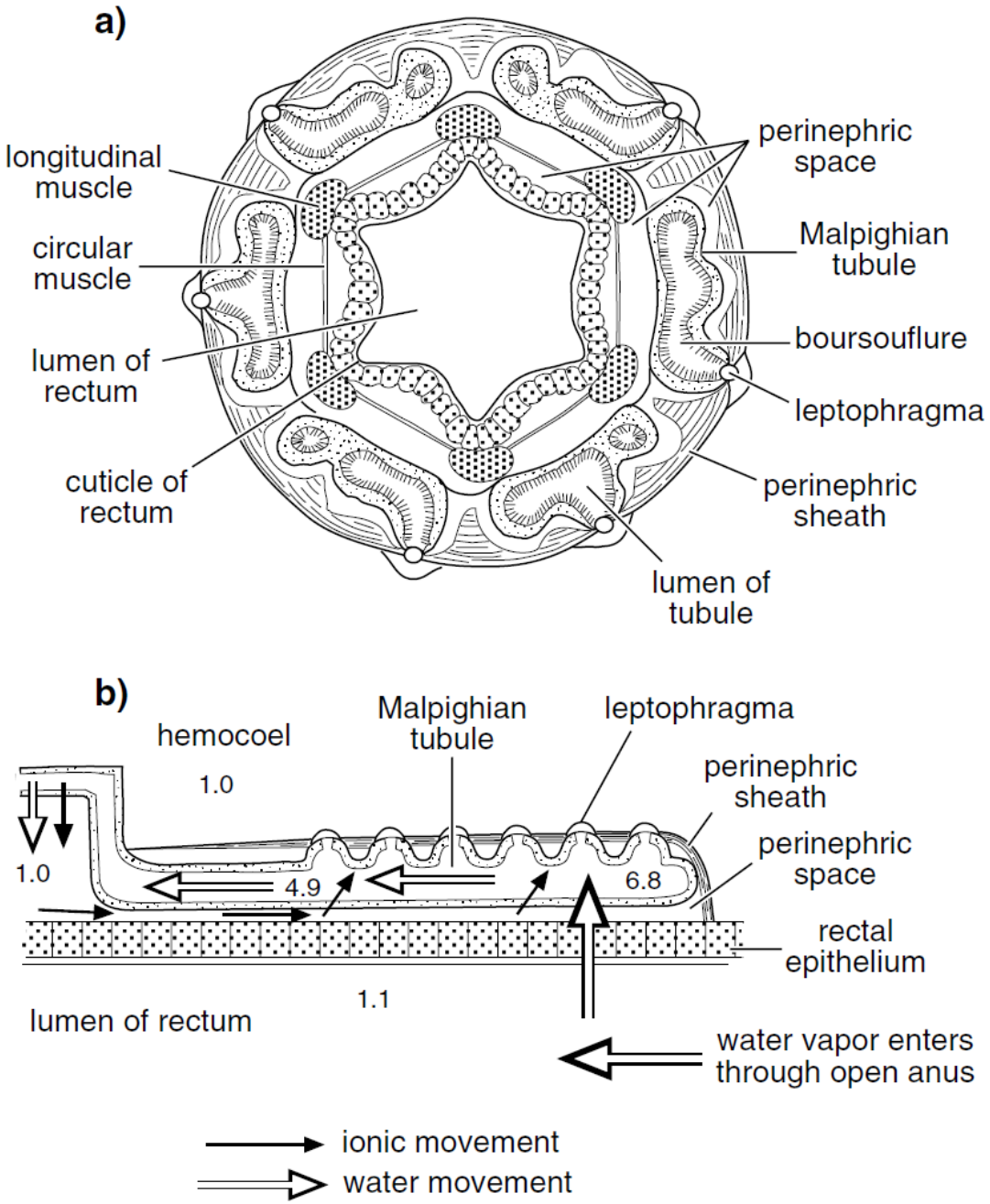

Obr. 10 Produkce moči u suchozemského hmyzu

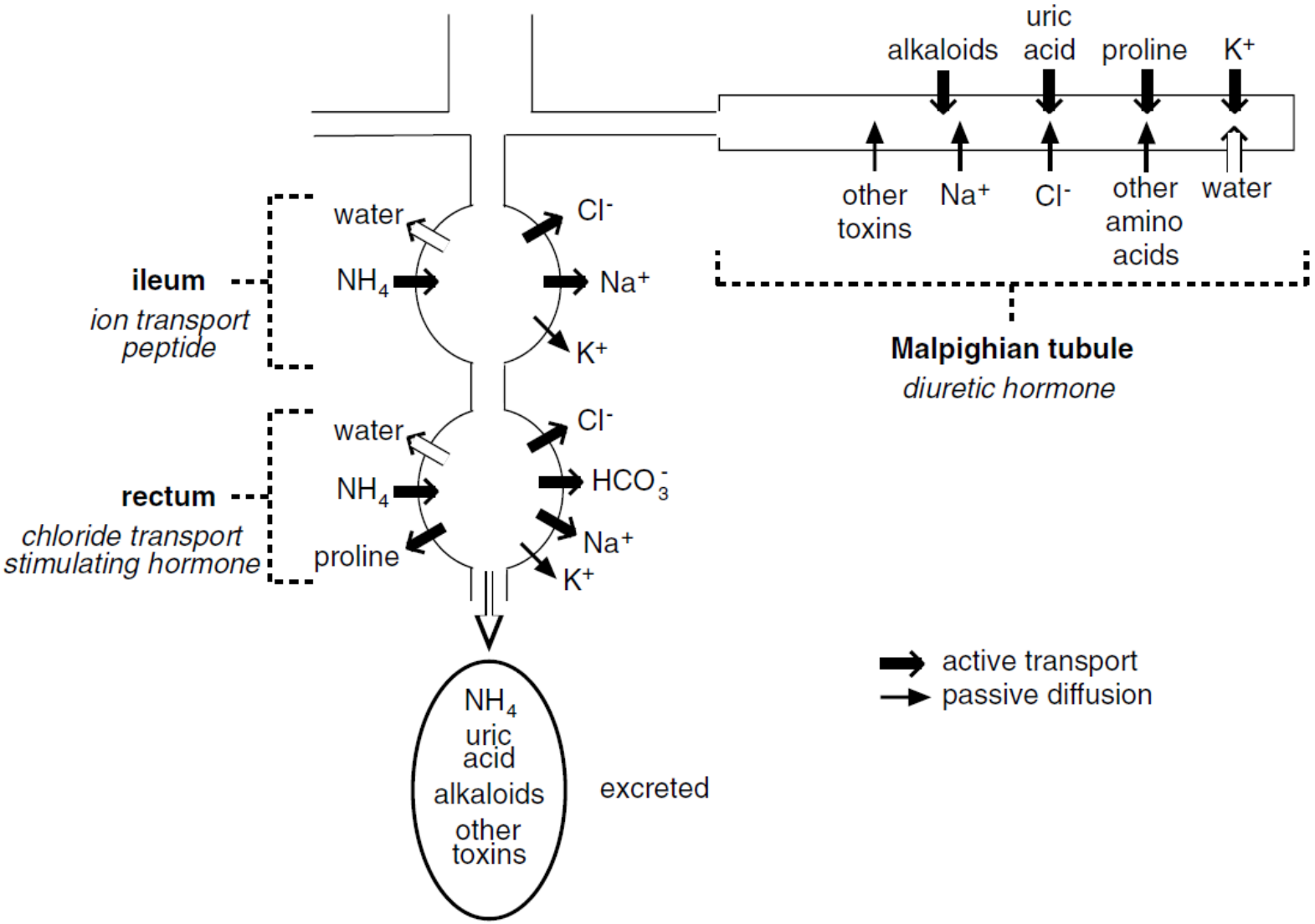

Fig. 18.7. Urine production and modification in a terrestrial insect (*Schistocerca*). Active transport of potassium into the Malpighian tubule leads to the osmotic movement of water and most other solutes follow passively. Many of the solutes are recovered as the urine moves through the hindgut, but ammonia is actively secreted into it. The hormones regulating the processes are shown in italics (partly based on Phillips & Audsley, 1995).

Obr. 11

Produkce moči u sladko- a slanovodního hmyzu

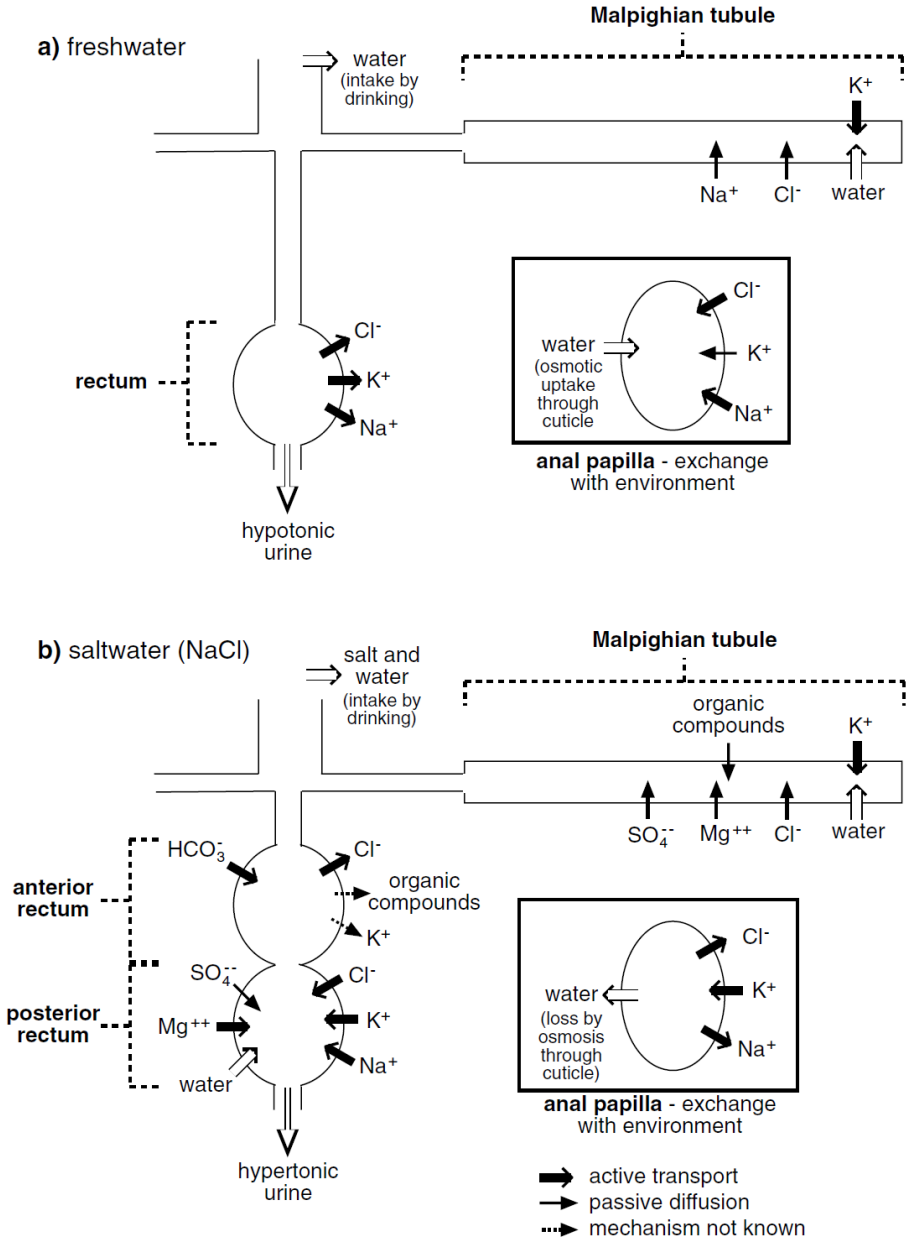

Fig. 18.8. Urine production and modification in aquatic insects (mosquito larvae). Nitrogenous excretory products not shown. **(a)** A freshwater insect, such as *Aedes aegypti*. The larva gains water by drinking and through the permeable cuticle of the anal papillae; excess water is removed as urine. **(b)** A saltwater insect, such as *Aedes campestris*. The gain of water due to drinking is greater than osmotic loss through the cuticle. Further water is lost in the urine. Note that although water is moved into the posterior rectum, the fluid produced there is hypertonic to the hemolymph and the medium (partly based on Bradley & Phillips, 1977b).

5. Oběh tělních tekutin

Obr. 1 Schéma oběhu tělních tekutin u hmyzu

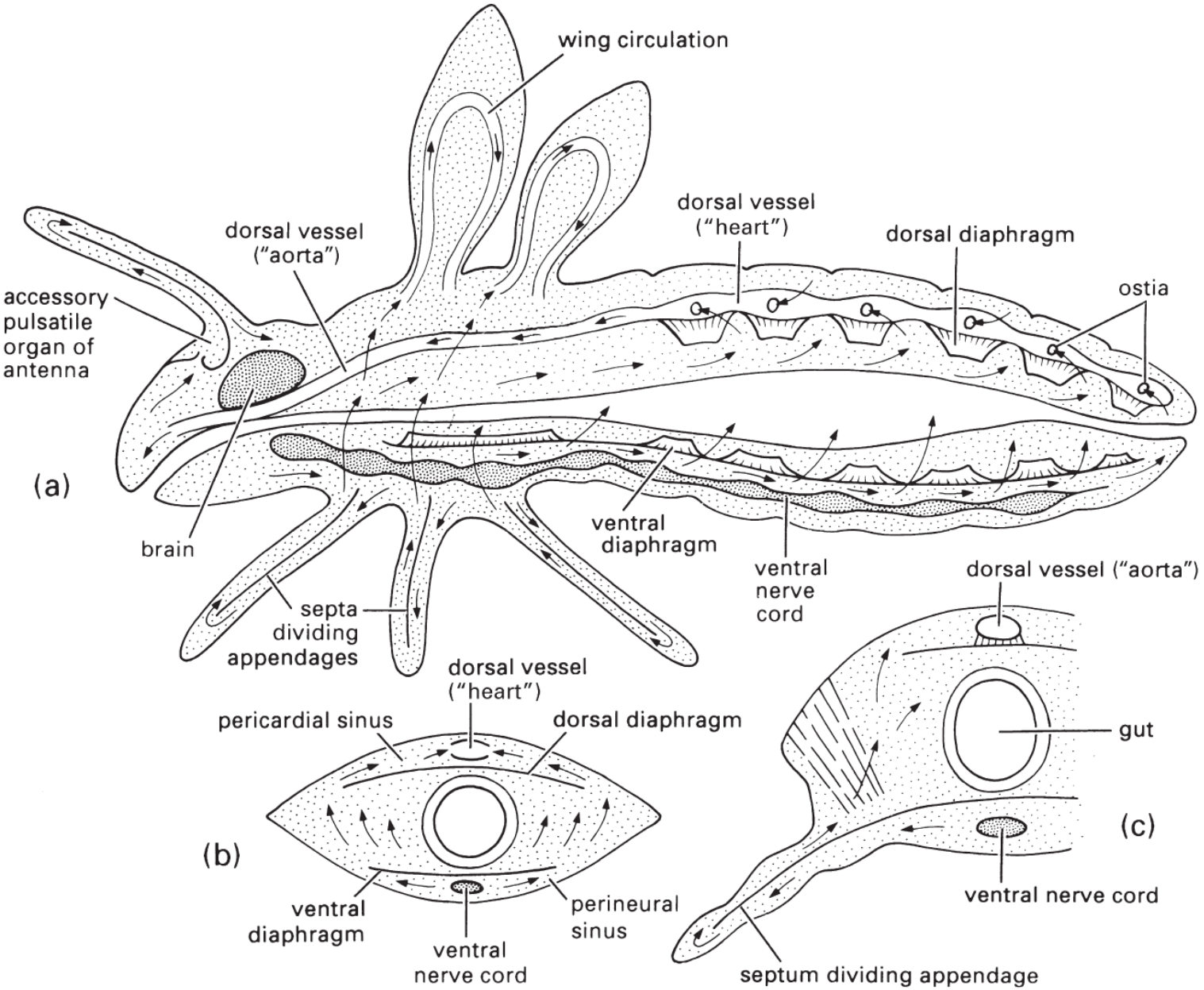

Fig. 3.9 Schematic diagram of a well-developed circulatory system: (a) longitudinal section through body; (b) transverse section of the abdomen; (c) transverse section of the thorax. Arrows indicate directions of hemolymph flow. (After Wigglesworth 1972.)

Obr. 2 Transport hydrofobních molekul v hemolymfě

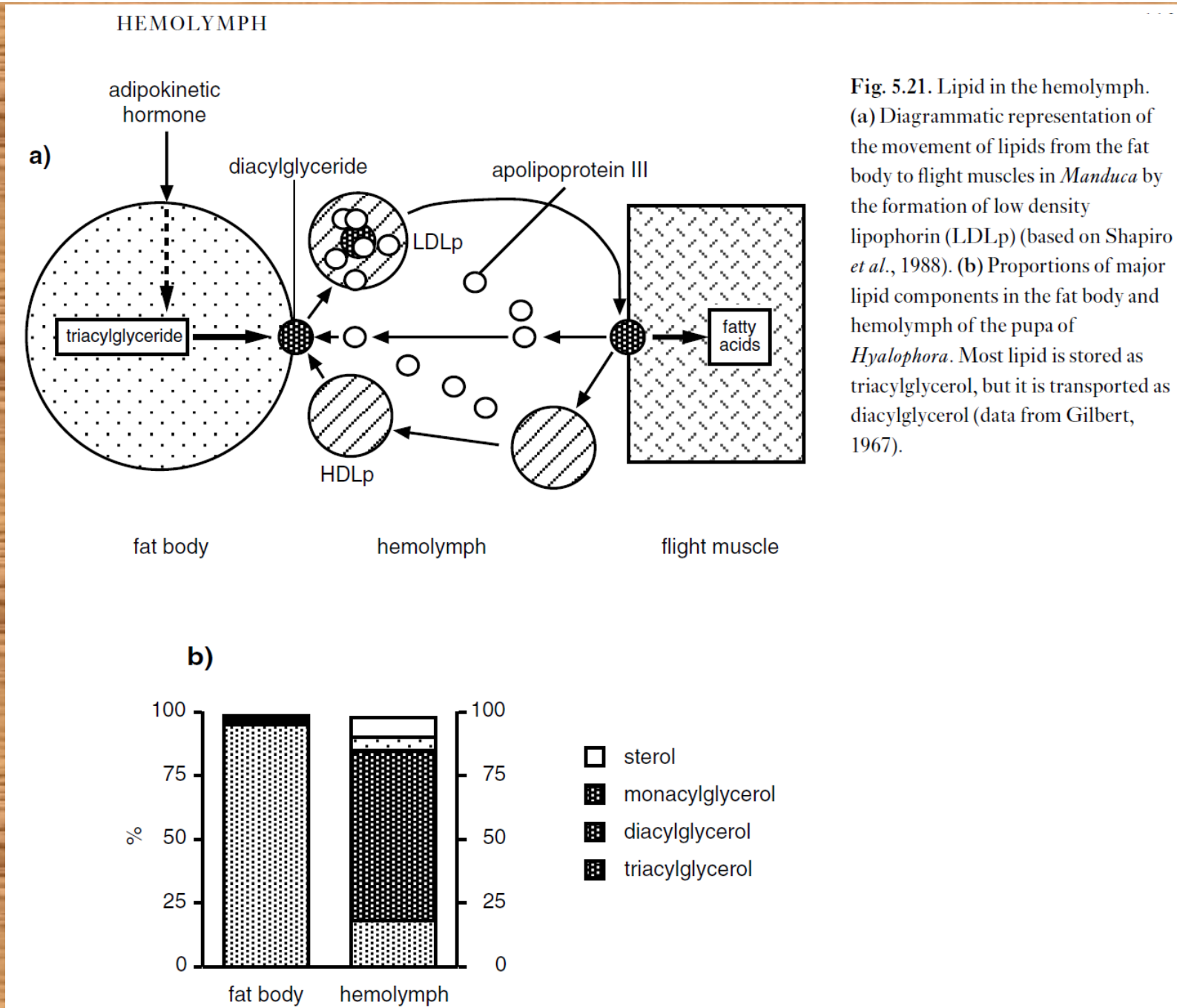

Fig. 5.21. Lipid in the hemolymph. **(a)** Diagrammatic representation of the movement of lipids from the fat body to flight muscles in *Manduca* by the formation of low density lipophorin (LDLp) (based on Shapiro *et al.*, 1988). **(b)** Proportions of major lipid components in the fat body and hemolymph of the pupa of *Hyalophora*. Most lipid is stored as triacylglycerol, but it is transported as diacylglycerol (data from Gilbert, 1967).

Obr. 3

Hlavní typy hmyzích hemocytů

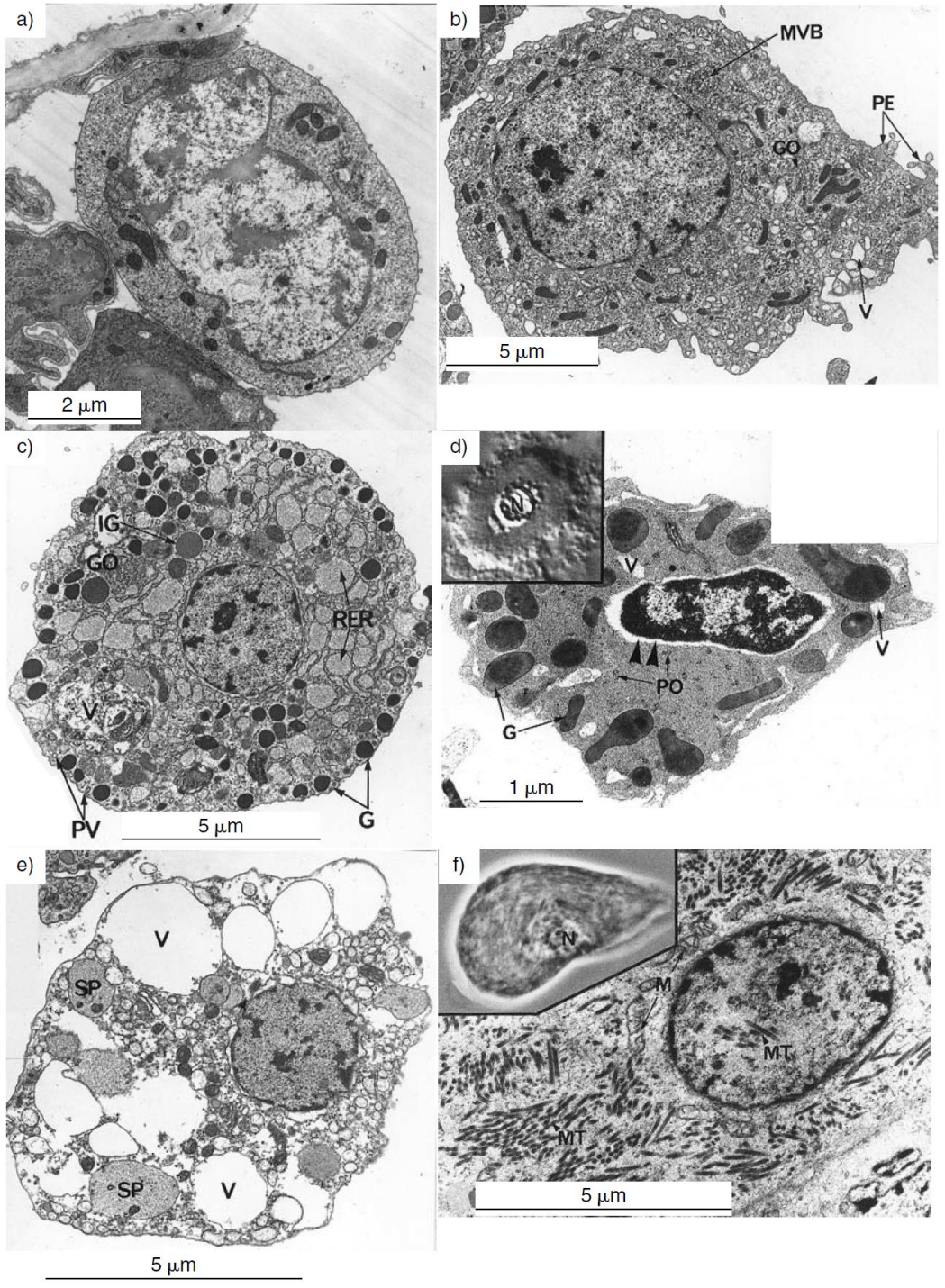

Obr. 4

Nefrocyty

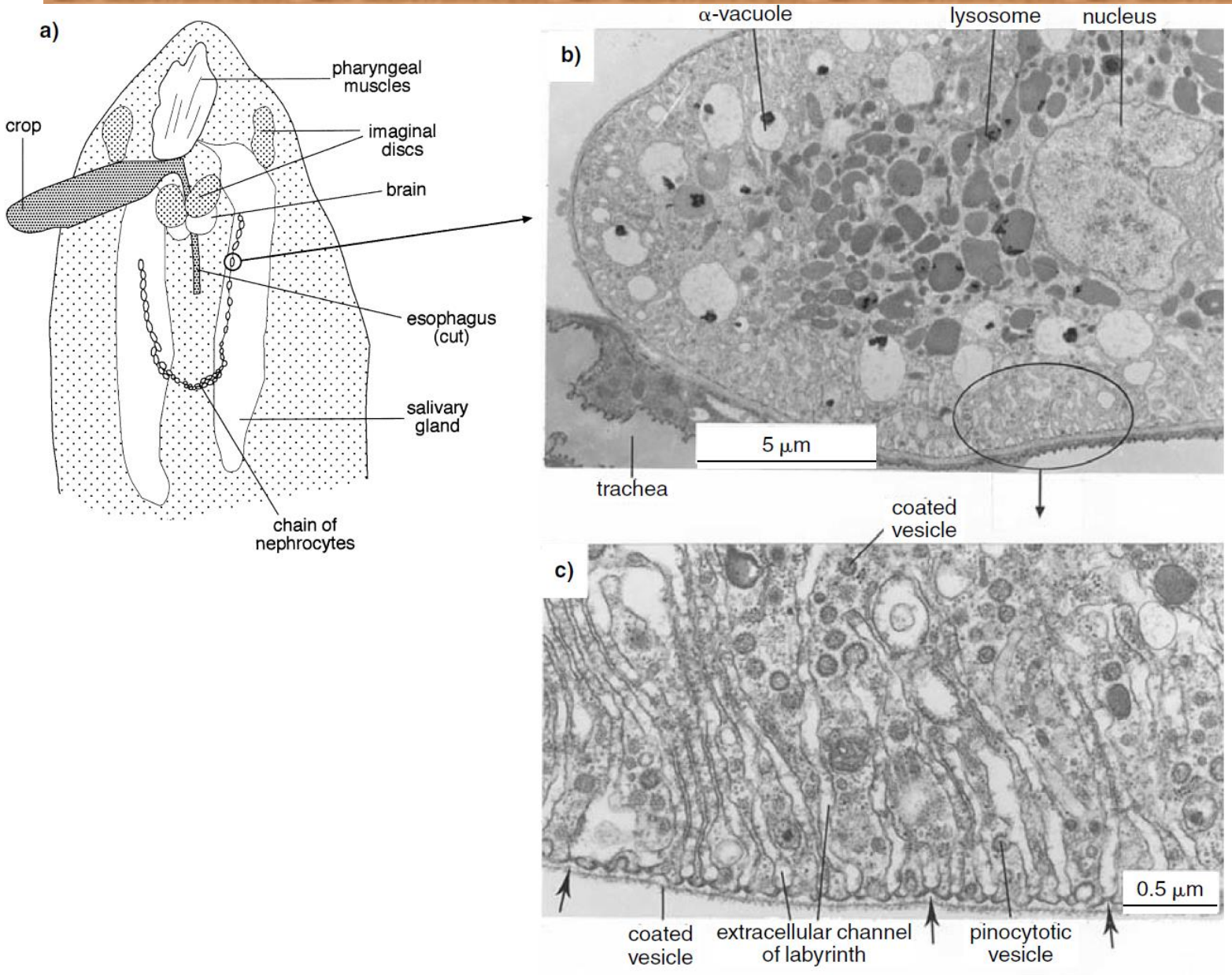

Fig. 18.19. Nephrocytes. **(a)** Dissection of the anterior part of a blowfly larva showing the chain of nephrocytes known as a garland. **(b)** Nephrocyte from the garland of *Drosophila* larva. α-vacuoles are formed from the amalgamation of pinocytotic vesicles formed in the labyrinth (after Koenig & Ikeda, 1990). **(c)** Cortical region of a nephrocyte of *Drosophila* larva showing the labyrinth. Arrows show the desmosome-like connections between adjacent projections of the cell (after Koenig & Ikeda, 1990).

Obr. 5 **Hemopoetické orgány hmyzu**

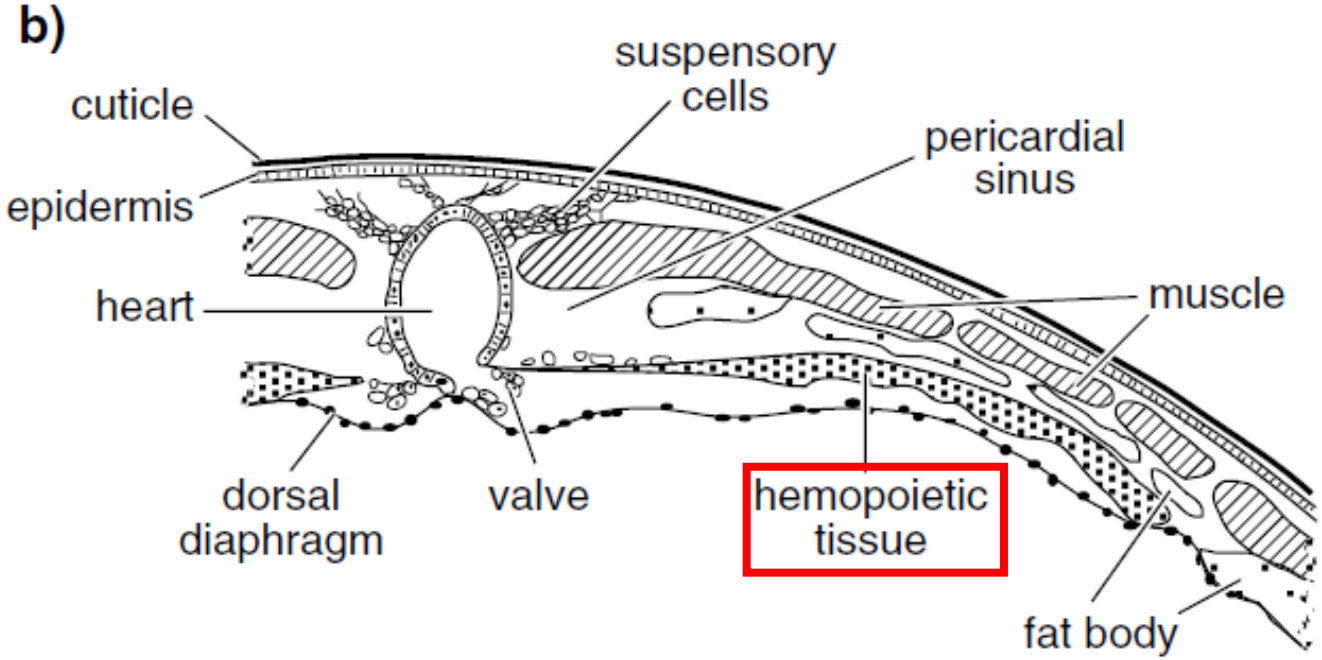

Fig. 5.2. Dorsal vessel and hemopoietic organs of the mole cricket, *Gryllotalpa* (after Nutting, 1951). **(a)** Ventral dissection. The dorsal diaphragm is continuous over the ventral wall of the heart, but is omitted from the drawing for clarity. Arrows show positions of incurrent ostia. **(b)** Transverse section through the pericardial sinus in the abdomen. Pericardial cells form supporting elements (suspensory cells) for the heart dorsally.

Obr. 6 Cirkulace hemolymfy

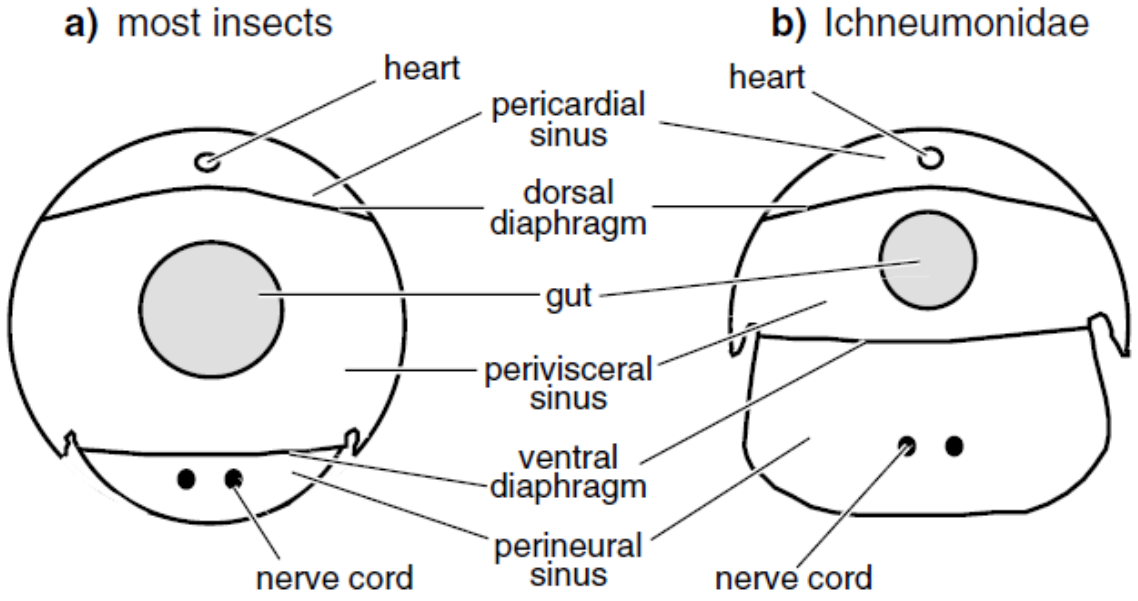

Fig. 5.1. Main sinuses of the hemocoel shown in diagrammatic cross-sections (after Richards, 1963).

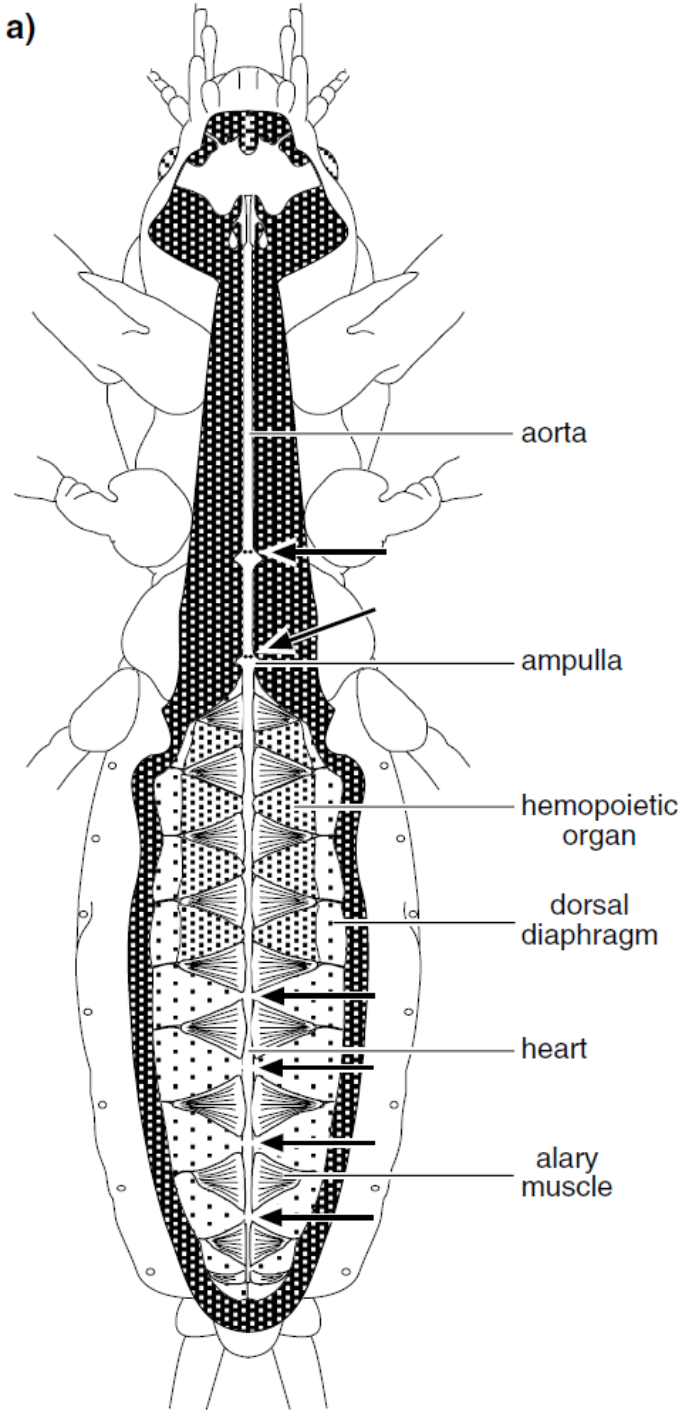

Obr. 7 Přepážky a přídatné pulsující orgány u hmyzu

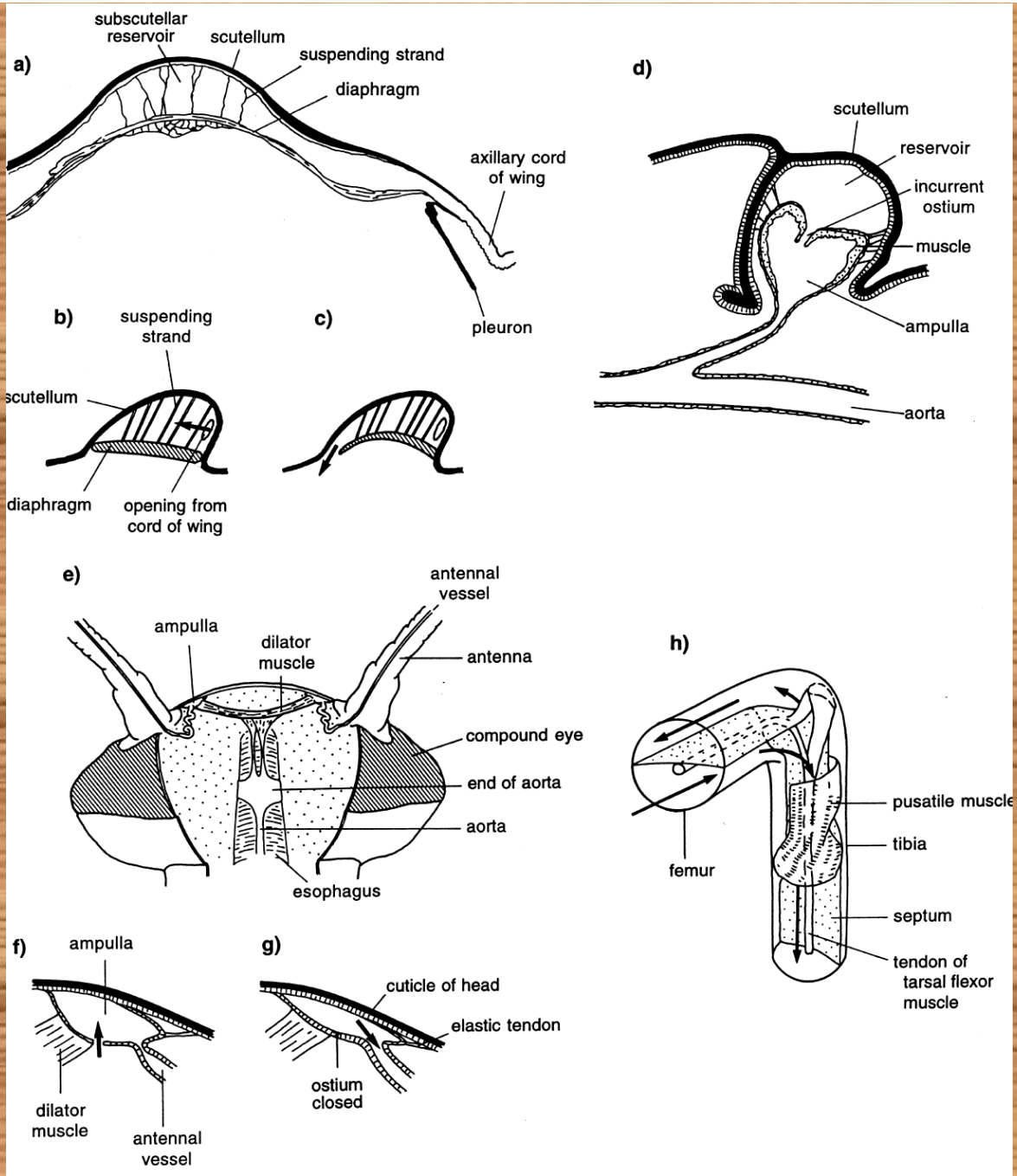

Obr. 8 Přídatný pulsující orgán a funkce vzdušného vaku v cirkulaci hemolymfy

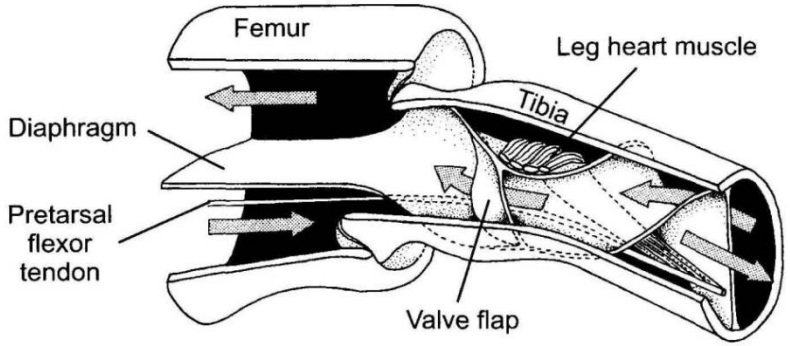

FIGURE 7.5. An accessory pulsatile organ in the insect leg. Arrows show the direction of hemolymph flow. From Hantschk (1991). Reprinted with permission.

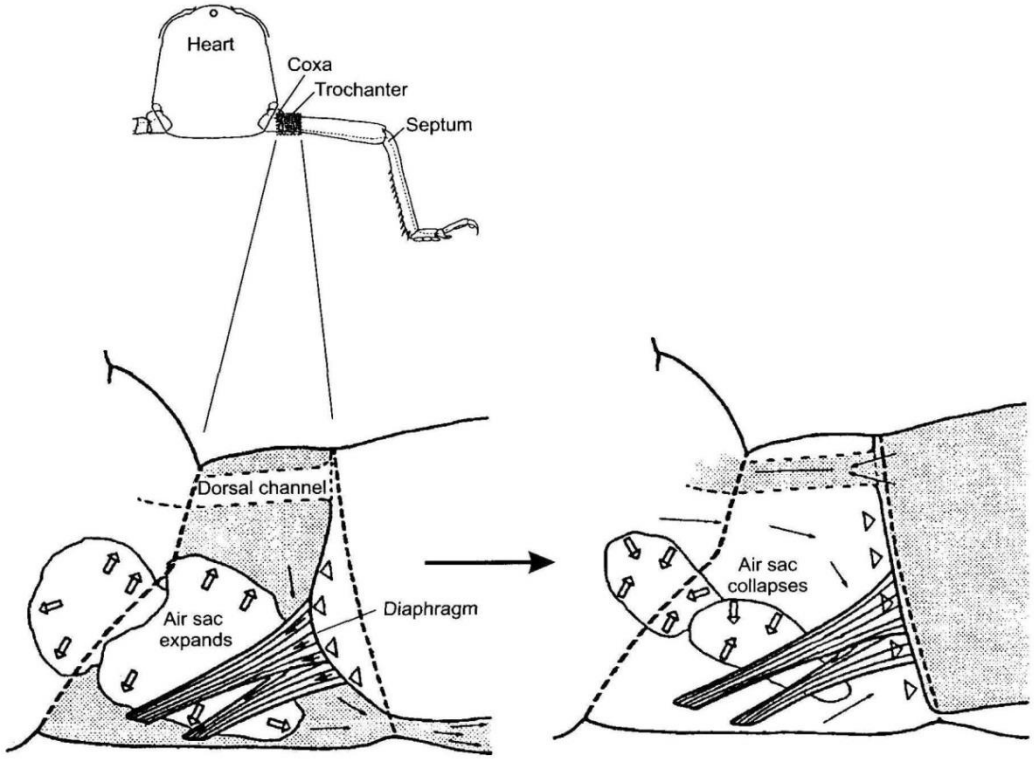

FIGURE 7.6. Tracheal air sacs can regulate the movement of hemolymph into the leg. From Hustert (1999).

http://www.youtube.com/watch?v=KCC_FrbuR3U&feature=plcp

Obr. 9 Hmyzí imunitní systém

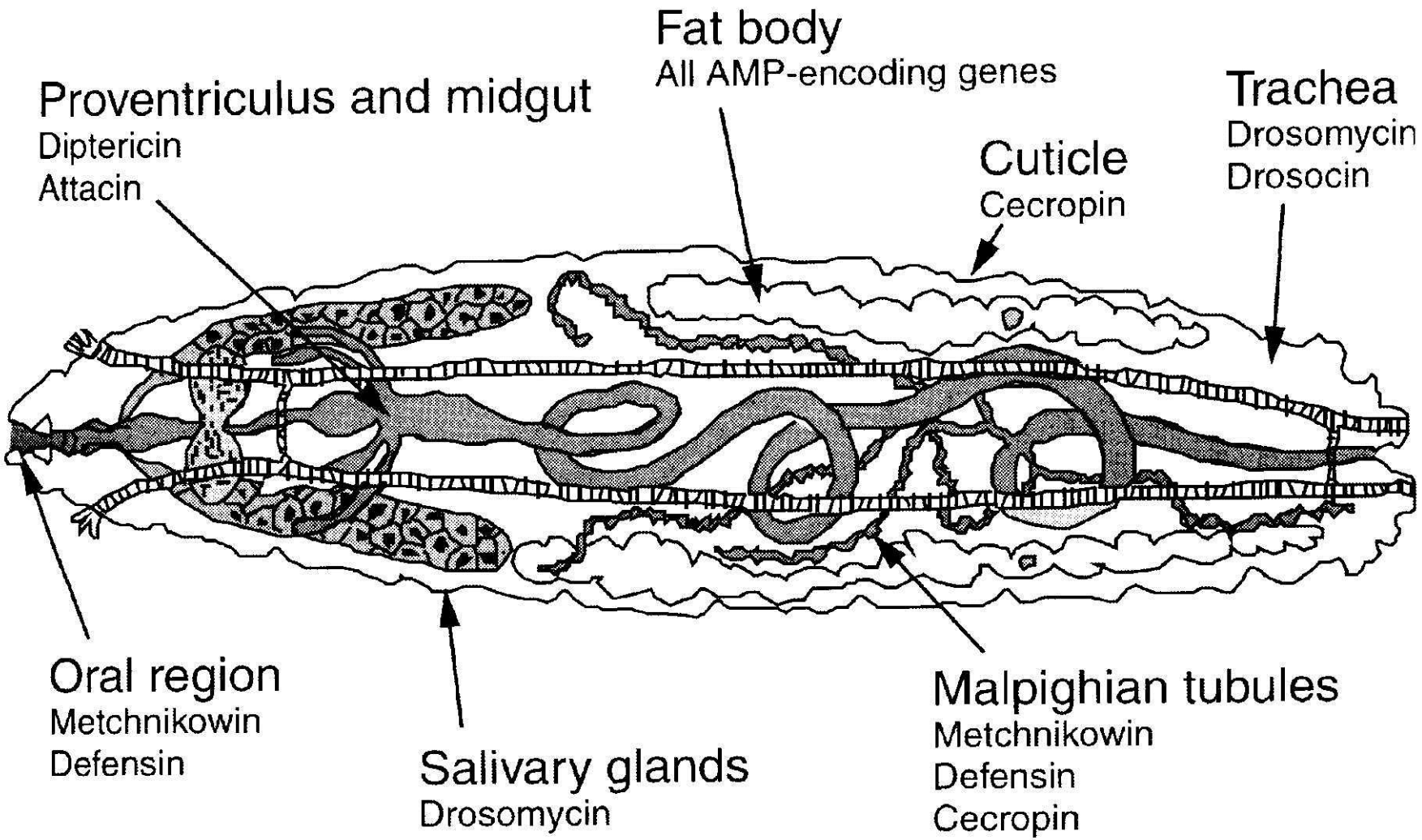

FIGURE 7.16. Biological defense barriers to infection in *Drosophila* larvae. From Tzou et al. (2002). Reprinted with permission.

Obr. 10 Tvorba nodulů

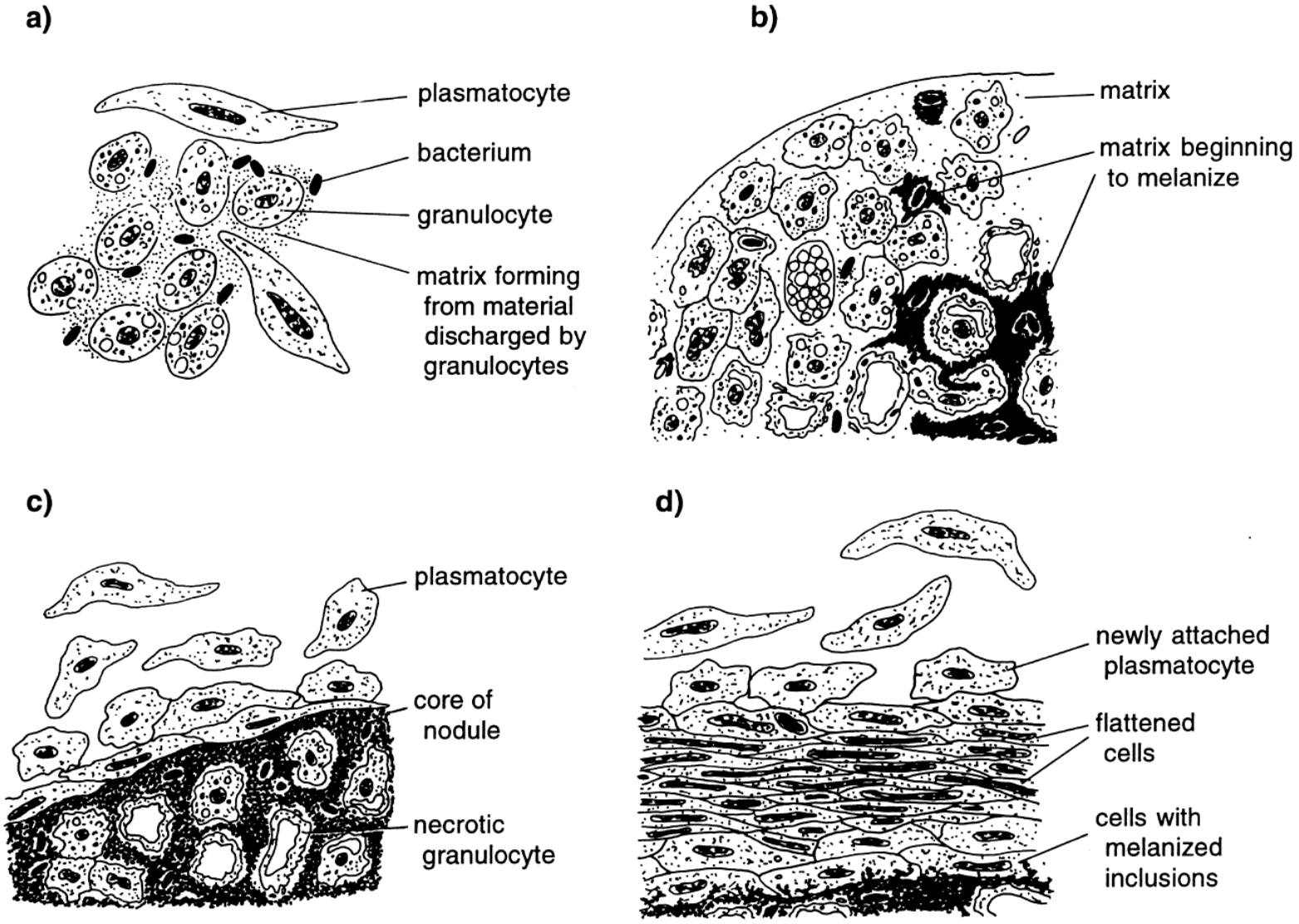

Fig. 5.33. Nodule formation (after Ratcliffe & Gagen, 1977). (a) One minute after injection of bacteria. Granulocytes have degranulated and bacteria are trapped in the flocculent material produced by the cells. (b) Thirty minutes after injection. The clumps of granulocytes and bacteria have compacted, and melanization of the matrix is beginning. (c) Plasmatocytes arrive at the nodule and melanization of the matrix is advanced. (d) Twenty-four hours after injection. Nodulation is complete. Three regions are recognizable in the layers of plasmatocytes.

Mechanismus enkapsulace: syntéza melaninu

Obr. 11

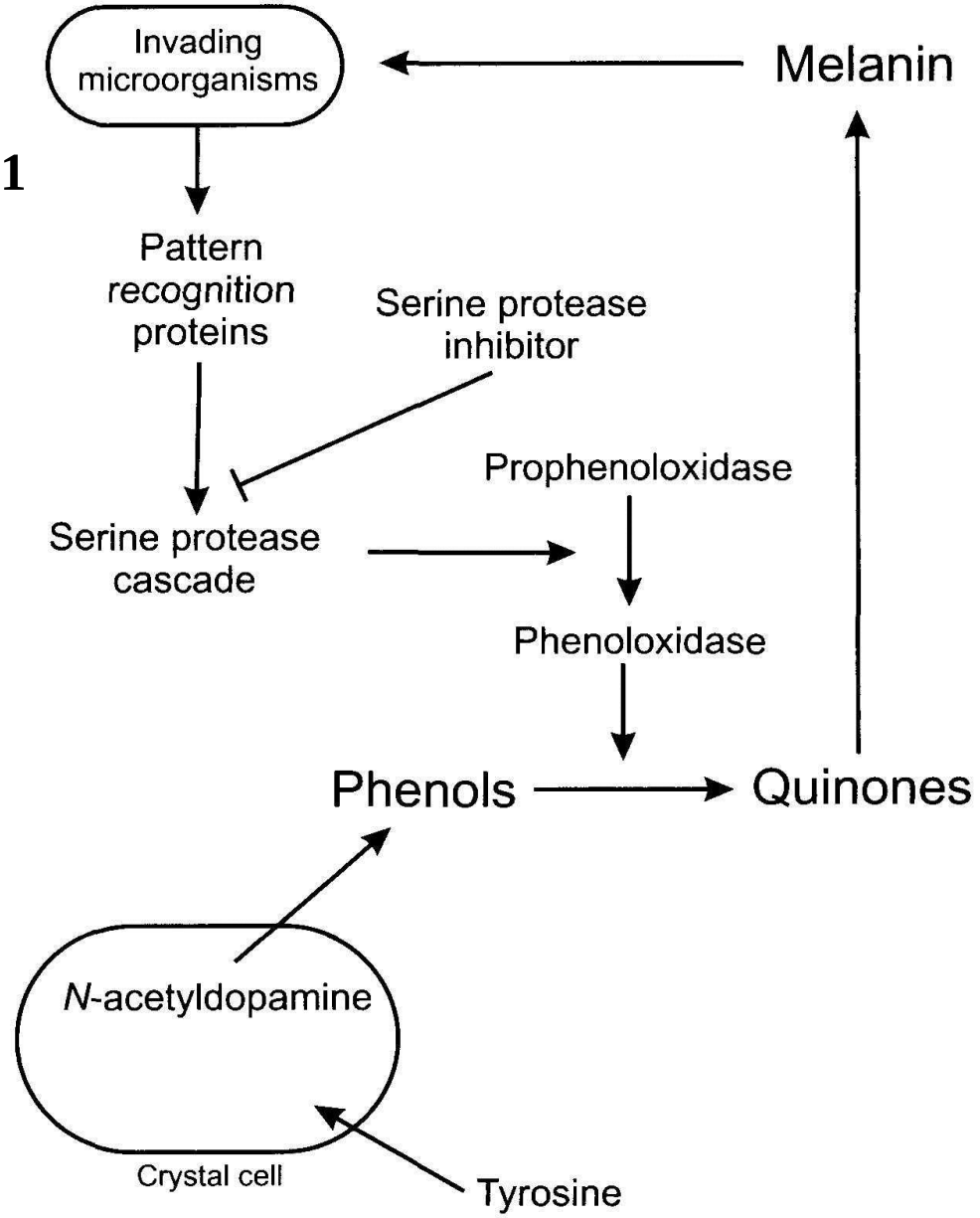

FIGURE 7.18. Mechanism of humoral encapsulation by the deposition of melanin on foreign invaders. The serine protease inhibitor restricts phenoloxidase activity to the site of the infection.

Syntéza hmyzích antimikrobiálních peptidů

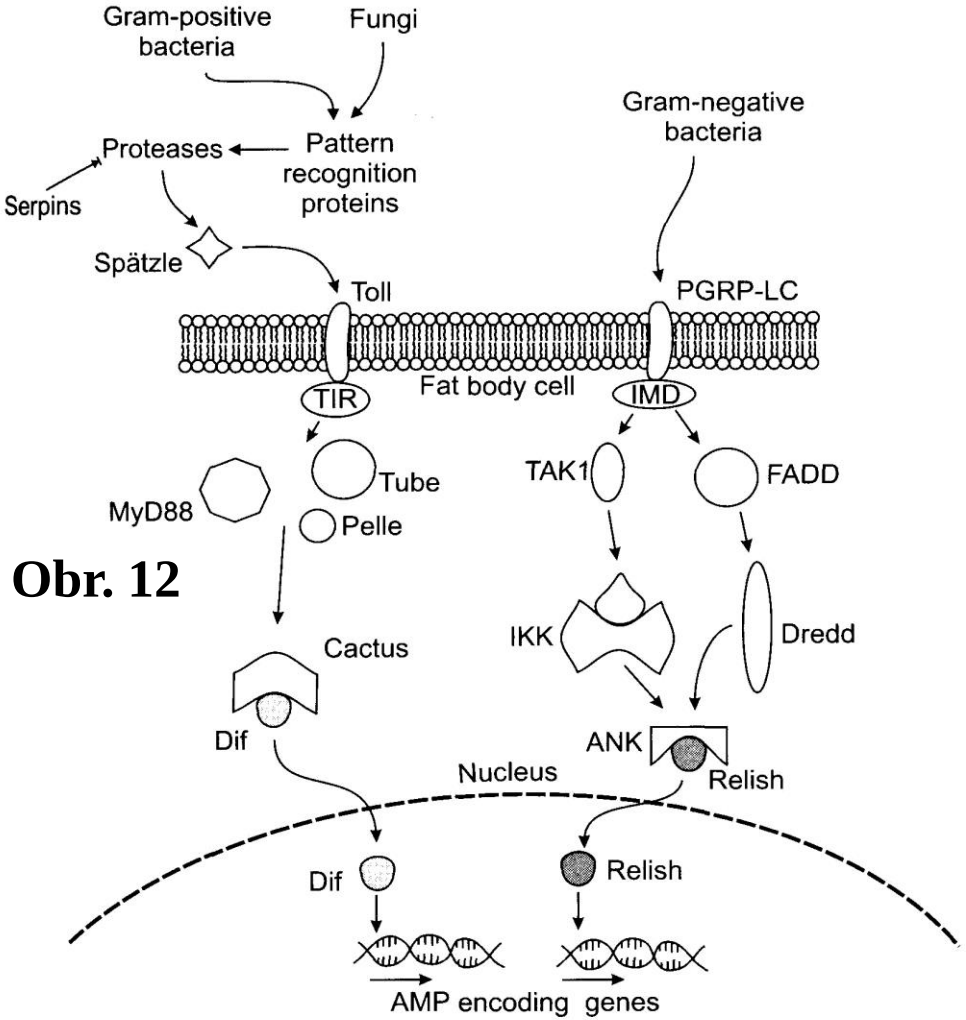

Obr. 12

FIGURE 7.20. The Toll (*left*) and IMD (*right*) signaling pathways. In the Toll pathway, an infection activates proteases that in turn activate Spätzle. Serpins inhibit the proteases in the absence of an immune challenge. When Spätzle binds to the Toll receptor, an intracellular signaling cascade causes the degradation of Cactus and the translocation of the Dif protein to the nucleus, where it initiates the transcription of antimicrobial peptides (AMP). In the IMD pathway, bacteria bind to a transmembrane peptidoglycan recognition protein (PGRP-LC) that activates the IMD protein and initiates a signal transduction that ultimately leads to the translocation of the Relish transcription factor that regulates AMP genes.

Obr. 12 **Komplexní imunitní reakce u hmyzu**

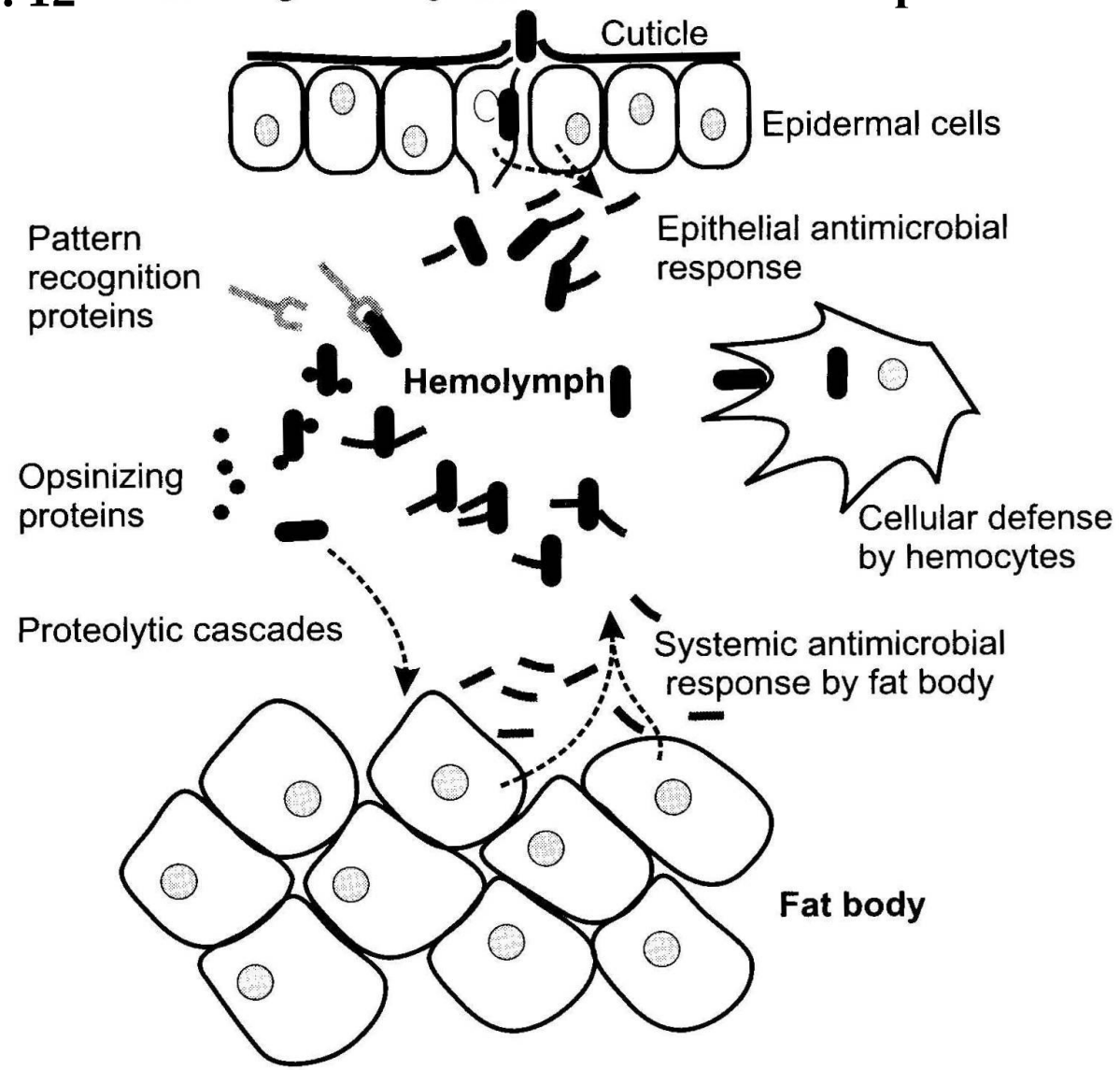

FIGURE 7.17. Possible mechanisms of response to invading parasites by epidermal cells, hemocytes, and fat body. Epidermal cells produce antimicrobial compounds, and pattern recognition and opsinizing proteins target invaders for attack by hemocytes. Fat body cells can also mount a systemic antimicrobial response.

Obr. 13a. Vliv jedu vosičky *Habrobracon hebetor* na ultrastukturu hrudních svalů ruměnice pospolné *Pyrrhocoris apterus* a obranná reakce řízená adipokinetickým hormonem

Kontrola **Jed** **Jed + adipokinetický hormon**

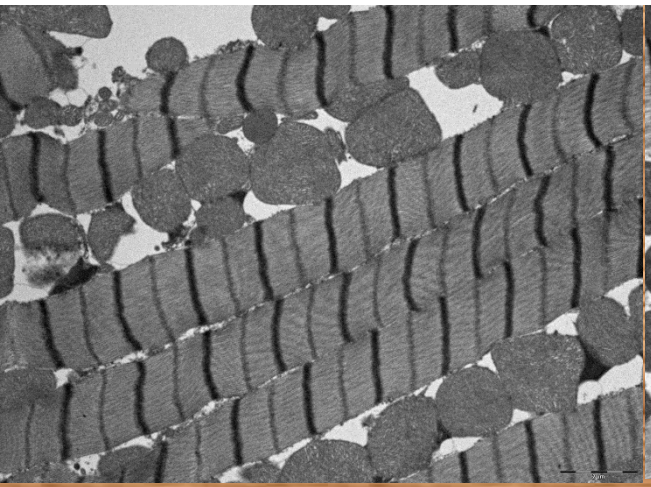

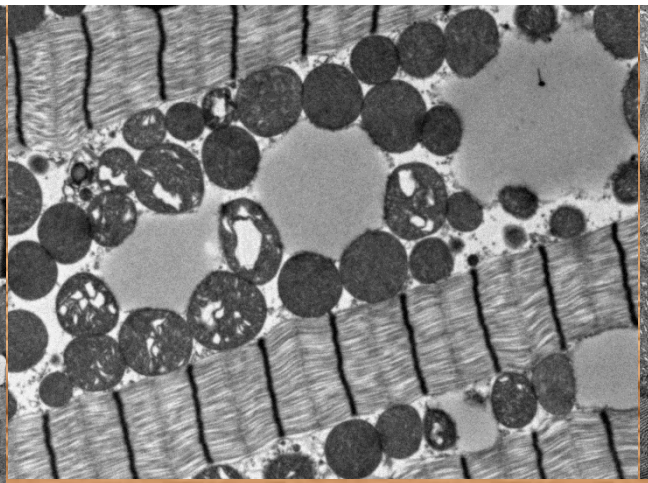

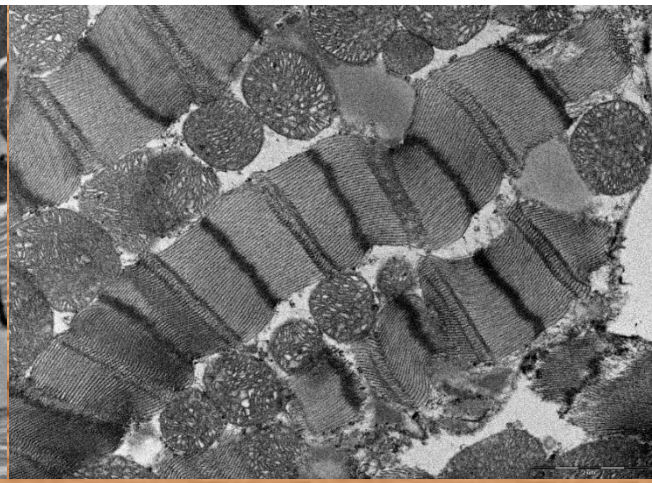

Obr. 13b. Vliv jedu vosičky *Habrobracon hebetor* na ultrastukturu mitochondrií z hrudních svalů ruměnice pospolné *Pyrrhocoris apterus* a obranná reakce řízená adipokinetickým hormonem

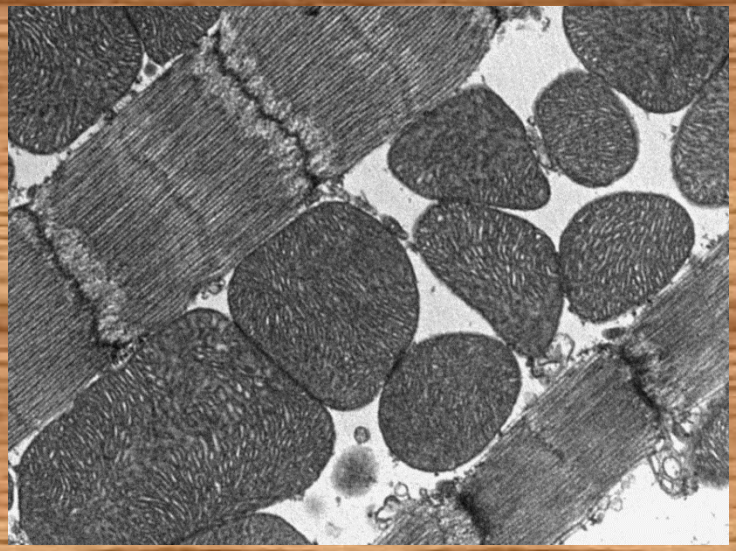

Kontrola ←

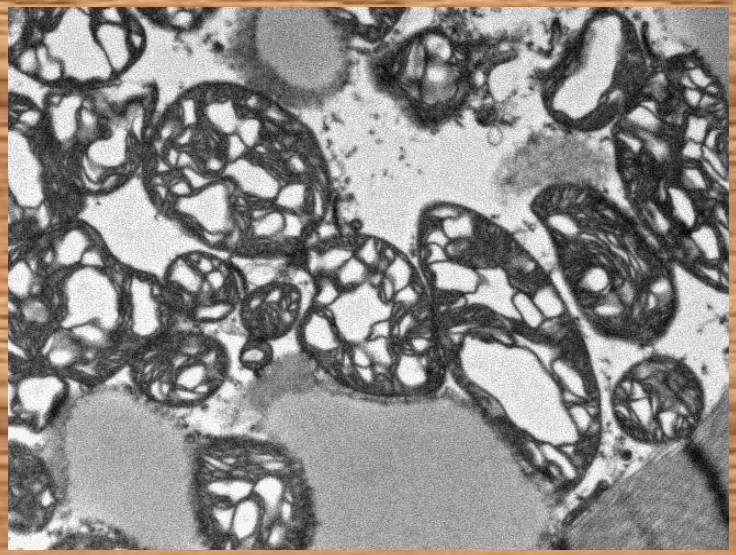

Jed ←

Jed + adipokinetický hormon →

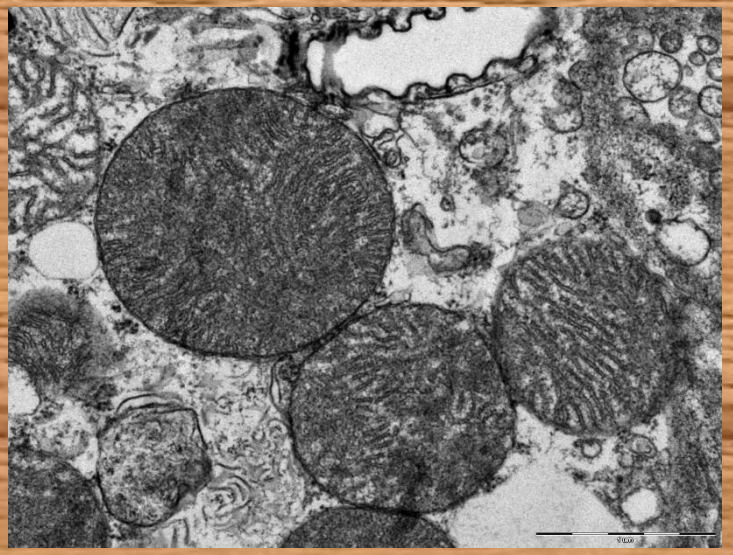

6. Bioluminiscence - svítivé orgány

Obr. 1 Svítivé orgány

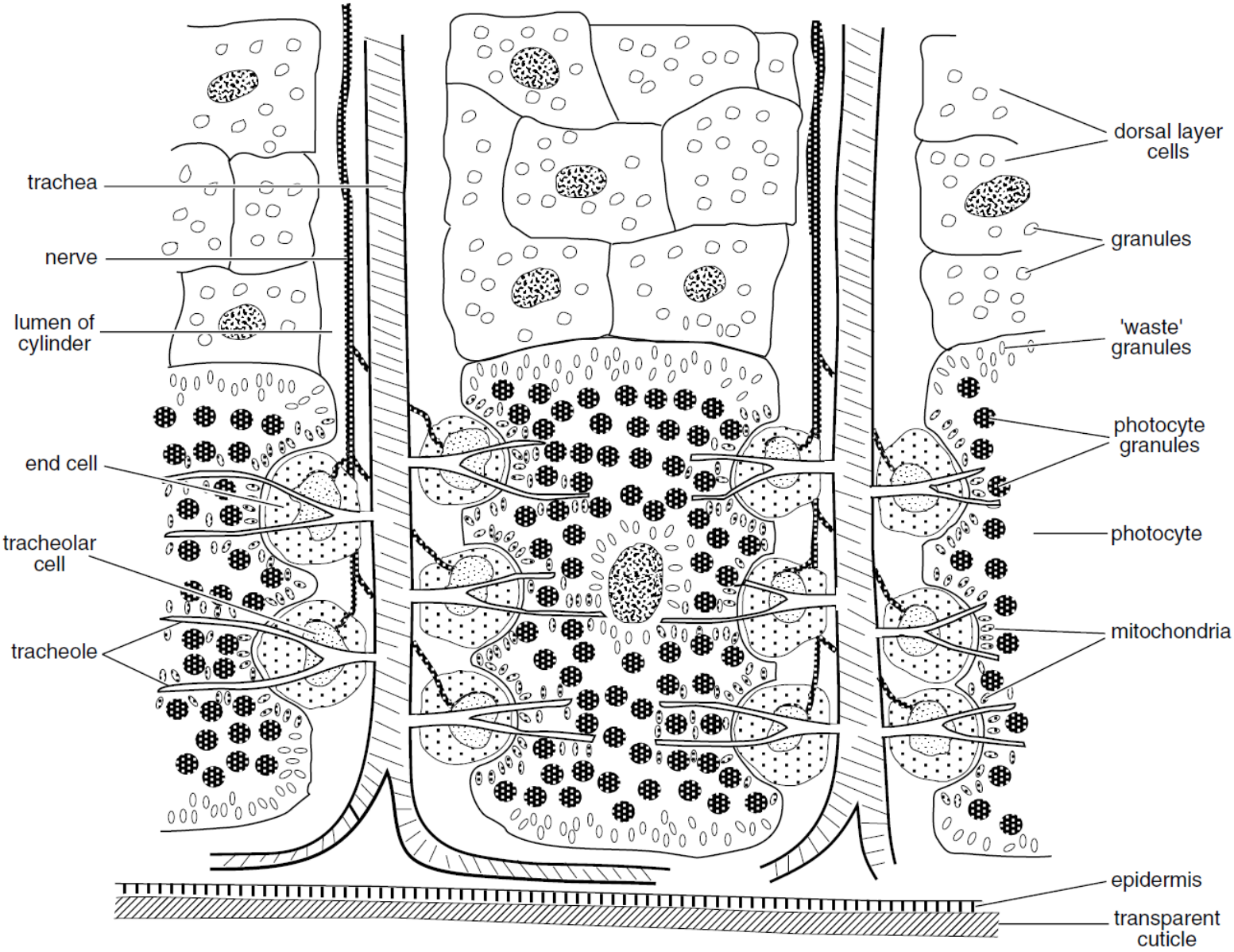

Fig. 25.16. Diagrammatic section through part of the light organ on the ventral side of an adult *Photuris*. The tracheoles pass between the photocytes, but do not penetrate into the cells (based on Smith, 1963).

Obr. 2

Mechanismus produkce světla

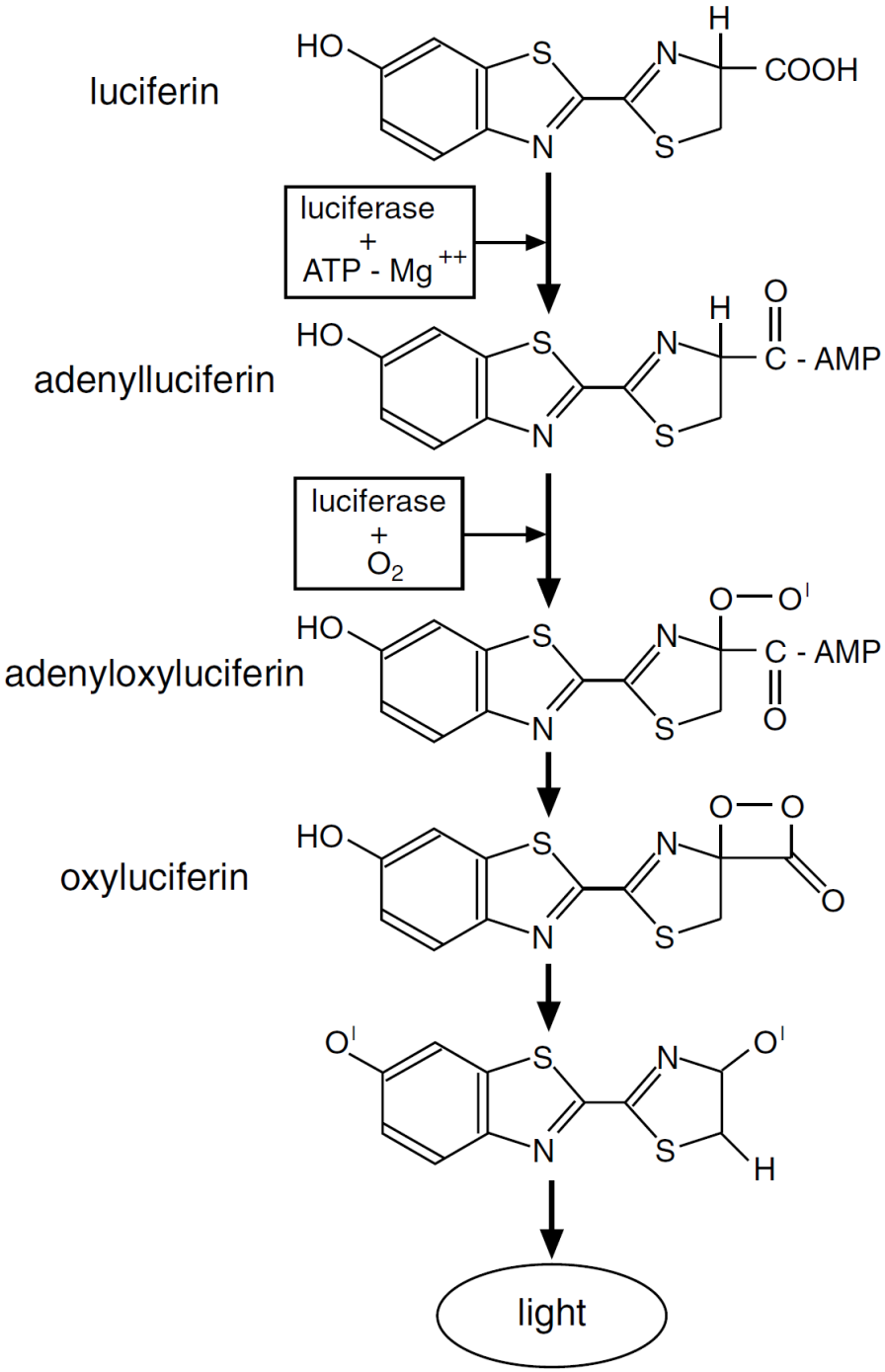

Obr. 3 Průřez světélkujícím orgánem světlušky *Phyusis splendidula* (Coleoptera)

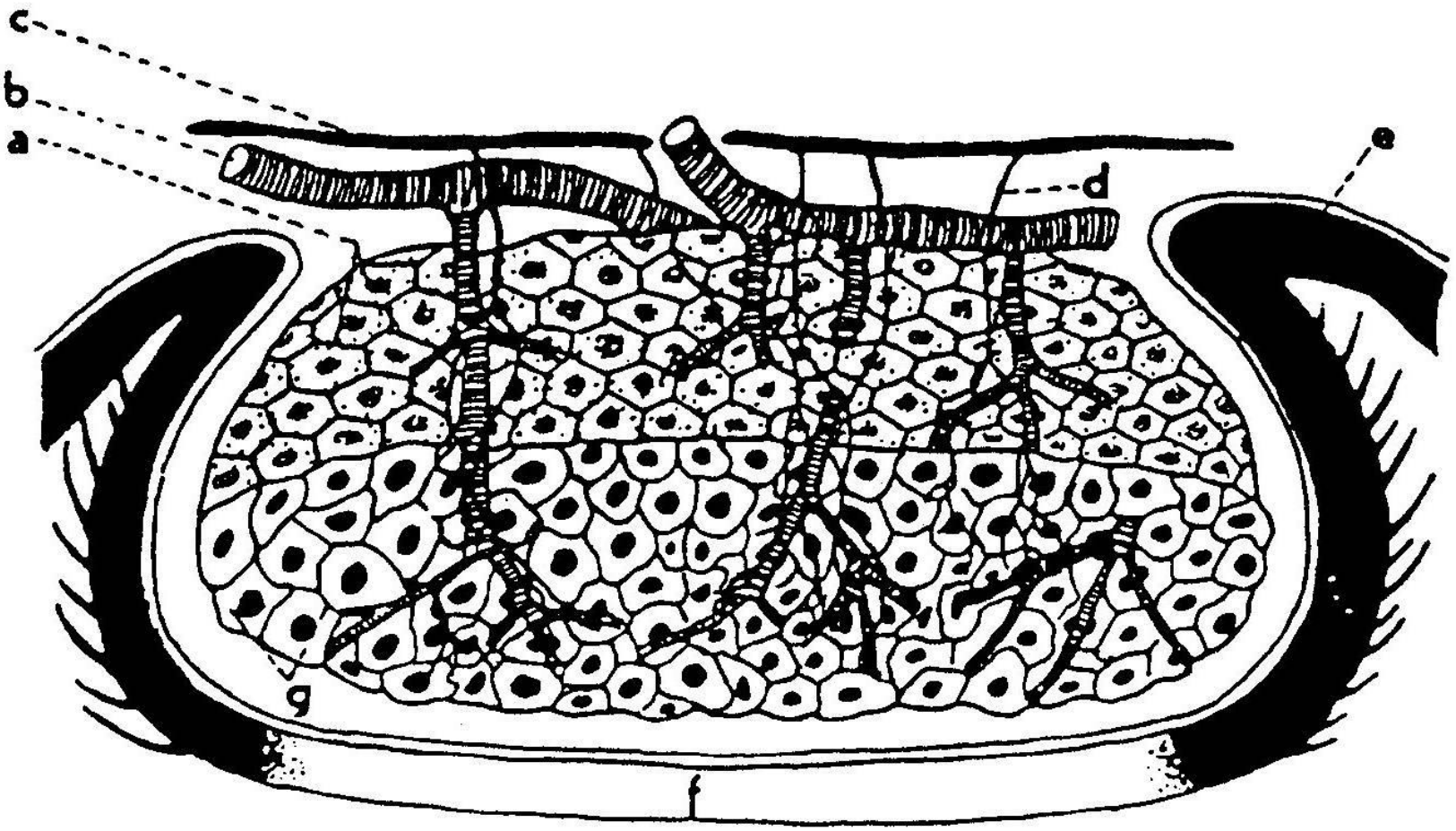

a = vrstva neprůhledných, bíle zbarvených buněk, které slouží jako reflexní vrstva - urátová vrstva, b = trachea, c = nerv, d = neurit, e = kutikula, f = průhledná vrstva kutikuly, která propouští světlo navenek, g = světelná vrstva, která vydává krátkovlnné světlo

Obr. 4 Příklady střídavé produkce světla (vzory blikání) u různých druhů hmyzu

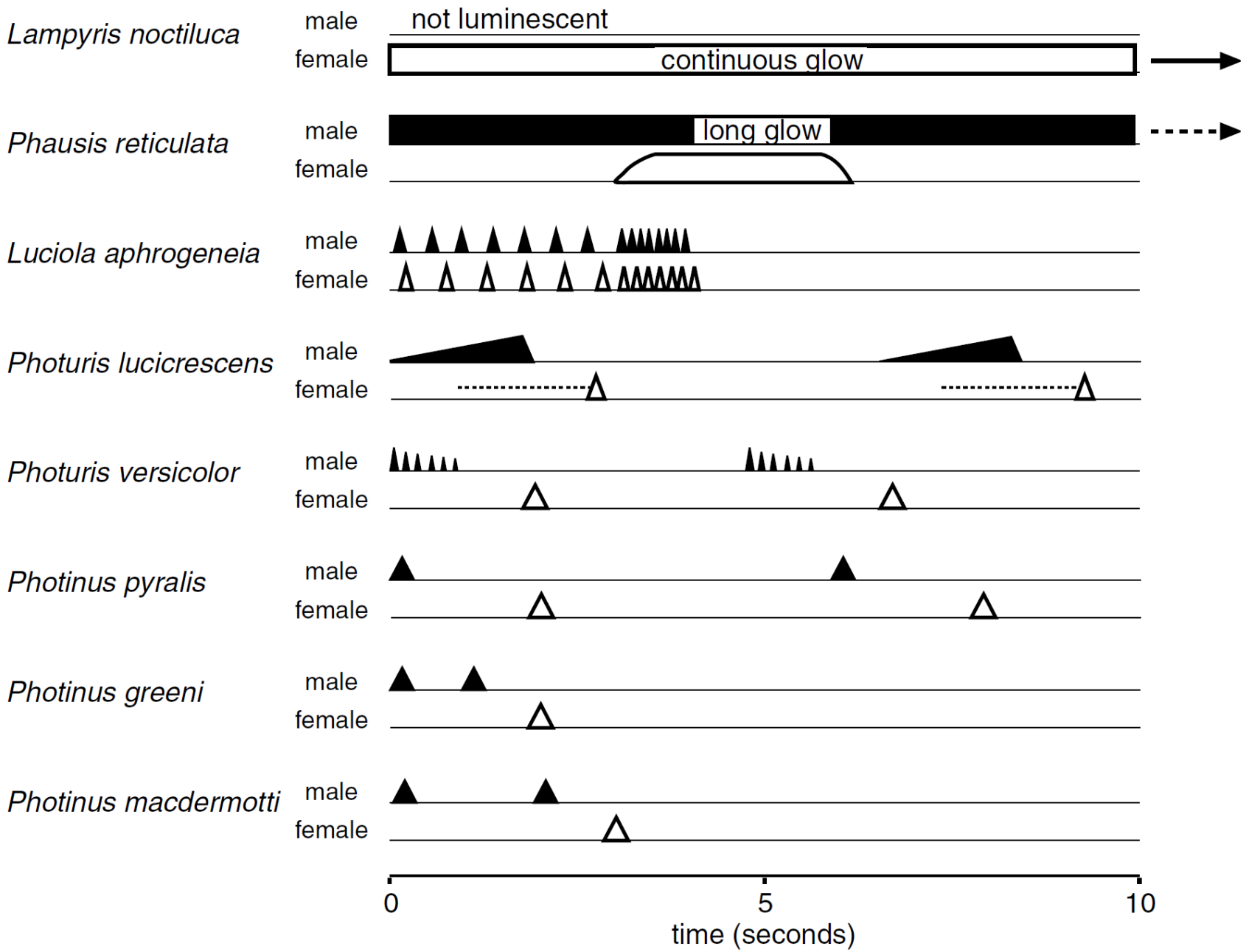

https://www.youtube.com/watch?v=HAiosJLdlUA

7. Vnější faktory ovlivňující fyziologické děje

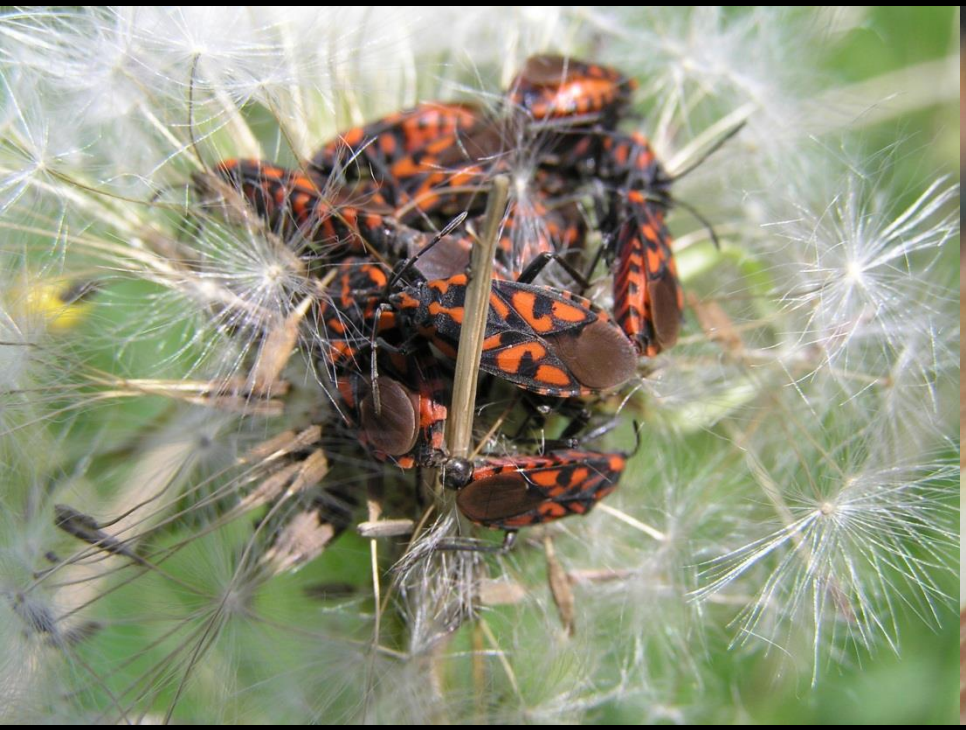

Obr. 1

Fyziologická termoregulace

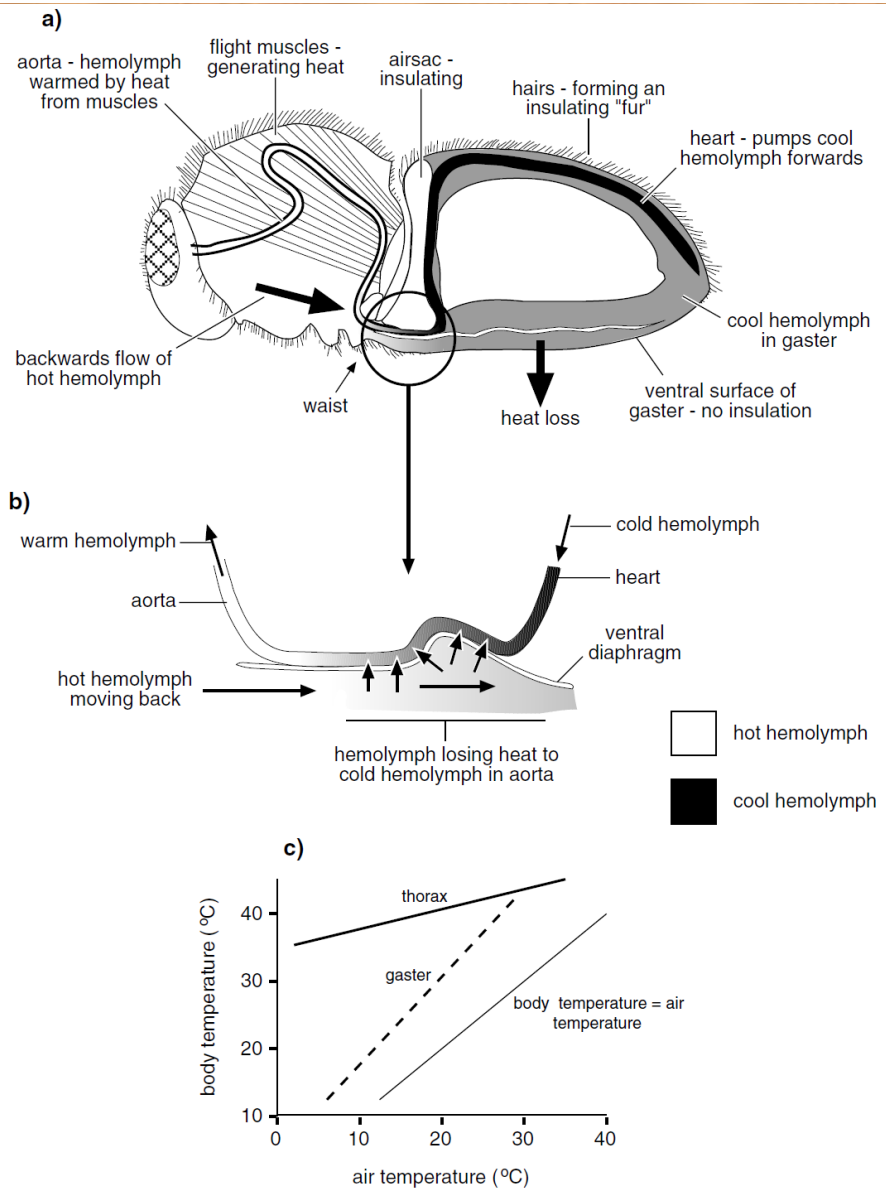

Fig. 19.3. Thermoregulation in a bumblebee (*Bombus*). **(a)** Sagittal section of a bee showing the features involved in regulating thoracic temperature (after Heinrich, 1976). **(b)** Detail of the heat exchange system in the waist region. As hot hemolymph flows back under the ventral diaphragm it loses heat to the cool, forwardly flowing hemolymph in the aorta (after Heinrich, 1976). **(c)** Temperature of the thorax and gaster of bumblebees in flight. As air temperature rises, the gaster gets markedly hotter. The insect cannot fly without overheating when thoracic temperature exceeds 45 °C. (after Heinrich, 1975).

Obr. 2 Svalová aktivita a produkce tepla při přípravě k letu a během vlastního letu

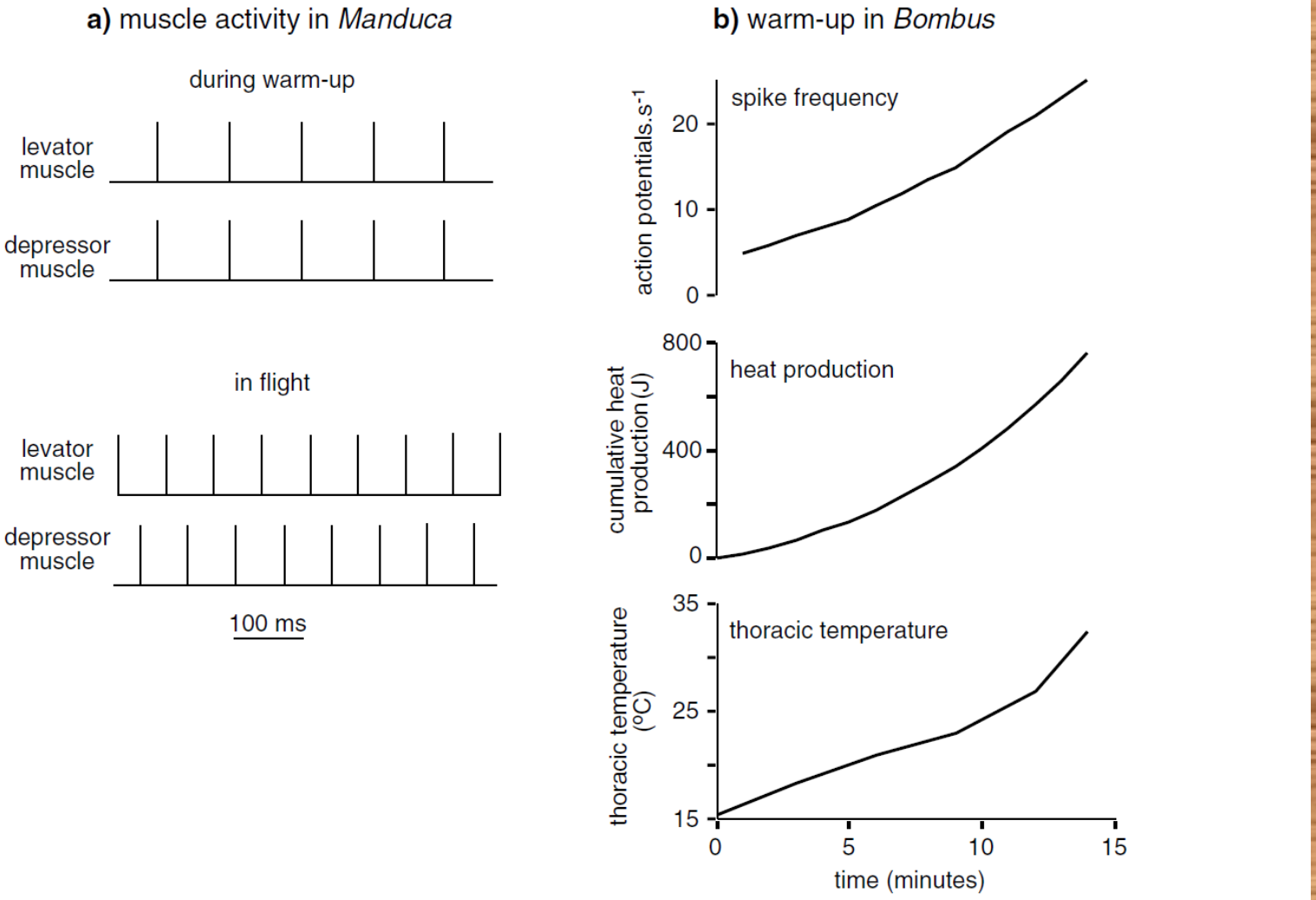

Fig. 19.2. Heat production during warm-up. **(a)** Activity of the flight muscles of a moth (*Manduca*). During warm-up, levator and depressor muscles contract at the same time; during flight they are in antiphase. **(b)** Warm-up in a bumblebee (*Bombus*). Time 0 is the start of warm-up behavior. Muscle activity (shown as spike frequency) increases over time as the thorax warms up. Notice that the total amount of heat produced, about 800 joules, is sufficient to raise the thoracic temperature by about 200 °C; it does not do so because more heat is lost as the difference between thoracic and air temperature increases. Air temperature in this experiment was 11 °C. The thorax was already hotter than this at the beginning of the experiment (after Heinrich & Kammer, 1973).

Obr. 3 **Vzrůst spotřeby kyslíku se zvyšující se teplotou**

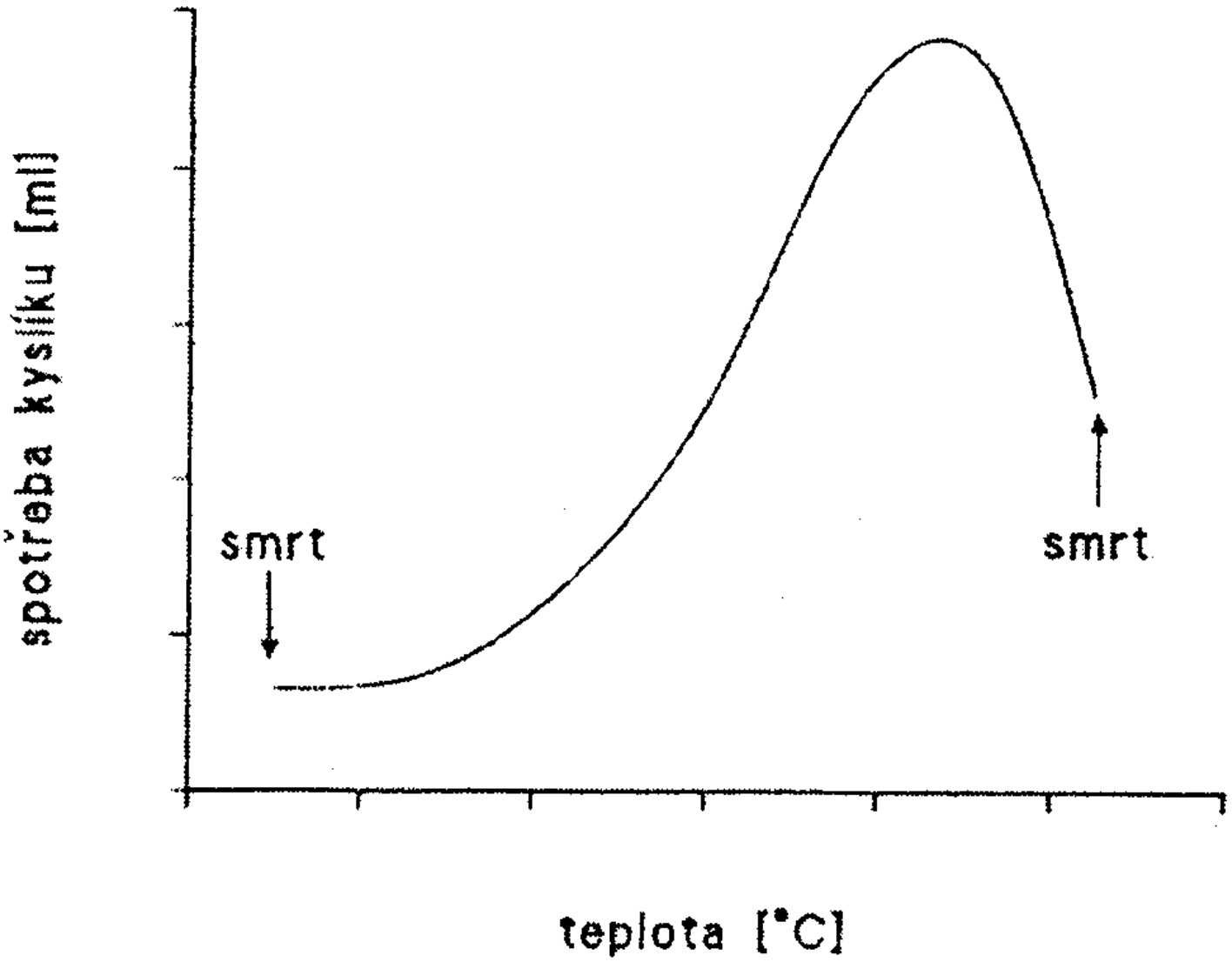

Fyziologický čas

Obr. 4

BOX 6.1
CALCULATION OF DAY-DEGREES

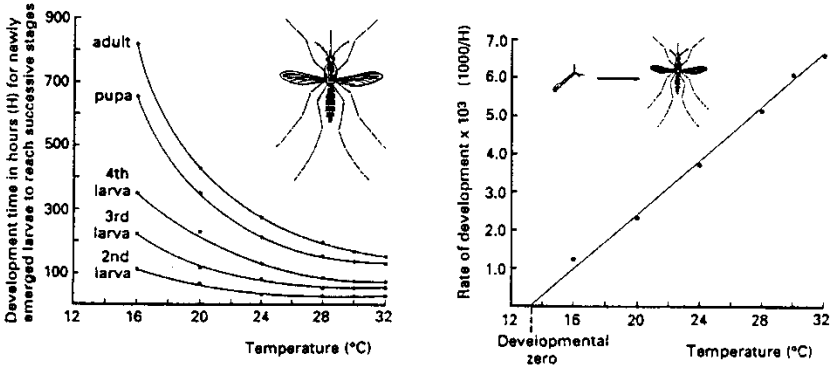

An outline of a simple method to estimate day-degrees (after Daly *et al.*, 1978) is exemplified by data on the relationship between temperature and development in the yellow fever mosquito, *Aedes aegypti* (Diptera: Culicidae) (after Bar-Zeev, 1958).

1. In the laboratory, establish the average time required for each stage to develop at different constant temperatures. The graph on left shows the time in hours (H) for newly hatched larvae of *Ae. aegypti* to reach successive stages of development when incubated at various temperatures.
2. Plot the reciprocal of development time (1/H), the development rate, against temperature to obtain a sigmoid curve with the middle part of the curve approximately linear. The graph on the right shows the linear part of this relationship for the total development of *Ae. aegypti* from the newly hatched larva to the adult stage. A straight line would not be obtained if extreme development temperatures (e.g. higher than 32 °C or lower than 16 °C) had been included.
3. Fit a linear regression line to the points and calculate the slope of this line. The slope represents the amount in hours by which development rates are increased for each one degree of increased temperature. Hence the reciprocal of the slope gives the number of hour-degrees, above threshold, required to complete development.
4. To estimate the developmental threshold, the regression line is projected to the x-axis (abscissa) to give the developmental zero, which in the case of *Ae. aegypti* is 13.3 °C. This zero value may differ slightly from the actual developmental threshold determined experimentally, probably because at low (or high) temperatures the temperature–development relationship is rarely linear. For *Ae. aegypti*, the developmental threshold actually lies between 9 and 10 °C.
5. The equation of the regression line is $1/H = k(T° - T')$, where H = development period, T° = temperature, T' = development threshold temperature, and k = slope of line.

Thus the physiological time for development is $H(T° - T') = 1/k$ hour-degrees; or $H(T° - T')/24 = 1/k = K$ day-degrees, where K = thermal constant or K-value.

By inserting the values of H, T° and T' for the data from *Ae. aegypti* in the equation given above, the value of K can be calculated for each of the experimental temperatures from 14–36 °C:

Temp.(°C)	14	16	20	24	28	30	32	34	36
K	1008	2211	2834	2921	2866	2755	2861	3415	3882

Thus the K-value for *Ae. aegypti* is approximately independent of temperature, except at extremes (14 and 34–36 °C), and averages about 2740 hour-degrees or 114 day-degrees between 16 and 32 °C.

Obr. 5 Přežívání nízkých teplot

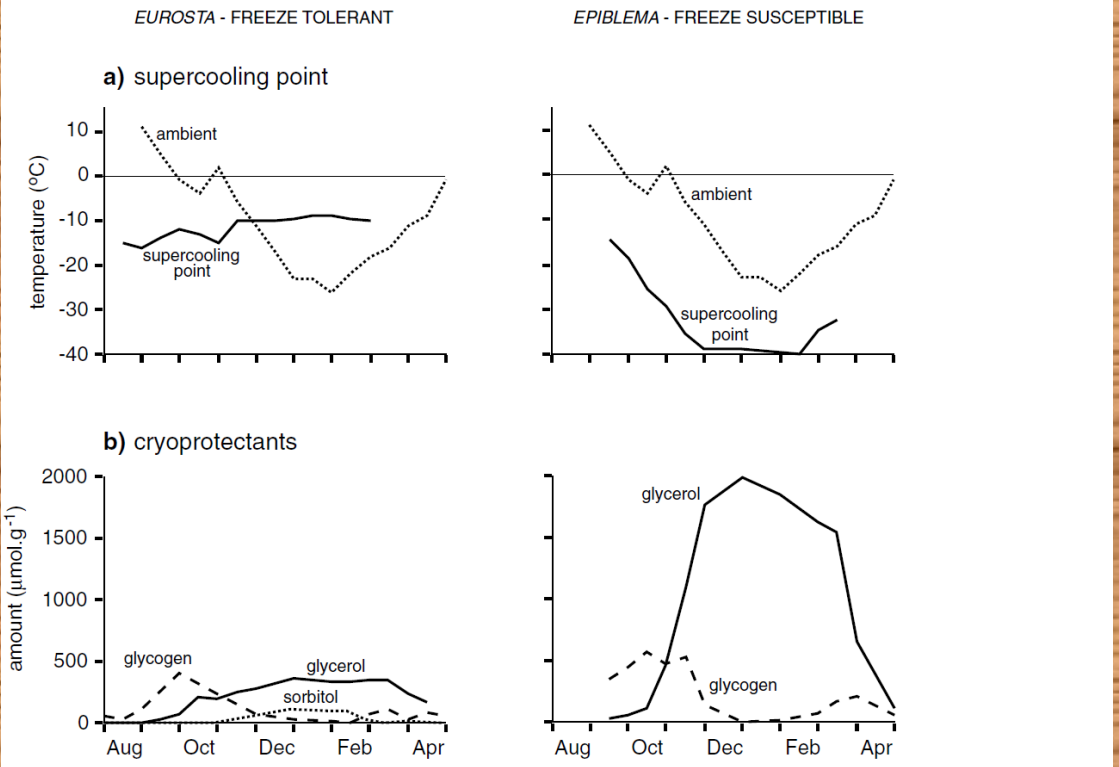

Fig. 19.12. Supercooling points and cryoprotectants of two insects that use different strategies to survive low temperatures during the winter. *Eurosta* is a gall fly that tolerates freezing. *Epiblema* is a gall moth that is freeze susceptible, but has a low supercooling point. Both species overwinter in the last larval stage in galls on the host plant, and both may occur on the same plant. Data in the figure relates primarily to insects overwintering near Ottawa, Canada. (a) Variation in supercooling points over the winter. Ambient temperatures are the minima occurring over a two-week period in one year. Notice that minimum temperatures are below the supercooling point of *Eurosta* for several months; the supercooling point of *Epiblema* is always well below the environmental minima (based on Morrissey & Baust, 1976; Rickards, Kelleher & Storey, 1987). (b) Seasonal changes in glycogen and the cryoprotectants, glycerol and sorbitol, that are derived from it. Notice that glycerol levels in the freeze susceptible insects reach levels five times higher than in the freeze tolerant insect. *Epiblema* produces very little sorbitol. Amounts are expressed in relation to the wet weights of the insects (based on Rickards, Kelleher & Storey, 1987; Storey & Storey, 1986).

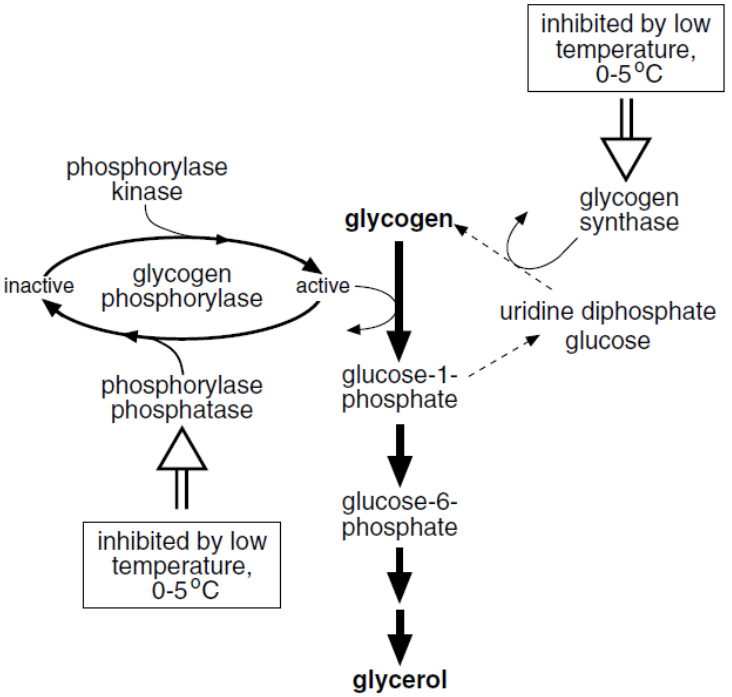

Fig. 19.13. Synthesis of glycerol from glycogen. At low temperatures, the conversion of glycogen phosphorylase from the active to the inactive form is inhibited; the production of the active form continues. As a result, the proportion of this enzyme in the active form is greatly increased so glycogen is metabolized to glucose-6-phosphate. Other enzymes (not shown) then lead to the synthesis of glycerol or sorbitol. Reconversion of glucose-1-phosphate to glycogen does not occur because the activity of glycogen synthase is inhibited by low temperature.

Obr. 6

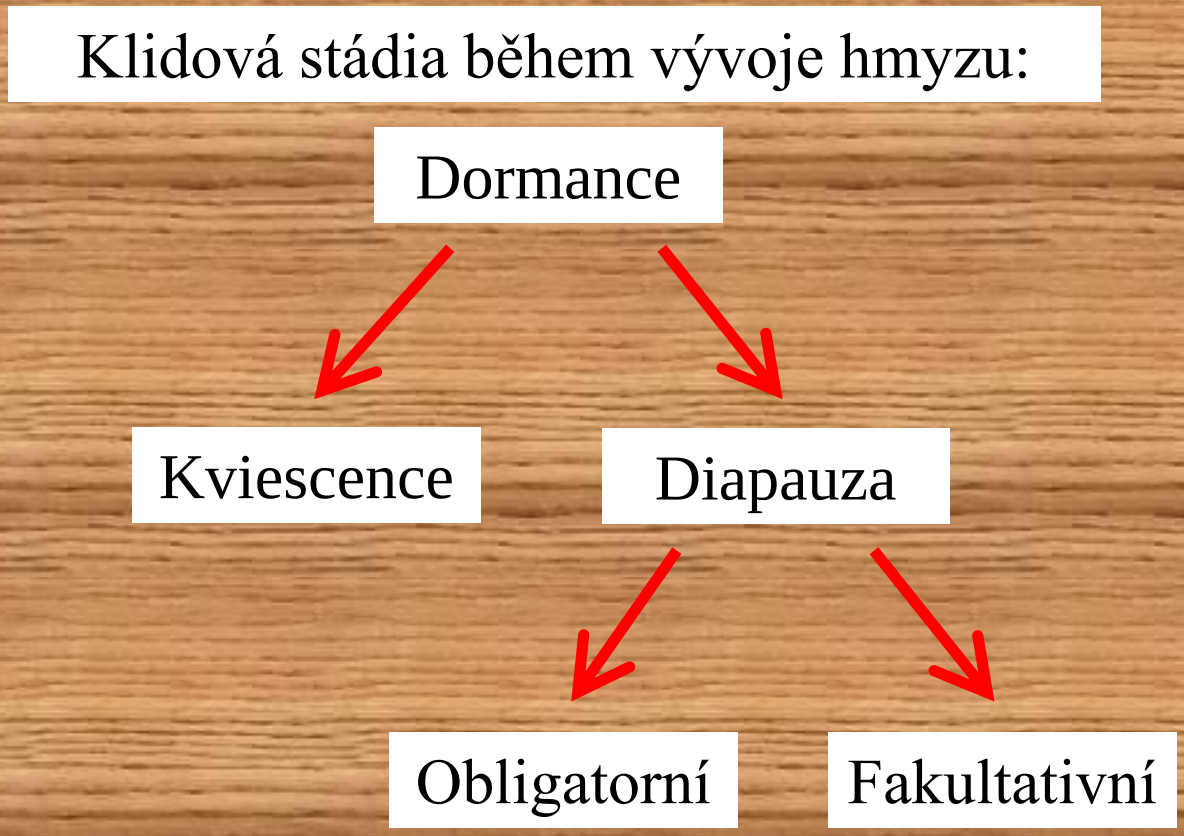
Klidová stádia během vývoje hmyzu:
Dormance
Kviescence
Diapauza
Obligatorní
Fakultativní

Fázový dimorfismus u saranče pustinné *Schistocerca gregaria*

Soliterní fáze **Gregarinní fáze**

Obr. 7

8. Nervová činnost

Obr. 1

Reflexní oblouk

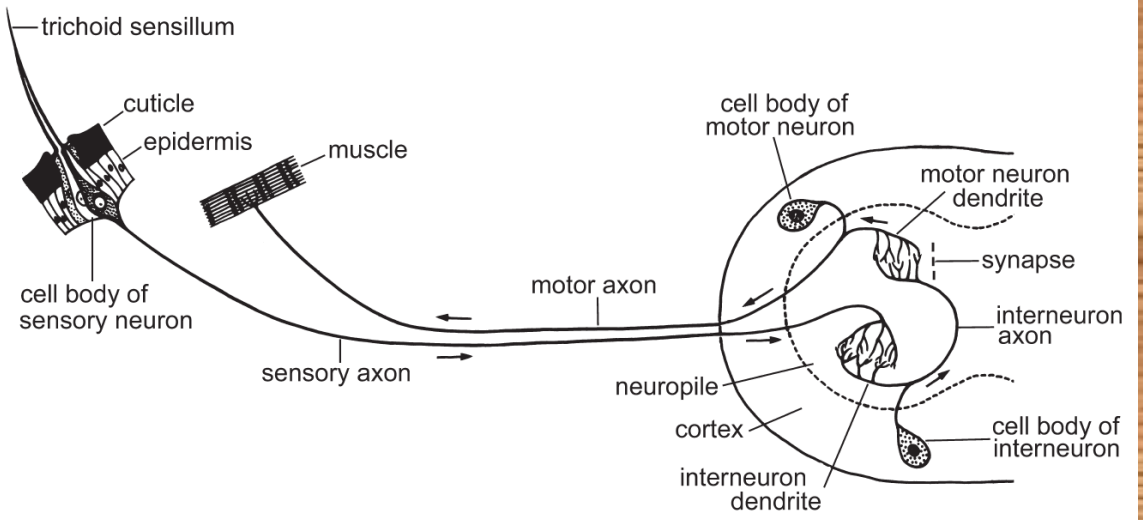

Fig. 3.5 Diagram of a simple reflex mechanism of an insect. The arrows show the paths of nerve impulses along nerve fibers (axons and dendrites). The ganglion, with its outer cortex and inner neuropile, is shown on the right. (After various sources.)

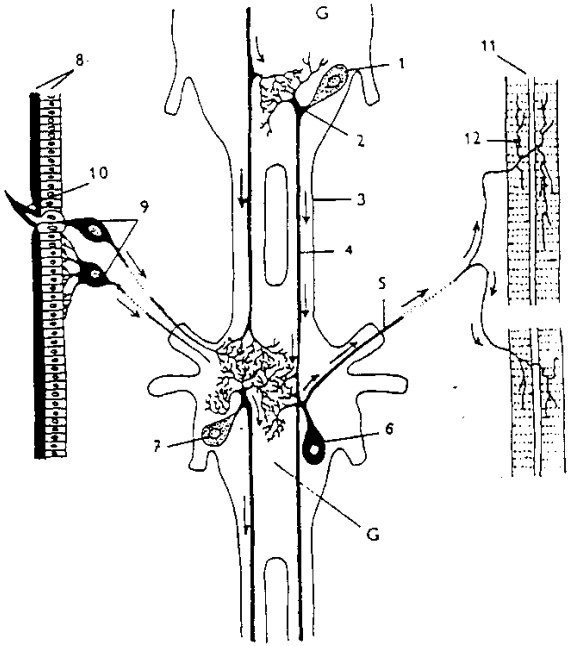

Obr.142.Schéma histologické stavby nervového systému hmyzu. Šipky udávají směr vedení podráždění. - (G - ganglion, 1 - asociační buňka, 2 - dendrit, 3 - konektiv či nervová spojka dvou zauzlin, 4 - axon, výběžek, 5 - axon motorické buňky, 6 - motorická buňka, 7 - asociační buňka, 8 - epidermis a kutikula, 9 - sensitivní buňky, 10 - sensilla, 11 - svalové vlákno, 12 - motorická nervová zakončení).

Obr. 2 Hmyzí neurony a stavba ganglia

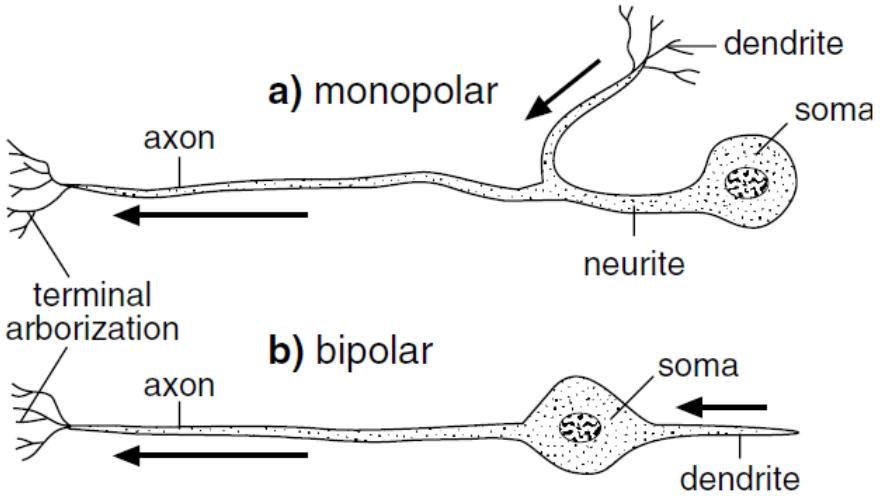

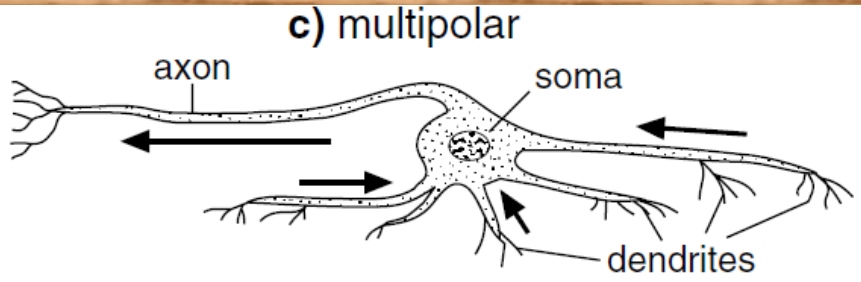

Fig. 20.1. Neurons. Diagrammatic representation of basic types of neuron. Arrow shows direction of conduction.

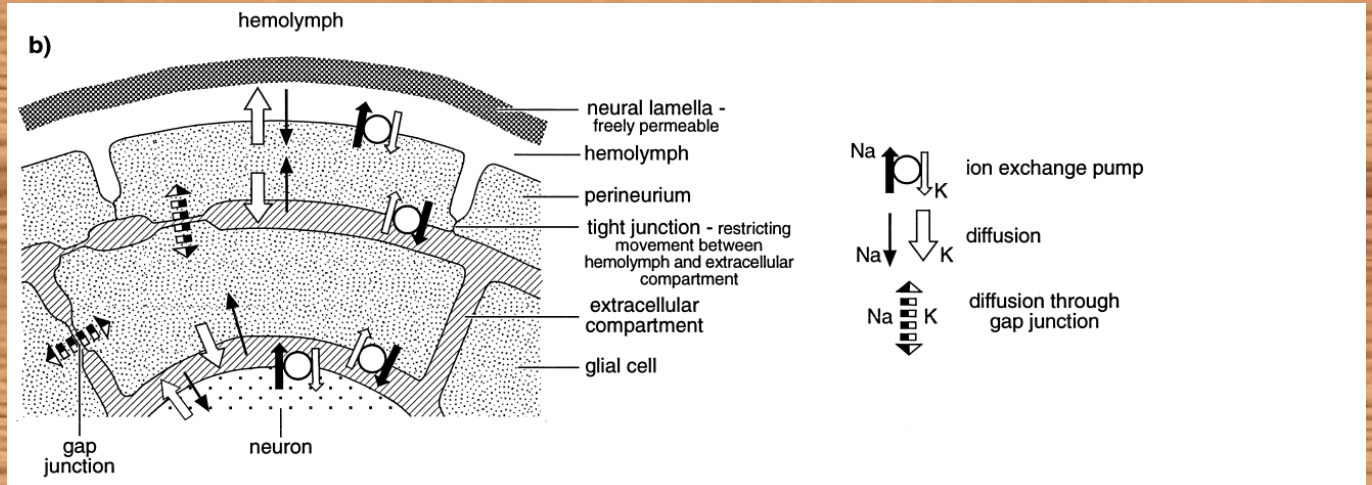

Fig. 20.3. Glia. **(a)** Diagrammatic section of part of an abdominal ganglion showing glial cells (light shading) that play different roles. Axons A and B are referred to in the text (after Smith & Treherne, 1963). **(b)** Representation of the role of glial cells in maintaining a constant ionic composition of the fluid bathing the neurons in a ganglion. The extracellular compartment is shown hatched to emphasize its isolation from the hemocoel. The pumps maintain a high concentration of sodium and low potassium in this compartment despite the diffusive movements of the ions. Broad open arrows indicate greater permeability to potassium than to sodium ions (after Treherne & Schofield, 1981).

Obr. 3

Akční potenciál a biologicky aktivní látky produkované neurony

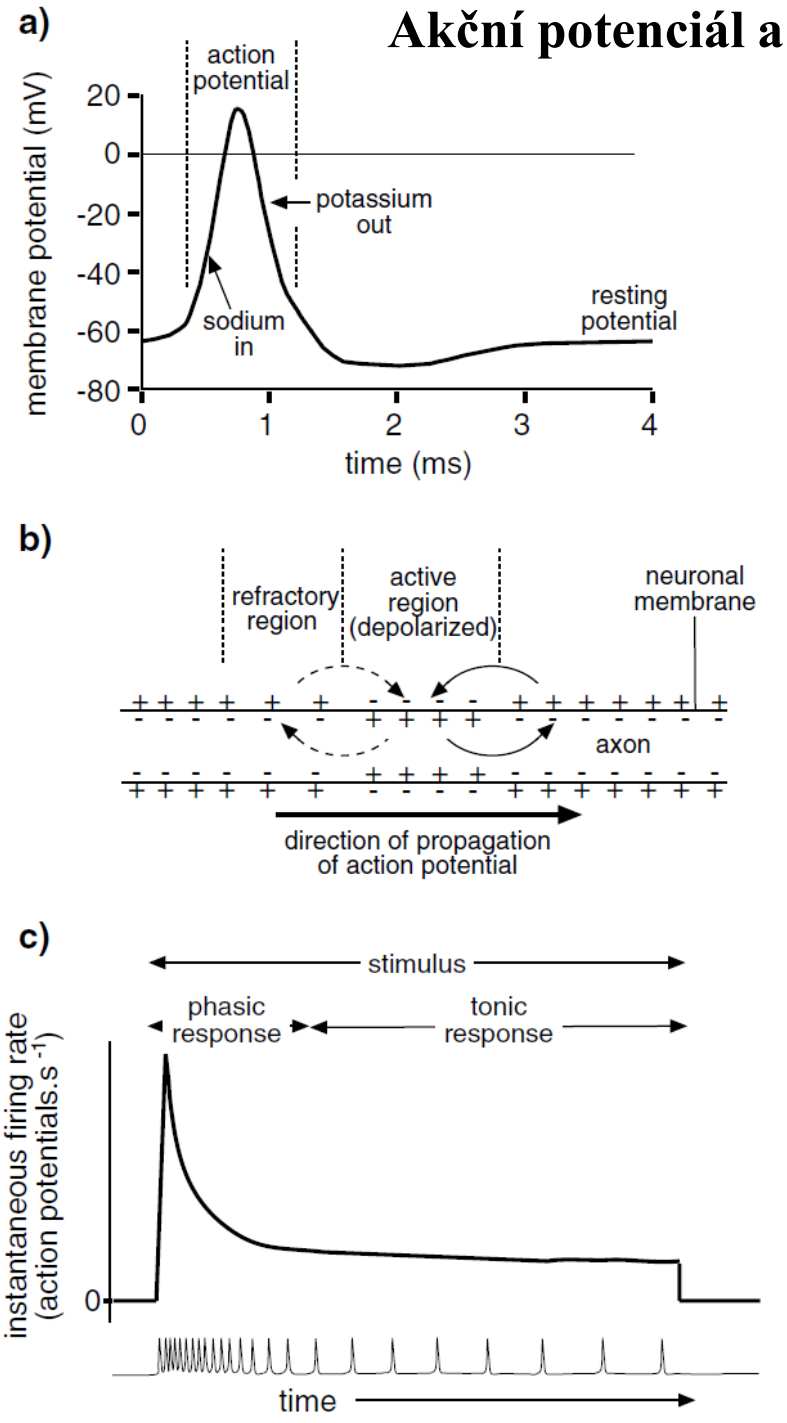

Table 20.2. *Substances secreted by neurons in the central nervous system and their principal functions*

Chemical	Neurotransmitter	Neuromodulator	Neurohormone
Acetylcholine	+++ (excitatory in CNS)		
Biogenic amines			
Dopamine	+	+	
Histamine	+		
Serotonin (5-hydroxytryptamine)		++	+
Octopamine	+	+++	+
Amino acids			
γ-aminobutyric acid (GABA)	+++ (inhibitory)		
Glutamate	+++ (excitatory at muscles)		
Peptides			
Adipokinetic hormone			+++
Allatotropin		+	+
Allatostatin		+	+
Cardioactive peptide			+++
Diuretic peptide			+++
FMRFamide		+	
Leucokinin		+	
Pheromone biosynthesis (PBAN)		+	++
Proctolin	+	+++	+
Prothoracicotropic hormone			+++

Note:
+++, major function; +, occasional function.

Obr. 4 **Synapse**

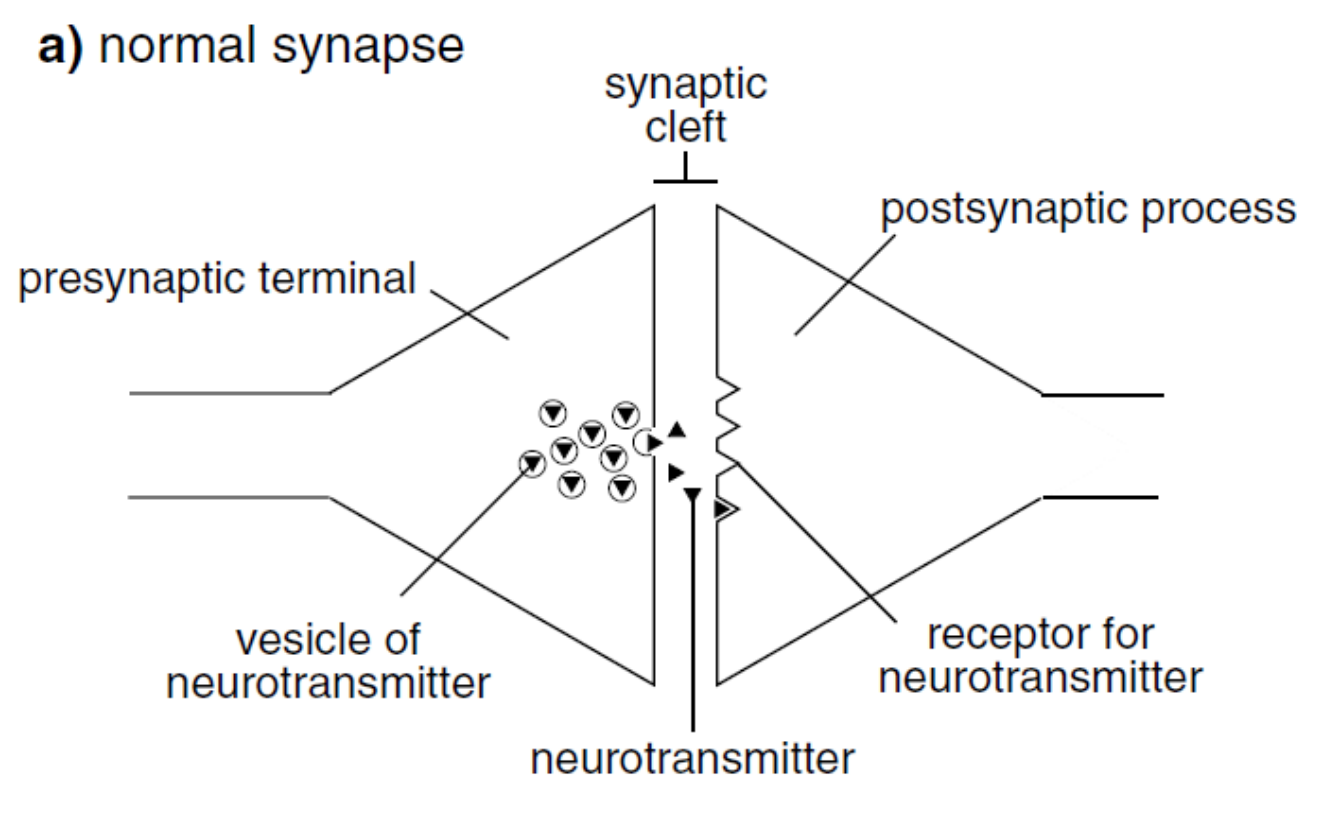

Typy biogenních aminů

Obr. 5

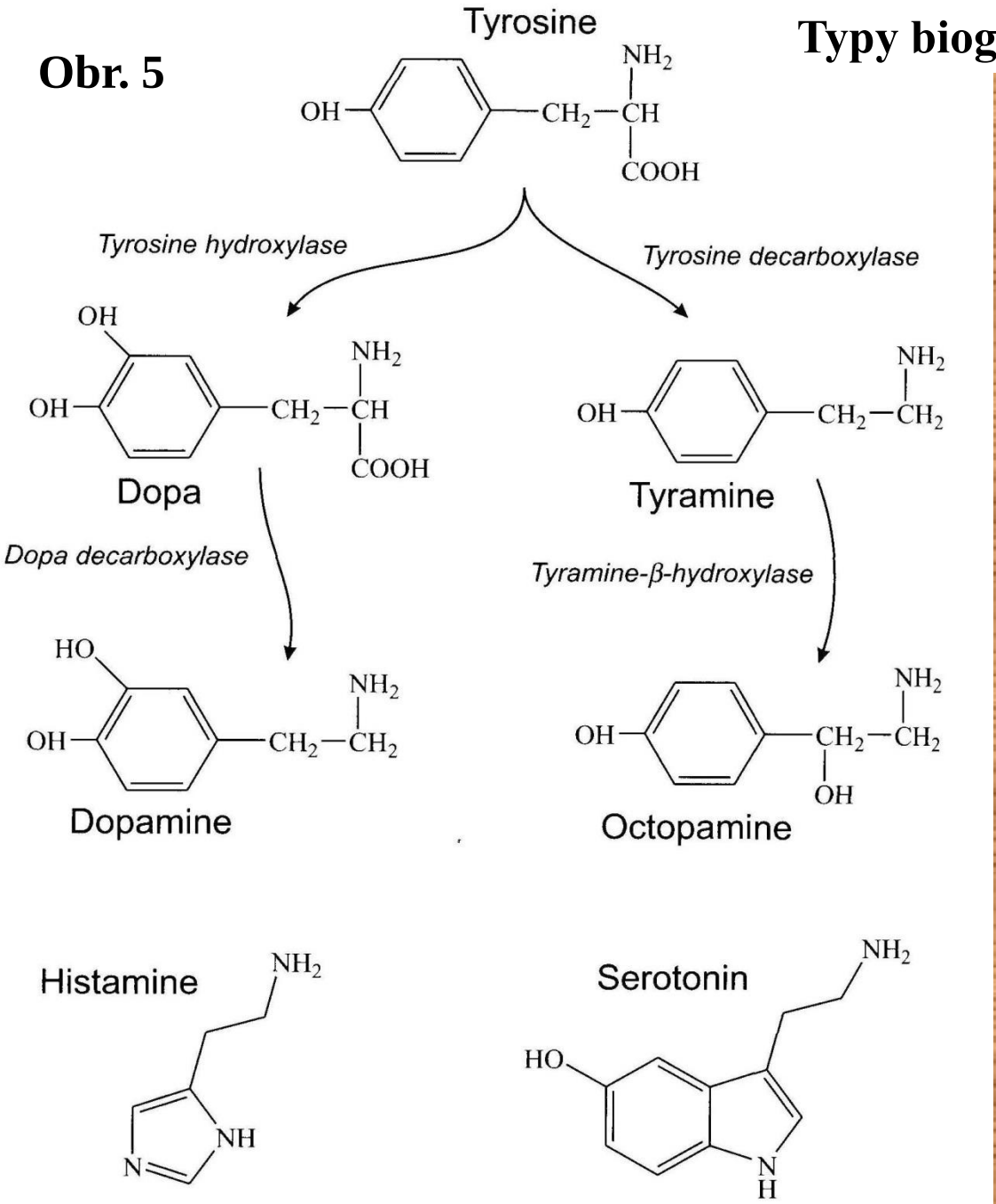

FIGURE 11.7. Synthesis of biogenic amines from tyrosine.

Obr. 6 Typy mediátorů

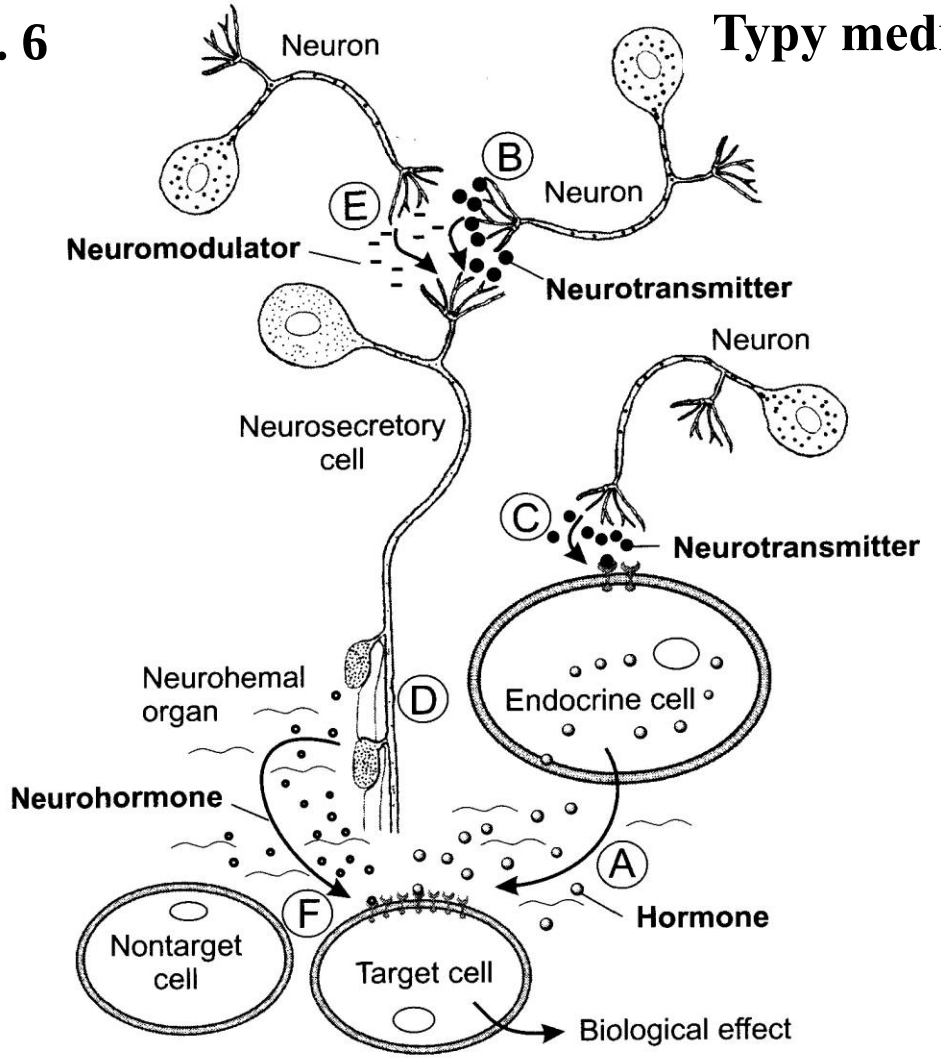

FIGURE 1.1. Some examples of neurotransmitter release. A. An endocrine cell releasing a hormone into the circulatory system. B. A neuron synapsing with a neurosecretory cell, releasing a neurotransmitter at the synapse. C. A neuron synapsing with an endocrine cell, releasing a neurotransmitter. D. A neurosecretory cell releasing a neurohormone into the circulatory system at a neurohemal organ. E. An inhibitory neuron synapsing with a neurosecretory cell, releasing a neuromodulator at the synapse. F. Receptors on target cells recognize specific neurohormones in circulation, resulting in a biological effect. The absence of receptors on nontarget cells results in the cell not being able to respond to the circulating chemical messages, and any molecules taken up nonspecifically are degraded.

Obr. 7 Děje na synapsích

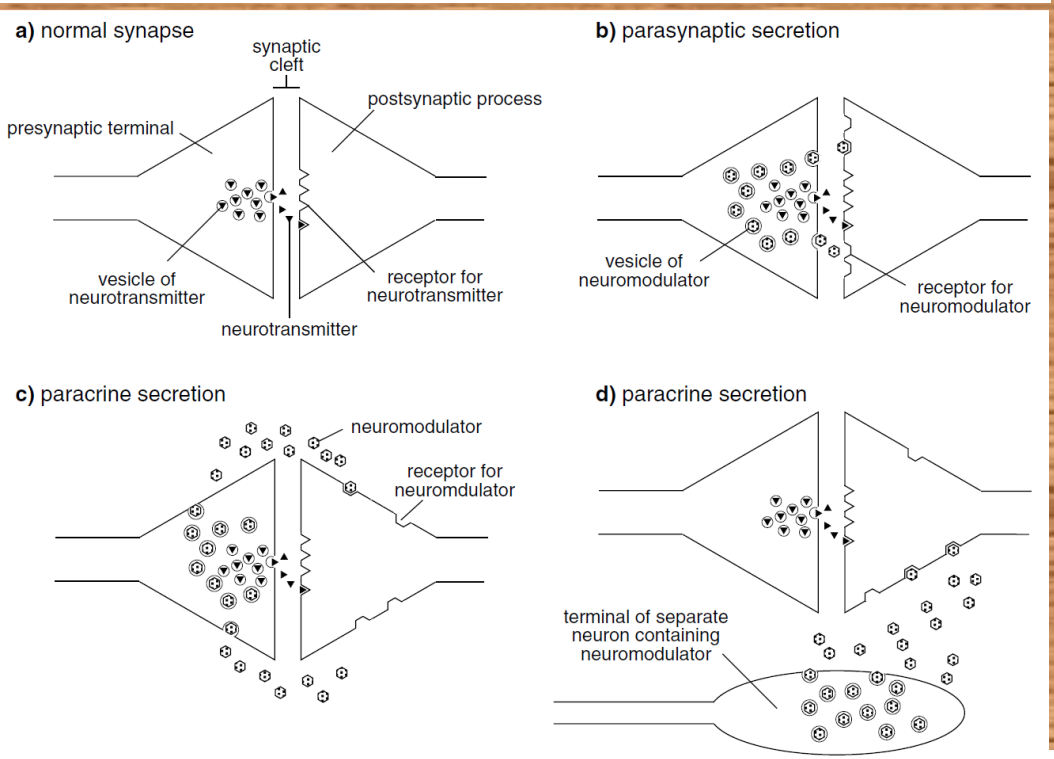

Fig. 20.7. Neuromodulation at a synapse. Diagrammatic representation of different pathways by which neuromodulators may affect the postsynaptic element. Transmitter compound is shown as black triangles; neuromodulator as shaded hexagons. **(a)** A synapse with no neuromodulators. **(b)** Parasynaptic secretion. The neuromodulator co-occurs with the transmitter and acts close to the synapse. **(c)** Paracrine secretion. The neuromodulator co-occurs with the transmitter but is released round the area of the synapse. It may affect other neurons in the vicinity. **(d)** Paracrine secretion. The neuromodulator is produced by a separate neuron and affects the general environment around the synapse.

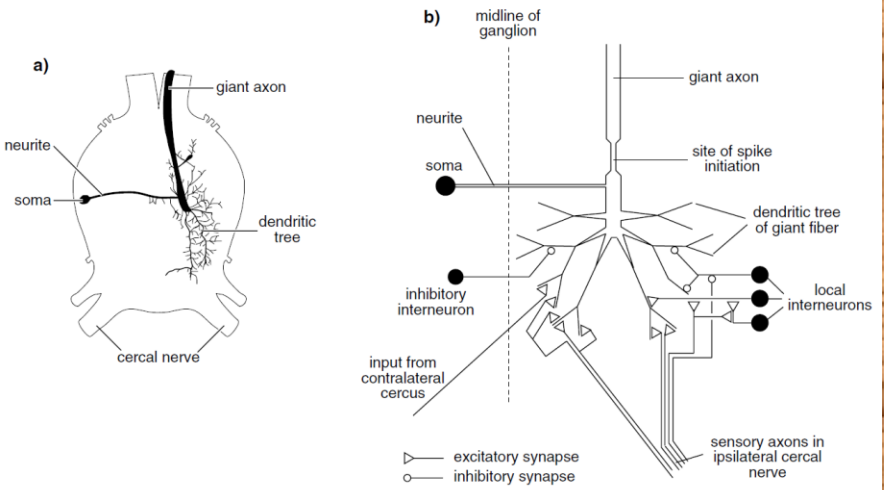

Fig. 20.14 Integration at synapses. A giant fiber in the terminal abdominal ganglion of *Periplaneta* (after Callec, 1985). **(a)** Diagram showing the dendritic arbor and contralateral position of the soma. **(b)** The neuron with the giant axon receives direct input on to its dendritic branches from sensory neurons in both the ipsilateral and contralateral cerci as well as from local interneurons. Inputs are both excitatory and inhibitory.

Obr. 8 Vývoj koncentrované nervové soustavy

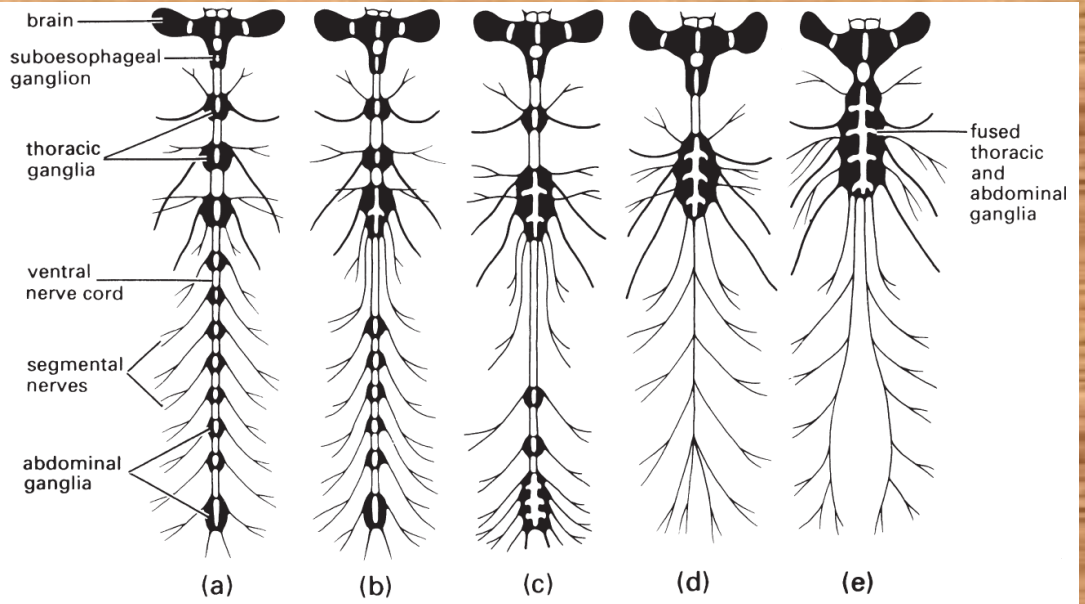

Fig. 3.6 The central nervous system of various insects showing the diversity of arrangement of ganglia in the ventral nerve cord. Varying degrees of fusion of ganglia occur from the least to the most specialized: (a) three separate thoracic and eight abdominal ganglia, as in *Dictyopterus* (Coleoptera: Lycidae) and *Pulex* (Siphonaptera: Pulicidae); (b) three thoracic and six abdominal, as in *Blatta* (Blattodea: Blattidae) and *Chironomus* (Diptera: Chironomidae); (c) two thoracic and considerable abdominal fusion of ganglia, as in *Crabro* and *Eucera* (Hymenoptera: Crabronidae and Anthophoridae); (d) highly fused with one thoracic and no abdominal ganglia, as in *Musca*, *Calliphora*, and *Lucilia* (Diptera: Muscidae and Calliphoridae); (e) extreme fusion with no separate suboesophageal ganglion, as in *Hydrometra* (Hemiptera: Hydrometridae) and *Rhizotrogus* (Scarabaeidae). (After Horridge 1965.)

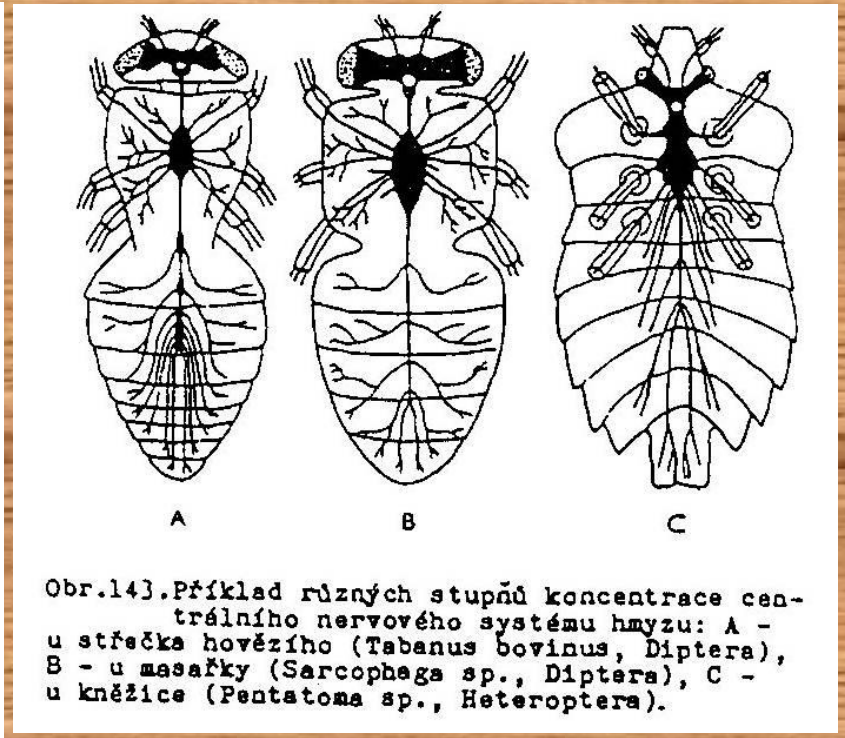

Obr.143.Příklad různých stupňů koncentrace centrálního nervového systému hmyzu: A - u střečka hovězího (Tabanus bovinus, Diptera), B - u masařky (Sarcophaga sp., Diptera), C - u kněžice (Pentatoma sp., Heteroptera).

Obr. 9

Obecná struktura hmyzího ganglia

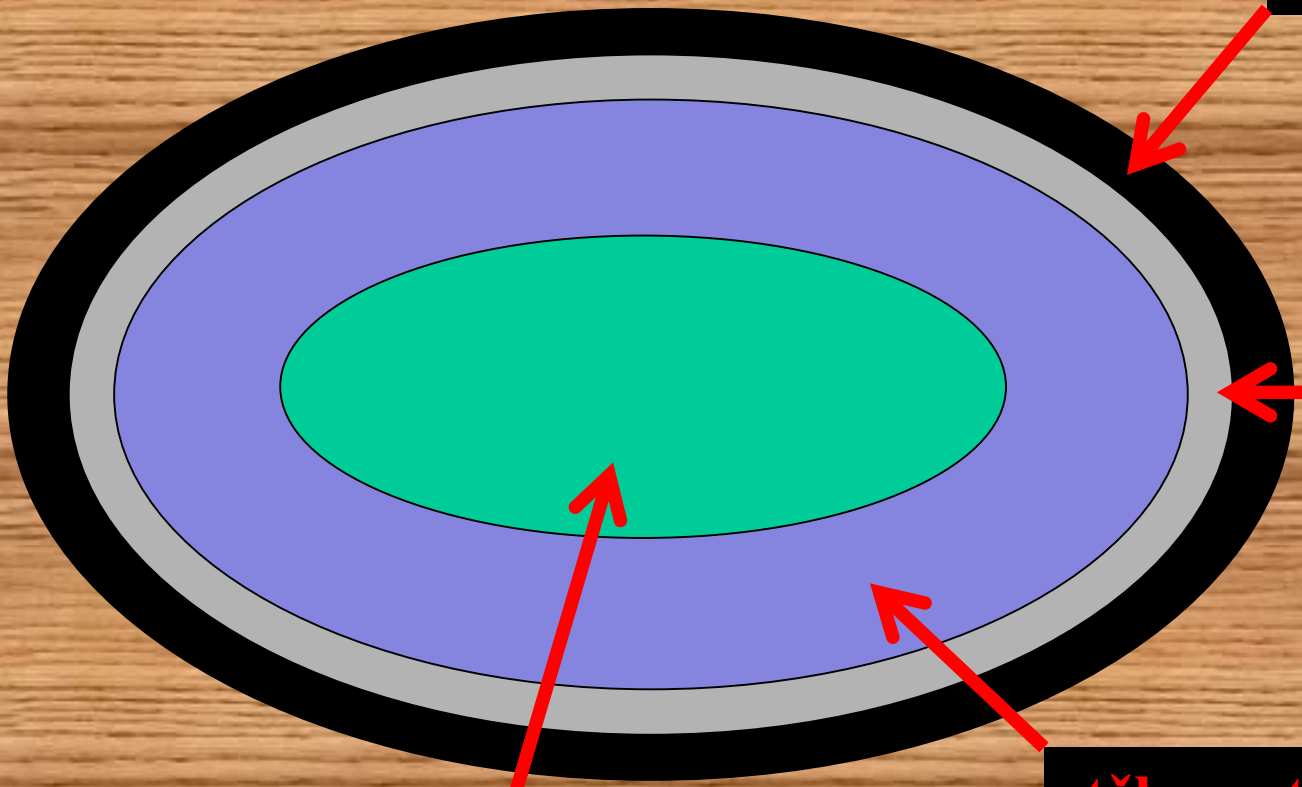

neurální lamela

perineurium

těla motorických neuronů a interneuronů

neuropile

Obr. 10

Řez hmyzím gangliem

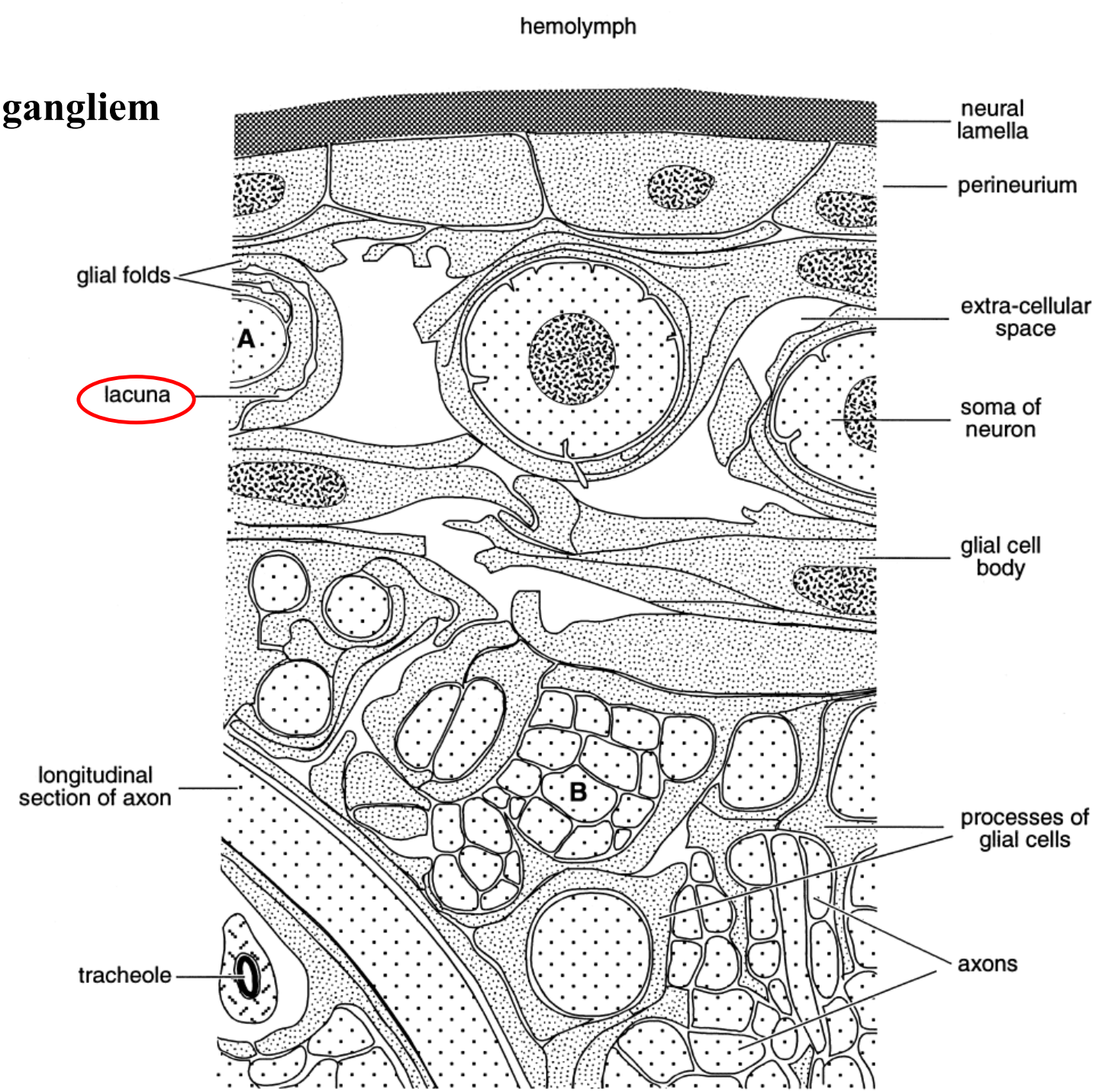

Obr. 11 Mozek ruměnice pospolné *Pyrrhocoris apterus*, SEM, foto - F. Weyda

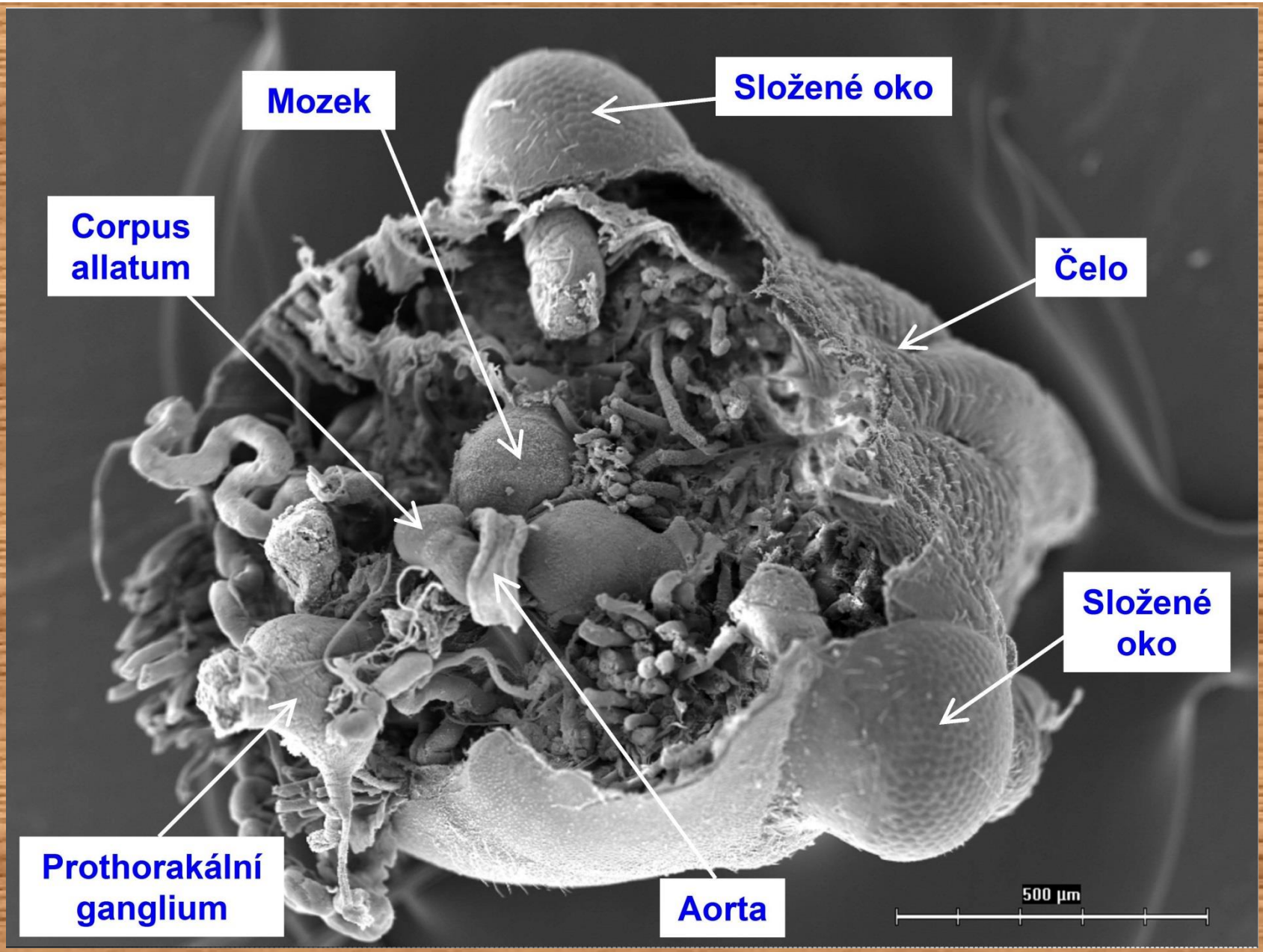

Obr. 12

Schématická zobrazení hmyzího mozku

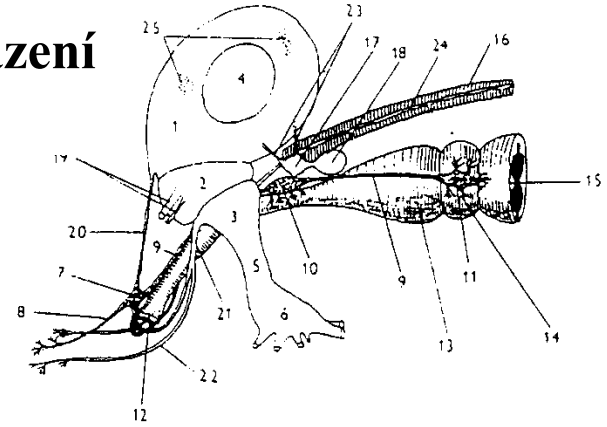

Obr.144.Schéma mozku a stomatogastrického systému hmyzu - pohled z boku. (1 - protocerebrum, 2 - deutocerebrum, 3 - tritocerebrum, 4 - oční lalok, 5 - obloukovitá spojka mozku a podjícnového ganglia, 6 - podjícnové ganglion, 7 - čelní ganglion, 8 - nervus procurrens, 9 - nervus recurrens, 10 - hypocerebrální ganglion, 11 - ventrikulární ganglion, 12 - jícen, 13 - vole, 14 - žvýkací žaludek, 15 - střední střevo, 16 - aorta, 17 - corpora cardiaca, 18 - corpora allata, 19 - motorická a sensitivní větev tykadlového nervu, 20 - nervus connectivus, 21 - čelní konektiv, 22 - pyskový nerv, 23 - nervus corporis cardiaci, 24 - boční srdeční nerv, 25 - skupiny neurosekretorických buněk).

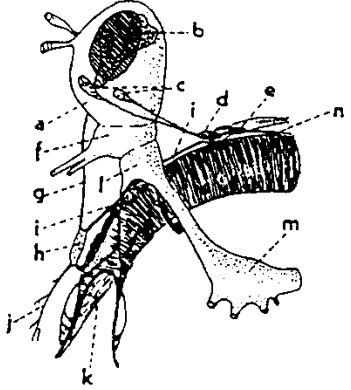

Mozek hmyzu

a = protocerebrální lalok, b = houbovité těleso, c = neurosekreční bunky mozku, d = corpora cardiaca, e = corpora allata, f = deutocerebrum, g = nervus connektivus, h = frontální uzlina, i = nervus recurrentis, j = nervus procurrens, k = cibarium, l = tritocerebrum, m = podjícnová (subesofageální) uzlina, (g, h, i, j) = součásti stomatogastrického vegetativního nervstva, n = viscerální nerv

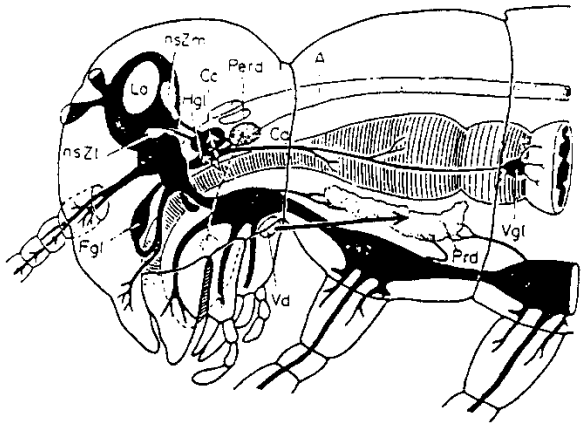

Obr.145.Schéma přední části těla larvy s nervovým systémem (vyznačen černě) a s inkretorickými orgány, jejichž ontogenetický původ je naznačen šipkami. (A - aorta, Ca - corpora allata, Cc - corpora cardiaca, Fgl - čelní ganglion, Hgl - hypocerebrální ganglion, Lo - oční lalok, Nr - nervus recurrens, nsZl+nsZm - skupiny neurosekretorických buněk v mozku, Oes - jícen, Perd - perikardiální žláza, Prd - prothorakální žláza, Tr - vzdušnice, Usgl - podjícnové ganglion, Vd - ventrální žláza, Vgl - ventrikulární ganglion).

Obr. 13 Hmyzí mozek a umístění neuropil v něm

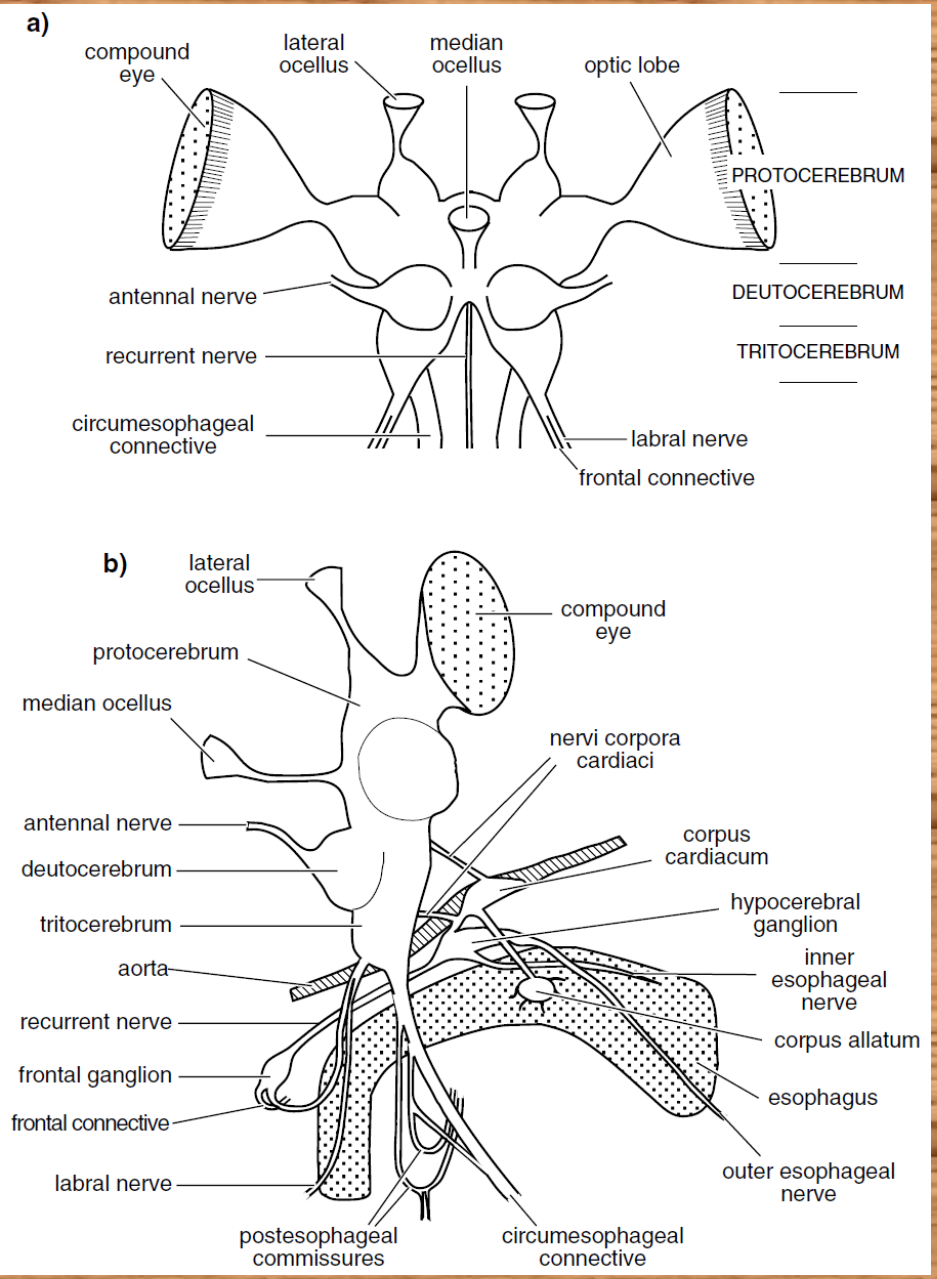

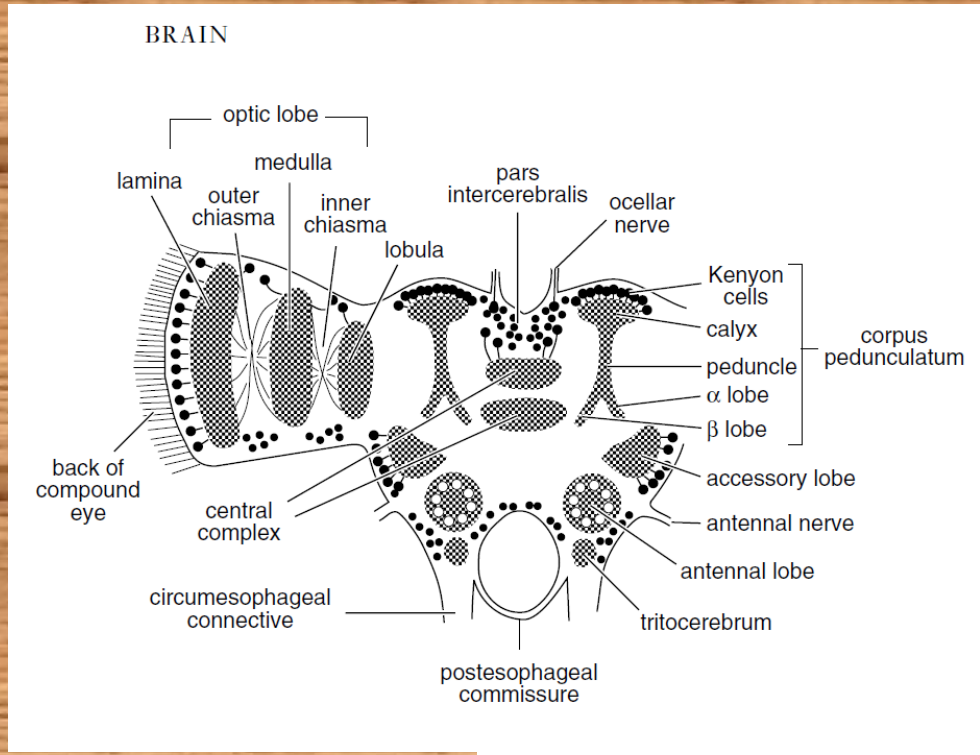

Fig. 20.17. Brain. The main regions of organized neuropil (shaded). The distribution of somata is indicated by the black dots.

Imunochemická lokalizace prothoracicotropního hormonu v mozku kukly *Manduca sexta*

Obr. 14

Obr. 15

Model paměti u *Drosophila*

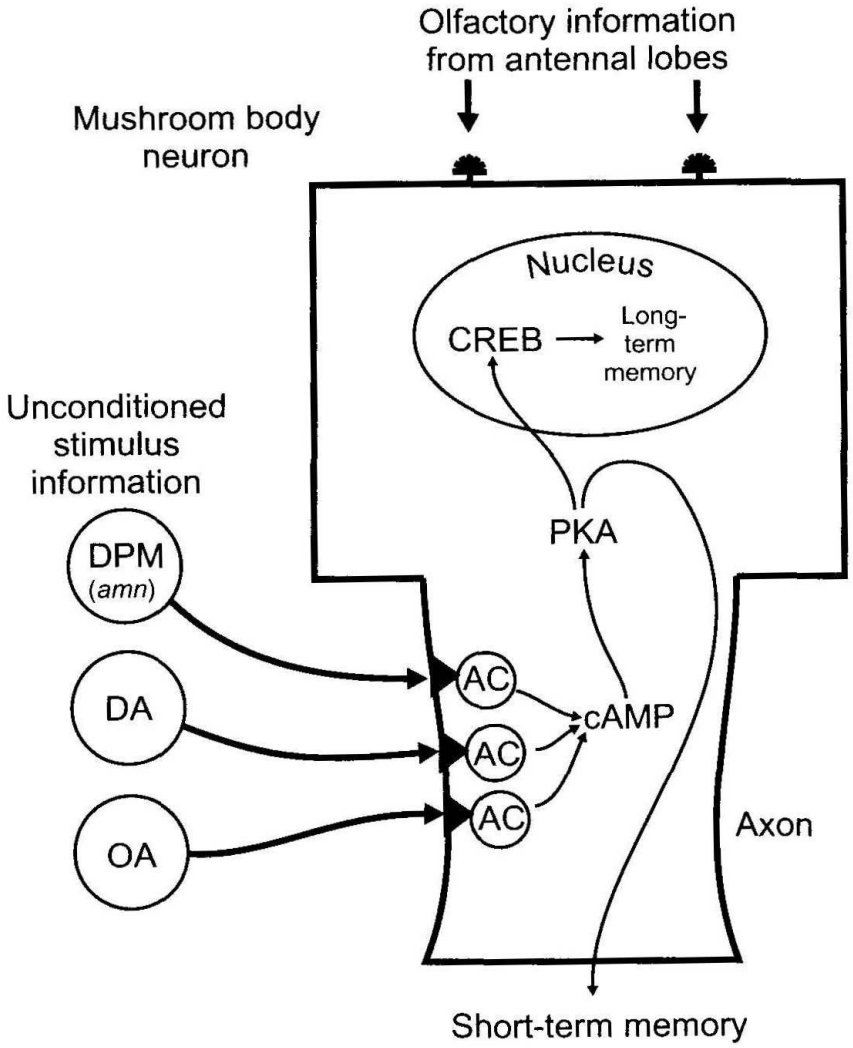

FIGURE 5.3. A model for short- and long-term memory in *Drosophila*. The antennal lobes receive olfactory information that can be associated with unconditioned stimulus information from dorsal paired medial (DPM), dopaminergic (DA), and octopaminergic (OA) neurons. DPM neurons express the *amnesiac* (*amn*) peptides. These neurons can activate adenylate cyclase (AC) that elevates cAMP, which then activates protein kinase A (PKA). PKA can establish short-term memory by phosphorylating other proteins or by phosphorylating cAMP response element binding protein (CREB) and establishing long-term memory.

Obr. 16a

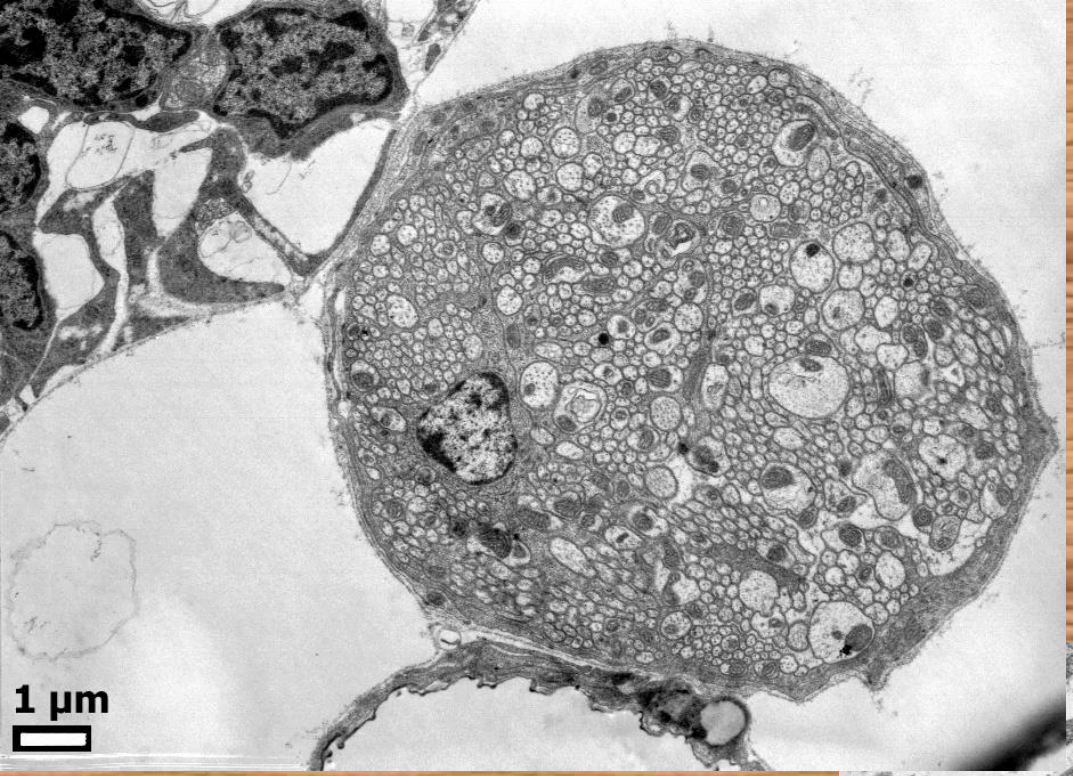

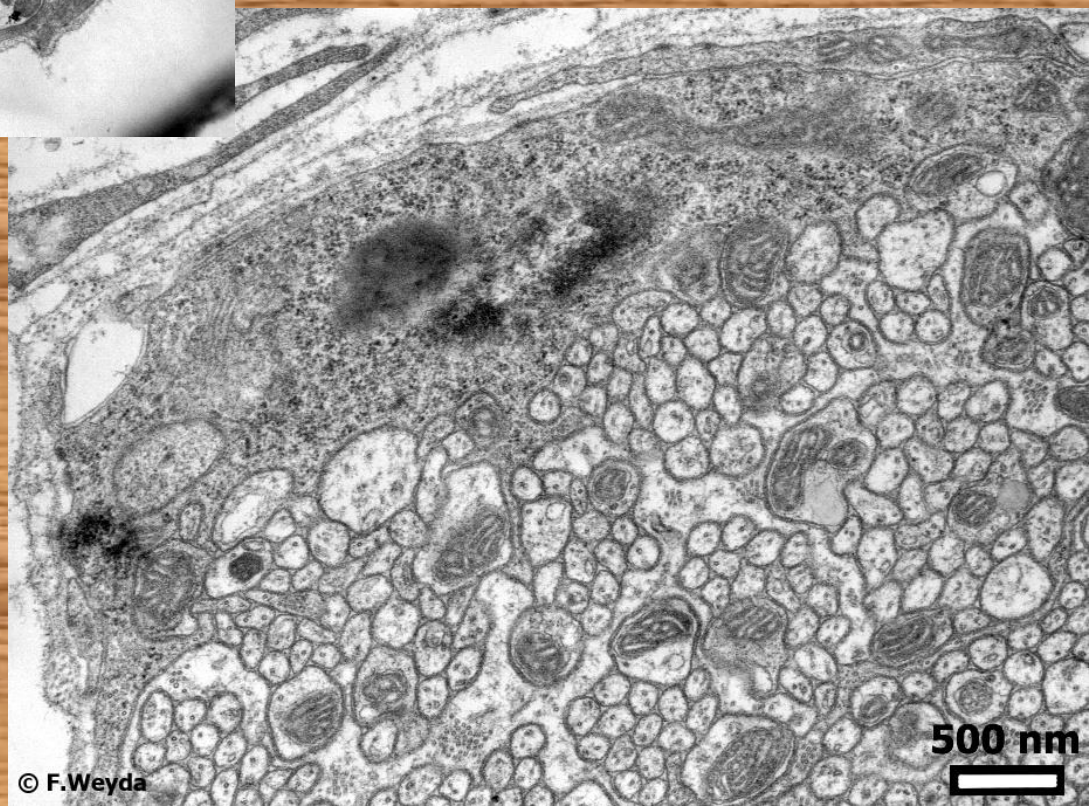

Antenalní nerv - svazek axonů procházejících tykadlem a inervujících antenální sensily (nahoře) a detail (vpravo)

Nerv femuru ruměnice pospolné *Pyrrhocoris apterus*, TEM, foto - F. Weyda

Obr. 16b

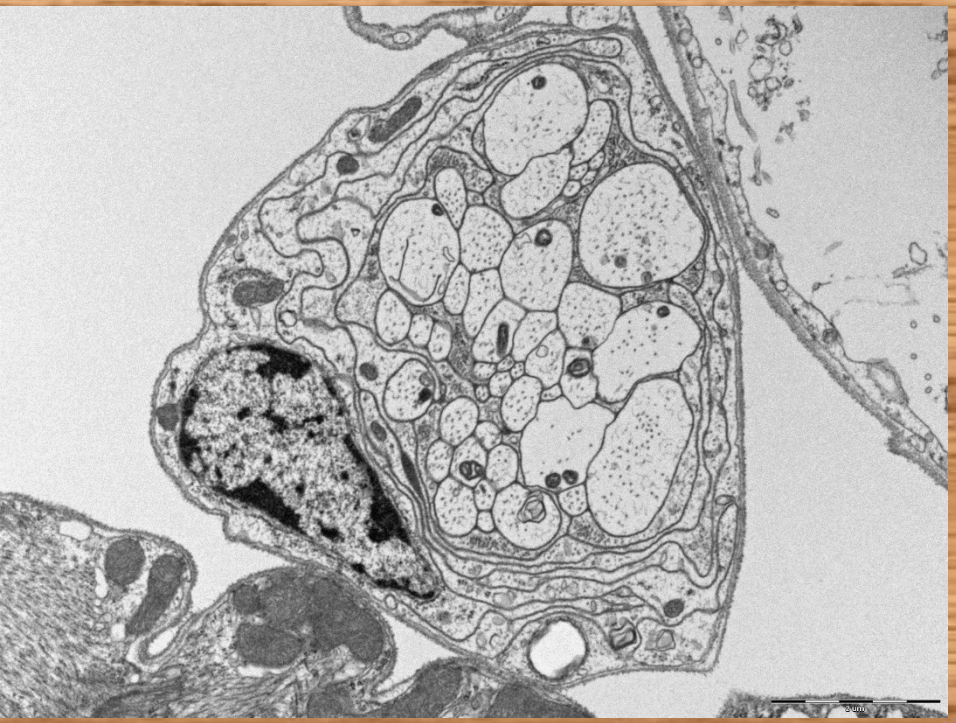

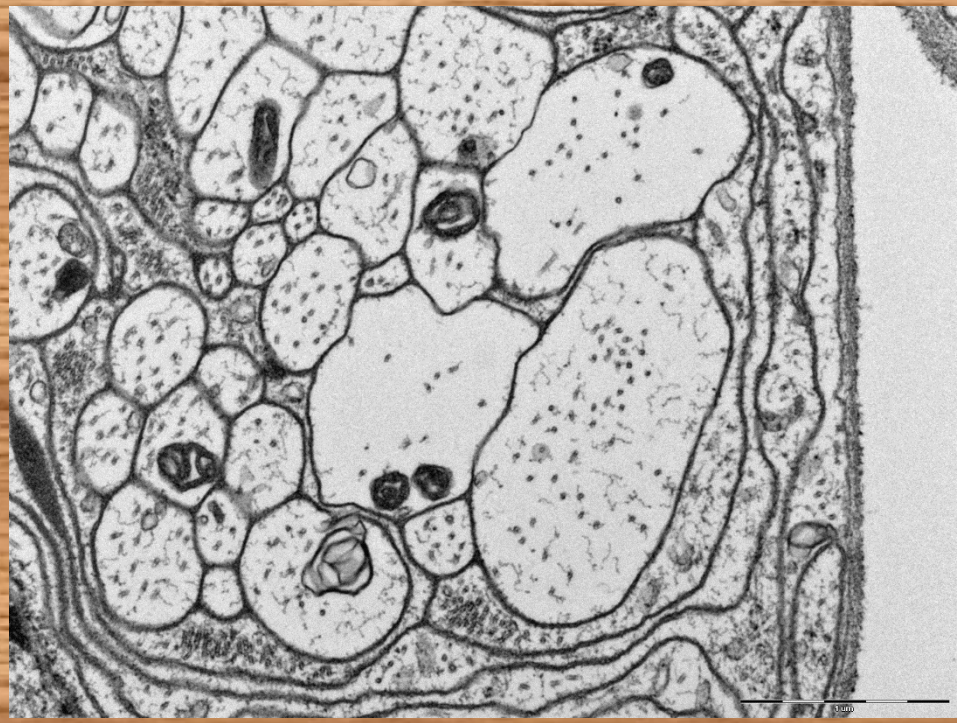

Nerv femuru ruměnice pospolné *Pyrrhocoris apterus* (podélný řez), TEM, foto - F. Weyda

Obr. 16b

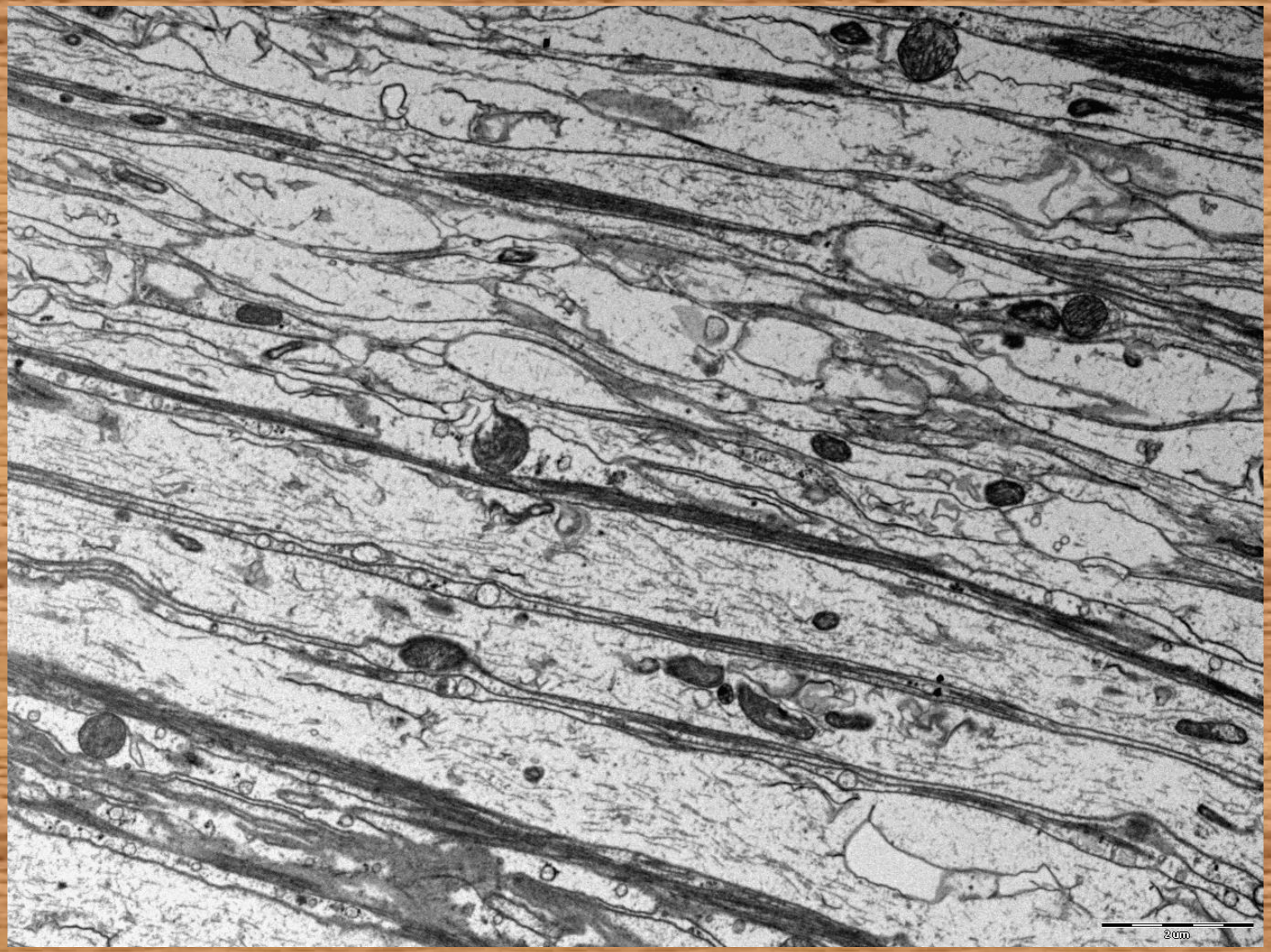

http://www.youtube.com/watch?v=pNCMz2HzKRg

Obr. 17

Orientace v prostoru

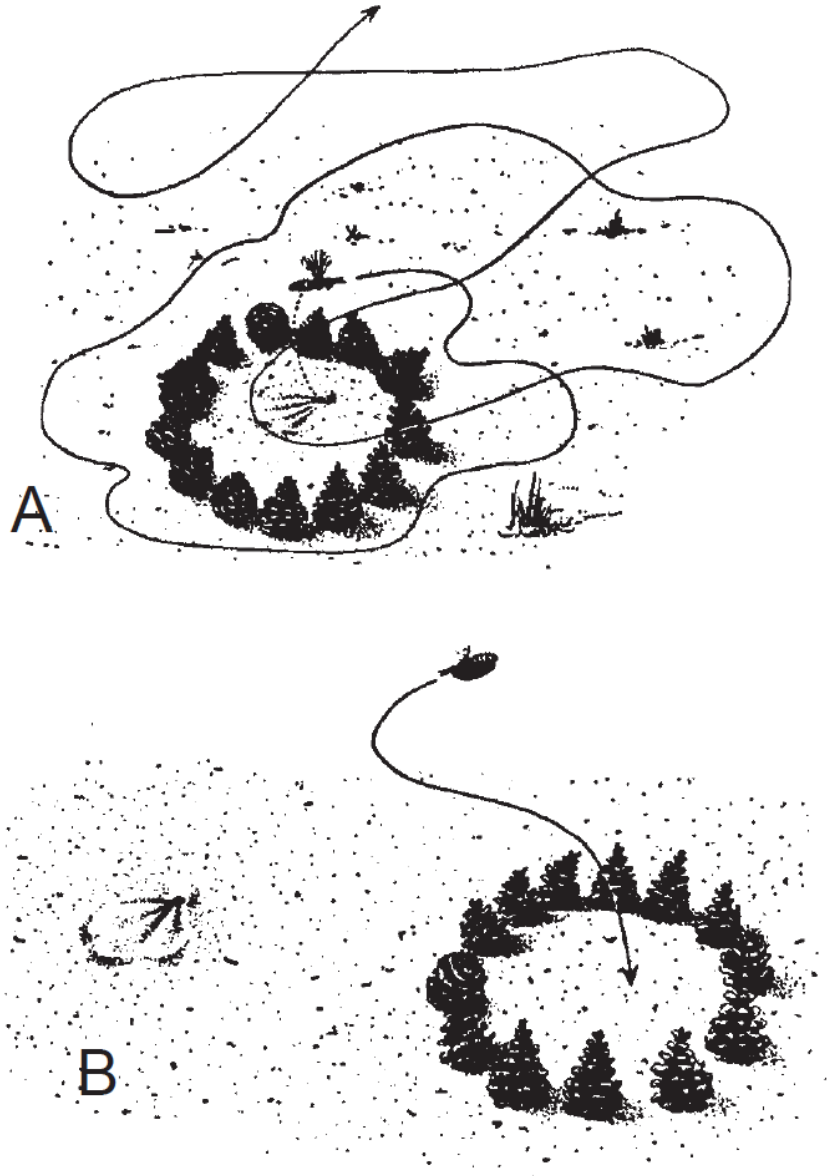

FIGURE 5.4. A. The path followed by a wasp while on an orientation flight, after its nest is circled by pinecones. B. The circle of pine cones is moved while the wasp is away foraging. When it returns, it attempts to enter the nest at the center of the cones instead of the real entrance. The wasp associates the nest opening with the pattern of cones after its orientation flight. Reprinted from Matthews, R.W., and J.R. Matthews. 1978. *Insect behavior*. Reprinted with permission from John Wiley & Sons.

Obr. 18

Včelí tance

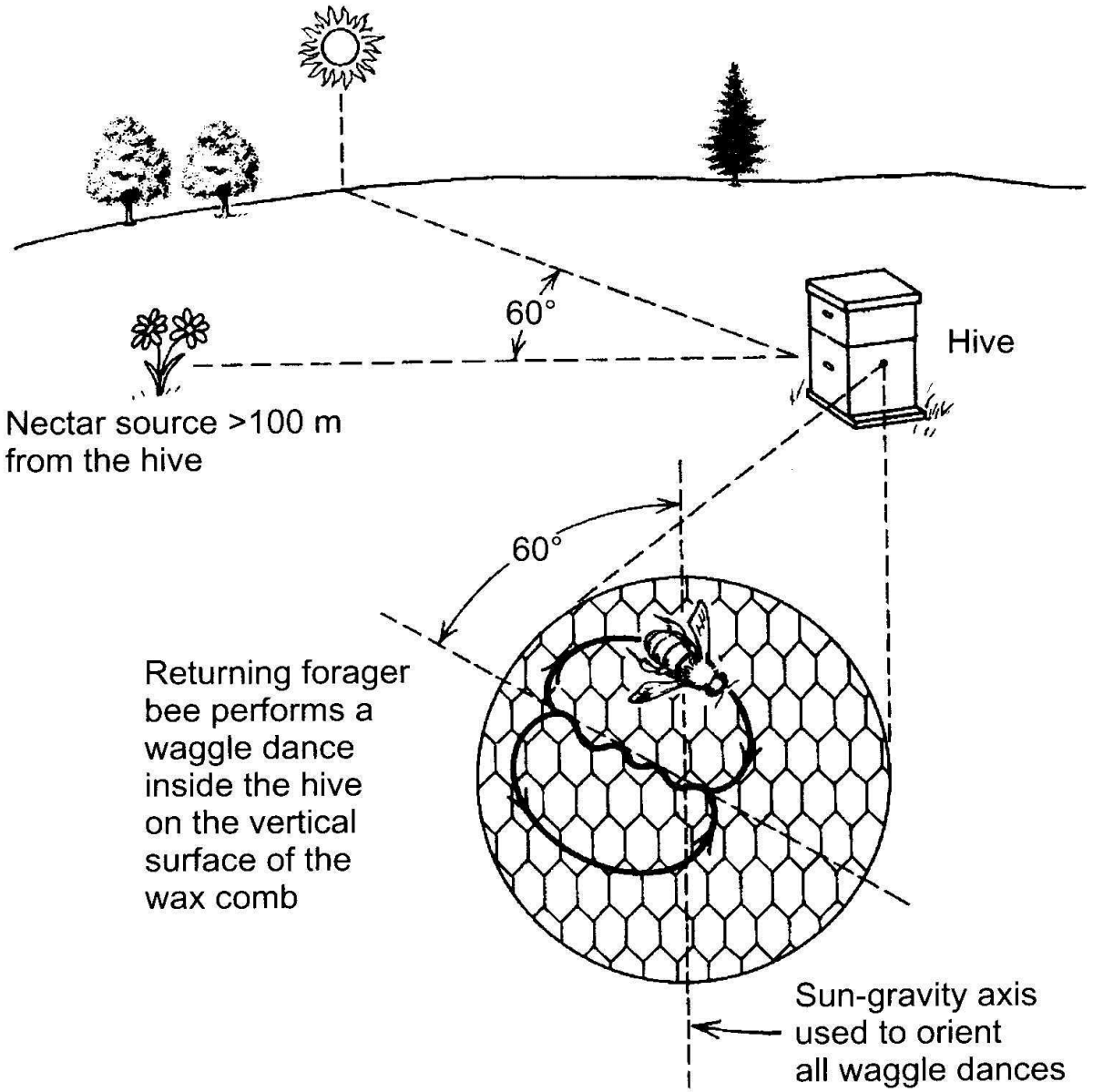

FIGURE 12.20. The waggle dance of the worker bee on the vertical comb of the hive is performed at an angle equal to the angle of the nectar source from the hive. From Matthews and Matthews (1978). Reprinted with permission.

Obr. 19 Příklad cirkadiánních rytmů – denní změny pohybové aktivity u samic cvrčka *Gryllus bimaculatus*

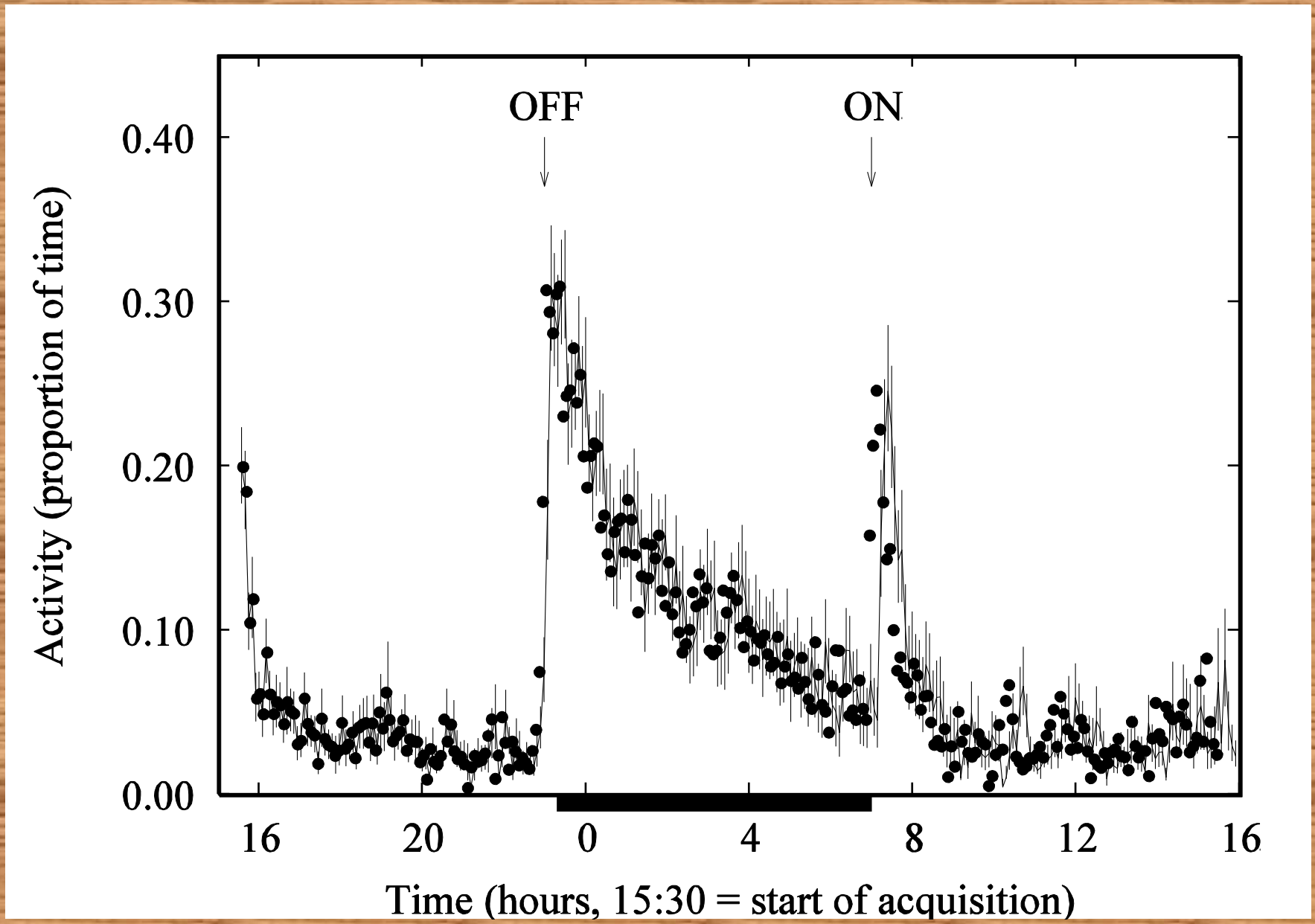

Obr. 20 Příklad cirkadiánních rytmů – denní kolísání hladiny adipokinetického hormonu (AKH) v CNS a hladiny lipidů po injekci 10 pmol AKH v hemolymfě ruměnice pospolné *Pyrrhocoris apterus*

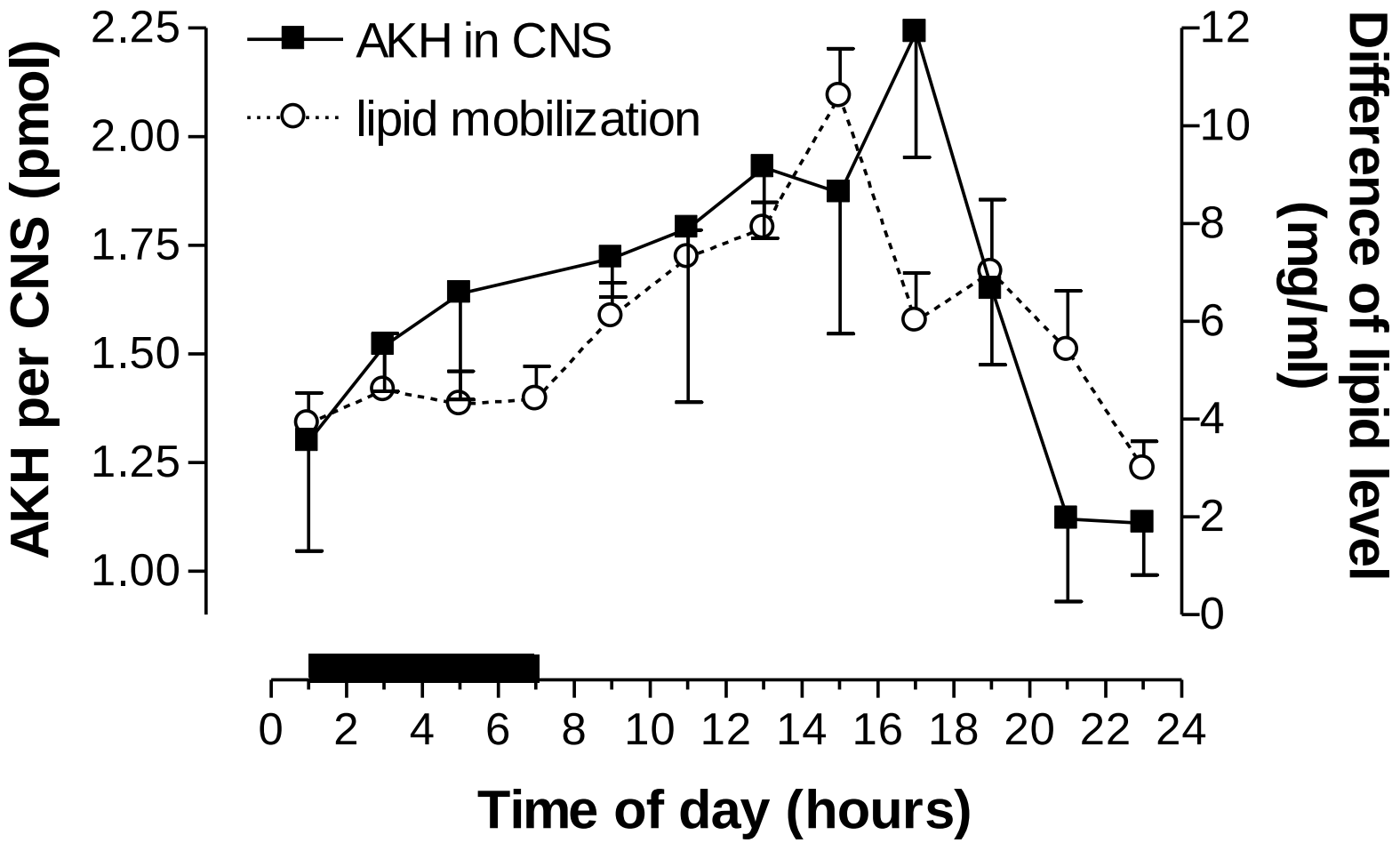

Možná centra circadiánních hodin

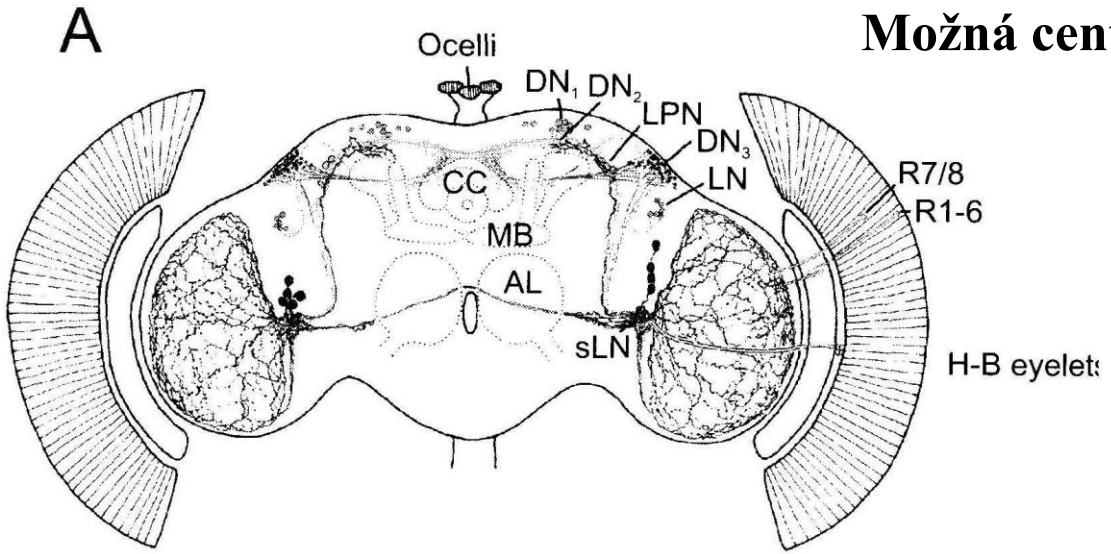

Obr. 21

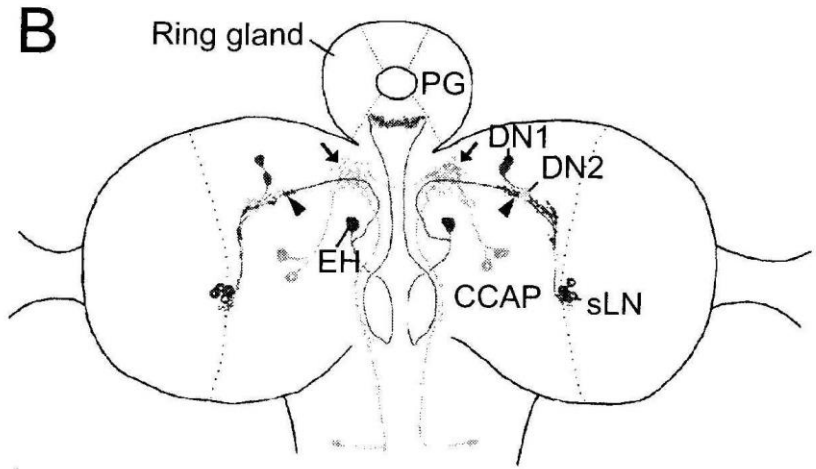

FIGURE 5.8. Neurons in the *Drosophila* adult (A) and larval (B) brains that express genes involved in circadian rhythmicity. Groups of dorsal neurons (DN), lateral posterior neurons (LPN), and large (LN) and small (sLN) ventral lateral neurons express *period* and *timeless* genes. The larval neurons that express crustacean cardioactive peptide (CCAP) and eclosion hormone (EH) are also shown. The photoreceptor cells R1-6 and R7/8 in the compound eyes and the H-B eyelets contain cryptochrome and contribute to circadian entrainment. The prothoracic gland (PG) is contained within the larval ring gland. From Helfrich-Förster (2005). Reprinted with permission.

Mechanismus působení biologických hodin

Obr. 22

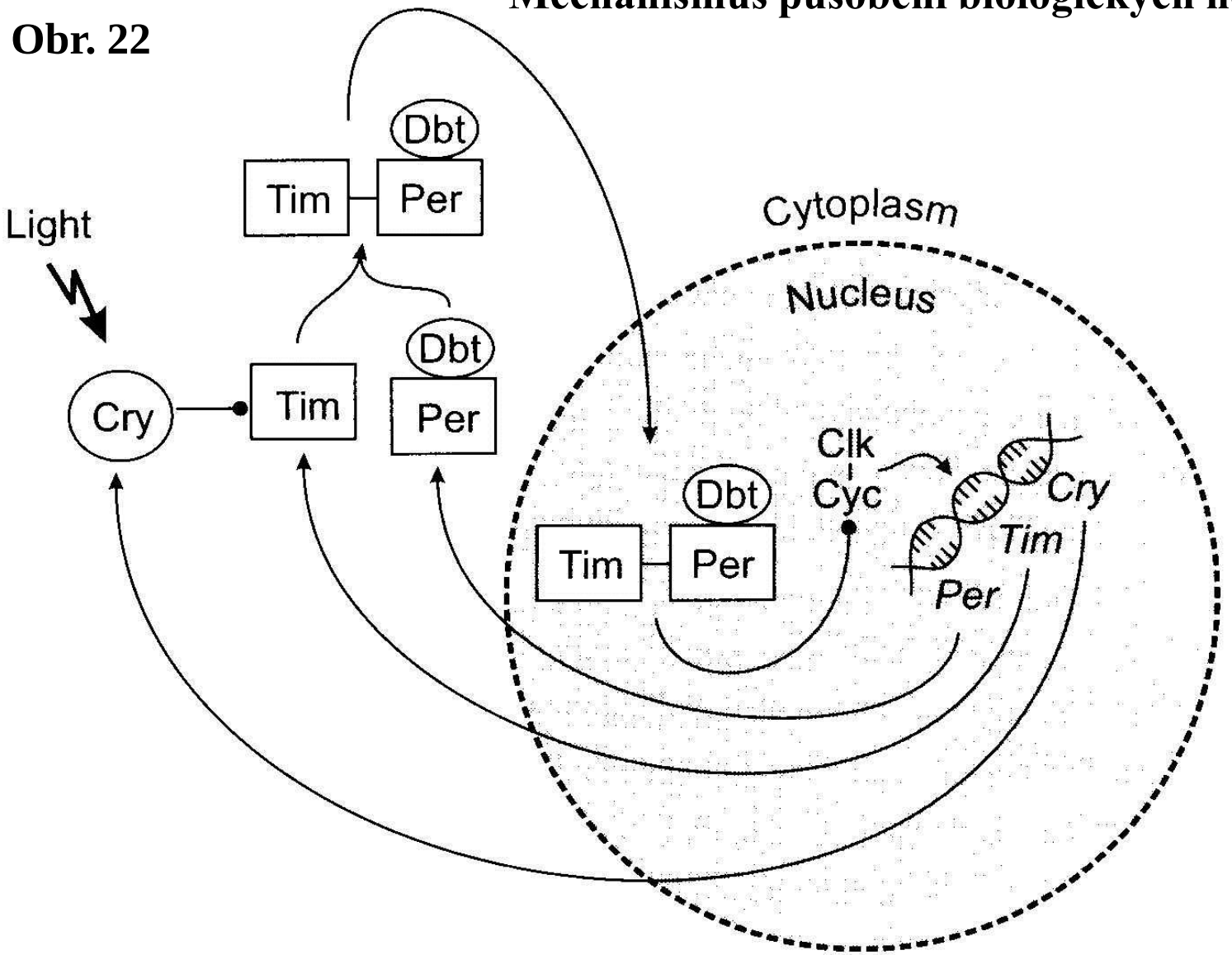

FIGURE 5.9. Components of the circadian clock. See the text for details.

9. Fyziologie smyslové soustavy

Obr. 1

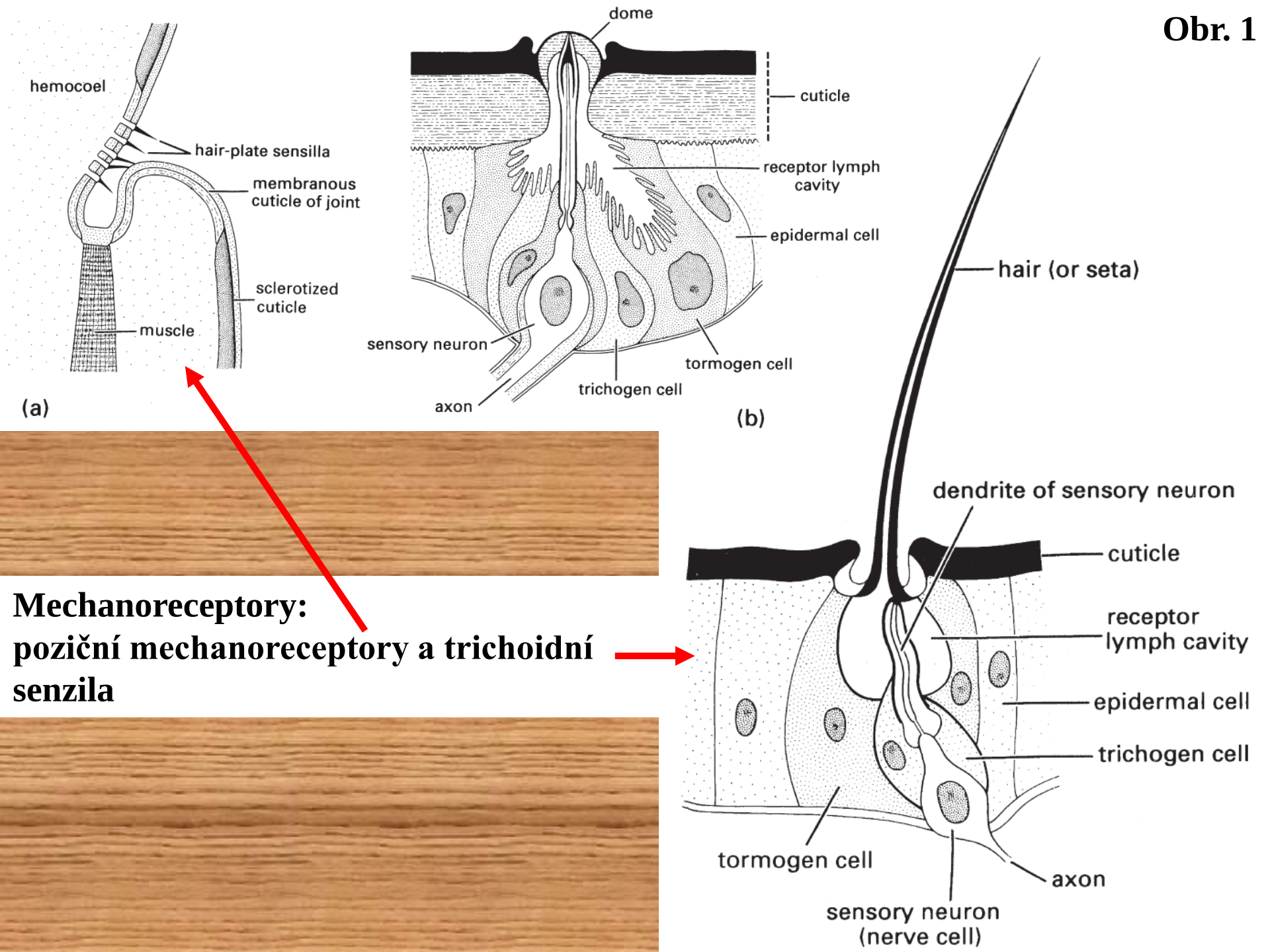

Mechanoreceptory: pozční mechanoreceptory a trichoidní senzila

Obr. 2 Mechanoreceptory

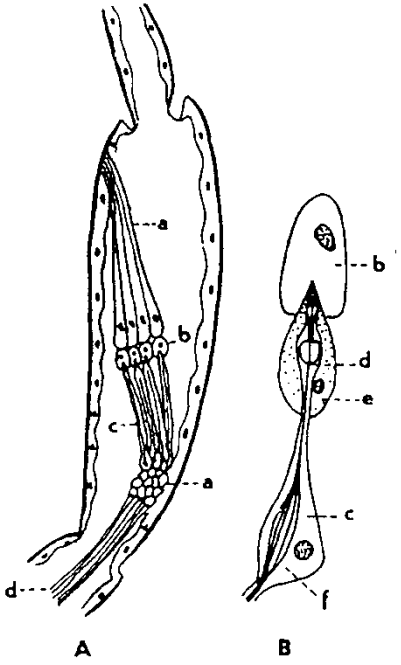

Chordotonální ústrojí hmyzu

A - chordotonální orgán zavěšený v dutině holeně hmyzu,
B - scolopophor z tympanálního orgánu sarančete

a = upevňovací buňky, b = krycí buňky, c = smyslové buňky s čípky, d = čípek smyslové buňky, e = obalová buňka, f = neurofibrily

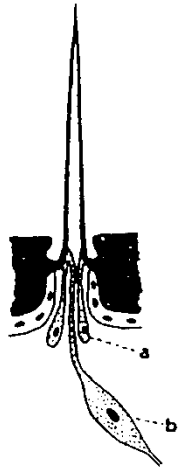

Hmatový chlup hmyzu

a = epiteliální buňky, které vylučují štětinu,
b = smyslová buňka

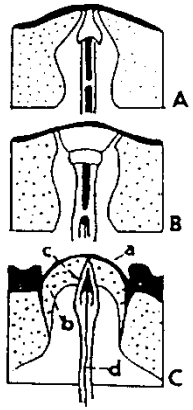

Companuliformní sensilli

A - s úzkým zakončením kutikulárního spoje,
B - se širokým zakončením kutikulárního spoje,
C - obecné schéma

a = vnější lamella stříšky, b = vnitřní lamella stříšky, c = artikulární přípojka, d = distální výběžek smyslové buňky

Obr. 3 Řez skolopidiem

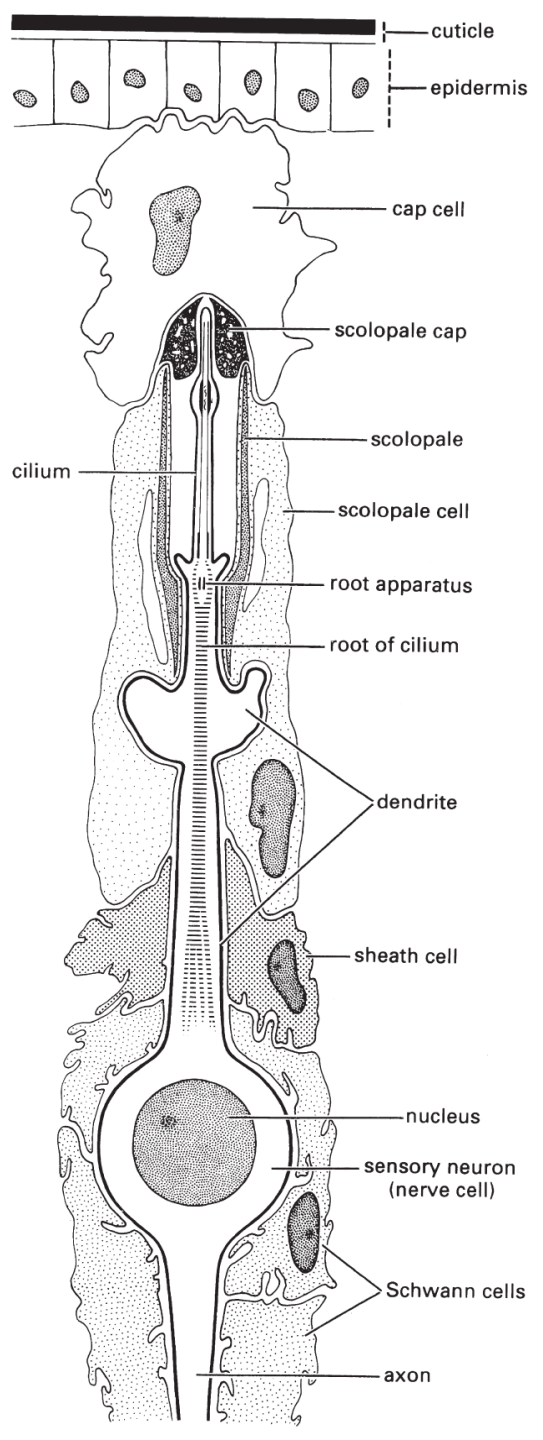

Obr. 4 Tympanální orgány

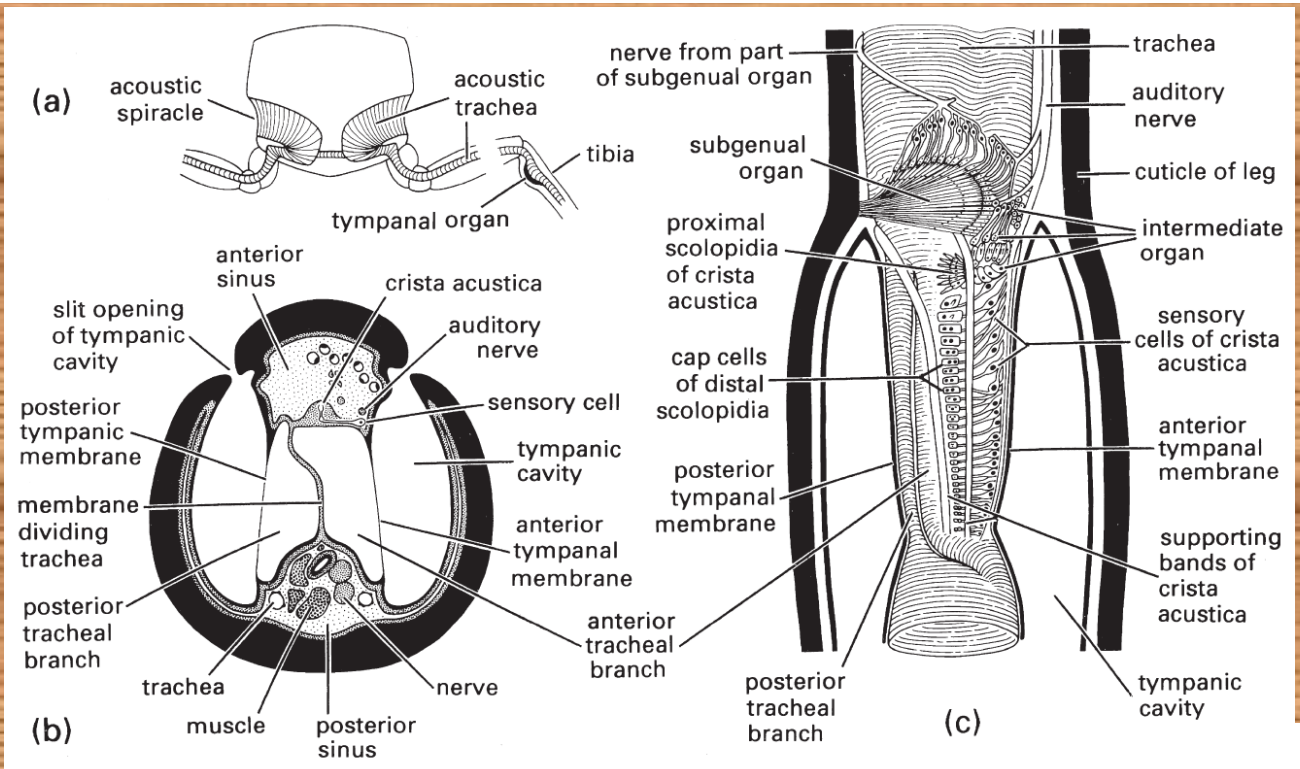

Fig. 4.4 Tympanal organs of a katydid, *Decticus* (Orthoptera: Tettigoniidae): (a) transverse section through the fore legs and prothorax to show the acoustic spiracles and tracheae; (b) transverse section through the base of the fore tibia; (c) longitudinal breakaway view of the fore tibia. (After Schwabe 1906; in Michelsen & Larsen 1985.)

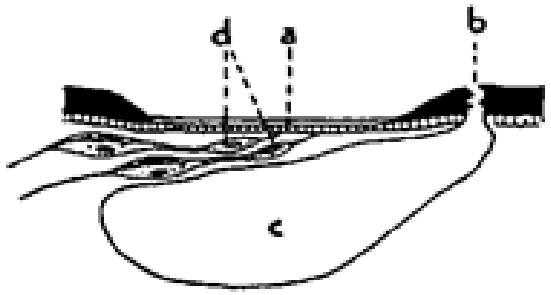

Tympanální ústrojí hmyzu (saranče)

a = bubínek, b = stigma vzduš-nice, c = rezonátor (váček nadmuté vzdušnice), d = smys-lové buňky (crista acustica)

Obr. 5

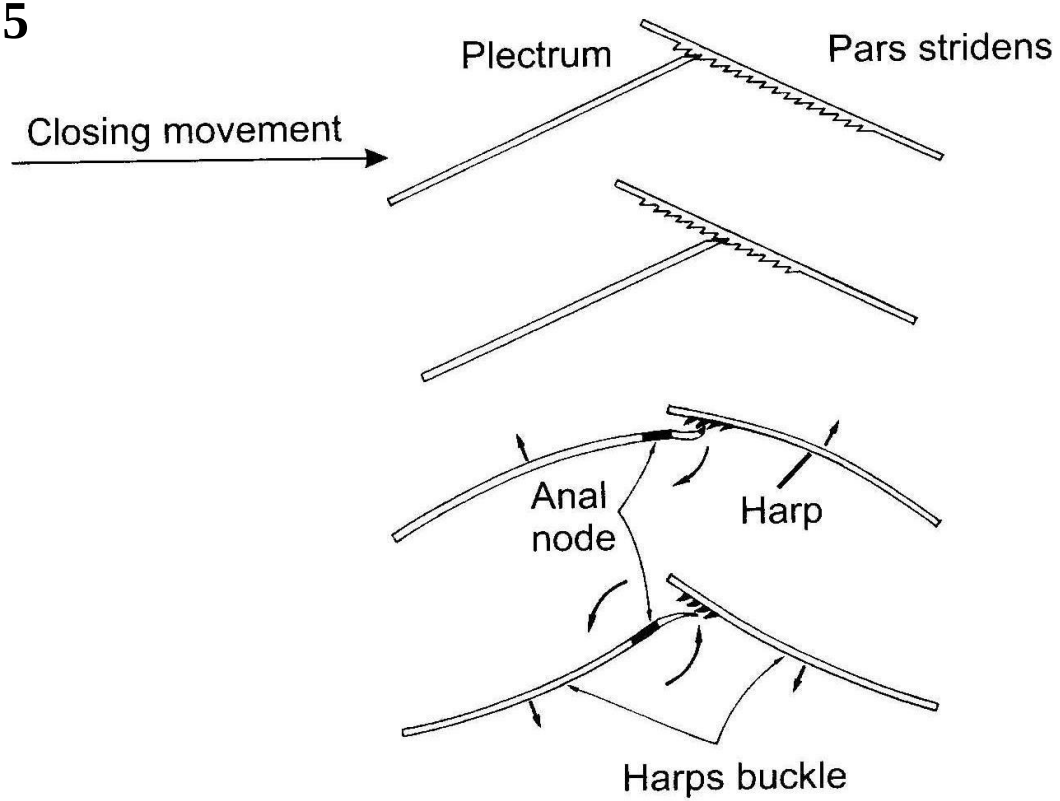

Produkce zvuku u Orthoptera

FIGURE 12.6. (*Top*) The stridulatory apparatus of a katydid. The mirror frame vibrates as the file on one elytron is moved across the plectrum. (*Bottom*) The stridulatory apparatus of a cricket. From Ewing (1989) and Bennet-Clark (1989). Reprinted with permission.

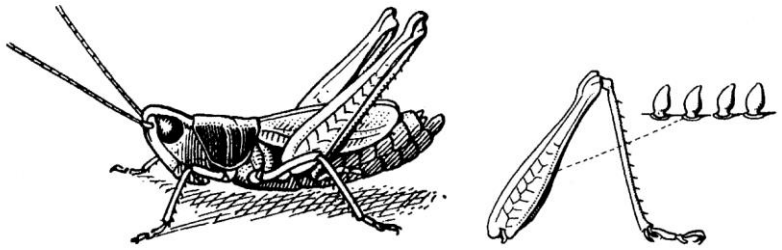

FIGURE 12.9. (*Right*) The stridulatory pegs on the legs of a grasshopper. From Haskell (1961). Reprinted with permission.

Obr. 6 Zvýšení intenzity produkce zvuků pomocí vibrací substrátu

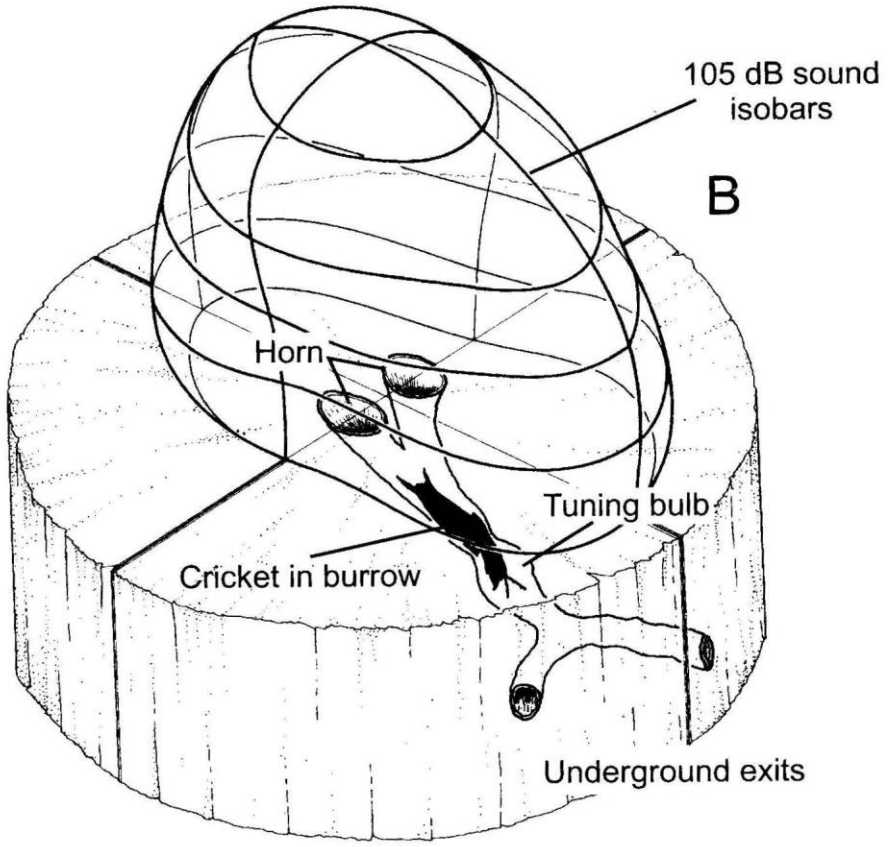

FIGURE 12.7. A. A cross section of a mole cricket burrow. B. A three-dimensional view of the acoustical chamber that amplifies the stridulations. From Bennet-Clark (1989). Reprinted with permission.

https://www.youtube.com/watch?v=TPAJLouL-d4

Obr. 7
Produkce zvuku pomocí rezonanční destičky (tymbal) u cikád

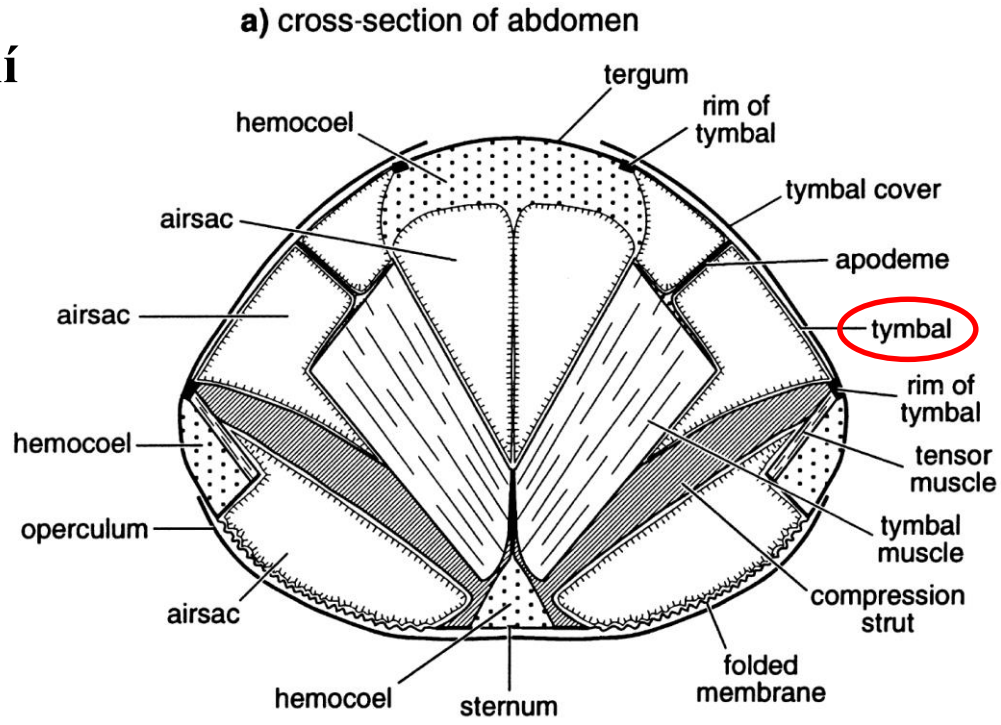

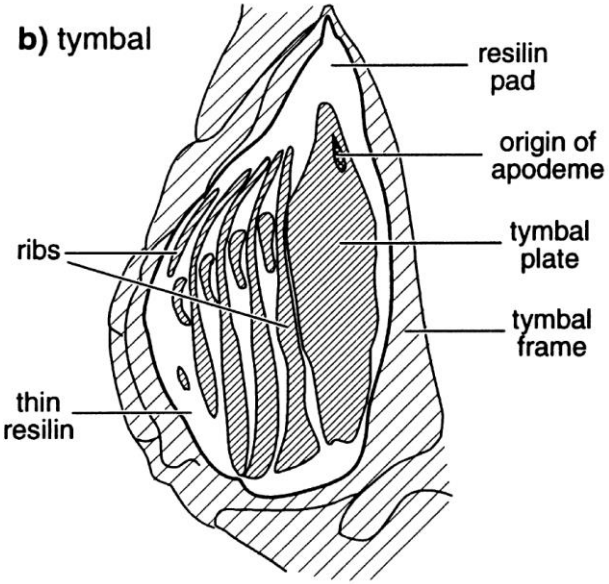

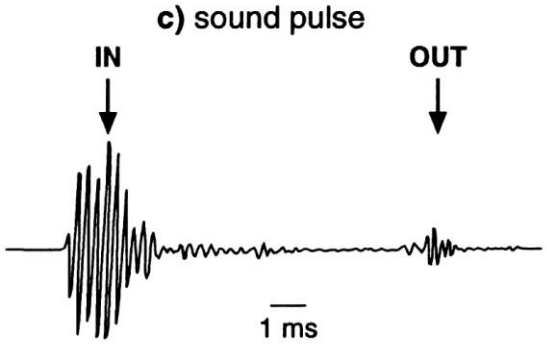

Obr. 8 Schéma termohydroreceptoru

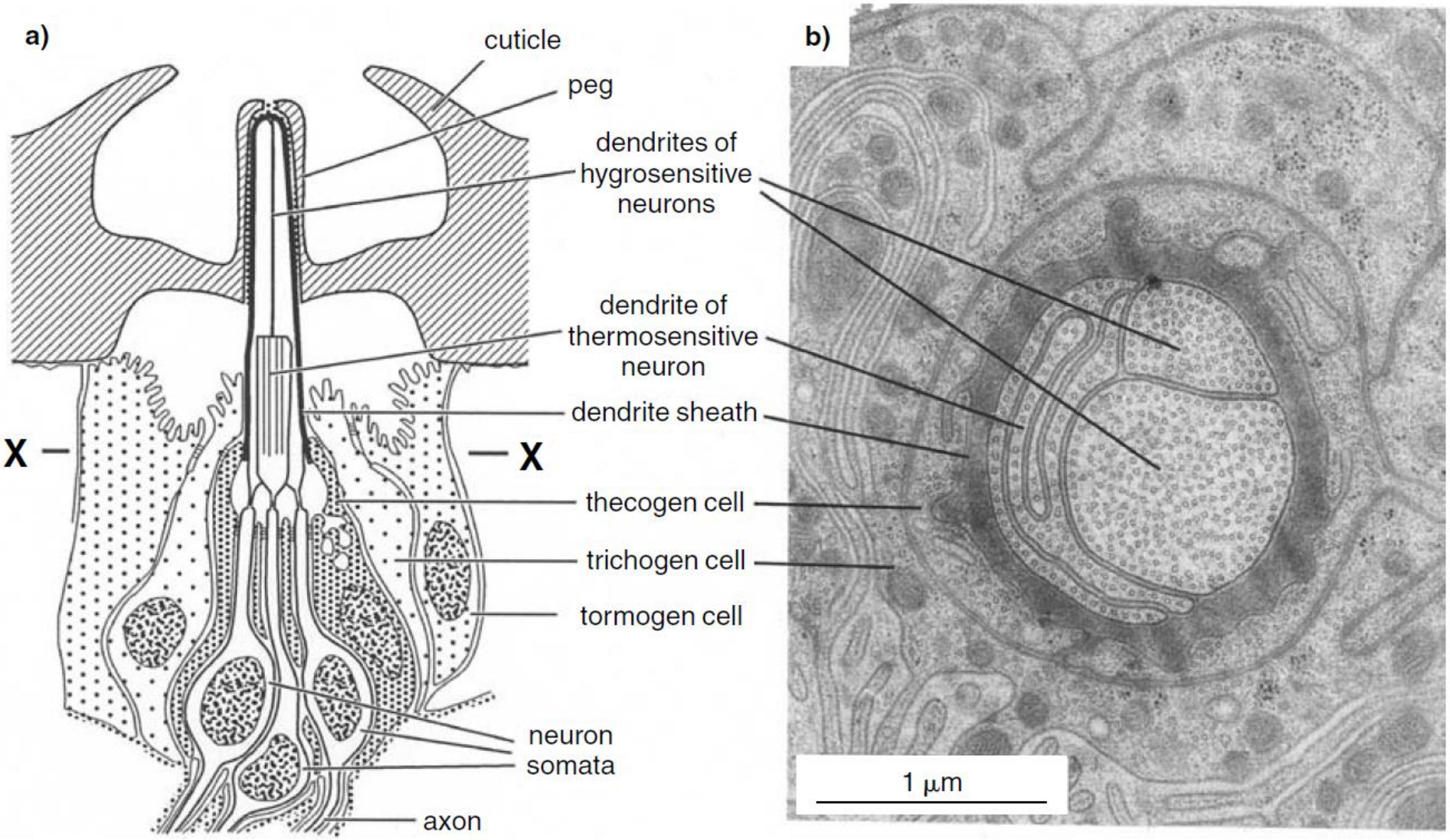

Fig. 19.15. Thermohygroreceptor. **(a)** Diagrammatic longitudinal section through a coeloconic sensillum. **(b)** Electron micrograph of a transverse section of a thermohygroreceptor at the level of X–X in **(a)**. Notice the dendrites of two hygrosensitive neurons and folds of the dendrite of a thermosensitive neuron completely occupying the space in the dendrite sheath (*Bombyx*) (after Steinbrecht *et al.*, 1989).

Obr. 9 Chemosensila (vpravo) - čárka ukazuje komunikaci dutiny válce s vnějším prostředím; vlevo dole - podélný řez bází chemosensily (nervy, smyslové buňky, trichogenní a tormogenní buňky); vpravo dole - příčný řez pod bází upevnění sensily ke kutikule

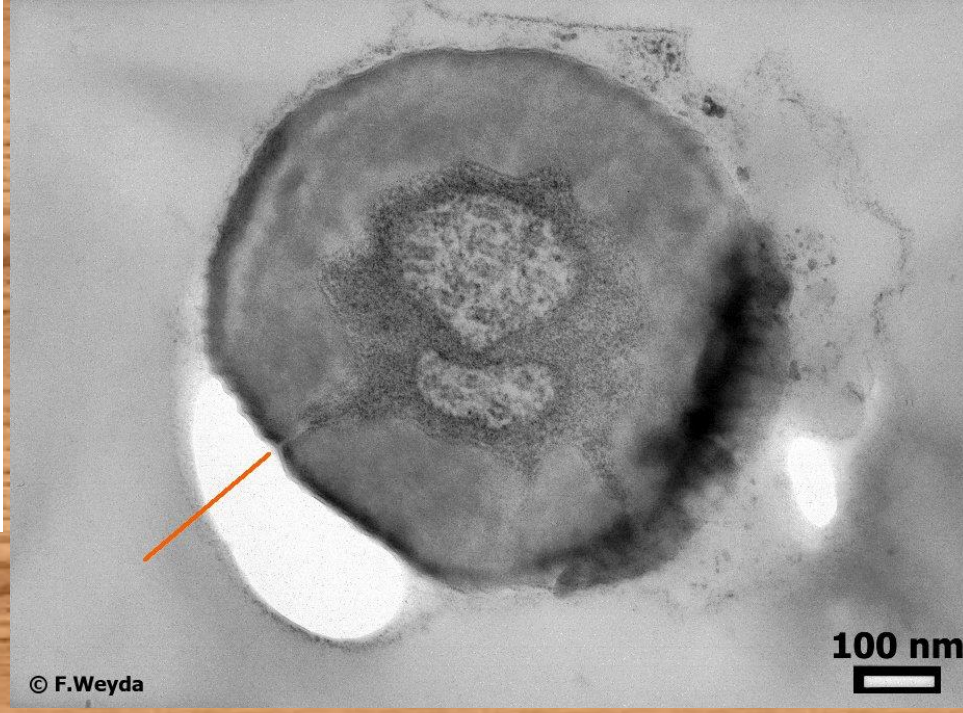

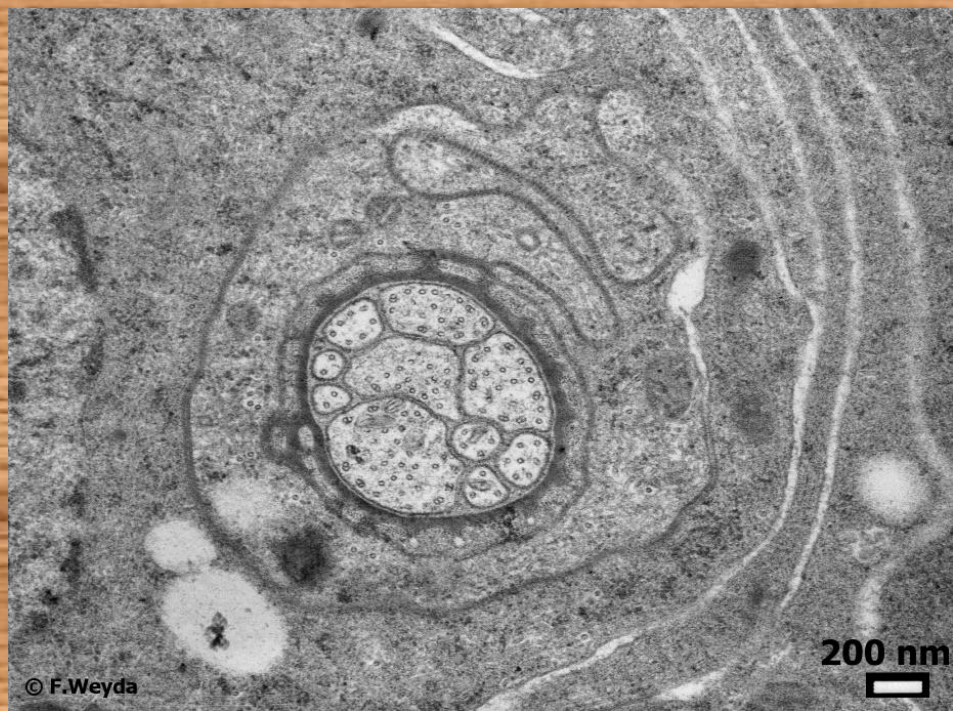

Obr. 10 Hmyzí čichové senzily

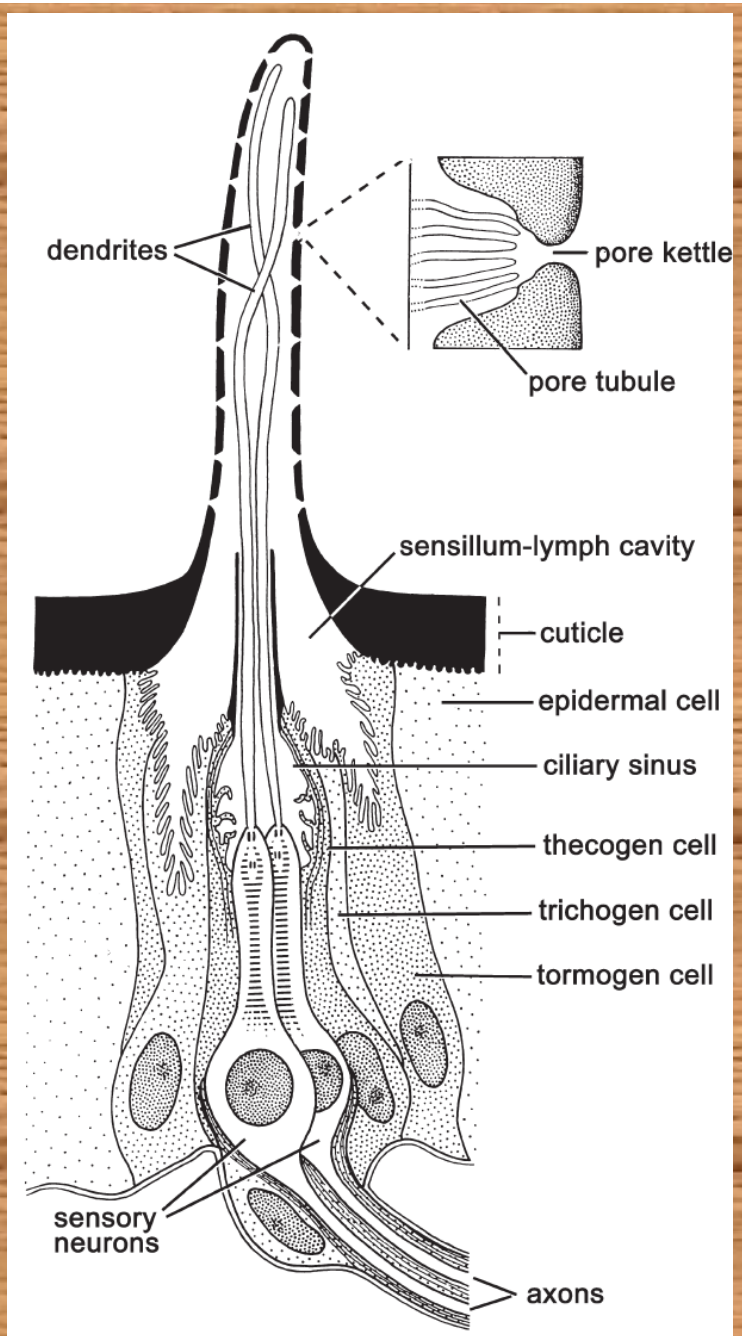

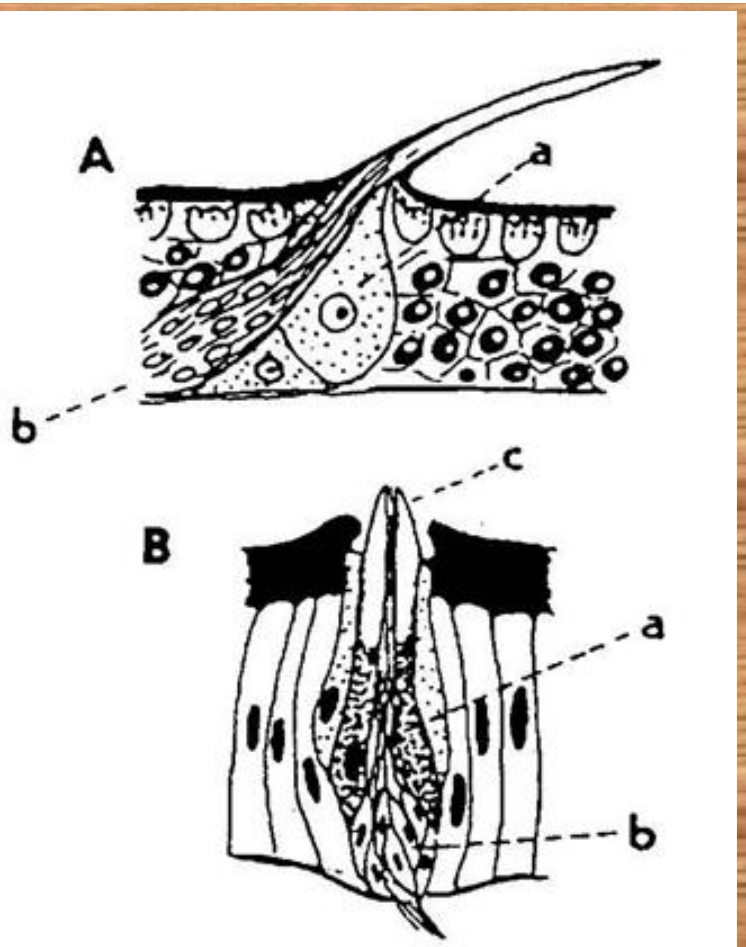

Čichové senzily hmyzu
A - čichová brva
B - čichový kužel

a = trichogenní buňky
b = smyslové buňky
c = čichová tyčinka

Obr. 11 **Umístění čichových senzil na tykadlech**

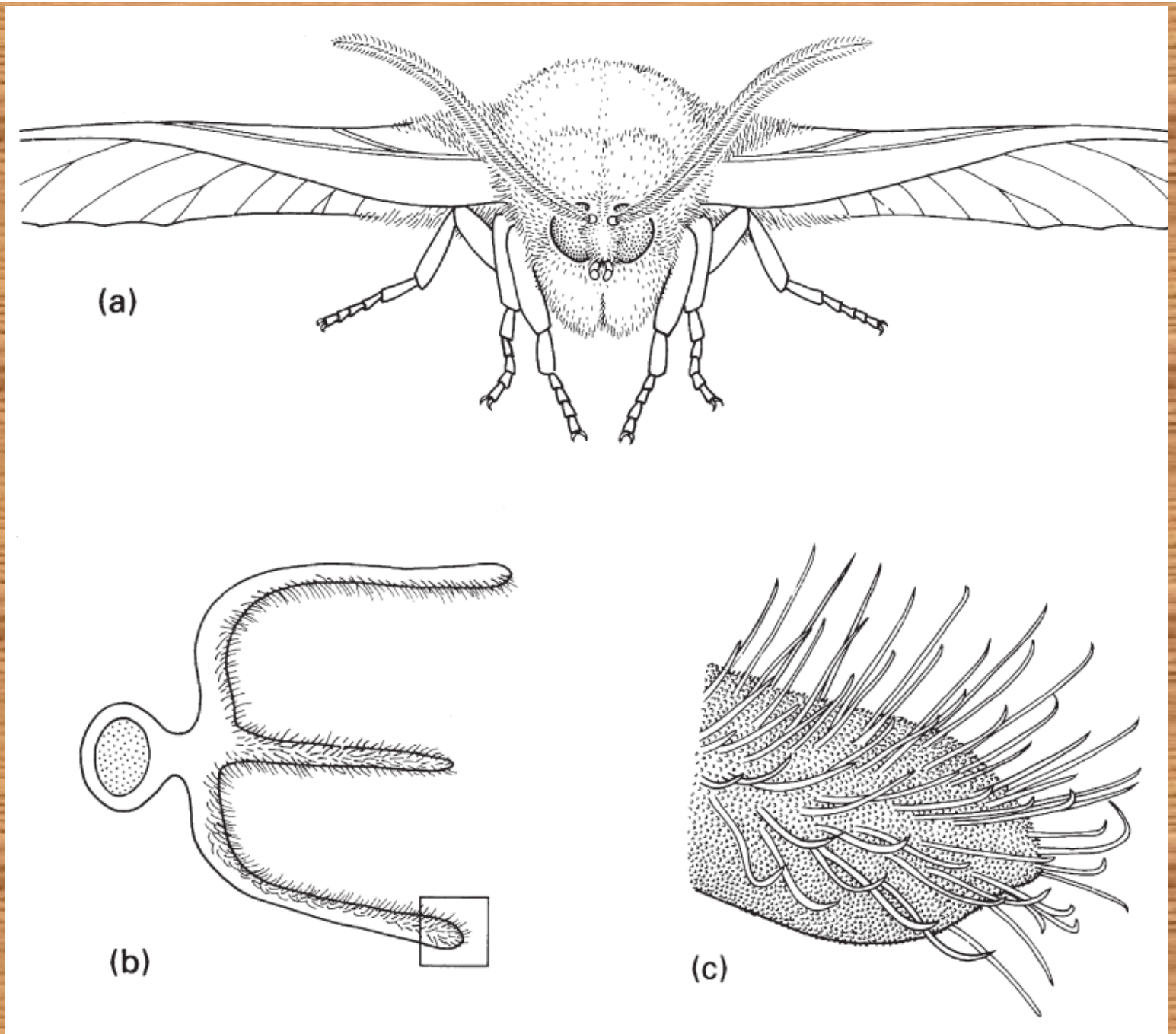

Obr. 12

Typy hmyzích zrakových orgánů

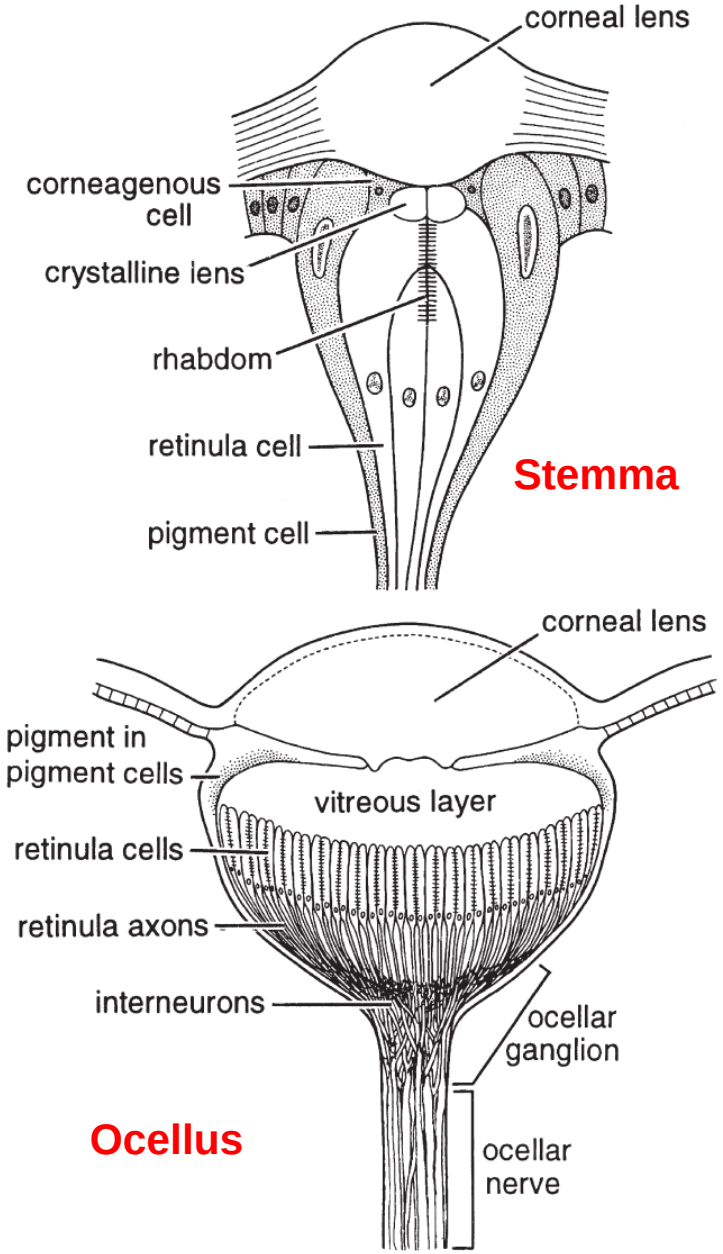

Fig. 4.9 Longitudinal sections through simple eyes: (a) a simple stemma of a lepidopteran larva; (b) a light-adapted median ocellus of a locust. ((a) After Snodgrass 1935; (b) after Wilson 1978.)

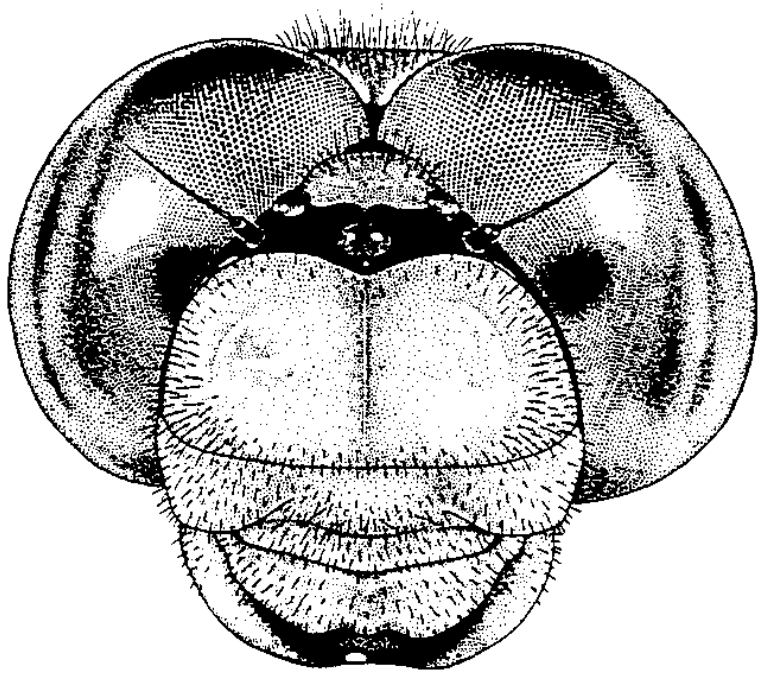

Head of a dragonfly showing enormous compound eyes

Obr. 13

Složené oko hmyzu

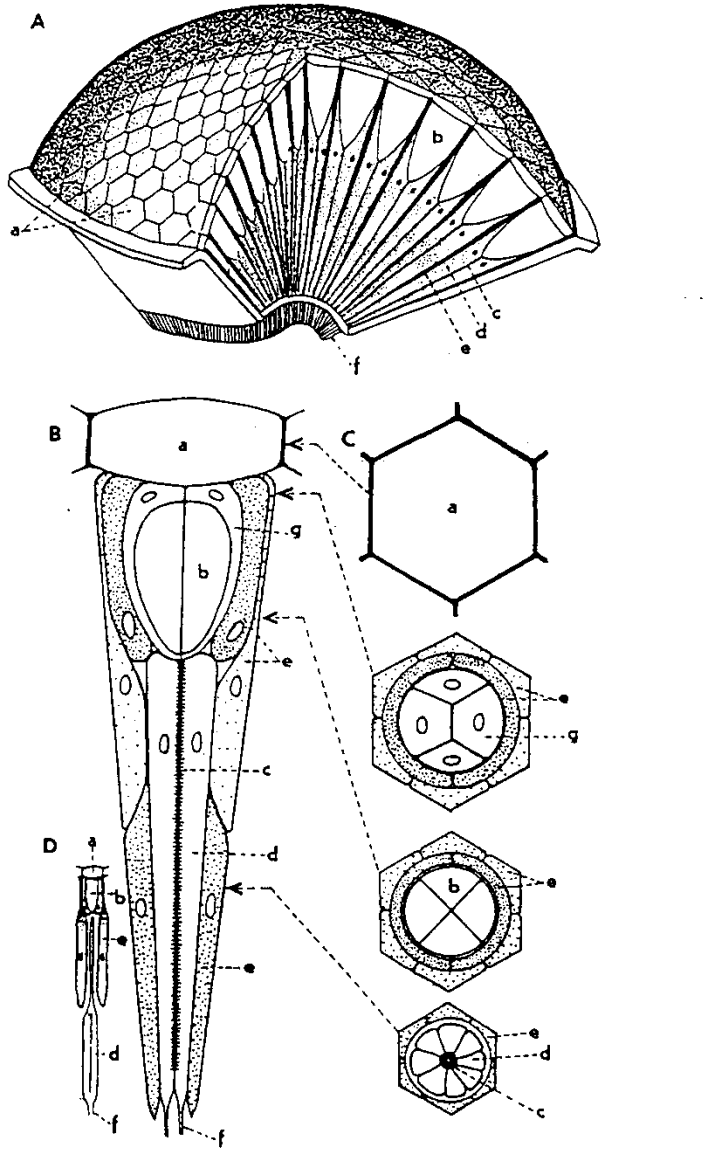

Složené oči členovců

A - celkový pohled na složené oko,
B - detailní stavba apozičního omatidia na podélném řezu,
C - na příčných řezech v úrovních označených šipkami,
D - superpoziční omatidium při malém zvětšení

a = facęta, b = křišťálový kužel, c = rhabdom, d = zraková buňka (primární buňka smyslová), e = pigmentová buňka, f = nervové výběžky zrakových buněk, g = křišťálotvorná buňka

Obr. 14

Poměrná velikost hmyzího oka vůči hmyzímu tělu aplikovaná na člověka

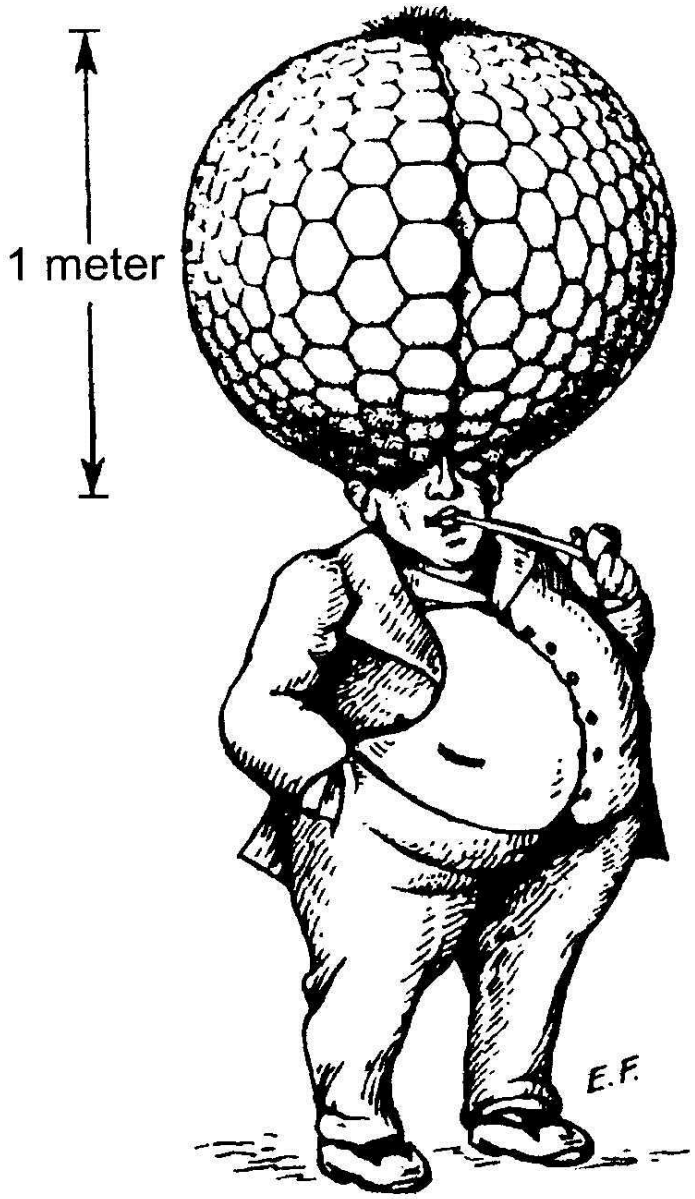

FIGURE 11.45. The approximate size of a compound eye in humans if the same resolution were to be obtained as for a lens eye. From Kirschfield (1976). Reprinted with permission.

Obr. 15

Rhabdomery a jejich funkce polarizačních filtrů

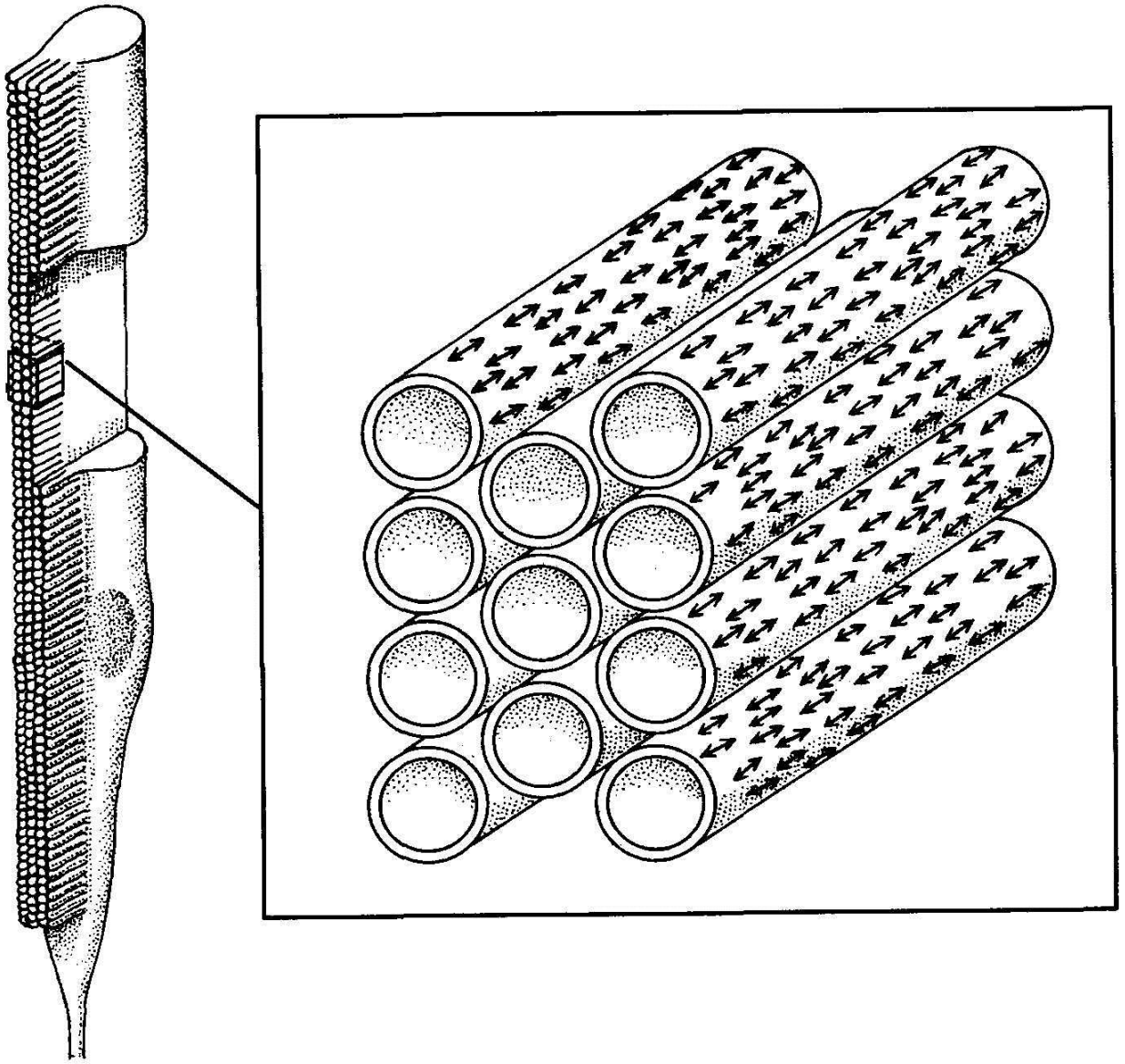

FIGURE 11.53. (*Left*) An elongated rhabdomere. (*Right*) The uniform orientation of rhodopsin within the microvilli of the rhabdomere that allows the reception of polarized light. From Wehner (1976). Reprinted with permission.

http://www.youtube.com/watch?v=TU6bgQnTi18&feature=plcp

Obr. 16 Struktura rhodopsinu

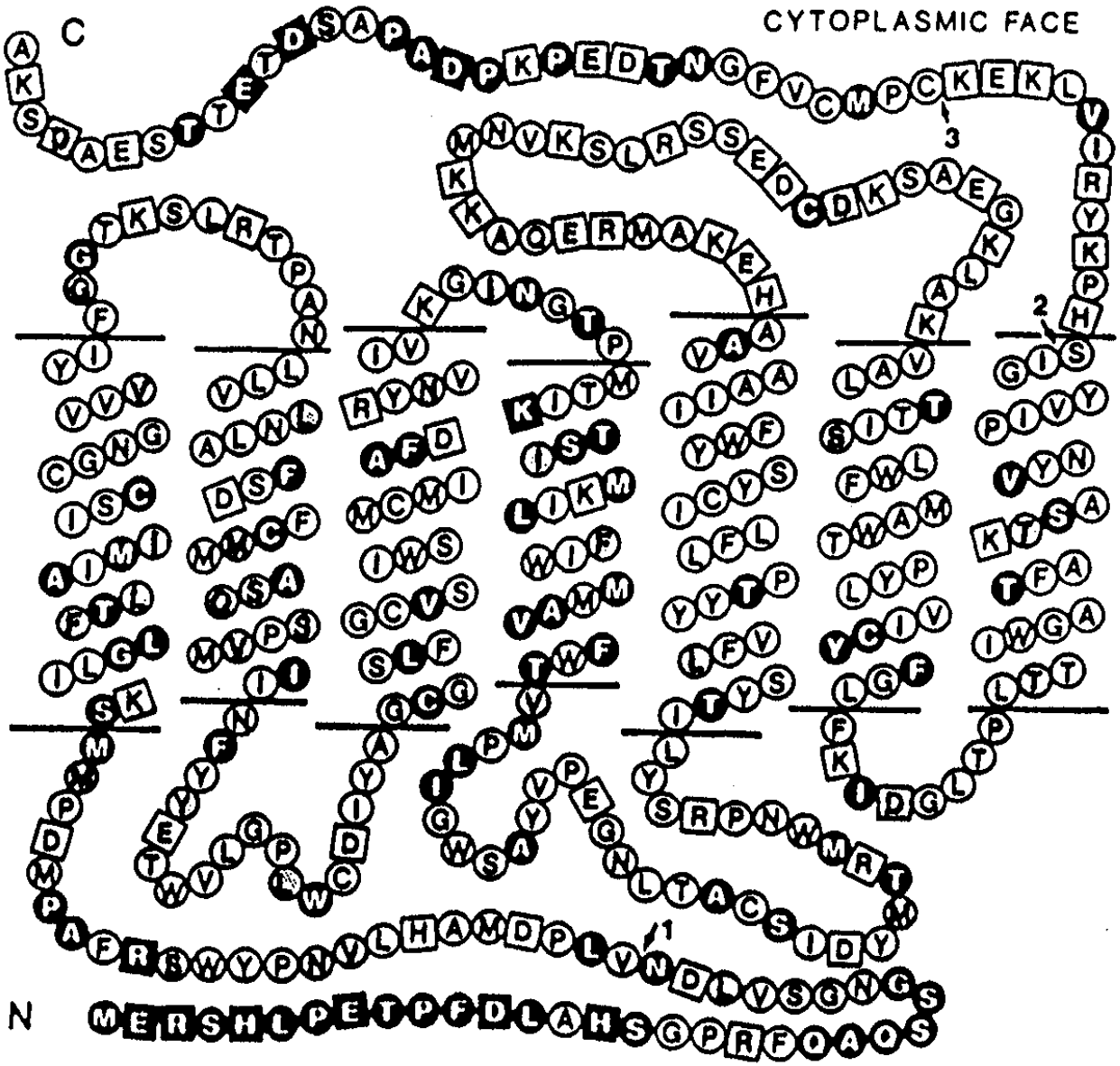

FIGURE 10.18 A diagram of the transmembrane nature of rhodopsin in the membranes of the rhabdomeres of retinular cells. (Reproduced with permission from Mizunami, 1994.)

Obr. 17 Mechanismus vnímaní světla u hmyzu - schéma

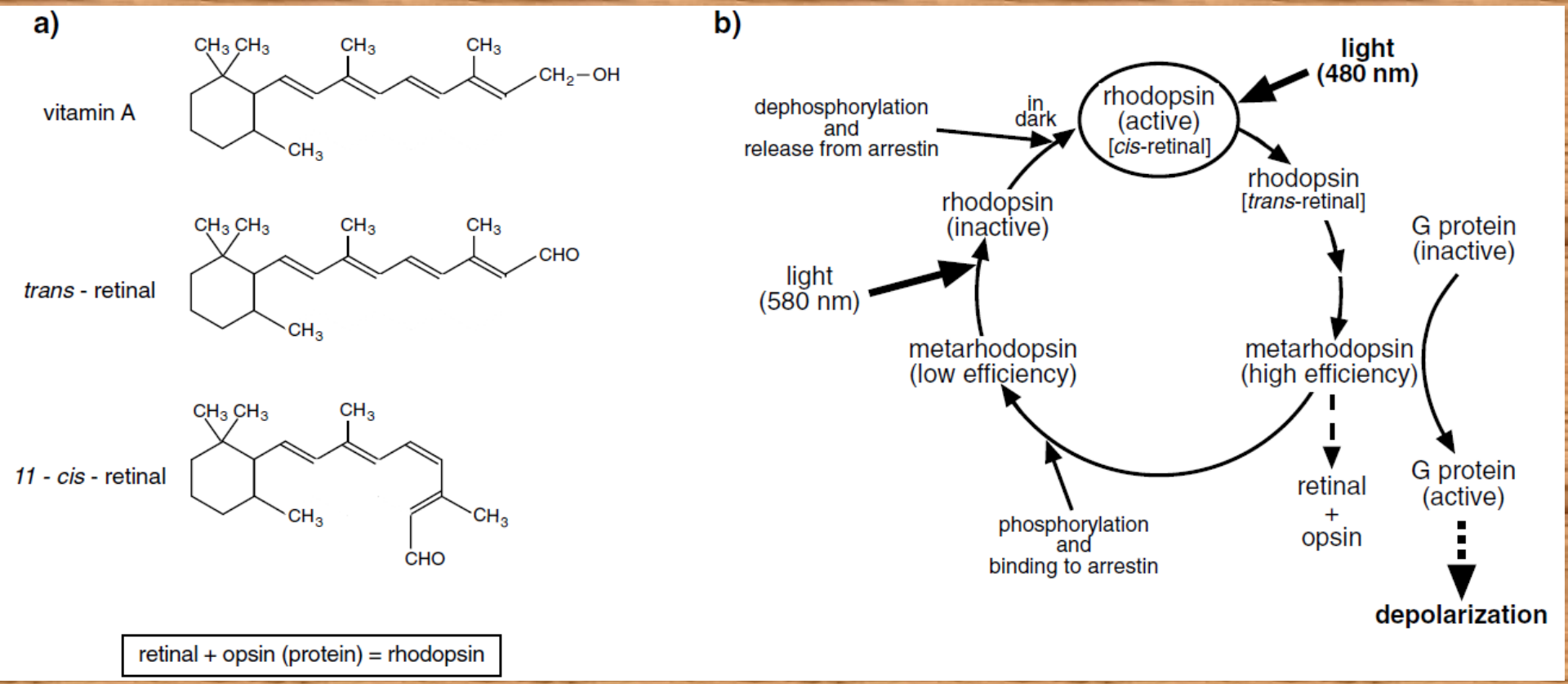

Obr. 18 **Mechanismus vnímaní světla u hmyzu - detail**

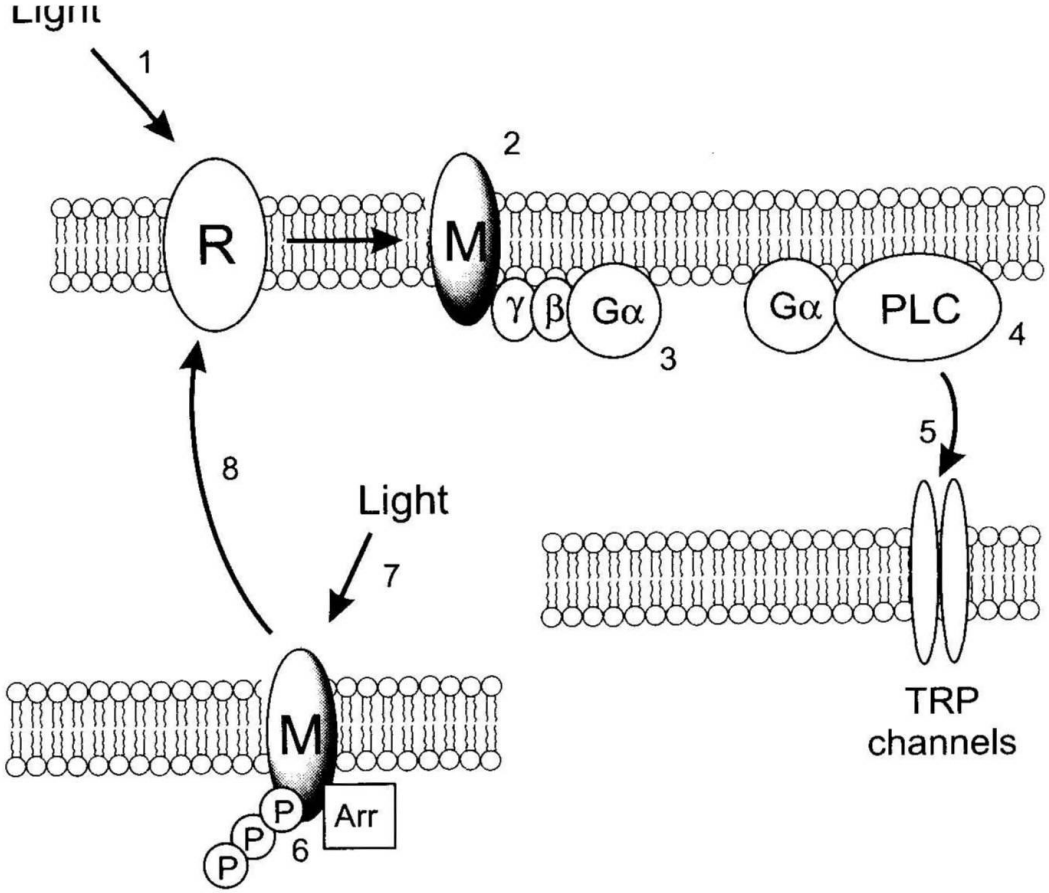

FIGURE 11.51. The transduction cascade on the *Drosophila* rhabdom membrane. (1) When a photon of light is absorbed by the rhodopsin (R) and mediates the isomerization to the *trans* form and (2) ultimately the stable metarhodopsin M, a G-protein cascade (3) is activated. This activates phospholipase C (PLC) (4) that ultimately activates transient receptor potential (TRP) channels (5) to allow the influx of sodium and calcium and generate a receptor potential. Phosphorylation and arrestin binding inactivates the metarhodopsin (6), but light (7) regenerates the rhodopsin once again (8).

10. Endokrinní soustava

Obr. 1 Vztah mezi nervovou a endokrinní soustavou

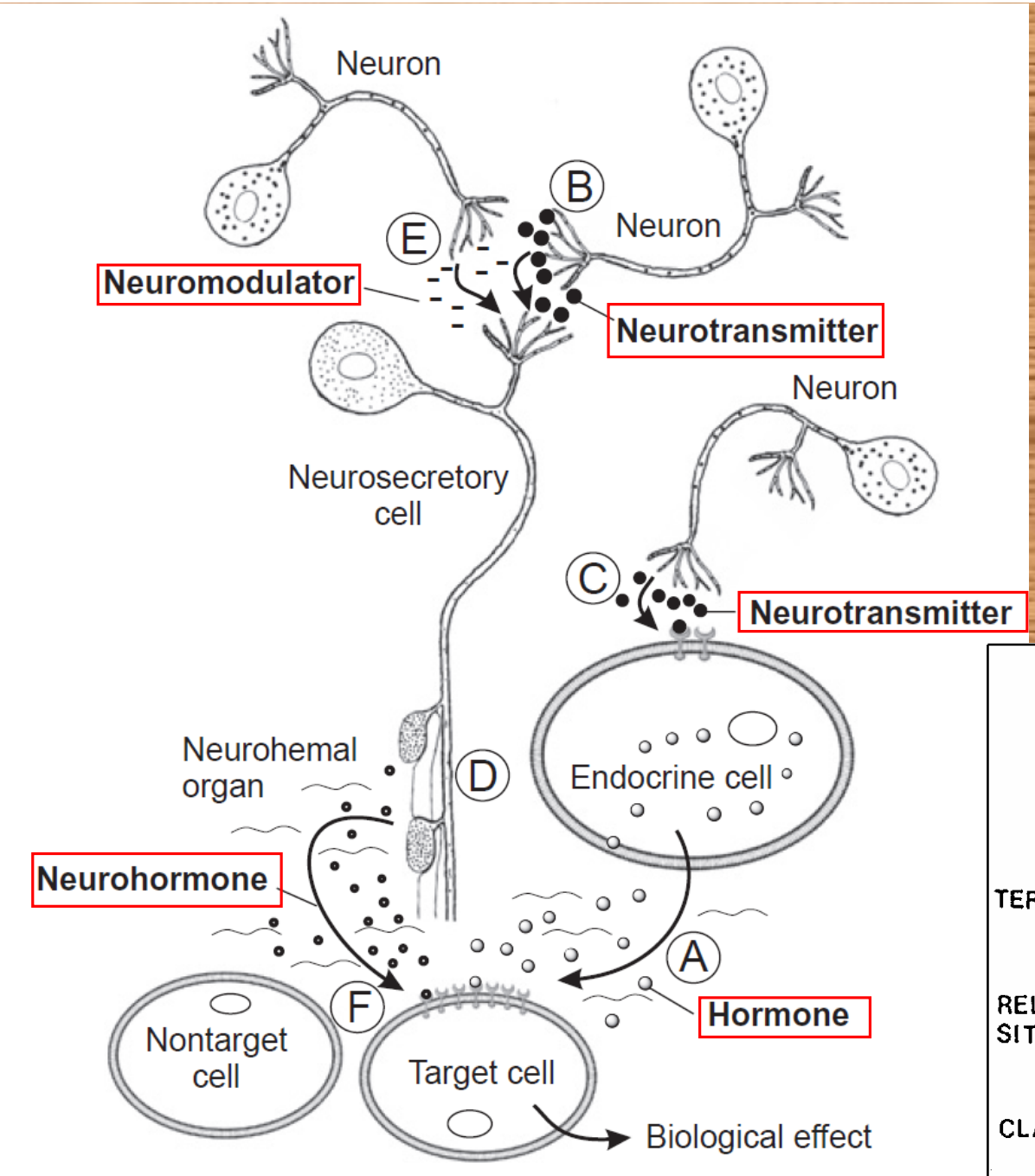

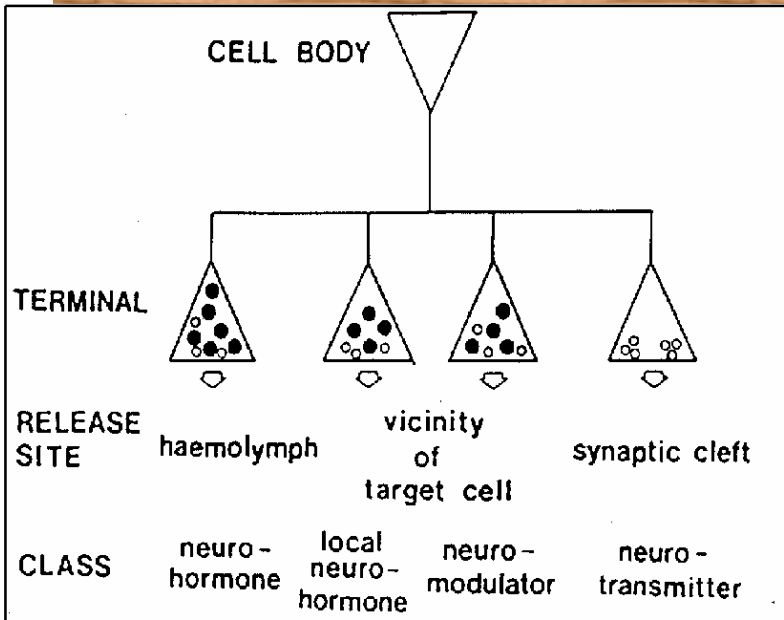

Působení hydrofilních hormonů - signální dráha aktivovaná cAMP

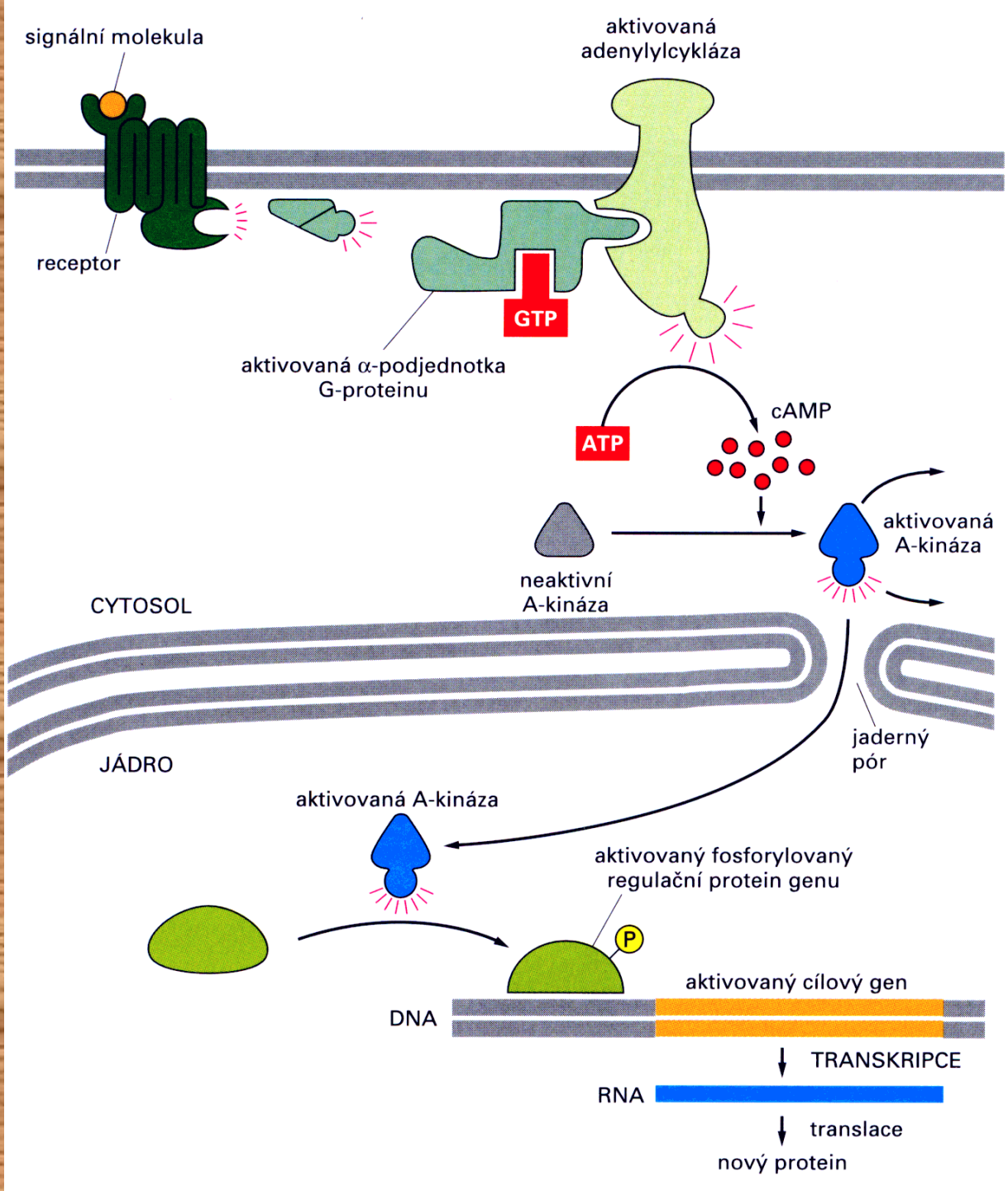

Obr. 2

Působení hydrofilních hormonů signální dráha aktivovaná fosfolipázou C

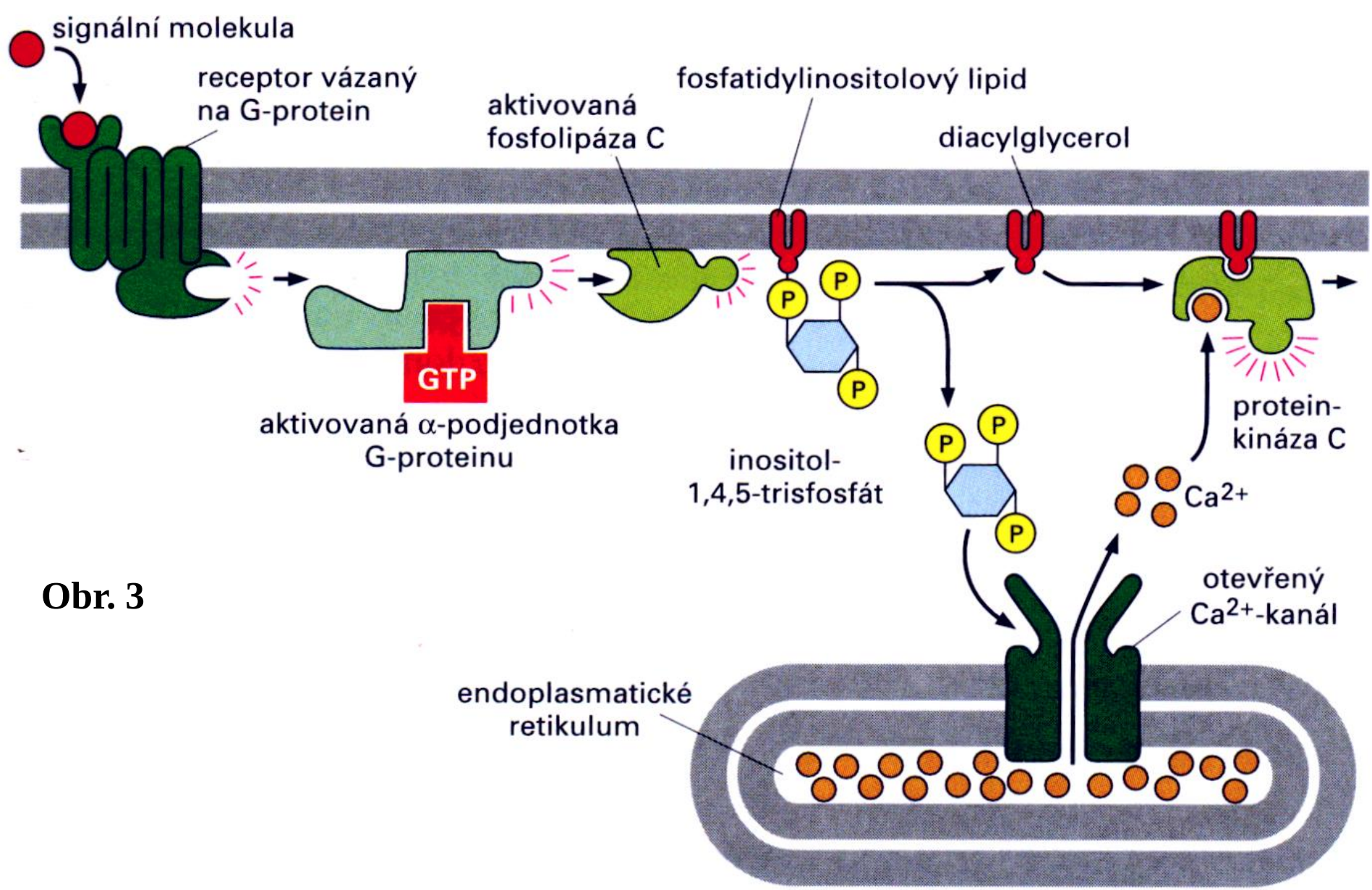

Obr. 3

Mechanismus působení lipofilních hormonů – ekdysteroidy, juvenilní hormony

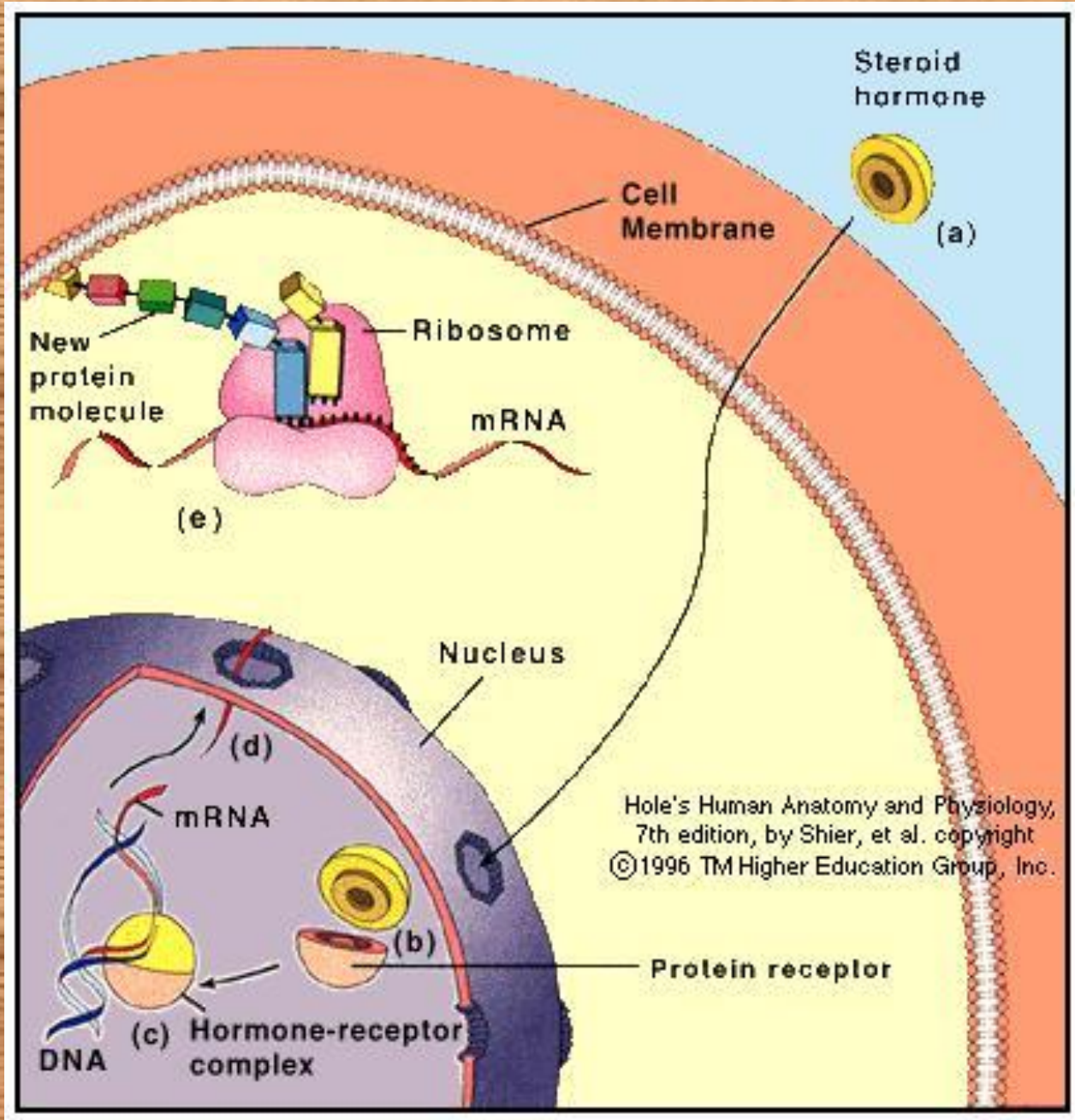

Obr. 4

Hormonální soustava korýšů

Obr. 5

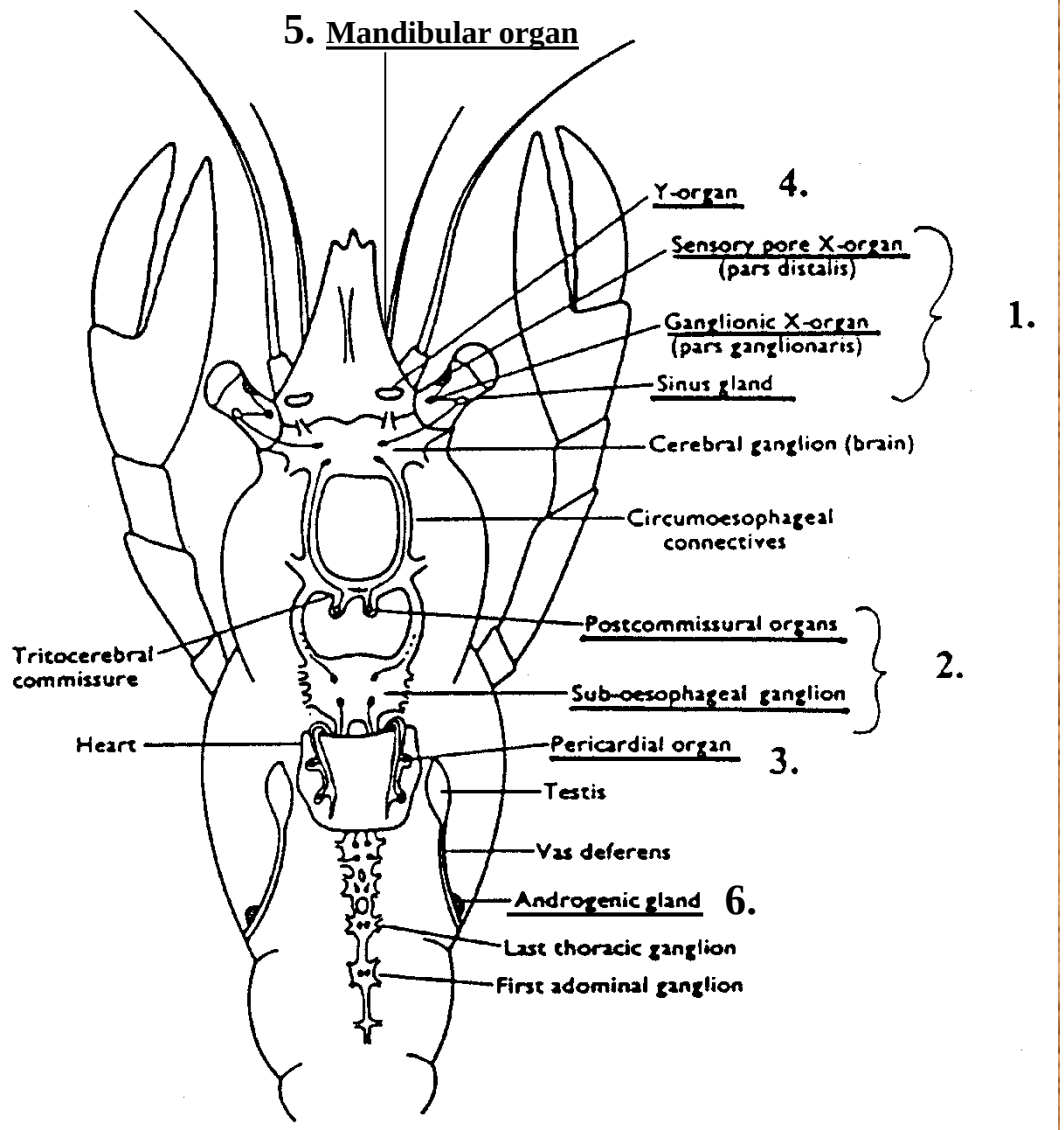

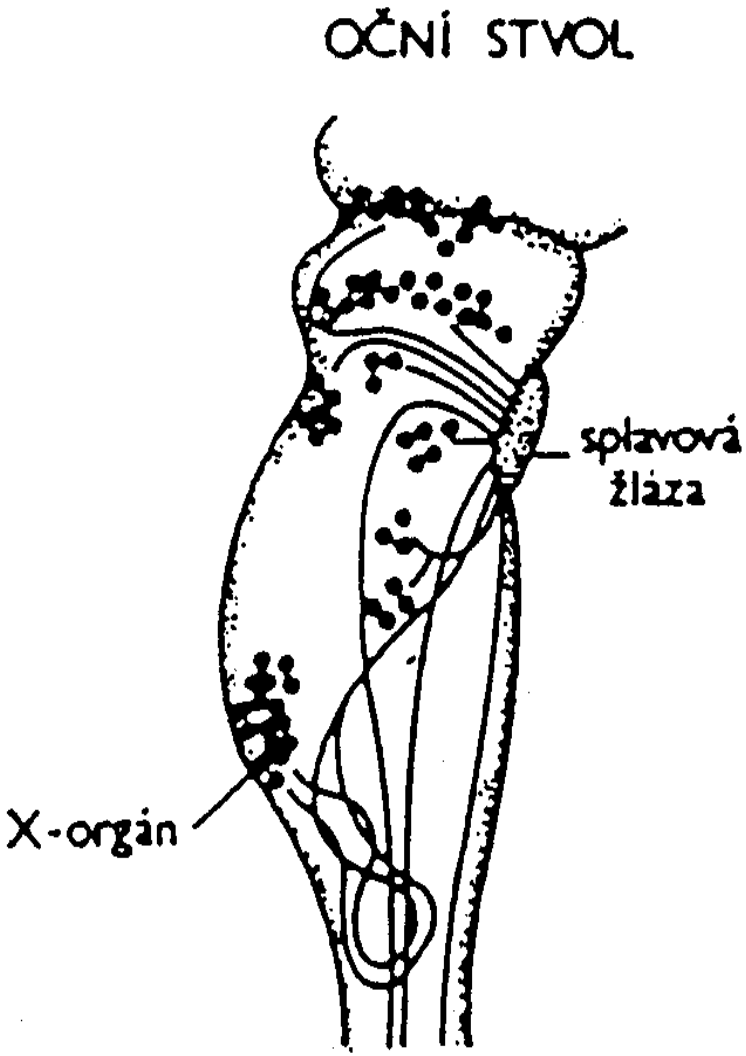

Obr. 6 Endokrinní soustava hmyzu

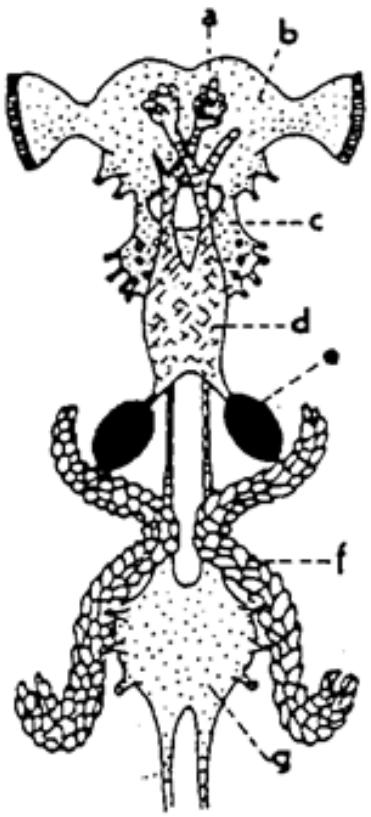

Endokrinní soustava hmyzu
a = neurosekreční buňky
b = mozek
c = podjícnová uzlina
d = corpora cardiaca
e = corpora allata
f = prothorakální žláza
g = I. hrudní ganglion

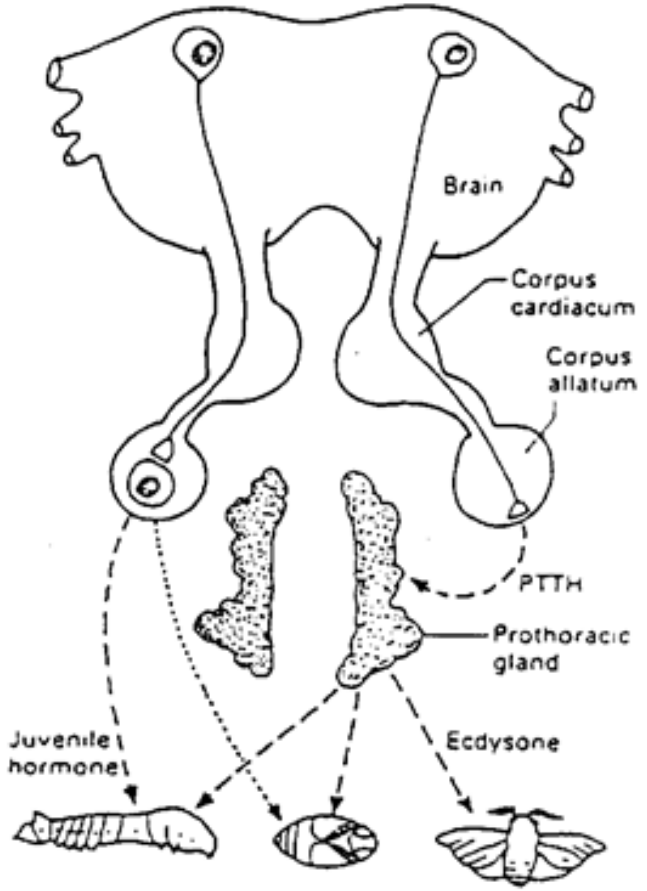

Neuroendocrine control of development in the endopterygote insect *Manduca*. Neurosecretory cells in the brain (one shown, right), with terminals in the corpus allatum, secrete the hormone PTTH which controls the prothoracic glands. Other neurones (one shown, left) control the gland cells of the corpus allatum by, at least in part, the local action of their secretory products. The progression larva–pupa–adult is controlled by ecdysone and juvenile hormone. (For further details, see Box 16.11.)

Obr. 7

Endokrinní soustava hmyzu

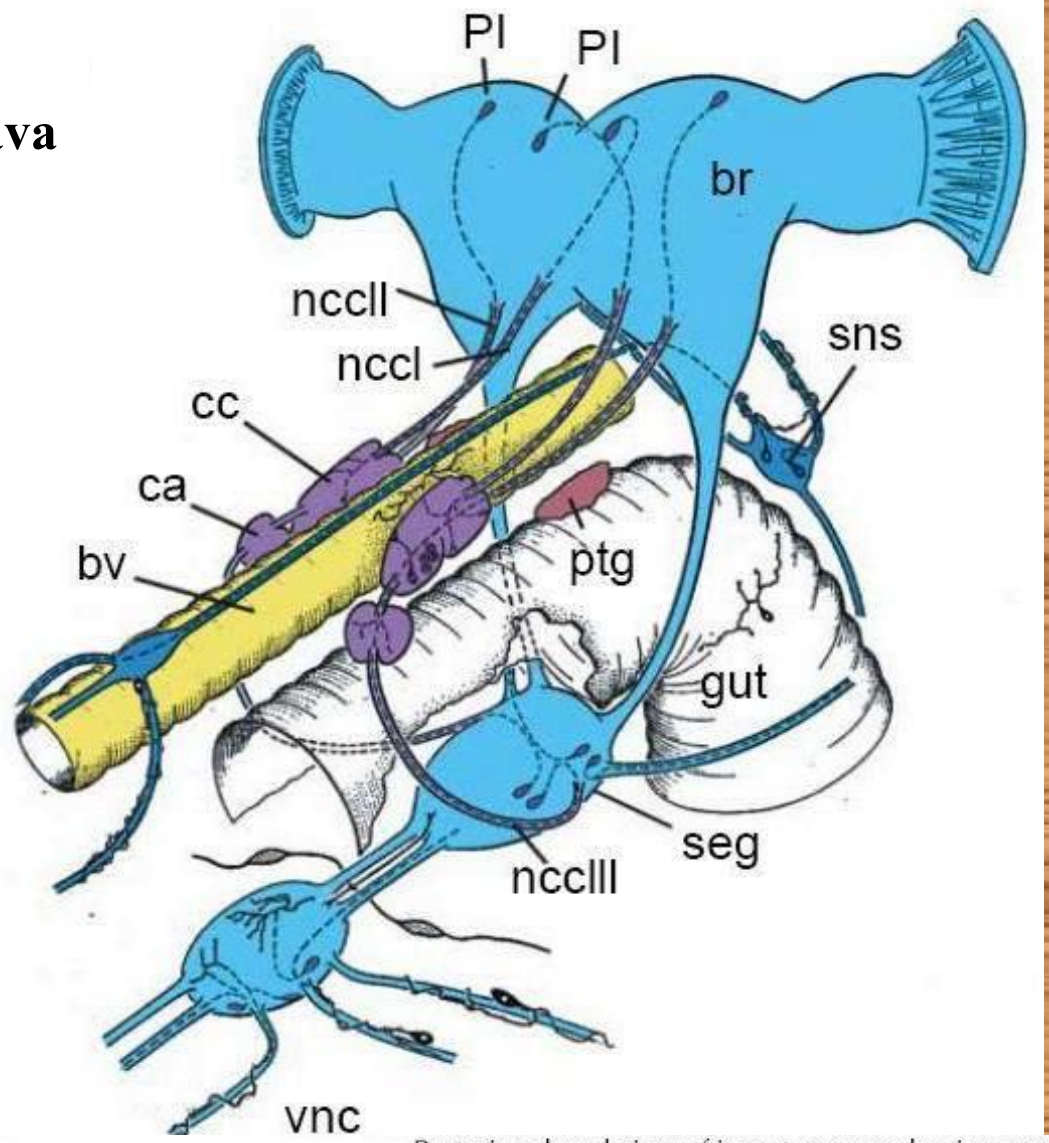

Posterior–dorsal view of insect neuroendocrine system. Central NSCs are located in the pars intercerebralis (PI) and pars lateralis (PL) of the protocerebrum, the tritocerebrum and subesophageal ganglion (seg), and the ventral nerve cord (vnc). Peripheral axons of these cells innervate the retrocerebral complex of endocrine glands via the nccI nerve (from PI), nccII (from PL), and nccIII (from subesophageal ganglion/tritocerebrum). Secretory axons of NSCs located in the ventral nerve cord terminate at neurohemal release sites associated with the glial sheath surrounding the nerve cord and peripheral nerves. The retrocerebral complex receiving NSC axons consists of the corpora cardiaca (cc) and corpora allata (ca), both of which are located close to the dorsal blood vessel (bv). The corpora allata produce juvenile hormone which, together with the steroid ecdysone produced and released by the prothoracic gland (ptg), control growth and molting. The stomatogastric nervous system (sns) contains further NSCs and is functionally closely connected to the corpora allata and corpora cardiaca.

Obr. 8

Hmyzí endokrinní žlázy

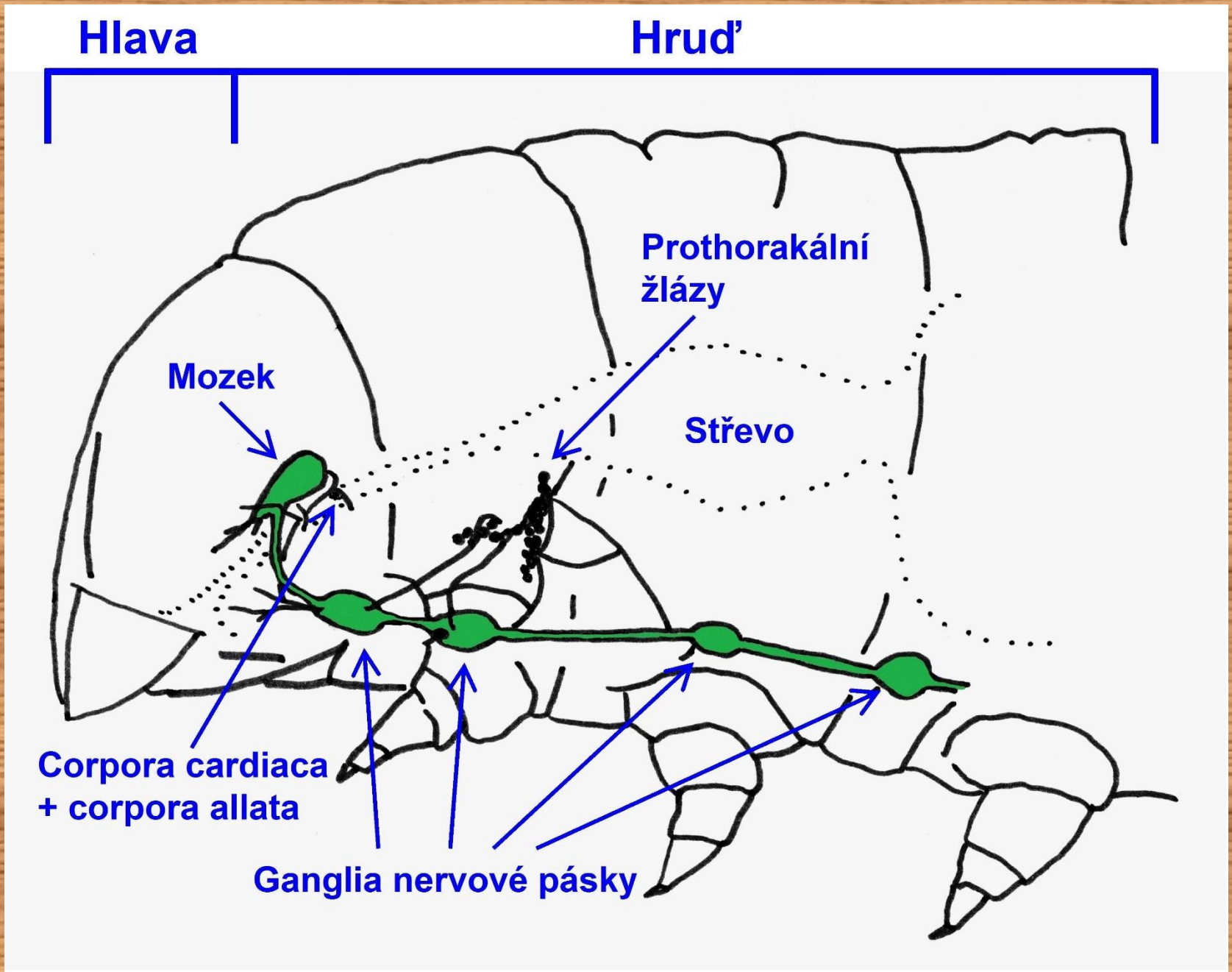

Obr. 9 Neuresekretorické buňky

Granule v neurosekretorických buňkách mozku ploštice *Pyrrhocoris apterus* obsahující adipokinetický hormon (TEM, foto F. Weyda)

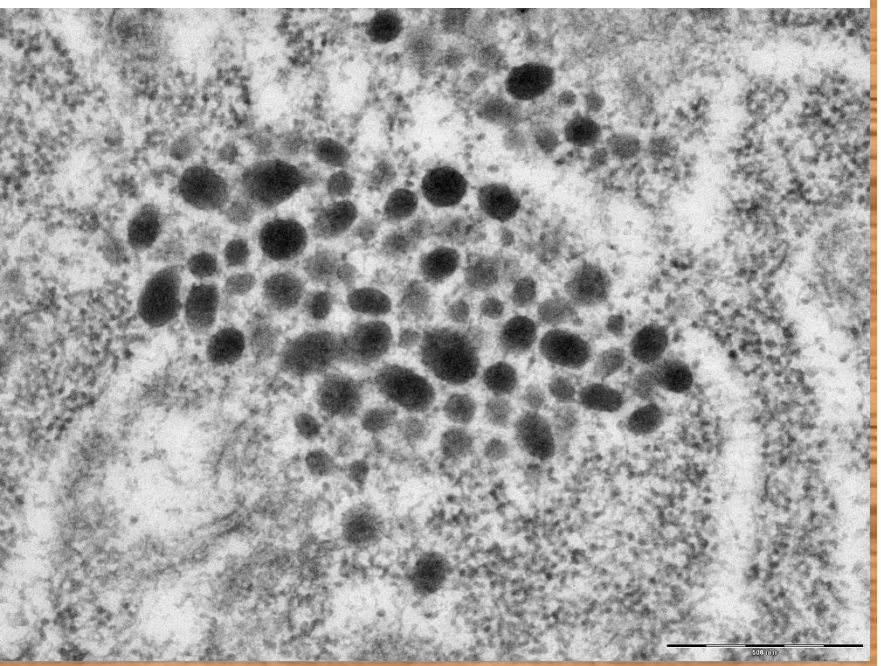

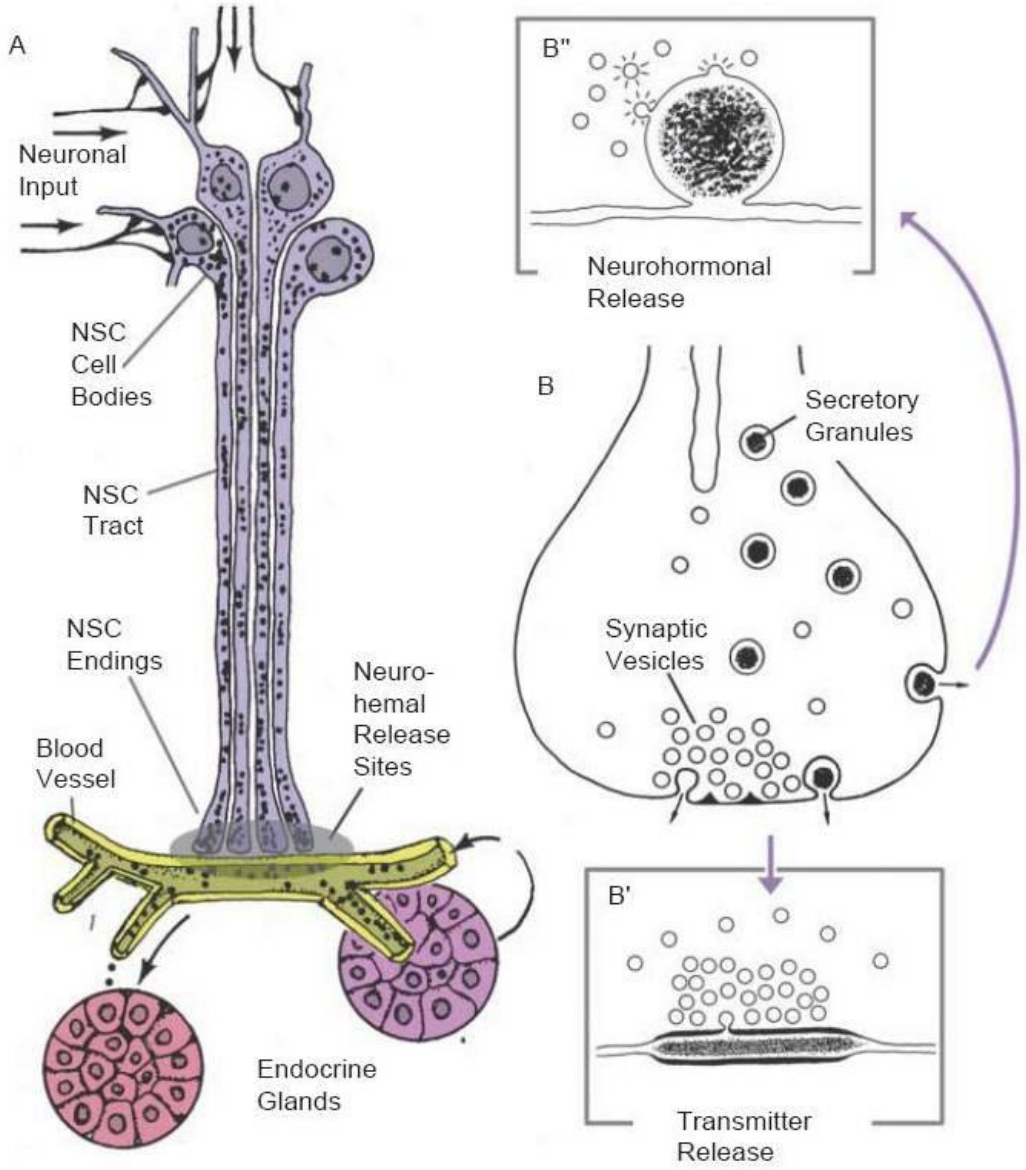

Figure 1 Structure of the neuroendocrine system. (A) Somata of neurosecretory cells (NSCs) are located in the central nervous system and receive neuronal input from presynaptic neurons. NSC axons project to peripheral neurohemal release sites that are frequently in close contact with endocrine cells targeted by the neurohormones released at the NSC terminals (after Scharrer & Scharrer 1963). (B) Ultrastructural aspects of neurotransmitter release (B′) and neurohormonal release (B″). Neurotransmitter release occurs exclusively at presynaptic sites from 50 nm vesicles. Neurohormones are stored in large vesicles found throughout the NSC and released outside synapses (after Golding & Pow 1988).

Prothorakální žlázy u sarančete *Locusta migratoria*

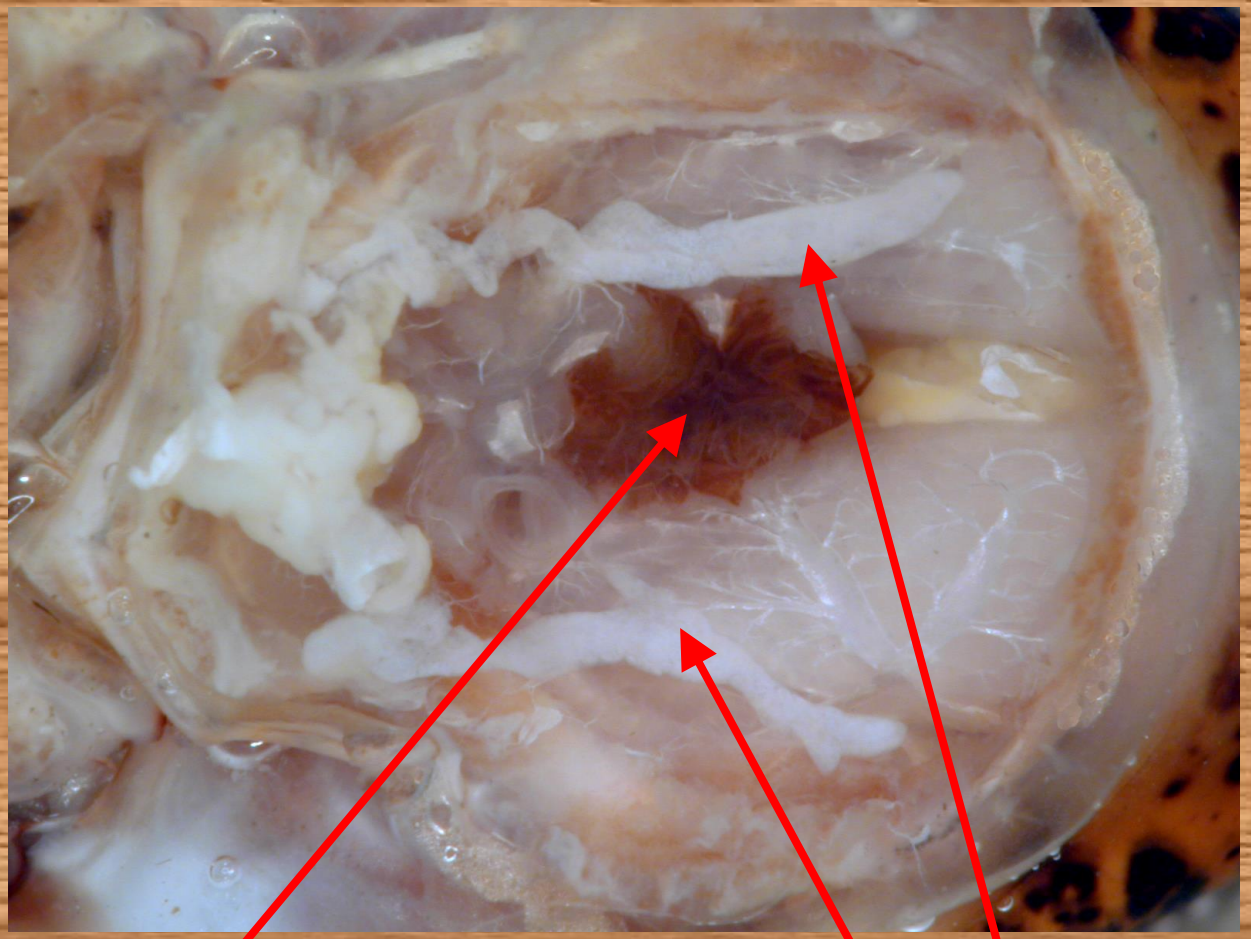

Obr. 10

Prothorakální žlázy u sarančete *Locusta migratoria*

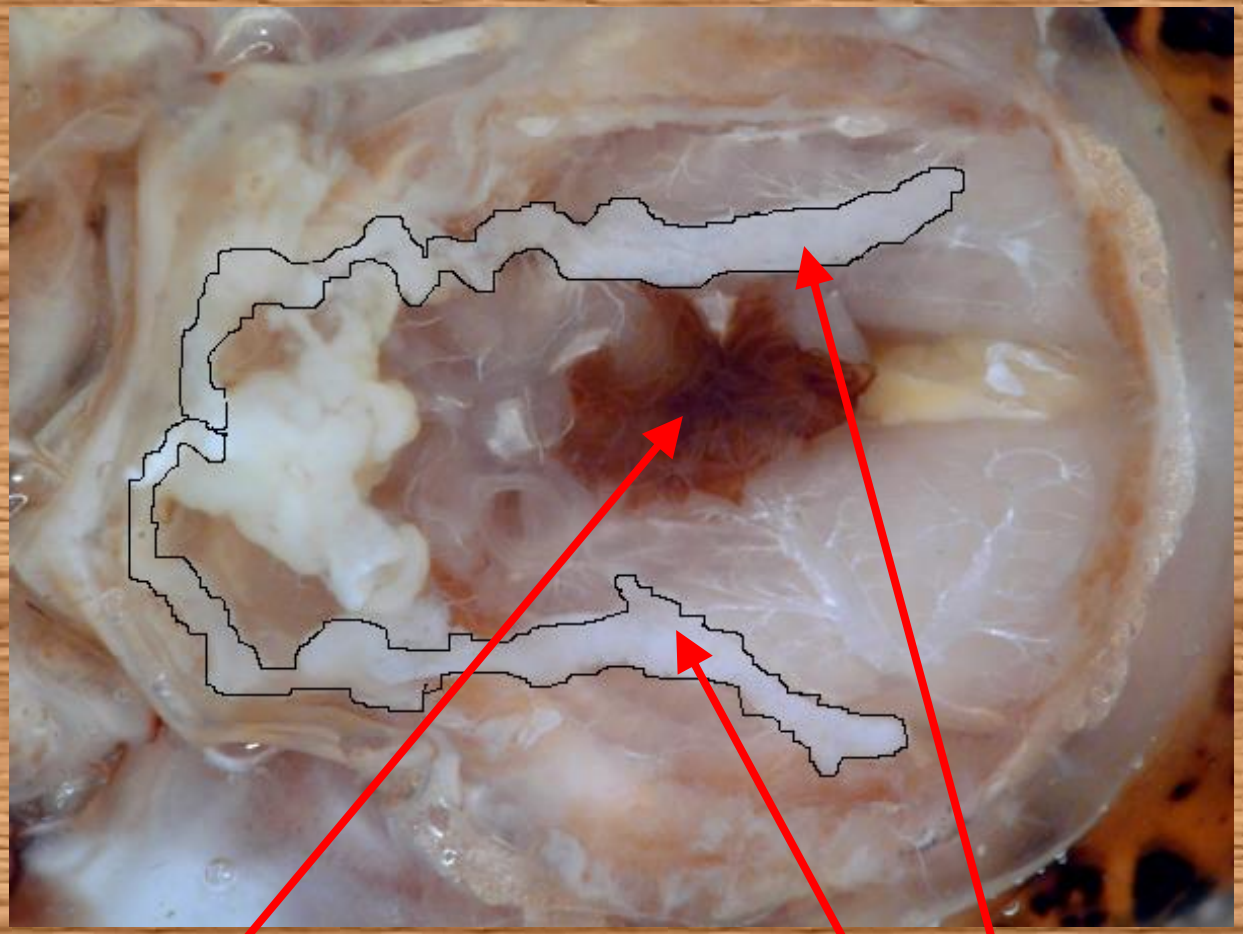

Obr. 11

Obr. 12 Prothorakální žlázy hmyzu

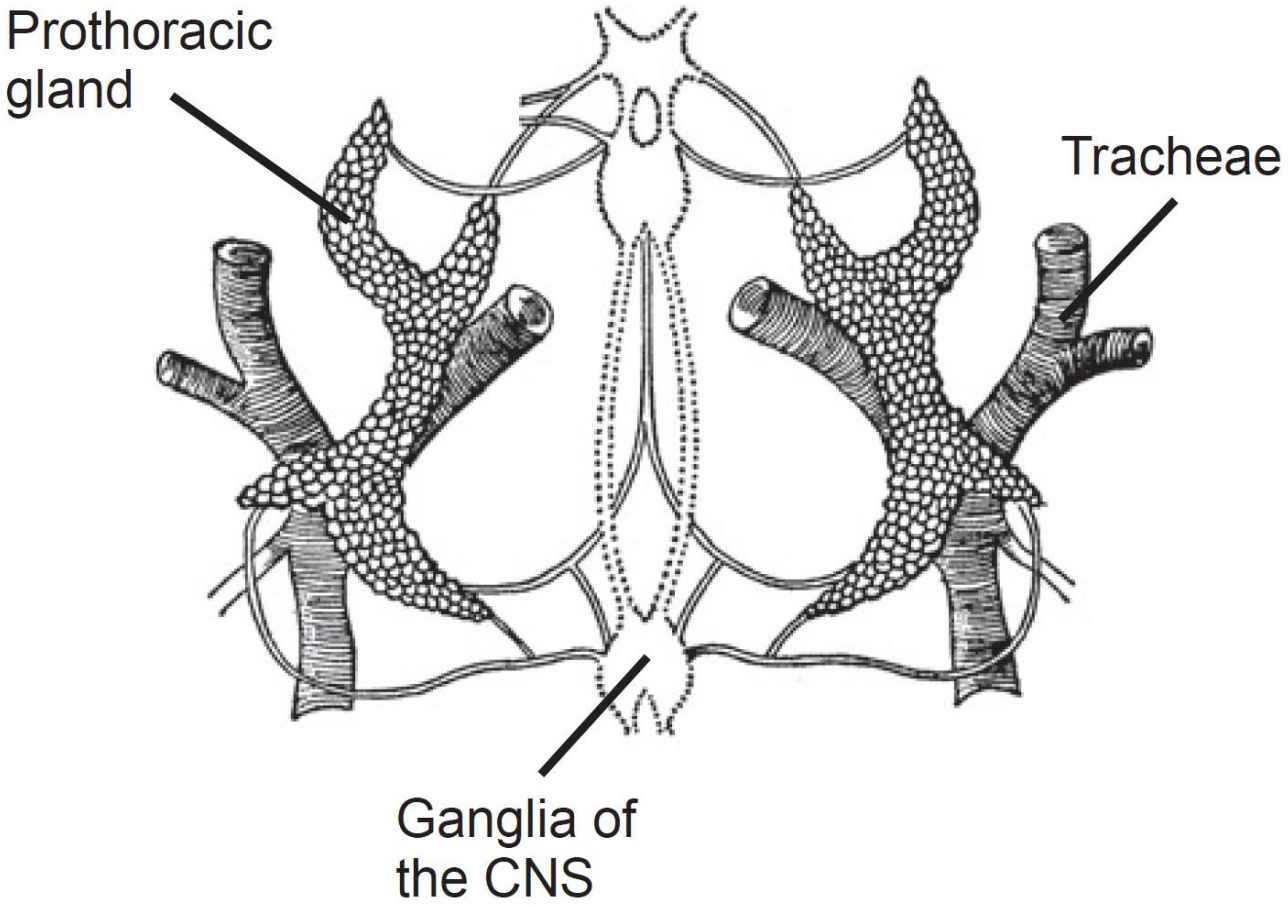

FIGURE 1.22. Location of the prothoracic glands around the thoracic tracheae. From Cymborowski (1992). Reprinted with permission.

Obr. 13 Kruhová žláza Dipter

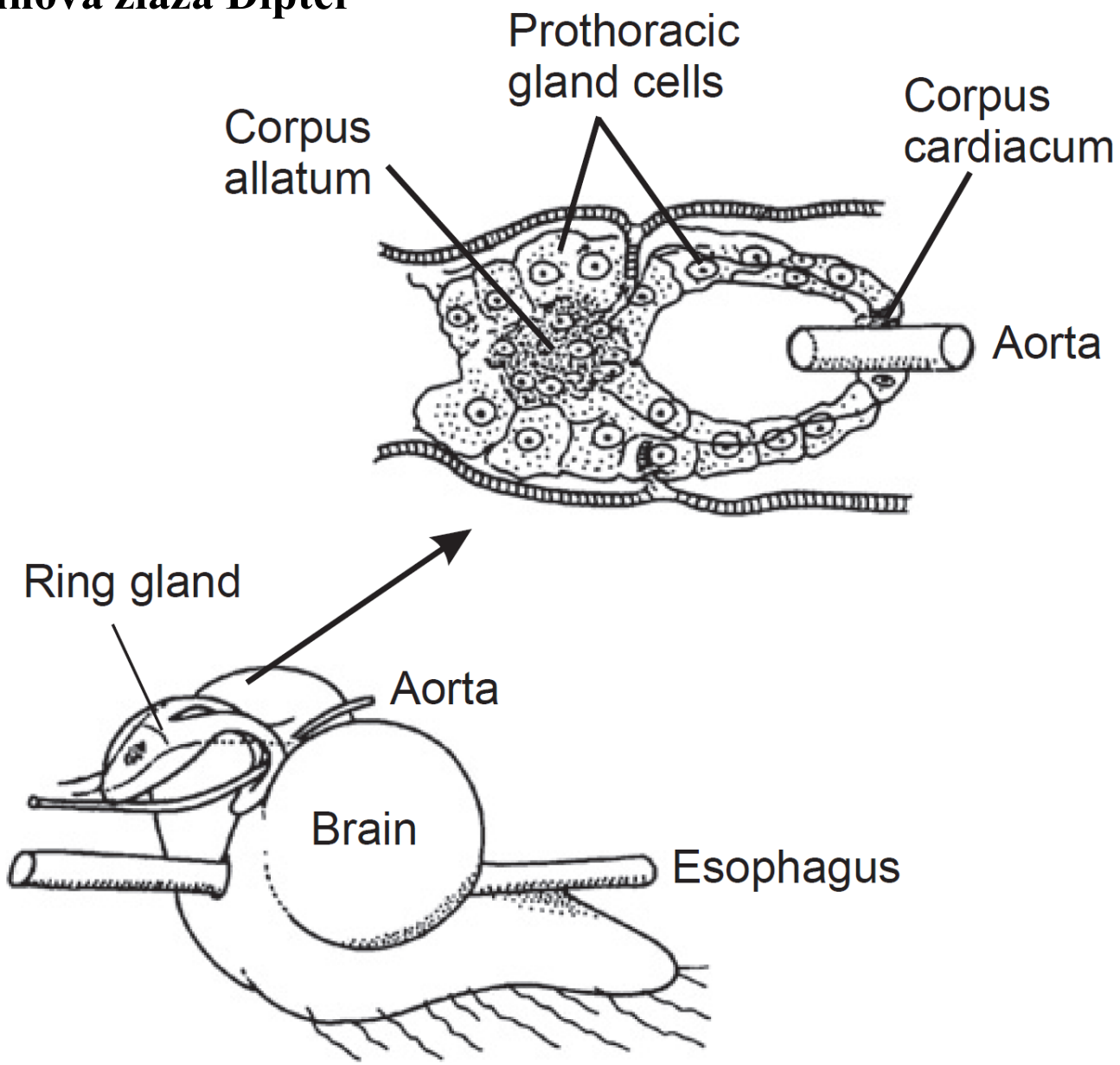

FIGURE 1.21. The ring gland of higher dipterans, consisting of the corpus cardiacum, corpus allatum, and the prothoracic gland assembled in a ring structure. From Wigglesworth (1984).

Obr. 14

Mozek a kruhová žláza u Diptera

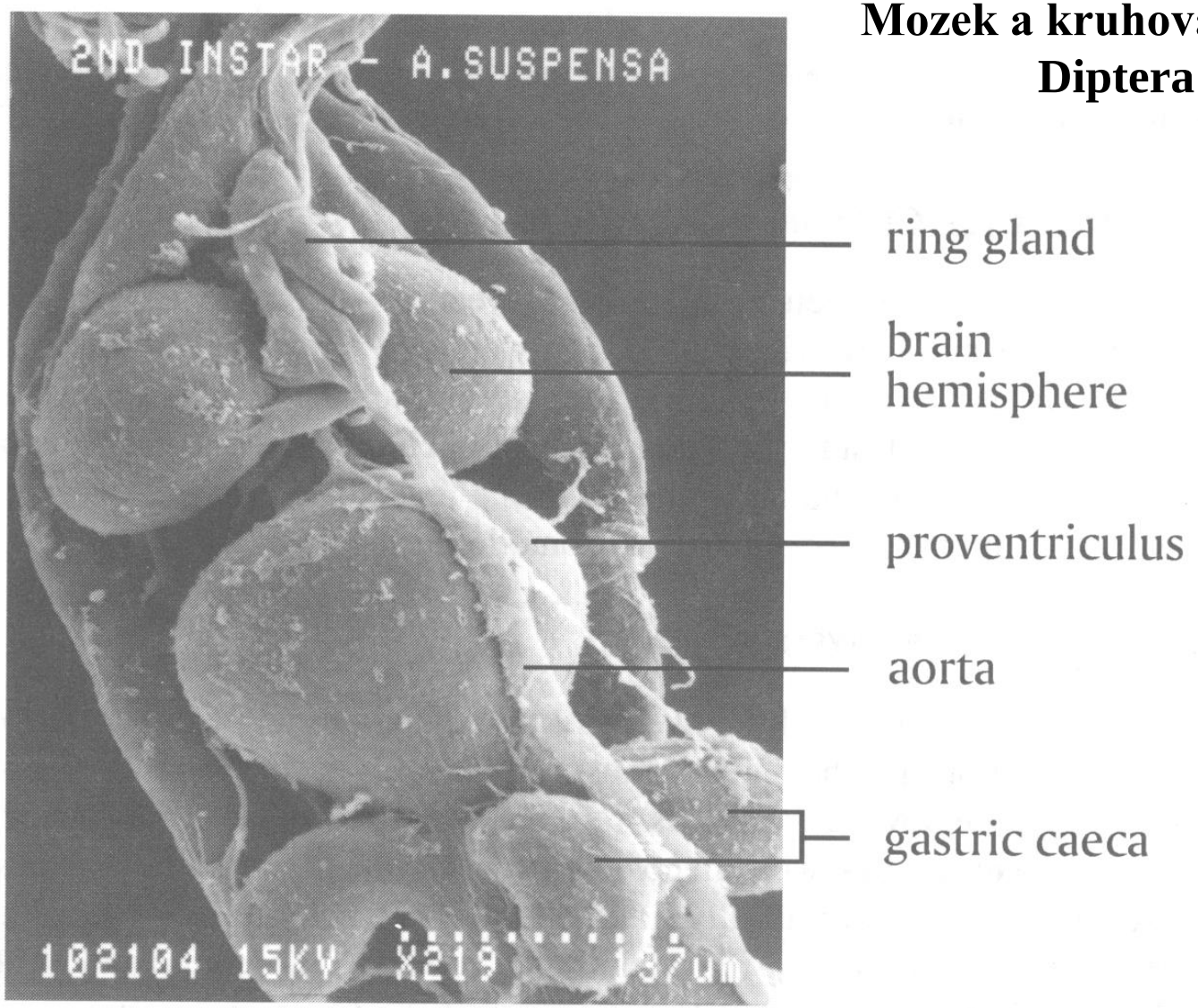

FIGURE 5.10 A scanning electron micrograph of the larval ring gland and brain in a 2nd instar of the tephritid fruit fly *Anastrepha suspensa*. Note the aorta passing through the ring gland.

Obr. 15 Neurosekretorické buňky a neurohemální orgány u housenek *Manduca*

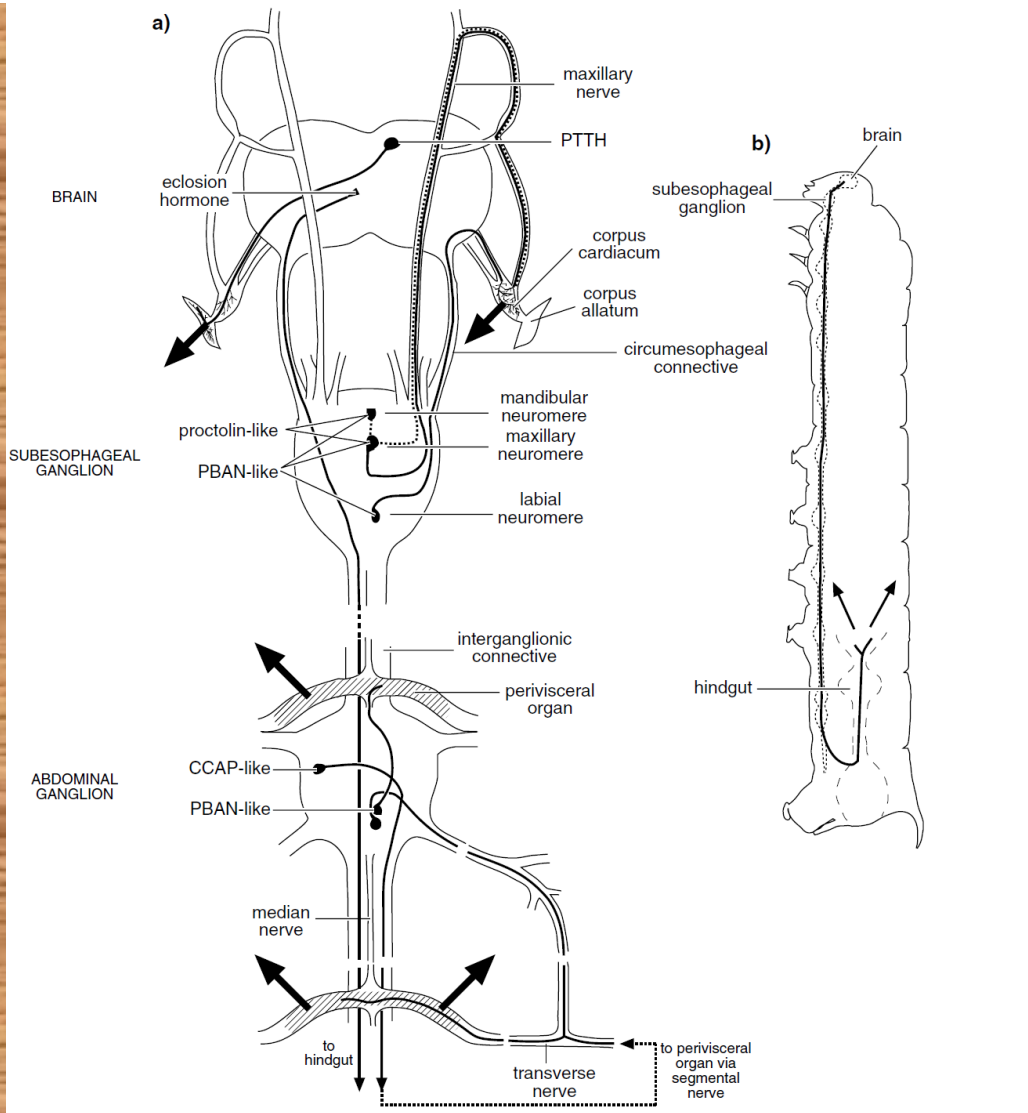

Fig. 21.7. Examples of neurosecretory cells and neurohemal organs in the larva of *Manduca*. **(a)** Connections of some neurosecretory cells with their neurohemal organs. Bold arrows indicate release of peptides into hemolymph. Only a few of the cells are shown. Note that, in most insects, the corpora cardiaca are the neurohemal organs for prothoracicotropic hormone (PTTH); the Lepidoptera are unusual in using the corpora allata for this purpose. It is important to note that the suffix 'like' on some labels indicates that the peptides in the labelled cell are similar to, but not necessarily the same as the named peptide. Their functions are generally unknown. Abbreviations: CCAP, crustacean cardioactive peptide; PBAN, pheromone biosynthesis activating neuropeptide (based largely on data of Dr. N.T.Davis). **(b)** Eclosion hormone is released from neurohemal areas on the hindgut. The position of the soma in the brain is shown in (a) (after Truman & Copenhaver, 1989).

Obr. 16

Přehled hmyzích hormonů

1. Ekdysteroidy

- ekdyson, 20-hydroxyekdyson (20-E), makisteron A (=24-metyl-20E), 2-deoxyekdyson, 26-hydroxyekdyson a další

2. Juvenilní hormony

JH-I, JH-II, JH-III, JH-0, 4-metyl-JH-I, kyselina juvenilního hormonu

3. Peptidické neurohormony

I. Hormony řídící metabolismus a homeostázu

1. Adipokinetické hormony (AKH) a hypertrehalosemické hormony
2. Diuretické hormony
3. Antidiuretické hormony
4. Chloride transport stimulating hormone a ion transport peptide

II. Hormony řídící metamorfózu, vývoj a růst

1. Prothoracikotropní hormon (PTTH) a bombyxin
2. prothoracikostatický hormon (PTSH)
3. Allatostatiny a allatotropin
4. PBAN I, II, III (pheromone biosynthesis activating neuropeptide)
5. Eklozní hormon a *ecdysis triggering hormone (ETH)*
6. Burzikon
7. Faktory regulující puparizaci much
8. Diapauzní hormon

III. Hormony řídící pohlavní funkce

1. stimulační gonádotropní neurohormony (gonadotropiny):
   - ovary maturing parsin (OMP)
   - egg development neurohormone (EDNH) (=ovarian ecdysteroidogenic factor)
2. inhibiční neurohormony (antigonadotropiny, folikulostatiny):
   - neuroparsin
   - oostatické hormony a TMOF (trypsin-modulating oostatic factor)

VI. Hormony modifikující svalovou kontrakci (myotropní peptidy)

1. Proctolin
2. Kardiostimulační hormony - crustacean cardioactive peptide (CCAP)
3. Skupiny myotropních neurohormonů - myokininy, sulfakininy, pyrokininy, tachykininy, myoinhibiční peptidy, periviscerokininy, FMRF-amid

V. Hormony řídící barvoměnu (chromatotropiny)

1. PDF - pigment dispersing factor
2. MRCH - melanization and reddish coloratig hormone (identický s PBAN)

https://www.youtube.com/watch?v=XMzoq9fUyiE

Obr. 17

Ekdysteroidy

Ecdyson, 20-hydroxyecdyson (20-E), makisteron A (=24-methyl-20E), 2-deoxyecdysone, 26-hydroxyecdysone a další

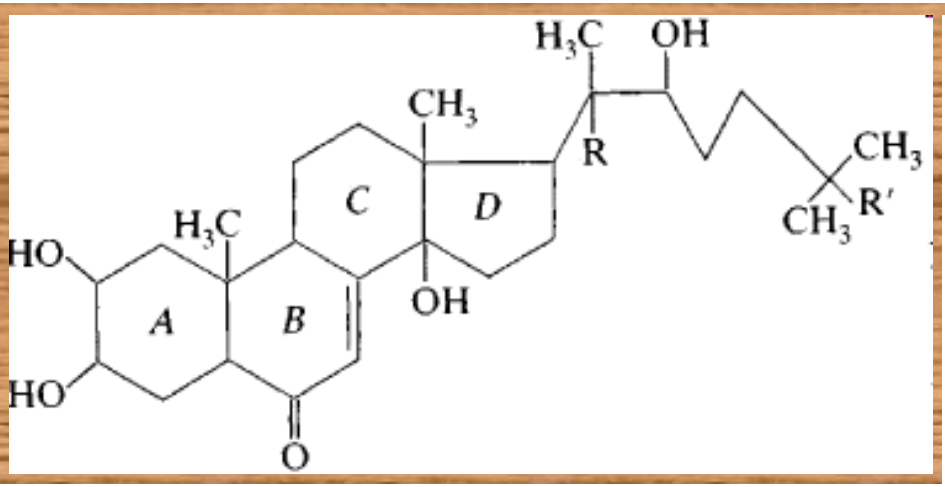

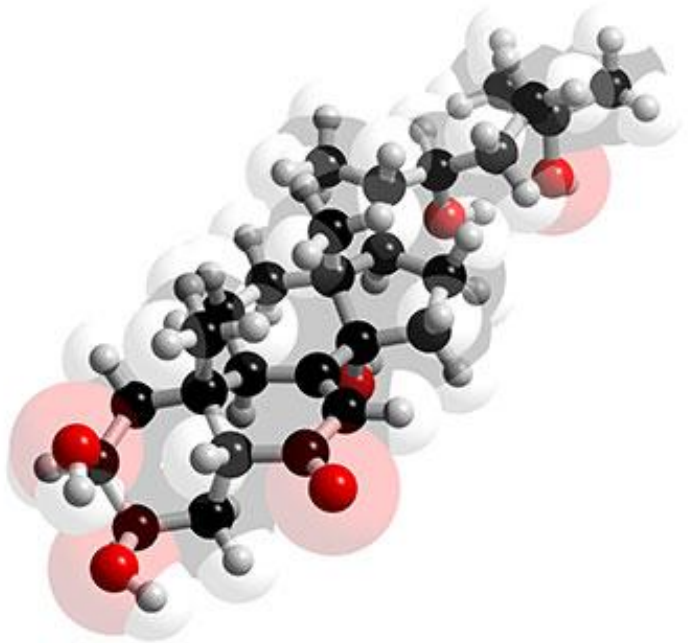

Funkce

- Řízení svlékaní a metamorfózy
- Řízení reprodukce - tvorba gamet

- Další funkce – ovlivnění metabolických procesů, diapauzy, proteosyntézy atd.

Obr. 18 Přehled hlavních ekdysteroidů

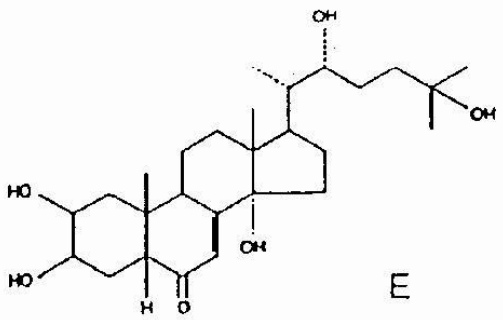

E

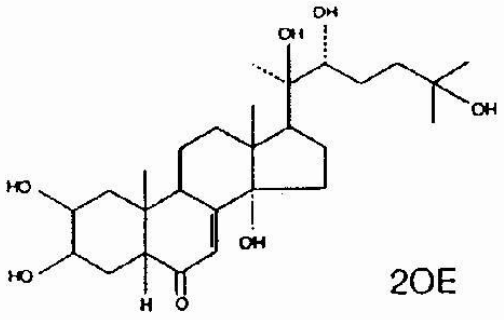

20E

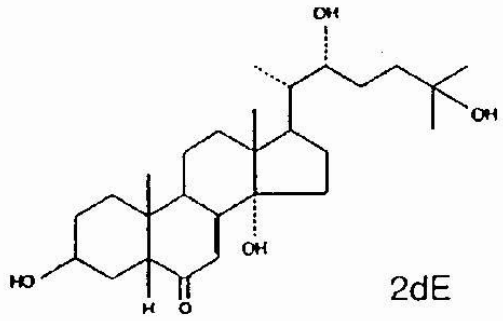

2dE

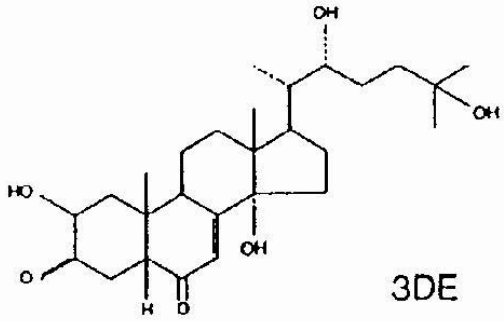

3DE

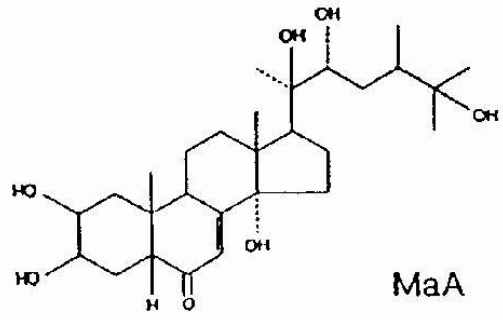

MaA

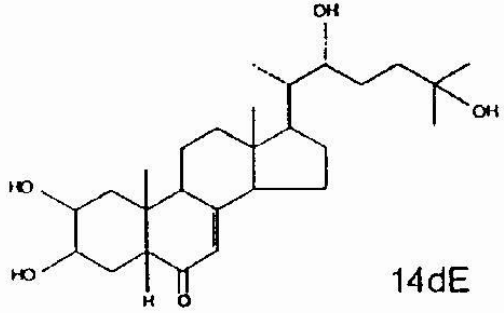

14dE

FIG. 2. Structural formulas of some major zooecdysteroids. E, ecdysone; 20E, 20-hydroxyecdysone; 2dE, 2-deoxyecdysone; 3DE, 3-dehydroecdysone; MaA, maldsterone A (24Me20E); 14dE, 14-deoxyecdysone.

Obr. 19 Struktura ekdysonového receptoru

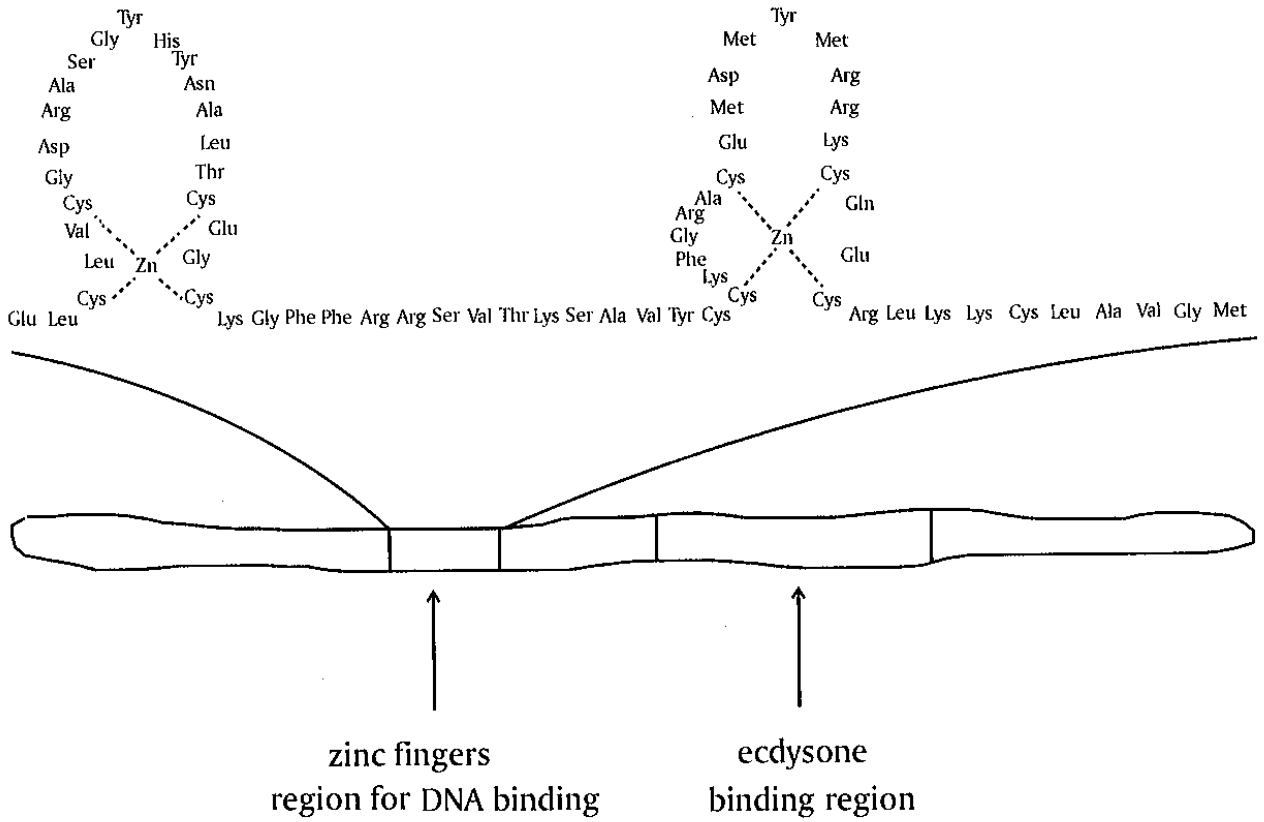

FIGURE 5.19 Representation of the amino acid sequence and Zn atoms in the two zinc fingers in the DNA binding region of the ecdysone receptor isolated from *Drosophila* cultured K_c cells. Additional portions of the receptor molecule (bottom diagram) are involved with actual binding of the ecdysteroid hormone and possibly with transactivation after binding to the DNA.

Obr. 20

Prothorakální žlázy a metabolismus ekdysteroidů

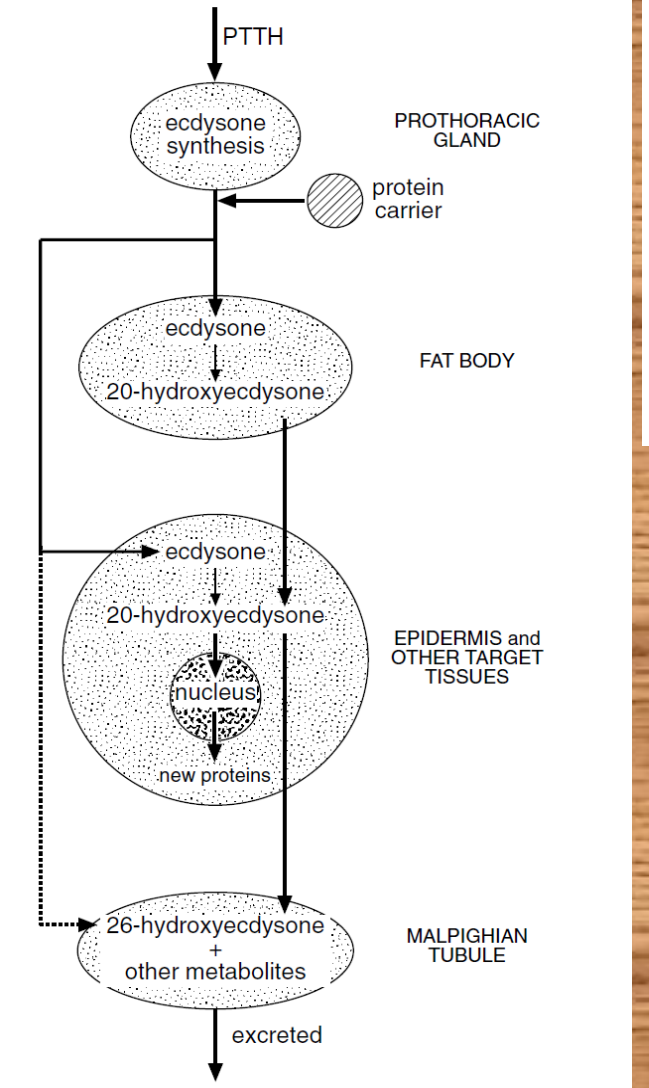

Fig. 21.9. Ecdysteroids. The principal stages in the production, activity and degradation of ecdysteroids.

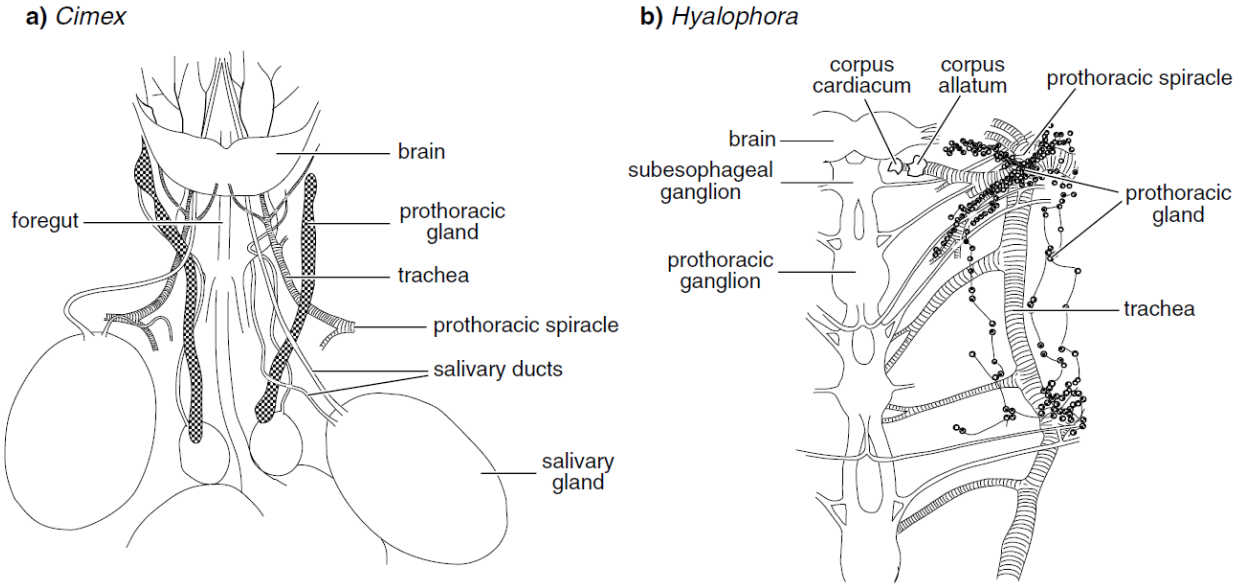

Fig. 21.4. Prothoracic glands shown by dark shading. General arrangement: **(a)** in larval bed bug, *Cimex* (after Wells, 1954); **(b)** in pupal silk moth, *Hyalophora* (after Herman & Gilbert, 1966).

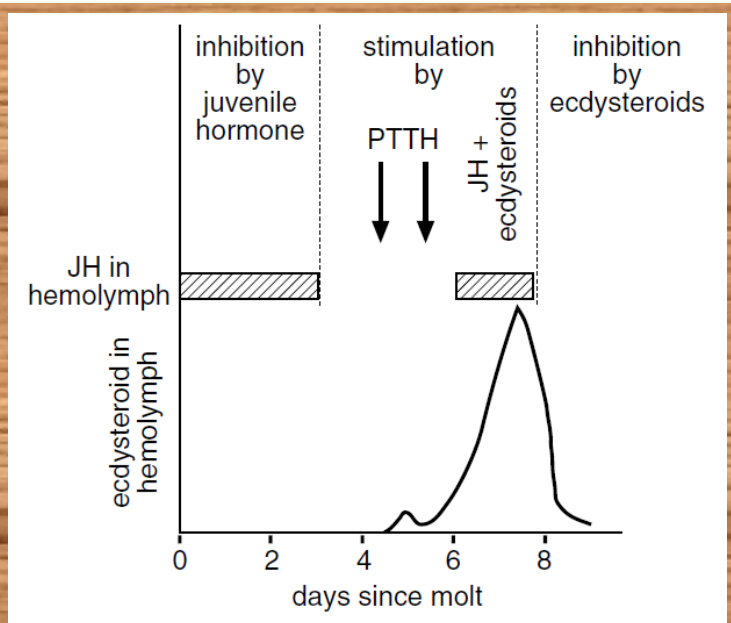

Fig. 21.8. Prothoracic glands: regulation of synthetic activity in the final stage larva of *Manduca* (based on Smith, 1995).

Obr. 21 Změny hladin metamorfozních hormonů během vývoje

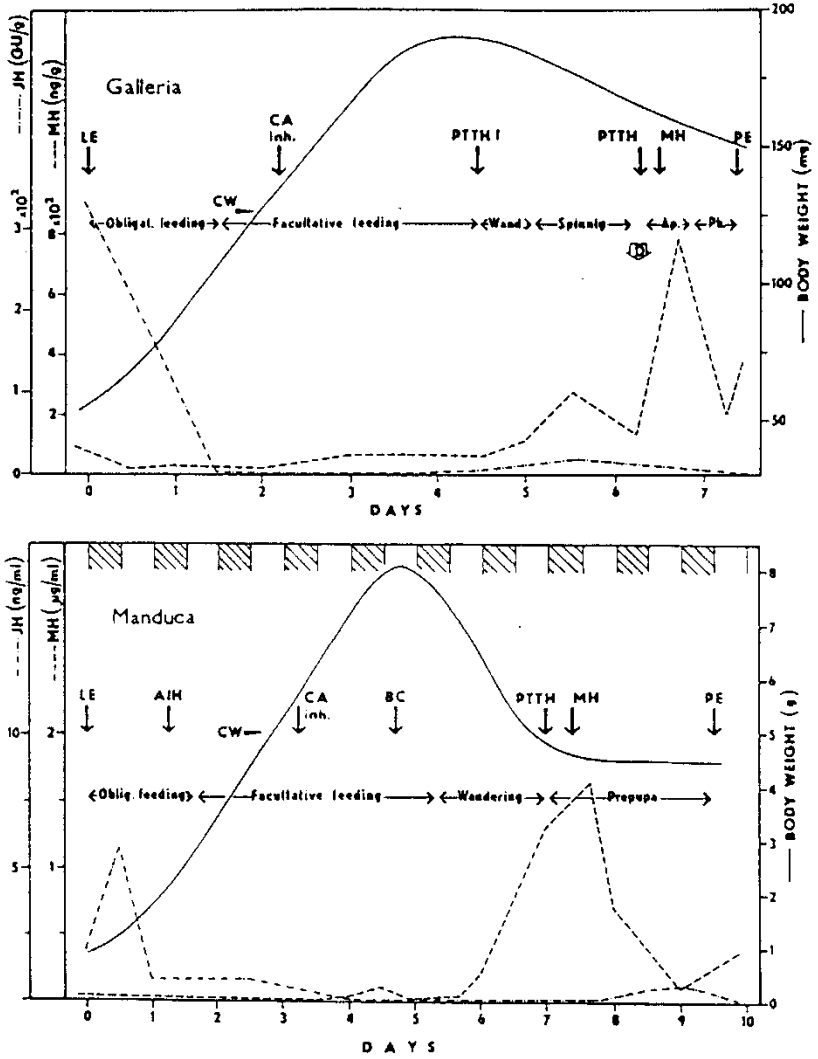

FIG. 20. The timing of crucial developmental events in the last larval instar of *Galleria mellonella* and *Manduca sexta* (Lepidoptera) in relation to body weight and hormone concentrations. Explanations from left to right: *LE*, last larval ecdysis; AIH-release of allatohibin; CW, critical weight (metamorphosis cannot be reversed to larval development any more); *CA inh.*, inhibition of corpora allata; *BC*, brain critical period for several events (gut purge, exposure of dorsal vessel) which precede wandering in *Manduca*; *PTTH?*, – possible release of prothoracicotropin at the termination of feeding in *Galleria*; *PTTH*, brain (and presumably further PTTH secretion) becomes dispensable for pupal moult; *MH*, prothoracic glands (and presumably further ecdysone secretion) become dispensable; *D*, *Galleria* can enter diapause at this time; *Ap.*, apolysis; *Ph.*, pharate pupa, *PE*, pupal ecdysis. Many developmental events in *Manduca* are precisely synchronized with photoperiod (hatched intervals indicate scotophase). Concentration of juvenile hormone is expressed in equivalency of JH I in *Galleria* units or in ng ml^{-1} haemolymph; concentration of ecdysteroids (MH) is expressed in equivalents of 20-hydroxyecdysone as ng g^{-1} body weight or µg ml^{-1} haemolymph. The chart for *Galleria* was compiled from Peferoen, M. and De Loof, A. (1980), Sehnal, F. (1966b); Sehnal, F. and Granger, N. (1975), and Sehnal, F. *et al.* (1981); that for *Manduca* is based on the papers by Bhaskaran, G. (1981); Bollenbacher, W. *et al.* (1981); Riddiford, L. and Truman, J. (1978); Truman, J. and Riddiford, L. (1974) and Williams, C. (1976).

Obr. 22

Juvenilní hormony

JH-I, JH-II, JH-III, JH-0, 4-methyl-JH-I

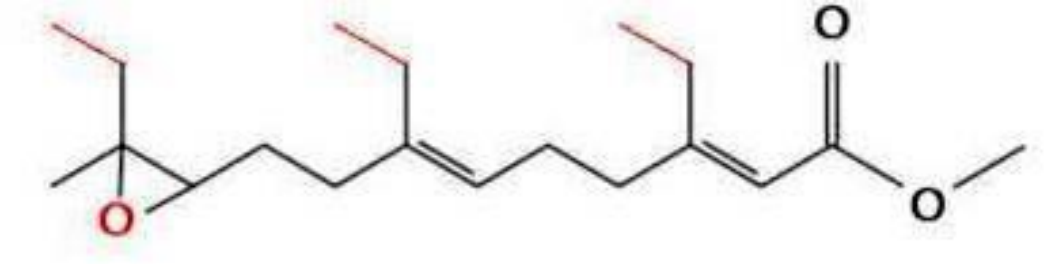

Funkce

- Udržování jedince v juvenilním stádiu = bránění metamorfóze

- reprodukce – tvorba žloutku (vitellogeninu - Vg)

Další funkce – diapauza, syntéza bílkovin, metabolismus, pigmentace, polymorfismus, barvoměna atd.

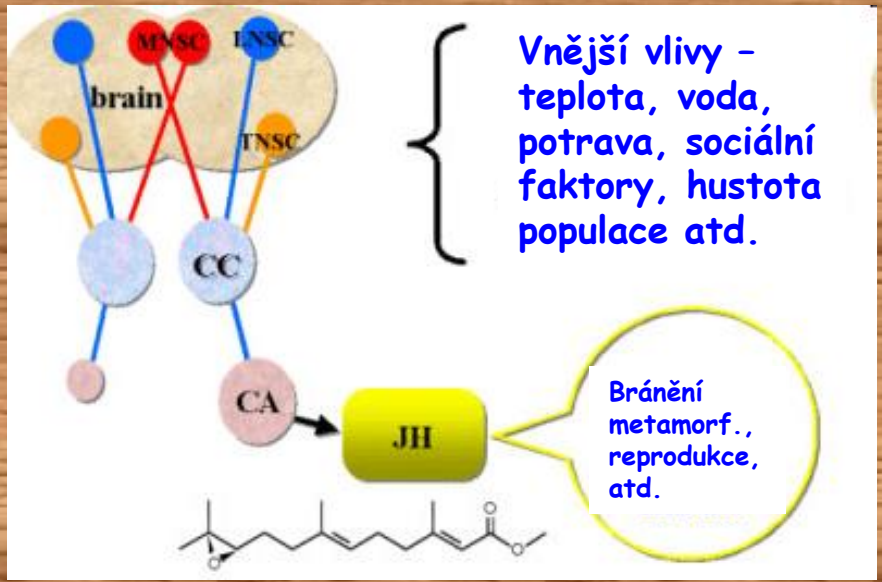

Obr. 23 Juvenilní hormony

JH-0	$R_1=R_2=R_3=C_2H_5$
JH-I	$R_1=R_2=C_2H_5$, $R_3=CH_3$
JH-II	$R_1=C_2H_5$, $R_2=R_3=CH_3$
JH-III	$R_1=R_2=R_3=CH_3$

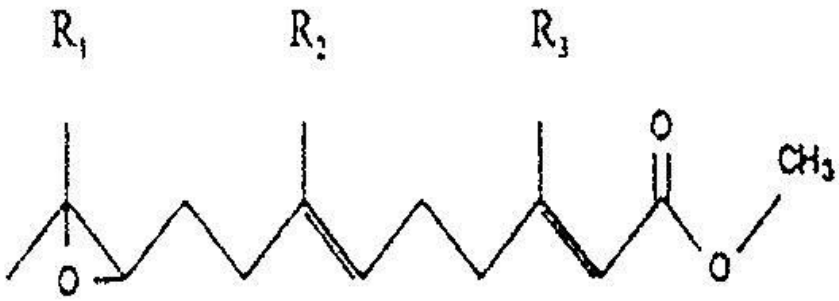

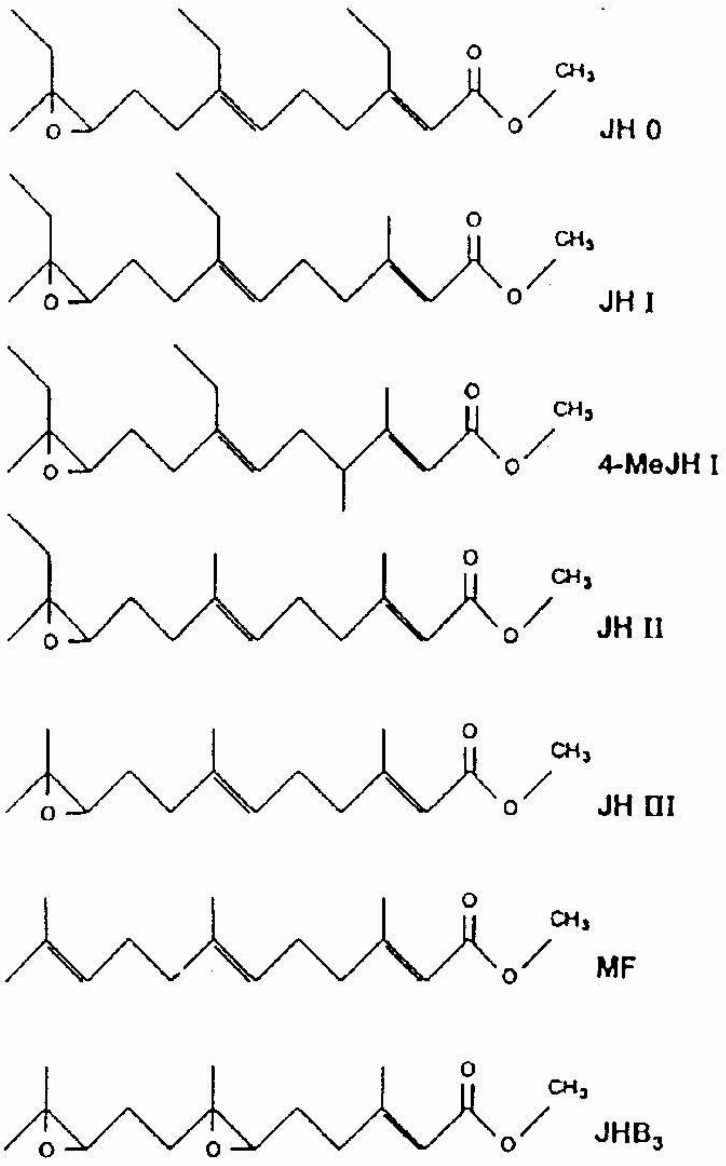

FIG. 1. Juvenile hormone homologs. JH 0-III, juvenile hormone 0-III; 4 MeJH 1, 4-methyl JH I; JHB_3, JH III bisepoxide; MF, methyl farnesoate.

Obr. 24 **Imaginální disky**

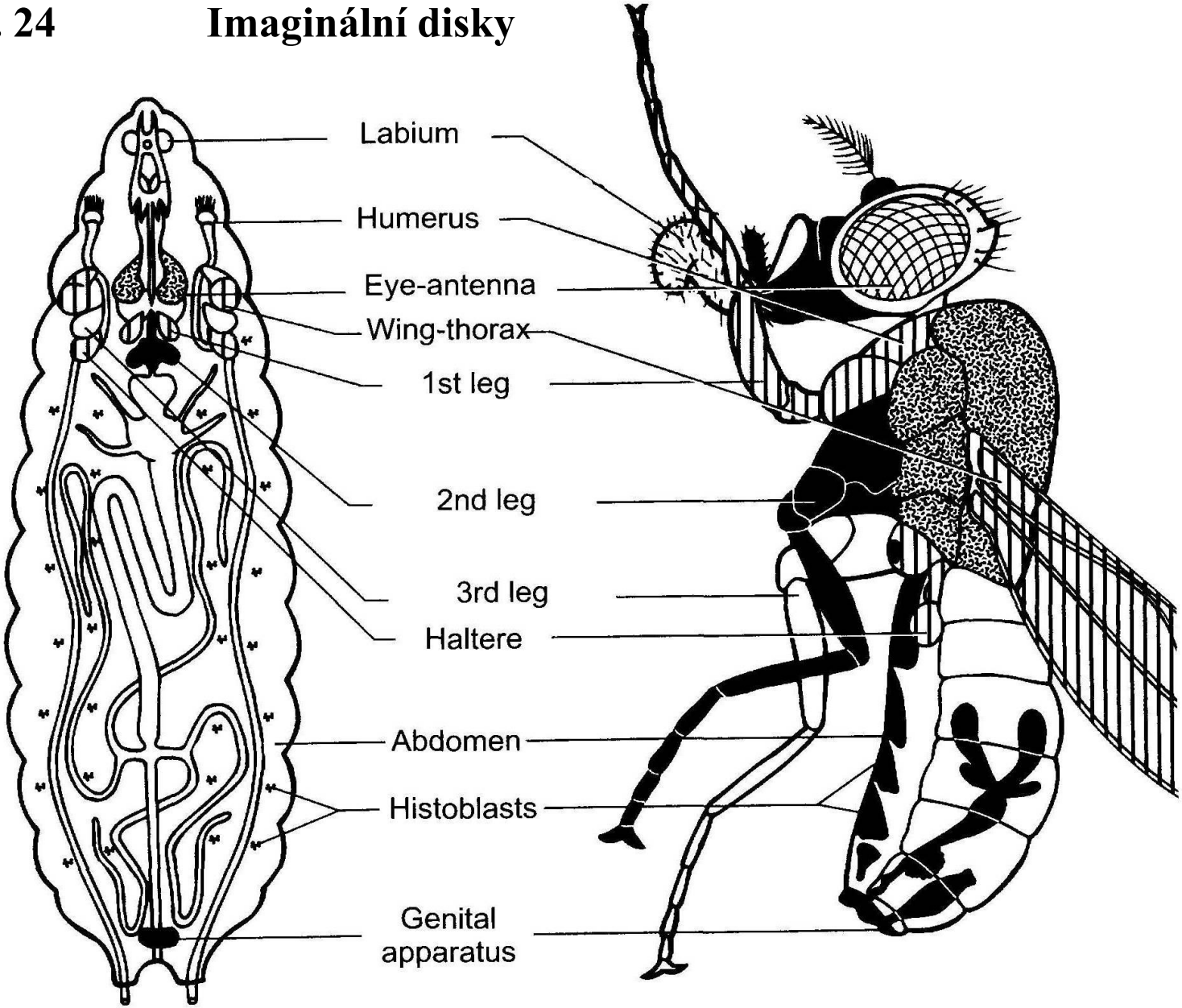

FIGURE 2.28. The imaginal discs of a larval *Drosophila* (left) and the corresponding structures in the adult (right) to which they give rise. From Nothiger (1972). Reprinted with permission.

Obr. 25 **Řízení hladiny juvenilního hormonu**

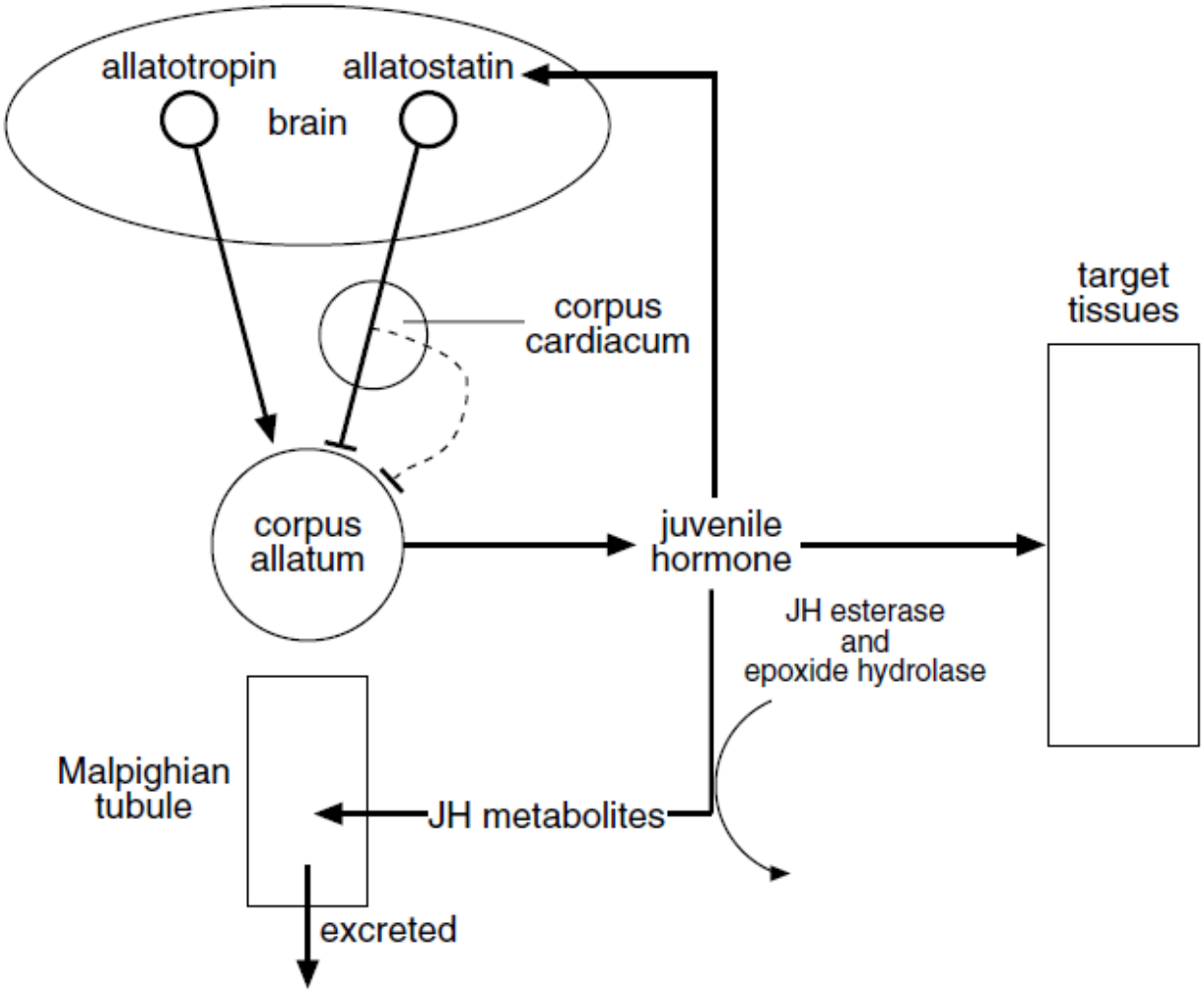

Fig. 21.11. Juvenile hormone. Regulation of hemolymph titer involves the balance between synthesis in the corpora allata and degradation and excretion by the Malpighian tubules.

Obr. 26

Hladina juvenilního hormonu během vývoje Holometabol

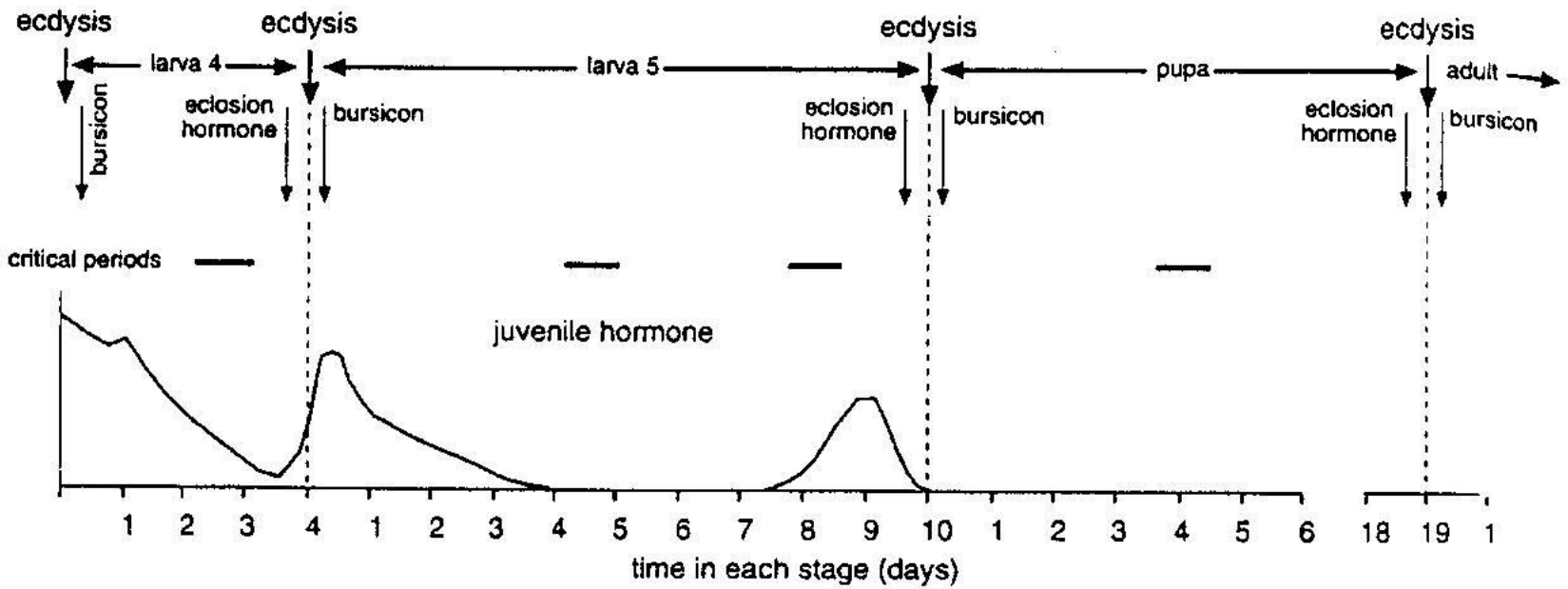

Tvorba přechodných forem larva-kukla po aplikaci juvenoidu u potemníka moučného Tenebrio molitor

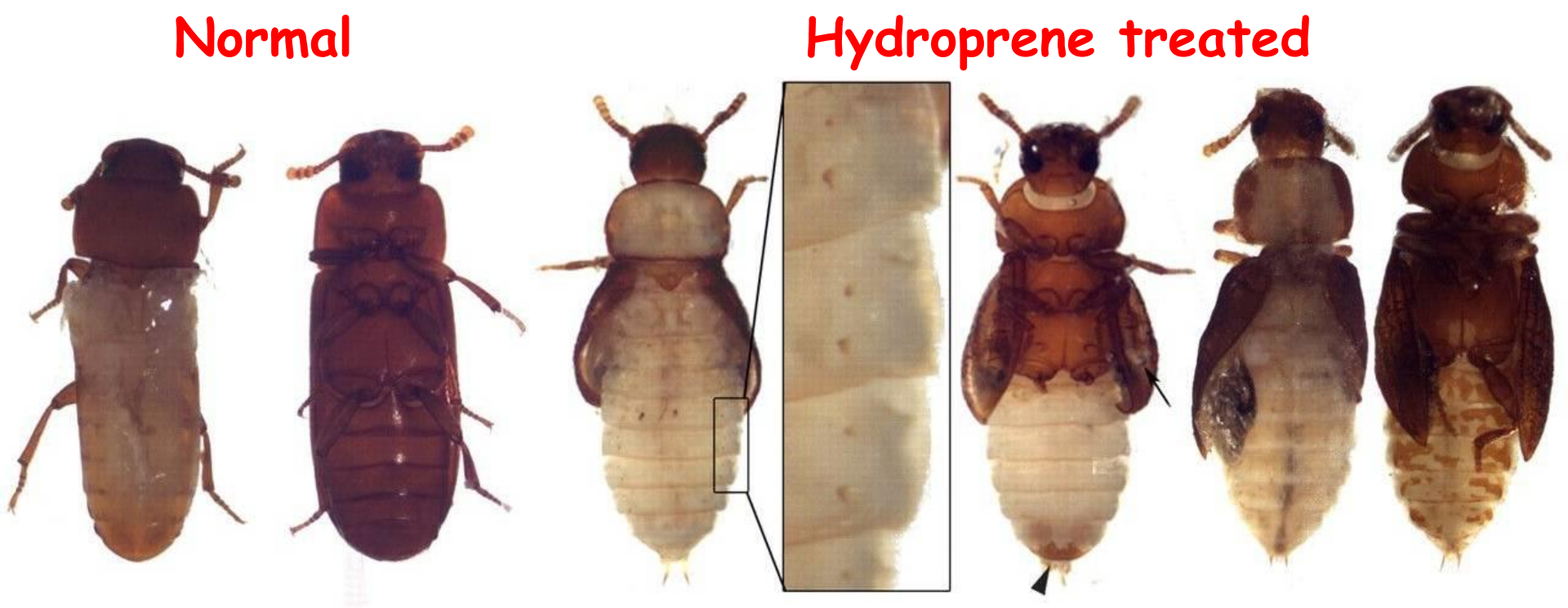

Obr. 27

Účinek juvenoidů u zavíječe voskového Galleria mellonella

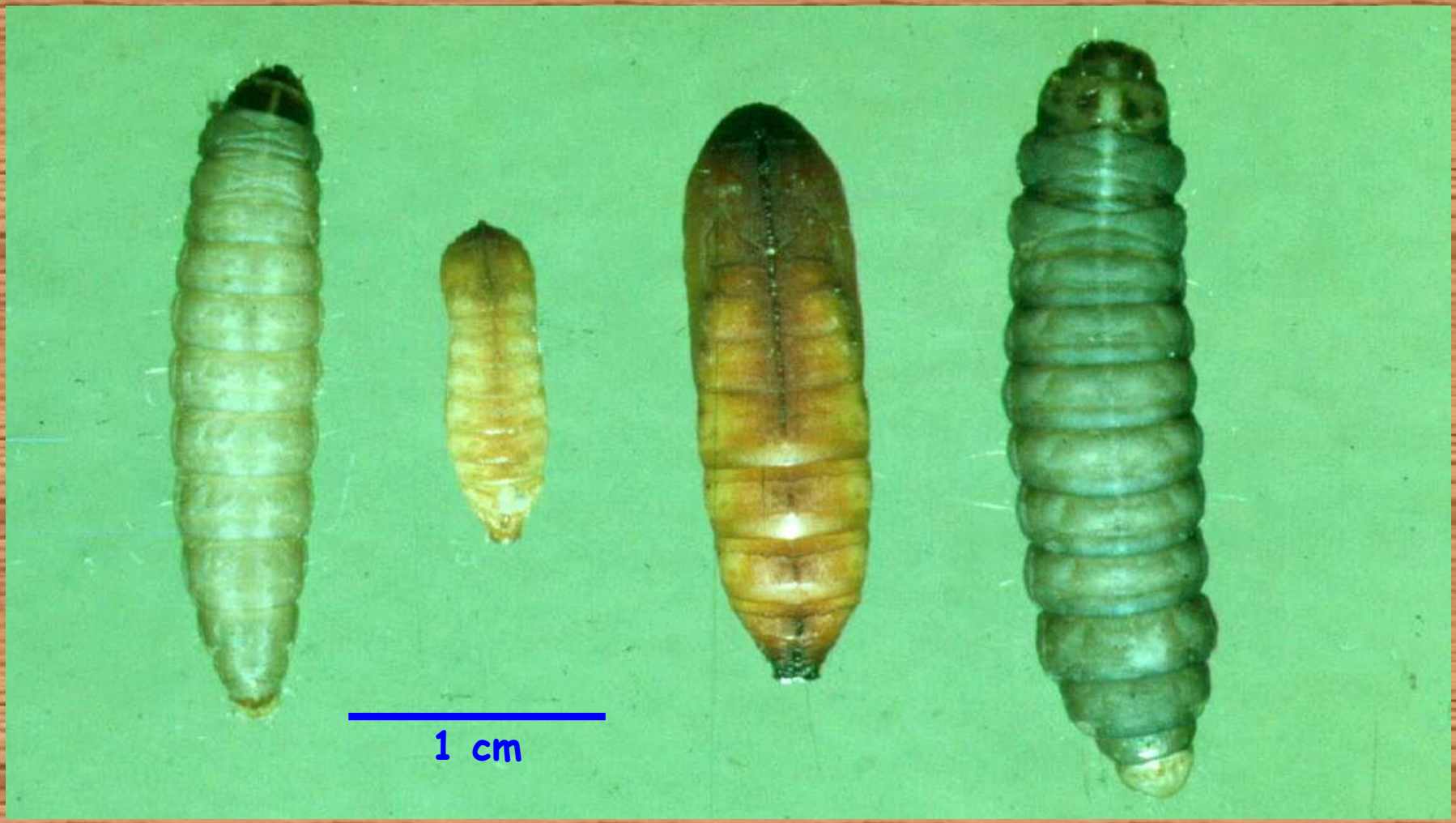

Obr. 28

Obr. 29 Přehled hlavních funkcí neurohormonů

Figure 3.16 Major physiological functions regulated by neurohormones in insects. Hormonal distribution is accomplished chiefly by release into the hemolymph, but localized secretion from nerves does occur. CC = corpora cardiaca; CA = corpora allata; PG = prothoracic gland.

Modified from Cook and Holman (1985).

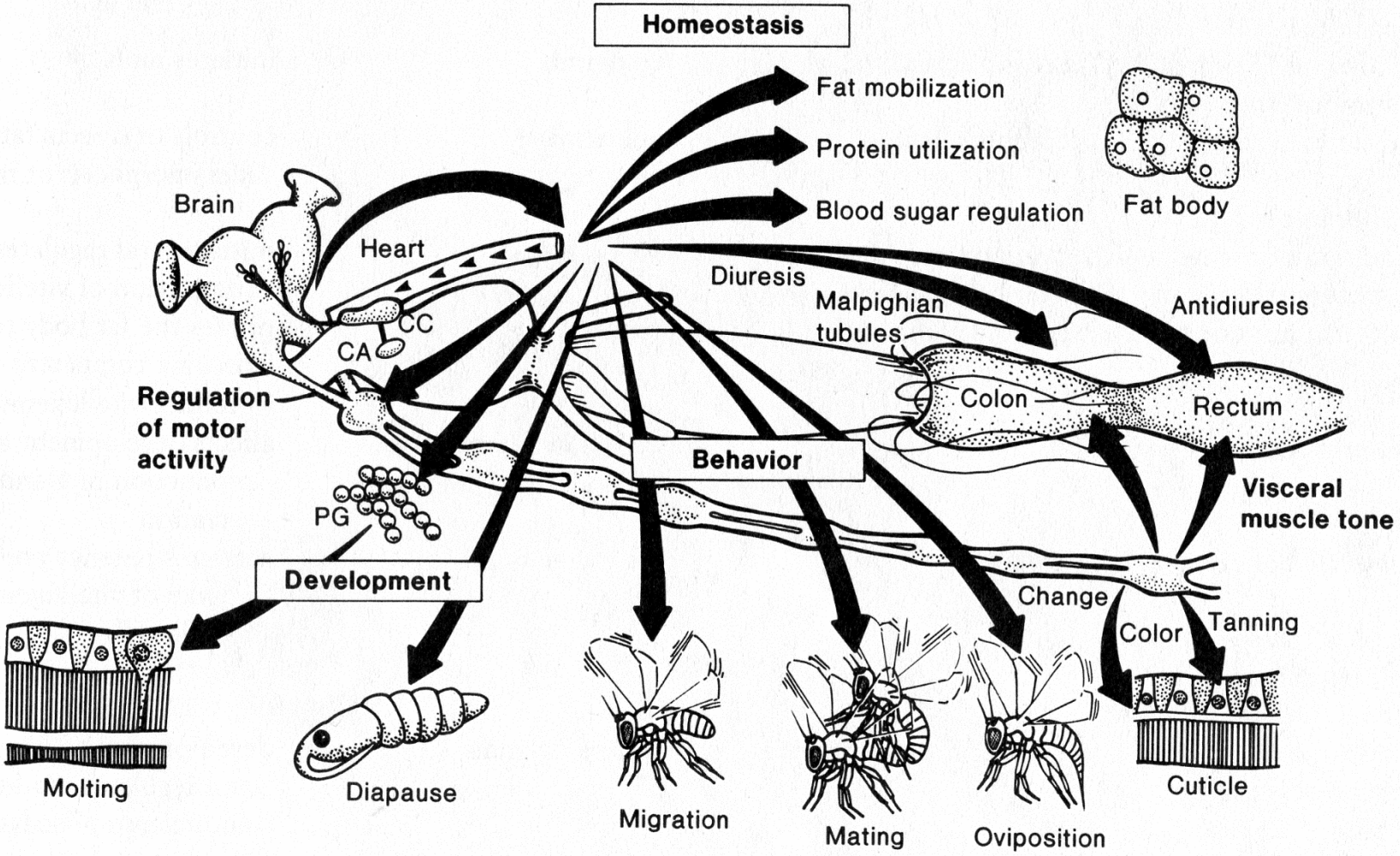

- HPLC - purifikace - LC/MS analýza
- Metody molekulární biologie - DNA, RNA, PCR, RT-PCR, in situ hybridizace, RNAi atd.
- Imunometody - ELISA, Western bloting, RIA, imunohistochemické metody atd.

Příklad identifikace a charakterizace adipokineckých hormonů z CNS ruměnice pospolné *Pyrrhocoris apterus*

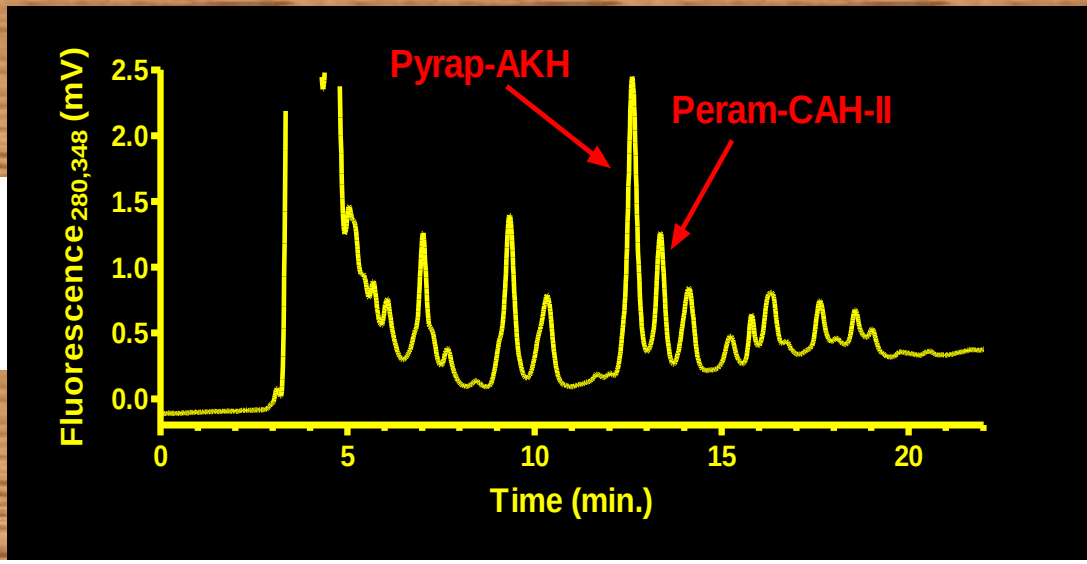

Pyrap-AKH structure:

DNA

AGTATTCTCGACGGCGCATCCCAGAGGACAACTACAATGGACAAATATATCATCACCTTGTACGTAATACTGGTTGTTGGTACAGTACAGTGTCTGGGGCAGC
TTAACTTTACACCTAACTGGGGAAAACGTATGGCCGTGACCCAGGACGAATGTAAAATTGGCGGCGAAGCTATTATTTACATATTATCTACGATTGAGAACG
GAATTAAAAAAATAATGGAGTGTGAGAAGCTGAGAACTTCAAGTGGATTACAATAGACCCAAAGCTGTTACCAATAATTTTAGTCTTACTACATTACCAGT
TTCAATAATGTCAATTGTATTCTAGTGTAATAAATATGTTCTAATTCGAAGTGTATTTATCAAATATAATTATTAAAAATAAAAAAAAAAAAAAAAAA

Amino acid composition

MDKYIITLYVILVVGTVQCLGQLNFTPNWGKRMAVTQDECKIGGEAIIYILSTIENGIKKIMECEKLRTSSGLQ

Peram-CAH-II structure:

DNA

AGTATTCTCGAAGGCGCATCCCAGAGGAGAACTACAATGGACAAATATATGATCAGTTTGTACGTATTACTGGTTCTTAGTACAGTACAGTGTCTGGGGCAG
CTTACCTTTACACCTAACTGGGGAAAACGTATGACCGTGAGCCAGGACGAATGTAAAATTGGCGGCGAAGCTATTGTTTACATATTATCCACGATTGAGACC
GGAATTAAAAAAATAATTGAGTGTGAAAAGCTGAGGATTTCAAGTGGATTACAATAGACGCATAGCTGTTACCAATAATTGTAGTCTTACTACATTAACC
AGTTTCATAAAAATGCATTATTGTATTCTAGTGTAATAAATATGTTCTAAATCGAAAAAAAAAAAAAAAAAA

Amino acid composition

MDKYMISLYVLLVLSTVQCLGQLTFTPNWGKRMTVSQDECKIGGEAIVYILSTIETGIKKIIECEKLRISSGLQ

Obr. 31

Geny hnyzích neurohormonů

1. Preprohormony obsahují – signální peptid a neuropeptid (eklozní hormon)

2. Preprohormony obsahují – signální peptid, neuropeptid a další strukturně nepříbuzné peptidy (adipokinetický hormon)

3. Preprohormony obsahují – signální peptid a řadu kopií stejnéo nebo příbuzného neuropeptidu (allatostatin)

Obr. 32

Dělení hmyzích neurohormonů

1. Hormony řídící metabolismus a homeostázu

2. Hormony řídící metamorfózu, vývoj a růst

3. Hormony řídící pohlavní funkce

4. Hormony modifikující svalovou kontrakci

5. Hormony řídící barvoměnu (chromatotropiny)

Obr. 33

Hormony řídící metabolismus a homeostázu

1. Adipokinetické hormony (AKH)

2. Diuretické hormony

3. Antidiuretické hormony

4. Chloride transport stimulating hormone

5. Ion transport peptide

Obr. 34 Adipokinetický hormon a jeho funkce v mobilizaci lipidů

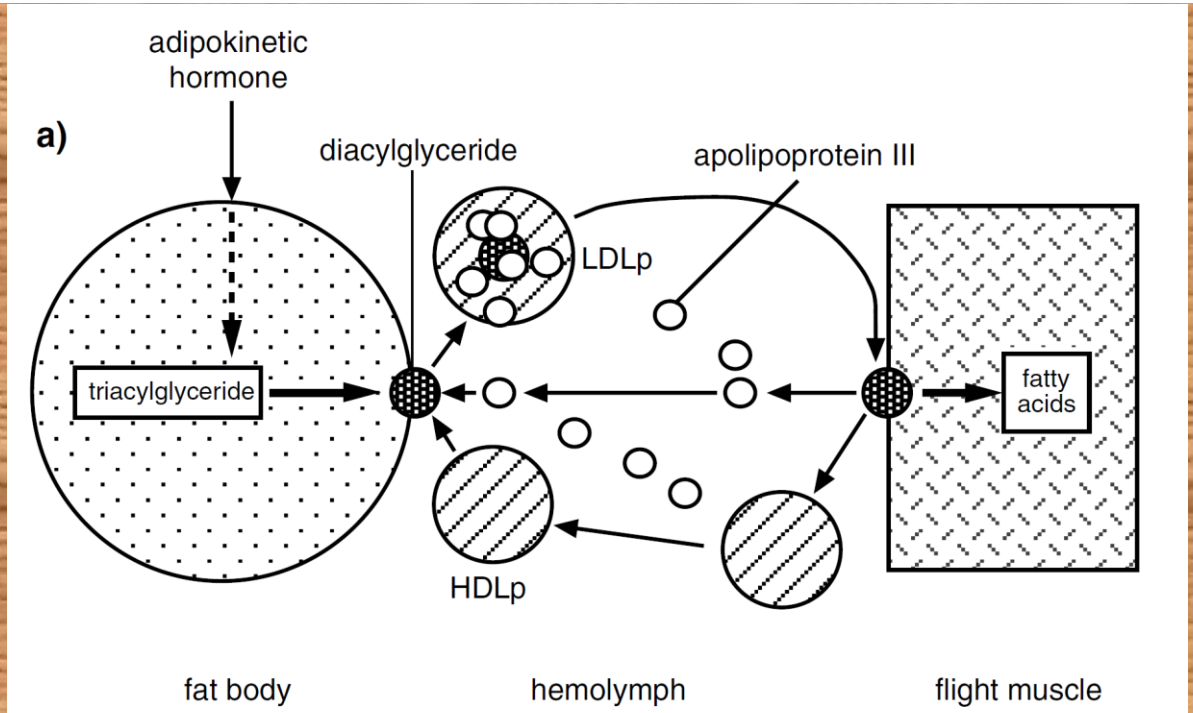

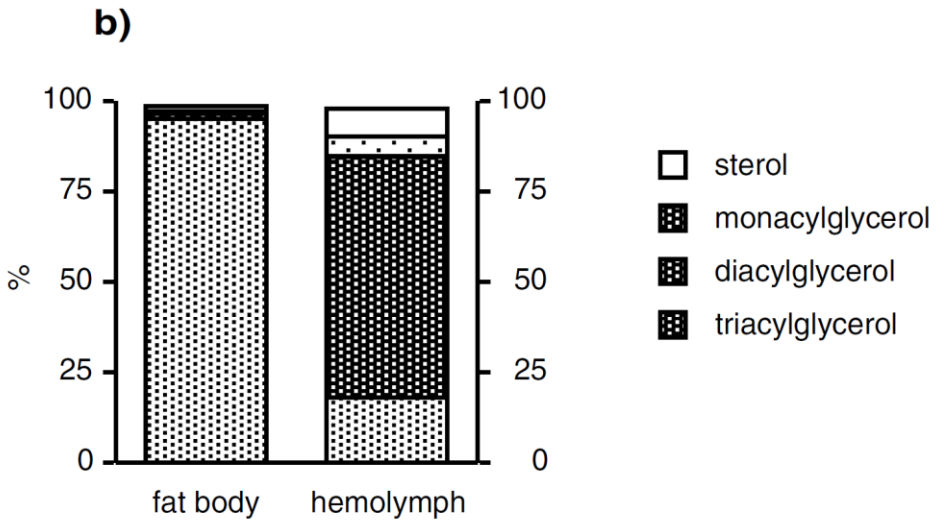

Mechanismus působení adipokinetického hormonu – 1. alternativa

Obr. 35

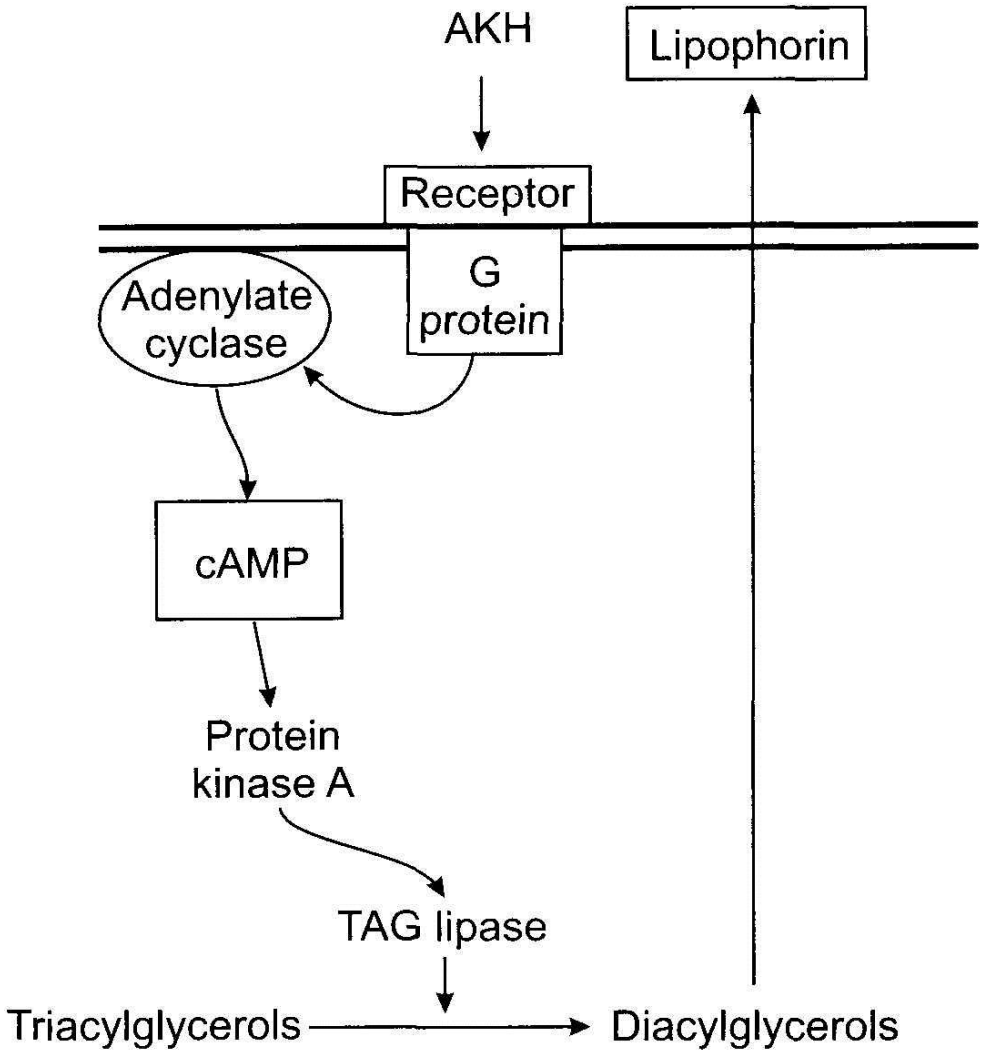

FIGURE 6.34. AKH activates the enzyme TAG lipase that hydrolyzes stored triacylglycerols to diacylglycerols. The diacylglycerols are transported to target tissues by lipophorin.

Obr. 36 Transport lipidů

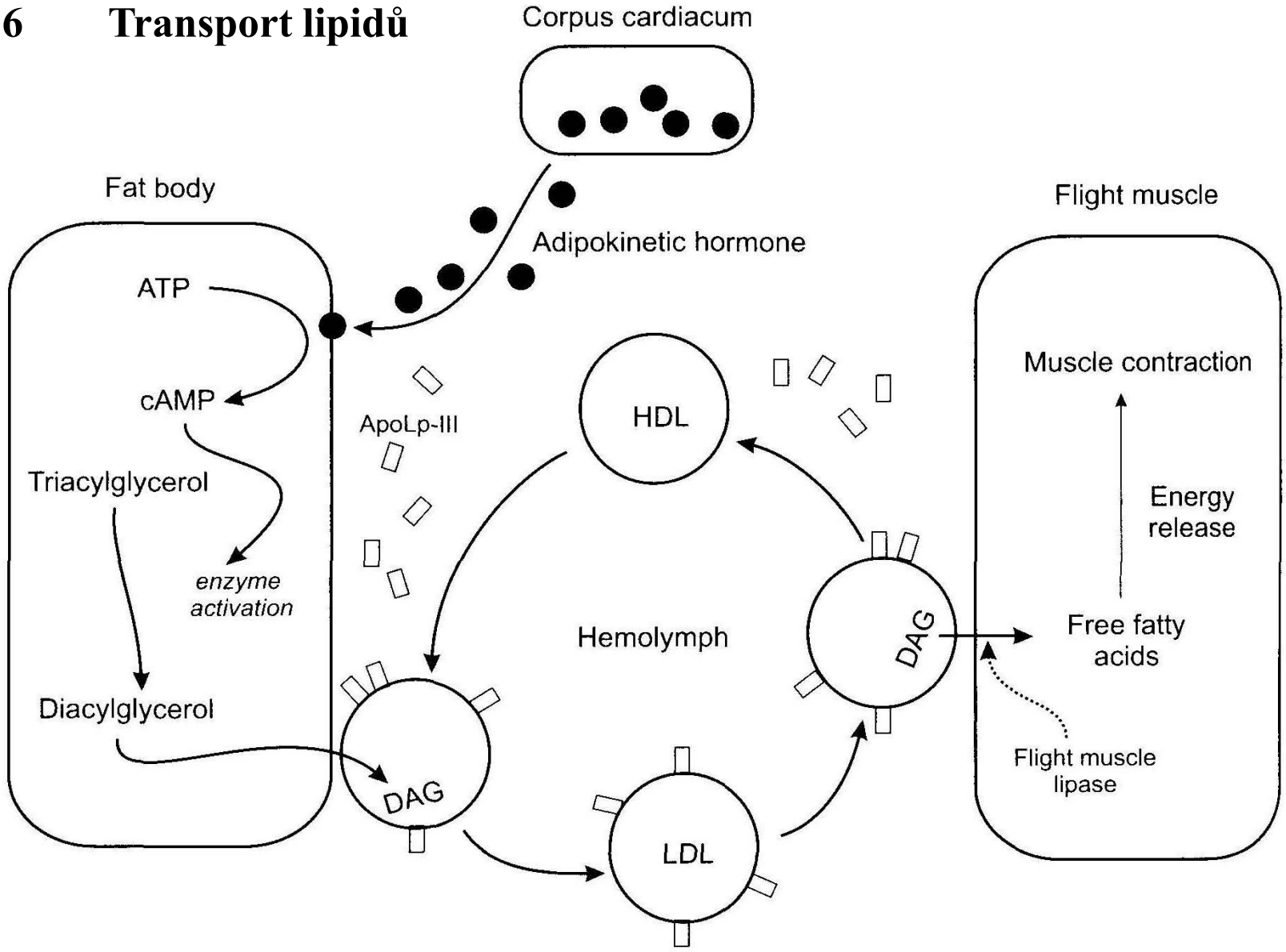

FIGURE 6.33. The transport of lipid from the fat body to flight muscles. Apolipophorin III circulates in the hemolymph and is taken up by the high density lipophorin (HDL) when it acquires the diacylglycerols (DAG) from the fat body. This transforms the HDL into a low-density lipophorin (LDL), which transfers the DAG to the flight muscles.

Obr. 37 Mechanismus působení adipokinetického hormonu – 2. alternativa

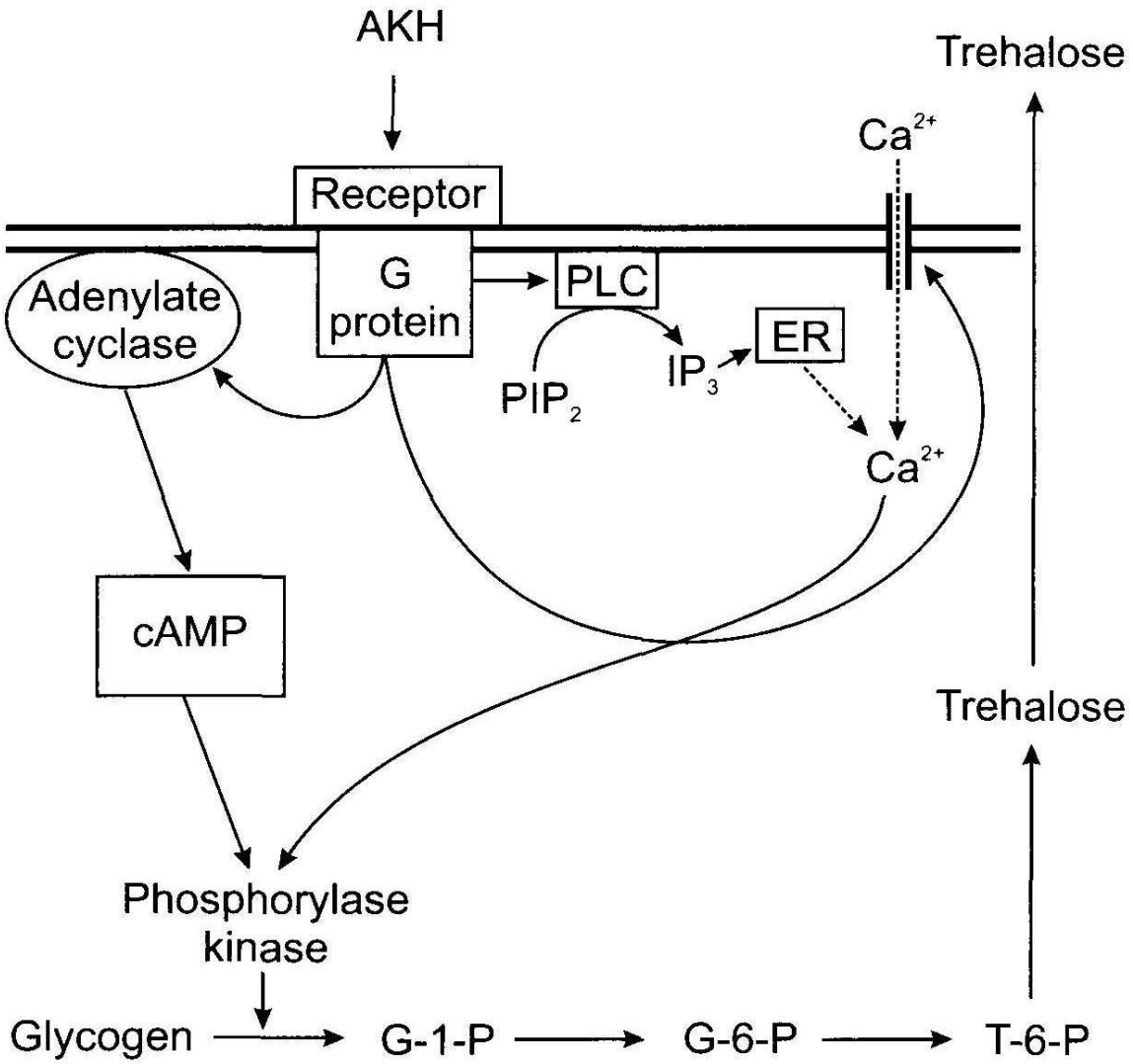

FIGURE 6.35. AKH activates the enzyme phosphorylase kinase that hydrolyzes glycogen to trehalose released into the hemolymph.

Obr. 38

Hormony řídící metamorfózu, vývoj a růst

1. Prothoracikotropní hormon (PTTH)

2. Allatostatiny a allatotropiny

3. Eklozní hormon (EH) a ecdysis triggering hormone (ETH)

4. Burzikon

5. Faktory regulující pupariaci much

6. Pheromone biosynthesis activating neuropeptide (PBAN)

7. Diapauzní hormon

Obr. 39 **Struktura PTTH z *Bombyx mori***

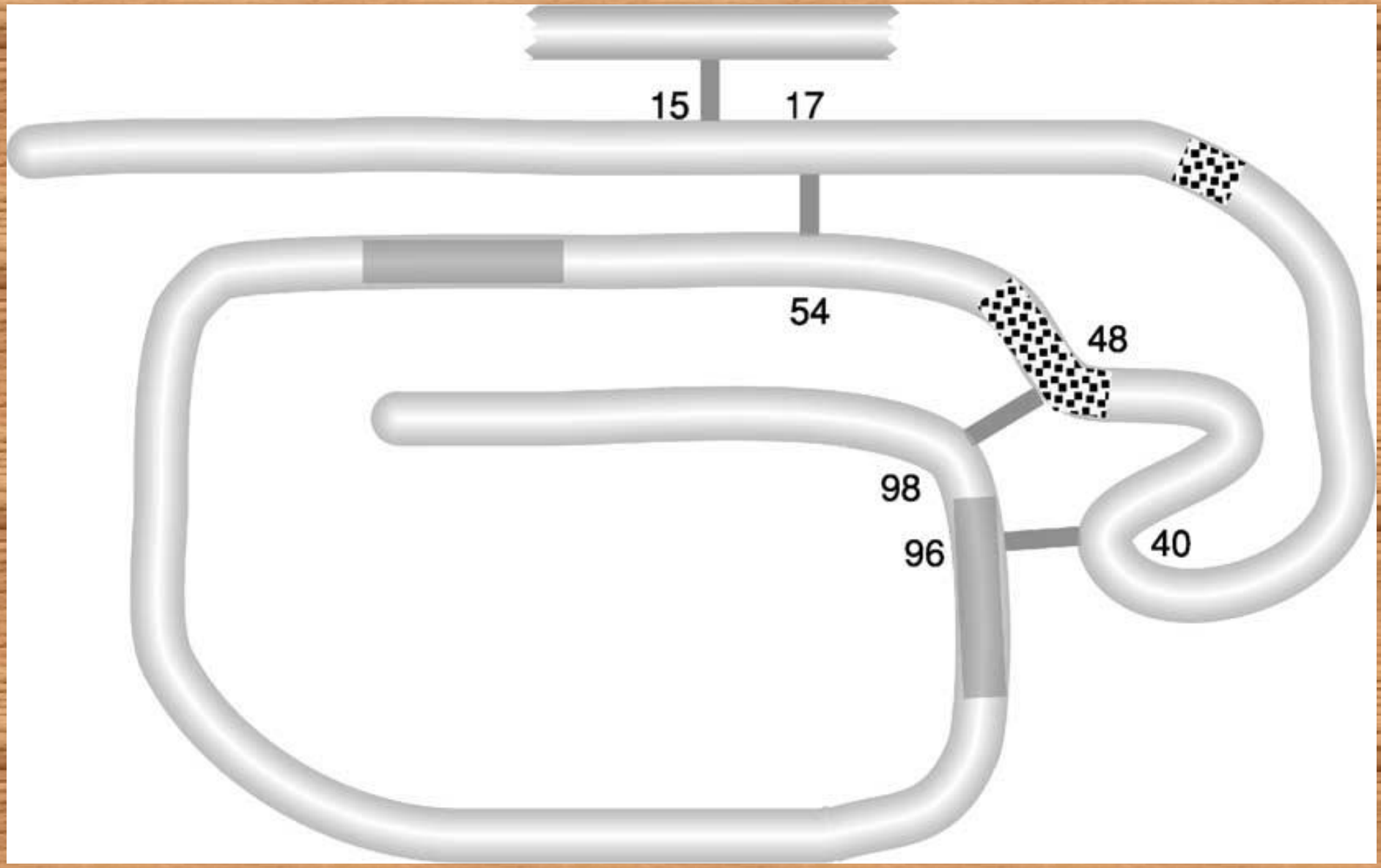

Obr. 40 Mechanismus působení PTTH v prothorakálních žlázách

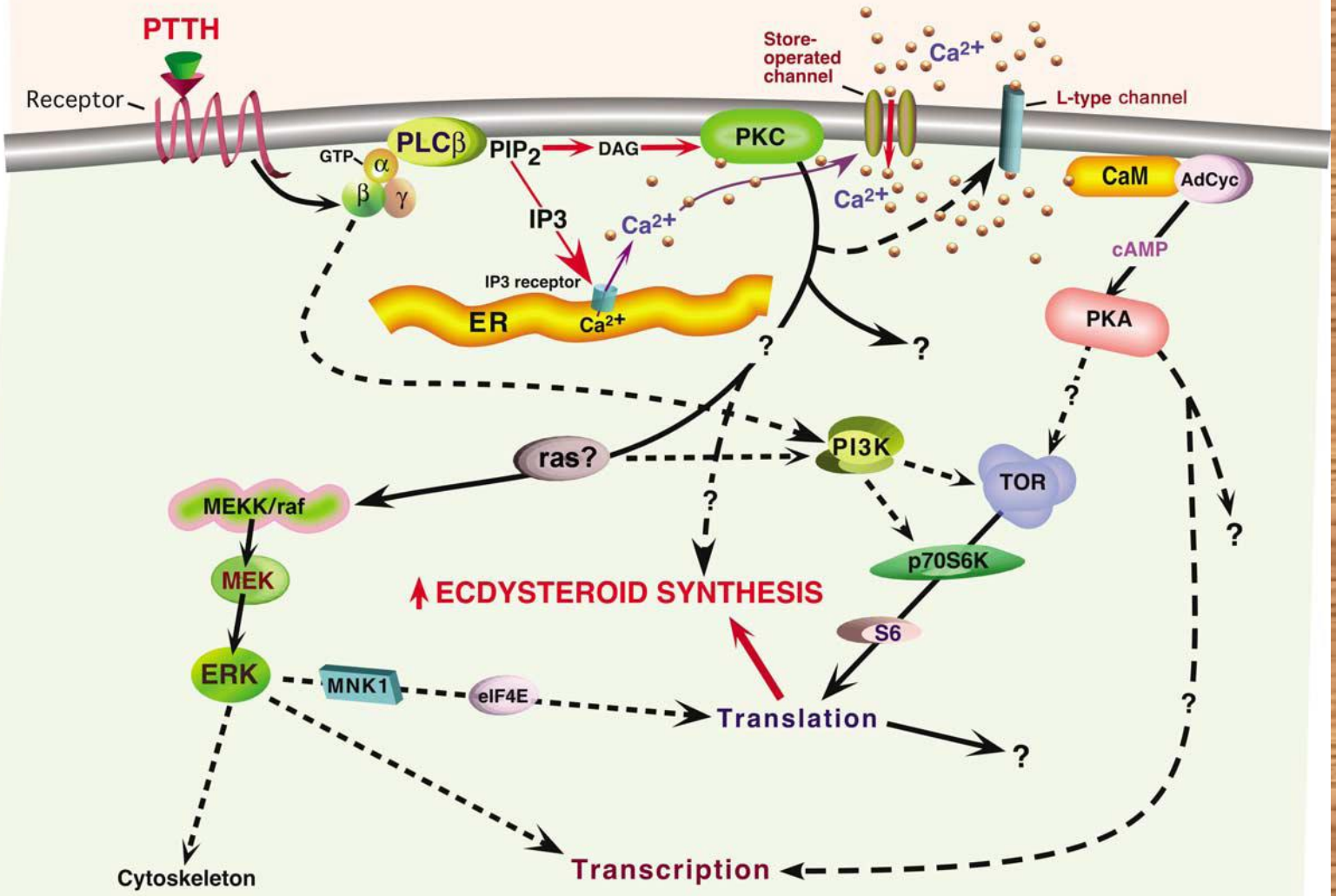

Obr. 41 Mechanismus působení PBAN

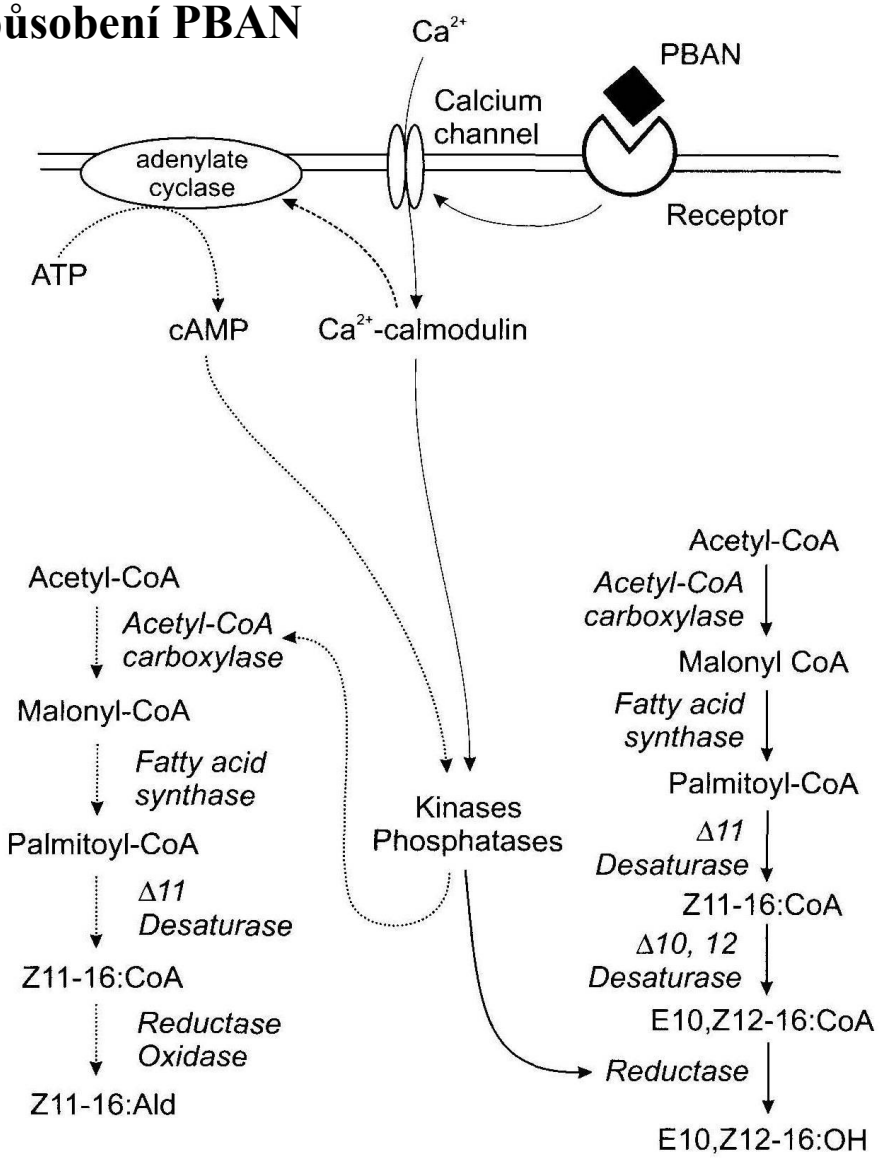

Figure 12.14. The activation of key enzymes in pheromone synthesis by pheromone biosynthesis activating neuropeptide (PBAN) in two lepidopteran species. (*Right*) The phosphatase dephosphorylates and activates a reductase as the last step in bombykol biosynthesis in *Bombyx*. (*Left*) cAMP activates a kinase that activates the enzyme acetyl-CoA carboxylase, the first in the synthetic pathway in *Helicoverpa*.

Obr. 42 Změny hladin hormonů během metamorfózy

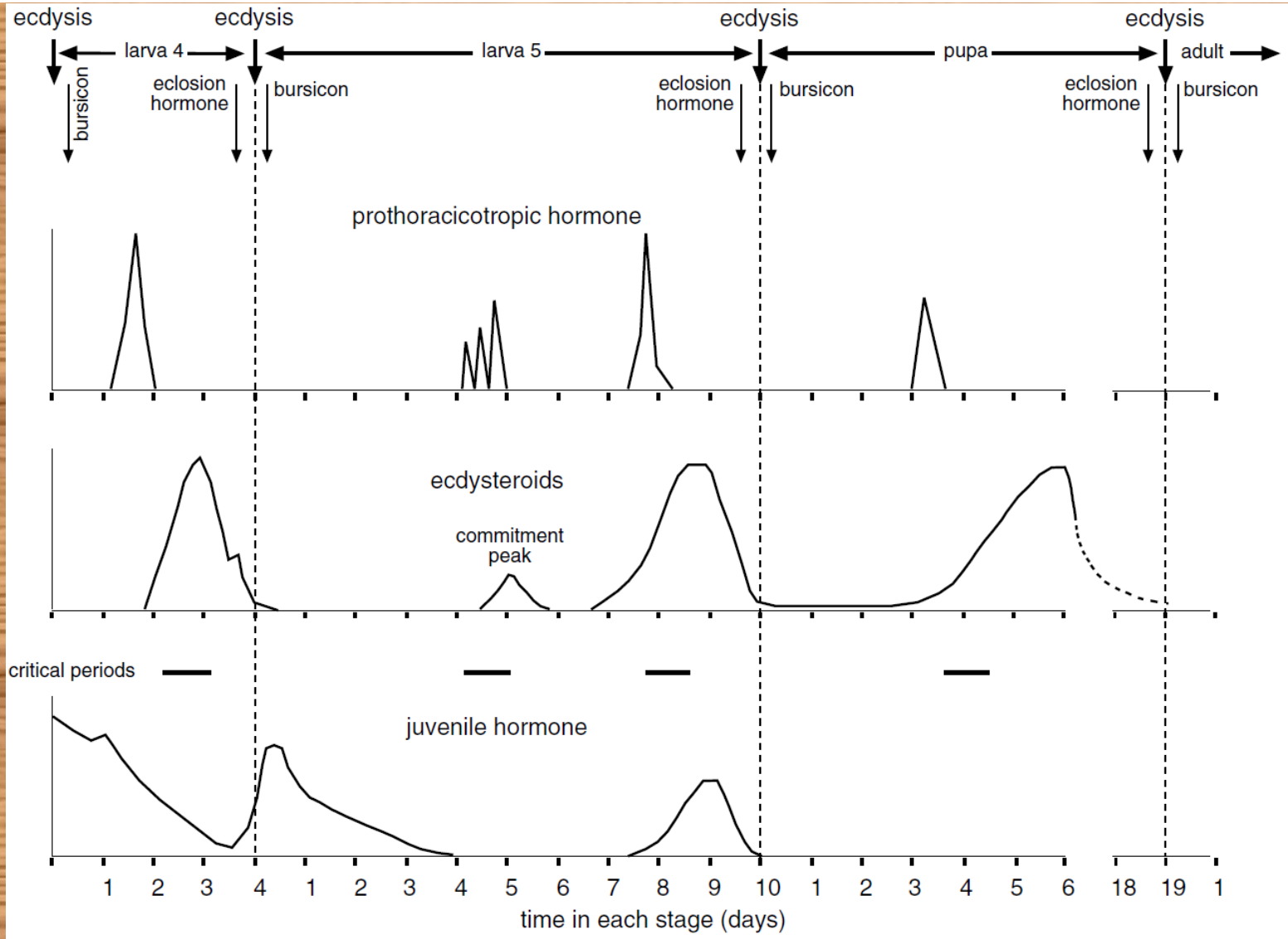

Fig. 15.30. Changes in hormone titers regulating molting and metamorphosis in a holometabolous insect. At the molt from larva to larva, juvenile hormone is present during the critical period; at the molt from larva to pupa, no juvenile hormone is present at the first critical period. The second critical period of sensitivity to juvenile hormone in the fifth stage larva regulates development of the imaginal discs. Eclosion hormone and bursicon are produced for a brief period before and after each ecdysis (based on data for *Manduca*, Lepidoptera).

Obr. 43 Hormonální řízení ekdyse

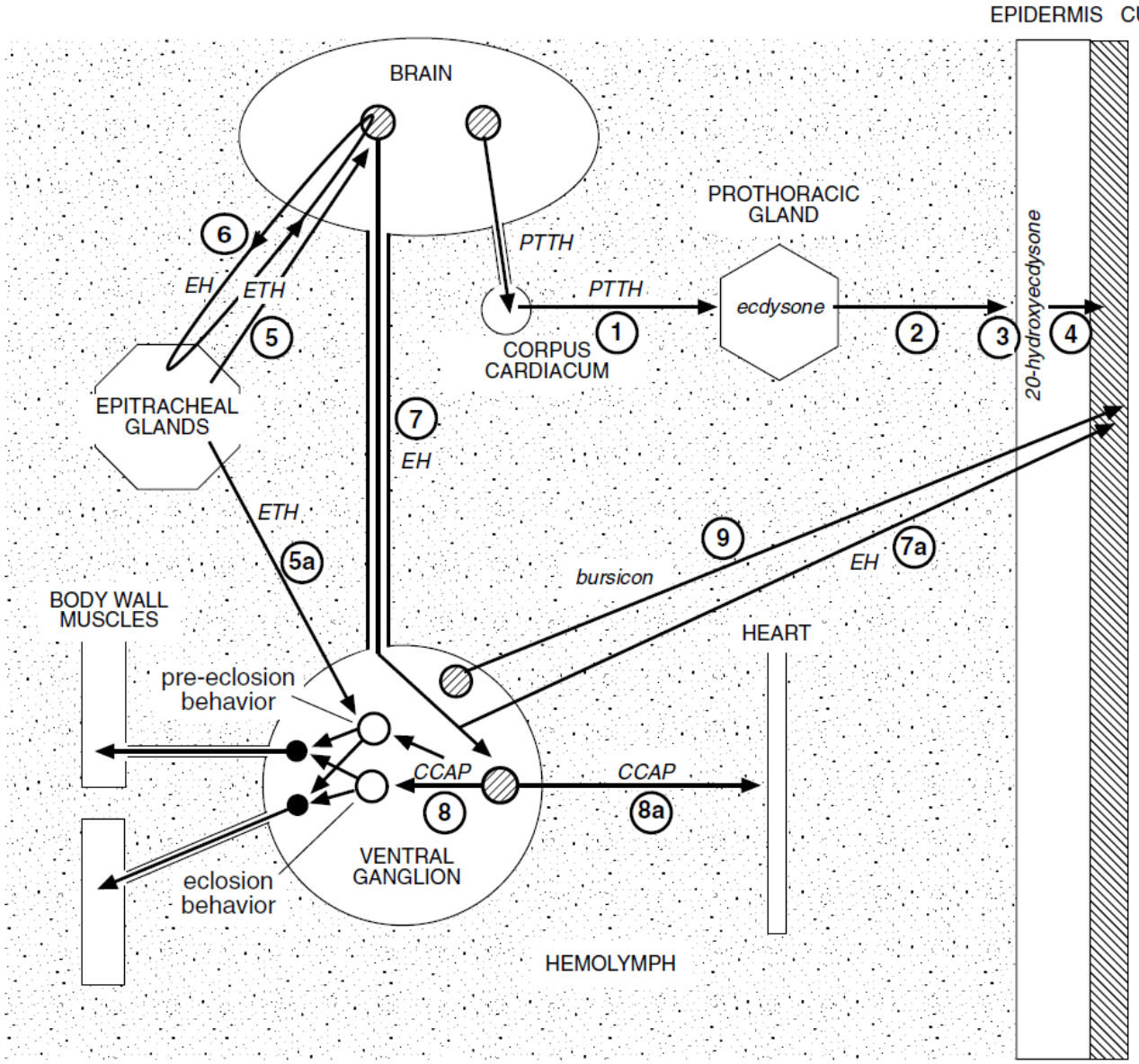

CONTROL OF APOLYSIS AND CUTICLE PRODUCTION

1 PTTH stimulates synthesis and release of ecdysone

2 ecdysone in hemolymph

3 ecdysone hydroxylated at tissues

4 20-hydroxyecdysone regulates genes producing cuticle

CONTROL OF ECDYSIS

5 ecdysis triggering hormone causes release of eclosion hormone

5a ecdysis triggering hormone switches on pre-eclosion behavior

6 positive feedback loop between ETH and EH results in massive release of EH

7 central release of EH causes release of CCAP

7a EH acting via hemolymph plasticizes cuticle

8 CCAP switches on eclosion behavior and switches off pre-eclosion behavior

CONTROL OF EXPANSION AND SCLEROTIZATION

8a CCAP acting via hemolymph increases heartbeat

9 bursicon first plasticizes cuticle, then switches on cuticular sclerotization

Obr. 44

Hormony regulující pohlavní funkce

1. Stimulační neurohormony (gonadotropiny)
   - ovary maturing parsin (OMP)
   - egg development neurohormone (EDNH)

2. Inhibiční nerohormony (gonadostatiny)
   - neuroparsin
   - oostatické hormony a trypsin-modulating oostatic factor (TMOF)

Obr. 45

Hormony modifikující svalovou kontrakci

1. Proctolin

2. Corazonin

3. Další kardiostimulační hormony (CCAP, AKH)

4. Skupiny myotropinů a myoinhibinů - myokininy, sulfakininy, pyrokininy, tachykininy, periviscerokininy, FMRF-amid

Obr. 46

Hormony řídící barvoměnu

1. Pigment dispersing faktor (PDF)

2. Melanization and reddish colorating hormone (MRCH)

Obr. 47

Feromony

HMG-CoA: 3-hydroxy-3-metyl glutaryl koenzym A

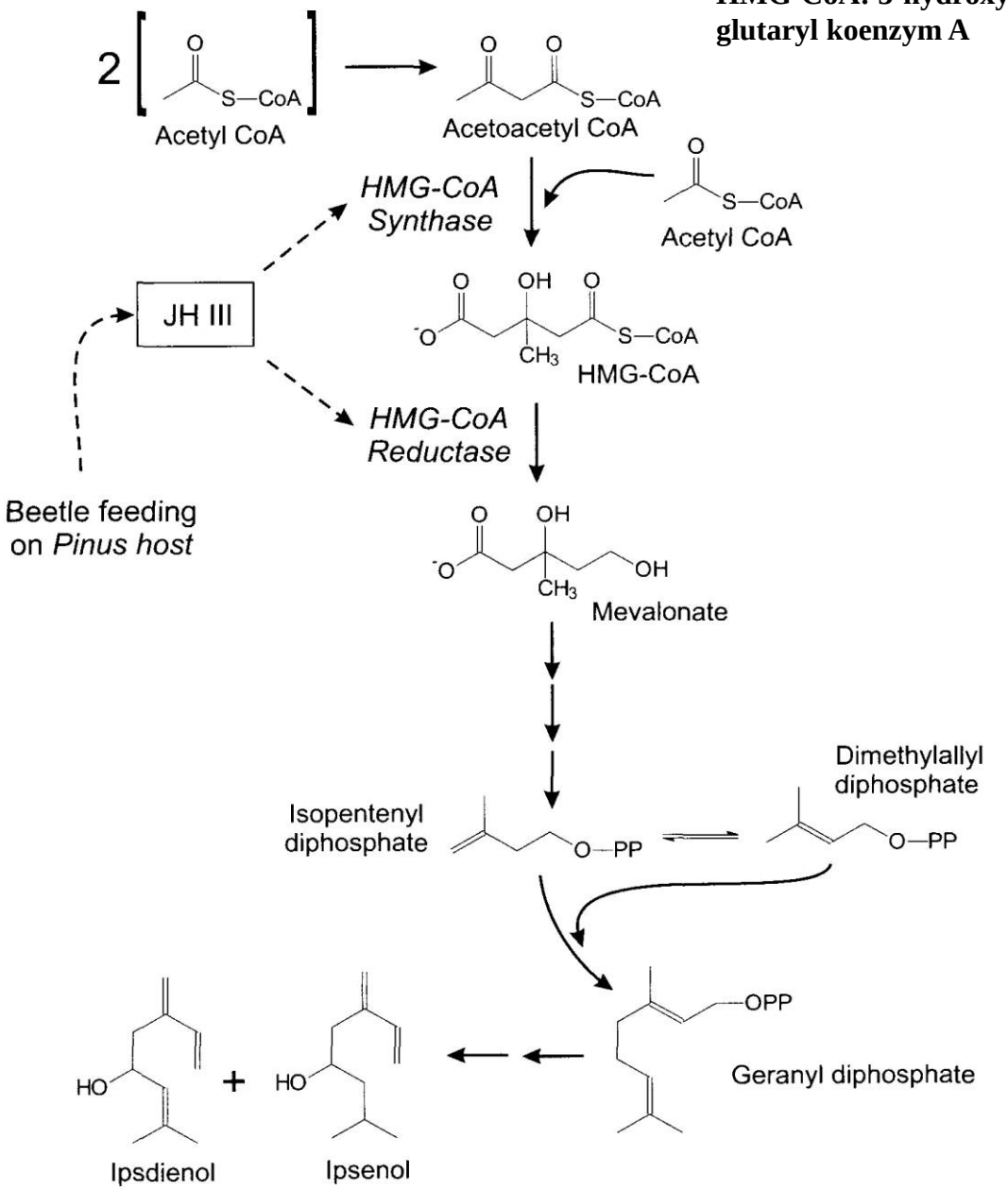

FIGURE 12.16. Pheromone biosynthesis in bark beetles and its control by JH. Two key enzymes involved in the pathway toward the synthesis of ipsenol and ipsdienol are activated by JH. From Tillman et al. (1999).

Obr. 48

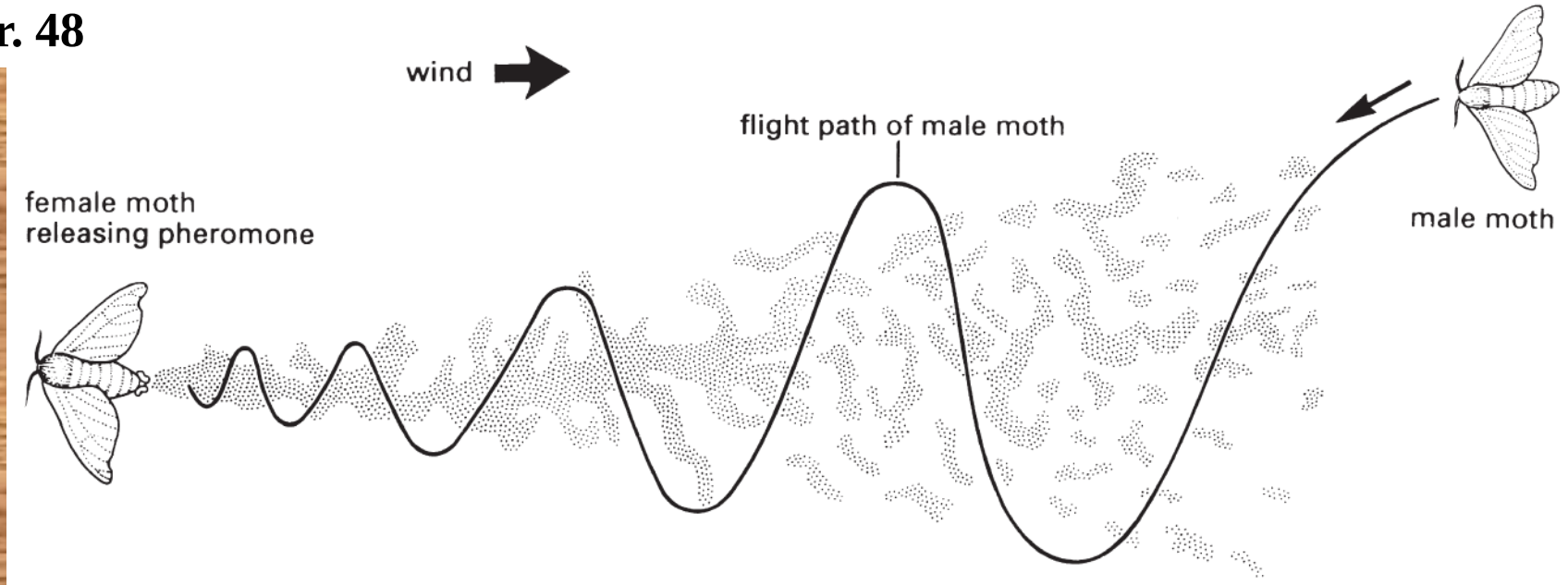

Fig. 4.7 Location of pheromone-emitting female by male moth tacking upwind. The pheromone trail forms a somewhat discontinuous plume because of turbulence, intermittent release, and other factors. (After Haynes & Birch 1985.)

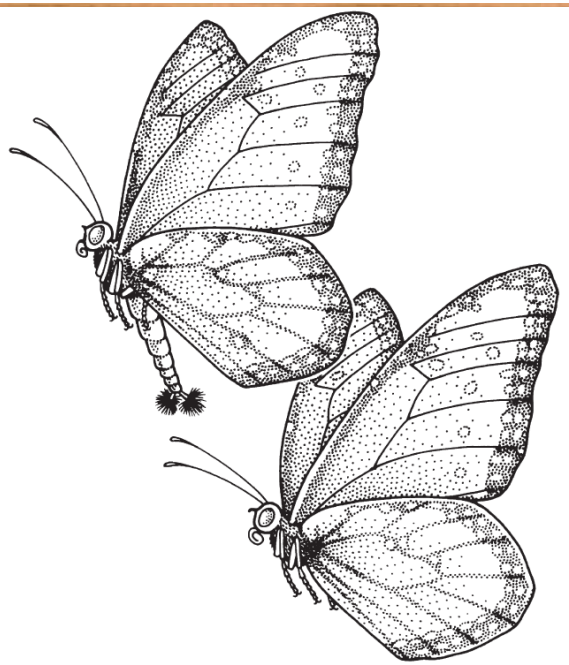

Fig. 4.8 A pair of queen butterflies, *Danaus gilippus* (Lepidoptera: Nymphalidae: Danainae), showing aerial "hairpencilling" by the male. The male (above) has splayed hairpencils (at his abdominal apex) and is applying pheromone to the female (below). (After Brower et al. 1965.)

Obr. 49 **Allelochemikálie**

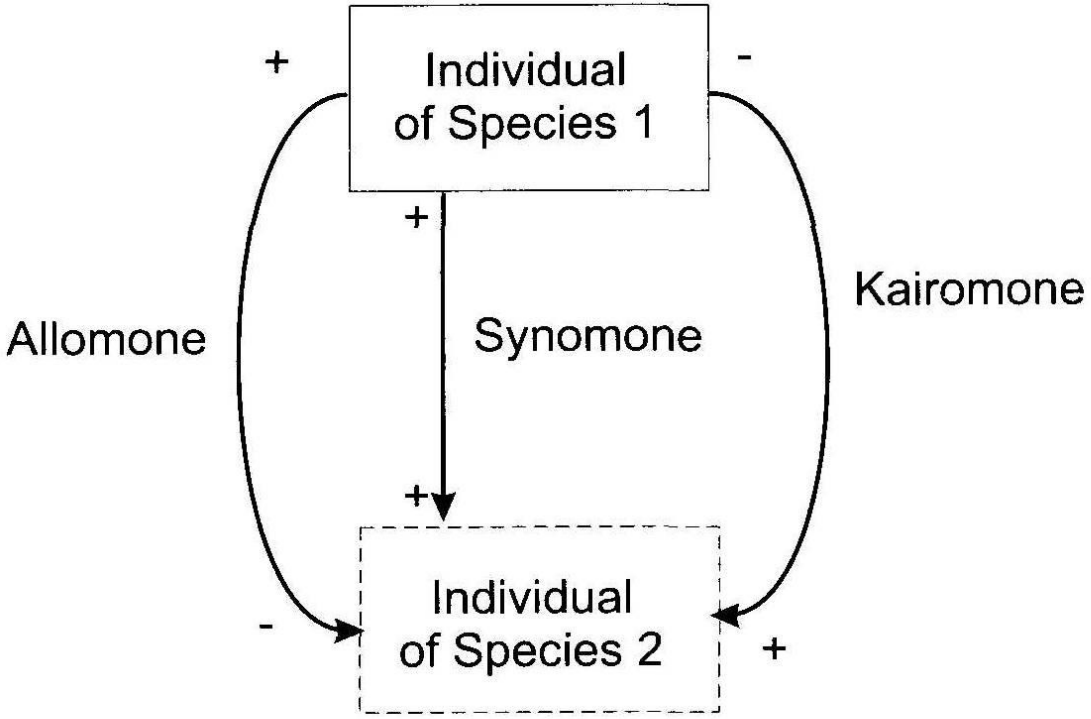

FIGURE 12.17. Allelochemicals, which mediate interspecific interactions. Allomones are allelochemicals that are adaptively favorable to the emitter but not the receiver. Kairomones are adaptively favorable to the receiver and not the emitter. Synomones are adaptively favorable to both the emitter and the receiver.

11. Činnost pohlavních orgánů a rozmnožování

Obr. 1 Pohlavní orgány hmyzu

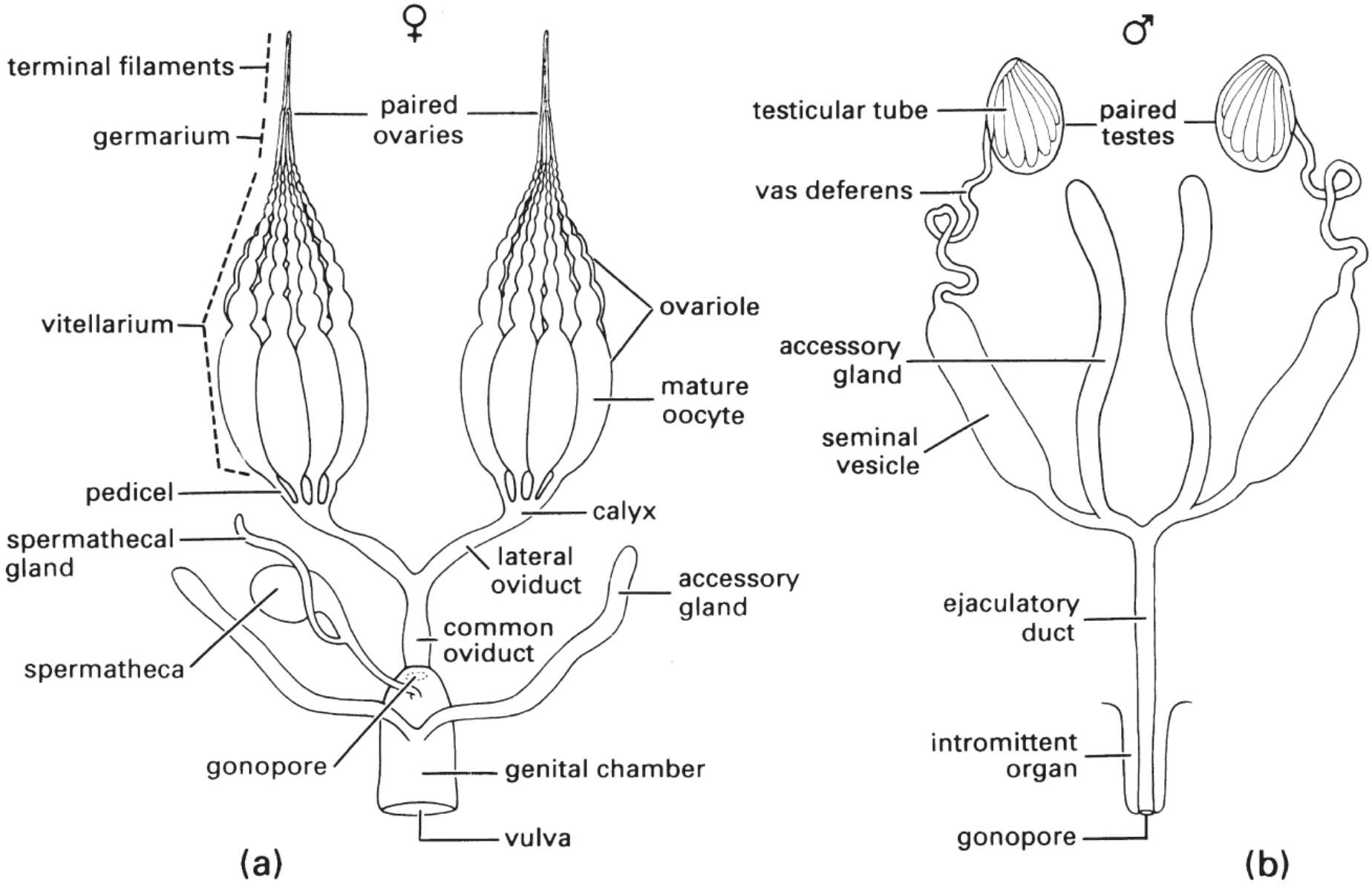

Fig. 3.20 Comparison of generalized (a) female and (b) male reproductive systems. (After Snodgrass 1935.)

Obr. 2 Typy hmyzích ovariol

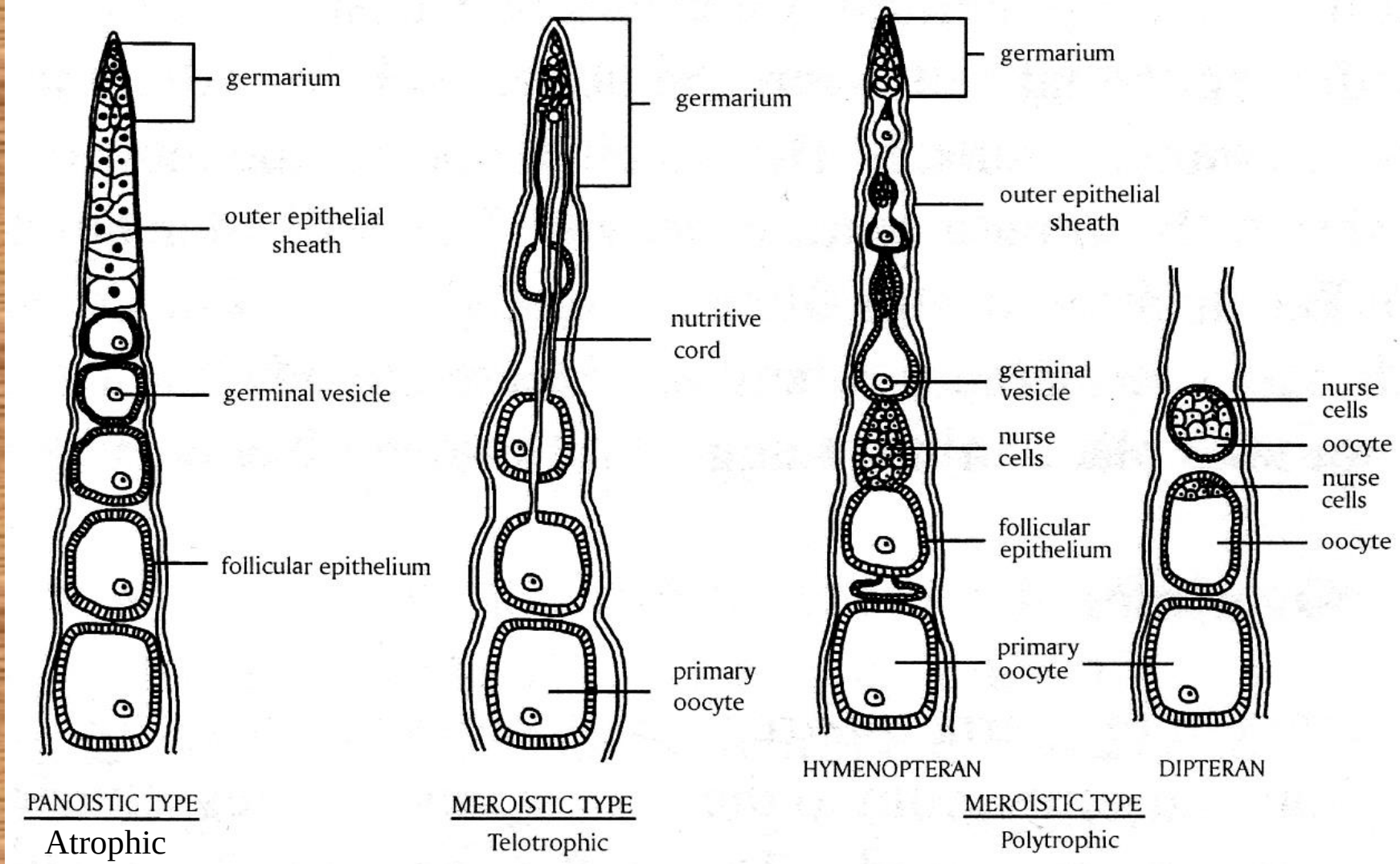

FIGURE 15.2 Major types of ovary structure in insects. The panoistic ovary is typical of Orthoptera and Dictyoptera with no nurse cells. Meroistic telotrophic ovaries have nurse cells in the germarial region and cytoplasmic strands extend to the developing oocytes. Coleoptera and Hemiptera have telotrophic ovaries. Meriostic ovaries may be polytrophic, as for example in Hymenoptera and higher Diptera. In polytrophic ovaries, the nurse cells occur in an adjacent follicle (Hymenoptera) or in the follicle with the developing oocyte (higher Diptera). In all cases, the nurse cells pass nutrients and gene products (mRNAs) to the developing oocyte.

https://www.youtube.com/watch?v=lopc1CrGCX4&feature=plc

Obr. 3

Kopulace

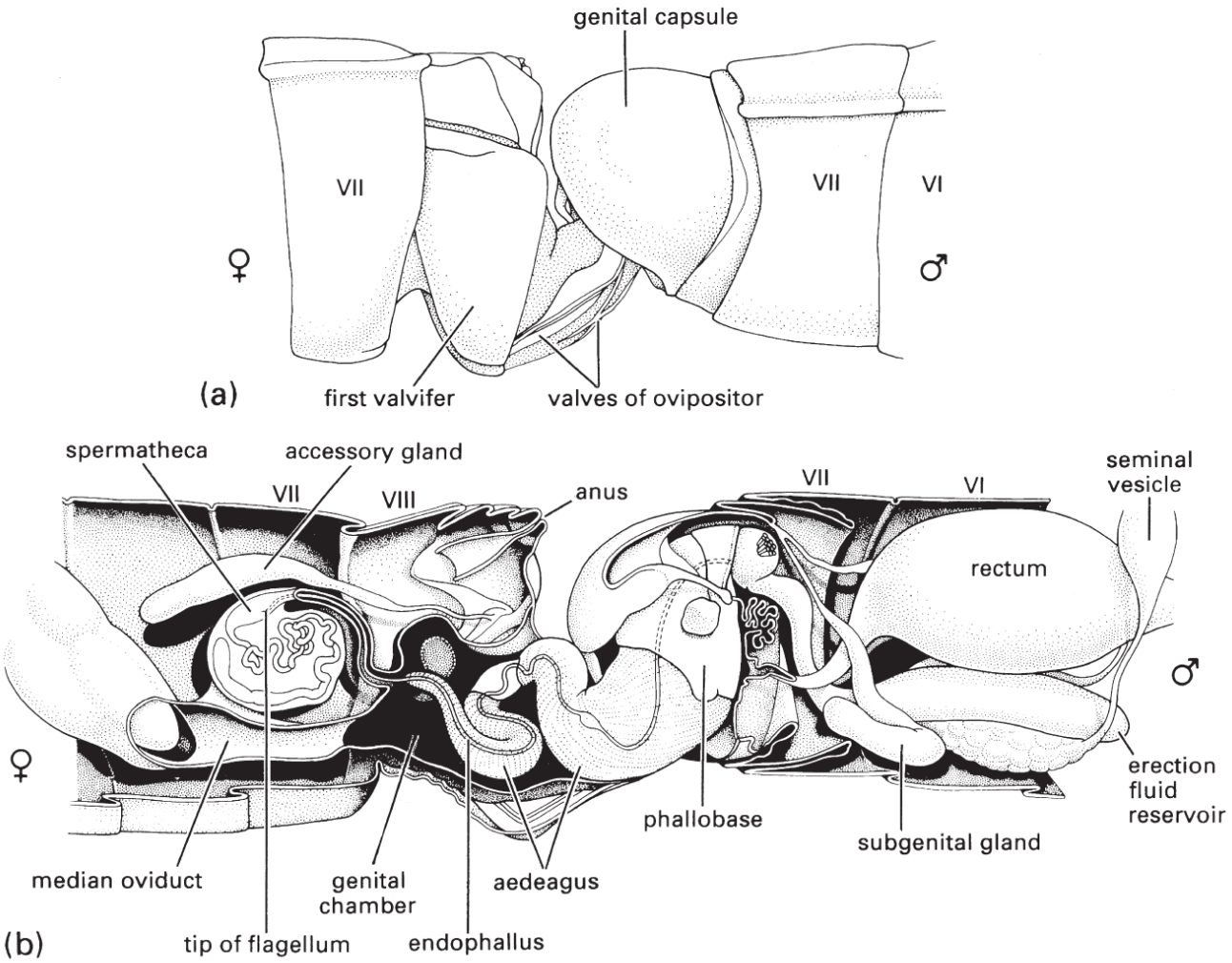

Fig. 5.4 Posterior ends of a pair of copulating milkweed bugs, *Oncopeltus fasciatus* (Hemiptera: Lygaeidae). Mating commences with the pair facing in the same direction, then the male rotates his eighth abdominal segment (90°) and genital capsule (180°), erects the aedeagus and gains entry to the female's genital chamber, before he swings around to face in the opposite direction. The bugs may copulate for several hours, during which they walk around with the female leading and the male walking backwards. (a) Lateral view of the terminal segments, showing the valves of the female's ovipositor in the male genital chamber; (b) longitudinal section showing internal structures of the reproductive system, with the tip of the male's aedeagus in the female's spermatheca. (After Bonhag & Wick 1953.)

Obr. 4

Hormonální regulace hmyzí reprodukce

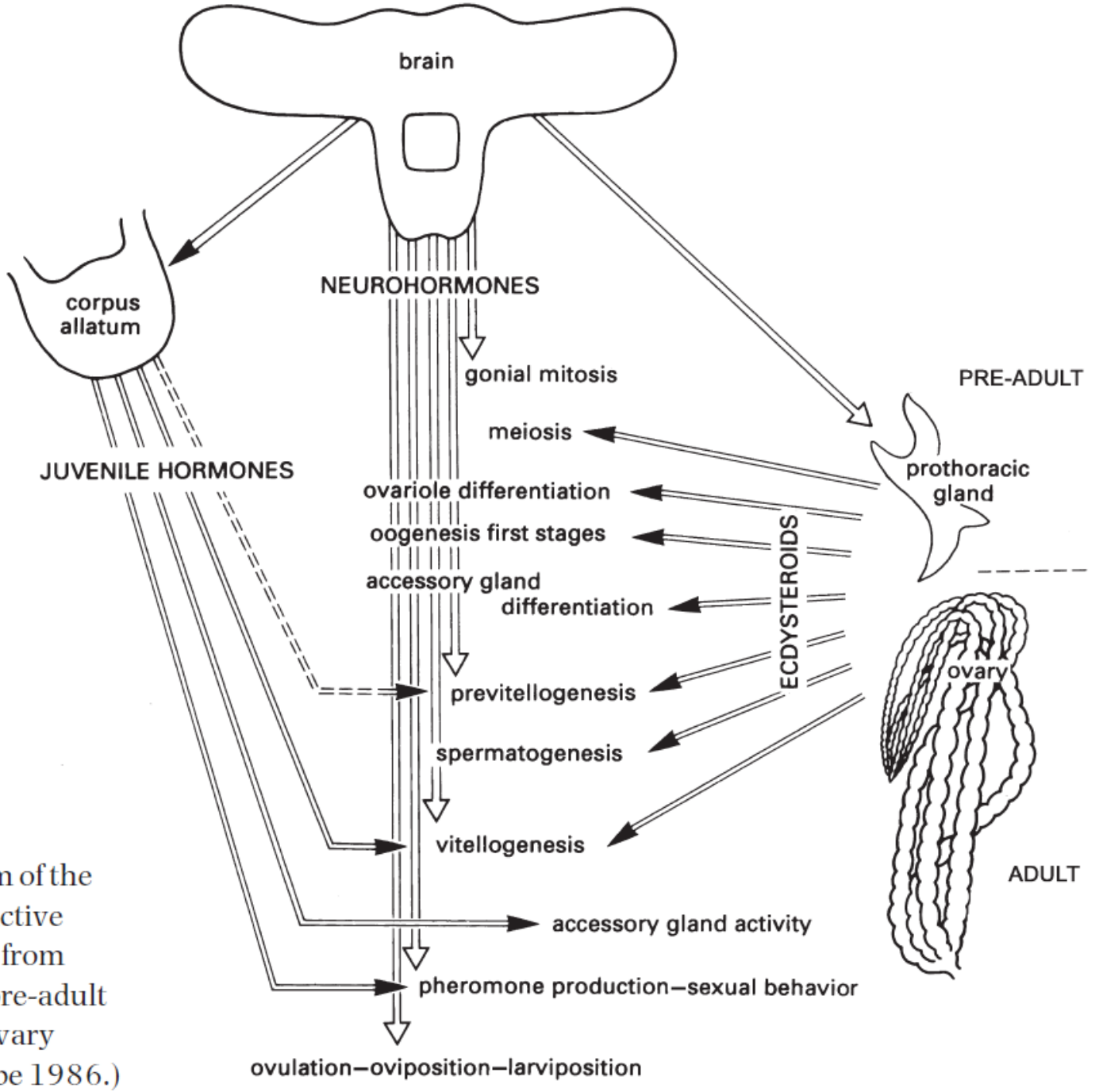

Fig. 5.13 A schematic diagram of the hormonal regulation of reproductive events in insects. The transition from ecdysterone production by the pre-adult prothoracic gland to the adult ovary varies between taxa. (After Raabe 1986.)

Obr. 5

Tvorba vitelogeninové mRNA

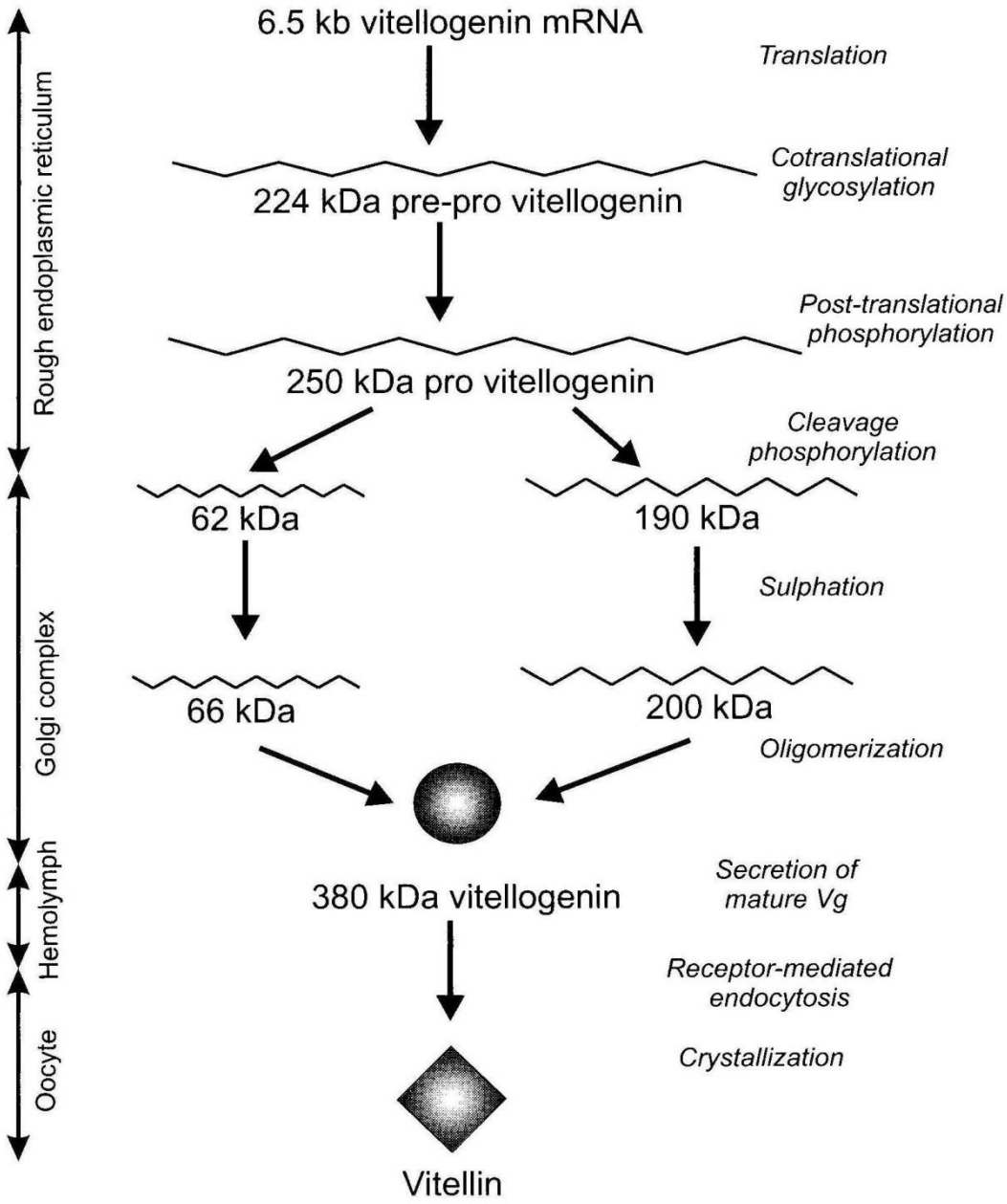

FIGURE 4.10. The processing of vitellogenin mRNA to form the vitellin deposited in the mature yolk body of the mosquito. From Sappington and Raikhel (1998). Reprinted with permission.

Obr. 6

Přesun vitellogeninů u Dipter

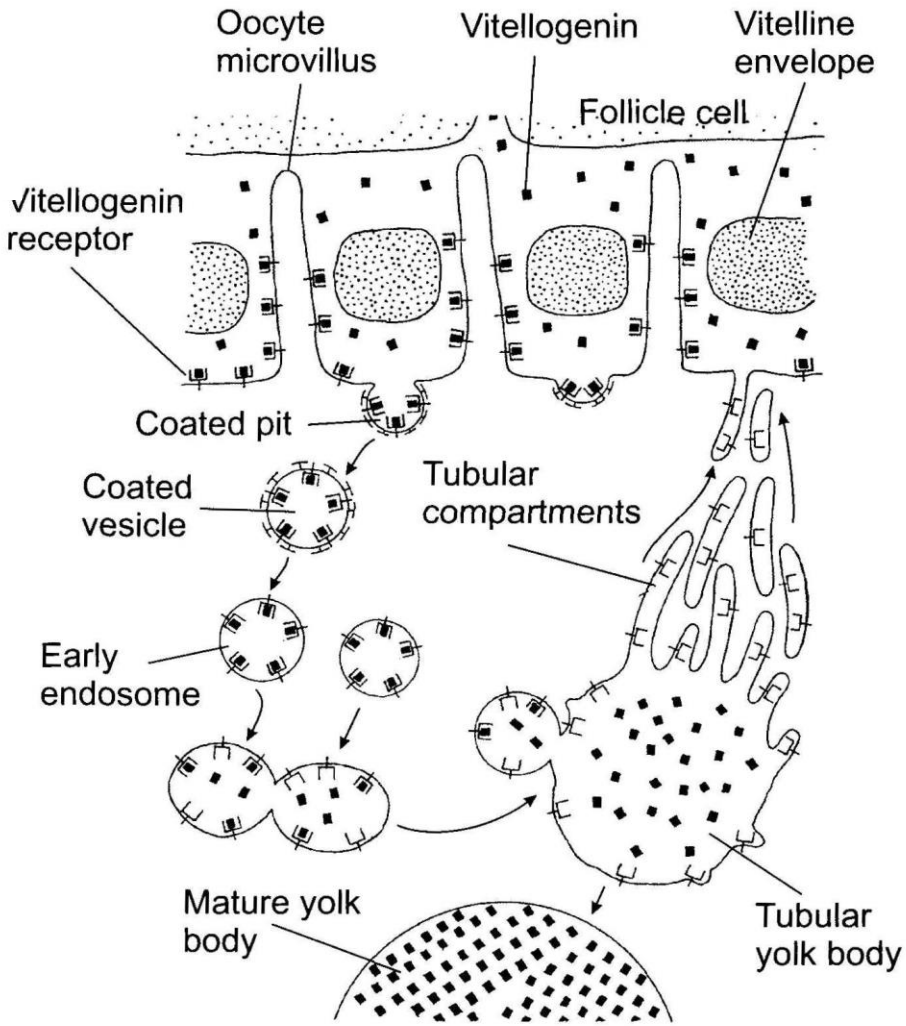

FIGURE 4.9. The process of receptor-mediated endocytosis during vitellogenesis in mosquitoes. The vitellogenin enters from the hemolymph between follicle cells through pores within the vitelline envelope. It binds to receptors on the oocyte plasma membrane, accumulating in clathrin-coated pits that invaginate into the oocyte cytoplasm and form coated vesicles. When the coated vesicles lose their clathrin, they become early endosomes, which fuse to form a larger tubular yolk body. The vitellogenin is crystallized as vitellin, forming a mature yolk body. The vitellogenin receptors are recycled to the plasma membrane by way of the tubular compartments. Modified from Snigirevskaya et al. (1997). Reprinted with permission.

Obr. 7 Řízení syntézy vitellogeninů - většina druhů hmyzu

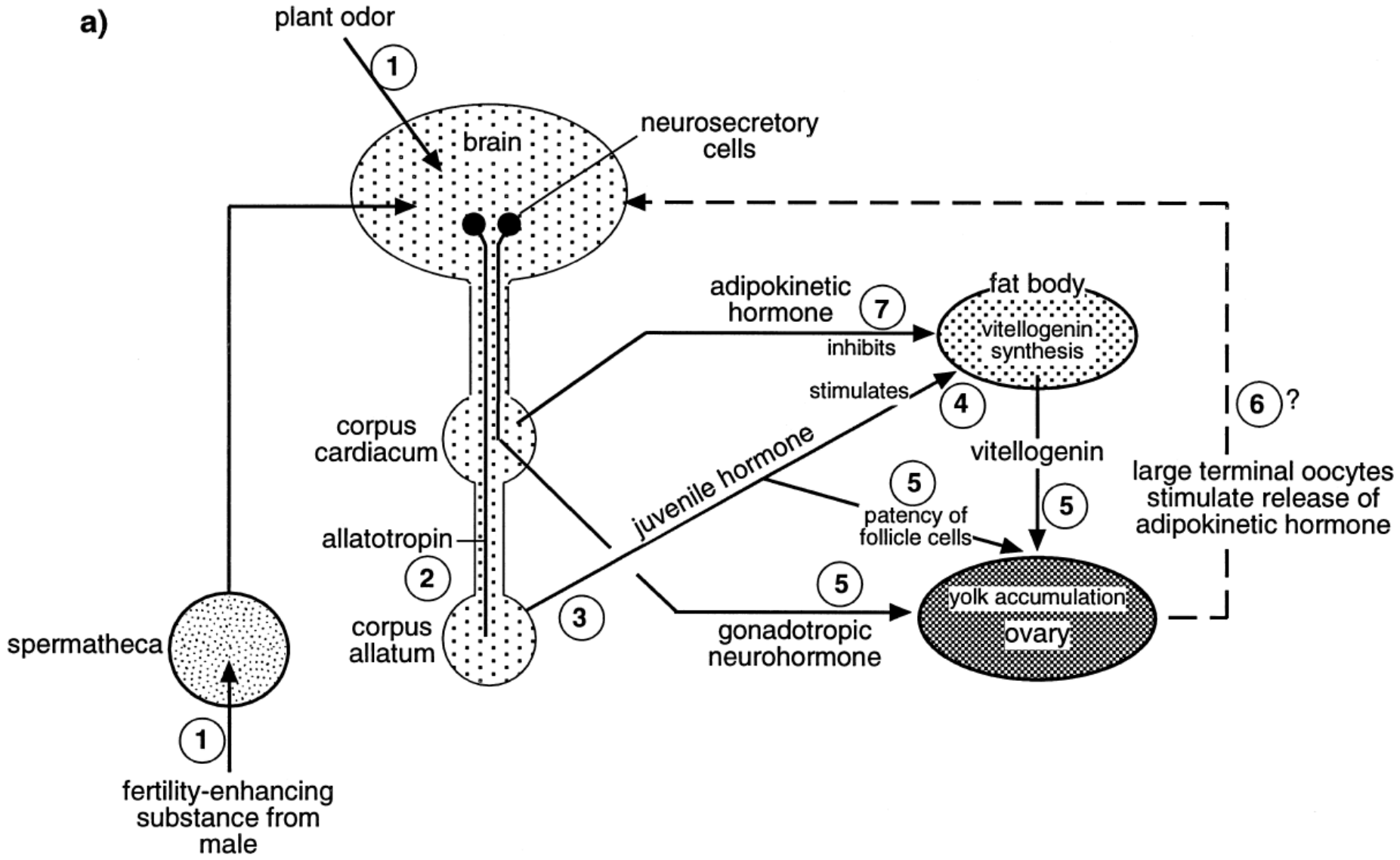

Obr. 8 **Řízení syntézy vitellogeninů - Diptera**

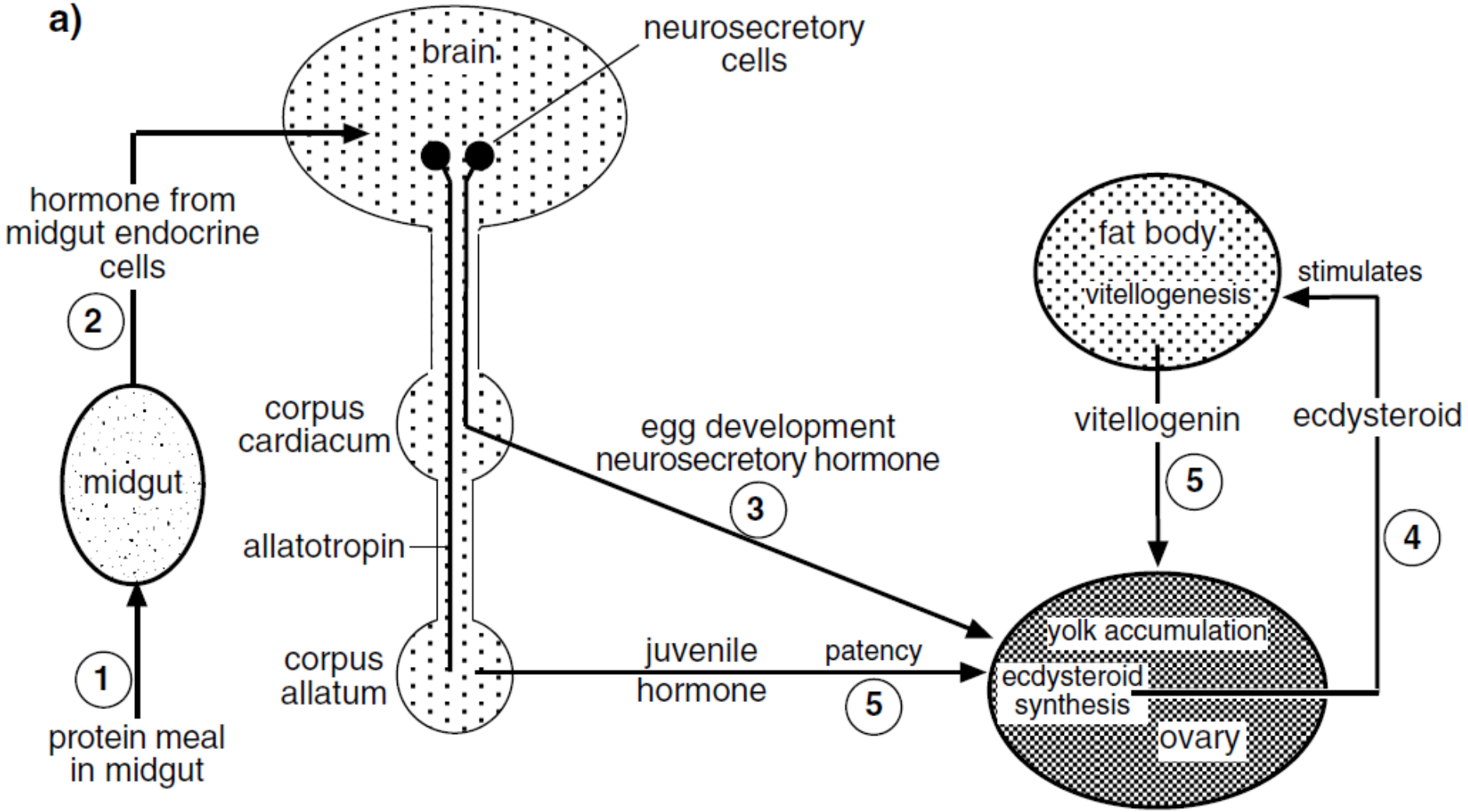

Obr. 9

Hormonální a nervové řízení kladení vajíček

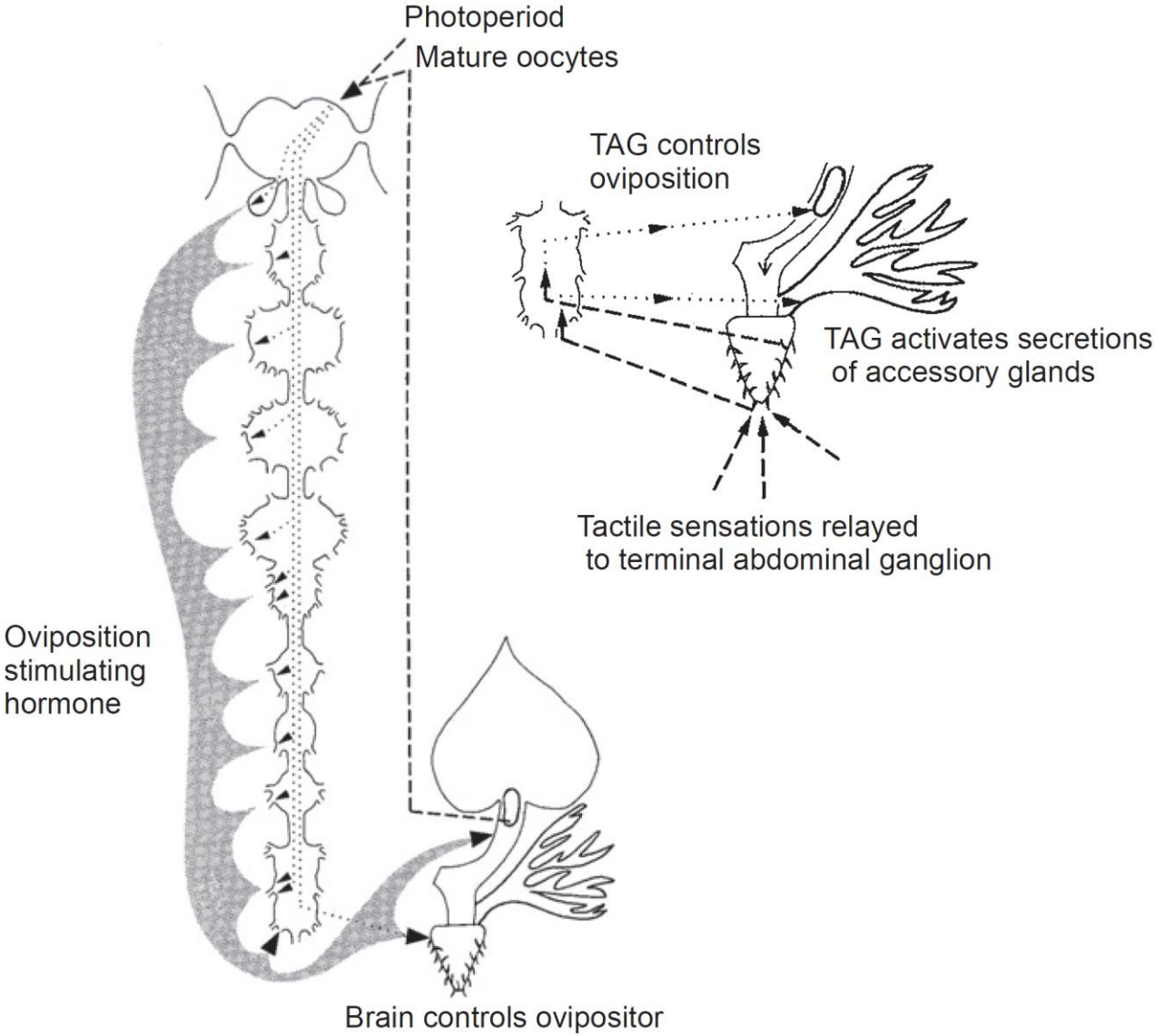

FIGURE 4.16. The control of oviposition in the cockroach, *Sphodromantis lineola*. The proper photoperiod and the presence of mature oocytes are perceived by the brain, which triggers the release of an oviposition-stimulating hormone from the ventral ganglia that causes the oviduct muscles to contract. The brain also controls the searching movements of the ovipositor. Tactile sensations of the ovipositor are relayed to the terminal abdominal ganglion, which activates the secretions by the accessory glands. The perception of all these components by genital receptors causes further contractions of the oviducts and oviposition. From Mesnier (1984). Reprinted with permission.

Obr. 10

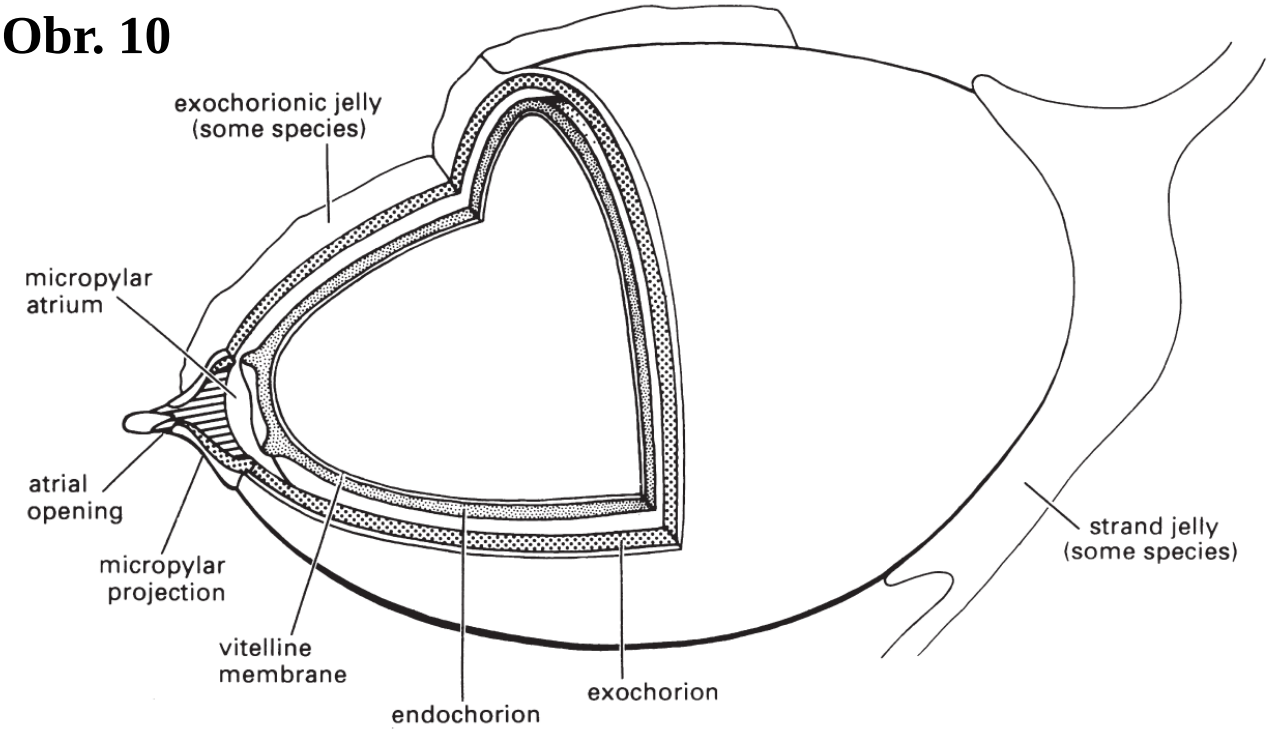

Fig. 5.10 The generalized structure of a libelluloid dragonfly egg (Odonata: Corduliidae, Libellulidae). Libelluloid dragonflies oviposit into freshwater but always exophytically (i.e. outside of plant tissues). The endochorionic and exochorionic layers of th eggshell are separated by a distinct gap in some species. A gelatinous matrix may be present on the exochorion or as connecting strands between eggs. (After Trueman 1991.)

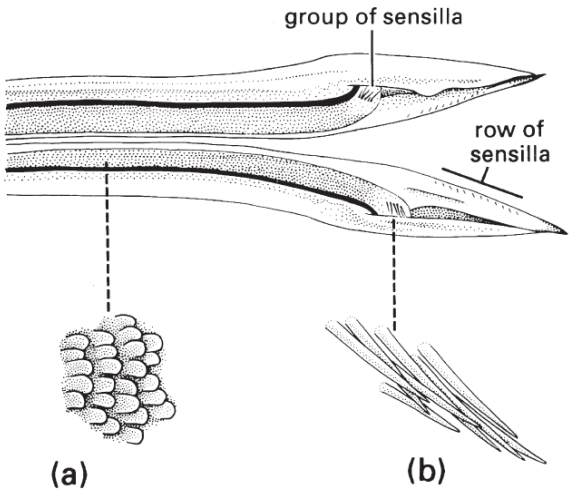

Fig. 5.12 Tip of the ovipositor of a female of the black field cricket, *Teleogryllus commodus* (Orthoptera: Gryllidae), split open to reveal the inside surface of the two halves of the ovipositor. Enlargements show: (a) posteriorly directed ovipositor scales; (b) distal group of sensilla. (After Austin & Browning 1981.)

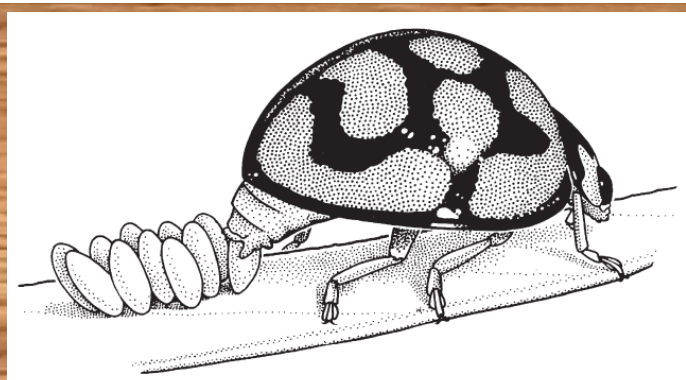

Fig. 5.9 Oviposition by a South African ladybird beetle, *Chilomenes lunulata* (Coleoptera: Coccinellidae). The eggs adhere to the leaf surface because of a sticky secretion applied to each egg. (After Blaney 1976.)

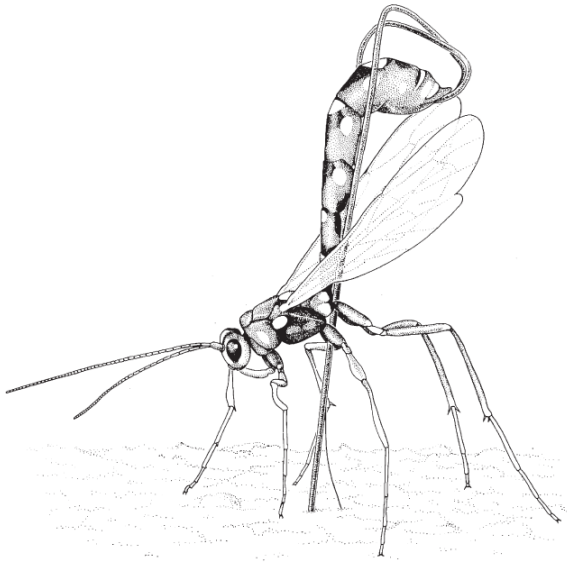

Fig. 5.11 A female of the parasitic wasp *Megarhyssa nortoni* (Hymenoptera: Ichneumonidae) probing a pine log with her very long ovipositor in search of a larva of the sirex wood wasp, *Sirex noctilio* (Hymenoptera: Siricidae). If a larva is located, she stings and paralyses it before laying an egg on it.

Obr. 11 **Hemocelická inseminace**

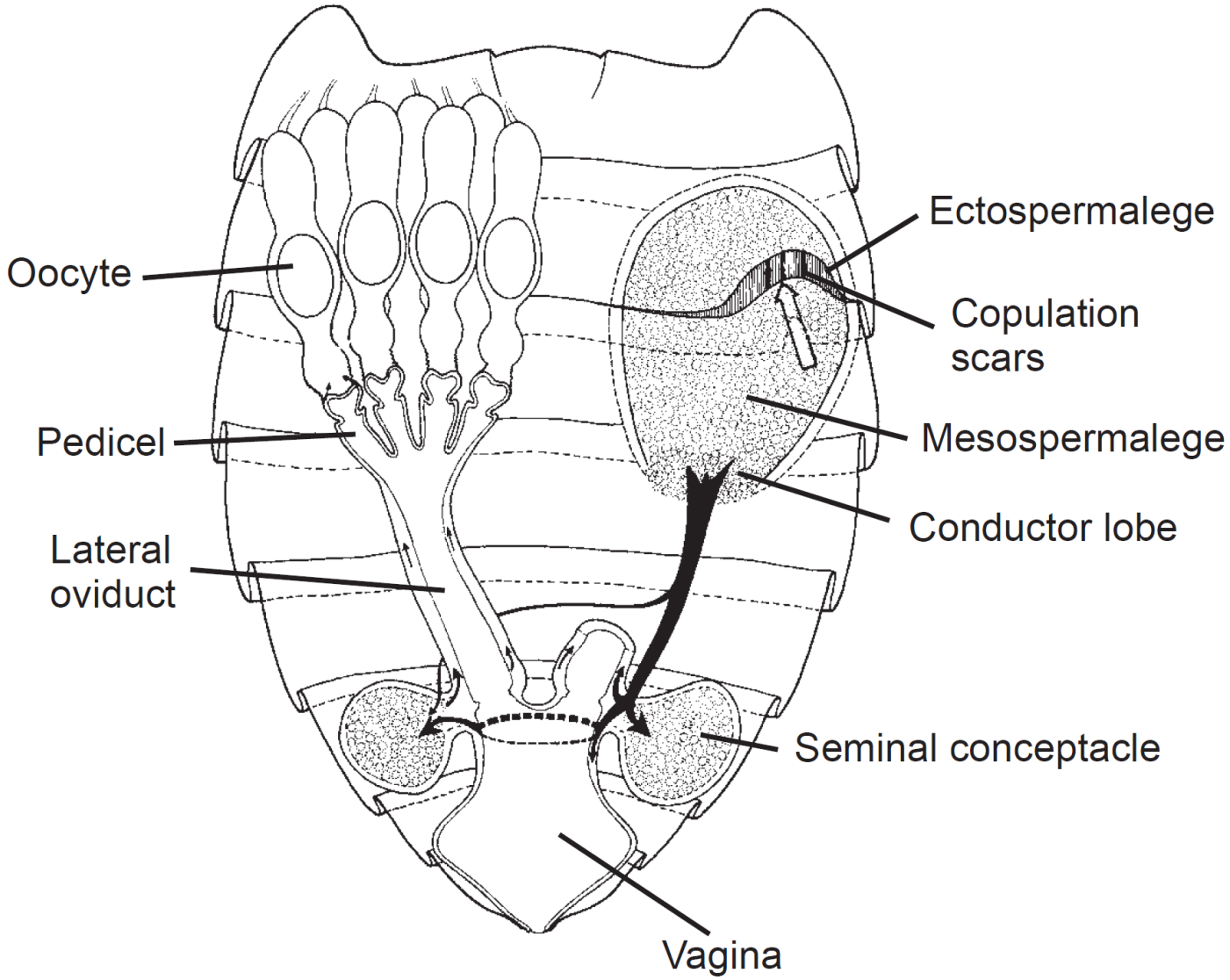

Figure 4.30. The abdomen of the bed bug, containing the reproductive tract. The ectospermalege, a cuticular pouch on the abdomen, is a special reception site for sperm introduced by hemocelic insemination. From Carayon (1966). Reprinted with permission.

12. Hmyzí produkty využitelné člověkem

Obr. 1 Hmyz jako potrava

Obr. 2 **Nutritivní skladba některých druhů hmyzu**

Table 1.2 Proximate, mineral, and vitamin analyses of four edible Angolan insects (percentages of daily human dietary requirements/100 g of insects consumed). (After Santos Oliviera et al. 1976, as adapted by DeFoliart 1989.)

Nutrient	Requirement per capita (reference person)	*Macrotermes subhyalinus* (Termitidae)	*Imbrasia ertli* (Saturniidae)	*Usta terpsichore* (Saturniidae)	*Rhynchophorus phoenicus* (Curculionidae)
Energy	2850 kcal	21.5%	13.2%	13.0%	19.7%
Protein	37 g	38.4	26.3	76.3	18.1
Calcium	1 g	4.0	5.0	35.5	18.6
Phosphorus	1 g	43.8	54.6	69.5	31.4
Magnesium	400 mg	104.2	57.8	13.5	7.5
Iron	18 mg	41.7	10.6	197.2	72.8
Copper	2 mg	680.0	70.0	120.0	70.0
Zinc	15 mg	–	–	153.3	158.0
Thiamine	1.5 mg	8.7	–	244.7	201.3
Riboflavin	1.7 mg	67.4	–	112.2	131.7
Niacin	20 mg	47.7	–	26.0	38.9

Obr. 3 Snovací žlázy bource morušového

Obr. 4 Snovací žlázy bource morušového

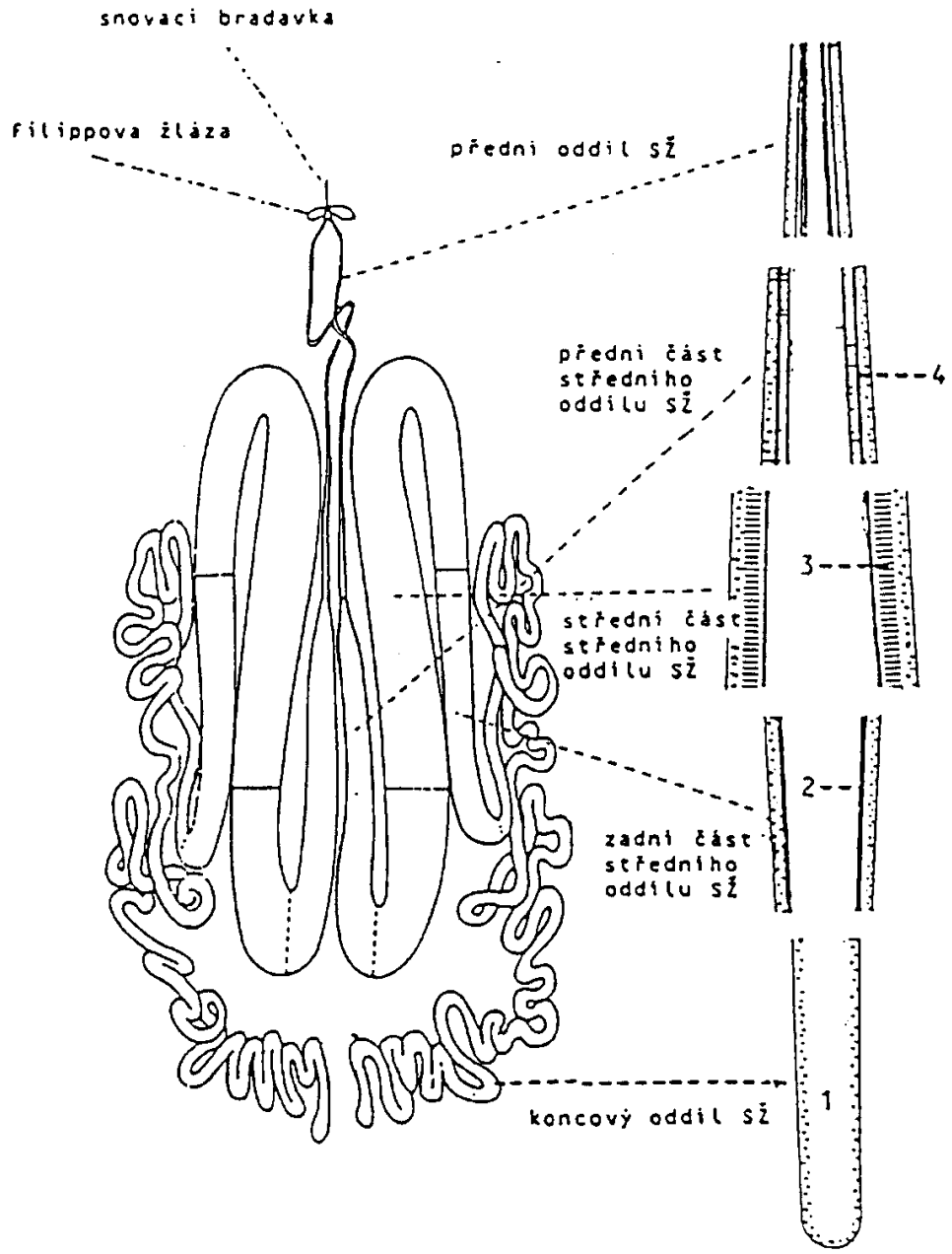

Obr. 5 **Bourec morušový – hlavní producent komerčného přírodního hedvábí**

https://www.youtube.com/watch?v=77ktNSPFbwQ

Obr. 6 Hedvábná vlákna martináče dubového *Antheraea yamamai*, SEM foto - F. Weyda

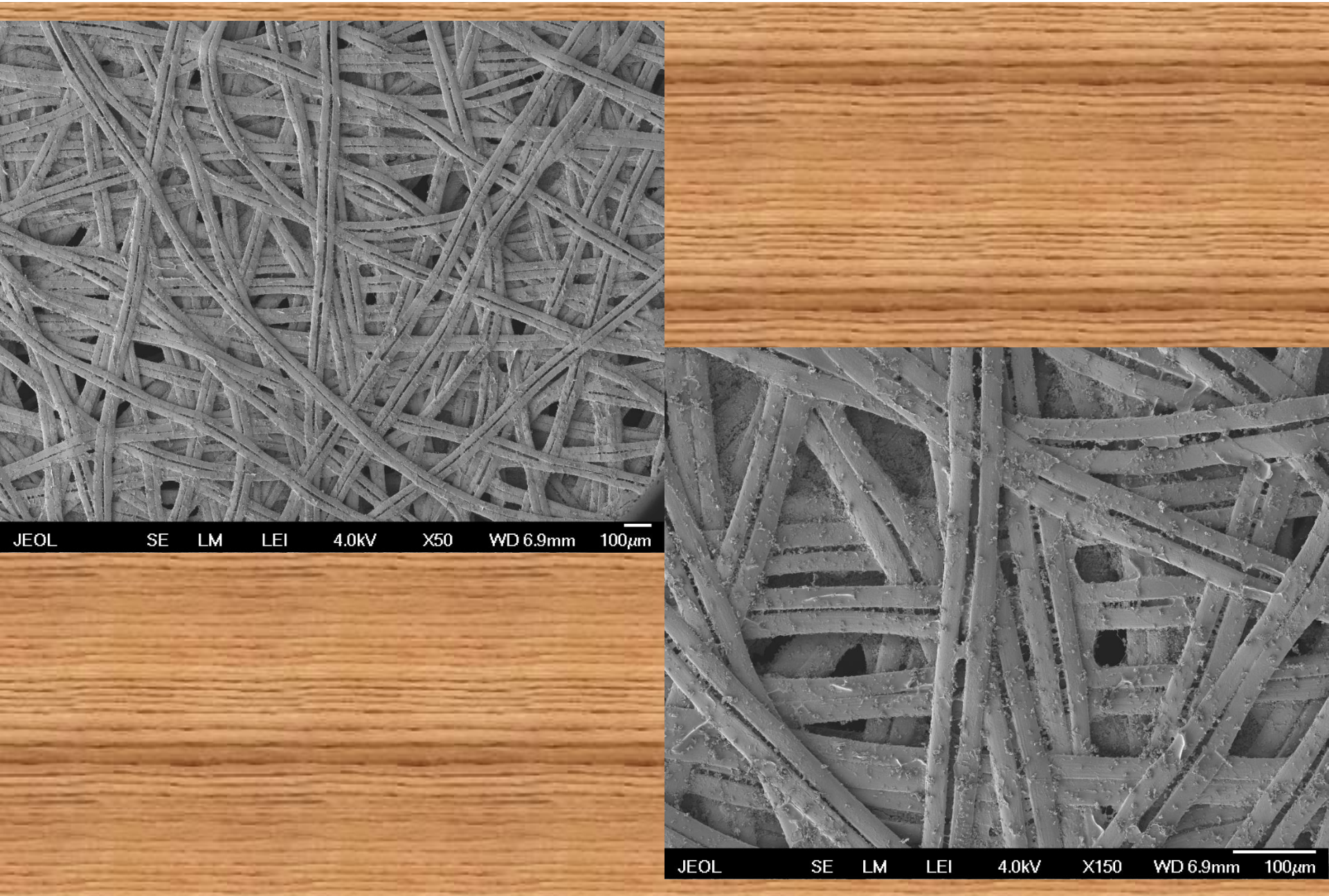

Obr. 7 Hedvábná vlákna martináče dubového *Antheraea yamamai* s krystalky šťavelanu vápenatého, SEM, foto – F. Weyda

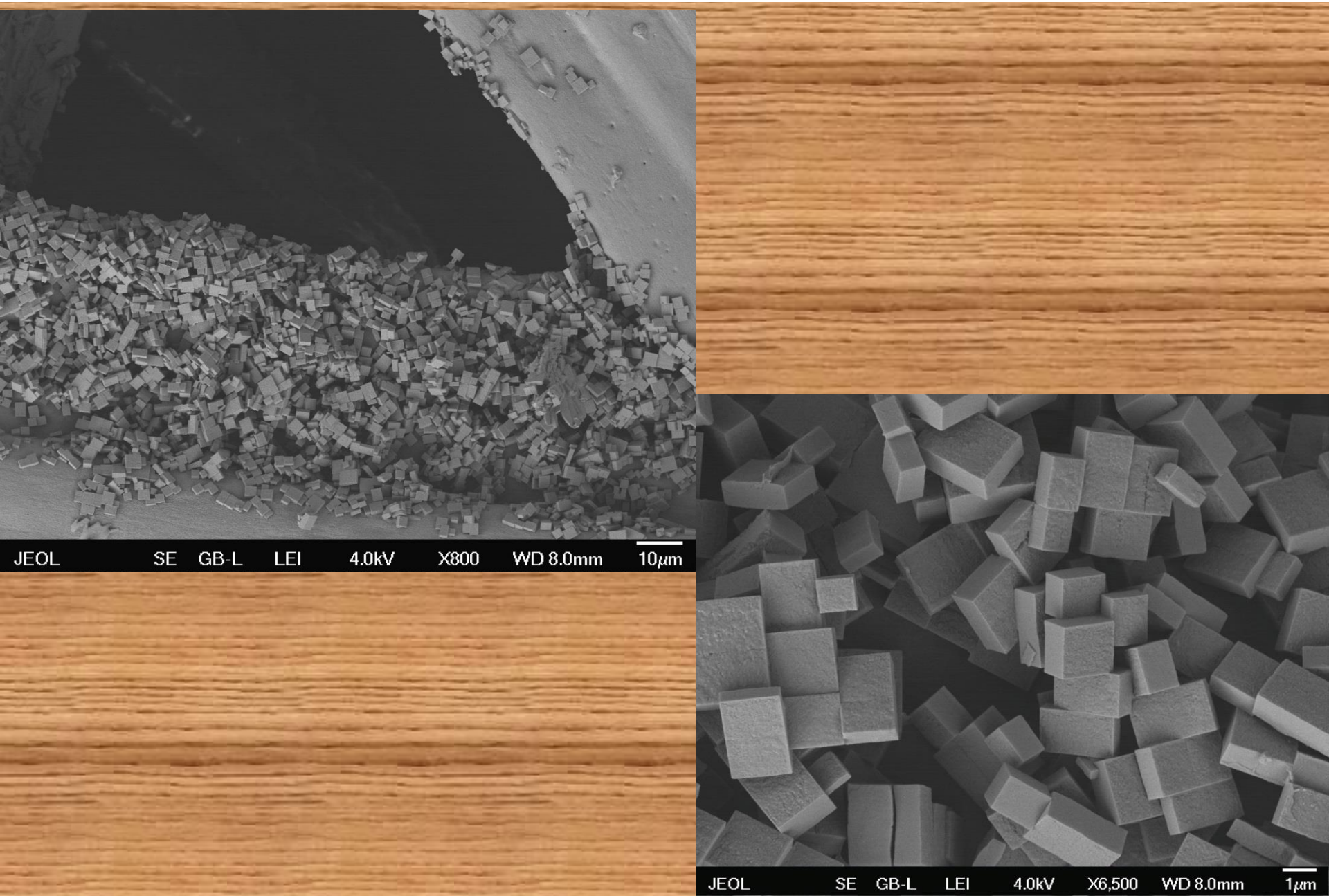

Obr. 8 Včelí med a jeho složení

SLOŽKA	KVĚTOVÝ	MEDOVICOVÝ	jednotka
JEDNODUCHÉ CUKRY			
Fruktóza	38,2	31,8	%
Glukóza	31,3	26,1	%
SLOŽITÉ CUKRY			
Sacharóza	0,7	0,5	%
Ostatní	9,5	22,1	%
MINERÁLNÍ LÁTKY			
Draslík	205	1676	mg/kg
Sodík	18	76	mg/kg
Vápník	49	51	mg/kg
Hořčík	19	35	mg/kg
Železo	2,4	9,4	mg/kg
Mangan	0,3	4,1	mg/kg
Křemík	9	14	mg/kg
Zinek	1,2	2,5	mg/kg
VITAMÍNY			
B_1, B_2, B_3, B_5, B_6, C - vše v malém množství			
OSTATNÍ			
Voda	18		%
Antioxidanty	2		mmol/kg
Tuky	0,015		%
pH	3,4	6,1	

A dále: pylová zrna, bílkoviny, kyseliny, aminokyseliny, barviva, aromatické látky, acetylcholin, adrenalin, peroxid vodíku, ...

Obr. 9 Včelí vosk

Obr. 10 Šelak

Obr. 11 Vosí žihadlo a orgány produkující vosí jed

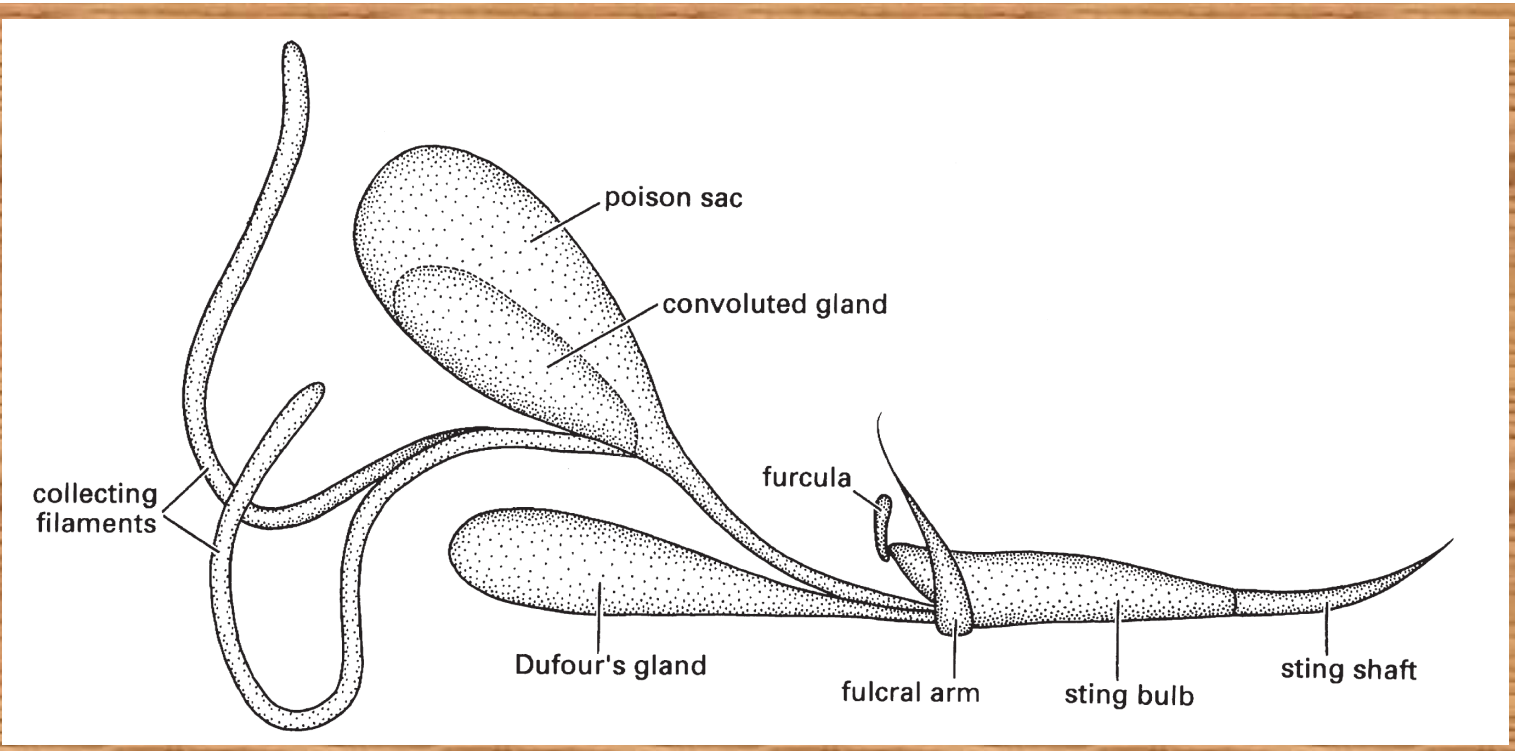

Včelí žihadlo je vybaveno zpětnými háčky

Obr. 12 Složení včelího jedu

SLOŽKA	PODÍL
sušina	20 – 30%
melittin	50% sušiny
fosfolipáza	12% sušiny
apamin	2% sušiny
minimin	2% sušiny
MCD peptid	2% sušiny
hyaluronidáza	2% sušiny
quinin, secapin, procamin, adolapin, terpiapin, fosfomonoesteráza, lysofolipáza, alfa-glucosidáza, histamin, dopamin, noradrenalin, kyselina tau-aminomáselná	do 1% sušiny

Děkuji za pozornost a hodně štěstí u zkoušky!